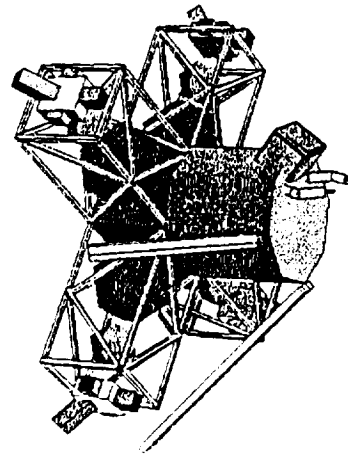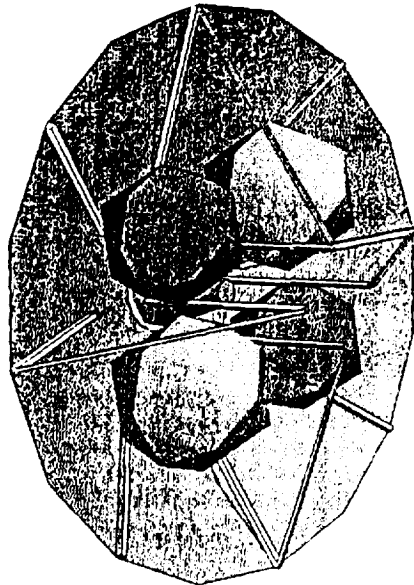*IN-18-CR
26130
415P*

# MOOSE

## Manned On-Orbit Servicing Equipment

University of Maryland College Park
Department of Aerospace Engineering
ENAE 412 Design Project
Spring 1993

Professor David Akin, Sc.D.

# Abstract

The ability to service satellites has thus far been limited to Low Earth Orbit (LEO) platforms within reach of the Space Shuttle. Other orbits, such as Geosynchronous Orbits (GEO) containing high-value spacecraft have, thus far, not been attainable by a servicing vehicle. The useful life of a satellite can be extended by replacing spent propellant and damaged Orbital Replacement Units (ORUs), forestalling the need for eventual replacement. This growing need for satellite on-orbit servicing can be met by the Manned On-Orbit Servicing Equipment (MOOSE). Missions requiring orbit transfer capability, precision manipulation and maneuvering, and man-in-the-loop control can be accomplished using MOOSE. MOOSE is a flexible, reusable, single operator, aerobraking spacecraft designed to refuel, repair, and service orbiting spacecraft. MOOSE will be deployed from Space Station Freedom, (SSF), where it will be stored, resupplied, and refurbished.

# Acknowledgements

Executive Summary

# MOOSE
## Manned On-Orbit Servicing Equipment

**University of Maryland, College Park**
**Department of Aerospace Engineering**
**College Park, Maryland**

Professor David L. Akin, Sc.D.
Tharen Rice, Teaching Assistant

Jason Budinoff, J. Corde Lane, Nicole Leontsinis, Ram C. Singh,
and the MOOSE Design Team

## ABSTRACT

The ability to service satellites has thus far been limited to Low Earth Orbit (LEO) platforms within reach of the Space Shuttle. Other orbits, such as Geosynchronous Orbits (GEO) containing high-value spacecraft have, thus far, not been reachable by a servicing vehicle. The useful life of a satellite can be extended by replacing spent propellant and damaged Orbital Replacement Units (ORUs), forestalling the need for eventual replacement. This growing need for satellite on-orbit servicing can be met by the Manned On-Orbit Servicing Equipment (MOOSE). Missions requiring orbit transfer capability, precision manipulation and maneuvering, and man-in-the-loop control can be accomplished using MOOSE. MOOSE is a flexible, reusable, single operator, aerobraking spacecraft designed to refuel, repair, and service orbiting spacecraft. MOOSE will be deployed from Space Station Freedom, (SSF), where it will be stored, resupplied, and refurbished.

## INTRODUCTION

### MOOSE Description

The MOOSE spacecraft is an orbiting vehicle capable of sending an astronaut on three day satellite servicing missions to GEO or LEO and back to SSF. The astronaut is housed in a "shirt-sleeve" environment, Extravehicular Activities (EVAs) are not permitted from the MOOSE, since the vehicle is a single-person vessel.

In order to conduct the servicing tasks, MOOSE is equipped with a seven degree of freedom (DOF) Telerobotic Manipulator Arm (TMA), a four DOF Telerobotic Grappling Arm (TGA), and a Manual Manipulation System (MMS). MOOSE will employ a 9m reusable aerobrake in order to return rendezvous with SSF from GEO.

The MOOSE vehicle can be separated into two distinct parts. The first is the MOOSE Manned Module (MMM), shown in Figure 1 (top). It consists of the crew cabin, the Reaction Control System (RCS), spider truss, and the Manipulator/Grappler System (Man/Grap). The second part is the MOOSE Propulsion Module (MPM), shown in Figure 1 (bottom). It consists of the aerobrake, main spinal truss, and main propulsion unit.

The MOOSE flight vehicle operates in 2 modes. The first is the primary operational configuration for servicing missions to GEO. It entails using the entire flight vehicle, consisting of MPU and the MMM fully fueled. The second is the "cab-only" mode, in which the MMM flight vehicle separates from the MPU. This configuration is used to conduct servicing missions in LEO, or in close proximity to SSF, and enables MOOSE to be more maneuverable and cost-effective.
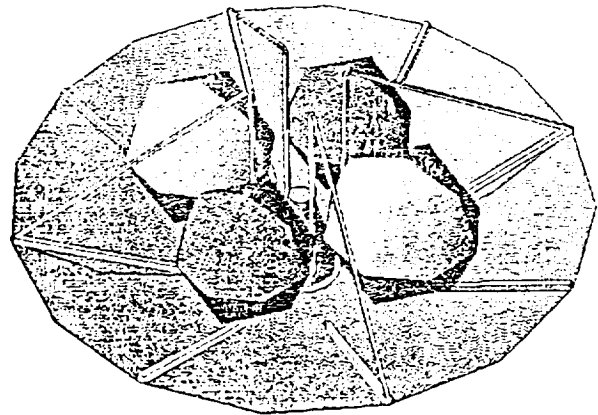


Figure 1. MMM (top) and MPM (bottom)

MOOSE subsystems are designed as ORUs which can be changed out via the SSF Remote Manipulator System (RMS). All significant systems are configured to make access, test, and change-out as simple as possible.

### SSF-Based Operations

MOOSE operations increase the frequency of SSF departing/arriving spacecraft. Propellant Maneuvering Vehicles (PMVs), shuttles, and MOOSE will be utilizing SSF airspace, possibly simultaneously. A SSF traffic management scheme has been developed based upon the Johnson Space Center (JSC) Orbital Maneuvering Vehicle plan for SSF terminal control zone management.

Dedicated MOOSE support personnel on-station will be minimal. MOOSE maintenance, check-out, and refurbishment tasks will be as automated as possible. Dedicated Inter-Vehicular Activities/Extra-Vehicular Activities (IVA/EVA) would be performed by the available crew as needed.

A second crew member is required, in addition to the astronaut operating the MOOSE, to operate the SSF RMS during berthing and de-berthing operations.

## Expendable Launch Vehicle (ELV) Operations

ELV operations are essential to the MOOSE mission. Regular propellant delivery must be maintained if flexibility is desired. PMVs would be delivered to SSF from their respective launch sites.

## VEHICLE OVERVIEW

In its standard configuration (MPU mated to the MMM), the MOOSE vehicle weighs 3067 kg (dry) and 14481 kg (wet). This configuration is the maximum weight for a three-day GEO servicing mission. For LEO missions, the MPU can be left at *Freedom*, creating a vehicle that would weigh a maximum of 1235 kg (dry) and 1980 kg (wet).

MOOSE is capable of carrying 800 kg of payload to orbits inclined up to 70° at altitudes from 185 km to 40,000 km. Consumables are provided for a nominal 3-day mission, with contingency mission duration of 10 days.

## COSTING OVERVIEW

*Develop Cost*
| | | |
|---|---|---|
| RDT&E | $2,374.70 | M93 |
| First Unit | $203.90 | M93 |
| Flight Unit | $203.90 | M93 |

*Development Operations Costs*
| | | |
|---|---|---|
| ASE RDT&E | $1,100 | M93 |
| ELV Support | $1,182 | M93 |
| Ground Support | $375 | M93 |

*Mission Operations Cost*
| | | |
|---|---|---|
| 3 sorties/year | $294 | M93 |
| 6 sorties/year | $432 | M93 |
| 13 sorties/year | $780 | M93 |

*Program Cost @ IOC*
| | | |
|---|---|---|
| | $5,439.50 | M93 |

*Median Operations Cost/year*
| | | |
|---|---|---|
| | $432 | M93 |

Table 1 Overview of projected costs

## NAVIGATION AND TRACKING

### Orbit and Attitude Determination

Orbit information must be accurate enough at geostationary orbit to bring the vehicle within tracking distance of the target. The working range of the selected rendezvous system will be 4.5 nmi. The error in position at GEO added to the error in the target's known position must therefore be less then this range. Using a .75 safety factor, the requirement for GEO position determination accuracy will therefore be 6 km.

At LEO and below, the main positioning requirement will be determined by the aerobraking maneuver. Non-inertial navigation systems will be blacked out during this maneuver, so inertial guidance will be need to be

accurately calibrated before the maneuver. From GEO, an accuracy of 2 km will be required for the aerobraking window. On approach to the maneuver, the window will be smaller, requiring an accuracy of 100 m for necessary course adjustments.

### Inertial Measurement Units (IMUs)

Two IMUs will be used on MOOSE, and will consist of sensors that measure both rotational motion (using gyroscopes) and translation motion (using accelerometers). Strapdown units will be used instead of gimbaled platforms because they have less mechanical complexities and mass, while maintaining accuracy comparable to that of gimbaled systems.

The Inertial Measurement Unit (IMU) was chosen as the primary navigation system for its high accuracy. The main drawback of IMUs are the time degradation that they undergo. To keep their accuracy, position and orientation information must be updated before the data is no longer useful. Immediate updates would be required immediately after large $\Delta V$ burns.

### Global Positioning System (GPS)

GPS provides 25 m accuracy at LEO, but it is not designed to work above 8000 nmi altitude. This system will be used to meet the 100 m aerobrake accuracy requirement. GPS will be used in LEO for calibration of the IMUs. All LEO and GEO transfer orbits will be calculated using GPS and Kalman filtering software. A GPS update occurs at the rate of 2 updates per second. GPS information is used to verify the aerobraking maneuver approach orbit.--updates are fast enough to allow for mid-course corrections.

### Microcosm Autonomous Navigation System (MANS)

This system provides 600m to 1.5 km accuracy using 2 sensors. This system is necessary for long term navigation in GEO, and to meet the 2 km aerobrake window requirement. It can provide orientation updates to an accuracy of 0.01 degrees, using the sun as a reference. For 11.4% of the time in GEO, the sun will be blocked out, but the horizon sensors will still be functional, providing an accuracy of 0.1° to 0.25°. For 4.6% of the time, no orientation updates are possible. For the first 20 hours after GPS updates are lost, the IMUs are more reliable than MANS. After this point, MANS must begin linear navigation updates at its returning frequency of 0.5 Hz.

### Star Trackers

This system can provide updates to an accuracy of 0.01° when the sun's glare does not affect the sensor. Although it can be used at other points, the star trackers will definitely be able to be used during the 16% MANS blackout/partial blackout time. Star trackers are useful in increasing the accuracy of the altitude measurement, and for determining the angle and angle rate to a target for rendezvous purposes.

### OMV Rendezvous Radar

Although the Orbital Maneuvering Vehicle project has been canceled, its rendezvous radar has been fully designed. This system was specifically designed to assist the rendezvous tasks that MOOSE is required to do. It has a range of 4.5 nmi, and an accuracy of better then 20 ft, or <2% of the range. It also provides a range rate accuracy of greater than 0.1 ft/sec, or 2% of the range rate.

## CONTROL MOMENT GYROSCOPES

External torques, such as those produced by solar radiation and gravity gradients, and internal torques, such as that produce by positional uncertainty of the center of gravity, must be compensated for. A trade study was done comparing the mass of the fuel required to do orientation adjustment for a typical three day mission versus the mass of the control moment gyroscopes (CMGs) required to do the same job. The required fuel mass was 150 kg for the cold gas thrusters and 242 kg of hydrazine for the RCS. This compares with a CMG mass of 76 kg.

The MOOSE vehicle was designed to use double-gimbaled CMGs for three-axis control. The CMGs are located near the center of gravity for maximum performance. Three CMGs are used for redundancy considerations—should one fail, the other two will be able to maintain three-axis control. The primary RCS can be used to desaturate the CMG wheels. The impulse torques caused by gravity gradients, solar pressure, and aerodynamic effects are well below the impulse torques that the moment gyros were designed for.

The model used to design the wheels was a thin-rim, high-speed flywheel. It was found that AISI 4340 (normalized at 1600°F, quenched in oil from 1525°F) would give the smallest wheel radius and the maximum performance. For high-speed bearings, (>3000 rpm), a closed loop oil system should be used to give an active flow through lubrication system which would enhance the bearing life by continuously supplying additional oil to the spinning ball bearing at a controllable rate. A DC brushless motor will be used for its high torqueing capability. A tachometer will be used to monitor the wheel speed.

## REACTION CONTROL SYSTEM

The manned module must be able to maneuver around and approach the target satellite from any angle to capture and repair it. The reaction control system is comprised of primary and secondary thrust chambers. The need to ensure a contamination-free environment about the SSF and satellite hardware drove the two-system design.

### Primary RCS

The primary thrusters are utilized for attitude control, course corrections, orienting the MOOSE vehicle for proper guidance & navigation sensing and aerobrake-maneuver positioning, desaturating the control moment gyros, and collision avoidance.

The primary thrust chambers utilize monopropellant liquid anhydrous hydrazine and operate in pressure blow-down mode with helium as the pressurant gas. The hydrazine system does not require an oxidizer for combustion, it spontaneously decomposes as it flows over the Shell 405 catalyst bed and produces hot gases which are expelled through the nozzle. The selected level of ammonia dissociation is 0.6 and the resulting performance level, Isp, is 240 seconds.

A total of 24 520 N (100 lbf) hydrazine thrusters will be utilized. Four thrust chambers will be on the lower truss struts, with one on each strut. Twenty thrust chambers will be on the spider truss booms with five on each boom. The total monopropellant mass is 512 kg, and the total mass of the 24 hydrazine thrusters is 44.74 kg. The figure below is a schematic of a typical hydrazine thruster configuration.
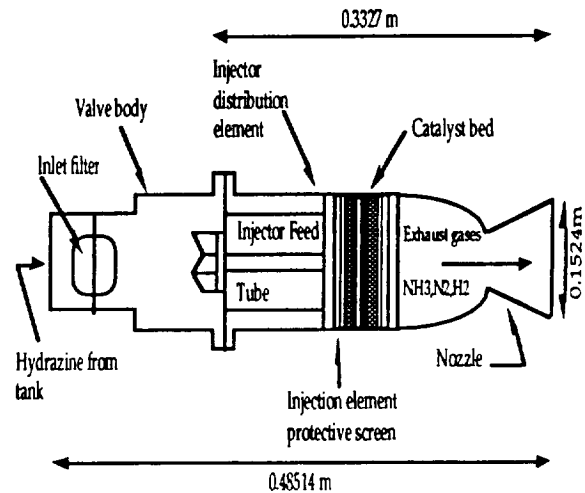


Figure 2 Hydrazine Thruster Configuration

### RCS Spider Truss

The RCS Spider truss serves as a platform for the MOOSE RCS. The boom extends for only 2.6 m from the center line of the MOOSE, to protect the nozzles during the aerobraking maneuver. It houses the RCS tanks within its members and acts as a boom for the reaction control nozzles to ensure their operation as far away from the c.g. of the MOOSE vehicle as possible. The trusses and the avionics box are an integrated structure which attaches to the bottom of the MOOSE crew cabin.

The material selected for the truss is a high-strength graphite/epoxy with a 45° fiber orientation to ensure the composite's strength in bending. The resulting configuration for the spider truss consists of two different cross sections. The inner and outer cross members both have circular cross sections of outer radius 1.25 cm and inner radius of 1.0 cm. The remaining spider truss members have circular cross sections of outer radius 7 mm and inner radius 5 mm. The mass per spider truss is 9.36 kg, therefore, the total mass for all four spider trusses is 37.5 kg.

### Primary RCS Tanks

Two tanks are necessary to store the hydrazine monopropellant and helium gas pressurant. The blow-down ratio is 4.2 , with a beginning of life tank pressure of 420 psi and an end of life pressure of 100 psi. The total volume for hydrazine propellant is 0.5005 m$^3$ and the helium pressurant volume is 0.1564m$^3$. The radius of each of the tanks is 0.428m and the material is Al 1100-0 which is resistant to the corrosive effects of hydrazine.

Hydrazine freezes at 273K so line heaters were used to ensure the operability of the thrusters.

### Secondary RCS

Due to the sensitivity of the SSF and satellite hardware to contamination from thruster exhaust products, a helium cold gas thruster system is utilized for all GEO satellite-servicing operations and for separation and docking maneuvers. The mass of the helium for the secondary thrusters is 223 kg. The total mass of the 40 thrusters is 3.4 kg. The thrusters on the lower truss struts are grouped

in threes with one grouping per strut. Seven cold gas thrusters were located on each boom of the spider truss. These thrusters produces 20 lbf (89 N) at a pressure-at-thrust of 1000 psi. The area expansion ratio is 25:1.
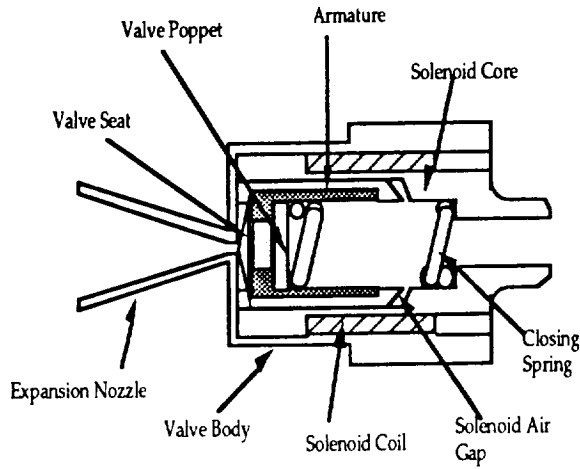


Figure 3 Single Seat Cold Gas Thruster

## Secondary RCS Tanks

The helium cold gas for the secondary thrusters will be stored in four (4) Ti 8-1-1 tanks at a tank thickness of 1.66 cm and a mass per tank of 55.75 kg. The tank pressure is $41.4E6 \text{ N/m}^2$.

## MAIN PROPULSION SYSTEM

The main propulsion system of MOOSE will perform four burns on a typical mission. These burns include GEO transfer injection, GEO circularization, LEO transfer injection, and LEO circularization after the aerobrake maneuver.

Propellant Transport Cost vs. Structural Mass
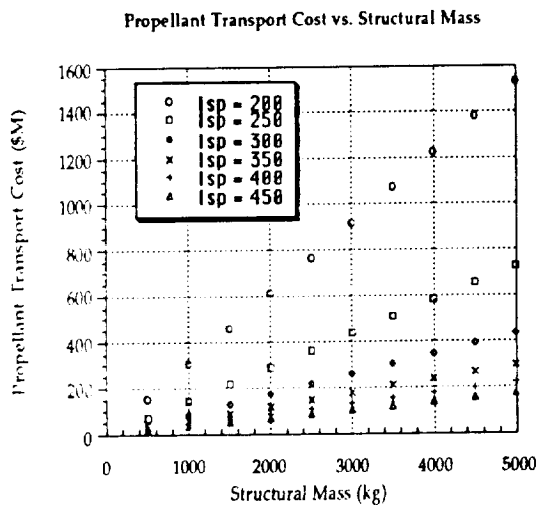


Figure 4 Propellant Transport Costs vs. Structural Mass

The main propulsion system utilizes cryogenic liquid hydrogen and liquid oxygen as the fuel and oxidizer respectively. To achieve cost efficiency in propellant

transport cost so the customer price tag does not exceed 100 $Million, the performance level, Isp, must be 450 seconds. The figure below demonstrates the relationship between cost and performance level. The mixture ratio is optimized at 7:1 which maximizes the Isp, and assures complete combustion of the liquid oxygen while not running too hydrogen rich, where some of the hydrogen does not combust.

The dimensions of the combustion chamber are as follows: chamber diameter is 0.281 m, chamber volume is 0.022 $m^3$, and chamber length is 0.355 m.

### Injector Design

The injector is designed to deliver the propellants to the combustion chamber and to sufficiently mix and atomize the propellants to form a homogeneous fuel-oxidizer mixture.

The injection system selected is a coaxial non-impinging configuration which is the most common for Oxygen/Hydrogen engines, including the SSME, and provides good combustion stability. Low velocity liquid oxygen (LOX) is fed through a tube which is surrounded by high velocity gaseous hydrogen (GH2). The GH2, already warmed from the regenerative cooling cycle, warms the liquid oxygen in the tube and vaporizes it. The gaseous hydrogen and oxygen then readily mix in the combustion chamber.

### Ignition System

The ignition system is of critical concern for it must ensure rapid ignition of the propellant mixture and equally rapid thrust increase to the designed rating.

A spark-torch igniter was selected for the ignition system. It is highly reliable, has multiple restart capability (a must for MOOSE), and performs well at high altitude. The spark-torch igniter allows some propellant in, then supplies a spark for ignition. The flame is then ducted to various locations on the injector face to ignite the main propellant flow.

### Nozzle Design

The expansion nozzle is designed to take the high temperature exhaust gas flow and expand it to allow the thermal energy of the flow to be transformed into kinetic energy, i.e. useful propulsive energy.

The MOOSE will use a bell shaped nozzle with an area expansion ratio of 40:1 at a design mach number of 4.22. This expansion ratio relates to an exit area of 0.99 $m^2$ and a throat area of 0.0248 $m^2$.

The large heat flux to the nozzle walls from the combustion products requires a cooling process that will preserve the nozzle contour, its material integrity, and allow for an indefinite firing duration. A regenerative cooling system was selected over nozzle-material ablation since it satisfies the above mentioned requirements and the vehicle has available coolant, the LH2 fuel. This cooling method is relatively lightweight since additional on-board cooling subsystems are not required and the desire to achieve a maximum Isp, to successfully perform the MOOSE mission requirements, is achieved through augmenting the energy content in the combustion chamber by utilizing the thermal energy picked up by the LH2 in cooling the nozzle. The high heat flux capacity, necessary for LOX/LH2

combustion, is also accounted for by the regenerative cooling system.

## Turbopump Feed System / Plumbing

The pump system selected is an expander cycle turbopump feed system. An Auxiliary Power Unit (APU) is used to initiate the propellant flow to the combustion chamber. The hydrogen fuel exiting the nozzle cooling-jacket will drive both the oxidizer and fuel turbines which drive the fuel and oxidizer pumps. Once initiated, the propellant pumping process is self perpetuating and is sustained by the turbine generating 82.7 kW of power to drive the pumps at the required pressure of $2.66 \times 10^6 N/m^2$.
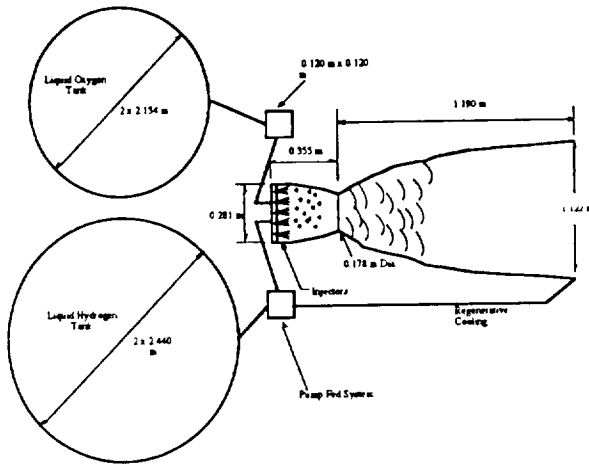


Figure 5 Main Propulsion System Configuration

## Thrust Vectoring Control

Thrust vectoring will be controlled by the RCS for pitch, yaw and roll motions of the MOOSE vehicle The thrusters are located at the ends of each boom of the spider truss and on each of the lower truss struts. The location of the thrusters will provide three axis stability.

## Main Propulsion Malfunctions

The MOOSE can survive a main propulsion system malfunction if it occurs either after the first or after the third main engine burn. In the event that a malfunction occurs after the first main engine burn, the astronaut will remain in the elliptical Hohmann transfer orbit until the vehicle returns to the SSF. It will take ten and a half hours to return to SSF. The astronaut can survive this since the MOOSE is designed and equipped for a three day mission. If the malfunction occurs after the third burn for LEO injection, the RCS will handle the necessary maneuvers to return the astronaut safely to the SSF.

Malfunctions occurring after the GEO circularization and prior to the LEO transfer injection burns will require the astronaut to wait for a rescue vehicle in order to return to the space station.

## Main Propulsion Tanks

The main propellant tanks will be launched empty from Earth using the NASA Space Shuttle launch platform and will be integrated with the MOOSE system on orbit at Space Station Freedom. For the launch from Earth, the tanks will be pressurized to stiffen the structure against

loads resulting from the launch. The tank walls will consist of Al-1100 at thicknesses of 3.5 mm and 3.0 mm for the liquid hydrogen and liquid oxygen tanks respectively, and corresponding tank masses of 178 kg and 99 kg.

The tanks will be integrated to the central support truss by a 10 cm x 5 cm, 1.1 kg Al-1100 disk threaded around its surface area and located at the top of each of the tanks. The bottom of the tanks rest on the aerobrake support arches and will be wrapped with a thermal protection foil to withstand the heat transfer from the nozzle and aerobrake maneuver and allow the Al-1100 alloy to maintain its actual yield strength. The final mass total for the liquid hydrogen tanks is 179 kg and 100 kg for the liquid oxygen tanks.

## AEROBRAKE
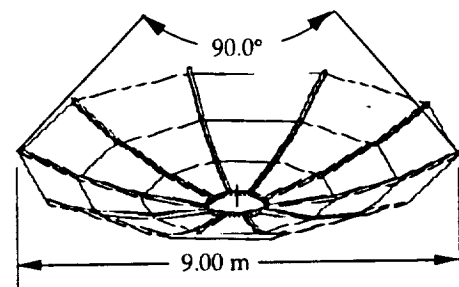


Figure 6 Aerobrake Structure

The design of MOOSE included the aerobrake used to partially reenter the atmosphere and use drag forces to modify its orbit instead of fuel, thus reducing mass. A spherical shape made of an aluminum honeycomb provided a lightweight thermally resistant structure. Ceramic thermal protection tiles were placed on the above structure. The design allowed for assembly and maintenance to easily be performed.

## Trajectory

A two shallow pass trajectory was chosen instead of a single deep pass. Although the chosen trajectory speed was Mach 34, because of a shallow pass of 80 km minimum altitude, the largest aerodynamic forces on the aerobrake were almost negligible, only a few hundred Pascals. The g forces on the brake during the two pass maneuver were less than the propulsive forces during an orbital burn, maximum of 1.5 gs.

## MAIN SPINAL TRUSS

This structure carried up to 2g loads. All major components the cabin, spider truss, fuel tanks, propulsion system, and aerobrake were connected to the spinal truss. The titanium longitudinal beams were welded to hard points on three spinal rings. These rings integrated the aerobrake, cabin, and fuel tanks.

## MANIPULATOR/GRAPPLER SYSTEM

### Introduction

The Manipulator/Grappler System is essential to the execution of MOOSE's duties as an on-orbit servicer. One of the driving requirements for MOOSE is that the astronaut must not have to do an EVA during the repair

process. To accomplish this, it is necessary to equip the vehicle with a manipulation system that he/she can control from within the spacecraft. The possible components of the Man/Grap System are: a Telerobotic Manipulator Arm (TMA), a Telerobotic Grappling Arm (TGA), and a Manual Manipulation System (MMS).

Many possible combinations of these subsystems were examined. The primary design criteria were mass, flexibility, complexity, and development/production costs. The culmination of the design process was a system that utilized all three subsystems.
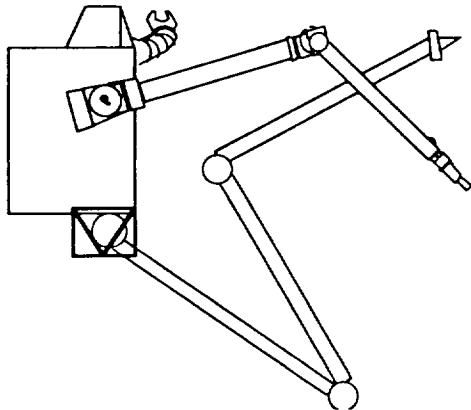


**Figure 7** View of Cabin & Manipulator/Grappler System

The TGA is a four DOF arm, with various possible end-effectors. It is necessary to have a grappling arm to maintain a fixed position and orientation, with respect to the target, during repair operations. The TGA has three links. Link 0 and link 1 are each 2 m long, while link 3 is 3 m long. It was determined that the TGA should be able to successfully maneuver a 6000 kg payload.

| Spacecraft Subsystem Anomaly | Number | Percent |
|---|---|---|
| Timing, Control, and Command | 55 | 9.1 |
| Telemetry and Data Handling | 112 | 19.1 |
| Power Supply | 56 | 9.2 |
| Attitude Control | 123 | 20.3 |
| Propulsion | 26 | 4.3 |
| Environmental Control | 16 | 2.6 |
| Structure | 6 | 1.0 |
| Payload/Experiment | 208 | 34.3 |
| | | |
| TOTAL | 602 | 100% |

**Table 2** Survey of 602 Satellite Failures

| Degree of Failure | Number | Percent |
|---|---|---|
| Negligible Effect | 447 | 74.3 |
| Small Effect | 117 | 19.4 |
| 1/3 to 2/3 Loss | 32 | 5.3 |
| 2/3 to near total loss | 5 | 1 |
| Total Mission Loss | 1 | — |

**Table 3** Failures' Effect on Mission

Based on the data shown in Tables 2 and 3 above (Shockey 1984), it was determined that a significant number of satellites (at least 25%) can be expected to has some loss of attitude or navigational control. Therefore, it would be desirable for MOOSE to be able to grapple with and control errant satellites, so long as the crew member is in minimal danger.

The TMA is a seven DOF arm, with interchangeable end-effectors. The TMA is expected to function as an

"assistant" to the astronaut, in that it can handle massive loads, hold "handed-off" tools and equipment, retrieve ORUs from storage, etc. By providing a variety of end-effectors, it can also be used to perform simple servicing tasks, such as on-orbit refueling. The TMA should be able to handle 450 kg ORUs.
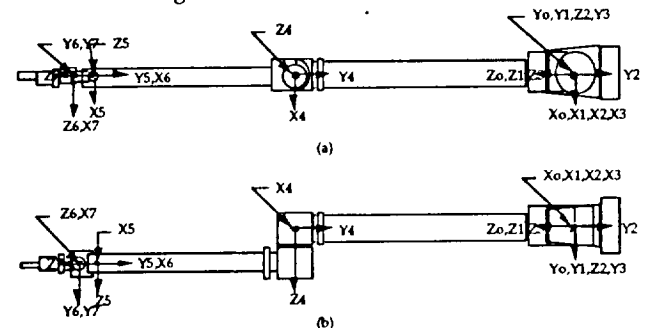


**Figure 8** Side and Top View of TMA Design

The MMS is basically astronaut space suit gloves that are attached to the outside of the vessel's cabin. The astronaut has the benefit of being able to use his/her over 50 DOF arms and hands to conduct repairs, without having to leave the cabin. While this option provides the ultimate in fine dexterity, the limited workspace envelop necessitates the provision of the TMA.

## Prismatic-vs-Revolute Joints

The main problem with using prismatic joints in space is the difficulty involved with sealing the linear bearings from the environment. Revolute joints are much easier to seal, and have large workspaces, and low energy and torque requirements. Inspite of the added complexities of the hardware and software, the jointed manipulator design has many benefits, are will from the basis of for the MOOSE TMA and TGA.

## Direct Drive-vs-Transmitted Drive

One of the main design drivers is that the vehicle systems have low mass. To illustrate the mass relationships of direct drive and transmitted arms, a rough cut analysis was conducted, yielding the following data. Substantial mass is saved by using a tramsmitted drive arm design.

### ARM MASSES-VS-TIP ACCELERATION
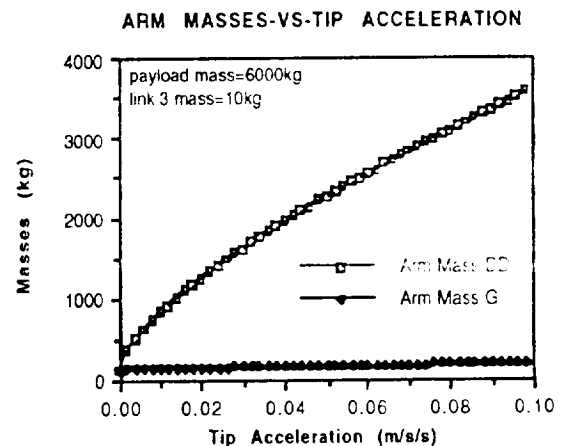


**Figure 9** Arm Mass in a Direct Drive Design vs. Geared Design

## ARM MASSES-VS-LINK MASSES
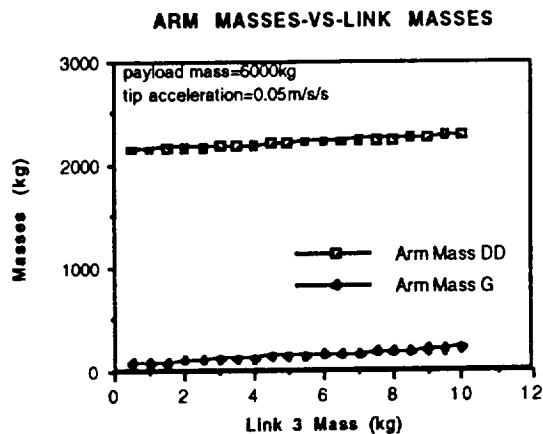


Figure 10 Arm Mass in a Direct Drive Design vs. Geared Design

## Material Selection

A variety of materials with which to construct the arms were investigated. The final decision was to fabricate the main links of the TGA and TMA from Graphite/Epoxy, and the joints from Titanium (T16 A1-4 V). The major driver in this selection was the thermal expansion compatibility of the two materials, as well as their large relative strength-to-weight ratios. The resistance to corrosion of Graphite/Epoxy and Titanium was an added bonus. The TMA will be subjected to highly unfavorable conditions during satellite fluid replenishment missions.
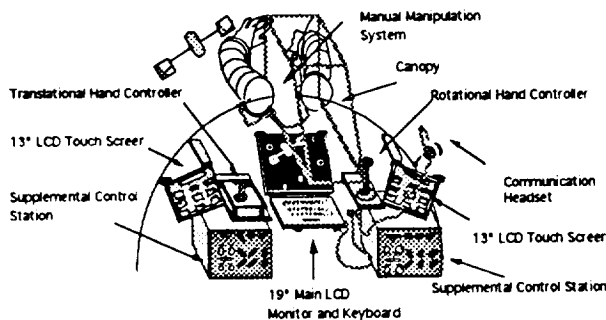


Figure 11 Control Station Design

## COMMUNICATIONS

MOOSE will not communicate with the space station directly during most of the mission. Rather, communications will be routed to SSF from ground links. If SSF were used as the main space relay link, a significant portion of its communication system would have to be devoted to MOOSE data during missions. In addition, MOOSE and SSF can be in a relative position where communications are blocked by the Earth for significant periods of time, requiring the use of relay satellites. Therefore, the communication system would have to be able to communicate with earth from altitudes ranging from LEO (250 km) to GEO (39.000 km).

The uplink, from ground to MOOSE, would consist of voice and command. Voice will be used to communicate with astronaut. The ground computers can communicate with the MOOSE computer system via the command link. In the

case of an emergency where ground control needs to control the vehicle, command communication will be essential.

The downlink will transmit voice, video, and telemetry information. Video information can be transmitted at any time, but may be especially useful during the repair phase of a mission. The telemetry information is essentially housekeeping data. Unlike other space vehicles, no experiments will be conducted on board MOOSE, therefore telemetry will not be as high as an STS, for instance.

Digital communications will be used instead of analog for two main reasons. One, digital signals are more reliable then analog signals. Second, several digital signals can be multiplexed onto one rf signal. For example, voice, video, and telemetry can be sent on one link.

| | | |
|---|---|---|
| Structure | 6400 | bps |
| Life Support | 540 | bps |
| Man/Grap | 5080 | bps |
| Propulsion | 288 | kbps |
| Attitude Control | 3380 | bps |
| Navigation/Tracking | 180 | bps |
| Reaction Control | 2900. | bps |

Table 4 Communication Data Rate Requirements

The breakdown, according to main systems, of transmission rate requirements are shown above. Note that most of the systems will not need to transmit at the maximum rate listed above for significant periods of time during the mission. To fulfill the above requirements, the Ku-band will be used for all transmissions.

At low altitudes, links will be established through TDRSS satellites. Direct communication to the surface would not be possible due to unacceptable blackout periods, and due to the difficulty that is experienced in locking onto ground stations from low altitude orbits. When MOOSE's altitude is between 12,000 km and 39,000 km, direct ground links will be used.

MOOSE requires 20 W transmitter to send voice, telemetry, and video from a GEO orbit. The communications system will consist of two transponders for redundancy. The antennae are mounted on telescoping booms, so that they can be pulled into the protective cone of the shield during the aerobraking maneuver.

## COMPUTATION AND DATA MANAGEMENT

The Computation and Data Management System (CDMS) has to provide sufficient processing power for all other systems. Computations and data transfers must be fast and reliable.

### Hardware

Distributed processor architectures offer attractive benefits such as reliability, ease of growth, and parallel processing. It also allows for processors with various capabilities and requirements to work together with ease. The physical distribution of hardware on MOOSE, combined with the natural delineations and relations of tasks, makes distribution of processes and processors a natural alternative to a centralized system.

Most system processing will be invisible to other systems, but some operations (such as orbital tranfer and attitude control, attitude control and manipulator/grappler, etc.) will span several system. This would require the coordination of some highly complex computing processes

over various processors. This would place a heavy burden on the lone crew member. The required level of automation is high, in order to reduce the workload for the astronaut.

Reliability has many facets, including probability of correct function over a period of time, probability of recovery (and recovery times) from minor, localized, or major systems breakdown, gracefulness of performance degradation when full service is not possible, and assurance that critical calculations and tasks will be computed in the face of unusual computing loads.

A carefully designed distributed processing system has intrinsic benefits for reliability and secure design, including: 1. enhanced physical, electrical, and logical fault isolation., 2. convenience of configuration for redundant computing resources, 3. well-defined and protectable constraints on information flow, and 4. easy redelegation of tasks as computational priorities shift in the face of changing requirements.

MOOSE's CDMS must be able to evolve and grow over time to meet different and more complicated mission requirements. Distributed processing provides uniform physical and logical techniques for interconnecting diverse processing activities.

The main processor bus would be required to transfer 32-bits of data at high-speed. The VME-bus has a sustained data tranfer rate of 40 Mbyte/s, and utilizes an asynchronous protocol, which allows for easy implementation of systems with parallel processors operating at different speeds.

A network standard was needed to interconnect the processors that were physically distributed throughout the MOOSE vehicle. Such as standard would have to have high data transfer rates, high data integrity, and low susceptibility to noise and Radio Frequency Interference/Electro-Magnetic Interference (RFI/EMI). The Fiber Distributed Data Interface provides very high transfer rates (12.5 Mbits/s, with the development of Gbit/s rates in the near future), very high data reliability, and no susceptibility to RFI/EMI . In addition, it has a low installation expense, and no sparking hazard. These benefits more than compensate for the high transmission media expense.
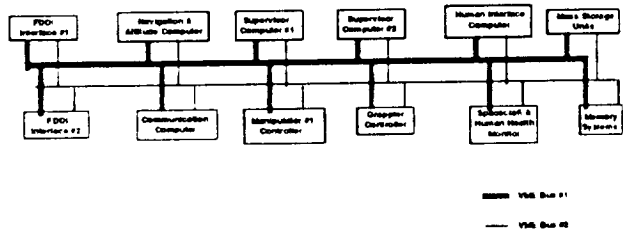


Figure 12 Double VME-bus

MOOSE will utilize a double (for redundancy) VME-bus backplane for its main processor bus. This configuration will yield a fast and mature system that is easily supported. It will also use a FDDI-based network in a double-ring architecture (to help eliminate single-point failures) to interconnect spatially distributed processors.
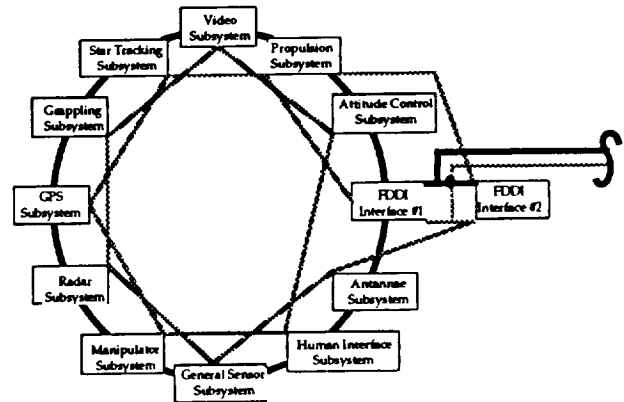


Figure 13 FDDI Double Ring Architecture

## Software

True modularization of hardware design ("plug-and-play") is a well-accepted and mature idea. Attempts to do the same on the software level using traditional procedural programming methods has yielded less than adequate results. The advent of Object-Oriented Programming (OOPs) has created tools that should be used to develop and maintain MOOSE software.

Using OOPs, a real-time programmer/team of programmers can: 1 deal more effectively with complexity, 2 create a library of readily reusable code, and 3 begin the design at a much higher level of abstraction, allowing trade-offs to be effectively examined before commiting to prototype development. OOPs also produces a system design and architecture that permits experts who are not programmers to contribute to the development process much easier.

There is much concern that OOPs programs suffer from performance bottlenecks. This stems from the misconception that real-time systems must be "fast". In reality, such systems need merely be "fast enough". In addition, raw speed does not necessarily equate to better performance.

Most problems with large systems have to do with the level of complexity. Programmers are not good at predicting where the bottlenecks will occur. OOPs combats this with fast development times, allowing performance data to be collected much earlier in the development cycle. The well-defined module interfaces that result from OOP practices allows for easy elimination of performance problems. This is much better than optimizing compilers. Optimizing compilers technology generally lags far behind hardware advances. They also create side effects that renders performance measurements difficult.

## POWER

The total available power on MOOSE is derived from the compilation of the individual subsystem power requirements. The table below outlines the system, power required, duration, and the resulting energy requirements.

The primary power source for MOOSE will be fuel cells. They will produce a maximum output of 2 kW with an allowable 10% loss due to power conditioning and full power for the mission. The fuel cells will operate on gaseous hydrogen and oxygen stored as cryogens. The oxygen needed for life support will be stored in the same oxygen tanks as for the fuel cells. The mass of the fuel,

tanks, and fuel cell will be 63 kg, including life support's oxygen mass. Fuel tanks will be stowed in the avionics box below the command module.

The lightest weight power source for the 7 kW hr needed for backup is nickel cadmium batteries. The energy density of these batteries is 0.4 kW/kg so 17.5 kg of batteries will be used.

| System | Power Required (W) | Time | Energy Required (kW hr) |
|---|---|---|---|
| Data Recording | 0120 | all | 8.64 |
| Optical Sensors | 0022 | all | 1.584 |
| *Computer | 0200 | all | 14.4 |
| *Control Station and LCD Screens | 0008 | all | 0.576 |
| Lights | 0040 | all | 2.88 |
| *Inertial Measuring Unit | 0030 | all | 2.16 |
| *Life Support | 0350 | all | 25.2 |
| *Smoke Detector | 0005 | all | 0.36 |
| Communications | 0025 | all | 1.8 |
| *Rendezvous Radar (Rendezvous) | 0060 | 1 hr | 0.06 |
| *GPS Sensors (LEO) | 0006 | 72 hr | 0.432 |
| *Main Fuel Valves and Pumps (burns) | 0020 | 12 min | 0.004 |
| *Star Sensor (every 8 hrs) | 0003 | 1 hr | 0.003 |
| *Control Moment Gyros (drifting & working) | 0030 | 4 hrs | 0.72 |
| Grappler Arm (grappling satellite) | 1000 | 1 hr | 1.0 |
| Manipulator Arm (repairing satellite) | 1000 | 6 hr | 6.0 |
| *Reaction Control System | 0072 | 10 hr | 0.72 |

Maximum Power Required 1.830 kW   Total Energy Required   66.539 kW hr
Backup Power Required   0.746 kW   Backup Energy Required   7 kW hr

* Necessary for safe return of astronaut

Table 5 Outline of Power Requirements

## CABIN STRUCTURE
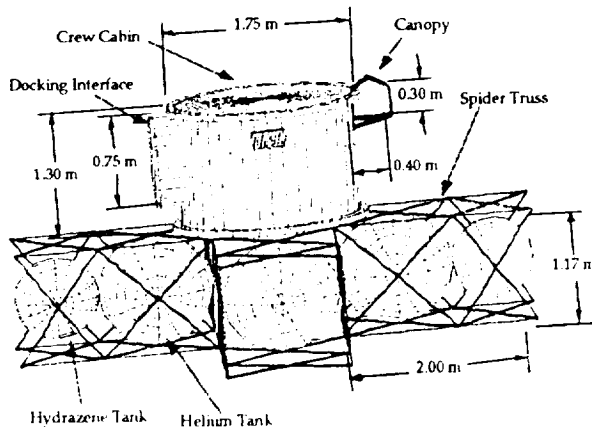


Figure 14 Main components of the MMM

The cabin's design was a simple monocoque cylinder made from aluminum 7075. Two aluminum crossbeams gave structural support at the endplates to eliminate most deflections. The one centimeter thickness needed for radiation protection provided ample structural safety when carrying propulsive 3g loading. The stress concentration of the docking ring, also made out of aluminum, were well below material strength. A debris shield surrounding the cabin was design as a lightweight

protection for the aluminum walls from micrometeor impacts. The viewport canopy, made of five centimeter Lexan plastic was designed to survive impacts without debris shielding. The base of the cylinder was mounted to the spider truss completing, the structure for the separated vehicle.

## RADIATION SHIELDING

Using NASA limits for radiation, the cabin walls were designed as one centimeter thick aluminum. The average dose for a two day mission in GEO was approximated from four to eight rem. For a LEO or polar mission the radiation dosage is below 0.2 rem.

Most radiation protection was needed during solar particle events where a dosage of 10000 rem during a day may occur. At GEO with the current shielding, the largest solar flares were able to deliver 130 to 200 rem. However since these flares have been predicted 10 to 20 hours prior to the event, the protocol allowed the crew member to take evasive maneuvers. By orienting the aerobrake toward the solar flare, more protection was offered by the aerobrake and propulsive materials. When the vehicle was directed to a lower orbit, less than a 50 rem dosage was delivered.

## CABIN COMPONENTS
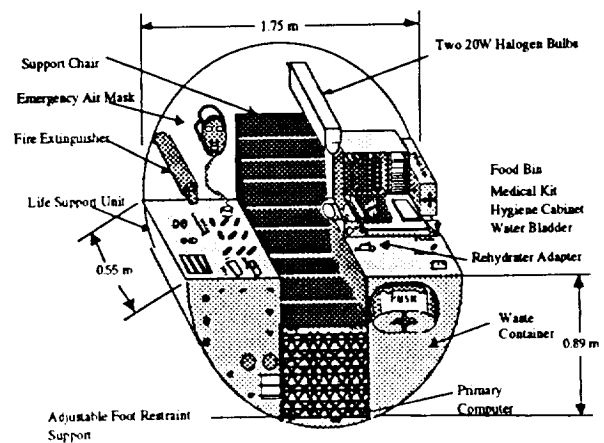


Figure 15 Cabin Layout

## OXYGEN AND NITROGEN SUPPLY

A 50/50 atmosphere of oxygen and nitrogen inside of the cabin had a design total pressure of 41.5 kPa (0.41 atm). This provided a low pressure, which leads to low overall mass, fire safe atmosphere, that did not affect the crew member's performance.

The oxygen and nitrogen supply system monitored the levels of oxygen in the cabin feeding gas when needed to maintain the above specifications. Pressure valves in the cabin released air into space when necessary. The oxygen was supplied from the cryogenic fuel cell tanks, however an emergency high pressure tank could have been used. Two other backup valves were design to send the oxygen to the emergency air mask or directly out of the life support unit. The crew member then would have monitored the oxygen flow directly using the sensors.
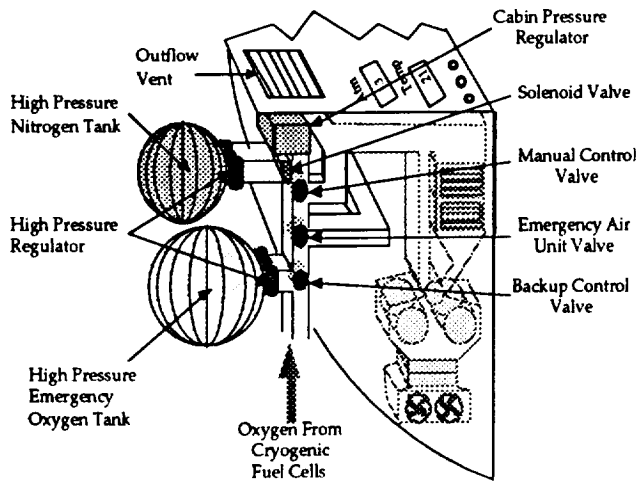
**Figure 16** Oxygen and Nitrogen Supply System Layout

## ATMOSPHERIC REVITALIZATION

The crew member was expected to produce 1.02 kg of $CO_2$, 2 kg of water vapor, and excess heat each day. The atmospheric revitalization system (ARS) was designed to extract the above and maintain an environment of less than 2000 Pa (0.02 atm) of $CO_2$, about 40% relative humidity, and around 21°C.
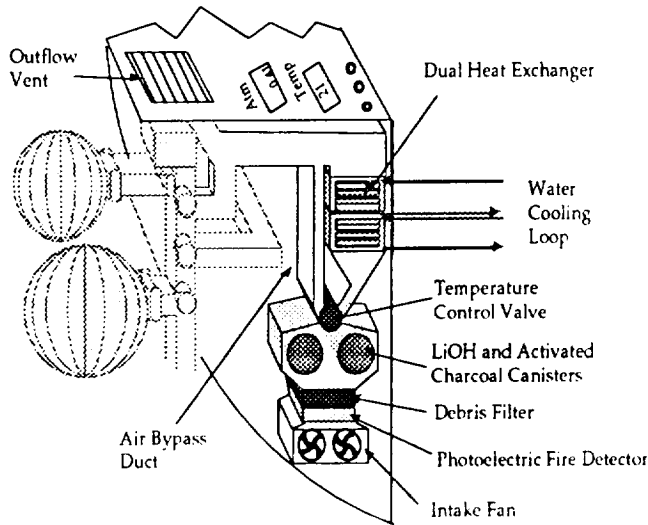


**Figure 17** ARS Layout

The design for an airflow rate of 9.5 m³ per minute was achieved by using either of two intake fans. The air passed through a photoelectric fire detector and debris filter. Containers holding lithium hydroxide (LiOH) and activated charcoal extracted the $CO_2$ and trace contaminants respectively. At the temperature control valve the flow was directed, either bypassed directly to the cabin or guided to the dual heat exchanger. Here the air was cooled, water vapor extracted, then reheated to the proper temperature, and returned to the cabin.

## FOOD SYSTEM

The food system was a modified version of the MRE (Meal, Ready-to-Eat)., current used by the US Armed Forces,. MREs were storable for a long duration, easy to prepare, inexpensive, compact, and were palatable with a variety of menu selections. Beverages consisted of powdered drinks in prepackage containers. Rehydration occurred when a hose with an adapter penetrated the container, filling it with water. Beverage containers can be reused for water consumption.
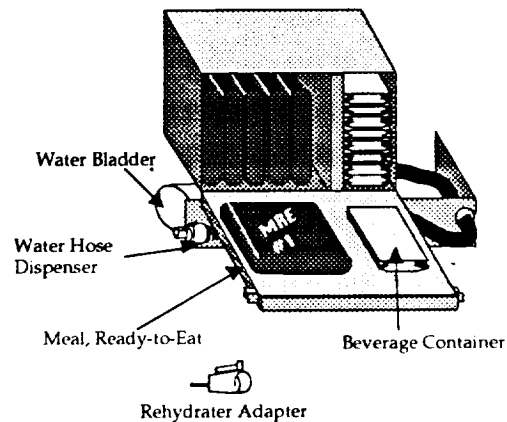


**Figure 18** Food System Layout

## HYGIENE AND WASTE

A hygiene cabinet held personal hygiene articles including wetnaps for minor clean up, toothbrush and paste, toilet paper, comb, and other amenities. Also chemically treated waste disposal bags were stored here. A urine container held a solid substance that absorbs and chemically treated the urine. A bag was provided to solid matter. After use, a chemical pack was placed into the bag. The bag was then sealed and mixed.

All disposal containers were placed in the waste container. A hatch was sealed so that no fumes from the waste diffused into the cabin. The waste container was design to be able to exposed its contents to the vacuum of space as an auxiliary waste stabilization technique.

## FIRE SUPPRESSION

For prevention of fires, flame retardant cabin materials were integrated into the design. The small cabin interior allowed the crew member to detect most fires quickly. However, to detect smoldering fires, which are difficult to visually notice, and as a general safety precaution, a photoelectric smoke detector was installed in the life support unit. These detect smoke particles precisely and were not affected by temperature or humidity that would yield false alarms.

A small fire extinguisher holding 1.13 kg of halon 1301 was placed in the cabin. This instantly cooled and smothered the fire without damaging electrical equipment. Protocol demands the crew member don the emergency air mask within five minutes after activating the halon,. until the life support unit replaced the atmosphere in the cabin.

## MASS BREAKDOWN

| Component | Mass (kg) |
|---|---|
| Structure | 200 |
| Cabin | 355 |
| Cabin Systems | 663 |
| Aerobrake | 650 |
| Tankage | 610 |
| Power | 52 |
| Avionics | 196 |
| Propulsion | 300 |
| ACS | 41 |
| LOX | 1334 |
| LH2 | 9335 |
| Hydrazine | 522 |
| Helium | 223 |
| Crew | 90 |
| Payload | 500 |
| | |
| Dry Mass | 3067 |
| Flight Mass | 15071 |

**Table 6** Mass Budget Summary

## OPERATIONS

MOOSE has the ability to perform ORU change-outs, refueling of consumables (including cryogens), and Multi-Layer Insulation (MLI) repair to client spacecraft.

### Trajectory

MOOSE can service satellites in most orbits, with the exception of polar/sun-synchronous orbits. MOOSE can execute plane changes of up to 42˚. Plane changes are accomplished by a combined burn at 35,740 km apogee in order to minimize fuel consumption. A two-pass aerobraking maneuver then adjusts for the proper target altitude. All propulsive orbit transfers utilize Hohmann minimum energy transfer.

### Target Proximity Operations

In the vicinity of the target, the standard closing technique is the +V-bar approach. This approach provides good target visibility.

### Support Equipment

Successful MOOSE operations require a storage/refurbishment facility on SSF. The MOOSE facility can store large amounts of cryogenic for extended periods of time, possibly on the order of months. In contains berthing hardware and racks for storage of tools and payloads. The entire facility is partially enclosed with a micro-meteorite shield.

The cryogenic storage facility can store LO2 and LH2. Boil-off losses are countered through the use of a Stirling cycle refrigerator. Other cryogens are stored in the secondary cryogenic storage tank, when required. Hydrazine is contained in two other tanks. Fluids are transferred via positive expulsion, using high-pressure GHe is the pressurant. The pressurant supply also contains the GHe supply for the MOOSE flight vehicle.

The berthing area contains the lock-down and securing hardware for the MOOSE vehicle. Crew ingress/egress is provided by a retractable pressurized docking assembly. This assembly attaches to SSF at one of the resource nodes. The MOOSE vehicle, once berthed, may be rotated around the flight axis to provide the SSF RMS access to all vehicle components.

## CONCLUSION

MOOSE was designed to fulfill a primary mission of servicing satellites in GEO, a task that can be done by no system in operation today. The MOOSE design team had the foresight to design a vehicle that can fulfill a host of secondary missions (astronaut EVA resuce, Space Station *Freedom* assembly and servicing, Hubble Space Telescope (and other LEO satellites) servicing, for instance). In addition, MOOSE can conduct multiple missions per outing, servicing two or more satellites at once. MOOSE is a small, inexpensive, and flexible system that can greatly expand the types of activities that can be conducted in space, with a minimal risk to the crew member.

## REFERENCES

Shockey, Edward. *Analysis of Spacecraft On-Orbit Anomalies and Lifetimes*. PRCR-3579. February 10, 1984.

Wertz, James R. and Wiley J. Larson, ed. *Space Mission Analysis and Design*. Kluwer Academic. Boston. 1991.

## ACKNOWLEDGMENTS

# 1.0 Systems Integration

## 1.1 Introduction

### 1.1.1 MOOSE

The Manned On- Orbit Servicing Equipment spacecraft is an orbiting vehicle capable of sending an astronaut on satellite servicing missions to geosynchronous orbit and returning safely to low earth orbit, where it will be stationed at Space Station Freedom. The astronaut is housed in a cylindrical crew cabin that will provide a "shirt-sleeve" environment, thus precluding the need for extravehicular activities. In order to conduct the servicing tasks, MOOSE is equipped with a seven degree of freedom manipulation apparatus, a seven degree of freedom grappling apparatus, and a manual manipulation system free of mechanical actuation. MOOSE will employ a reusable aerobrake to bleed the necessary amount of kinetic energy into the atmosphere in order to return rendezvous at Freedom. The reusable aspect of the aerobrake allows the entire vehicle to become integrated within its confines. Figure 1.1.1 illustrates the important features of the spacecraft.

### 1.1.2 Mission Statement

The project assigned to this class is the design of a reusable spacecraft capable of transporting one astronaut and necessary equipment from Space Station Freedom (SSF) at Low Earth Orbit (LEO) to Geosynchronous Earth Orbit (GEO) for a satellite service mission. The mission at GEO is to rendezvous with a target satellite, grapple the uncooperative target, and perform on-site servicing. Furthermore, the MOOSE will be an autonomous system capable of free-flight maneuverability independent of SSF.

MOOSE will be designed with a technology cut-off date of 1993. Demonstrable technologies will be implemented in order to produce a viable, low-cost design solution. For this mission, ENAE 412 has developed a set of objectives in order to proceed with this vehicle design. They are presented as follows.

### 1.1.3 Mission Objectives

1. *To extend the serviceable range of satellites reachable by humans beyond LEO.* To reach GEO satellites will be the MOOSE primary objective. The reference mission and subsequent vehicle design will reflect this objective.
2. *On-orbit satellite servicing*
   Providing the means to repair faulty hardware, replenish fuel and/or power systems, and modify existing hardware. MOOSE will be designed incorporating the necessary equipment and supplies to accomplish these tasks.
3. *Maximize the number of satellites serviceable by MOOSE.*
   Without changing the overall magnitude of the scale of the design, it would
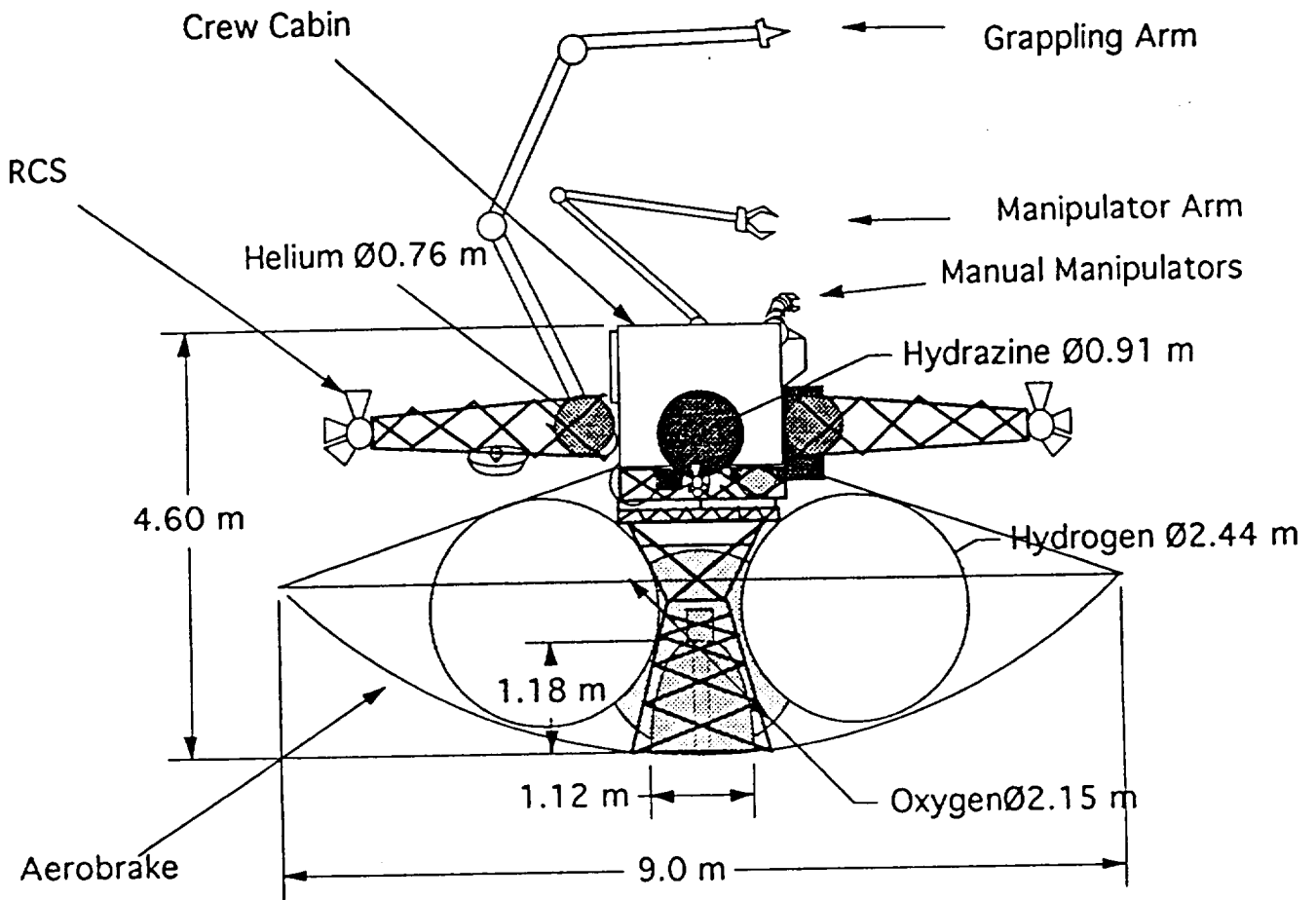
Figure 1.1.1
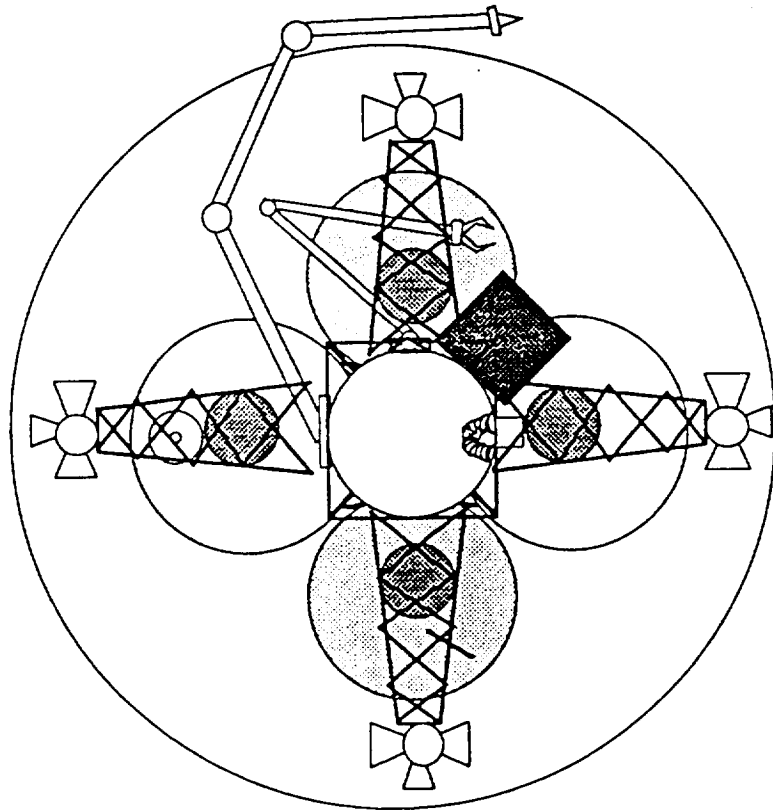
Figure 1.1.2

be desirable to have the capability to service satellites in orbits other than GEO. Satellites in polar orbits, and high value satellites, such the Gamma Ray Observatory (GRO) and the Hubble Space Telescope (HST) will be target objectives for mission and vehicle design. Furthermore, the capability to service multiple satellites per mission would be desirable in order to further reduce launch cost per customer.

4. *Economic viability*

Cost of course is a high priority. The design of a vehicle such as MOOSE must provide a cost effective method of satellite maintenance. In order to meet realistic and prudent design criteria, the technology cut-off will be 1993 . In order to reduce the liability costs of satellite missions, MOOSE design will strive to meet the following rule of thumb :

COST to use MOOSE $\leq$ 25% COST satellite replacement  [1]

## 1.1.4 Design Requirements

In order to meet the outlined objectives, the following necessary design requirements were derived or assumed:

### Table 1.1.4a

| Maximum operational | | |
|---|---|---|
| cost per mission | $100M 1993 | (DERIVED) |
| Functional Requirements | | |
| Crew | 1 astronaut | (GIVEN) |
| Design Mission time | 3 days | (DERIVED) |
| $\Delta$V mission | 9.54* km/s | (DERIVED 1.2.1) |
| Max. g loading | 2.0 g's | (ASSUMED) |
| Deliverable | | |
| Payload mass | 500 kg | (DERIVED 1.4.1) |

* NOTE: Propulsive $\Delta$V =7.00 km/sec

## 1.1.5 Design History

Initial guess masses for the MOOSE were based on previous vehicles and previous studies of manned spacecraft and their applications. Conservative estimates of component masses gave a preliminary vehicle dry mass. Using the rocket equation for the reference mission requirement $\Delta$V, propellant and then total vehicle masses were obtained. An iteration of parametric component equations were worked through to obtain new masses. When convergence was obtained the final component mass estimates were compiled as mass budget ceilings.

The major subsystems required for MOOSE were broken down into life support, propulsion, and structure. The vehicle configuration then became dependent on what solutions to the requirements these systems could provide. Vehicle concepts for MOOSE initially included staging configurations, single stage vehicle

configurations, and expendable tank (blow-off tanks) at LEO configurations. The conventional staged vehicle that would detach a first stage at GEO was immediately deemed too environmentally hazardous for consideration. From Figure 1.1.3[2]. The number of eventual Ku-band satellites in GEO may reach 113. With a mean angular separation of 3.2°, the probability of very large orbital debris in the form of propellant tanks colliding with any satellite was too high of a risk and was not in agreement with space debris precautions recommended by DoD and NASA policy studies[3]. It was determined by later calculations (Figure 1.2.4c) that GEO objects with very small ΔV drifts, such as those imparted by an stage ejection system, would eventually travel about the GEO arc with a precessing node at GEO orbit, thereby constituting a real hazard to existing GEO satellites and MOOSE itself during subsequent missions. Alternatives including deorbiting and orbital escape ejection were also deemed unfavorable due to the additional propellant mass and mission complexity.

A spinoff of the staging concept was to examine the advantages of a configuration with expendable tanks to be ejected upon LEO insertion, thus establishing a savings in propellant required for LEO insertion. Early disadvantages foreseen were the added failure possibility for the ejection mechanisms. This concept was eventually excluded from the final configuration due to the complexity required when an aerobraking shield was included in the design.

Originally it was assumed that storable cryogenic propellants were not demonstrable technology. At the time the design incorporated a deliverable propulsion system that required a launch vehicle per mission. Upon further inspection, the proposed cost per mission was prohibitively high and too unreliable due to the mission single point failure scenario at launch.

By demonstrating reliable storability (8.25.2.6), the MOOSE design may now incorporate more flexibility due to less reliance on launch per mission. In addition, the capability of the aerobrake to accommodate ΔV savings provides a smaller mass budget for the vehicle, wherein a larger mass margin than a conventional single stage vehicle is obtained.

Finally, the decision to incorporate a marketable degree of mission flexibility led to the design maximum ΔV capability of 7.0 km/sec. As outlined in section 1.2.5, a trade study conducted found that promising GEO coverage is possible for additional satellite missions within small mass penalties for increasing the vehicle's ΔV capability.

# Appendix B

## Ku-band Geosynchronous Satellites

GALAXY K2 F18 US-HUGHES 130° W
ASC I US (1985) 128° W
MARTIN MARIETTA MMC-II US-Martin Marietta (1989) 126° W
FEDEX B US-Federal Express (1988) 124° W
SBS V US-SBS (1986) 122° W
SPACENET I US-GTE 120° W

DOMINION US-Dominion (1988) 119° W
ANIK C3 Canada-Telesat 117.5°
MORELOS F2 Mexico (1985) 116.5°
W MORELOS F1 Mexico 113.5°
W ANIK C2 Canada-Telesat 112.5°

110° W STC 1 & STC 2 US-Comsat (1986)
110° W USSB 1 US-USSB (1988)
109° W ANIK C1 Canada-Telesat (1985)
107.5° W ANIK C1 US-GTE
105° W GSTAR A1 US-GTE
103° W GStar A2 US-GTE (1985)
101° W GALAXY DBS 1 & 2 US-Hughes Comm (1989)
101° W FORDSAT I US-Ford Aerospace (1987)
99° W SBS I US-SBS
97° W SBS II US-SBS
95° W SBS III US-SBS
93° W FORDSAT II US-Ford Aerospace (1987)

85° W SATCOM K1 US-RCA (1985)
83° W ASC II US (1985)
81° W SATCOM K2 US-RCA (1985)
79° W MARTIN MARIETTA MMC-I US-Martin Marietta (1989)
77° W FEDEX A US-Federal Express
75° W COMSTAR K1 US-Comsat (1988)
73° W WESTAR A US-Western Union (1988)
71° W GALAXY K1 US-Hughes (1987)
69° W SPACENET II US-GTE
67° W SATCOM K3 US-RCA (1987)

57° W PANAMSAT I US (1987)
58° W U.S.A.-SAT US (1988)
60° W INTELSAT IVA, V (1986)
61° W SATCOM K4 US-RCA (1989)
61° W TDRS B US-Spacecom (1985)
62° W SBS 6 US-SBS (1987)
64° W ASC 3 & ASC 4 US-ASC (1987, 1989) 41° W TDRS A US-Spacecom

56° W INTELSAT IVA, V, VA (1987)
56° W U.S.A.-SAT US (1987)
53° W INTELSAT VF8
50° W ORION III US (1987)
47° W ORION II US (1987)
45° W CYGNUS II US (1988)
43° W CYGNUS I US (1988)

27.5° W INTELSAT
34.5° W INTELSAT VF4
37.5° W VIDEOSAT 2 France (1988)
37.5° W ORION I US (1986)
40.5° W INTELSAT VB (1986)

24.5° W INTELSAT
20° W GOL4
19° W
19° W

YAF10
Luxembourg (1986) GOL 5 Luxembourg 01° E
SARIT Italy (1986)

01° W TELECOM F2 France
05° W TELECOM F1 France
08° W F-SAT 2 France (1986)
11° W GORIZONT 4 STATSIONAR 11 USSR
14° W GORIZONT 7 (STATSIONAR 4) USSR
16.5° W INTELSAT VF6 (1986)
18.5° W INTELSAT VF6 MCS B

19° W TVSAT A3 & A5 W Germany (1986)
19° W TDF 1A & 1B France (1986)
19° W OLYMPUS ESA (1986)

YAF11

AMS 1 & 2 Israel (1986) 15° E
07° W EUTELSAT I F2 ESA
05° E TELE X Nor/Swe/Finland (1986)
05° E OTS 2 ESA
03° E TELECOM F3 France (1985)
10° E EUTELSAT I F3 ESA (1985)
13° E EUTELSAT I F1 ESA
16° E SIRCAL 1A Italy (1987)
17° E SABS Saudi Arabia (1988)
19° E GDL 6 Luxembourg
22° E SICRAL 1B Italy (1987)

DFS 1 W Germany (1987) 23.5° E
ZOHREH 2 Iran 26° E
DFS 2 W Germany (1987) 29.5° E
VIDEOSAT 1 France (1987) 32° E
PAKSAT 1 Pakistan (1986) 38° E
PAKSAT 2 Pakistan (1986) 41° E

INTELSAT V (1985) 66° E

47° E ZOHREH 3 Iran
34° E ZOHREH 1 Iran
57° E INTELSAT VF1
41° E ZOHREH 4 Iran
60° E INTELSAT VF7
63° E INTELSAT VF5

90° E STATSIONAR 13 USSR
GORIZONT 8 (STATSIONAR 6) USSR 90° E
80° E CHINASAT China (1988)
92° E YURI (BS-2B) Japan
110° E BS-3A Japan (1989)
110° E BS-2A Japan
167° E PAPAU NEW GUINEA SAT

173° E INTELSAT V (1987)

III Australia OTC (1985) 160° E
II Australia OTC (1990) 164° E
INTELSAT V (1986) 176° E
NAR 10 USSR 170° W
C (1987) 166° W
(1995) 160° W
(1987) 157° W

W WESTAR B US-Western Union (1988)
W COMSTAR K2 US-Comsat General (1989)
136° W SPACENET 4 US-GTE-Spacenet (1989)
136° W GSTAR A3 US-GTE (1989)
147.5° W COLSAT 2 US-GoC (1987)
148° W USSB2 US-STC (1987)
148° W DBS SATELLITES US-various (1988)

SSS US-Spm
ESDRN USSR
SCS 2 US-SPACE
STATSO

AUSSAT
AUSSAT

132'
134'

| BAND | C | K | BOTH |
|------|---|---|------|
| EXISTING | ◆ | ▲ | ● |
| PROPOSED | ◇ | △ | ○ |

FIGURE 1.1.3

1-6

# References

1. Akin, Dr. David, classroom lecture, April 1993.

2. Wirin, William B., "Limits on Mission Design. Law and Policy Considerations", Space Mission Design and Analysis, ed. Wertz, J., and Larson, W.,1991, Kluwer Academic Publishers, Boston, pp. 699-700.

3. Wilson, Andrew, Intervia Space Directory , Jane's Information Group, Virginia, 1990, pp. 490-491.

## 1.2 Trajectory Analysis

The trajectory analysis was done using standard orbital mechanics equations. The Vis-Viva equation combined with vector addition analysis for plane changes was used to calculate the total optimal $\Delta V$.

The types of transfers that were considered are high energy, low thrust, spiral, hohmann, and aerobrake/assist. Each of these trajectories were analyzed to see if they could meet the mission objectives while conforming with the following constraints. The total $\Delta V$ will need to be minimized in order to reduce the amount of propellant needed which will reduce the total mission cost. The time of the transfers will also need to be minimized in order to save on cost. However, MOOSE will be crewed by an astronaut and crew safety will be the number one constraint. Appendix 1.2 has the detailed breakdown on the trajectory analysis.

### 1.2.1 Mission Objectives

MOOSE's main mission will be to repair satellites in geosynchronous orbit. At a minimum, the OTV will need to perform the following mission. The spacecraft will be stationed at Space Station Freedom (SSF) in a 333x444 kilometer altitude low earth orbit and at 28.5° inclination. MOOSE will then transfer to geosynchronous orbit at 35,286 km altitude and at 0° inclination. After the spacecraft performs the satellite repair, it will deorbit and rendezvous with SSF.

### 1.2.2 Mission Analysis

MOOSE will use a Hohmann transfer to GEO as it is the most energy efficient type of transfer. However, it was determined that MOOSE will utilize an aerobrake maneuver on the return leg. By using an aerobrake, the total $\Delta V$ can be reduced by about 25% as the aerobrake is used to replace the final LEO Circurilization burn. This offers a substansial savings in propellent mass over conventional all propulsive transfers. Figure1.2.1 shows that up to 40% of the total propellent mass can be saved. The aerobrake mass on MOOSE is about 22% of the total vehicle mass so about



Propellent Savings From Aerobrake
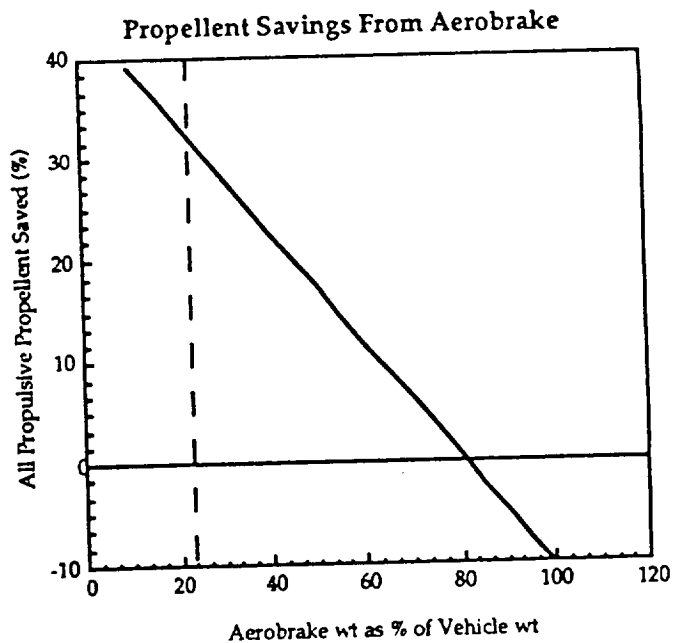
Figure 1.2.1

32% of propellent mass is saved over a comparible all propulsive vehicle. This significantly reduces the per mission cost of the OTV. From figure 1.2.2 it can be seen that MOOSE will be about 26% lighter than an all propulsive vehicle.

**Total Vehicle wt Saved (%) vs All Propulsive Vehicle**



Aerobrake wt as % of Vehicle wt
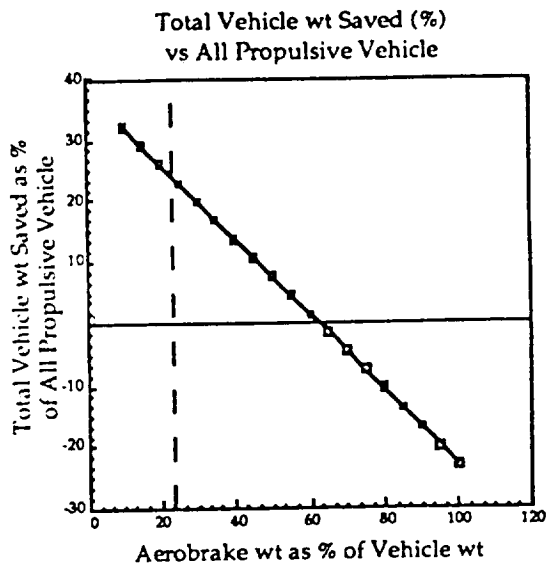
**Figure 1.2.2**

Further DV savings can be obtained by combining the plane change burns with the GEO/LEO tranfer burns and optimizing the inclination change by splitting the inclination changes at apogee and perigee. Figure 1.2.3 shows that 2.25° is the optimal inclination change when comined with the GEO transfer burn at perigee. Then at apogee, a 26.25° inclination change will be combined with the GEO circurilization burn.

**ΔV vs Angle of Inclination Change at Perigee**



Angle of Inclination Change at Perigee (deg
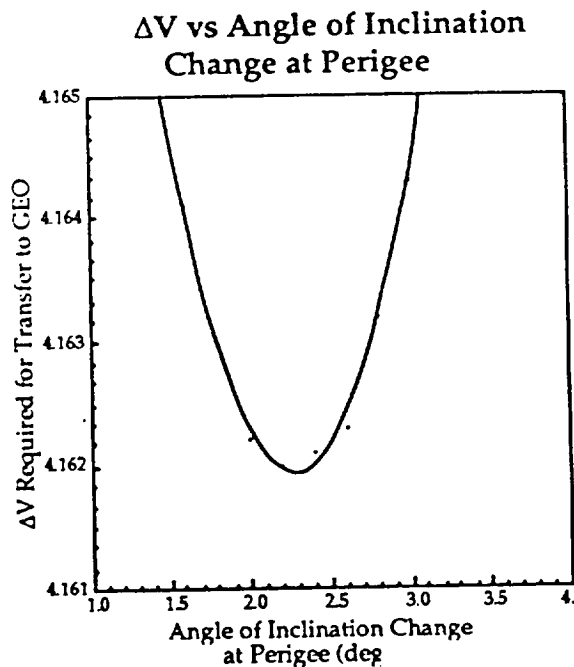
**Figure 1.2.3**

In order to reduce the heat and force loads on the spacecraft during the aerobrake manuever, two atmosperic passes will be used. This will add about 4.6 hours to the total mision but at no energy cost (ΔV wise).

## 1.2.3 Reference Mission

MOOSE will be docked at SSF in a 333x444 km altitude, 28.5° inclination orbit. After MOOSE clears SSF the spacecraft will make a combined GEO inject and a 2.25° plane change burn. 5.3 hours later MOOSE will make a GEO circ, 26.25° plane change burn and rendevous with the target satellite. After the repairs, the spacecraft will make a

combined LEO inject and a 26.25° plane change burn. 5.3 hours after this burn MOOSE will make a first pass into the atmosphere to slow down. The second pass will occure in about 4.6 hours and place MOOSE at SSF altitude at apogee. MOOSE will make a final LEO circ burn and manuever back to SSF. The total $\Delta V$ used will be 6468 m/s and the total transfer time will be 15.2 hours. MOOSE will have 532 m/s in reserve which can be used to extend its capabities in the future.

## 1.2.4 $\Delta V$ Budget

| Event | $\Delta V$ (m/s) |
|---|---|
| Separate | 3 |
| GEO Transfer Inject | 2400 |
| Midcourse | 15 |
| GEO Circ | 1762 |
| Orbit Trim | 9 . |
| GEO Ops | 208 |
| LEO Transfer Inject | 1844 |
| Midcourse | 20 |
| Aeromaneuver | 67 |
| LEO Circ | 122 |
| Rend & Dock | 18 |
| Reserves | 532 |
| | |
| Total | 7000 |

## 1.2.5 ΔV vs. Mass Trade

With the goal in mind of providing a marketable product for production, investigation into mission flexibility was conducted. The first step in this study Using the rocket equation, a variation of ΔV for an initial dry mass yielded a new propellant mass. In addition, the tank mass was modeled using a parametric equation as a function of the propellant mass. Thus, through iterative convergence a new dry mass was obtained.

Then a costing estimate of the resulting propellant mass required was run. The effect of small and large ΔV additions to the ΔV required for one GEO mission is seen in Table 1.2.5a. Preliminary conclusions were that ΔV design for MOOSE could increase substantially with a small mass penalty. For ΔV required to service one GEO satellite (ΔV$_{GEO 1}$) equal to 6.568 km/sec, an additional "Δ(ΔV)" of 0.5 km/sec integrated into the design would cost approximately $ 21M (FY93) per mission. The advantages of such added performance are explained in the next section.

### Table 1.2.5a

| Δ(ΔV) km/sec | M dry kg | M tanks kg | M propellant kg | Propellant Cost $M 93 | M vehicle kg |
|---|---|---|---|---|---|
| 0 | 3782 | 1157 | 13381 | 94 | 17163 |
| 0.2 | 3869 | 1244 | 14512 | 102 | 18381 |
| 0.5 | 4015 | 1390 | 16413 | 115 | 20428 |
| 0.8 | 4180 | 1556 | 18600 | 130 | 22780 |
| 1.0 | 4304 | 1679 | 20245 | 142 | 24549 |
| 2.0 | 5138 | 2513 | 31694 | 222 | 36832 |
| 3.0 | 6616 | 3991 | 52992 | 371 | 59608 |
| 4.0 | 9705 | 7080 | 100184 | 701 | 109889 |

## 1.2.6 Phasing Orbit Study

In order to realize any advantage from designing off of optimum requirements, the use of the extra ΔV, hence propellant, must be quantified. By attempting to service more than one satellite, a reduction in cost per satellite mission may be realized. The constraints on this study were determined to be phasing orbit perigee altitude, phasing orbit period (transfer time), and "Δ(ΔV)"(additional ΔV to ΔV$_{GEO 1}$ ). These limits were determined as follows.

Phasing orbit perigee altitude, h$_p$, was constrained by design to be no smaller than 1000 km. This altitude was picked without full appreciation of the concerns of a highly elliptical orbit. It is unknown at this time the hazards, if any (i.e. collisions, communications degradation, radiation effects) of deploying a crewed spacecraft in an orbit about earth with apogee at 42000 km and perigee at h$_p$, or 1000 km. This altitude was selected as approximately twice LEO altitude, for safety in avoiding collision with SSF.

Phasing orbit period, $T_{transfer}$, was constrained by the maximum mission time of three days, or 72 hours. This mission time drives the amount of radiation protection incorporated in the vehicle. For the reference mission (1.2.3) the mission duration is 25 hours (allowing 10 hours for service/repair operations). This leaves a maximum of 47 hours allowable for transfer, rendezvous, and repair. Allowing another 10 hours for service/repair operations, the total maximum transfer time, or $T_{transfer}$, is 37 hours.

The additional $\Delta V$ constraint for this study is 0.532 km/sec. This figure arises from the last design iteration prior to this report and does not reflect optimum flexibility. The advantages to this "$\Delta(\Delta V)$", however, will be quite clear. The sample calculations in Appendix 1.2.6 may be implemented to suit the mission designer for other general cases. The new $\Delta V$, $\Delta V_{GEO\ II} = \Delta V_{GEO\ I} + \Delta(\Delta V) = 7.000$ km/sec.

Using orbital mechanics calculations outlined in Appendix 1.2.6, Figures 1.2.4a-c were obtained. These graphs illustrate the effects of the constraints on coverage capability within the GEO arc (Figure 1.2.5). The phase separation between MOOSE and the target satellite in GEO is $\Phi$. GEO Arc Coverage is defined as the percentage of an assumed circular orbit with radius = 42000 km that MOOSE could reach. The results of the Phasing Orbit Study are as follows:

Table 1.2.6a

| Constraint | $\Phi$ Range | GEO Arc Coverage |
|---|---|---|
| $h_p$ | $\Phi \leq 150°$ | 100 % |
| $T_{transfer}$ | $-200° \leq \Phi \leq 360°$ | 100 % |
| $\Delta(\Delta V)$ | $-120° \leq \Phi \leq 72°$ | 53 % |

Clearly, for the constraint conditions chosen, the limiting factor is $\Delta(\Delta V)$. From Figure 1.2.4c. the effect of increasing $\Delta(\Delta V)$ can be seen by widening the $\Delta V_{available}$ band. Note that excluding $\Delta(\Delta V)$, the other constraints place the range at $-220° \geq \Phi \geq 150°$. More coverage is obtained in the $+\Delta(\Delta V)$ range, indicating that a "burn-in" transfer orbit provides more $\Phi$ per $\Delta(\Delta V)$.

## Perigee Altitude vs. Phase Angle

$h_{perigee}$ (km)

$\Phi$ (°)

Figure 1.2.4a

## Transfer Time vs. Phase Angle

$T_{transfer}$ (hrs)

$\Phi$ (°)

Figure 1.2.4b

## $\Delta V$ vs. Phase Angle

$\Delta V_{available}$ Limits

$\Phi_{range}$, $\Delta V$ limited

$\Delta V_{transfer}$ (km/sec)

$\Phi$ (°)

Figure 1.2.4c

1-13
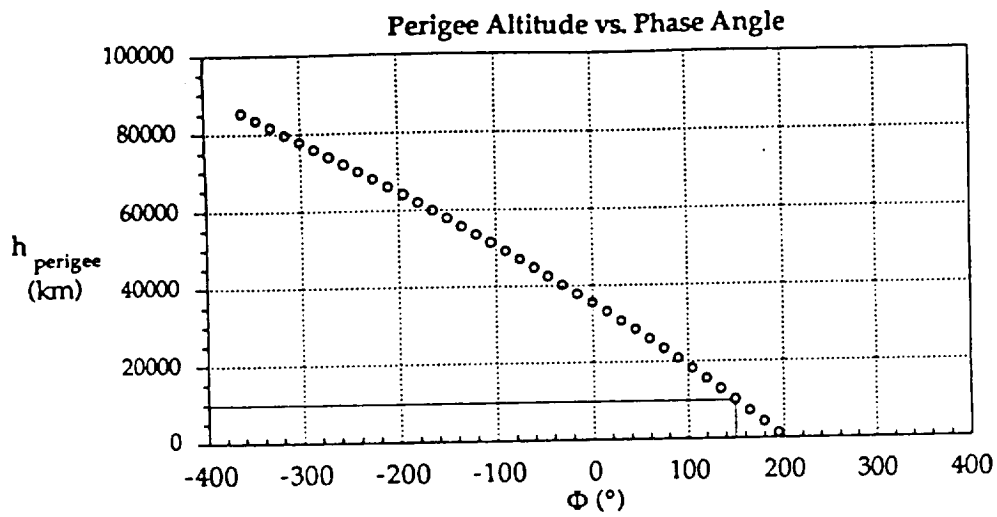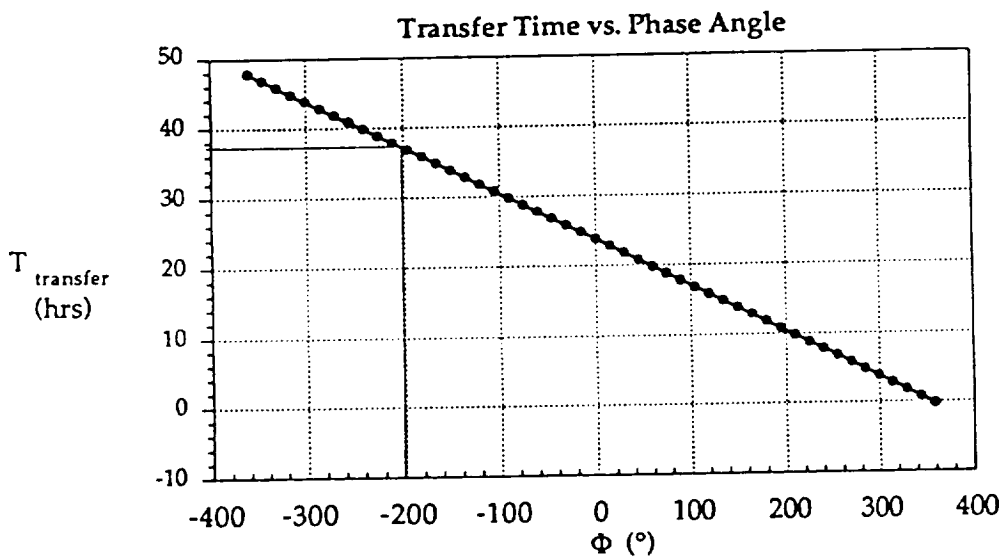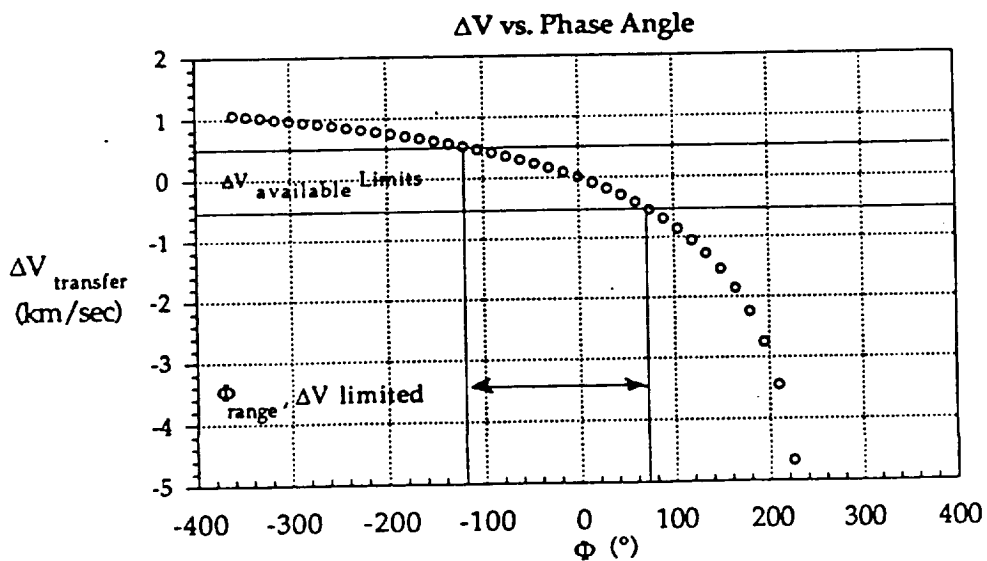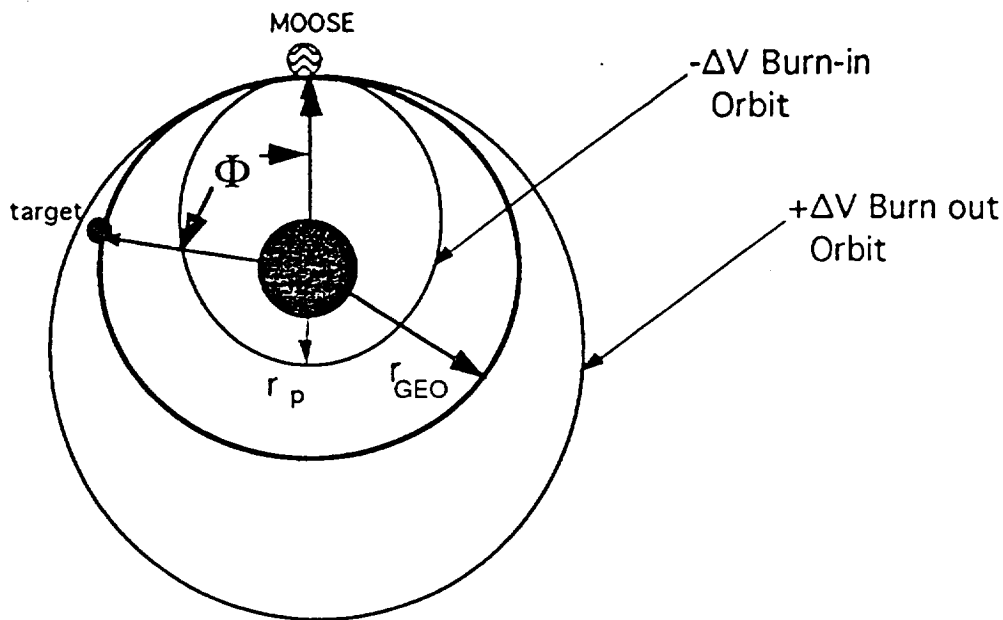
Figure 1.2.5

**Conclusions:**

With the perscribed $\Delta V_{GEO\ II} = 7.000$, or $\Delta(\Delta V) = 0.532$ km/sec, over half of the GEO Arc is coverable. This in rough terms means 60 of the 113 Ku-band GEO satellites at present are reachable from GEO after one GEO satellite servicing mission. The trade off in mass gain to obtain this capability translates to a full vehicle mass of 16700 kg, a propellant mass of 13650 kg fully loaded, and a dry mass of 3047 kg. Note that the Mass Budget (1.4.1) itemizes propellant masses for a GEO I mission, or one satellite servicing and return. Any additional performance is outlined here. In summary, the capability demonstrated here is presented as a performance characteristic of the vehicle with full confidence that it establishes market value for servicing.

## 1.3 Costing

Costing estimates for the MOOSE were computed using the NASA JSC costing model format with several modifications for systems or components not included in the original model. A detailed breakdown of the original model and the applied modifications is presented in Appendix 1.3.1. Research, design, testing and evaluation (RDT&E) costs as well as first unit costs were estimated using the modified format. Major subsystems such as the crew cabin, avionics and the aerobrake were broken down into their component subsystems and evaluated. These component subsystem costs and total program costs are presented in Tables 1.3.1 and 1.3.2. Total program cost is approximately 2.6 billion dollars (FY93) with a first unit production cost of 204 million dollars (FY93) and a discounted total cost of 2.0 billion dollars (FY93). Program development costs were spread over a seven year period such that the MOOSE will be operational when Space Station Freedom is completed in the year 2000. A standard discount rate of 10% was assumed over this seven year funding period and when applied in conjunction with time spreading of costs the values given in Appendix 1.3.2 were obtained.

### 1.3.1 Cost per Mission

At the conclusion of a mission expendables such as propellant and food must be replaced. In addition, refurbishment and repair of the vehicle if necessary must be accomplished before another mission can be attempted. Propellant costs are the major driver of these turnaround costs as large amounts (on the order of 13,500 kg) are expended during the majority of satellite repair missions. Several launch vehicles were examined with factors such as launch frequency, reliability and payload capacity being the major concerns (see Section 8.2.5). Based on these trade studies it was determined that the Titan IV would be the primary launch vehicle to resupply the MOOSE. Considering launch cost and payload capacity it was determined that cargo can be delivered to Freedom for approximately 7000 dollars per kilogram. A breakdown of cost per mission is given below in Table 1.3.3.

Table 1.3.3: Cost per Mission

| System | Cost Parameter | Cost per Mission ($M93) |
|---|---|---|
| 13,650 kg Propellant (LOX & LH2) | $7000 per kg | 95.6 |
| Refurbishment and Repair | estimated 10% of fuel cost | 9.6 |
| Misc. Resupply and Maintenance | estimated 5% of fuel cost | 4.8 |
| **Total Cost per Mission** | | **110.0** |

Note that these costs can vary greatly from mission to mission depending on vehicle condition and thus it is very difficult to estimate a standard cost per mission. The above figure is the best estimate available for a typical mission to GEO with minimal structural repair necessary. Also very difficult to predict are major lifecycle repair costs such as a new engine or major aerobrake repair which may become necessary during the vehicle's projected 20 year lifespan.

1.3.2 Cost Recovery and Profit Potential

During the first few years of MOOSE missions it is expected that there will be enough satellites already in need of repair such that two or more may be serviced during a single mission. This will greatly decrease production cost recovery time and increase profit potential. Based on the mission cost requirement, an upper limit of 100 million dollars (FY93) per satellite repair can be expected to be paid by the customer. Given a cost per mission of 110 million dollars (FY93) and conservatively projected revenues of 175 million dollars (FY93) from two customers, the project clears a 65 million dollar (FY93) profit per mission. Assuming three missions per year due to Station servicing constraints and vehicle turnaround, this results in a 195 million dollar (FY93) profit per year. In order to recover the first unit production costs of 204 million dollars (FY93) missions servicing multiple satellites must be performed. After those costs are recovered anything above and beyond mission cost can be used to reimburse RDT&E costs. Assuming optimal servicing conditions (i.e. two satellites serviced per mission and three missions per year) continue after first unit production costs are recovered this program could potentially generate as much as 270 million dollars (FY93) in revenue per year. Projected over the twenty year life span of the vehicle this results in total program revenues of 5.4 billion dollars (FY93).

## Table 1.3.1: Costing Model Summary I

| System | Mass (kg) | RDT&E Cost ($M93) | First Unit Cost ($M93) |
|---|---|---|---|
| **Cabin/Crew Accomodations** | | | |
| Cabin Structure | 240 | 80.4 | 14.0 |
| Insulation and Shielding | 75 | 56.8 | 10.5 |
| Crew Accomodations and Supplies | 180 | 292.7 | 33.6 |
| Subtotal | 495 | 429.8 | 58.0 |
| **Avionics** | | | |
| Control Moment Gyros | 56 | 38.1 | 2.3 |
| Computer Equipment and Sensors | 121 | 415.9 | 18.0 |
| Subtotal | 177 | 454.0 | 20.2 |
| **Propulsion** | | | |
| Main Engine, Pumps and Piping | 300 | 63.4 | 8.2 |
| 20 RCS Thrusters (N2H4) | 37 | 10.1 | 2.6 |
| 40 RCS Thrusters (He) | 4 | 1.4 | 0.8 |
| Subtotal | 341 | 75.0 | 11.6 |
| **Main Propellant and RCS Tanks** | | | |
| 2 LOX Tanks | 210 | 14.2 | 1.8 |
| 2 LH2 Tanks | 370 | 23.5 | 2.5 |
| 2 N2H4 Tanks | 10 | 1.0 | 0.3 |
| 2 He Tanks | 10 | 1.0 | 0.3 |
| Subtotal | 600 | 39.6 | 4.8 |
| **Aerobrake** | | | |
| Aerobrake Structure | 250 | 123.0 | 21.4 |
| Thermal Protection System | 400 | 154.9 | 26.3 |
| Truss Structure | 100 | 65.4 | 11.9 |
| Subtotal | 750 | 343.3 | 59.6 |
| **Docking Module** | 30 | 8.5 | 1.0 |
| **Upper Truss Structure** | 100 | 52.3 | 9.5 |
| **Power** | 52 | 19.1 | 3.5 |
| **Satellite Grappler and Robotic Arm** | 250 | 205.0 | 35.6 |
| Subtotal | | 1626.5 | 203.9 |

## Table 1.3.2: Costing Model Summary II

| System | Parameter | RDT&E Cost ($M93) |
|---|---|---|
| Software | kloc | 230.5 |
| Systems Engineering and Integration | RDT&E Cost ($M92) | 131.0 |
| Project Management | Total Direct Cost ($M92) | 52.6 |
| Subsystems Development and Testing | Total Direct Cost ($M92) | 128.1 |
| Support Equipment | Total Direct Cost ($M92) | 157.9 |
| Integration, Assembly and Check | First Unit Cost ($M92) | 48.0 |
| | | |
| Subtotal | | 748.2 |

| | |
|---|---|
| Total RDT&E Cost ($M93) | 2374.7 |
| Total First Unit Cost ($M93) | 203.9 |
| | |
| Total Program Cost ($M93) | 2578.6 |
| | |
| Discounted Program Cost ($M93) | 2026.3 |

## Figure 1.3.1
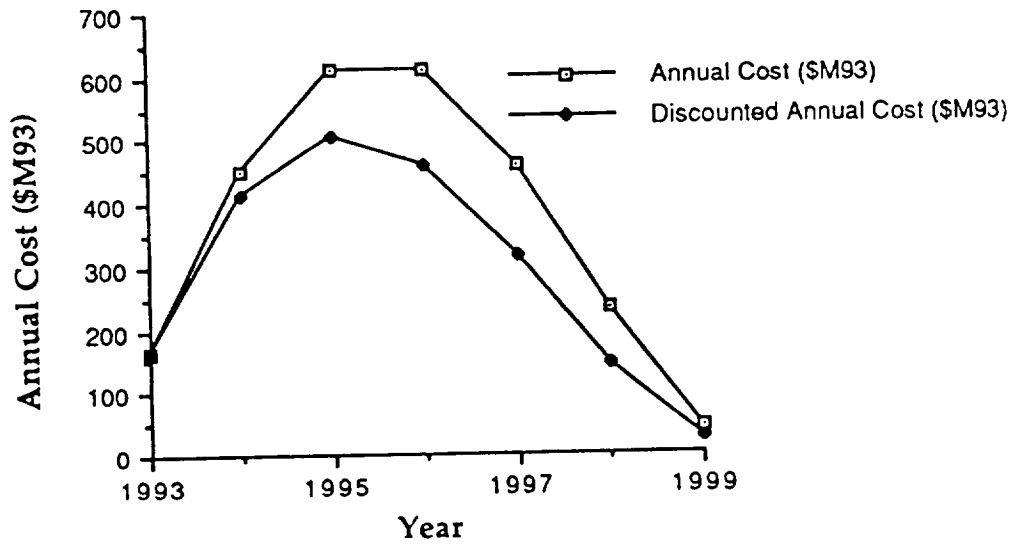


## Figure 1.3.2
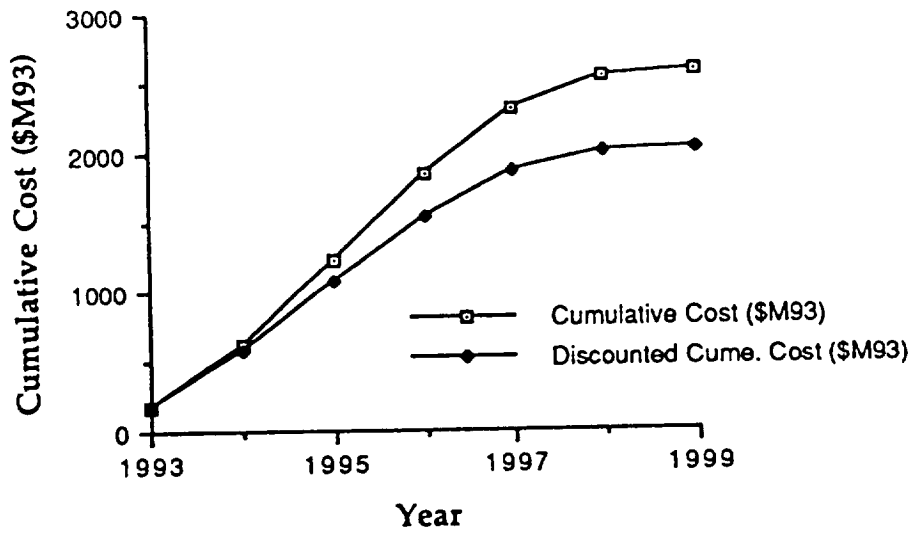
## 1.4   Mass Properties

## 1.41   Mass Budget

The mass budget for the vehicle lists each component of the vehicle and a mass for each value has been estimated or calculated. Total mass values for a dry and wet vehicle are given. The mass margin, which is an indication of how much the vehicle is allowed to increase in mass before effecting the design of the vehicle, is also given. The mass margin is important because a kilogram saved in structure is a kilogram that can be used to carry more payload; the payload for this vehicle being the equipment needed to repair the satellites. Below is the mass budget.

| SYSTEM | COMPONENT | MASS (kg) | STATUS |
|---|---|---|---|
| Avionics | | | |
| | gps | 7 | estimated |
| | sun sensors | 7 | estimated |
| | control moment gyros | 76 | estimated |
| | accelerometers | 1 | estimated |
| | outboard assembly | 34 | estimated |
| | (rendezvous radar) | | |
| | (antenna) | | |
| | star trackers | 3 | estimated |
| | data recorders | 28 | estimated |
| | primary computer | 40 | estimated |
| Power | | | |
| | fuel cells | 52 | estimated |
| Propulsion | | | |
| | main thrust chamber assembly | 300 | estimated |
| | (injector) | | |
| | (ignition system) | | |
| | (inlet and distribution manifold) | | |
| | (mounting structure) | | |
| | (combustion chamber) | | |
| | (expansion nozzle) | | |
| | (filter for each tank) | | |
| | (pump fed system for main propulsion) | | |
| | (RCS pressure fed system) | | |
| | (plumbing, piping, and valves) | | |
| | (attitude and control thrusters) | | |
| | (thermocouples) | | |
| | (heaters for lines) | | |

|  |  |  |
|---|---|---|
| RCS thrusters | | |
| 20 N2H4 | 37 | calculated |
| 40 He | 4 | calculated |

Human Factors

|  |  |  |
|---|---|---|
| crew member | 90 | estimated |
| nitrogen and tank | 15 | estimated |
| water | 8 | estimated |
| communication headset | 1 | estimated |
| keyboard | 1 | estimated |
| manual manipulation arms | 6 | estimated |
| two 13" touch LCD monitor | 2 | estimated |
| 19" touch LCD monitor | 1 | estimated |
| rotational hand controller | 1 | estimated |
| supplemental control station | 3 | estimated |
| translational hand controller | 1 | estimated |
| emergency air mask | 2 | estimated |
| fire extinguisher | 5 | estimated |
| support chair | 8 | estimated |
| food | 5 | estimated |
| hygiene cabinet (full) | 3 | estimated |
| light system | 2 | estimated |
| life support Unit | 50 | estimated |
| medical kit | 1 | estimated |
| waste container | 5 | estimated |
| water bladder | 3 | estimated |

Structures

|  |  |  |
|---|---|---|
| LH2 tank | 185 | calculated |
| LH2 tank | 185 | calculated |
| LOX tank | 105 | calculated |
| LOX tank | 105 | calculated |
| RCS tank | 5 | estimated |
| RCS tank | 5 | estimated |
| cold gas tank | 5 | estimated |
| cold gas tank | 5 | estimated |
| cold gas tank | 5 | estimated |
| cold gas tank | 5 | estimated |
| crew module | 240 | calculated |
| insulation and debris shield | 75 | estimated |
| docking ring | 30 | estimated |
| window | 10 | estimated |

|                          |        |           |
|--------------------------|--------|-----------|
| aerobrake                | 250    | estimated |
| aerobrake TPS            | 400    | estimated |
| grappler and manipulator | 250    | estimated |
| spider truss             | 100    | estimated |
| lower truss              | 100    | estimated |

Operations

|                                            |     |           |
|--------------------------------------------|-----|-----------|
| end effectors, tools, ORU, and extra propellant | 200 | estimated |

Propellant

|          |      |            |
|----------|------|------------|
| Oxygen   | 1334 | calculated |
| Hydrogen | 9335 | calculated |
| $N_2H_4$ | 522  | calculated |
| He       | 223  | calculated |

The overall dry mass of the vehicle is the sum of all the component masses excluding the propellant mass. The fully loaded mass is the sum of all the component masses including propellant mass.

The total mass of the vehicle excluding payload, which will vary depending on the particular servicing mission to be performed, is:

| | |
|---|---|
| Vehicle Dry Mass | 3067 Kg |
| Vehicle Fully Loaded | 14481 Kg |

| | |
|---|---|
| MASS MARGIN | 12.9% |

One of the capabilities of MOOSE is to do servicing around Space Station Freedom itself. To become more maneuverable for servicing around the station, MOOSE separates beneath the spider truss, from the aerobrake and the main propulsion system. The components which comprise the separable portion of the vehicle are listed below.

| Component          | Mass (Kg) | Status    |
|--------------------|-----------|-----------|
| gps                | 7         | estimated |
| two sun sensors    | 5         | estimated |
| control moment gyros | 76      | estimated |

| | | |
|---|---|---|
| accelerometers | 1 | estimated |
| outboard assembly (rendezvous radar) (antenna) | 34 | estimated |
| star trackers | 3 | estimated |
| data recorders | 28 | estimated |
| primary computer | 40 | estimated |
| fuel cells | 52 | estimated |
| RCS thrusters | | |
| 20 N2H4 | 37 | calculated |
| 40 He | 4 | calculated |
| crew member | 90 | estimated |
| nitrogen and tank | 15 | estimated |
| water | 8 | estimated |
| communication headset | 1 | estimated |
| keyboard | 1 | estimated |
| manual manipulation arms | 6 | estimated |
| two 13" touch LCD monitor | 2 | estimated |
| 19" touch LCD monitor | 1 | estimated |
| rotational hand controller | 1 | estimated |
| supplemental control station | 3 | estimated |
| translational hand controller | 1 | estimated |
| emergency air mask | 2 | estimated |
| fire extinguisher | 5 | estimated |
| support .chair | 8 | estimated |
| food | 5 | estimated |
| hygiene cabinet (full) | 3 | estimated |
| light system | 2 | estimated |
| life support unit | 50 | estimated |
| medical kit | 1 | estimated |
| waste container | 5 | estimated |
| water bladder | 3 | estimated |
| RCS tank | 5 | estimated |
| RCS tank | 5 | estimated |
| cold gas tank | 5 | estimated |
| cold gas tank | 5 | estimated |
| cold gas tank | 5 | estimated |
| cold gas tank | 5 | estimated |
| crew module | 240 | calculated |
| insulation and debris shield | 75 | estimated |

| | | | |
|---|---|---|---|
| docking ring | 30 | estimated | |
| window | 10 | estimated | |
| grappler and manipulator | 250 | estimated | |
| spider truss | 100 | estimated | |
| N2H4 propellant | 522 | calculated | |
| He propellant | 223 | calculated | |

For this separable portion of the vehicle the total masses are:

| | |
|---|---|
| Vehicle Dry Mass | 1235 Kg |
| Vehicle Fully Loaded | 1980 Kg |

## 1.42 The Center of Gravity

The center of gravity of each component is determined by formulae for the centroid of homogeneous bodies. Listed below are the Xc.g., Yc.g., and Zc.g. station numbers associated with each component used to determine total vehicle center of gravity for the wet vehicle.

| COMPONENT | Zc.g. station no. (m) | Yc.g.(m) | Xc.g. (m) |
|---|---|---|---|
| LH2 tank | 1.56 | 2.19 | 0 |
| LH2 tank | 1.56 | -2.19 | 0 |
| LOX tank | 1.25 | 0 | 2.19 |
| LOX tank | 1.25 | 0 | -2.19 |
| RCS tank | 3.6 | .96 | 0 |
| RCS tank | 3.6 | -.96 | 0 |
| cold gas tank | 3.6 | 1.15 | 1.15 |
| cold gas tank | 3.6 | 1.15 | -1.15 |
| cold gas tank | 3.6 | -1.15 | 1.15 |
| cold gas tank | 3.6 | -1.15 | -1.15 |
| crew module | 4.85 | 0 | 0 |
| aerobrake | .375 | 0 | 0 |
| grappler/arm | 5.5 | 0 | 0 |
| insulation and shield | 4.85 | 0 | 0 |
| spider truss | 4.2 | 0 | 0 |
| window | 5.6 | 1.05 | 0 |
| lower truss | 2.97 | 0 | 0 |
| interior of cabin | 4.75 | -.04 | .66 |

| | | | |
|---|---|---|---|
| upper sun sensor | 4.2 | 1.03 | 0 |
| upper sun sensor | 4.2 | -1.03 | 0 |
| gps | 3.6 | 0 | 0 |
| lower sun sensor | 1 | 4.45 | 0 |
| lower sun sensor | 1 | -4.45 | 0 |
| control moment gyros | 3.6 | 0 | 0 |
| accelerometers | 3.6 | 0 | 0 |
| star trackers | 4.2 | .95 | 0 |
| rendezvous radar | 4.2 | 0 | 1.03 |
| data recorders | 3.6 | 0 | 0 |
| main thrust assembly | .31 | 0 | 0 |
| N2H4 & He thrusters | 3.6 | 2.06 | 0 |
| N2H4 & He thrusters | 3.6 | -2.06 | 0 |
| N2H4 & He thrusters | 3.6 | 0 | 2.06 |
| N2H4 & He thrusters | 3.6 | 0 | -2.06 |
| N2H4 & He thrusters | 3.6 | 3.36 | 0 |
| N2H4 & He thrusters | 3.6 | -3.36 | 0 |
| N2H4 & He thrusters | 3.6 | 0 | 3.36 |
| N2H4 &He thrusters | 3.6 | 0 | -3.36 |

The overall center of gravity of the vehicle is determined by Xc.g. vehicle = [$\Sigma$mass components*X c.g. of component]/[$\Sigma$mass], Yc.g.= [$\Sigma$ mass*Yc.g./$\Sigma$mass], Zc.g. = [$\Sigma$mass* Zc.g./$\Sigma$mass].

The overall center of gravity as indicated on figures 1.421 and 1.422 is located at :

| | Zc.g. (m) | Yc.g. (m) | Xc.g. (m) |
|---|---|---|---|
| Total vehicle before geo | 1.77 | 0.00 | 0.01 |
| Total vehicle after geo | 2.03 | 0.00 | 0.03 |
| Separable vehicle | 3.85 | 0.00 | 0.09 |

## 1.43 Moments of Inertia.

The moment of inertia for each component is calculated using the formulae for moment of inertia of homogeneous bodies. The moment of inertia about the center of gravity is determined from Ixx c.g. = Ixx + mass*distance to the center of gravity^2, Iyy c.g. = Iyy + mass*distance to the center of gravity^2, Izz c.g. = Izz + mass*distance to the center of gravity^2  where the moment of inertia about the center of gravity is increased by the parallel axis term [mass*distance to the center of gravity^2]. The cross moments of inertia about the center of gravity is Ixzc.g.= Ixz +mass*(xdistance to c.g.^2 + zdistance to c.g.^2)^1/2, Iyzc.g.=Iyz +mass*(ydistance to

c.g.^2 + zdistance to c.g.^2)^1/2, Ixyc.g.=Ixy + mass*(xdistance to c.g.^2 + ydistance to c.g.^2)^1/2.  Moments of inertia for individual components can be found in appendix 1.4.   Below are listed the moments of inertia for the total vehicle before and after servicing and for the separable vehicle fully loaded.

| | Izzc.g. * | Iyyc.g. | Ixxc.g. | Ixzc.g. | Iyzc.g. | Ixyc.g. |
|---|---|---|---|---|---|---|
| Vehicle before geo mission | 56386 | 22819 | 15504 | 11756 | 28524 | 25861 |
| Vehicle after geo mission | 14085 | 15085 | 53233 | 6985 | 9855 | 5903 |
| Separable vehicle | 1193 | 1481 | 24843 | 1533 | 1861 | 1203 |

* units are m^4

References:
Greenwood, Donald T. 1988.  Principles of Dynamics. New Jersey: Prentice-Hall,Inc.
Hibbeler, R.C. 1989. Engineering Mechanics. New York: Macmillan Publishing Co.
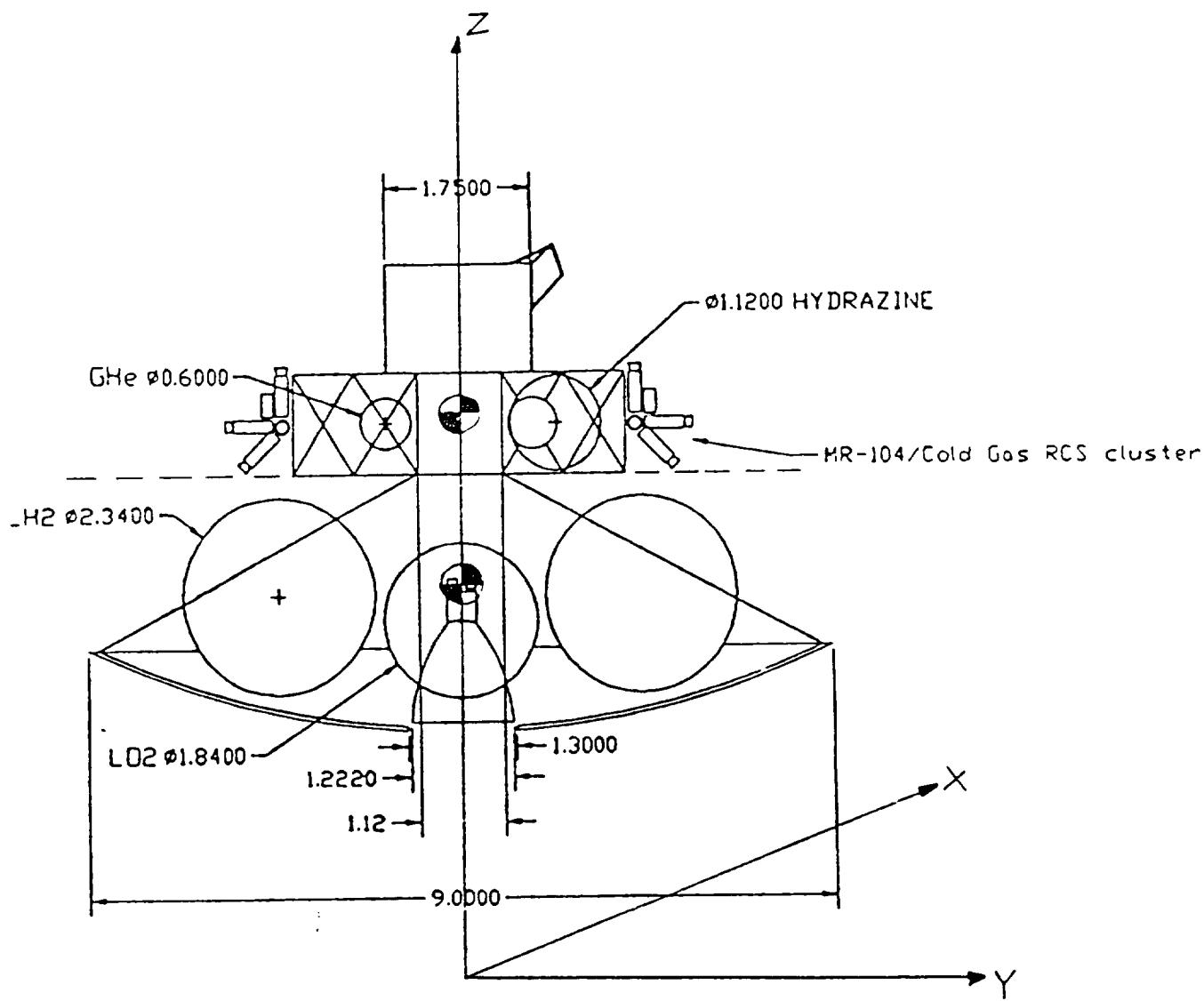
FIGURE 1.421: Center of Gravity for Fully Loaded Total Vehicle and Separable Vehicle
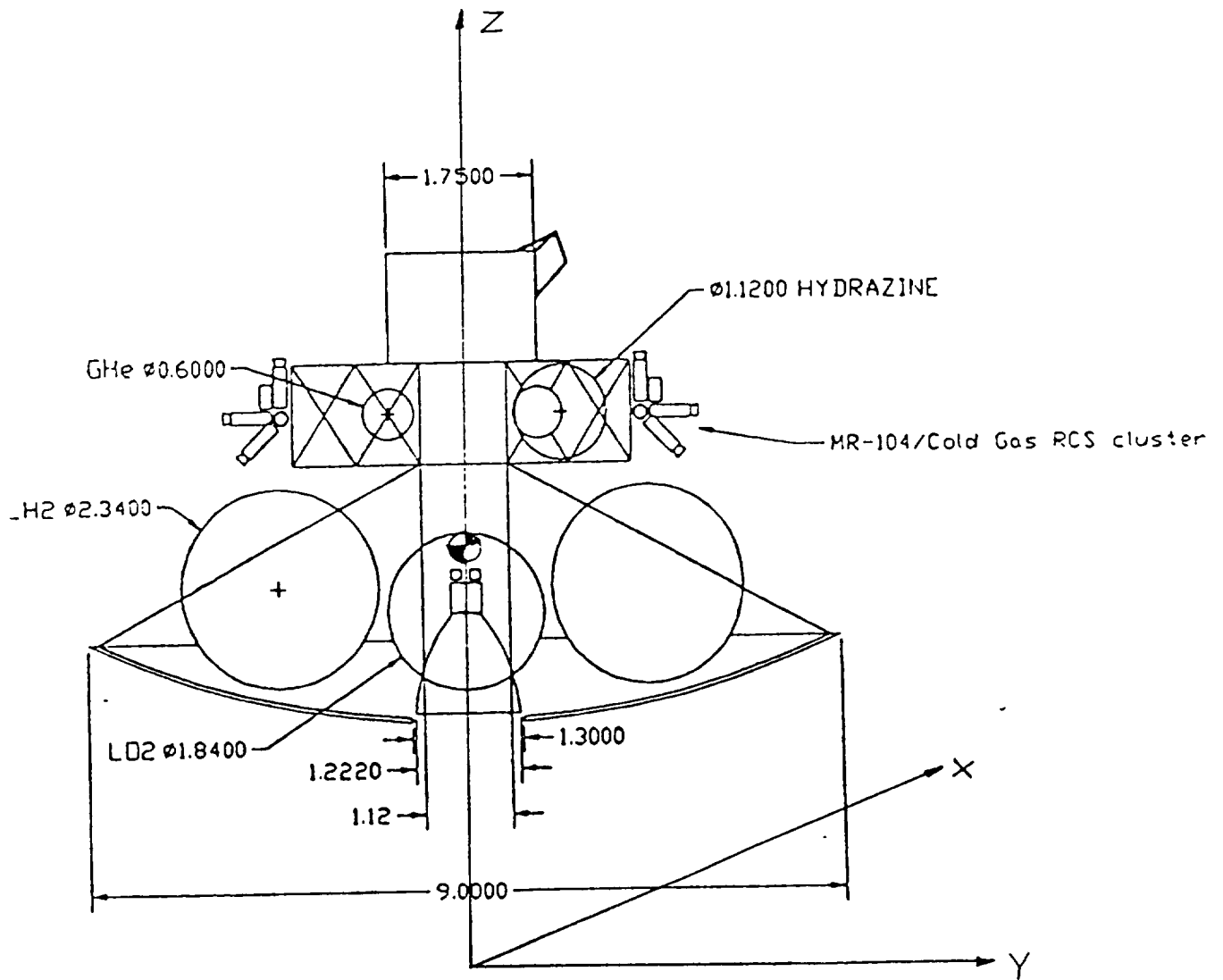
FIGURE 1.422:  Center of Gravity for Vehicle After Geo Servicing

1-28

# 2.0 Manipulator/Grappler System

## 2.1 Introduction

### 2.1.1 System Requirements

The Manipulator/Grappler System is essential to the execution of MOOSE's duties as an on-orbit servicer. One of the driving requirements for MOOSE is that the astronaut should not have to do an EVA during the repair process. To accomplish this, it is necessary to equip the vehicle with a manipulation system that he/she can control from within the spacecraft. The possible components of the Man/Grap System are: a Telerobotic Manipulator Arm (TMA), a Telerobotic Grappling Arm (TGA), and a Manual Manipulation System (MMS). There are several ways to fulfill the requirement using these subsystems.

### 2.1.2 Two Telerobotic Manipulator Arms and a Telerobotic Grappling Arm

This design is the most complicated in terms of implementation and control, but it offers more flexibility then the other options. The TGA is a four degree of freedom (DOF) arm, with various possible end effectors. It is necessary to have a grappling arm in order to maintain a fixed position and orientation, with respect to the target, during repair operations. The TMAs are both seven DOF arms (including end effectors).

In this design, the TMAs are capable of fine, dexterous tasks. The astronaut has to conduct all repairs using these arms, so the TMAs have to be able to perform all the functions an astronaut in EVA can perform. The need for a highly dexterous arm design would drive development and production costs very high, and complicate the control hardware and software. In addition, the astronaut would need extensive practice with the arms and end effectors in order to become effective at conducting repairs.

As the need to lower the total mass and size of the vehicle became more pressing, it became clear that the mass resulting from having three arms would have to be reduced. In addition, the issue arose as to whether enough power could be provided to maintain the operation of two TMAs at the same

time, and whether there was enough space on the outside of the cabin to mount three arms.

### 2.1.3 One Telerobotic Manipulator Arm and a Telerobotic Grappling Arm

This design does away with a TMA, leaving just two arms with which to perform the repair tasks. The TMA is just as complicated as in the 2TMA/1TGA configuration. Unfortunately, the types of repairs that can be performed with just one arm is limited to on-orbit refueling. Not having another manipulator to "hand-off" to is a severe limitation.

### 2.1.4 Manual Manipulator System and a Telerobotic Grappling Arm

In this design, the TMAs are replaced with a MMS, which consists of, basically, astronaut gloves that are attached to the outside of the vessel's cabin. The astronaut has the benefit of using most of the flexibility of his/her over 50 DOF arms and hands to conduct the repairs, without having to leave the cabin. While this option provides the ultimate in fine dexterity, the limited workspace envelope leaves much to be desired. The Orbital Replacement Units (ORUs) and refueling facilities would have to be within the arms' reach if this configuration is to be useful. In addition, it may be difficult for the astronaut to conduct repairs on objects that have great size or mass.

### 2.1.5 Final Configuration

The culmination of the design process was a system that utilized all three subsystems. The TGA remains unchanged, as does the MMS. These systems provide the stable environment and flexibility necessary to conduct the repairs. The TMA can now be simplified, however.

Since the astronaut is expected to handle the bulk of the fine manipulation using the MMS, the TMA does not need to have the fine dexterity that was required in the first two configurations. This means that the mass and complexity that would have been required to create a very stiff (non-compliant) arm can be eliminated. The TMA is to function as an "assistant" to the astronaut, in that it can handle massive loads, hold "hand-off" tools and equipment, retrieve ORUs from storage, etc. By providing a variety of end effectors, the TMA can still perform simple repair tasks, such as refueling, etc.

The current design of the Man/Grap system is shown below (Figure 2.1.a). The MMS is mounted directly below the cupola. The TGA is shown with an optional third link/stinger end effector.
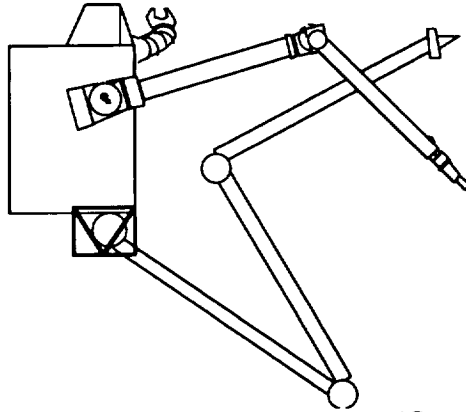
**Figure 2.1.a** View of Cabin & Manipulator/Grappler System

## 2.2 Telerobotic Manipulator Arm (TMA)

### 2.2.1 Functional Requirements

The primary functional requirement of the TMA is that it act as a secondary system to the Manual Manipulation System (MMS). It will assist the MMS in servicing operations by retrieving MMS tools and providing hand-off capability.

A secondary functional requirement of the TMA is to maneuver the Satellite Fluids Replenishment System (SFRS) during a satellite replenishment mission. The TMA will connect to the SFRS fluid transfer hose and position the nozzle for attachment.

The TMA will retrieve satellite ORU's from the MOOSE payload area and transfer them to the MMS workspace.

The TMA shall also have maximum functional flexibility to perform unforeseen satellite servicing tasks. The TMA shall have 7 degrees of freedom as well as a 4 meter reach capability to allow for unexpected tasks.

### 2.2.2 Design Requirements

The TMA shall be designed primarily as an assistant to the MMS, performing tasks that the MMS cannot achieve.

The TMA shall have a maximum payload capability of 425 kg. This payload mass is based on the largest possible satellite ORU needed.

The total mass of the TMA will be a maximum of 50 kg. This is a result of a vehicle requirement to minimize mass.

The TMA shall have 7 degrees of freedom and consist of 2 major links.

2-3

The TMA shall have a joint braking system to limit continuous servicing power consumption.

The TMA shall have an Interchangeable End Effector System ( IEES).

## 2.2.3 TMA Configuration

The TMA configuration consists of 2 major links containing 7 degrees of freedom. A schematic of the TMA is shown in Figure 2.2.a. The arm has seven revolute joints located down its length starting with the shoulder roll at the base. The shoulder has three degrees of freedom in a roll, pitch, roll setup where all three axes intersect at the base. The elbow has a pitch degree of freedom that contains an offset between the two major links. The first degree of freedom at the wrist is a pitch, followed by a yaw that is offset from the pitch joint, and finally a roll joint whose axis intersects the previous two joint axes.



(a)

(b)
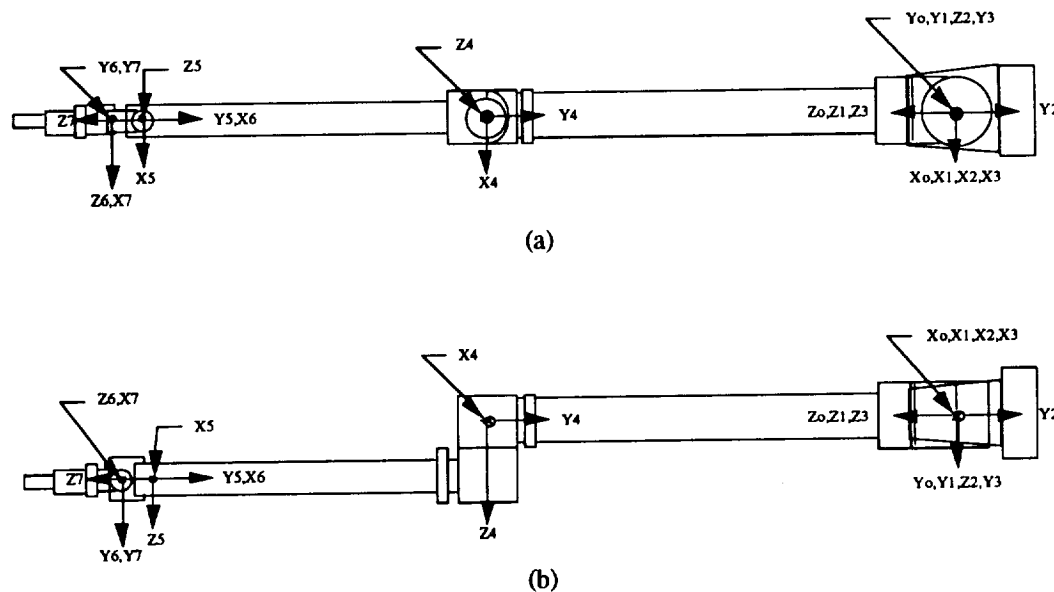
Figure 2.2.a Telerobotic Manipulation Arm (TMA): (a) side view; (b) top view

To fully characterize the kinematics of the TMA, the Denavit-Hartenburg notation is given in Table 2.2.a. These values are called the D-H parameters.

| Joint # i | $a_{i-1}$ (meters) | alpha$_i$ (deg) | d$_i$ (meters) |
|-----------|--------------------|-----------------|-----------------|
| 1 | 0.000 | 0 | 0.000 |
| 2 | 0.000 | +90 | 0.000 |
| 3 | 0.000 | -90 | 0.000 |
| 4 | 0.000 | -90 | 0.150 |
| 5 | 2.000 | 0 | 0.000 |
| 6 | 0.100 | -90 | 0.000 |
| 7 | 0.000 | +90 | 0.000 |

**Table 2.2.a** Denavit-Hartenburg (D-H) Parameters for TMA

There are 3 parameters for each joint that are required to completely describe the fixed portion of the TMA's kinematics. The first is link length, represented in D-H notation by (a). It is defined as the mutually perpendicular distance between the rotation axes of joint i - 1 and joint i . The second parameter is link twist, represented by (alpha). It represents the angle formed by the rotation axes of joint i - 1 and joint i . The third parameter is the link offset, represented by (d). Neighboring links have a common joint axis between them. The distance along this common axis from one link to the next is defined as the link offset.

If we were to add one more parameter (q ), the revolution angle of all joints, to the above list we would have a full kinematic description of our arm.

## 2.2.4 Configuration Drivers

The TMA configuration summarized above evolved from the desire for a versatile manipulator system. A configuration using two telerobotic manipulators was considered as well. In the interest of mass savings and manual dexterity the TMA/MMS configuration was chosen. There was also a trade-off between manipulator and grappler complexity. A choice was made to have a versatile manipulator and to sacrifice some grappler complexity to achieve this. Complexity is defined here as maneuvering capability (degrees of freedom, link lengths).

## 2.2.5 Physical Arm Characteristics

The 2 main links of the TMA are to be fabricated from Graphite/Epoxy. The joint material is Titanium (T16 A1-4 V). The thermal expansion compatibility of these materials was a major driver in their selection. Each material has a large strength-to-weight ratio as well as a good resistance to corrosiveness.

The arm will be subjected to an unfavorable environment during satellite fluid replenishment missions. Graphite/Epoxy provides a suitable stiffness for the TMA links.

## 2.2.5.1 Outer Link

The outer link of the TMA is a 2 meter long thin-walled beam made of Graphite/Epoxy. It has a skin thickness of 0.002 m and radius of 0.05 m. This link has a mass of 3 kg. The maximum tensile stress on this link is approximately $2 \times e7$ N/sq. meter. The critical stress level for this link is $1.337 \times e9$ N/sq. meter. Therefore there is a factor of safety of at least 10 on this beam. The inside of the beam has a section of multi-layer insulation for thermal control. Extensive wiring will pass through the center of the beam.



.002 m skin thickness

R.070 m

Insulation
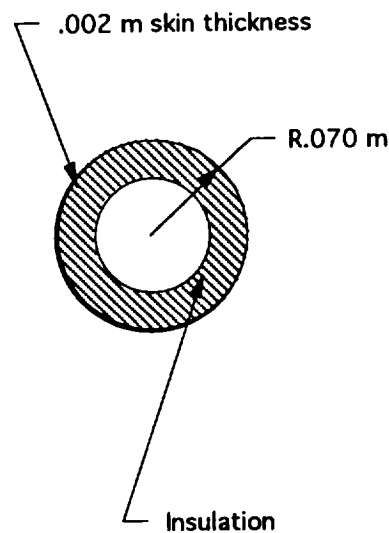
**Figure 2.2.b** Outer Link Cross-section

## 2.2.5.2 Inner Link

The inner link of the TMA is a 2 meter beam made of Graphite/Epoxy. It has a skin thickness of 0.01 m and a radius of 0.08 m. The link has a mass of 34 kg. The inside of the beam has a section of multi-layer insulation for thermal control. The inner beam has sufficient space for the increasing amount of wiring that will run up the length of the arm.

.01 m skin thickness

R.080 m

Insulation
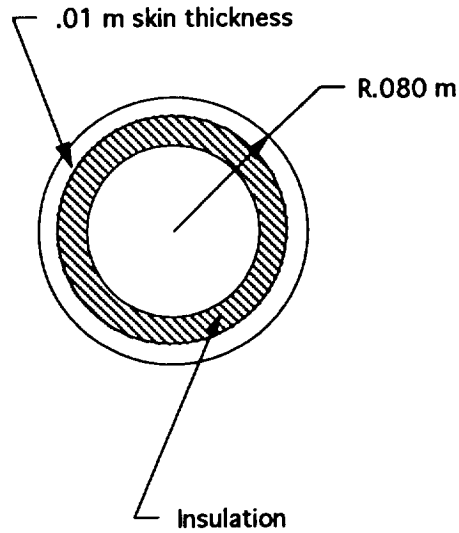
**Figure 2.2.c** Inner Link Cross-section

## 2.2.6 TMA Motors

The TMA will use a set of brushless DC motors in each of its joints. The 3 motors for the TMA wrist have been estimated at approximately 0.5 to 1 kg per motor. The masses of the gearboxes for these motors will be in the range of 1 kg each. The elbow motor has been estimated at 1.2 kg. Its gearbox mass is 1.3 kg. The shoulder motors will be more massive due to the larger torques they supply. The motors will have a mass of approximately 1.5 kg each. Their gearbox masses will be in the neighborhood of 2 kg each.

## 2.2.7 TMA Power Requirements

Power requirements for the TMA were estimated from the torques that must be supplied by the motors. A range of motors that could satisfy the torque requirements was identified. From the power requirements of these motors a maximum power requirement of approximately 700 Watts was estimated.

## 2.2.8 TMA Braking System

The TMA will contain a braking system to brake the arm during any non-use periods. Each joint will contain an individual brake. This braking system is essential to limit the maximum power requirements for the entire telerobotic system. This will allow the TMA to draw minimal power while the TGA is in use.

## 2.2.9 TMA Dynamics

Several TMA movement parameters have been set in order to design the arm. The maximum tip acceleration for the TMA is 0.05 m/sec sq. This leads to a maximum angular acceleration of 0.025 rad/sec sq. A maximum angular velocity of 0.1 rad/sec was set to limit the load on the TMA when translating a payload.

The TMA takes approximately 5 seconds to reach the maximum angular velocity. The TMA can traverse a fully extended 180 degree movement in approximately 45 seconds. Movement of a payload will in all likelihood increase travel time.

## 2.2.10 TMA End Effectors

The TMA will employ the use of the NASA Mobile Servicing System ORU/Tool Changeout Mechanism (OTCM). The OTCM will be permanently mounted at the tip of the TMA. The OTCM allows simple changeout of the TMA's two primary end effectors as well as the attachment to any H-Handle Interface. The OTCM has an electrical interface built in that will allow power interface to any end effector similarly equipped.

## 2.2.10.1 Fluid Transfer Nozzle End Effector

This end effector will be an H-Handle interface built into the Fluid Transfer System (FTS) that will be used when replenishing satellites. The FTS is a self contained unit containing a fluid tank, a fluid transfer mechanism, and a fluid transfer hose. The fluid transfer hose will run from the FTS mounted at the MOOSE payload attachment point. The payload attachment point is located on the attitude control system truss. The fluid transfer hose will run from this point to the base of the crew cabin. It then runs vertically up the crew cabin and is secured to the cabin wall by several powered attachments.

**Nozzle End Effector**

**Fluid Transfer Hose**
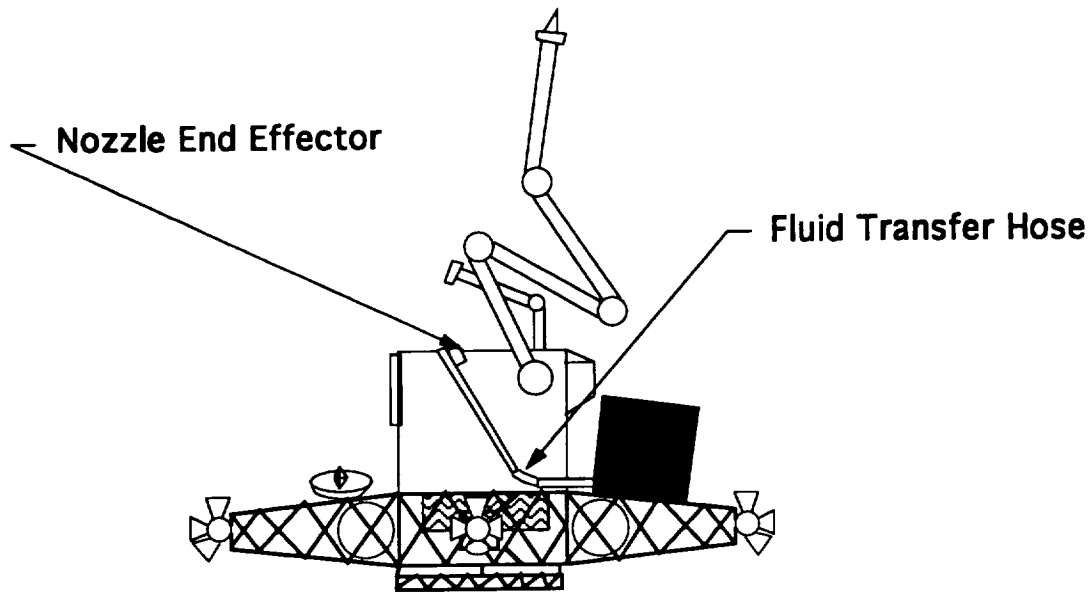
Figure 2.2.d  Fluid Transfer Hose Configuration

The TMA use of the fluid transfer will involve several steps that begins with the OTCM mating with an H-Handle interface mounted on the fluid transfer hose. The mating will connect power to the FTS and the FTS will then be powered up. The fluid transfer hose will then be released from the crew cabin wall. The TMA will translate the hose to the satellite work area. The fluid transfer hose will have a nozzle attached to the end of the hose. This nozzle will be mated to the satellite fluid interface. After the mating is verified, the fluid will be transferred to the satellite. De-mating will then occur, and the fluid transfer hose will be translated back to the crew cabin side. The hose will be re-attached to the crew cabin and the FTS will then be powered down. The TMA will then de-mate from the FTS's H-Handle interface.

### 2.2.10.2  Parallel Gripper End Effector

This end effector will be the baseline end effector launched in place on the TMA. It consists of a parallel gripping mechanism (see Figure 2.2.e) that will be capable of retrieving tools and other objects for the Manned Manipulation System (MMS). When the TMA is functioning as an assistant to the MMS this end effector will be used. This end effector can also be used for any unforeseen tasks involved in a satellite servicing. The end effector will have and H-Handle interface on the mounting side for mating with the OTCM.

2-9
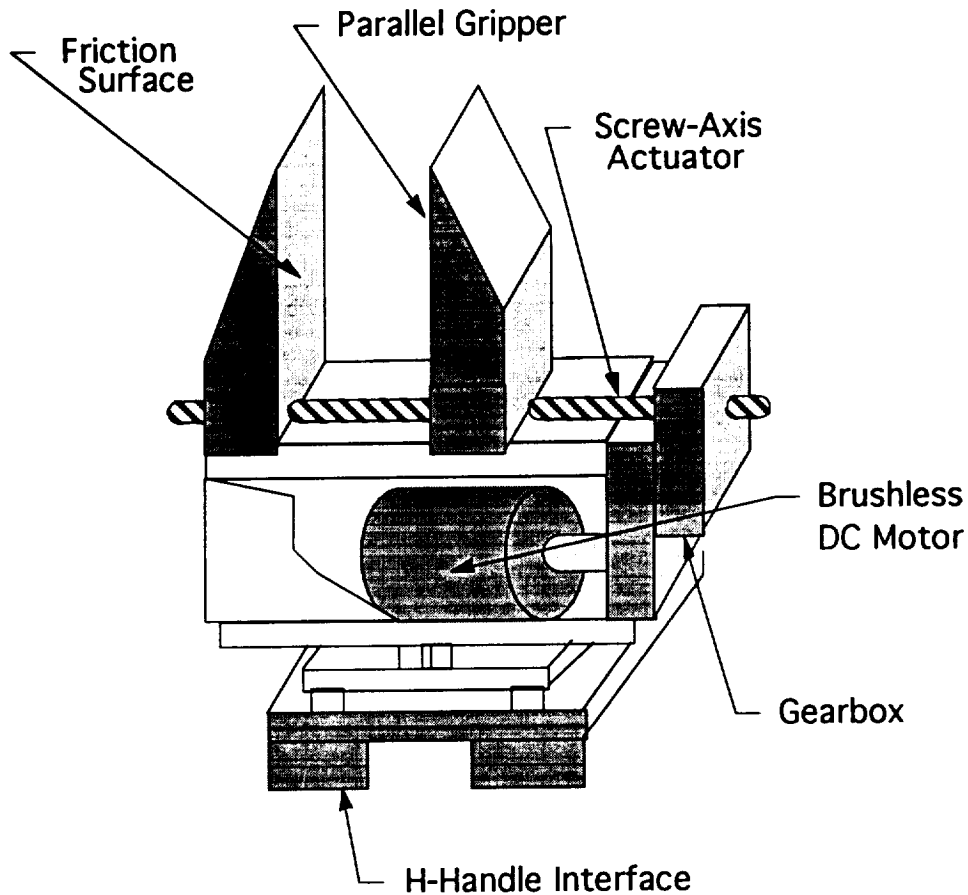
**Figure 2.2.e** Parallel Gripper End Effector

### 2.2.11 TMA Stowage

The TMA will be put into stowage position during any MOOSE transfer burns. The stowage position for the TMA is with link 1 down the crew cabin side at a slight angle, the elbow located at the base of the crew cabin, and link 2 continuing along the base of the crew cabin. When the TMA is in stowed position, it will have the braking system applied.

## 2.3 Telerobotic Grappling Arm (TGA)

### 2.3.1 Functional Requirements

- Provide the ability to firmly grapple and hold a cooperative satellite (i.e. a satellite with fully functioning Attitude Control System, Reaction Control System, and Communication System).

- Provide ability to grapple, stabilize, and hold an errant satellite in pure (or near pure) spin.

- Be compact in design, so as to be stowable when not in use.

- Minimize the risk of damage to MOOSE and the target satellites.

- Maintain appropriate distance and orientation between MOOSE and target satellites during operations.

## 2.3.2 Design Issues

### 2.3.2.1 Revolute-vs-Prismatic Joints

In Appendix 2.a, several robotic manipulator design criteria are discussed, including the relative benefits/detriments of revolute-vs-prismatic joints. The main problem with using prismatic joints in space is the difficulty that one has in sealing the linear bearings from the space environment, to allow the joint to remain well lubricated. This contrasts with revolute joints, which are much easier to seal. In addition, jointed manipulators are very flexible, with large workspace and low energy and torque requirements. In spite of the added complexities of the hardware and control software, the jointed manipulator design has much going for it, and will form the basis for the MOOSE grappler mechanism.

### 2.3.2.2 Direct Drive-vs-Transmitted Drive

One of the main design drivers is that the vehicle systems have low masses. In order to get a basic idea of how direct drive drive manipulators compare to transmitted drive manipulator in term of mass, a rough cut analysis was conducted, using the program listed in Appendix 2.b. The resulting data is shown below (Figure 2.3.a).

ARM MASSES-VS-TIP ACCELERATION
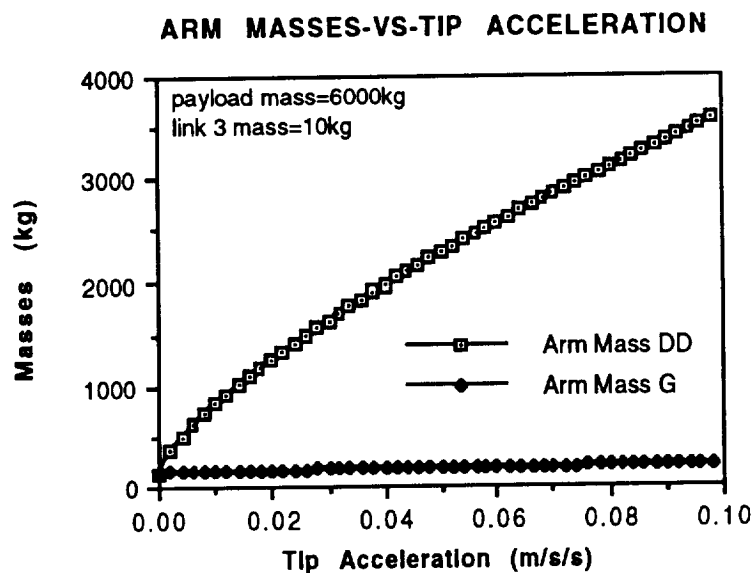


Figure 2.3.a  Arm Masses -vs-Tip Acceleration for Direct-Drive and Geared Designs

2 - 11

For the sake of computation, it was assumed that the maximum payload mass to be handled was 6000 kg, and that the mass of link 3 would be 10 kg. It can be seen from this chart that as the desired tip acceleration increases, the required mass of the transmitted drive manipulator system grows very quickly, while the geared drive manipulator system mass stays almost constant, at around 250 kilograms.

A second chart (Figure 2.3.b) shows that increasing the mass of the third link increases the overall mass of both the direct-drive and the gear mechanism by the same rate. Note, again, that the direct-drive arm has a much higher mass than the geared arm.

## ARM MASSES-VS-LINK MASSES
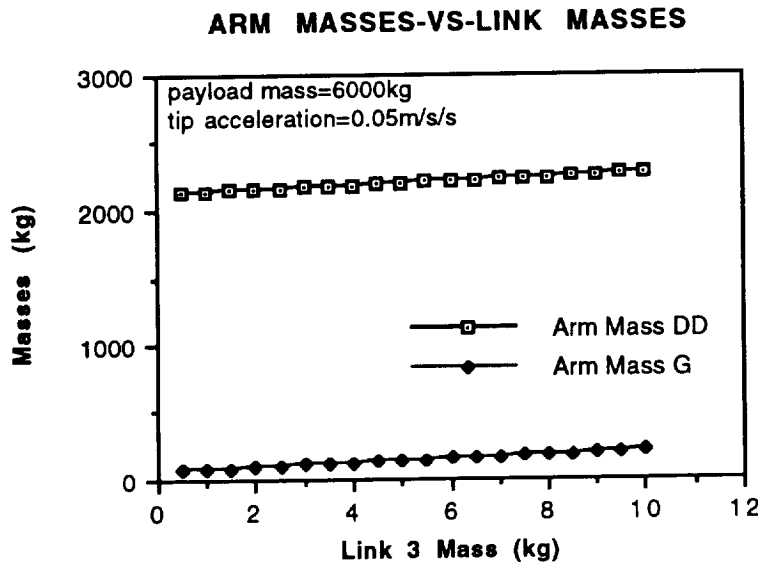


Figure 2.3.b Arm Masses-vs-Link 3 Masses for Direct-Drive and Geared Designs

The mass savings that is experienced by using geared mechanisms instead of direct-drive mechanisms far out weighs the problems that would result from transmission losses, compliance in the gears, etc.

### 2.3.2.3 High torque/low speed Requirement

Figure 2.3.c below shows the required torques from the motors at joints one and two. The data was calculated using the program listed in Appendix 2.c. The torques were calculated for the entire spread of angles. Figure 2.3.c presents only one set of the data, where theta1 = 0 radians, the tip accelerates at 1 m/s in the x- or y- direction, is the link lengths were 2.5 m, and the payload was 6000 kg. (NOTE: This program does a two-dimension approximation of the arm).

## Torques -vs- Angular Position
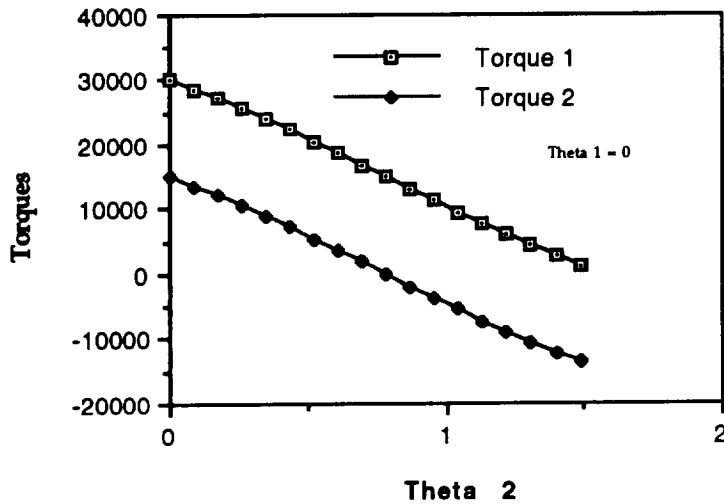


Figure 2.3.c Torques-vs-Angular Position at Joints 1 an d 2

### 2.3.2.4 Active-vs-passive braking

In order to minimize the required power, it is necessary to use a passive breaking mechanism in all the joints. The grappling arm is estimated to require 1kW of power.

### 2.3.2.5 Interchangable end effectors

Since there is no standard interface employed by all satellites, it is necessary to allow for interchangeable end effectors that can be deployed according to the mission. Currently, only two designs for end effectors are baselined. The first is a "stinger" mechanism, which can be use to grapple with the apogee kick motor of a satellite. The second is a generic gripper type mechanism, which can be used to grab any sturdy structure in a grapple attempt.

### 2.3.2.6 Degrees of Freedom (DOF) required

The arm is going to require 4 degrees of freedom: a turn-table type mechanism, and a revolute joint, at the base, another revolute joint at the end of the first link, and a revolute joint at the end of the second link. End effectors can have as many as 4 more degrees of freedom.

### 2.3.3 Arm Design

Dimensions
  5 m extended length (2.5 meters per link)

Work Envelope

Analysis
  Stress Distributions
  Material Selection
  Maximum Loading
  Torque Analysis
  Motor Selection
  Power Consumption
  Braking Requirements

Mass of Linkages/Motors

Handle (max.) 6000 kg payload--this is the mass of the largest satellites
  in LEO

### 2.3.4 End Effector Design

Stinger/Despinner

Gripper

### 2.3.5 Grappling Arm Stowage

## 2.4 Manual Manipulation System (MMS)

### 2.4.1 Configuration

The MMS consists of two spacesuit-type arms coming out of the capsule. The crew member slides their arms into MMS and can actually touch, grab and hold objects outside the vehicle. The major advantage is the many degrees of freedom inherent to the human arm and hand that can be used without the need to provide any control or computational hardware/software other than the astronaut's brain. The shoulder joint is included in the MMS to use the maximum natural degrees of freedom as possible.
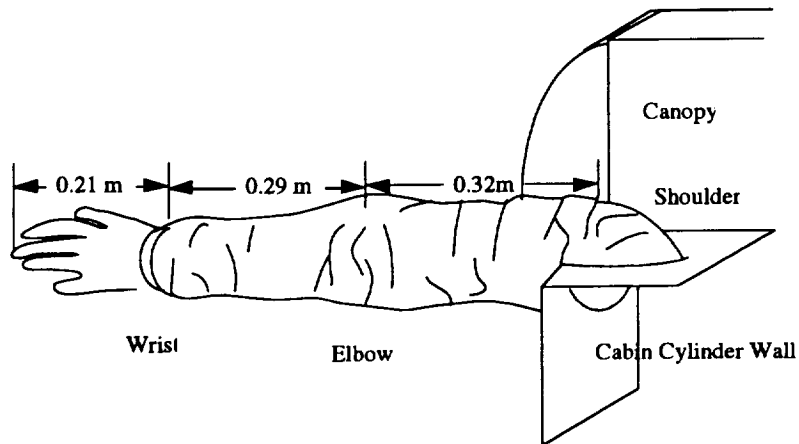
Figure 2.4.a Detailed View of an Manual Manipulator

Mass (both arms)                    6kg

Most maintenance and other manipulation tasks will be performed using the MMS. A canopy is provided so that the crew member will have the maximum viewing area possible when observing the worksite. However because of the short length of a human arm, the MMS is placed at the extreme end of the vehicle. This way, the crew member can work close to the satellite without other parts of MOOSE interfering.
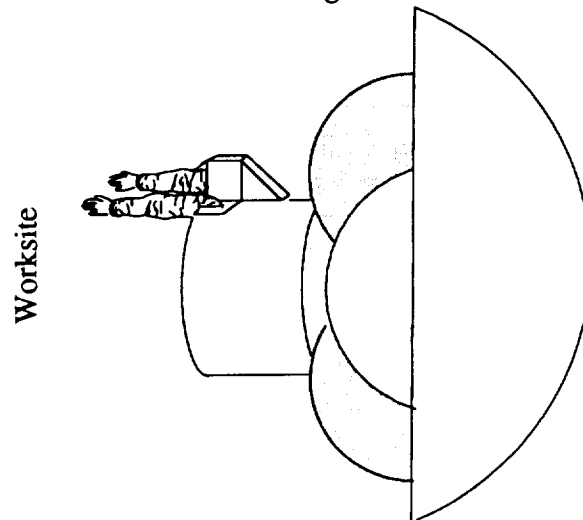


Figure 2.4.b Location of MMS on MOOSE

This system is similar to an astronaut suit, and is extremely bulky. The range of motion and work envelop is extremely limited when compared to a robotic manipulator. The elbow is able to keep much of its range of motion; however the shoulder's mobility is hindered considerably. This is due to the integration of the shoulder to the cabin cylinder. As an example of how the workspace of the left shoulder is limited, see Figure 6.4.c below.

2 - 15
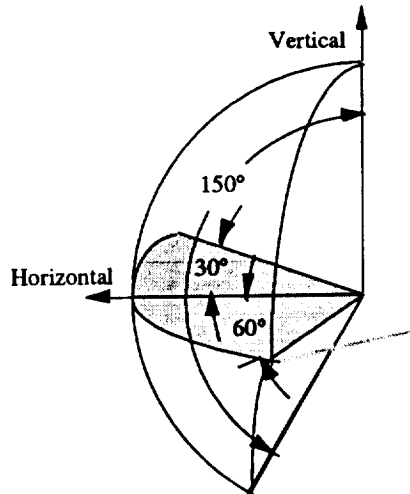
**Figure 2.4.c** Range of Motion of Left Shoulder of MMS

The right shoulder workspace is a mirror image. Although the full freedom of the crew member can not be perfectly achieved, the MMS will be able to perform most tasks need to complete the mission.

## 2.5 Control Station

### 2.5.1 Functional Requirements

The control station must command the manipulator and grappler. Vehicle control will also occur here, as will adjustments to the environmental system, communication operations, and emergency overrides. Effective utilization of tools and equipment accessible to the manipulator system will be integrated to the design.

### 2.5.2 Design Requirements

Human factors, especially ergonomics, will be used to ease operation by the crew member. Multiple alternative control devices will be placed on the system so that a task may be performed using the preferred device. The manipulator worksite (outside the canopy), the essential controls, and the monitors should be within the optimal range of view of the crew member. The comfort of the crew member while performing task for a long time becomes a factor. The crew member should be in the neutral position during most of the working time.

The control station is simple and lightweight--the total mass of the station is about 10 kg. The view of the control station is provided in Figure 2.5.a below.

2 - 16
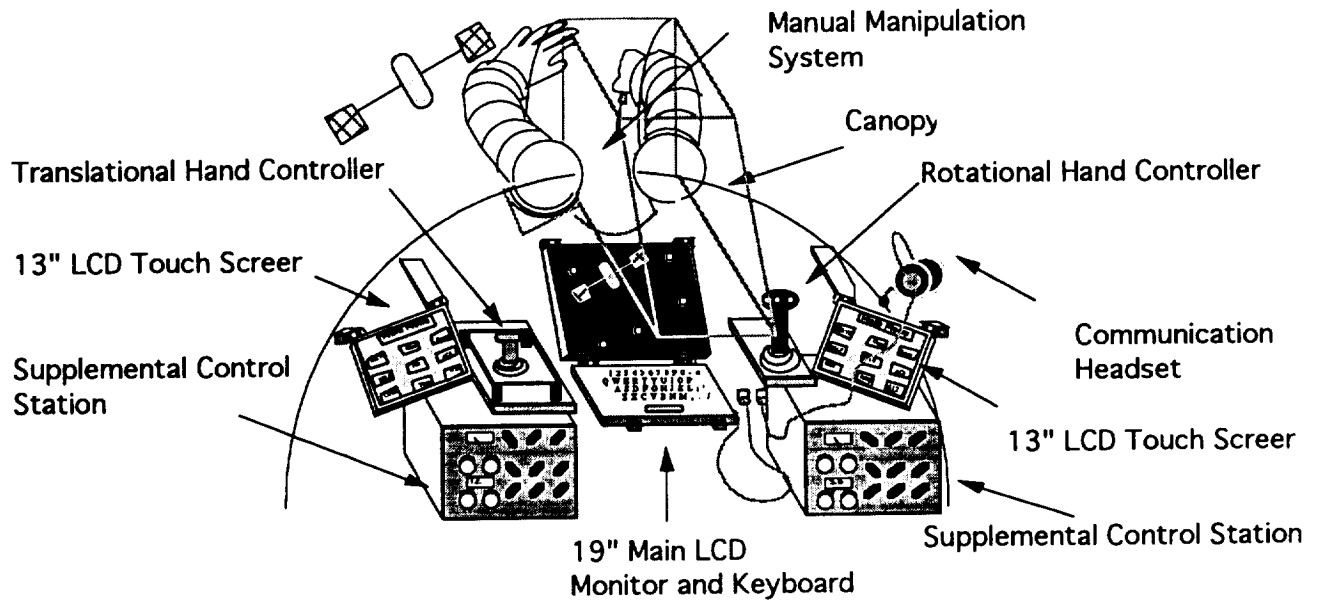
Figure 2.5.a Control Station Layout

## 2.5.3 Control Systems

Many control system are provided for the crew member. The systems overlap, causing many redundancies. This allows the crew member to chose a prefered system to accomplish a given task. In addition, the reliability of the control station is high due to the many backup control systems

### 2.5.3.1 Joystick Control

Most manipulation control will occur using the transitional and rotational hand controllers. Both manipulation and vehicle movement can be controlled using these joysticks. It is possible to toggle between vehicle, grappler, and manipulator control. This is the primary control of the vehicle. Astronauts are already familiar with this style of control. In general, they will not need to get accustomed to using the joysticks, only how the joysticks effect the the manipulation and vehicle control systems. Due to its simplicity, this is a very compact and lightweight system as compared to other mean of controlling the manipulators or vehicle.

### 2.5.3.2 Touch Screen

To help eliminate the need for many switches, monitors using touch screen technology will be used as a major control component. Three LCD touch screen monitors are provided. The main 19" will be used primarily for video imaging. Pictures sent from the end effectors cameras will show the worksite here. Two 13" LCD screens will be used for interactive touch control. Exact menus for specific tasks, such a grappling, could be brought up and used, then

switched for another task, as dictated. This will save space by having many menus available to the crew member. What is more important, the touch screen monitors will be in optimal viewing range so that the important controls and readouts will be easily seen and used during a task.

### 2.5.3.3 Voice Control

When both of the crew member's arms are using the MMS, it may be necessary to adjust the manipulator arm, the grappling arm, or even the entire vehicle. Since the joystick control or any other system requiring the crew's hands can not be used, necessary control is established through voice control. The crew member will wear headphones with a microphone during most operations. This headset will be linked into the communication system that will be used to talk to ground control or space station. Using the voice recognition system, certain simple control can be activated by the crew member orally. These tasks would include closing an end effector, relative positioning of a manipulator, hand-off of an ORU or tool, etc. With joystick, touch screen, and voice control, all tasks can be completed with redundancies creating high reliability for mission success.

### 2.5.3.4 Keyboard Control

A keyboard interface with the primary computer is provided. As another means of control, joint angles or tip positioning can be input into the computer. Additional menus can be brought up and utilized using the keyboard. More complex menus requiring the keyboard will be used. General control of the vehicle and manipulators can be performed at the expense of efficiency. However, this system provides another control style and backup system.

### 2.5.3.5 Supplemental Control Station

Hardwire controls using traditional switches, knobs, and gauges provide auxiliary control for particularly sensitive systems. Life support can be controlled from one of the stations that is physically attached to the life support unit. The two stations shown above (Figure 2.5.a) control the vehicle propulsion and avionics systems directly. Although this system can be used for primary control, it is designed as a backup system.

### 2.5.3.6 Video Cameras

Although the canopy provides a real viewing range of the worksite, cameras will be used to augment vision during certain tasks. Both the manipulator and grappler will have cameras to give a local frame of reference to the end effector. This will aid in grappling satellites, ORU changeout and installation, and inspection of the worksite from another view besides the canopy.

# 3.0 Crew Cabin

## 3.1 Introduction

MOOSE design included carrying a crew member to perform the maintenance tasks on a satellite. The cabin not only housed the equipment necessary to perform the task, but protected the crew member from the hostile environment of space. The target probability to complete the mission was 95%. However the probability for crew survival was 99.9%. Therefore the crew cabin was designed with many redundancies in critical systems. Also, the human factors were involved, attempting to make the crew member best able to complete the mission. Finally, the constraint of weight was traded off with the above; excess in niceties was avoided. The amenities provided in the cabin were needed to complete the mission and increase crew safety.

## 3.2 Ergonomic Requirements

### 3.2.1 Temperature Requirements

To accommodate a crew member, performing mostly light work, wearing normal light clothing, the cabin temperature should be around 21°C (70°F). As humidity, duration, and other factors vary, human tolerance to temperature is shown in figure 3.2.a.

Most of the thermal control will come from exchanging heat between the structure and space, through radiation transference. The shape, color, and texture of the external structure will determine the general thermal balance. A circulation system can be developed to exchange heat between the cabin and electronic areas with that of the skin of the vehicle.

### 3.2.2 Humidity Requirements

At a temperature of 21°C, the recommended relative humidity is 50%. Control is needed to take out excess water vapor, which is placed into the air by human wastes. Calculations can show that a human exhales more than one pound of water a day. However, perspiration is the major cause of moisture loss for a crew member. Figure 3.2.b below shows the total amount

of moisture loss as temperature varies. For a typical day, at about 21°C, a standard amount of rest, and while performing hard and light work, four to five pounds of water would need to be extracted from the air.[1]
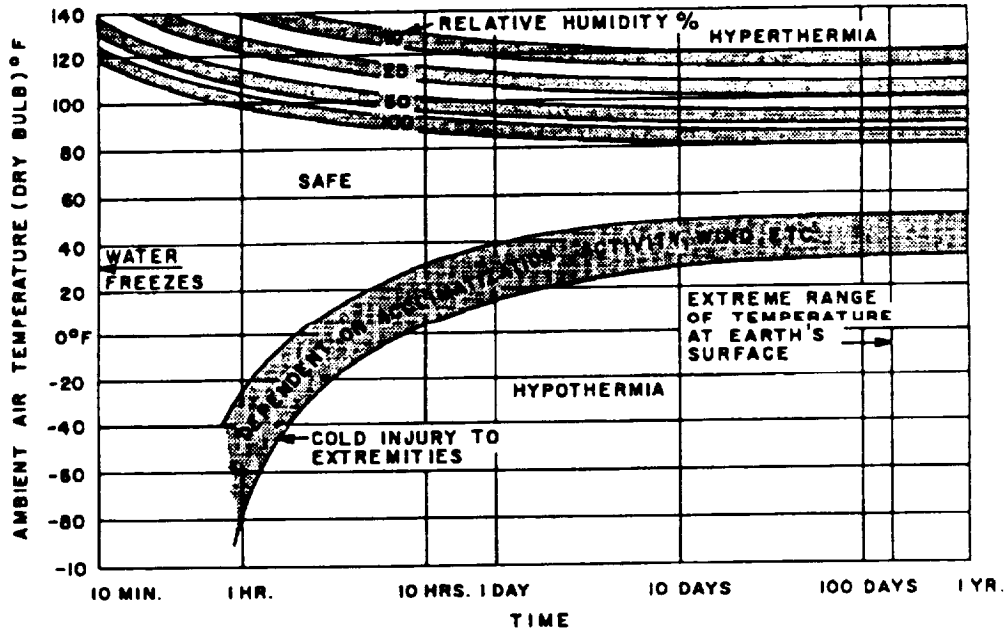
Figure 3.2.a  Human Temperature Exposure Limits[2]
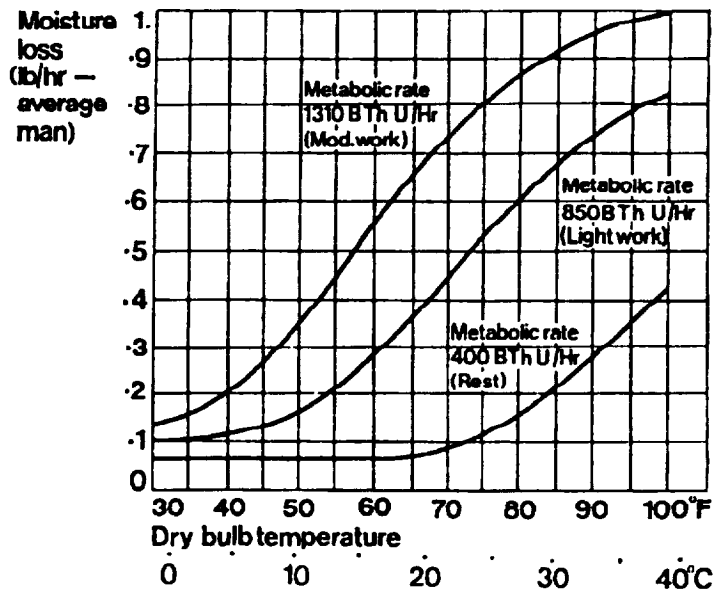
Figure 3.2.b Hourly Moisture Loss of a Crew Member[3]

## 3.2.3 Acceleration Requirements

In figure 3.2.c, a crew member's tolerance to acceleration is shown to vary with duration and body position. The acceleration, in g's, represents a conservative safe limit. Many astronauts can tolerate three times this value; however the graph is the lower limit of non-selected crew.

The body position relative to the acceleration force
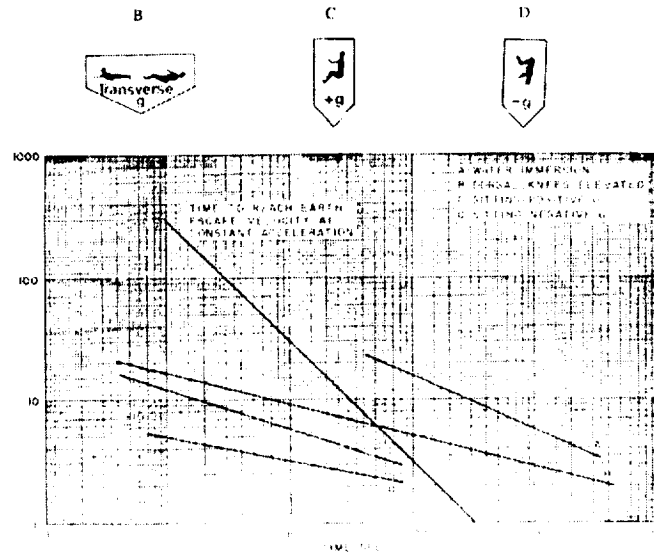


Figure 3.2.c  Safe Duration For Varying Accelerations[4]

## 3.2.4 Vibration Requirements

Below figure 3.2.d shows a crew member's sensitivity to vibration. This threshold vibration may occur with very little adverse effects to the crew. A tolerable limit may be established at ten times the amount given below; however fatigue and other psychological factors develop. Design should dictate below this threshold.
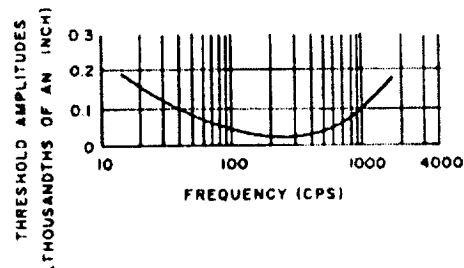


Figure 3.2.d  Vibration Limits[5]

## 3.2.5 Illumination Requirements

Although the total visual range is from $1.6 \times 10^{-12}$ W/cm$^2$ ($10^{-9}$ Lamberts) to 0.0256 W/cm$^2$ (16 Lamberts) fatigue will be induced if the illumination levels are not controlled. The following lighting conditions, shown in table 3.2.a, should be taken into account for the work area.

|  | Foot-candles |
|---|---|
| Emergency Lighting | 3 |
| Bulk Storage Areas | 5 |
| Passageways | 10 |
| Small Parts Areas | 20 |
| General Work Area | 30 |
| Light Reading Area | 30 |
| Study Reading Area | 50 |
| Drafting | 100 |
| Inspection | 200 |

**Table 3.2.a** Minimum Illumination Values[6]

These are minimum values; reduction in fatigue will occur with increase of illumination by a factor of 2 to 4. The immediate surrounding should not be brighter than the work area nor less than a tenth the illumination of the work area. The general surroundings should be between one tenth and ten times the illumination of the work area. The type of light is also important. White light is needed, Sunlight is the best, however halogen light is acceptable, and florescent should be avoided.

With the following information known, the standard cabin illumination should be around 100 foot candles; therefore being three times the general work area, but minimum light for more detailed work. The illumination should be able to reach levels of two or three hundred so that fine detailed work can be accomplished efficiently.

## 3.2.6 Audio and Sound Requirements

The sensitivity range of the human ear is $10^9$:1, but sound levels must be monitored. Exceedingly loud noises can cause temporary or permanent deafness. Alternately, if an area is too quiet, the crew member will be able to hear annoying incidental noises, such as those produced by blood circulation through the ear. In table 3.2.b, recommended background noise levels are given depending on the activity performed.

| Location | Level, dB |
|---|---|
| Sanctuaries | 30 |
| Sleeping area | 35 |
| Rest, reading | 40 |
| Restaurant | 45 |
| Sports | 45 |
| Detail work | 45 |
| Heavy work | 50 - 70 |

**Table 3.2.b** Recommended Background Noise[7]

## 3.2.7 Interior Volume

A very important dimension of this spacecraft is its interior free volume. Without a certain minimum amount of living space, there may be a negative psychological effect on the astronaut. This volume is very sensitive to mission duration for missions under 30 days, and an approximate relation is given by figure 3.2.e, which is a power fit to several data points. This fit has a correlation coefficient of .99997.



$$Y = 1.1604 \, X^{.4884}$$
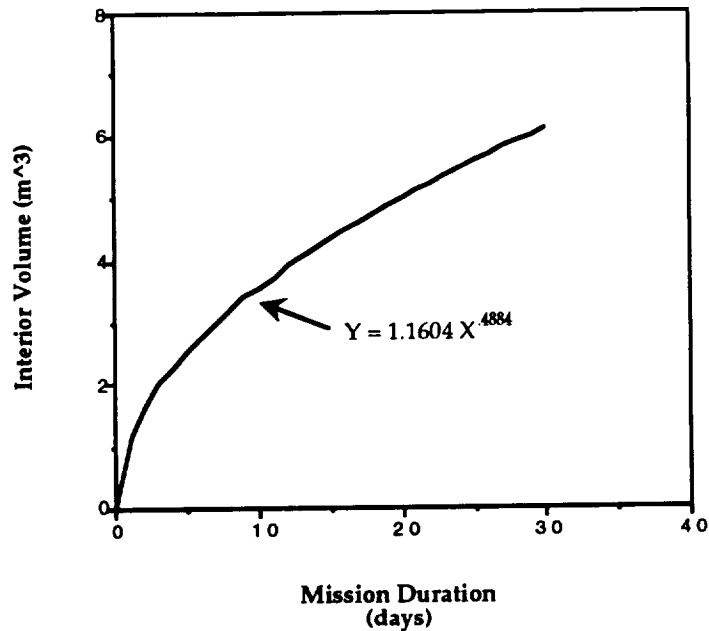
**Figure 3.2.e** Minimum Interior Volume

For a two to three day mission, the necessary interior volume is approximately two cubic meters. When crew and equipment volume is taken into account, this results in a crew cabin which is approximately 2.75 meters tall, 1.22 meters wide, and .91 meters deep.

### 3.2.8 Clothing

In order to best perform the mission, the astronaut should be dressed as comfortably as is possible. Currently, the anticipated attire consists of shorts, a T-shirt, and special shoes. These shoes will allow the astronaut to lock themselves into position on a height adjustable platform for easy access to the controls for manipulation of the satellite. These shoes are similar to those worn by competition bicycle racers, which click into place, and release with a simple twist of the foot. Another alternative considered was the possibility of simple Velcro foot restraints. Problems with this system included possible slippage, and the difficulty in tightening the restraints onto the foot.

### 3.2.9 Ergonomics

In order for the astronaut to perform their mission to the best of their abilities, their working environment must be safe, comfortable, and well organized. To allow the astronaut to adapt to the working environment as quickly as possible, a traditional vertical layout has been maintained in the crew cabin. Although not necessary in micro gravity, this layout is psychologically more familiar to the astronaut, and therefore it is easier for the astronaut to adapt.

## 3.3 Cabin Components

The rear of the cabin holds most of the components that will be used by the crew member. If the crew member faces away from the control station the figure 3.3.a would be seen.

Outlined below is each system including estimates on mass and dimensions and a description of that component.

### 3.3.1 Adjustable Foot Restraint Support

Mass:                             2 kg

Attached to the primary computer, this stand can be swung forward, up to 90 degrees, and propped up to support the crew member when at the control station. The stand has a triangle grid which will be used with the crew member's shoes to latch themselves to the grid. More discussion is included in 3.2.8.

**Cabin Layout**
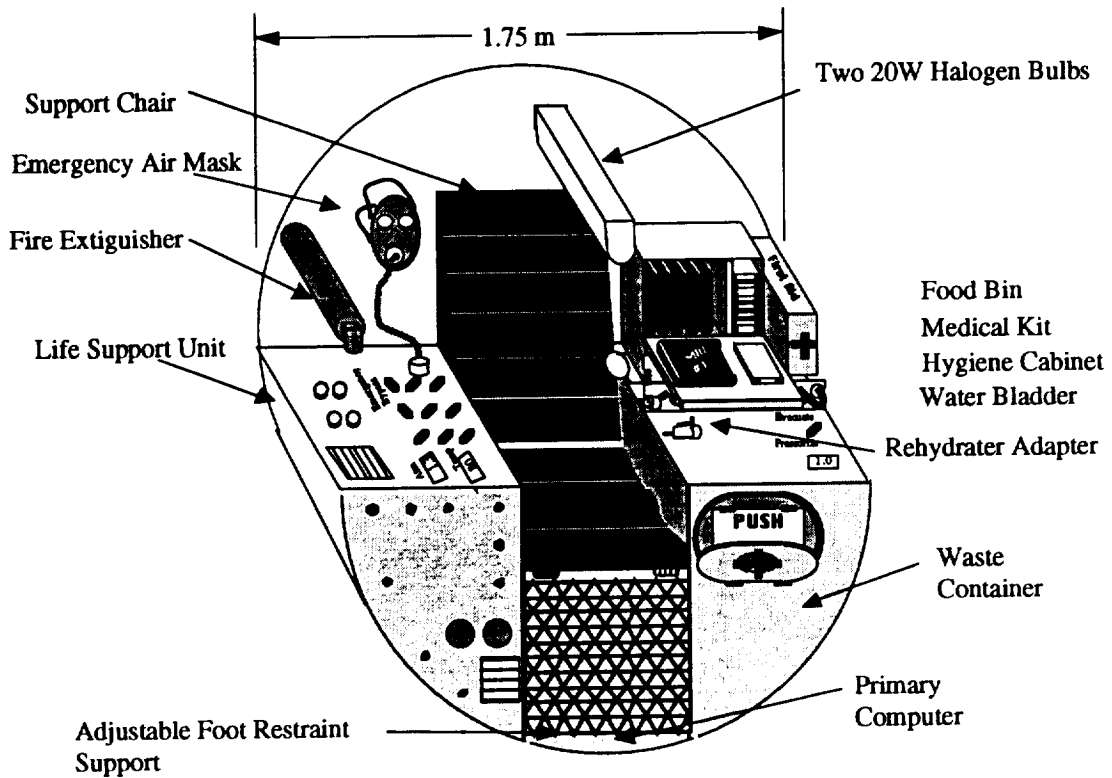


**Figure 3.3.a** Cabin Layout

## 3.3.2 Docking Ring

Dimensions:          0.75m dia. x 0.1m thick

       Mass:                 30 kg

This will be used by the crew member to enter and exit the vehicle. A standard airlock design will be able to mate to Space Station.

## 3.3.3 Emergency Air Mask



**Figure 3.3.b** Emergency Air Mask

Mass:                   2 kg

In the case where airborne contaminants have saturated the cabin atmosphere such that it is unsafe to breathe. Standard procedure will be to

use the air unit. This system is hooked into the cabin's life support; therefore the crew member can breath directly off life support. A hose leads from the full face mask to a connector, hooking the air unit into the life support system. The cabin could then evacuate the contaminants slowly while replenishing the atmosphere. This method will keep the cabin pressure constant. However the contaminants are never completely removed; much atmosphere is wasted in the attempt to saturate with good atmosphere. The crew member is able to breathe directly off the oxygen and nitrogen tanks through the air mask. More will be explained about this system in 3.4.7.

### 3.3.4 Extra Storage Mesh Bags

|  |  |
|---|---|
| Dimensions: | 0.5m x 0.5 m |
| Mass: | 1 kg |

These large capacity bags can be used to store personal items. For extended missions extra food and hygiene materials can be kept there.

### 3.3.5 Fire Extinguisher
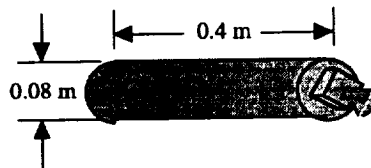


**Figure 3.3.c** Halon Fire Extinguisher

|  |  |
|---|---|
| Mass: | 2.5 kg |

A description of this extinguisher will be given later along in 3.6.3 with fire suppression procedures.

## 3.3.6 Food Storage Bin
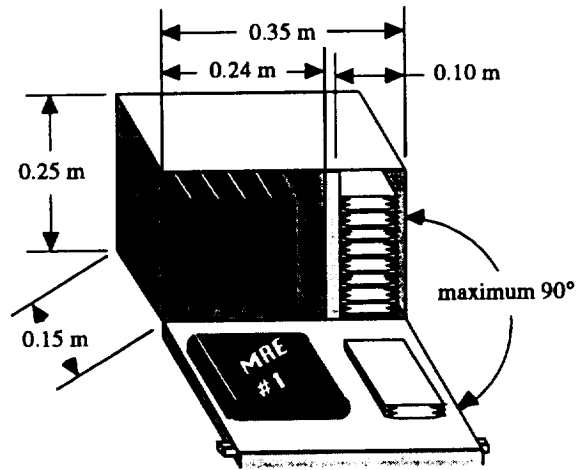


**Figure 3.3.d** Food Storage Bin

Mass:                                   5 kg (filled)

This bin holds food and beverage containers for a standard mission duration of two days. This consists six Food pouches and 20 beverage containers. The door has two latches keeping it closed during normal vehicle operation. The door swings down and can be used as a food preparation table. More details on the food system will be given in 3.7.

## 3.3.7 Hygiene Cabinet
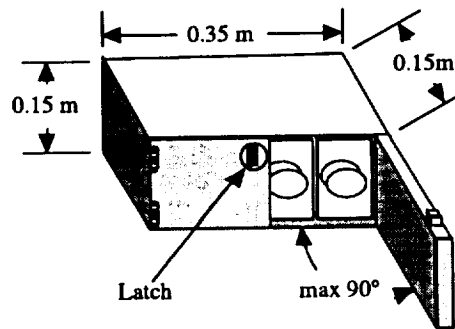


**Figure 3.3.e** Hygiene Cabinet

Mass:                                   2 kg

This cabinet holds the waste disposal bags for a 2 day mission. Personal hygiene articles are also provided; these include wetnaps, toothbrush, toothpaste, toilet paper, hair brush, a pocket mirror, and other amenities. Greater explanation is provided on the waste disposal bags in 3.8.1.

## 3.3.8 Life Support System
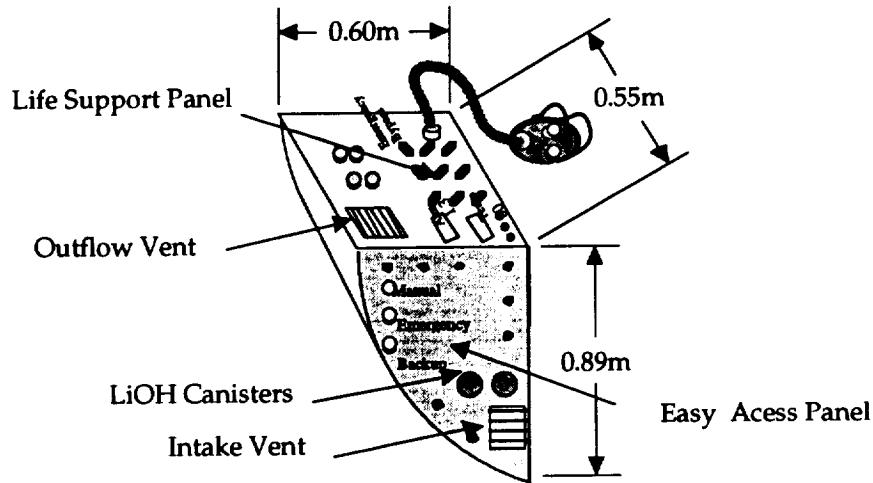


**Figure 3.3.f** Life Support Unit

Mass:                                    20 kg

The main unit provides the apparatus that controls the cabin temperature and humidity, scrubs out the $CO_2$, filters the water supply, and monitors any smoke particles indicating a fire hazard. Due to its importance, it can be accessed easily by the crew member. An in depth analysis on the whole life support system will be provided in 3.4.

## 3.3.9 Lighting System
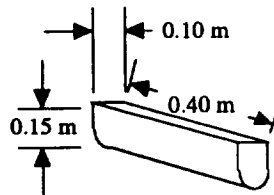


**Figure 3.3.g** Halogen Light

Mass:                                    2 kg

Two 20 Watt halogen lights will be used for cabin lighting. Halogen lights emanate a near white light illumination that is a need for the ergonomics. Halogen lights are also quite power efficient.

## 3.3.10 Medical Kit
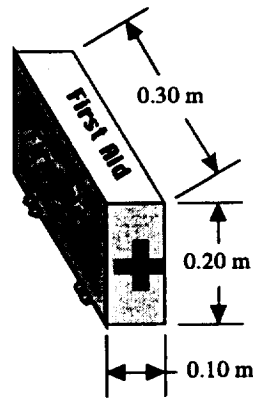


**Figure 3.3.h**  Medical Kit

Mass:                          1 kg

This is a combination of a first aid kit and medicine cabinet.  Contents include materials for treating burns (electrical and thermal), bleeding, and muscular/skeletal injuries (sprains, contusions, broken bones). Medications are provided including pain relievers, cold pills, anti-diuretic, infection control, etc.

## 3.3.11 Primary Computer

Dimensions:              0.55m x 0.55m x 0.55m
Mass:                        20 kg

The computer will be used to accept commands from the control station and implement them to the various avionics and propulsion systems.  Due to the fast pace technology advancement in computers, the exact type of computer is not given so that a computer can be chosen later that can fulfill its requirements with minimal cost.  Space has been allotted for radiation shielding.

## 3.3.12 Support Chair
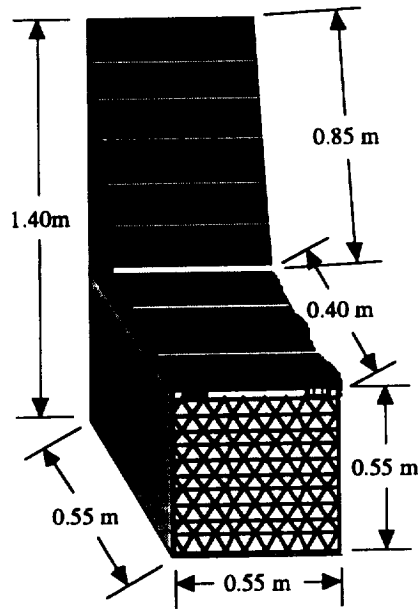


**Figure 3.3.i** Support Chair

Mass: 8 kg

A support chair is integrated to the back wall and primary computer. The crew member will use this during transfer orbit burns of the propulsion system. Elastic straps are also used to secure the crew member to the chair when they are sleeping. This will prevent the likelihood of injury during propulsive burns or sleeping.

## 3.3.13 Waste Container
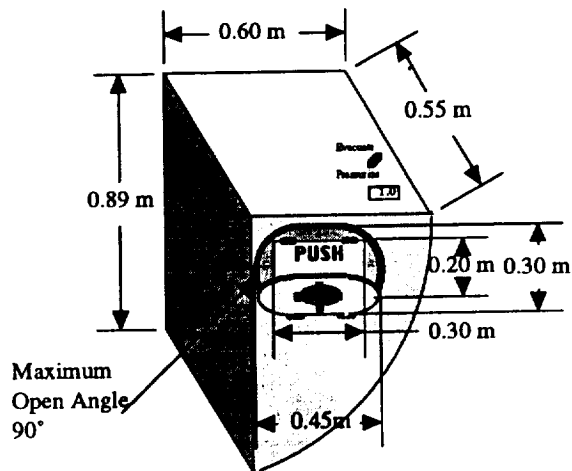


**Figure 3.3.j** Waste Container

Mass: 5 kg

This is the collection and storage of dry waste (i.e. paper products), wet waste (i.e. unused food, discarded beverage containers, wetnaps, etc.), and the waste disposal bags. The discussion on the waste container occurs later in 3.8.2.

### 3.3.14 Water Bladder
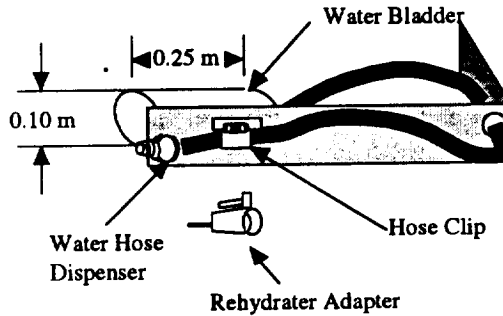


**Figure 3.3.k** Water Distribution Unit

Mass: 2 kg

This canister collects water produced by the fuel cells. After the water has been filtered in the life support unit, it will be placed here until the crew member uses it. Inside, a bladder expands until it reaches full capacity, at which time the life support unit will no longer divert water to the bladder. One half a gallon can be stored at a time. When the crew member uses the water dispenser, the bladder decreases volume so that the fluid is under continual pressure. The water is forced through a hose out the dispenser. A rehydrater adapter is included for food preparation. The hose is secured by a clip so that it will not float around.

## 3.4 Life Support Systems

The life support systems for MOOSE should provide a shirt sleeve working environment in the manned module for the astronaut to work in. The environment should provide the most optimum living and working conditions for the astronaut during a standard three day mission.

### 3.4.1 Atmospheric Requirements

Allowing the astronaut to wear a t-shirt and shorts, the atmosphere for the most optimal conditions should be as similar to the earth's atmosphere, at sea level, as possible. Providing an atmosphere of 79% nitrogen and 21% oxygen is possible and would provide the same atmosphere makeup as here on earth. The atmospheric pressure at sea level is one atmosphere (14.7 psi) and can be supplied for the astronaut.

However when supplying a pressure of one atmosphere in the manned module the thickness of the end plates on the manned module increases greatly to protect from end deflections. This becomes a limiting factor because the ultimate goal is to achieve our objectives with maximum mass efficiency. Therefore the pressure in the manned module should be reduced while still providing the most optimum environment for the astronaut.

In providing an environment for the astronaut to work in with unimpaired performance the lower the total pressure in the manned module the higher the percentage of oxygen necessary. However, the larger the percentage of oxygen in the atmosphere the greater the fire hazard, and the more a health hazard it becomes to the astronaut. An astronaut that is exposed to pure oxygen or atmospheres with large percentages of oxygen runs a great risk of oxygen toxicity, or anoxia. This becomes a trade off, one wants to keep the percentage of oxygen low to reduce the fire hazard.

In trying to keep the oxygen percentage and the total pressure low the most optimum pressure would be a total pressure of 0.41 atm (6 psi). With this pressure, the percentage of oxygen should be anywhere from 42% to 95% for unimpaired performance of the astronaut; 55% being the sea level equivalent. In trying to provide with the least percentage of oxygen possible while maintaining the most optimum conditions for the astronaut an atmospheric composition of 50% oxygen and 50% nitrogen will be provided. With a total pressure of 0.41 atm and a composition of 50% oxygen and 50% nitrogen the partial pressures of oxygen and nitrogen will be 0.205 atm. This composition will provide the astronaut with the most optimum working conditions while maintaining the lowest internal pressure possible to help reduce the mass of the end plates on the manned module.

### 3.4.2 Atmospheric Control

The manned module needs to be filled with 50% oxygen and 50% nitrogen both at partial pressures of 0.205 atm. The internal volume of the manned module is 16 cubic meters and to initially fill the module will require 2.2 kg of oxygen and 2.0 kg of nitrogen. An astronaut will use 0.9 kg of oxygen per crew member per day. For a three day mission one astronaut will use 2.7 kg of oxygen. In the event of a fire the manned module will have to evacuate the atmosphere and replenish it with new oxygen and nitrogen. This will require refilling the module with fresh oxygen and nitrogen increasing the amounts necessary. The amount of oxygen and nitrogen necessary will be 7.1 kg and 4.0 kg respectively.

### 3.4.3 Temperature and Humidity Control

The temperature and humidity in the manned module should be controlled to provide the optimum conditions for the astronaut to live and work in. The

safest conditions for the astronaut are a temperature from 18°C to 32°C with a humidity of 30% to 50% with an airflow rate of 9.0 m/min to 15 m/min. These conditions will keep the astronaut free from any health hazards such as hypothermia and hyperthermia. These are the safe living conditions for the astronaut to survive in but they are not the optimum working conditions. The ideal working environment for the astronaut, where they will have no impairment, is at a temperature from 21°C to 24°C with a humidity of around 40% and an airflow rate of about 9.5 m/min. This temperature and humidity are the conditions in which the astronaut will be most comfortable and able to concentrate the best on their work. It will provide the crew member with an environment in which their hands should not get cold, and an environment in which they should not sweat.

Maintaining an airflow rate of 9.5 m/min is crucial for odor control, noise control, and especially for carbon dioxide removal from the atmosphere. A slower airflow rate of 5 m/min would not circulate the air sufficiently to do a proper job of removing carbon dioxide quick enough to keep it below its maximum partial pressure. Odors would tend to linger in the module and the air would become stale at the lower airflow rate. The circulation of the air is important for the resupply of oxygen and an airflow rate this slow would not keep fresh oxygen in the module at all times.

On the other hand an airflow rate of over 15 m/min. would not be desired for several reasons. Supplying an airflow rate that fast would cause unwanted noise for the astronaut. The airflow would create a disturbing breezy environment. Therefore a sufficient airflow rate in between these two values has been chosen, 9.5 m/min. This rate will sufficiently recirculate the air for removal of odors and carbon dioxide while not disturbing the astronaut with undesired noise and excess breeze within the module.

### 3.4.4 Carbon Dioxide

The crew will produce 1.02 kg of carbon dioxide per astronaut per day. For the astronaut to be free and safe from carbon dioxide poisoning the maximum allowable percentage of carbon dioxide in the atmosphere should be less than 0.5%. To much carbon dioxide in the atmosphere becomes dangerous to the astronaut and can cause carbon dioxide narcosis, which causes impairment or even death to the astronaut. Allowing carbon dioxide concentrations above 0.5% of the atmosphere may also alter the astronauts physical response to radiation. Understanding these requirements shows that the carbon dioxide removal system must remove 1.02 kg of carbon dioxide per crew member per day keeping concentrations below a maximum of 0.5% (0.02 atm) of the atmosphere. The most efficient method of removing the carbon dioxide for the standard three day mission will be through the use of lithium hydroxide canisters with activated carbon inside. A resulting trade study that shows why lithium hydroxide should be used can be found in appendix A3.1. The

lithium hydroxide will remove the carbon dioxide and the activated carbon will remove other trace contaminants found in the air.

Each canister will contain enough supply of LiOH to remove $CO_2$ for 1.5 days. In each canister will also be added activated carbon to filter out impurities in the air such as odors and other chemicals found in the atmosphere. Each canister will carry 13 kg of LiOH and 0.09 kg of activated carbon. The amount of activated carbon necessary to filter out impurities is 0.06 kg per crew member per day. The activated carbon will be used to remove odors and numerous chemical compounds found in the atmosphere such as acetic acid, methanol, ammonia, chlorine, carbon monoxide, and many more.

### 3.4.5 Life Support Panel
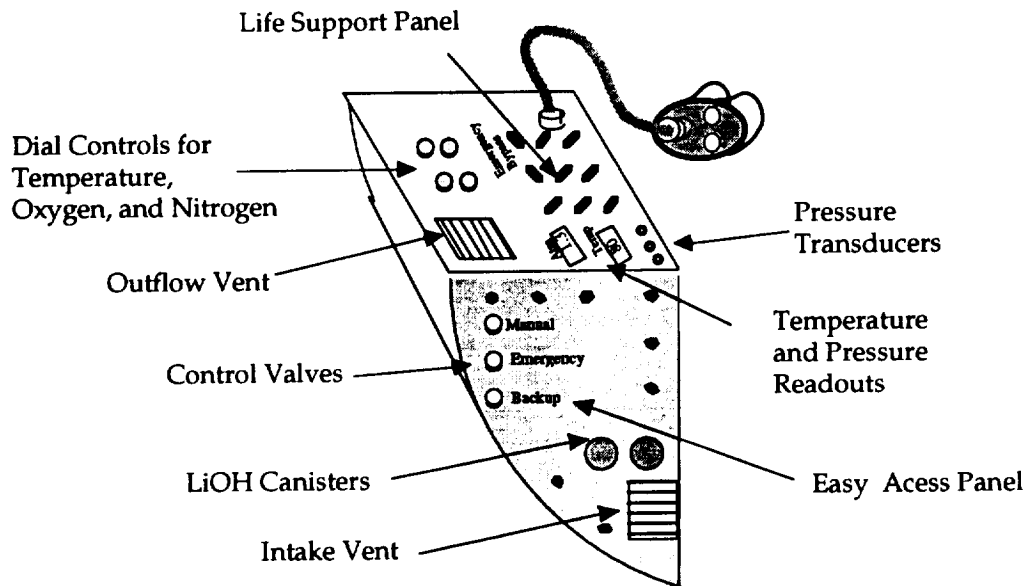


**Figure 3.4.a** Life Support Unit

The life support panel above is housed in the manned module on the atmospheric revitalization system (ARS) and the oxygen and nitrogen supply system. The air from the cabin will be drawn into the life support unit through the intake vent and will be released back into the module through the outflow vent. On this panel will be a temperature sensor that will show the astronaut the cabin temperature. A temperature dial control will be provided so the astronaut can control the temperature inside the cabin within one degree Celsius. The lithium hydroxide canisters, which will be used for the removal of carbon dioxide will be housed in the unit and can be changed when necessary. Transducers will be on the panel to tell the astronaut the partial pressure of the oxygen and nitrogen and the total pressure in the manned module. The oxygen control valve can be used by the astronaut if the

oxygen partial pressure falls below a certain pressure. This valve will release oxygen into the cabin until the desired pressure is maintained.

### 3.4.6 Atmospheric Revitalization System

The atmospheric revitalization System or ARS, in figure 3.4.b, will be used for circulation of the air in the manned module, temperature and humidity control, and carbon dioxide removal. The air can be drawn into the system by two intake fans. Only one fan will be used. The second fan will automatically switch on if the first fan fails. The fan will draw the air into the system and circulate the air at the required rate of 9.5 m/min.
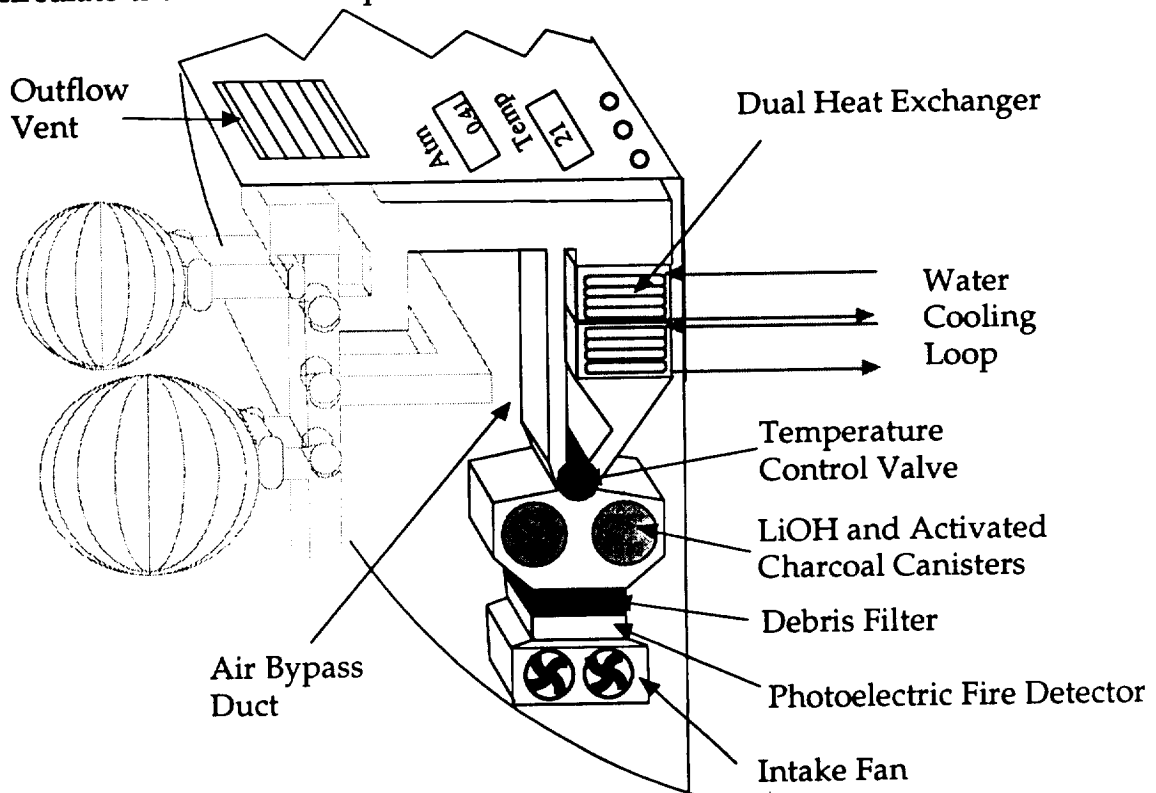


**Figure 3.4.b** Atmospheric Revitalization System

The air will then pass through a debris filter where dust and fine particles will be removed. Once past the debris filter the air will pass through the LiOH canisters for the removal of carbon dioxide and other trace contaminants. The ARS system holds two LiOH canisters which last for 32 hours. The canisters can be removed and replaced by the astronaut when necessary. The excess canister will be carried inside the manned module attached to the life support panel. The air will then come to a temperature control valve.

The temperature control valve will be controlled by the temperature dial on the exterior of the life support panel and the temperature sensor. If the temperature in the cabin is the desired temperature, the control valve will

3 - 17

close the airflow and force the air into the bypass duct where it will go back into the cabin. If the temperature in the cabin is not the desired temperature, the control valve will remain open allowing the airflow to enter into the heat exchanger. In the case of the control valve failing, the airflow will automatically go into the heat exchanger where the manual temperature control dial will control the temperature of the airflow in the heat exchanger.

The heat exchanger will use a water cooling loop to cool the air below the dew point to remove the moisture from the air. The moisture will then be collected and added into the water cooling loop. If the cabin temperature is too warm the airflow will remain cool and be returned to the cabin. If the cabin temperature is too cool the heat exchanger will heat the air to the desired temperature as determined by the astronaut with the temperature control dial. The heater in the heat exchanger will consist of two separate heaters that will both operate together at the same time to heat the air. If one of the heaters should fail, the other would be able to maintain the necessary emergency temperature within the cabin to keep the astronaut healthy until return to the space station.

In the event of an emergency such as a power failure, the system can run on the one fan necessary and only one heater conserving on the power necessary.

### 3.4.7 Oxygen and Nitrogen Supply

The oxygen and nitrogen supply system in figure 3.4.c, will take the oxygen and nitrogen being sent from their storage tanks and regulate their pressure. Then the proper amount is released into the manned module. The oxygen and nitrogen will flow into the life support panel from the exterior of the manned module. Both gases will be entering the panel at high pressures. The cabin pressure regulator will take the gases and reduce their pressure to a total pressure of 0.41 atm and partial pressures of 0.205 atm.

A solenoid valve will be used to help regulate the gas flow into the manned module. If the nitrogen pressure is too low the solenoid valve will close allowing nitrogen into the cabin until the desired pressure is reestablished. Otherwise, the solenoid valve will remain open allowing oxygen into the cabin as necessary. If the solenoid valve should fail the astronaut has manual control over the release of the oxygen in the cabin to maintain the necessary supply of oxygen. This manual control valve releases oxygen directly into the cabin from storage after it has been reduced in pressure. If the pressure inside the cabin gets too high, two pressure relief valves will be used to vent out the excess pressure to space. These pressure relief valves will also be used in the event of evacuating the atmosphere from the cabin.

The oxygen necessary for a three day mission with one astronaut will be 7.1 kg at a pressure of 0.205 atm. A major concern for this project is mass and

volume. To save on redundancy of oxygen storage tanks, the oxygen will be stored in the cryogenic storage tanks being used for the fuel cells. This will save on both space and the excess mass of adding more tanks.
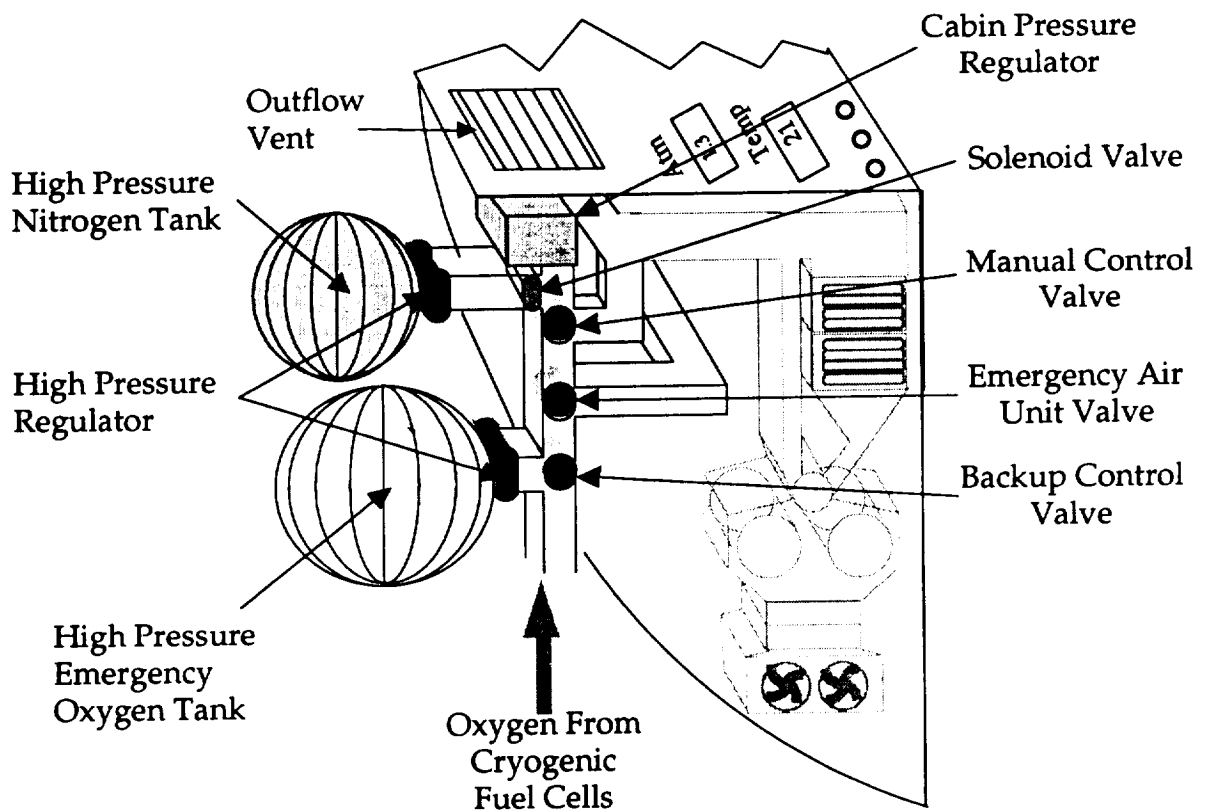


**Figure 3.4.c** Oxygen and Nitrogen Supply System

The oxygen will be stored cryogenically and pass through a high pressure regulator where the pressure will be reduced down to 4 atm. The oxygen will then be released into the oxygen and nitrogen supply system where it will be regulated and reduced in pressure even further before being released into the cabin. Monitors and alarms will be provided so that the astronaut can tell when the oxygen partial pressure is too low. Upon hearing these alarms, the astronaut can open the manual control valve to restore the oxygen pressure in the manned module.

Upon the failure of the cryogenic storage tanks used by the fuels cells, the spacecraft would have to return to Space Station Freedom. If the cryogenic storage tanks failed, the oxygen supply would be cutoff. Therefore an emergency oxygen storage tank is necessary for the safe return of the astronaut to the space station. In the event of failure it would take the spacecraft a maximum of twelve hours to return to the space station, so an oxygen supply for those twelve hours would be necessary. This would be done by a small high pressure storage tank that would contain 1 kg of oxygen

for emergency purposes. This tank would be similar to the nitrogen tank and would only weigh about 1 kg. The release of this oxygen into the manned module would be done by a backup control valve on the life support panel.

The mass of nitrogen needed is so small that the storage of the nitrogen by cryogenics would be inefficient; therefore the most desirable type of storage would be high pressure. A tank weighing only 5 kg will be used to store the 5 kg of nitrogen necessary. The tank will store the nitrogen at a pressure of 81 atm and needs a volume of only 0.1 cubic meters. The nitrogen will be released into the oxygen and nitrogen supply system where the pressure will be reduced down to 0.205 atm before being released into the module. The tank used for the nitrogen storage will be made of a titanium liner with a kevlar/epoxy composite over wrap on the outside. This accounts for the tanks lightweight and high pressure capabilities. The total weight of this system is approximately 10 kg. Two pressure lines would come out of the tank and go into the supply system. This redundancy is used when fone of the lines fail. The other will take over and supply the cabin with the necessary nitrogen.

The life support system will supply the astronaut with the most optimum working conditions that can be provided. The system has backup systems and components to keep the astronaut safe and give them the ability to return to the space station unharmed during most failure modes. Scenarios would have to be designed to determine what failure would result in the abortion of the mission and immediate return to the space station. However, the emergency systems will allow for the astronaut to be able to return to the space station.

## 3.5 Radiation Shielding

Appendix A3.2 discusses many aspects of the radiation environment and how it affects the crew member. When considering radiation shielding, several factors must be included to estimate the shieldings appropriate thickness. Extra aluminum thickness for capsule walls means more weight and more cost to launch a MOOSE mission. Not enough thickness on a capsule traveling to geostationary orbit could prove fatal, or at least raise the risk of an astronaut contracting latent cancers.

Radiation in Earth orbits come from three areas; galactic cosmic radiation or cosmic rays, trapped particle radiation from the Van Allen belts, and radiation from Solar Particle Events (SPEs). The Van Allen belts stretch to about 10,000 kilometers for largest doses, but do reach 75,000 kilometers at their greatest extent. Cosmic rays make up approximately 5-10% of effective radiation doses at all altitudes. SPEs are the most dangerous element of the space environment, with anomalously large SPEs delivering on the order of 1500 rem to an unprotected astronaut. SPEs are usually the limiting factor in designing spacecraft shielding.

The most important factor in determining proper shielding is the radiation environment, depending on where the mission will be heading. For Low Earth Orbit (LEO), radiation will be a minor factor, with most particles shielded by the geomagnetic field. The majority of the radiation will come from the trapped protons in the Van Allen belts and galactic cosmic rays. Little radiation will be encountered from the majority of SPEs.

For a polar orbit mission, the dose from trapped particles will be small, considering the Van Allen belts do not extend in any great concentrations in such orbits. SPEs, however will be more of a factor here, with an astronaut incurring significant doses of radiation if not properly shielded.

For geostationary orbit (GEO), radiation doses will be by far the highest. For a two day mission, doses received from the Van Allen belts in traveling to and from GEO will be significant, around 4-8 rem. Additionally, the potential for massive radiation doses from SPEs will be high if proper precautions are not taken.

## 3.5.1 Radiation Limits

Radiation dose for an astronaut should not exceed certain career radiation limits set by NASA, according to the equations:

Male Max Career= 200 rem + 7.5 rem(age of astronaut - 30)
Female Max Car = 200 rem + 7.5 rem(age of astronaut - 38)

Additionally, dose should not exceed 25 rem for one month or 50 rem for one year.

Using these figures, the MOOSE astronaut should not be exposed to greater than 10 rem for one mission, or 75 rem emergency dose. These limits help keep the astronaut from undergoing too much radiation exposure and having to be either sent home after one mission or having to wait months or years in between missions. It would be much more cost effective to have one or two experienced astronauts manning the MOOSE capsule instead of many new astronauts that must continuously be trained to perform a MOOSE mission successfully.

## 3.5.2 Radiation Protection

Considering these dose limits, 2.5 grams per centimeter squared shielding is required to effectively keep an astronaut safe. This is approximately equivalent to 1.0 centimeter thick aluminum walls all around the capsule. In case of emergency, such as an anomalously large SPE, other precautions should be taken. These include orienting the aerobrake towards the largest particle concentration during an SPE. Also, solar activity should be studied at the time of the mission to determine the likelihood of a large SPE occurring.

The most dangerous solar flares can be predicted between 10-20 hours in advance. Therefore, to avoid overexposure of the astronaut to radiation, the mission should be aborted at the first sighting of a flare. The MOOSE capsule will have ten hours to either return to LEO, and thus reduce the radiation incurred by 50%, or if possible, return directly to the Freedom space station and allow the astronaut to enter the radiation storm shelter at the station. However, in the worst case scenario that a SPE strikes without warning, the astronaut will have sufficient shielding to return to Freedom with minimum immediate physical damage. No serious disability will prevent the astronaut from returning to medical attention, but minor radiation sickness may be contracted.

## 3.6 Fire Suppression

The protocol that must be followed to assure proper levels of safety aboard MOOSE consists of three steps; prevention, detection of fires, and extinguishment.

Prevention deals mainly with minimizing the amount of flammables allowed in the capsule. Fire resistant clothing, normal Earth-like atmosphere instead of 100% oxygen, and flame retardant fabric on the support chair solve most of the fire problems aboard the capsule.

Fire detection should occur smoothly and promptly to minimize the damage to the equipment in the capsule and the astronaut. The most effective means of detecting a fire aboard the MOOSE is using the astronaut's own senses. In the NASA space shuttle missions, three fires have occurred, and all have been detected and dealt with by the astronauts before the smoke detectors in the ship were tripped. In the MOOSE, human alertness will be even more prominent because on such a small capsule, most open flames will be instantly obvious. However, for less visible fires, such as smoldering fires that cannot be seen by the human eye, a smoke detector is necessary.

Extinguishment includes extreme measures to control fires and save the life of the astronaut. Usually, extinguishers involve either a fire suppression system like sprinklers, or manual means, such as a portable fire extinguisher. For the MOOSE, the cheaper and more direct tool, the portable fire extinguisher is more appropriate, as the capsule is not large enough to support a sprinkler system.

### 3.6.1 Photoelectric Smoke Detector

The fire detection mechanism chosen for the MOOSE will be a photoelectric sensor, continuously using 5 watts of power and measuring 4 cm length by 4 cm height by 2 cm in depth. The device will be attached to the

air revitalization system  directly after the intake fan in the loop. This device uses two light sources aimed at two photo receivers attached perpendicular to each other. If smoke particles are present in the air, some of the light will be obscured, and the sensors directly across from the light sources will receive less light. Smoke particles will also interfere with light rays to an extent, hence the sensors perpendicular to the sources will receive some light scattering of a different frequency. The device responds to a 1.6% per meter optical obstruction of the sensors and a $5.3 \times 10^{10}$ particle/$m^3$ smoke concentration detection of light scattering. This device was chosen because it is highly effective in detecting smoldering fires, it is attachable to the air revitalization system and therefore relatively cheap and simple to build, and it is unresponsive to temperature and humidity changes, which may fluctuate greatly in a small capsule like the MOOSE. Therefore, false alarms due to these changes will be avoided.  See appendix A.3 for a trade study on detectors for the MOOSE.

### 3.6.2  Fire Extinguisher

The portable smoke detector chosen for the MOOSE will  measure 40 cm length by 8 cm diameter and weigh 2.25 kg, 1.13kg of which will be the actual extinguishing chemical. The extinguisher will contain halon 1301 (bromotrifluoromethane) and create a local concentration of 7% halon in less than 1 second, effectively extinguishing the fire immediately. In the event of use, the astronaut will breathe through the emergency oxygen mask in place on the control panel. Halon 1301 may be breathed at 7% concentration for five minutes without ill health effects, more than enough time for the astronaut to affix the oxygen mask. Meanwhile, the capsule atmosphere will be bled into space and replaced with fresh oxygen and nitrogen from reserve supplies to avoid contaminating the air revitalization system. See appendix A.4 for a trade study on extinguishers for the MOOSE.

## 3.7  Food System

The food system for this mission must be easy to prepare, provide all of the necessary nutrients, and it must have as small a mass possible.  In addition, the meals should be palatable to the astronaut, and should allow for a variety of menu selections to avoid monotony and account for variation of tastes among astronauts.  Several systems were considered, including the current system in use on the space shuttle, and a decision was made based on several key factors.

### 3.7.1  Nutritional Requirements

During extended duration in space, the human body tends to burn more calories per day than during a similar day on Earth.  This is primarily due to the fact that more energy is necessary to complete tasks in an unfamiliar

environment, such as micro gravity. The food system for a mission of this type must provide this extra energy, as well as maintain the nutrient balance of the body. In order to do this, the food system must supply each of the following on a daily basis.

| | | | |
|---|---|---|---|
| Calories: | 2800 | Vitamin A: | 5000 IU |
| Protein: | 56 g | Vitamin D: | 400 IU |
| Calcium: | 800 g | Vitamin E: | 15 IU |
| Phosphorus: | 800 mg | Ascorbic Acid: | 45 mg |
| Sodium: | 150 mEq | Niacin: | 18 mg |
| Potassium: | 70 mEq | Riboflavin: | 1.6 mg |
| Iron: | 18 mg | Thiamin: | 1.4 mg |
| Magnesium: | 350 mg | Vitamin $B_6$: | 2.0 mg |
| Zinc: | 15 mg | Vitamin $B_{12}$: | 3.0 μg |

**Table 3.7.a** Daily Nutrient Requirements

## 3.7.2 MRE

The system of choice is a modified version of the MRE (Meal, Ready-To-Eat), currently in use by the United States Armed Forces. These meals will provide approximately 1500 calories per meal, allowing rationing to two meals per day if necessary.

### 3.7.3 Packaging, Mass, and Cost Requirements

The major modification to the MRE will be the inclusion of beverage powder in rehdratable pouches, instead of the current plastic pouch. This will allow the astronaut to rehydrate the beverage without transferring the powder to a different container. Another option considered was the food system currently in use by the Space Shuttle Program. The major problems with this system were mass and power consumption. The preparation equipment needed for the galley of the space shuttle was considered much too massive, and the power consumption was deemed excessive for this mission duration of two days. Based on these factors, the MRE system was a clear choice. This system requires no preparation, with the exception of beverage rehydration. Therefore, the entire food system for a two day mission can be kept to a fraction of the mass of the current shuttle food system.

|         | Individual MRE          | Total Food System       |
|---------|-------------------------|-------------------------|
| Mass:   | 1.0 kg (including water) | 8.0kg(including water)  |
| Length: | 0.05 meters             | 0.33 meters             |
| Height: | 0.23 meters             | 0.23 meters             |
| Width:  | 0.13 meters             | 0.13 meters             |

**Table 3.7.b** Food System Dimensions

The total food system dimensions include extra beverage packages for between meals, and the mass figure includes water for these beverages. The total food packaging can be placed in the food bin provided in the cabin. MREs can be easily stored for long duration. This may be necessary since the time between MOOSE repair missions is unpredictable and can be very long. The cost of the MRE food system is also one of its major benefits. Since it is off-the-shelf technology, the cost of providing this system to the proposed mission is negligible.

### 3.7.4 Food Preparation Requirements

As mentioned before, the MRE food system requires no preparation, with the exception of rehydration for the beverages. To accomplish this, a small hose can be unclipped from the wall. A rehydration needle assembly is attached to the end of the hose with a quick disconnect. This assembly consists of a stainless steel needle surrounded by a protective sheath. This needle is inserted into the pouch through a membrane on the container. The water is injected until the pouch is properly filled. The needle is then removed, the membrane reseals, and the beverage can then be mixed by kneading the package. The empty beverage container may then be reused for drinking water at a later time. In addition to this, the possibility of creating an adapter for the end of the hose to allow the astronaut to consume water directly, without the need for a used pouch, should be explored.

## 3.8 Hygiene and Waste Management System

A general summary of different waste management procedures is given in appendix A.5. The complexity of the hygiene and waste management system is a function of mission duration. Below is a table of recommended services for different mission lengths.

| Mission Duration | Waste Management | Hygiene Services |
|---|---|---|
| 1 - 2   days | Simple containment system | Minimal Clean Up |
| 3 - 10   days | Waste management system<br>Toilet facilities | Sponge Bath<br>Personal Hygiene Bubble |
| 10 - 31 days | Elaborate treatment<br>and Storage | Body Shower |

**Table 3.8.a** Hygiene and Waste Management Recommendations

Wet-naps are provided for general clean-up. They can be used for wiping down the control station, cleaning small articles, and for partial human hygiene. Articles for grooming and dental hygiene are provided and are discussed in 3.3.7.

### 3.8.1  Waste Disposal Bags

The waste management system consists of chemically treated disposable containers. Different bags for collection of urine and fecal/emesis matter will be included in the hygiene cabinet. A urine container, that can be used by either gender, holds a solid substance. This substance absorbs and chemically treats the urine. The container can then be sealed and discarded into the waste container. For solid waste, a bag is provided. After usage, a separate chemical bag is opened and thrown into the solid waste bag. The bag is then sealed, its contents mix thoroughly, and discarded into the waste container. Leftover food and beverage containers may be dealt with using the solid waste bags. However general paper waste, such as the food packaging, can be discarded directly into the waste container.

### 3.8.2  Waste Container

The waste container holds the collection of waste. The inside to this container is separated from the cabin's atmosphere. A hatch, to the container, will be sealed, so that no fumes from the container propagate into the cabin while closed. To discard additional waste into the waste container, first the hatch is opened. Another door, which has a weak torsion spring, has to be pushed open to deposit waste. This is very similar to a conventional trash can; the push door will mechanically close so that waste can not float into the cabin. The crew member must hold the hatch door to counter the force required to open the push door. Otherwise the spring door will merely push the crew member away. The contents in the container can be exposed to the vacuum of space through an outer airlock. When the hatch door is closed, the airlock can be opened using the control panel on the waste container. The inside is depressurized and exposed to the vacuum of space. This would be

performed before the crew member goes to sleep. This system has two means of waste stabilization, chemical treatment and desiccation. The evacuation of the container is not a necessity, the chemical treatment should suffice; however it can be used as a back-up or extra system if needed.

## 3.9 Structural Analysis of Crew Cabin

### 3.9.1 Crew Cabin Design Overview

The primary goal in designing the crew cabin is to develop a lightweight structure that could perform without failure under all possible loading conditions. Other factors that need to be considered are the cabin volume for astronaut comfort and the skin thickness for radiation protection. The following criteria must be met by any crew cabin design to be incorporated into moose.

1. Ability to withstand g loadings of 3g axial and 2g lateral
2. Ability to withstand an internal pressure of $4.33 \times 10^5$ Pa
3. Allow only 10 rem maximum radiation exposure per mission
4. Internal volume of 2.75 cubic meters

### 3.9.2 Materials Selection

Aluminum 7075 will be used almost exclusively for crew cabin construction. Initial studies involved the use of a thin skinned aluminum vessel reinforced with graphite epoxy tubes. Due to the strict radiation limitation (10 rem maximum/mission) the skin designed to be 1.0 cm thick aluminum. The debris interface and docking interface rings will also be aluminum. Aluminum was also chosen because of its high strength to weight ratio and low cost of around $8 per kg. Titanium was considered for use in high stress areas where aluminum would fail, but due to the thickness of the cabin, stresses were low enough to use aluminum.

### 3.9.3 Cabin Design History

Initial cabin design trade studies were done on two different structural designs. The first was a simple monocoque cylinder design with only the skin carrying load. The second design was a semi-monocoque stringer design, where the skin carried only shear loads, and anywhere from 4 to 12 evenly circumferentially arranged stringers carried the loads. With initial cabin dimensions at 2 m radius and 4 m height, the stringer design with 12 stringers proved to be more weight efficient, with a weight savings of almost 50%. As the cabin got smaller and thus lighter (~300 kg) the stringer design became less efficient with weight savings on the order of 1%. The final decision was made to build a monocoque cylinder with a 1.75 m diameter and 1.3 m height

crew cabin    man/grap interface
docking interface    1 2500
viewport
1 3000    0.9400    0.3000
2.0000    helium tank    hydrazene
1 700
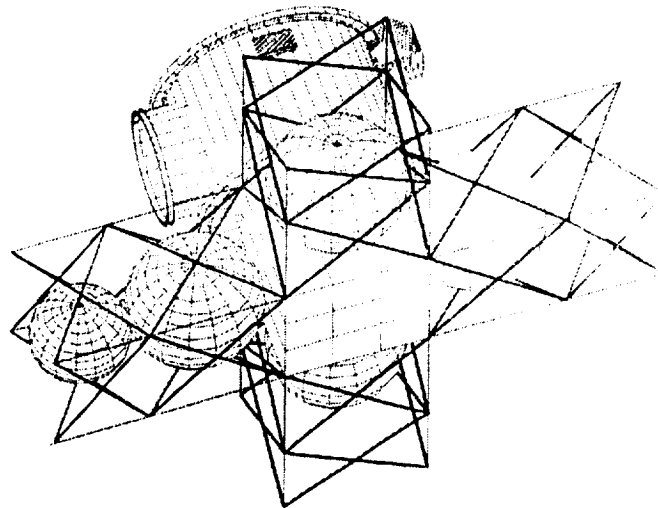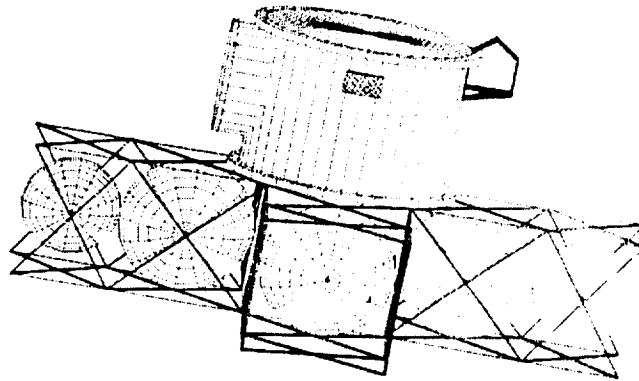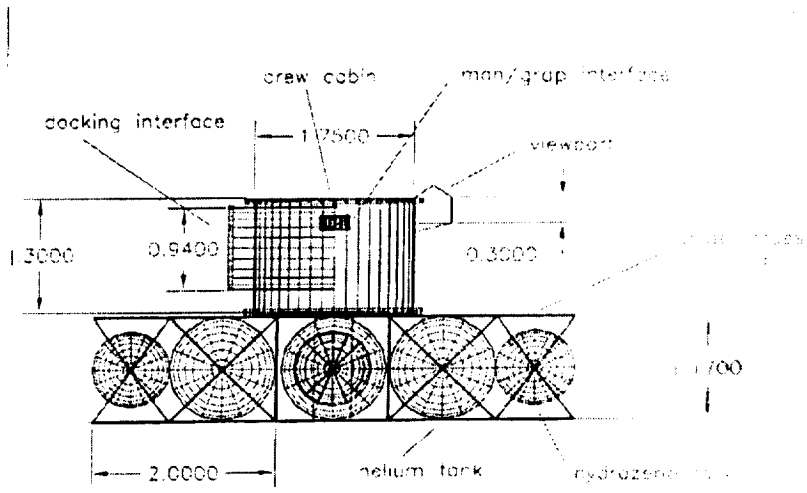
Figure 3.9.a  Cabin Structure

after an analysis showed it had met all load factors without any stringers added for stiffening.

### 3.9.4 Analysis Procedure

To get rough estimates of the stresses experienced by the vehicle during heavy g loading an analysis was performed on the cabin assuming the following:

1. Pure axial loading ( no eccentric loadings )
2. Bending moment about cabin neutral axis
3. Thin walled cylinder assumption ( radius/thickness > 50 )
4. Cylinder is symmetric about longitudinal and radial axes
5. Factor of safety of 1.5 used in all calculations

The axial loads were computed by multiplying the mass of all of the spacecraft below the bottom of the cabin including fuel (~10,000 kg) by a 3g axial load. The compressive load calculated was $4.41 \times 10^5$ N. A bending moment of 3188 N-m was also added acting at the junction of the cabin and the aerobrake spine truss, as a result of the 2.0 g lateral load  Using the general stress equation (see appendix A3.6) the maximum tensile stress was $8.2 \times 10^6$ Pa. This is much lower than the yield stress of $448 \times 10^6$ Pa for aluminum 7075. Using the equations for skin buckling (see appendix A3.6) the critical load was $1.6 \times 10^6$ N. This was much higher than the modeled load of $4.41 \times 10^5$ N.

### 3.9.4.1 Endplate Calculations

At CDR a question was raised concerning the validity of flat endplates on the cylinder. Fears were that the stresses at the junction of the plates and the cabin walls would be very high. By modeling the end plates as flat circular plates fixed at the edges an analysis was performed. By using a formula in Roark's the maximum stress on the plate was calculated to be $1.64 \times 10^8$ Pa. The stresses were the highest at the edges just as they were suspected to be. This value is well below the yield stress of $448 \times 10^6$ Pa for aluminum 7075. The main problem with the flat endplate design was the high deflections at the center of each plate. Two solutions were considered. One solution would be to increase the stiffness of the whole plate. To achieve an acceptable deflection the thickness would have to be raised to 1.75 cm per end plate. This would mean an increase of 50 kg per plate. Due to the strict mass budget another solution was investigated. Using the principle of super positioning a beam with square cross-section of 2.5 cm with a thickness of 2.5 mm was designed to satisfy the stiffness requirements of the deflecting plate. Two beams crossing at the center of the plate with length 1.75 m were used on each end of the cabin. The total mass added was only 8.0 kg.

### 3.9.4.2 Stress Concentrations Around Docking Ring

Another concern was the possibility of areas of high stress concentration near the docking ring. Knowing that stress concentrations can often reach 3 times the normal stress around holes, an analysis was performed using a set of equations from Roark's. The cabin was modeled as a thin walled cylinder with a hole at midpoint along the length. At the area of highest stress concentration the stress was only $1.74 \times 10^8$ Pa, well below the yield stress of Aluminum 7075. This stress took into account both axial loads and bending moments.

### 3.9.5 Cabin Interfaces

To connect with other cabin hardware the cabin has three interfaces. One of these is a docking ring. The docking ring has a diameter of 0.75 m and is designed for compatibility with the PDA docking modules at SSF. The second interfaces are the debris shield connecting rings. These are rings with a I-beam cross-section with a depth of 10 cm and a web with of 10 cm. They are designed to be welded to the cabin unit before shuttle places MOOSE in orbit. Finally the cabin is designed to interface with an avionics box at the base of the cabin. The avionics box is an aluminum 1.24 m square cross-section with a height of 1.17 m. The skin thickness was sized using a flat plate analysis for the bottom plate for Roark's. With a load of 100 kg assumed uniformly placed on the plate, an equation for plate stress and deflection determined the thickness to be 6.5 mm. The avionics box is mounted to the cabin with four pin connections at the corners of the box which line up with the edges of the cabin base.

### 3.9.6 Structural Masses

| | |
|---|---|
| cabin skin | 200 kg |
| endplates | 100 kg |
| endplate stiffeners | 8 kg |
| viewport | 20 kg |
| debris interface | 15 kg |
| docking interface | 30 kg |
| avionics box | 130 kg |
| | |
| Total | 503 kg |

Table 3.9.a  Cabin Structural Masses

## 3.9.7 Areas Under Research

One major concern was the mounting of the viewport to the cabin. As of
now the viewport is made of a 5 cm thick Lexan plastic. Testing will have to
be done on debris impact and bonding to cabin surface. The docking
hardware was merely sized for SSF docking capability and may be able to be
made lighter by using composites around the ring.

1   Howle, D.H. "Man in Space" *The Space Environment*. University of London Press Ltd.,
London, 1969. p200.

2   Merril, Grayson.*Handbook of Satellites and Space Vehicle*. D. Van Nostrand Company,Inc.
Princeton, NJ. 1965. p435.

3   Howle, D.H. "Man in Space" *The Space Environment*. University of London Press Ltd.,
London, 1969. p200.

4   Merril, Grayson.*Handbook of Satellites and Space Vehicle*. D. Van Nostrand Company,Inc.
Princeton, NJ. 1965. p441.

5   Ibid p443.

6   Ibid p438.

7   Ibid p439.

# 4.0 Aerobrake and Structure

## 4.1 Introduction

The main purpose of an aerobrake is to dissipate energy through aerodynamic drag instead of utilizing rockets (fuel) to provide the force necessary for braking the spacecraft. This leads to a considerable savings in fuel mass. The recent development of composite materials ( light weight) makes the aerobrake even more advantageous to propulsive braking than previously concluded. However, aerobraking requires a greater amount of structural design compared to a propulsive braking system.

The purpose of the aerobrake is to partially re-enter the atmosphere and use atmospheric drag forces to slow the vehicle down and modify its orbit. In this case, the aerobraking maneuver is used to change the orbit of the servicing vehicle from a geosynchronous orbit to a low earth orbit. This is done in order to rendezvous with Space Station Freedom, where it will normally be docked. There were several points taken into consideration in the design of the aerobrake.

- The shield should be re-usable.
- It should be able to be constructed using existing technology.
- Since it is unlikely that the shield could be sent up in one piece, it was required to be relatively easy to construct in orbit.
- It should be relatively easy to detect possible failures and repair them.

## 4.2 Shape Selection

The first major consideration in the design of the aerobrake shield is its shape. Both high L/D and low L/D configurations were examined. High L/D shapes, such as bi-conics, have the major advantage of being able to perform large plane changes. However, they generally require more structural support in addition to increased thermal protection than lower L/D configurations. Since it is not required that the vehicle be able to perform plane changes, a low L/D configuration was chosen.

The final shape of the shield was chosen to be spherical. Not only would this save weight in both the thermal protection system (TPS) and in the structure itself, but it would also allow for the application of past research and flight data. The spherical shield is similar in design to the Apollo command module.

## 4.3 Trajectory Analysis

Before the structural design and analysis of the aerobrake could begin, the loads that would be encountered during the maneuver had to be determined.

### 4.3.1 Equations of Motion

The loads were determined using the FORTRAN program shown in the Appendix A4.1. This program used the Runge-Kutta method to numerically integrate the equations of motion shown here.

$$\frac{dV}{dt} = \frac{-0.5\rho V^2}{\beta} - g\sin\gamma$$

$$\frac{d\gamma}{dt} = \frac{0.5\frac{L}{D}\rho V}{\beta} - \frac{g\cos\gamma}{V}(1 - \frac{V^2}{g(h+R)})$$

$$\frac{dh}{dt} = V\sin\gamma$$

### 4.3.2 One Pass versus a Two Pass Maneuver

By varying the initial conditions of the program, the ideal trajectory was determined for various vehicle masses and angles of attack as well as the loads associated with that trajectory. Both one and two pass maneuvers were considered for the trajectory. The loads associated with both types of maneuvers are shown in Figure 4.3.a and Figure 4.3.b respectively. These plots show that the loads are significantly higher for a one pass maneuver than for a two pass. A two pass maneuver involved the vehicle making two shallow passes into the atmosphere instead of one long deep pass. This type of maneuver only added approximately four hours to the total mission time, which is within the limits of the on-board life support equipment. Hence, the two pass maneuver was the method chosen for the vehicle.

### 4.3.3 Flow Impingement and Angle of Attack

One of the parameters which had to be determined to run the loads program was angle of attack. The size of the rest of the vehicle, especially the spider truss housing the reaction control thrusters, initially

4-2

**Deceleration vs Time
for various angles of attack
(Single Pass Maneuver)**



**Dynamic Pressure vs. Altitude
for various angles of attack
(Single Pass Maneuver)**
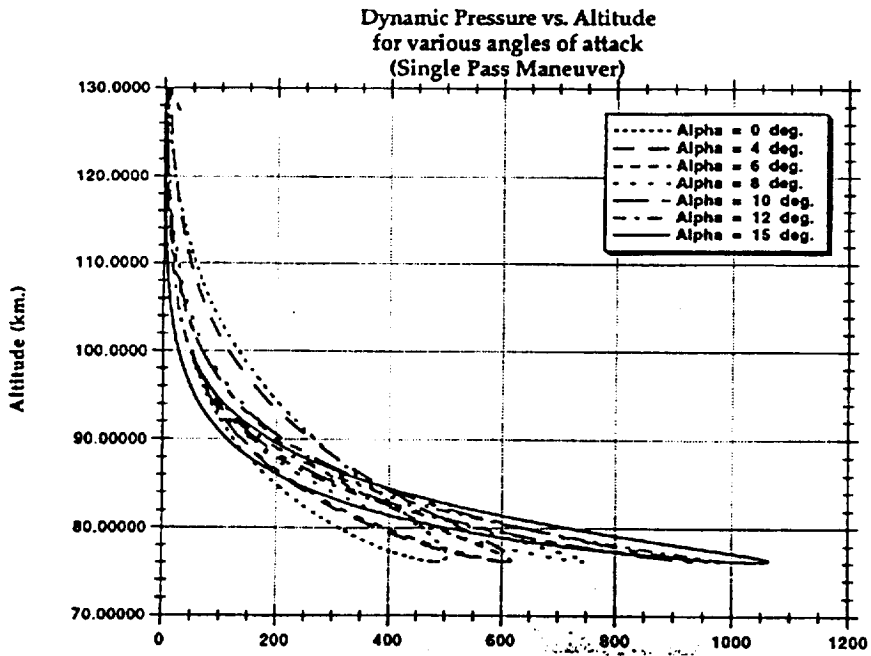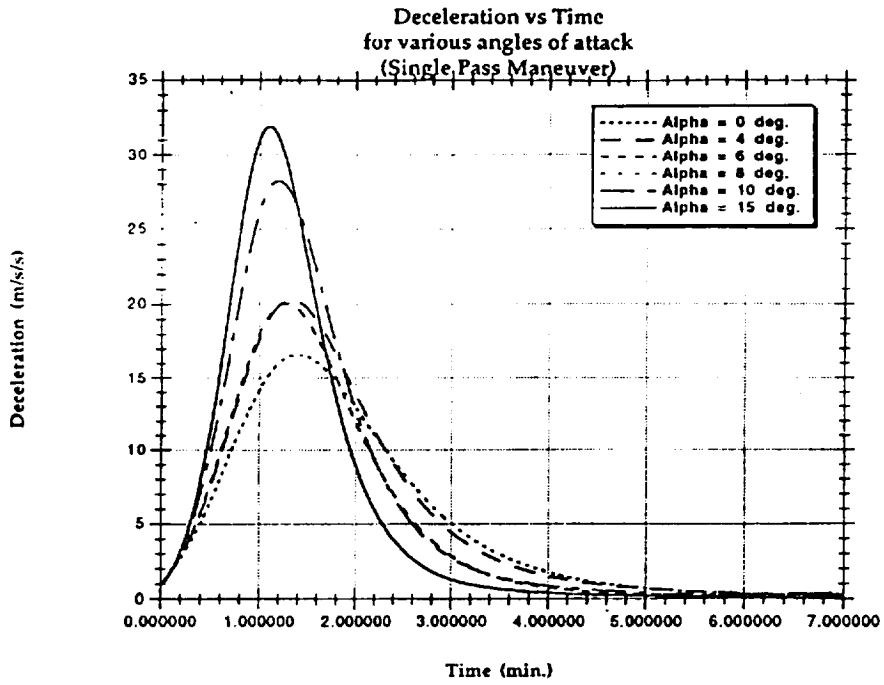


Dynamic Pressure (N/m$^2$)

**Figure 4.3.a** Single Pass Graphs

4 - 3

**Deceleration vs. Time
for various angles of attack
(Pass 1 of 2 pass maneuver)**



Legend:
— 0 deg
— 4 deg
— 6 deg
— 8 deg
— 10 deg
— 12 deg
— 16 deg

Y-axis: Deceleration (m/s/s)
X-axis: Time (min.)

**Dynamic Pressure vs. Altitude
for various angles of attack
(Pass 1 of 2 pass maneuver)**



Legend:
— 16 DEG
— 12 DEG.
— 10 DEG.
— 8 DEG.
— 6 DEG.
— 4 DEG.
— 0 DEG.

Y-axis: Altitude (km.)
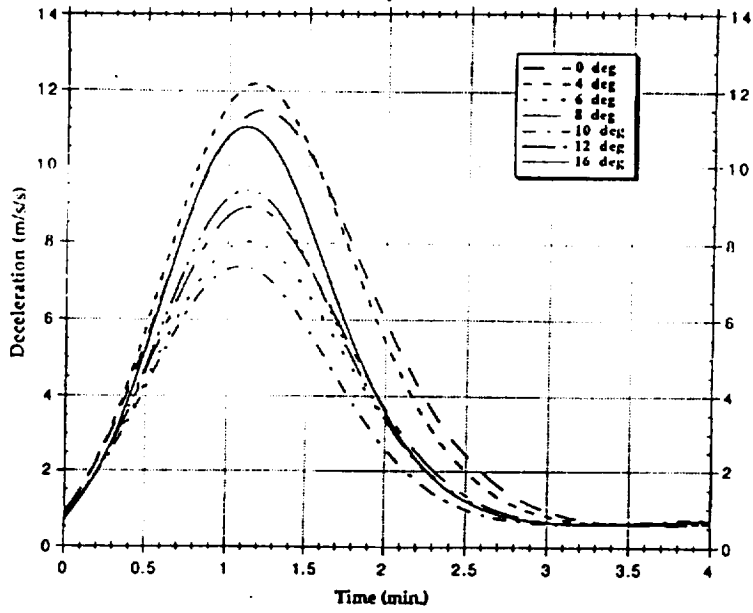
Dynamic Pressure (N/m$^2$)
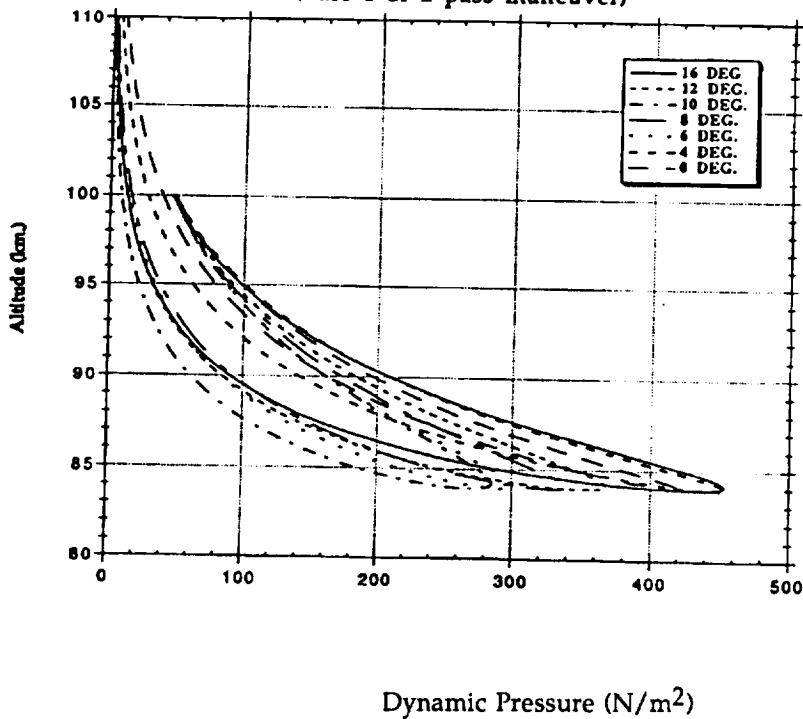
**Figure 4.3.b** First of Two Pass Manuever

determined the size of the shield. To stay within the given mass budget, the shield was downsized to a diameter of 9 meters. Figure 4.3.c shows the effect of angle of attack on flow impingement. Given that the diameter of the spider truss was slightly over 3 meters, simple geometry and Figure 4.3.c were used to determine that a maximum angle of attack of 16 degrees would prevent flow impingement on the spider truss. The location of the vehicle CG. determined the angle of attack. Since at the time of the analysis the location of the CG. was unknown, the program was run varying the angles of attack between 0 and 16 degrees.

### 4.3.4 Lift and Drag

Figure 4.3.b shows that the dynamic pressure loads increase as angle of attack increases. The shield was structurally sized to operate at an angle of attack of 16 degrees, since this is the maximum allowable angle of attack due to flow impingement effects.

As the vehicle travels at some angle of attack, both lift and drag are generated. The lift is given by :

$$L = \frac{1}{2}\rho V^2 A C_l$$

where:
L = lift
$\rho$ = density of the freestream atmosphere
V = velocity of the freestream
A = characteristic area of the aerobrake
$C_l$ = lift coefficient

The drag is given by :

$$D = \frac{1}{2}\rho V^2 A C_d$$

where:
D = drag
$C_d$ = drag coefficient

The lift generated allowed the pilot to make trajectory corrections during the maneuver. The larger the angle of attack, the larger the margin for error the pilot had. The lift and drag generated by the shield during the first pass of the maneuver assumes angles of attack between 0 and 16 degrees is shown in Figure 4.3.d.
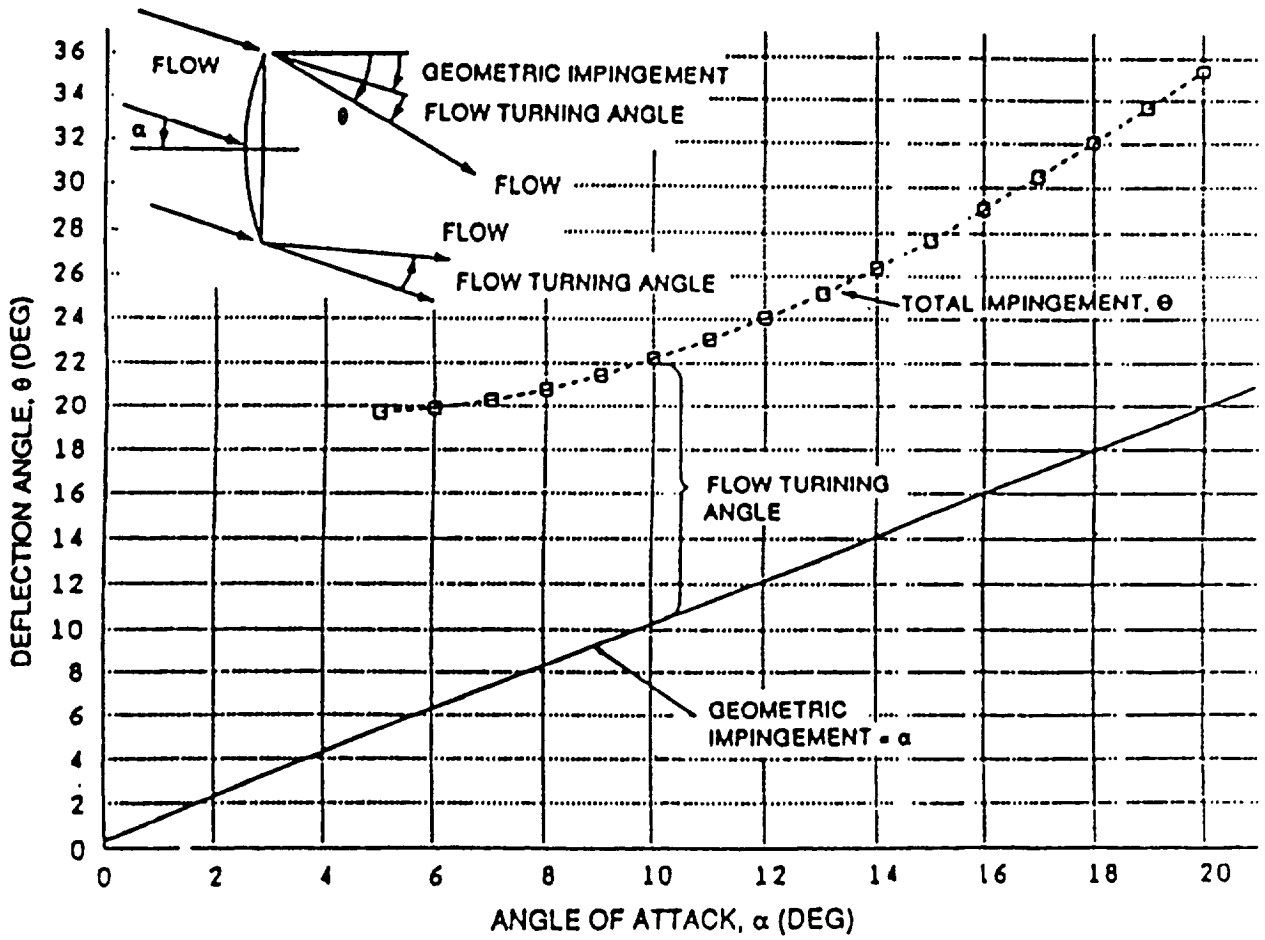
**Figure 4.3.c** Flow Impingement
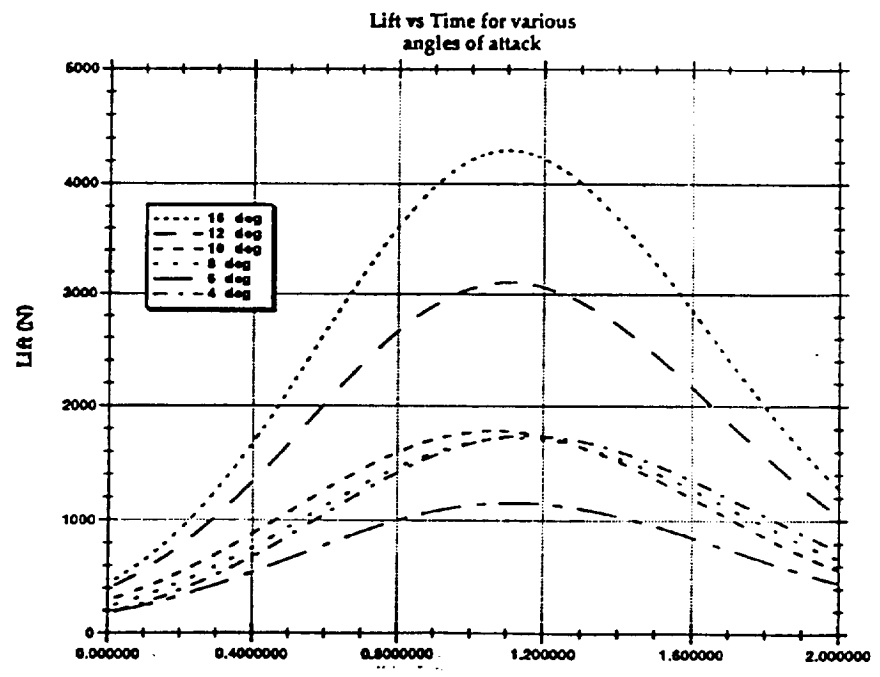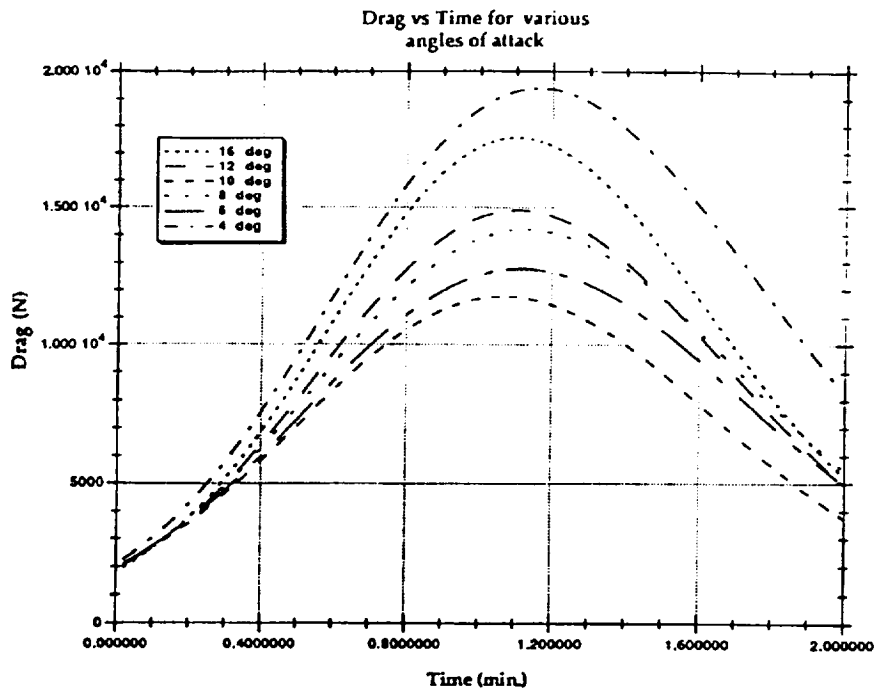
Figure 4.3.d  Lift and Drag on the Aerobrake

4 - 7

## 4.4 Aerodynamic Loads

For a two pass maneuver, the vehicle dips into the atmosphere about the same distance for both passes. However, the velocity is lower for the second pass. Therefore, the loads due to the dynamic pressure are higher during the first pass. The g-loads, however, are about the same for both. For this reason, the loads encountered during the first pass were chosen to be the critical aerodynamic loads.

The chosen trajectory gives a Mach number of 34. For a blunt body, the stagnation point value of the coefficient of pressure, $C_p$, can be determined using :

$$C_{pmax} = (\frac{2}{\gamma M^2})(\frac{P_{0,2}}{P_1} - 1)$$

The value for the ratio of pressures, $\frac{P_{0,2}}{P_1}$, can be obtained from a table of normal shock properties such as Anderson's *Fundamentals of Aerodynamics*. At M=34, the ratio was found to be $1.489 \times 10^3$. This gives

$$C_{pmax} = 1.839.$$

Since the vehicle is traveling at hypersonic speeds, modified Newtonian theory can be used. This theory states

$$C_p = C_{pmax} (cos^2(theta)),$$

where theta is the angle between a normal to the surface and the free stream velocity. While the maximum pressure would occur only at the stagnation point, the structural analysis was done assuming stagnation conditions over the entire shield. This provides an additional factor of safety. The total dynamic pressure loading was found to equal

$$C_{pmax} \times q = 1500 \, N/m^2$$

where q is the dynamic pressure. The next type of load to consider is the loading due to acceleration (g-loads). G-loads will be encountered on two occasions. The first will be during the thrusting maneuver to bring the vehicle to a geosynchronous orbit. According to the Propulsion group, this load will be no more than 2g. The second occasion is during the aerobrake maneuver. As shown in Figure 4.3.b, this load will not exceed 1.5g.

Due to time constraints, an analysis was not completed on how the nozzle hole in the shield would affect the aerodynamics.

## 4.5 Aerobrake Control

For purposes of control while performing the aerobrake maneuver, the torques of the brake were calculated. The torques that will contribute the most during this time is the aerodynamic torque and the gravity - gradient torque. The torques were calculated in a "worst case scenario." The worst possible thing that could happen is for the two torques to add to each other, however, it is possible for the two to work against each other.

### 4.5.1 Aerodynamic Torques

The aerodynamic torques occur in lower orbits or when entering the atmosphere. The torques are dependent on the density of the atmosphere and therefore on the orbit. At higher orbits, the density is too small to create a torque, therefore, the calculations of the torques were performed for the orbit altitudes of 80 km to 100 km, the region of the aerobrake maneuver.

The torques are also dependent on the locations of the center of pressure of the shield, Cp, the location of the center of gravity of the space craft, Cg, and the coefficient of drag of the shield, Cd. For the worst case, the Cp can be assumed to deviate 5% of the shield diameter from the Cg of the space craft. The Cg has been calculated to be the center of the shield.

### 4.5.2 Calculations of Aerodynamic Torques

The equation for the Aerodynamic torque is

$$Ta = F ( Cp - Cg )$$

where
Cp     = center of pressure
Cg     = center of gravity
F      = aerodynamic force.

The equation for the aerodynamic force is

$$F = .5\, \rho\, Cd\, A\, V^2$$

where

$\rho$ = atmospheric density
Cd = coefficient of drag
A = characteristic area of the aerobrake
V = velocity of the spacecraft.

The aerobrake maneuver will be done in two passes and the calculations for these passes are the following:

pass #1

| | | |
|---|---|---|
| @ 100 km. | F = 1073.6 N | Tg = 483.12 N - m |
| @ 80 km. | F = 34715.3 N | Tg = 15621.8 N - m |
| @ 100 km. | F = 868.3 N | Tg = 390.74 N - m |

pass #2

| | | |
|---|---|---|
| @ 100 km. | F = 868.3 N | Tg = 390.74 N - m |
| @ 80 km. | F = 27034.6 N | Tg = 12165.6 N - m |
| @ 100 km. | F = 643.5 N | Tg = 289.58 N - m |

The torques are now calculated and a control system can be developed to overcome these torques.

### 4.5.3 Gravity - Gradient Torques

Gravity - gradient torques are developed on space craft as they orbit the earth. These torques are usually quite small. They depend on the spacecraft's moments of inertia, and the orbit altitudes.

The torques were calculated using the formula

$$Tg = 3\,(\mu) / [2\,R^3]\ |I_z - I_y|\ \sin(2\,\theta)$$

where
$\mu$ = Earth's gravity constant = $3.986 \times 10^{14}$
R is the radius of the orbit in meters
Iz and Iy are the moments of inertia for the space craft
$\theta$ = angle between the Z - axis and the local vertical.

These calculations were made for the entire mission. Due to their length and their size, the reader can find these calculations in Appendix A4.3.

## 4.6 Material Selection

Titanium was first considered as a possible construction material. It has a high tensile yield strength and a low coefficient of thermal expansion. However, the structural members needed to support the aerodynamic and acceleration loads were far too heavy to merit further consideration. Since saving weight was a driving factor throughout the design process, solid aluminum was the next material considered for the shield and support structure. The brake was initially sized using aluminum I-beams for the support structure and covered with a thin aluminum skin on which to mount the thermal protection system (TPS). This configuration also had a final mass beyond the allowed mass budget.

The next choice was to use aluminum honeycomb. Hexcel Aerospace provided some material on designing honeycomb sandwich structures. Use of honeycomb in the shield and support structure decreased the weight of the brake to within the given mass limit. The overall thermal resistance of the honeycomb plate is the sum of the resistances of the core, facing, adhesive, and boundary layers on each side of the sandwich. This provides better insulation for the rest of the vehicle than the thin aluminum sheet originally considered.

## 4.7 Design Configuration

The aerobrake is composed of plating and a support structure.

The honeycomb plating gives the brake its solid spherical shape. It is also the surface onto which is mounted the TPS. The plating is composed of ten equally sized curved trapezoids, which fit together to form a spherical surface with a hole in the center for the engine nozzle. It was decided to divide the shield into ten segments because given the size of the brake, ten equal parts fit nicely in the shuttle cargo bay. The dimensions of the plates are as follows :

| | |
|---|---|
| Top width | = 0.352 m. |
| Bottom width | = 2.83 m. |
| Side edge lengths | = 4.88 m. |
| Plate area | = 7.50 sq. m. |
| Plate radius of curvature | = 10.63 m. |

| | |
|---|---|
| Honeycomb face sheet thickness | = 0.15 mm. |
| Honeycomb core thickness | = 15.66 mm. |

The support structure is composed of ten equally spaced arches and rods. The arches are basically curved beams which the curved plates are mounted to. These arches are also made of honeycomb. The dimensions of a typical arch are as follows :

| | |
|---|---|
| Beam width | = 0.15 m |
| Beam length | = 4.88 m |
| Beam radius of curvature | = 10.63 m |
| | |
| Honeycomb face sheet thickness | = 0.63 mm |
| Honeycomb core thickness | = 80 mm. |

The straight rods are pinned between the edge of the aerobrake and the main vehicle truss at an angle of 32 degrees to the horizontal. They mainly provide additional support against global buckling of the shield. It was decided to make the rods out of solid aluminum because at the time of the analysis, there was insufficient information on the behavior of honeycomb rods under tensile loading. Their use however should not be ruled out once more information is available. The dimensions of a typical rod are as follows :

| | |
|---|---|
| Rod length | = 4.67 m |
| Rod radius | = 0.018 m. |

The arches are pinned in a radial fashion to the nozzle ring (the ring shaped portion of the main vehicle truss surrounding the engine nozzle). The other end of the arches are pinned to the rods which in turn are pinned to the cabin ring (the ring shaped portion of the main vehicle truss below the crew cabin). The plates are simply pinned on to the arches. The shield and support structure (without the TPS) are shown in Fig. 5.

The structural analysis of the shield and supporting structure is shown in the appendix A4.2.

## 4.8 Mass Total

The total mass of the shield and support structure is tabulated as follows :

| | |
|---|---|
| Mass of plates | 156.72 kg |
| Mass of rods | 134.4  kg |
| Mass of arches | 56.8  kg |
| Adhesive and Aluminum Pins | 20.0  kg |
| | |
| Total Brake Mass | 367.92 kg    (does not include TPS). |

## 4.9 Assembly

The aerobrake will be shipped to space in pieces and then assembled on-orbit. The determination of in-space EVA/telerobotic assembly issues can be accomplished by testing a partial full-scale aerobrake structure. Such an experiment has previously been conducted at the McDonnell Douglas Space Systems Company Underwater Test Facility in Huntington Beach, California. Assembly procedures were tested underwater using two EVA astronauts and a telerobotic manipulator. Several extra divers assisted in the movement of the core in order to simulate the in-space movement of the "lazy Susan" structure.

### 4.9.1 Use of Telerobotics

Among the telerobotic systems that should be available at Space Station Freedom: Mobile Remote Servicer (MRS), Space Station Remote Manipulator System (SSRMS), Flight Telerobotic Servicer (FTS), Special Purpose Dexterous Manipulator (SPDM), and a Mobile Transporter (MT). The telerobots can be used to back up, assist, or replace EVA crew in the aerobrake assembly. The telerobots will primarily be used for transporting and holding large pieces of the aerobrake while the astronauts complete the tasks requiring more precision. The option of using telerobotics becomes feasible when one considers problems that may arise in space.

Space suit failures or the presence of solar flares would necessitate the use of telerobots. Therefore, a combination of EVA and telerobotics will be used in assembly, as a strictly automated assembly would not be cost effective. In addition, a structure commonly referred to as a "lazy Susan" is required for rotation of the aerobrake during assembly and maintenance.

### 4.9.2 Assembly Procedure

The individual pieces of the aerobrake are small enough to be brought into orbit on board the space shuttle. Once in orbit, the shield must be assembled. The first components that must be put on are the arches. These will simply be attached in a radial fashion by pins to the nozzle ring. The free ends of the arches will then be pinned to one end of the straight rods. The other end of the rods will then be pinned in a radial fashion to the cabin ring. Once this support structure is completed, the plates can be attached to the arches also using pins. The plates will be delivered to the station with the TPS already mounted on to them so no further assembly is required. All of the honeycomb structures will have small perforations in the core to allow for the release of pressure during the transition from the earth's atmosphere to the vacuum of space. Figure 4.9.a shows the aerobrake assembled.
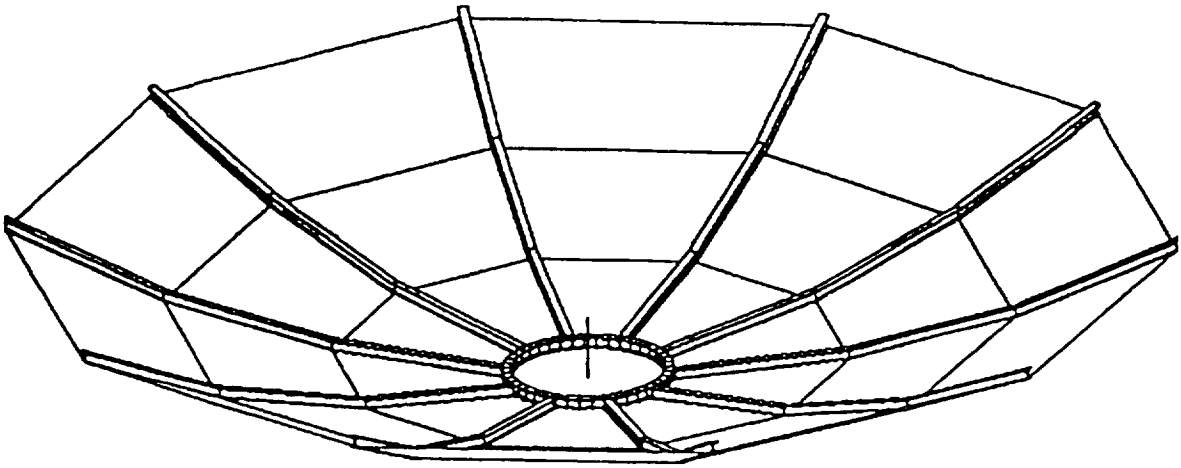
**Figure 4.9.a** Aerobrake Structure

### 4.9.3 Time for Assembly

Based on the results obtained from the underwater assembly of a three petal aerobrake , McDonnell Douglas proceeded to calculate the man-hours spent per task on a eight petal assembly. The graph on the following page (figure 4.9.b) depicts the man-hours to be spent per task on our ten petal assembly. The total time does not include time necessary for inspection after assembly. The inspection process involves checking the thermal protection tiles as well as using X-rays, computer enhanced imaging , or sensors to check the mechanical structure. Some extra time, however, has been allotted to allow the astronauts to become familiar with the assembly process. The graph shows the total time required to perform each assembly task: translate and ingress to PFR (portable foot restraints), alignment of the petal and soft dock, egress PFR and tether to the handrails, translate along the handrails and latch on the hard docking fasteners, and then attach the struts to conclude the assembly process. The total time to complete the aerobrake assembly is four hours and six minutes.

### 4.9.4 Maintenance

The simple pin configuration of the brake allows for easy servicing of the vehicle. For example, to remove a fuel tank, the appropriate pins can be removed and the rods that are in the way can simply be swung out. If the TPS on one of the plates is found to be defective or badly worn, that entire plate can just as easily be removed and replaced. The same applies for any of the rods or arches.

## 4.10 Main Spinal Truss

### 4.10.1 Requirements

The critical loading, of 2gs, for the main spinal truss is the buckling load induced during the third orbital burn. The spinal truss is 3.5 meters long and extends from the bottom of the aerobrake to the bottom of the avionics box and spider truss integrated system. The spinal truss must sustain the inertial loading of the complete MOOSE system seeing that it serves as the main load path for the vehicle. As was used for the buckling analysis for the crew cabin, a 10000 Newton force will be scaled by a factor of safety of 1.5. This force was applied in such a way that each of the four longitudinal members of the spinal truss would be required to withstand this load. This is a conservative analysis.

□ time in minutes per task
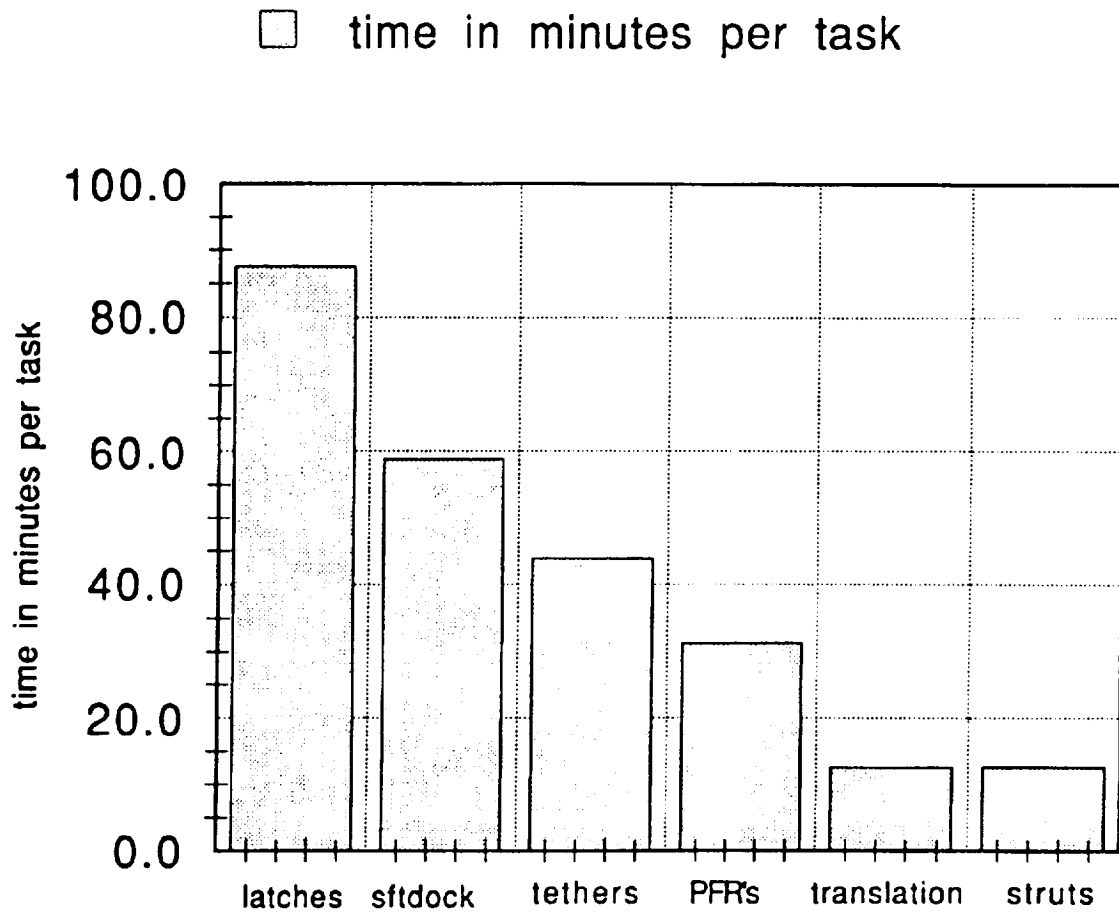


**Figure 4.9.b**  Aerobrake Assembly Time

## 4.10.2 Longitudinal Beams

Using the Euler buckling equation with a loading of 15000 Newtons on a beam of 3.5 meters length, a minimum moment of inertia for the beam can be found. The beams were assumed to be fixed at both ends with welds. This dictates an effective length of .71 times the actual length. A trade study was conducted between two materials, aluminum and titanium. Because of temperatures of 350°F behind the aerobrake, the aluminum beams were analyzed using 70% of their strength.

The circular tube cross section required for aluminum beams was found to have an outer radius of 5 cm and an inner radius of 4.4 cm. This cross sectional area yielded a mass of 17.35 kg per beam. The circular tube cross section required for the titanium beams was found to have an outer radius of 2.5 cm and an inner radius of 2.3 cm. This cross sectional area yielded a mass of 4.7 kg per beam. Clearly, titanium offers a distinct mass advantage for our system.

## 4.10.3 Cross Member Beams

The main longitudinal beams will be connected by 7 cross members of equal size. These members will have cross sections with half the dimensions of the main longitudinal members. Their total mass is 26.6 kg.

## 4.10.4 Spinal Rings

Three rings with box tube cross sections of outer radius 5 cm and inner radius 4.5 cm will be integrated between the four longitudinal members. Two of these rings will be located at the bottom and the top of the spinal truss configuration. The third would be attached at a height of 2.6 meters above the bottom of the aerobrake to serve as hard points for attaching the aerobrake, the crew cabin, and the tank interface beams. The total mass of these three rings is 24.7 kg. Titanium fittings will serve to interface the aerobrake members to the spinal truss.

## 4.10.5 Spinal Truss Interface

A cantilever beam analysis of the tank to spinal truss interface yields a circular tube cross section of outer radius 4 cm and inner radius of 3 cm. This beam must sustain the inertial loading created at the start of the first orbital burn since at this time the mass of the main propellant tanks is at a maximum. Although the g-loads here are not at a maximum, the loading at this point in our mission is still the critical loading for the tank to spinal truss interface beam. The mass of each of these beams is 5.2 kg. The total mass of the four beams is therefore 20.8 kg.

### 4.10.6 Spinal Truss Masses

| | | |
|---|---|---|
| Longitudinal Beams | 4 x 4.7 kg | 18.8 kg |
| Cross Member Beams | 7 x 3.8 kg | 26.6 kg |
| Spinal Rings | 3 x 8.2 kg | 24.7 kg |
| Spinal Truss Interface | 4 x 5.2 kg | 20.8 kg |
| | | |
| Total | | 90.9 kg. |

## 4.11 Thermal Protection System (Tile Sizing)

This section will strictly discuss how to determine the proper TPS tile size.

Shuttle-type TPS tiles are quite fragile and have to be separated by a strain isolation pad (SIP) from the underlying structure. There is a deflection limit in the support structure which if exceeded will cause the separation of the tiles from the structure. The separation occurs due to the failure of the SIP. A local induced radius of curvature is calculated from the normal panel deflections and then analyzed with respect to tile deflection ($W_{tps}$) and tile size ($L_1, L_2$) as illustrated in figure 4.11.a. `Using the following equation for a circle

$$Y^2 + Z^2 + C_1 Y + C_2 Z + C_3 = 0$$

and the positions of the three deflected points as determined from the diagram. We obtain solutions for $C_1$, $C_2$, $C_3$ upon substitution of the x and y values of each deflection point.

$$C_1 = 1/2L \; (-W_c^2 + W_a^2 + (W_c - W_a)(W_c^2 - W_b^2 + W_a^2 + 2L^2)/W_c - 2W_b + W_a)$$

$$C_2 = (W_c^2 - 2W_b^2 + W_a^2 + 2L^2) / W_c - 2W_b + W_a$$

$$C_3 = W_b [2L^2 + W_c (W_c - W_b) + W_a (W_a - W_b)] / W_c - 2W_b + W_a$$

The radius of curvature, ROC, related to the normal displacements on the structural panel is

$$ROC = 0.5 (C_1^2 + C_2^2 - 4C_3)^{0.5}.$$

The following equation relates tile size and tile deflection to obtain the ROC

$$(ROC - W_{tps,1})^2 + L_1^2 = ROC^2.$$
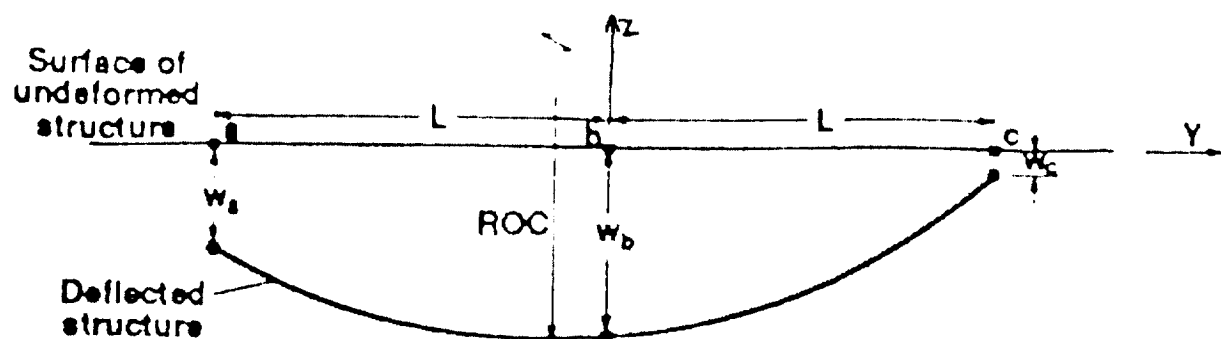
a. Geometry for calculating radius-of-curvature from 3 normal displacements.
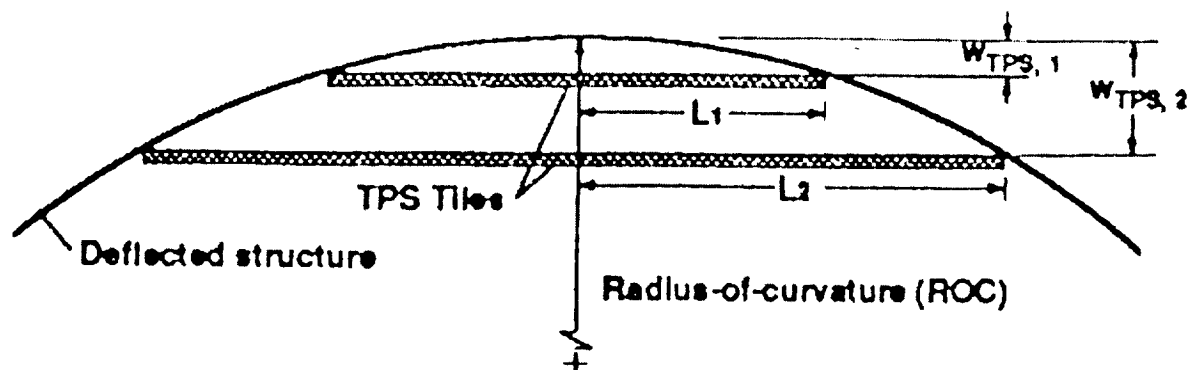


Figure 4.11.a   Relationship Between TPS Panel Size and Deflection Limit and ROC

# 5.0 Propulsion

## 5.1 Introduction to the MOOSE Propulsion Systems

This chapter outlines the propulsion systems utilized on MOOSE. The main propulsion system is complemented by a dual-propulsive reaction control system. Details of the components selected and each propulsive system's requirements further clarify the role and purpose of each system.

### 5.1.1 Optimum Propulsion System

Five different propulsion systems were considered for the MOOSE project. These propulsion systems included three different chemical propulsion systems (liquid, solid, and hybrid), a nuclear fission reactor, and a laser absorption process. It has been determined by the design group that the optimum propulsion system for the MOOSE project is a chemical system with liquid propellants. Section A.5.1 of the appendix, "Choosing the Optimum Propulsion System", details the four propulsion systems that were analyzed but not chosen for the MOOSE project. In addition to the results of section A.5.1, the analysis presented in section 5.1.2, "Propellant Transport Cost for Chemical Propulsion Systems," details the major factor in determining the optimum propulsion system for the MOOSE project.

### 5.1.2 Propellant Transport Cost for Chemical Propulsion Systems

In order to operate MOOSE the propellant needed for the vehicle must be transported from Earth to Space Station Freedom where MOOSE will be docked. Transporting the propellants to MOOSE turns out to be a primary cost for the customer, which can be lowered if the mass of propellants is reduced. The mass of propellants can be reduced by decreasing the structural mass or by increasing the specific impulse. Figure 5.1.a shows the relationship of propellant transport cost compared to the vehicle structural mass for various specific impulses.

The following design criteria was used for this analysis:

- Propellant transport cost = 8.9 $k/kg   (Typical for a Titan IV launch vehicle)
- $\Delta V$ = 7000 m/s
- Structural mass = 3047 kg

A chemical propulsion system that uses either solid or hybrid propellants would not be a cost efficient system for the MOOSE project. The performance level, Isp, for solid propellants ranges from 180 to 300 seconds. From Figure 5.1.a it can be seen that for a structural mass of 3047 kg it would cost between 300 to 1100 $Million just to transport the propellants from Earth to the space station. The performance level, Isp, for hybrid propellants ranges from 250 to 350 seconds. From Figure 5.1.a it can be seen that for a structural mass of 3047 kg it would cost between 200 to 510 $Million just to transport the propellants from Earth to the space station. The results show that it would not be cost efficient to use a chemical system with either solid or hybrid propellants. The design group can not expect the customer to pay over 100 $Million in transporting the propellants from Earth to the space station since the customer can build a new satellite and have it placed into orbit for an estimated 300 $Million. It would not even be cost efficient for MOOSE to repair two satellites during the same mission since each customer would still be paying over 100 $Million in propellant-transport cost.

A chemical propulsion system that uses liquid propellants can be cost efficient if the propellants chosen have a high enough performance level, Isp. From Figure 5.1.a it can be seen that for a structural mass of 3047 kg the performance level, Isp, must be about 450 seconds in order for the system to be cost efficient in propellant transport (assuming that MOOSE only repairs one satellite per mission). Propellants consisting of oxygen / hydrogen fit this criteria, costing slightly below 100 $Million in propellant-transport cost.

If MOOSE is to repair two satellites in one mission then the propellant-transport cost can be split among the two customers, allowing the propellant-transport cost to approach 200 $Million and the performance level, Isp, to lower to 350 seconds. A lower Isp would allow for various choices in liquid propellant combinations such as: oxygen / hydrogen, fluorine / hydrazine, and fluorine / hydrogen.
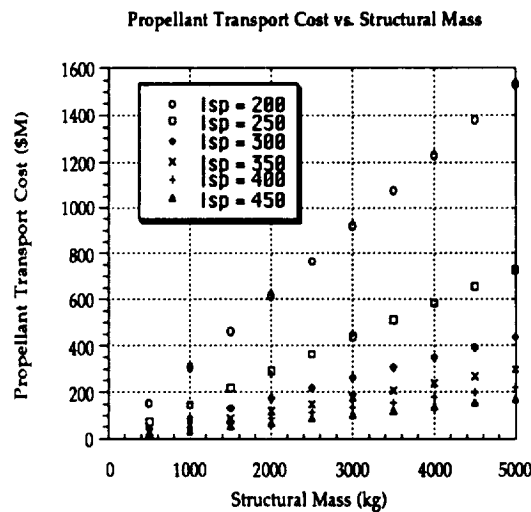


Figure 5.1.a Relationship of Propellant Transport Cost Compared to the Vehicle Structural Mass for Various Specific Impulses

### 5.1.3 Requirements for the Selection of Liquid Propellants

The selection criteria for the liquid propellants is based on many properties of the various potential propellants surveyed. These potential propellant combinations had to meet the requirements that follow before a final selection could be made based on the results of trade studies. The propellants must have high energy release per unit propellant mass as well as low molecular weight of the combustion gases to achieve high specific impulse. Ignition must be easily induced and stable combustion maintained. The propellant should have a high density to minimize the size and weight of the propellant tanks and feed systems. A low freezing point is desired to ease engine operations at low temperatures. The propellants must be compatible with the engine materials to assure the absence of corrosive effects. The ability to act as an effective coolant for the thrust chamber and nozzle is necessary (a combination of high thermal conductivity, high specific heat, and high critical temperature). Low viscosity is desired to minimize the pressure drops through the feed system and the injector. To reduce the risk of explosion and fire hazards, high thermal and shock stability is required. Low toxicity of the propellants and the combustion products is also desired. Finally, the propellants should be readily available at an acceptable price.

### 5.1.4 Liquid Propellant Analysis

From the above analysis on propellant transport cost it has been determined by the design group that if MOOSE can repair two satellites in one mission then the liquid propellant combinations that would provide a cost efficient system are: oxygen / hydrogen, fluorine / hydrazine, fluorine / hydrogen. However, if MOOSE only repairs one satellite for a given mission then the only liquid propellant combination that would provide a cost efficient system is oxygen / hydrogen. Note, for this analysis a cost efficient system is only referring to propellant transport cost under 100 $Million per customer.

The major disadvantage with using any of the above propellant combinations is that oxygen, hydrogen, and fluorine are all cryogenic propellants. The only alternative would be to reduce the structural mass of the vehicle such that liquid propellants with storability characteristics, such as hydrazine, can be used. However, since the performance level, Isp, of storable propellants drop below 350 seconds the structural mass would have to decrease below 2000 kg in order for the system to remain cost efficient, see Figure 5.1.a. Since the structural mass of MOOSE is 3047 kg the design group will be using cryogenic propellants, however, if the structural mass does drop below 2000 kg then using storable propellants needs to be considered.

The design group understands the difficulty in storing cryogenic propellants. Information on storing the cryogenics during flight can be found in section 5.10 of this chapter under the heading Propellant Tanks, and information for storing the cryogenics at the space station can be found in chapter 8. Again, the design group understands that storing cryogenic propellants is difficult, but no other propellant combinations are desirable from a cost efficient standpoint unless the structural mass

decreases below 2000 kg.

With the three cryogenic liquid propellant options available for the MOOSE project the design group decided to use oxygen / hydrogen for the main propulsion system. The major determining factor is that with an oxygen / hydrogen system MOOSE will not be limited to repairing two satellites in one mission. MOOSE can be sent out to repair one satellite on demand and still remain cost efficient. Note, the analysis for repairing two satellites in one mission can be found in chapter 1 under the mission analysis section. Another factor leading to the choice of an oxygen / hydrogen system is that the other two propellant options use fluorine as the oxidizer. Fluorine is extremely toxic and corrosive in addition to spontaneously reacting with many common spacecraft construction metals. Furthermore, fluorine has only been used in experimental rocket engines and not in production engines.

### 5.1.5 Chemical Propulsion with Liquid Propellants

A chemical propulsion system with liquid propellants generally consists of a combustion chamber, injectors, ignition system, nozzle, propellant feed mechanism, a power source for the feed mechanism, plumbing, and propellant tanks. In a chemical propulsion system with liquid propellants, the fuel and oxidizer reaction causes a high-pressure combustion which releases energy that heats the products of the chemical reaction to very high temperatures. These reaction products, which are in a gaseous state, are expanded in the nozzle and accelerated to high velocities, thereby imparting momentum to the system.

The main propulsion system for the MOOSE project is shown below in Figure 5.1.b.
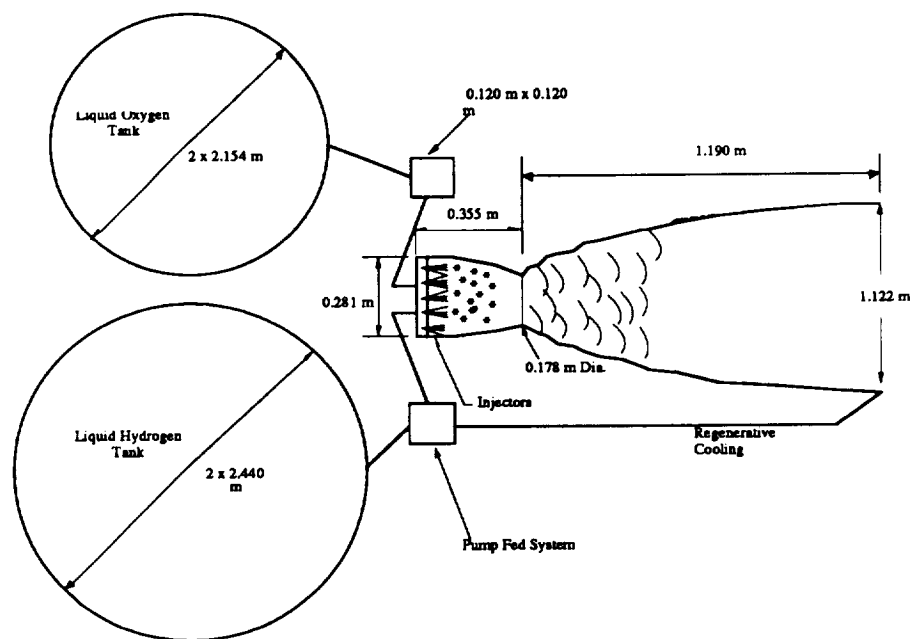


Figure 5.1.b  Main Propulsion System for the MOOSE Project

## 5.2 Mixture Ratio

The following expression is the chemical reaction of liquid hydrogen and liquid oxygen going to completion:

$$H_2 + \tfrac{1}{2}O_2 \rightarrow H_2O$$
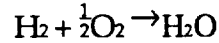
All of the hydrogen and oxygen are fully consumed to form water vapor. There is no reactant residue of either hydrogen or oxygen remaining after combustion since the reactants are in stoichiometric proportions. On a mass basis this stoichiometric mixture provides a stoichiometric mixture mass ratio of 8:1. The stoichiometric mixture mass ratio results in the highest combustion temperature and the highest release of energy per unit mass of propellant mixture. This does not automatically mean that operating at the stoichiometric mixture mass ratio provides the best performance. In fact, operating at hydrogen rich levels increases the performance level, Isp, of the engine. The hydrogen rich levels allow for some of the lightweight hydrogen molecules to remain unreacted. This reduces the average molecular weight of the reaction products, and therefore, increases the performance level, Isp, of the engine. The following equation shows the relationship between the performance level, Isp, and the average molecular weight of the propellants.

$$I_{sp} = \frac{1}{g} \sqrt{ \frac{2\gamma R}{\gamma - 1} T_o \left( 1 - \left( \frac{P_e}{P_o} \right)^{\frac{\gamma - 1}{\gamma}} \right) }$$

The "R" term in the above equation represents the propellant gas constant. The propellant gas constant is equivalent to the universal gas constant divided by the average molecular weight of the propellants. From this equation it is obvious that as the average molecular weight of the propellant decreases the propellant gas constant "R" increases, thus increasing the performance level, Isp.

Operating at hydrogen rich levels will increase the performance level, Isp, of the engine, as shown above, however, caution must be taken because if the hydrogen rich level is too high some of the hydrogen will be avoiding combustion. Any excessive hydrogen that avoids combustion is considered dead weight, meaning that it is undesirable to carry any additional propellant mass that is not useful. There is an obvious trade off on how high a hydrogen-rich level to use, but there are additional factors that need to be considered. In addition to increasing the performance level of the engine, hydrogen rich levels will also insure complete combustion of the liquid oxygen. Any liquid oxygen that does not combust can oxidize the nozzle causing corrosion, which in turn shortens the life span of the nozzle.

Even though it appears that operating at hydrogen rich levels has several advantages over operating at the stoichiometric mass mixture ratio, there is one major disadvantage that needs to be recognized. As the mixture ratio decreases from the

stoichiometric mass mixture ratio (any decrease from stoichiometric is considered as hydrogen rich levels) the size of the hydrogen tanks must also increase, therefore, increasing the mass of the hydrogen tanks. Since the density of the liquid hydrogen is 9.8% lower than the density of liquid oxygen, as the stoichiometric mass mixture ratio decreases the hydrogen tanks will increase in size more rapidly than the oxygen tanks can decrease in size, resulting in an overall net increase in size and mass of the tanks. Figure 5.2.a shows the relationship between total tank mass and mixture ratio, as well as the relationship between tank radii and mixture ratio. In order to keep MOOSE cost efficient from the standpoint of propellant transport cost, as explained in section 5.1.2, the design group has to be cautious when making design decisions that will increase the mass of the vehicle.
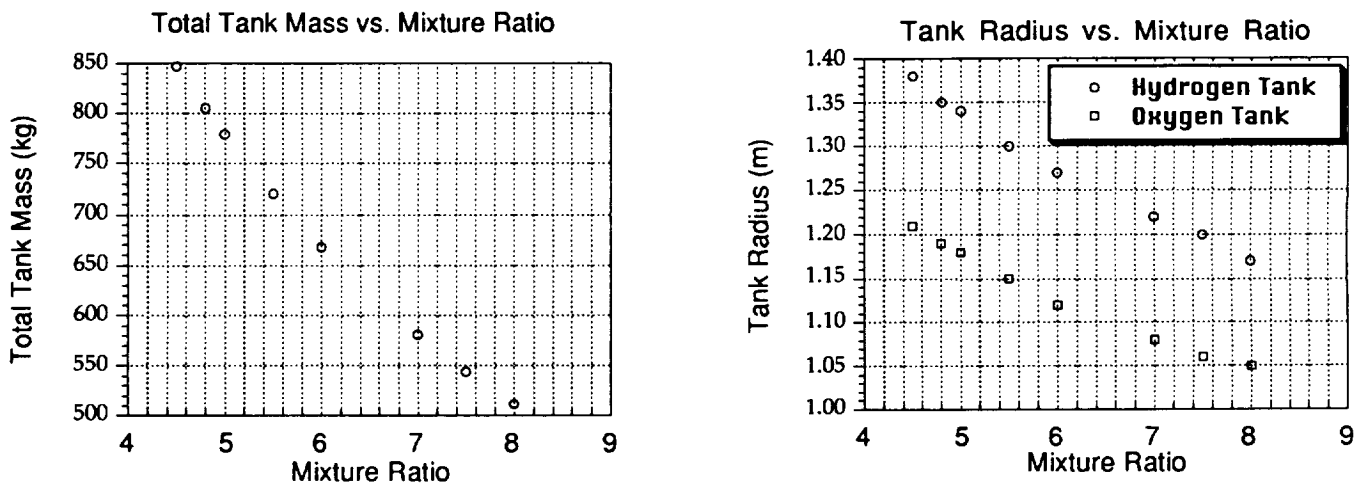


Figure 5.2.a Relationship Between Total Tank Mass and Mixture Ratio, as well as, the Relationship Between Tank Radii and Mixture Ratio

In order to avoid a significant increase in total tank mass (as compared to the total tank mass for a stoichiometric mass mixture ratio) the design group decided on a mixture ratio of 7:1. From Figure 5.2.a it can be seen that with a mixture ratio of 7:1 the total tank mass increases 12%, the hydrogen tank radii increases 4%, and the oxygen tank radii increases 3% as compared to the stoichiometric mass mixture ratio of 8:1. With a mixture ratio of 7:1 the engine will be operating at a hydrogen rich level that will insure the complete combustion of the liquid oxygen. The major disadvantage with a 7:1 mixture ratio is that the performance level, Isp, hardly increases. The performance level, however, can be increased other ways. For instance, by increasing total pressure and/or decreasing exit pressure (this can be seen from the above equation for Isp). More information on engine performance and design can be found throughout the remainder of this chapter.

## 5.3 Thrust Chamber

The thrust chamber is where the propellant is injected, mixed, and burned to produce a high temperature gas which is then expanded to transform the thermal energy into a

high velocity flow at the exit, hence useful thrust is imparted to the vehicle. A typical thrust chamber assembly consists of an injector, ignition system, propellant inlet and distribution manifolds, mounting structures, combustion chamber, and expansion nozzle.

## 5.3.1 Thrust Chamber Configuration

The results of the thrust chamber calculations are given below in Table 5.3.a; subsequent sections elaborate on how these results were obtained.

| | |
|---|---|
| Thrust, T | 87 kN |
| Mass flow rate, m | 28.8 kg / s |
| Exit area, Ae | 0.99 m$^2$ |
| Throat area, At | 0.0248 m$^2$ |
| Expansion Area Ration, Ae/At | 40 |
| Chamber diameter, Dc | 0.281 m |
| Chamber volume, Vc | 0.022 m$^3$ |
| Chamber length, Lc | 0.355 m |

Table 5.3.a Thrust Chamber Characteristic Values

## 5.3.2 The Combustion Process

In a liquid bipropellant rocket engine, the following basic steps characterize the conversion of the chemical energy of propellants into thrust. The liquid propellants, at the proper oxidizer fuel mixture ratio (O/F), are injected into the combustion chamber and atomized into droplets. The droplets are subsequently vaporized by heat transfer from the surrounding gas. The vaporized propellants are mixed rapidly, further heated, and react quickly, thus continuously increasing the mass flow rate within the combustion chamber. Combustion will essentially be complete upstream of the chamber throat, when all liquid droplets have been vaporized. Under certain conditions, shock and detonation waves may be generated by local disturbances in the chamber, possibly caused by fluctuations in mixing or propellant flow. These may trigger pressure oscillations that are amplified and maintained by the combustion processes. These amplified pressure waves are known as combustion instability and may produce high levels of vibration and heat flux that can be very destructive. As the gaseous products of the combustion process move toward and through the throat, they are accelerated to sonic, then supersonic velocities within the diverging nozzle section, and are finally ejected at the nozzle exit.

## 5.3.3 Thrust Calculation

The main propulsion system is designed to perform four burns: GEO transfer injection, GEO circularization, LEO transfer injection, and a small LEO circularization

after the aerobrake maneuver. A desired maximum acceleration of 2 g's or 19.62 m/s$^2$ is a design requirement for crew safety and comfort. The system mass and $\Delta V$ budgets as well as engine size constraints were used to calculate a good thrust level for the main engine system. With these criteria a nominal thrust level of 87 kN was selected for the thrust chamber design. At the proper O/F ratio, an Isp of 450 seconds can be obtained, yielding an ideal exit velocity of Ue = 4415 m/s. Losses associated with non-ideal expansion at the nozzle are unavoidable in the vacuum of space so a trade study looked at various exit pressures compared to the expansion ratio necessary to achieve these pressures; chamber pressure was also varied. As a result of this study, a chamber pressure of 25 atm was selected and an exit pressure of 0.4 atm was reached at an expansion are ratio of 40. For expansion area ratios greater than 40, the trend showed a diminishing effect on reducing the exit pressure; an area ratio of over 100 would be required to bring the exit pressure below 0.1 atm. This could be achieved through use of an extendible nozzle skirt, but this option was discarded as it added complexity, increased engine size envelope, and engine weight beyond its utility as a performance boost. According to the thrust equation T = mUe - (Pe-Pa)Ae a mass flow m = 28.8 kg/s is the nominal mass flow rate at 100% thrust.

| Burn | Thrust (N) | Maximum Acceleration (g's) | Burn time (s) | Mass flow rate (kg/s) |
|------|------------|----------------------------|---------------|-----------------------|
| GEO transfer injection DV=2400 m/s mf=10,240 kg | 87,000 | 0.87 | 360 | 28.8 |
| GEO circularization DV=1762 m/s mf=6770 kg | 87,000 | 1.30 | 170 | 28.8 |
| LEO transfer injection DV=1844 m/s mf=3980 kg | 78,000 @ 90% | 2.0 | 120 | 26.7 |
| LEO circularization DV=122 m/s mf=3660 kg | 72,000 @ 83% | 2.0 | 6.5 | 25.4 |

Figure 5.3.a  Main Propulsion System Burns

## 5.3.4 Combustion Chamber

The combustion chamber is the heart of the propulsion system. This is where the fuel and oxidizer are burned at high pressure adding thermal energy to the fluid which will later be transformed into useful kinetic energy in the expansion nozzle.

### 5.3.4.1 Requirements

The combustion chamber volume must be sufficient for mixing, vaporization, and

complete combustion of the propellants, i.e. large enough to allow adequate residence or stay time of propellants in combustion chamber. The cooling requirements are reduced by selecting chamber size and geometry such that the net heat transfer is a minimum. Weight should also be minimized; the weight depends on chamber geometry and pressure. A spherical shape minimizes weight but is difficult to manufacture. Fore ease of design and manufacture a simple chamber geometry is desired. Increasing chamber diameter to decrease length is acceptable, but a chamber that is somewhat longer (axial direction) than its diameter is desire to aid combustion stability and provide mixing turbulence. Chamber-pressure drops should be avoided as they lead to performance losses.

## 5.3.4.2 Combustion Chamber Calculations

The exact configuration of the combustion chamber tends not to be nearly as critical as the expansion nozzle. While a spherical chamber geometry has the least cooling surface and best weight, most U.S. designs favor the simpler cylindrical geometry for manufacturing considerations.

The combustion chamber volume is related to the throat area and a characteristic length $L^*$ according the equation $V_c = L^* A_t$, where $L^*$ is related to the combustion stay time. For $LOX/LH_2$ combustion typical $L^* = 76$ to $102$ cm, the design $L^*$ selected was 90 cm. For the throat area $A_t = 0.0248$ m$^2$ the chamber volume is calculated as $V_c = 0.022$ m$^3$. The chamber cross sectional area, then diameter, are determined from the contraction ratio (chamber area/throat area). From data on engines of similar size, a contraction ratio of 2.5 was chosen; the resulting chamber dimensions were then calculated for a cylindrical geometry: $A_c = 0.062$ m$^2$, $L_c = 0.355$ m, $D_c = 0.281$ m.
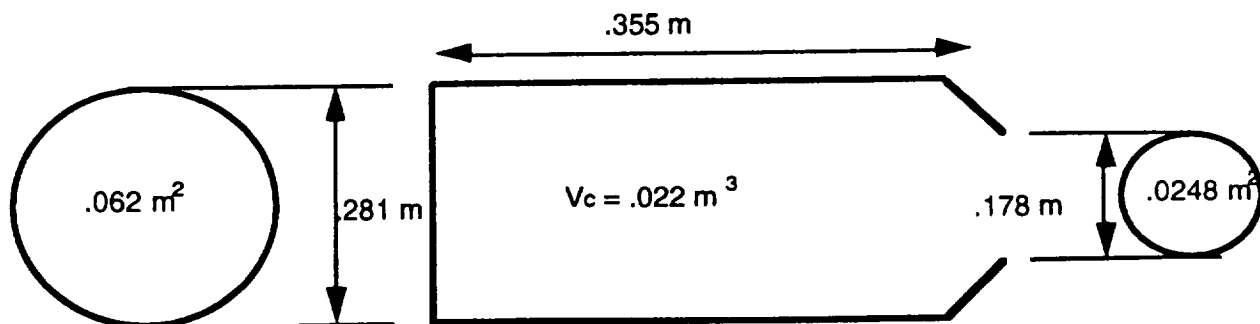


Figure 5.3.b Combustion Chamber Configuration

## 5.4 Injectors

A coaxial non-impinging injector configuration will deliver the propellant to the combustion chamber. The injector is designed to deliver the propellants to the combustion chamber and to sufficiently mix and atomize the propellants to form a homogeneous fuel-oxidizer mixture. Many injector configurations are possible; some of the more common ones include impinging-stream, shower head, splash plate, spray, and coaxial non-impinging type injectors. An impinging type injector has holes milled such that the fuel and oxidizer streams collide thus mixing together as well as assisting the atomization process. In a non-impinging injector the fuel and oxidizer generally exit normal the injector surface where mixing is promoted by turbulence and diffusion. The injection system most common to Oxygen-Hydrogen engines, including the SSME, is the coaxial non-impinging configuration. Low velocity LOX is fed through a tube which is surrounded by gaseous Hydrogen GH2 at high velocity. The GH2, already warmed from its regenerative cooling cycle, warms the liquid oxygen in the tube thus vaporizing it. The gaseous hydrogen and oxygen then readily mix in the combustion chamber; combustion stability is also good for coaxial injectors.
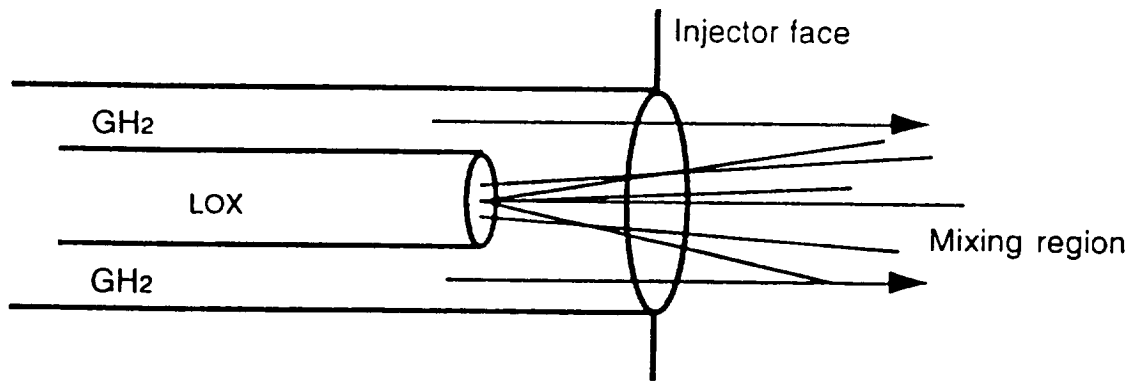


Figure 5.4.a Coaxial Non-Impinging Injector Schematic
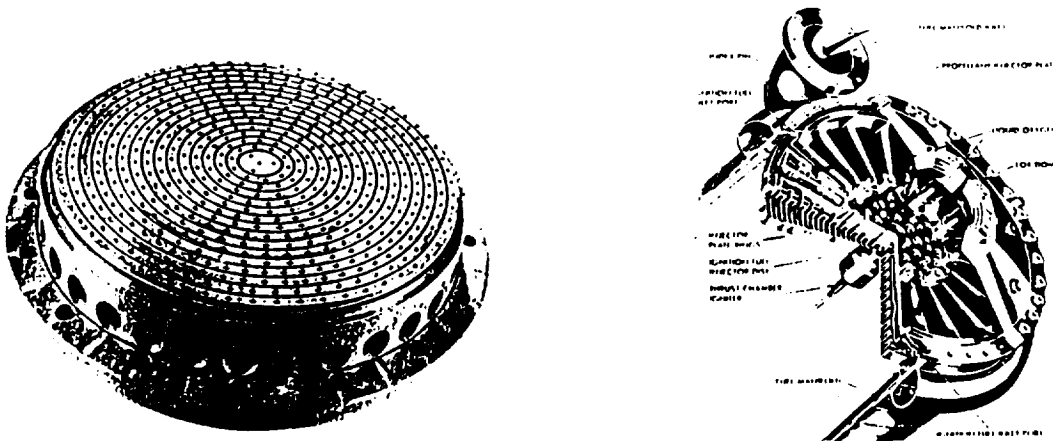


Figure 5.4.b Typical Injector Assembly[1] [2]

5 - 10

## 5.5 Ignition Systems

Ignition of the propellants is of critical concern. The ignition system must be able to ensure rapid ignition of the propellant mixture and equally rapid thrust increase to the design rating. Accumulation of propellants, not readily ignited, may lead to detonation of the propellant mixture. Any detonation may cause excessive stress to thrust chamber and possible loss of the engine system and or vehicle. The proper design and reliability of the hardware used in the ignition system are of primary importance.

A spark-torch type igniter was selected for the ignition system. Spark-torch systems are highly reliable, have multiple restart capability (a must for the MOOSE), and are good at high altitude. The spark-torch igniter allows some propellant in, then supplies a spark for ignition. The flame is then ducted to various locations on the injector face to ignite the main propellant flow. several igniters will be located around the injector face to ensure complete ignition of the propellant flow and to allow for loss of an igniter without loss of the mission. Other ignition systems were investigated such as multiple spark plugs and hypergolics. Spark plugs allowed flame to be introduced at one point only. Compared to the ducted flame of the spark-torch, the spark plug system would require more space and weight as more units would be necessary. Hypergolics are compounds which cause spontaneous ignition of the propellant; however, for multiple restarts a supply of the hypergolic compound must be maintained, as well as a mean for its injection. The added complexity of the system, as well as the possibility of clogging in the hypergolic lines, eliminated the hypergolic ignition system.

## 5.6 Nozzle Design

The expansion nozzles takes the high temperature exhaust gas flow and expands it. The expansion process allows the thermal energy of the flow to be transformed into kinetic energy, i.e. useful propulsive energy. The nozzle should be designed to produce uniform, axial gas flow at the nozzle exit for the maximum thrust. Minimum turbulence and hence separation are also design considerations. The shortest possible nozzle length is desired to reduce the size envelope, weight, and cooling requirements. The ease of manufacture is another necessary consideration.

### 5.6.1 Chamber and Nozzle Cooling

Regenerative cooling was selected due to the availability of good coolant, the LH2 fuel, and the desire to achieve a maximum Isp to perform the MOOSE mission. There is no cooling related performance loss since all the thermal energy absorbed by the coolant is returned to the combustion chamber. Noticeable performance losses are associated with dump, film, and transpiration cooling schemes. There is no change in wall contour with time (necessary for reusability); noticeable changes associated with ablative cooling. Regenerative cooling allows for an indefinite firing duration and is a relatively lightweight cooling method since the chamber and nozzle walls are

essentially hollow with the internal mass supplied by the fuel. The high heat flux capacity, necessary for LOX/LH2 combustion, is another factor which leads to the choice of regenerative cooling.

For the combustion chamber and throat, channel wall construction is necessary to handle the highest heat flux possible. Tubular wall construction (lighter weight) is satisfactory for the nozzle where the heat flux is lower. The channel wall is essentially a solid combustion chamber and throat with channels machined in place. A closeout plate or shell is then laid over this to complete the cooling channels. The tubular construction is comprised of tubes which are shaped into rings to form the nozzle contour. The tubing is then brazed together to finish the nozzle.

## 5.6.2 Nozzle Contour

In order to expand the propellant reaction products (gases) from subsonic to supersonic speeds the gases must travel through a convergent-divergent duct. The divergent section of the duct is considered to be the nozzle section of the engine. For the MOOSE vehicle the design group looked at conical nozzles, bell shaped nozzles, minimum length nozzles, and the method of characteristics to determine the appropriate nozzle contour.

Conical nozzle shapes are simple and easy to fabricate, however, losses are apparent from non-axial thrust components. A bell shaped nozzle, on the other hand, can be designed such that the overall losses are very small, however, it is difficult to fabricate the nozzle because of the nozzle contour. An analysis to determine whether or not the losses produced by a conical nozzle are negligible compared to a bell nozzle can be found in section A.5.3 of the appendix under the heading Conical vs. Bell Shaped Nozzles. It has been determined from this analysis that a conical half angle of 15 degrees is optimum in avoiding excessive thrust losses while minimizing nozzle length and weight. In fact the thrust for a conical half angle of 15 degrees is only 2% less than the thrust for an ideal bell nozzle. Even though conical nozzles are easier and cheaper to fabricate than bell shaped nozzles, the cost of a bell shaped nozzle is not significant when compared to the entire vehicle cost. In fact, a bell shaped nozzle would not represent more than 5% of the entire vehicle cost.

A bell shaped nozzle has a high angle expansion section immediately behind the throat. This expansion section is followed by a gradual reduction in slope so that the divergence angle at the nozzle exit is small. As the propellant reaction products (gases) travel through the expansion section weak expansion shock waves form. In addition, weak compression shocks form as the gases travel through the nozzle section where the contour slope is gradually reduced (this section of the nozzle causes a redirection of the gases which in turn causes weak compression waves). In order to make the bell shaped nozzle efficient, low thrust losses, the contour must be designed such that the weak expansion shock waves coincide and diminish the compression waves. By designing the contour such that the expansion and compression waves coincide it is possible to obtain a nearly even velocity distribution, but the nozzle length becomes

too long.

Using the idea of the bell shaped nozzle the design group implemented the method of characteristics technique to design the appropriate nozzle contour. The method of characteristics provides a technique for properly designing the contour of a divergent nozzle for shock free, isentropic flow. If the gradually increasing expansion section is shrunk to a point, then the expansion takes place through a centered Prandtl-Meyer wave emanating from a sharp-corner throat and the length of the nozzle is minimized. If the contour of the nozzle is made any shorter than the minimum length calculated, shocks can develop inside the nozzle. A minimum length nozzle reduces the weight of the nozzle, but for space applications the nozzle length should be as long as possible so that the exit pressure will approach ambient pressure. Therefore, a trade off is apparent between a minimum length nozzle and a nozzle length that will allow the exit pressure to approach ambient pressure. Considering the trade off in nozzle length the design group used the method of characteristics to design a nozzle for an exit mach number of 4.22 and an area expansion ratio of 40:1.

The nozzle contour is shown below in Figure 5.6.a The sonic line at the throat is assumed to be straight, and the first characteristic emanating from the sharp-corner throat was chosen to be inclined slightly from the normal sonic line ($\Delta\varnothing$ = 1.434 degrees). The remainder of the expansion fan is divided into 15 increments with $\Delta\varnothing$ = 3 degrees. The values of K+, K-, $\varnothing$, and v are tabulated in Table A.5.4.a for the first 33 grid points. The first 33 grid points are a good representation of the analysis, thus, it is unnecessary to list the properties for all 152 grid points. Note that a small inconsistency is involved with the properties at point 1. Figure 5.6.a shows point 1 on the centerline such that $\varnothing$ = 0 and Table A.5.4.a shows $\varnothing$ = 1.434 for point 1. This inconsistency is due to starting the calculations with the straight characteristic line, point A to point 1.
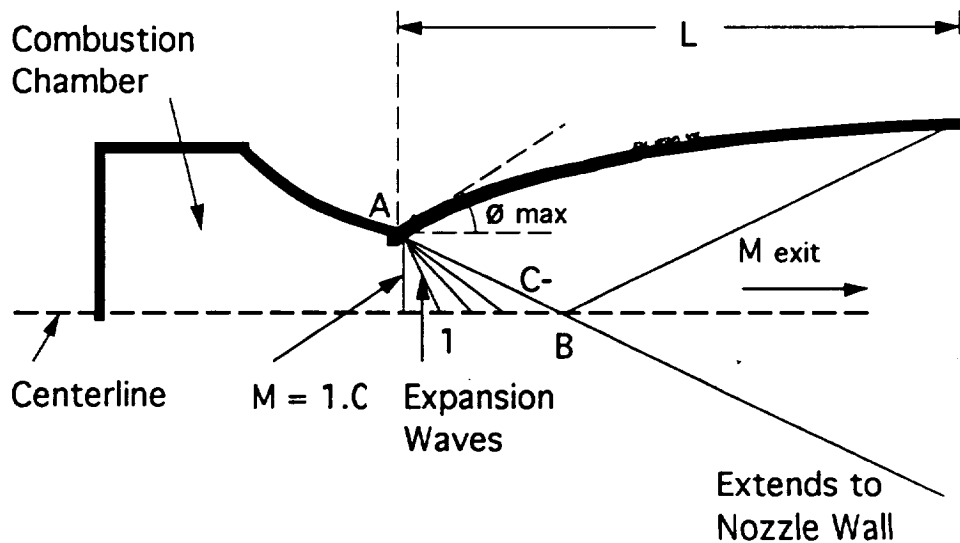


Figure 5.6.a Nozzle Contour

# 5.7 Turbopump Feed System/Plumbing

### 5.7.1 Pumps vs. Pressure

The magnitude of propellant tank pressures is considered in deciding whether to use a pumped or pressure fed system for transporting the fuel and oxidizer from their respective tanks to the combustion chamber. Tank pressures are much lower, approximately 10 to 40 times lower, for pumped than for pressure fed systems. This means that the tanks will not have to be as thick and heavy since the pressures are so much lower. In addition, since liquid hydrogen is being used as the fuel, which requires a larger volume tank due its low density, the final mass savings is appealing.

### 5.7.2 System Description

The pump system selected for MOOSE is an expander-cycle turbopump system shown in Figure 5.7.a. The system will be much more compact than what is shown, and will fit in the dashed-line, 1.2 m cylinder shown with dotted lines. Referring to Figure 5.7.a,
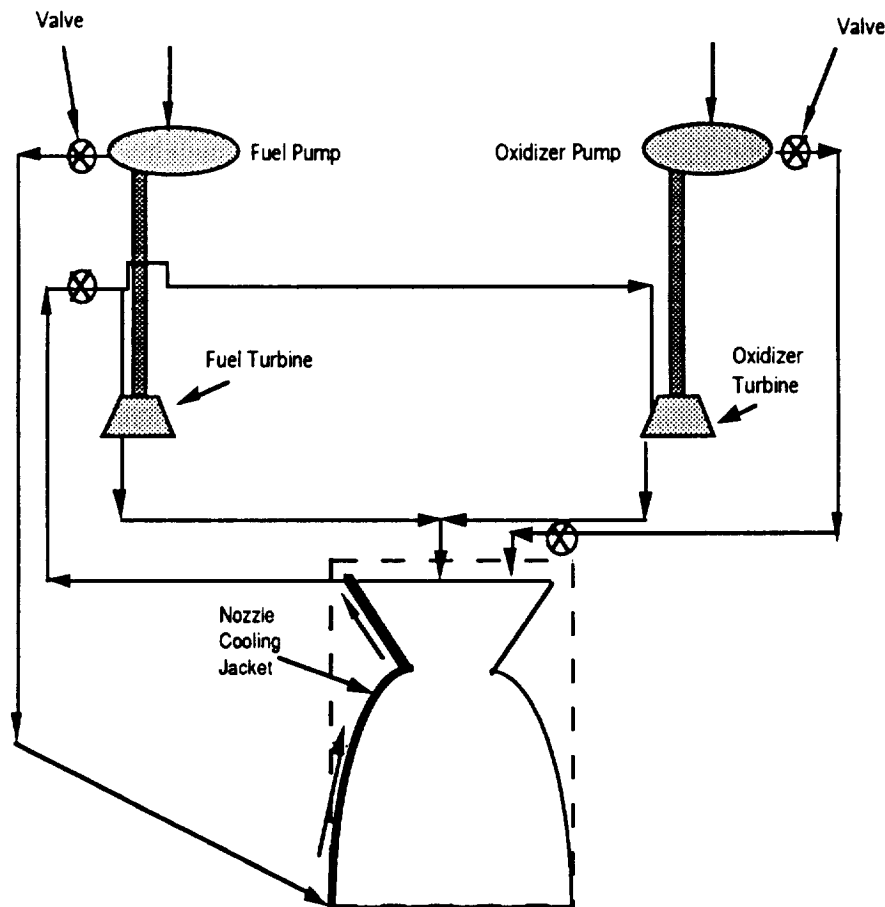


Figure 5.7.a Expander Cycle Turbopump

5 - 14

the hydrogen fuel enters through the fuel pump and then into the cooling jacket around the nozzle where the fuel will increase its thermal energy content in the process of cooling the hot nozzle and combustion chamber walls. After leaving the cooling jacket, the fuel flow splits and part of it strikes the fuel turbine which powers the fuel pump, and the remainder flows to the oxidizer turbine which powers the oxidizer pump. The hydrogen exhaust flow from both turbines recombines at the combustion chamber where it reacts with the oxygen.

This system requires auxiliary power to start since both pumps are driven by the turbines which are driven by the fuel flowing from the cooling jacket of the nozzle. The auxiliary power will come from the fuel cells and will be necessary during the four main-propulsion engine burns. In addition, two shut-off valves per line will be used for redundancy as shown in Figure 5.7.a.

### 5.7.3 Pump Pressure Requirements

The pumps will have to create a pressure rise, $\Delta P_{pump}$, that is greater than the sum of the pressure difference between the tanks and the combustion chamber, $P_{tank}$ & $P_{c.c.}$ respectively, and the pressure losses in the lines, $\Delta P_{loss}$.

$$\Delta P_{pump} \geq (P_{c.c.} - P_{tank}) + \Delta P_{loss}$$

$$P_{c.c} = 2.525 \times 10^6 \, N/m^2$$
$$P_{tank} = 1.010 \times 10^5 \, N/m^2$$

In order to find the $\Delta P_{loss}$ in the pipes, the Hagan-Poiseuille Law was used. It was assumed that the only place the flow lost pressure was in the cooling jacket since the other pipes were too short ($\Delta P_{loss} \sim \Delta L_{pipe}$).

When solving the equation, the cooling jacket was assumed to have 10 loops and an average circumference of 2.0 m. This meant a pipe length of 20 m. With a pipe radius of 3.0 cm, $P_{loss}$ was found to be just short of 8% of ($P_{c.c.}-P_{tank}$). This number was rounded up to 10% (or $2.42 \times 10^6 \, N/m^2$). The above equation yielded a required pump pressure of $2.66 \times 10^6 \, N/m^2$ driven by the turbines producing 82.7 kW of power.

Due to the low mass flow (3.6 kg/s) rate of the fuel and the high chamber pressure, two or three sets of compressor blades will be required to gradually raise the pressure.

### 5.7.4 Temperature and Material Considerations

In hydrogen cooled combustion chambers, where the wall surface to chamber volume ratio is relatively large, the temperature rise in the regenerative coolant will be large. Concern that the heat transfer to the pipes/fuel lines and especially to the turbine blades was too high lead to a materials trade study. Four materials with high yield

5 - 15

stresses were chosen for consideration and the results are presented in Figure 5.7.b and Figure 5.7.c.
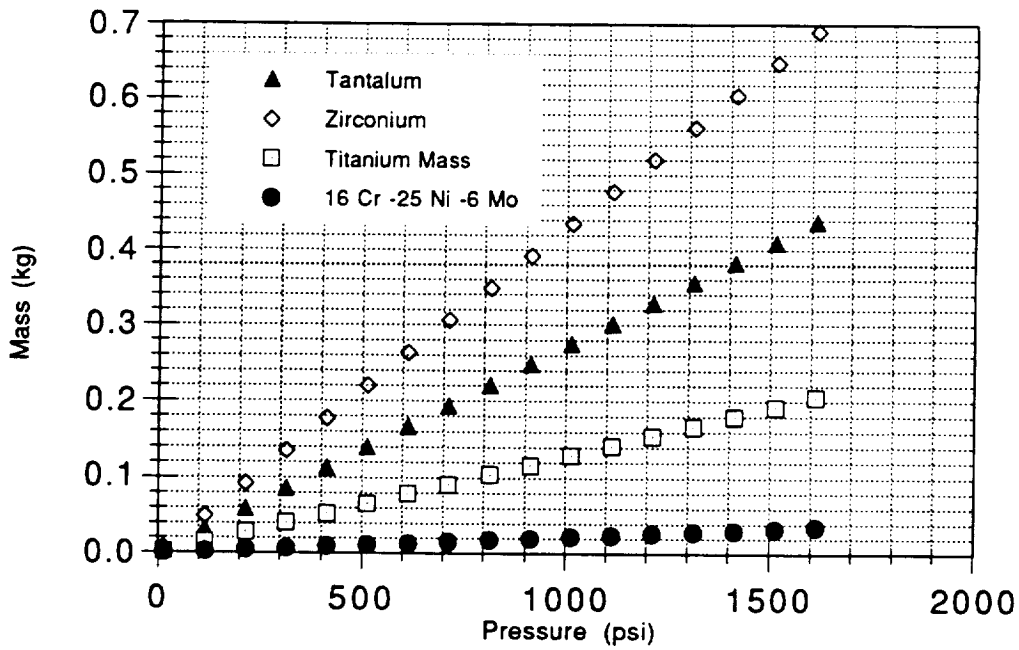


**Figure 5.7.b** Variation of Mass of Materials With Respect to Pressure
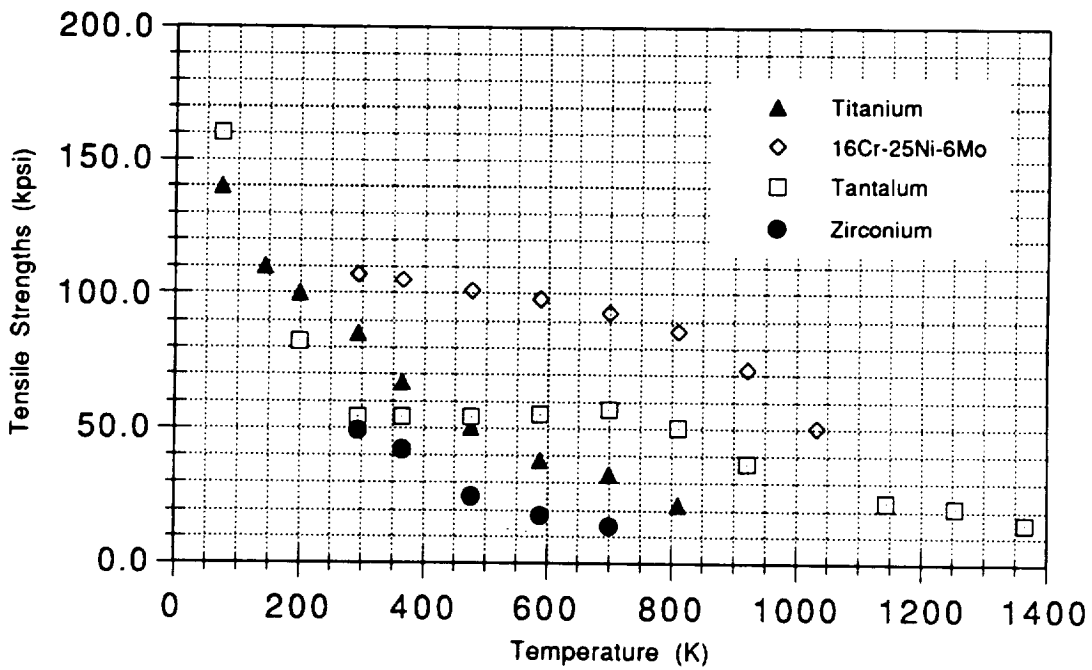


**Figure 5.7.c** Decrease in Yield Stress of Materials Due to Increase in Temperature

## 5.8 Thrust Vectoring Control

By controlling the direction of the thrust vector it is possible to control the pitch, yaw, and roll motions of the MOOSE vehicle. These motions can be controlled by the reaction control thrusters, which will perform as auxiliary thrusters when the main propulsion system is operating. By implementing the reaction control system as a thrust vectoring control system, the complexity and additional mass of either secondary fluid injection, jet vanes, or a gimbal system will be avoided. In addition, the chances of main engine malfunctions will be reduced if the thrust vectoring control system is a separate subsystem, rather than part of the main propulsion system.

The operation of the thrust vector control system will be determined by the guidance and control system. The guidance and control system will measure the three-dimensional position, velocity vectors, and rotational rates of the vehicle. These measurements are compared to the desired position, velocity, and rotations. The error signals between actual and measured parameters will be transformed by the computers into control commands for operating the thrust vector control system until the measured parameters match the desired parameters (i.e., until the error signals zero). More information about the guidance and control system can be found in Chapter 6.

## 5.9 Main Propulsion Malfunctions

The main propulsion system performs four burns for a typical mission. These burns include: GEO transfer injection, GEO circularization, LEO transfer injection, and LEO circularization.

The first burn, GEO transfer injection, propels the MOOSE vehicle from Space Station Freedom to geostationary orbit. Since this is an elliptical orbit, namely a Hohmann transfer orbit, if any malfunctions occur before the second burn then the MOOSE vehicle can follow the elliptical orbit back to the space station. It will take ten and a half hours to return to Space Station Freedom if the vehicle remains in the elliptical orbit. The astronaut can surely survive the ten and a half hour trip since MOOSE is equipped with enough supplies to last three full days.

If the MOOSE vehicle is in GEO circularization and a malfunction of the main propulsion system occurs then the astronaut will have to wait for a rescue vehicle in order to return to the space station. The reaction control system will not be able to perform the necessary $\Delta V$ of 1844 m/s necessary to propel the MOOSE vehicle into a LEO transfer orbit. It was determined from the rocket equation that the MOOSE vehicle could only weigh between 150 to 370 kg in order to enter a LEO transfer orbit and return to the space station. This structural mass varies from 150 to 370 kg depending on the amount of propellant used for attitude adjustments prior to the main engine malfunction. It is possible to reduce the structural mass of the MOOSE vehicle by dropping off detachable subsystems, such as the main engine, main propulsion tanks, and/or the aerobrake shield. However, by dropping off these subsystems it is not possible to reduce the structural mass below 370 kg. The only

option is for the astronaut to wait for a rescue vehicle.

The last burn performed by the main propulsion system is LEO circularization. This burn propels the MOOSE vehicle from the aerobraking maneuver to a circularized low Earth orbit. The $\Delta V$ for this burn is 122 m/s. If the main propulsion system fails before this burn, the reaction control system will be able to take over and perform the necessary maneuver.

## 5.10 Main Propulsion Tanks

### 5.10.1 Requirements

The main propellant tanks of the MOOSE vehicle house the liquid oxygen oxidizer and the liquid hydrogen fuel utilized by the primary propulsion system to execute the majority of MOOSE's orbital transfers. These tanks will be launched empty from Earth using the NASA Space Shuttle launch platform and will be integrated with the MOOSE system on orbit at Space Station Freedom. During this launch from Earth, the main propellant tanks will be pressurized to stiffen their structure against the loads induced during such a launch.

The structural requirements of the MOOSE main propellant tanks are developed through the analysis of the loading created both during the tanks' launch from Earth and during actual MOOSE operations while in orbit. While the categories of the loading created during these times are the same, the magnitudes of the loads are quite different. The loading categories are as follows:

1) Internal Pressure
2) G-Loading
3) Vibration Loading
4) Acoustic Loading

Table 5.10.a below illustrates the difference in the maximum magnitudes of these loadings between launch vehicle operations and MOOSE operations.

|  | Launch Vehicle | MOOSE Operations |
|---|---|---|
| Internal Pressure | needed for stiffening[3] | 2.6 MPa |
| G-Loading | 6.5 g's (empty) | 2.0 g's (93.6% empty) |
| Vibration Loading | 35 Hz | 35 Hz[4] |
| Acoustic Loading | 140 dB | 140 dB[5] |

Table 5.10.a Critical Structural Loading for Main Propulsion Tanks

### 5.10.2 Analysis

The first step towards developing the appropriate thickness for the main propulsion tanks was to determine the critical loading from the possibilities illustrated in Table 5.10.a. Initial calculations using the internal operating pressures of the main

propellants made the internal pressure loading an unlikely candidate. The analysis then continued on to address the G-Loading and Vibration Loading in the form of a trade study to determine which loading dictated the greater tank thickness. Since the G-loading during the delivery stage of the tanks to Space Station is significantly higher than the G-Loading during MOOSE operations with a similar configuration, it is quickly realized that, in terms of G-Loading, the selected launch platform creates the critical load.

Appendix A.5.7 illustrates, in detail, the trade studies performed to determine which was the critical load between G-Loading and Vibration Loading. Appendix A.5.7 also illustrates the trade study between the two candidate materials for the tank structure, Al-1100 and Ti-6Al-4V. This material trade study analysis was conducted with the single criteria of mass optimization. Al 1100-0 was chosen as a starting point because of the necessity of its use in the holding of hydrazine for the reaction control system. Al 1100-0 is resistant to the corrosive effects of hydrazine. To maintain uniformity of design, Al 1100-0 was then analyzed for use in all of the tank systems. Ti-6Al-4V was used as a comparison to determine if its positive material properties (high modulus with relatively low density) would offer a mass savings for the system. Both candidate materials were tested under the induced G-Loading and Vibration Loading from the launch vehicle. The material chosen was selected to perform under these loading with the minimum of mass increase to the overall MOOSE configuration.

### 5.10.3 Results

As Appendix A.5.7 shows, the vibration loading was the critical load and the best choice of material for the optimization of the MOOSE configuration mass was Al-1100. The plots of fundamental frequency versus tank thickness are shown below in Figure 5.10.a and Figure 5.10.b for the tank configuration used. Figure 5.10.a shows this plot for the liquid hydrogen fuel tanks. The liquid hydrogen tanks have an internal radius of 1.22 meters.[6]
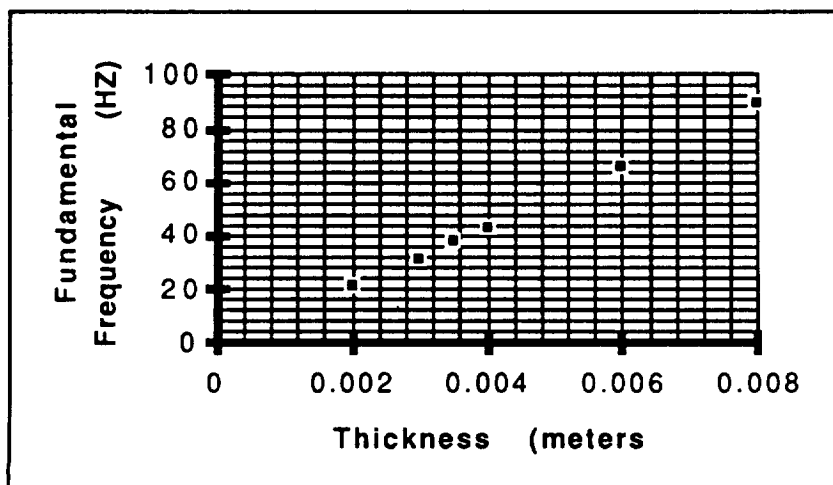


Figure 5.10.a Fundamental Frequency for Liquid Hydrogen Tanks

Figure 5.10.b shows this plot for the liquid oxygen oxidizer tanks. The liquid oxygen tanks have an internal radius of 1.077 meters.
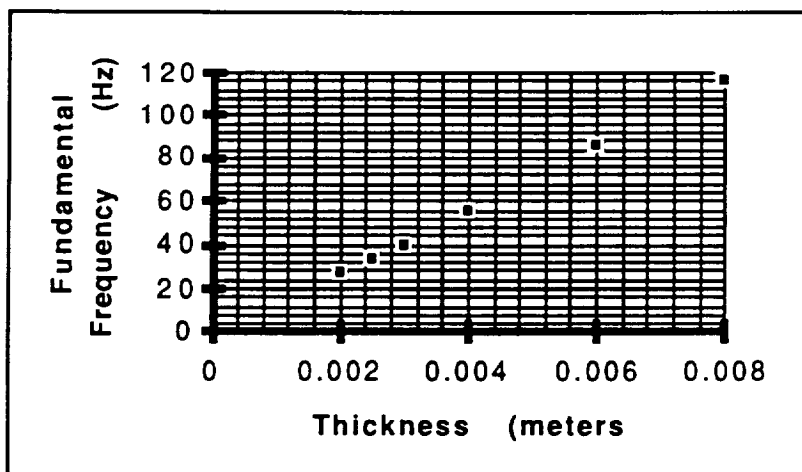


**Figure 5.10.b** Fundamental Frequency for Liquid Oxygen Tanks

Table 5.10.b below shows the required thickness for both the liquid hydrogen and the liquid oxygen tanks based on the data calculated in Figure 5.10.a and Figure 5.10.b. Table 5.10.b also shows the mass of each tank using these thicknesses with Al-1100 as the selected material for the tank walls. The MOOSE vehicle has two fuel tanks and two oxidizer tanks for its main propulsion configuration.

|  | Liquid Hydrogen Tanks | Liquid Oxygen Tanks |
|---|---|---|
| Required Thickness | 3.5 mm | 3.0 mm |
| Calculated Mass | 178 kg | 99 kg |

**Table 5.10.b** Main Propulsion Tank Thicknesses and Masses

### 5.10.4 Tank Integration to Central Spine Truss

Each of the main propulsion tanks has a 10 cm x 5 cm Al-1100 disk with threads around its surface area which is part of the tank structure located at the top of each of the tanks. Using this threaded disk, the tanks will be integrated with the central support truss by means of a cantilever tube which has a garden hose-like connector on its end. At Freedom, the main propulsion tanks are simply positioned and the adapters on the ends of the beams are thread onto the receptacle disks on each of the tanks. The bottom of the tanks rest on the aero-brake support arches. Due to the proximity of the tanks to the back surface of the aero-brake, the tanks will be wrapped with a thermal protection foil to allow the Al-1000 alloy to operate at its actual yield strength. Detailed drawings of the main propulsion tanks' structure can be found in Figure 5.10.c. All dimensions are in meters. Analysis and drawings of the beams which interfaces the tanks with the rest of the MOOSE vehicle are found in the aero-

brake section. The mass of the threaded disk interface for each tank is 1.1 kg. Adding these interface disks to the tanks brings the hydrogen tank mass to a final design total of 179 kg and the oxygen tanks to a final design mass of 100 kg.
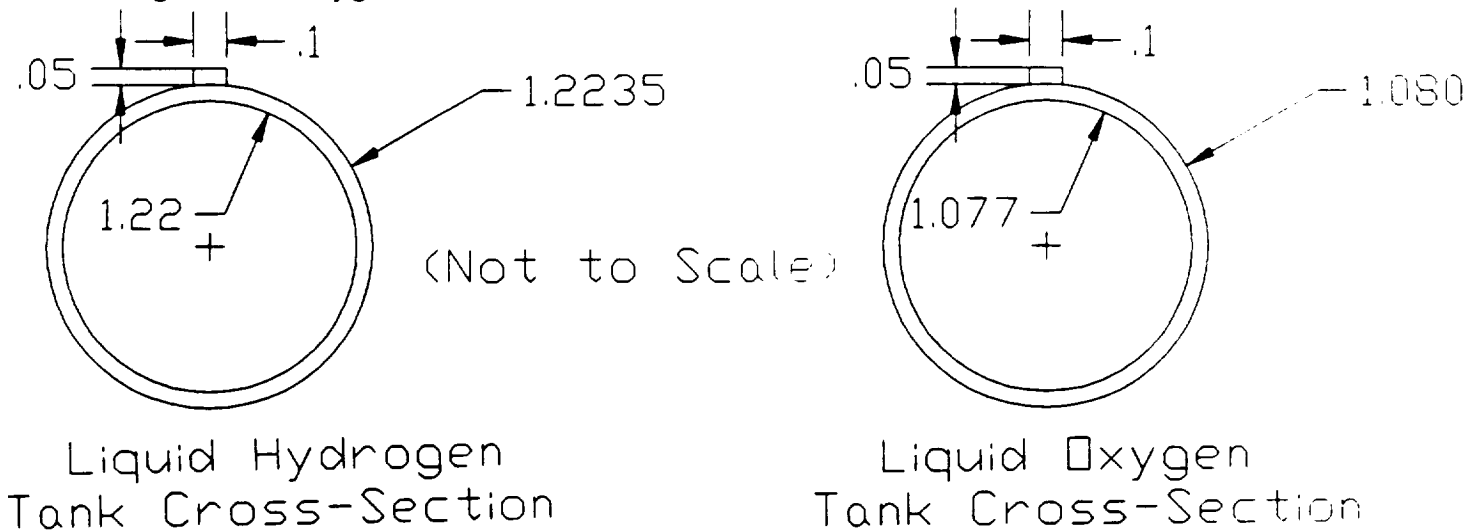


Figure 5.10.c Tank Structural Drawings

## 5.11 Introduction to the Reaction Control System

### 5.11.1 Requirements for the Selection of a Reaction Control System

The criteria for selecting an appropriate Reaction Control System (RCS) are derived from the MOOSE project's mission requirements. The fact that MOOSE is a manned vehicle requires three-axis stabilization and this places high demand on the reliability of the RCS. The baseline mission requirements of the RCS include the following capabilities: maneuverability in separating and docking with Space Station Freedom (SSF), rendezvous capability with the satellite to be serviced, control during grappling and release of the satellite, attitude control in maintaining proper orientation for the navigation and guidance sensors, counteracting adverse environmental / external / internal torques and disturbances, orienting the MOOSE for main engine burns and aerobraking, desaturating the control moment gyros, and collision avoidance.

Another critical requirement of the RCS is to avoid exhaust plume contamination of the SSF and the malfunctioning satellite hardware. In addition to complementing the main propulsion system in transferring the MOOSE to the appropriate satellite orbit, the RCS must be capable of handling small $\Delta V$ missions when the vehicle is in the "cab-only" mode, and must be capable of providing the high accuracy control and the necessary translational and rotational maneuvers as defined above.

### 5.11.2 RCS Systems Analysis

Servicing satellites in GEosynchronous Orbit (GEO) is the primary goal of the vehicle,

and a baseline ΔV budget was determined to meet the transfer requirements from the Low Earth Orbit (LEO) of the SSF out to the malfunctioning satellite and back. The overall ΔV requirements of the RCS system are given in Table 5.11.a.

Requirements of the primary RCS system include:

| | | |
|---|---|---|
| From LEO: | Mid Course Correction | 015 m/s |
| | Orbit Trim | 009 m/s |
| At GEO: | Satellite approach | 054 m/s |
| | Satellite departure & maneuver for main engine burn | 054 m/s |
| From GEO: | Mid Course Correction | 015 m/s |
| | Aerobrake Maneuver | 067 m/s |

Requirements of the secondary RCS system include:

| | | |
|---|---|---|
| From LEO: | Separation from Station | 003 m/s |
| At GEO: | Satellite Servicing | 050 m/s |
| From GEO: | Rendezvous & Docking | 018 m/s |

Table 5.11.a  ΔV requirements for the Primary and Secondary RCS

A more detailed break down of the baseline ΔV budget for all propulsion systems is given below.

| Maneuver | ΔV (m/s) | Propulsion System |
|---|---|---|
| Separation from Station | 0003 | COLD |
| GEO Transfer Injection | 2400 | MAIN |
| Main Propulsion Reserve | 0030 | MAIN |
| Mid Course Correction | 0015 | rcs |
| Attitude Control Reserve | 0005 | rcs |
| GEO Circularization | 1762 | MAIN |
| Main Propulsion Reserve | 0030 | MAIN |
| Orbit Trim | 0009 | rcs |
| GEO Operation | 0054 | rcs |
| GEO Operation | 0050 | COLD |
| GEO Operation | 0054 | rcs |
| LEO Transfer Injection | 1844 | MAIN |
| Main Propulsion Reserve | 0030 | MAIN |
| Mid Course Correction | 0020 | rcs |
| Attitude Control Reserve | 0005 | rcs |
| Aerobraking Maneuver | 0067 | rcs |
| Attitude Control Reserve | 0020 | rcs |
| LEO Circularization | 0122 | MAIN |
| Attitude Control Reserve | 0020 | rcs |
| Rendezvous & Docking | 0018 | COLD |
| Attitude Control Reserve | 0010 | COLD |

COLD=Secondary RCS
rcs=Primary RCS
MAIN=Main Propulsion

Table 5.11.b  Baseline ΔV Budget for LEO-GEO-LEO Mission with Aerobraking
and the Respective Propulsion System Utilized

## 5.11.3 Disturbance Torques

The space environment in which MOOSE will travel is not torque-free so external perturbations will cause deviations in the spacecraft's stability and intended trajectory. Environmental torques include aerodynamic, gravity gradient, solar pressure, and magnetic.

Aerodynamic torques are dominant at altitudes below 800 km and are due to the strong temperature gradients in the Earth's thermosphere which increases the atmospheric density at these lower altitudes. Increased temperatures due to ultraviolet heating from the Sun increases the density in this region due to the increased pressure from the thermosphere's expansion.[7] The aerobrake maneuver will be initiated at an altitude of approximately 100 km, and the RCS must counteract any torques resulting from a center of pressure offset from the center of gravity (c.g.).

The Earth's gravitational force is nonuniform which produces gravity gradient torques on non-symmetrical spacecraft orbiting the Earth. The magnitude of the torques vary with the inverse cube of the distance from the geocenter to the c.g. of the vehicle. Gravity gradient torques are minimized when the long axis of the spacecraft is directed along the nadir, otherwise, orientations deviating from this cause the vehicle to experience torques. Throughout the mission, the vehicle's orientation will vary to meet the demands of the guidance and navigation sensors, and to properly orient the MOOSE for main engine LEO/GEO injection burns, efficient satellite repair, and aerobraking. The sun and cone sensors require specific spacecraft orientations in order to provide the optimum accuracy in sensing the vehicle's attitude and meeting navigational control requirements.

The vehicle's exposure to solar pressure torques will occur primarily at GEO although the disturbance torques occur throughout the solar system. Solar pressure torques will be experienced whenever any component of the vehicle is exposed to the sun's radiation. Utilizing the aerobrake as a shade structure whenever possible will minimize the number of surfaces exposed to the sun's radiation and will help minimize the radiation exposure time of the astronaut.

Magnetic torques are the result of interactions between the spacecraft's residual magnetic field and the geomagnetic field.[8] Disturbances are primarily from the spacecraft's magnetic moment.

## 5.11.4 Primary RCS Propulsion Systems Considered

The various RCS systems considered had to meet the 1993 proven technology cut-off date, so analyses were conducted on the monopropellant and bipropellants found in Table 5.11.c.[9]

(o/f) = oxidizer mass flow rate to fuel mass flow rate
(mono) = monopropellant, no oxidizer
N2O4 = Nitrogen Tetroxide
UDMH = Unsymmetrical Dimethylhydrazine
50-50 = 50:50 mixture of UDMH and Hydrazine
LH2 = Liquid Hydrogen

| Propellant Name (oxidizer/fuel) | Isp (sec) | Mass Mixture Ratio (o/f) | Specific Gravity (g/cm$^3$) | Molecular Weight (kg/mol) |
|---|---|---|---|---|
| Hydrazine (mono) | 240 | - | 1.023 | 13.0 |
| Oxygen & UDMH | 295 | 1.39 | 0.96 | 19.8 |
| Oxygen & N2H4 | 301 | 0.74 | 1.06 | 18.3 |
| N2O4 & 50-50 | 288 | 2.00 | 1.21 | 22.6 |
| Fluorine & LH2 | 398 | 4.54 | 0.33 | 08.9 |

Table 5.11.c  Primary RCS Propellant Contenders and their Chemical Composition

From the baseline ΔV budget sequence, total masses were calculated for each of the potential primary and secondary RCS propellants. The sequential calculations are found in appendix A.5.9, and the final results are shown in Figures 5.11.a and 5.11.b. Referring to these figures, the liquid fluorine (LF) and liquid hydrogen (LH2) primary bipropellant combination has the lowest mass requirements (irrespective of the cold gas used) relative to the other potential propellants, followed by the hydrazine derivative bipropellant combinations, followed by the monopropellant hydrazine.

Propellant Masses with Helium as Cold Gas
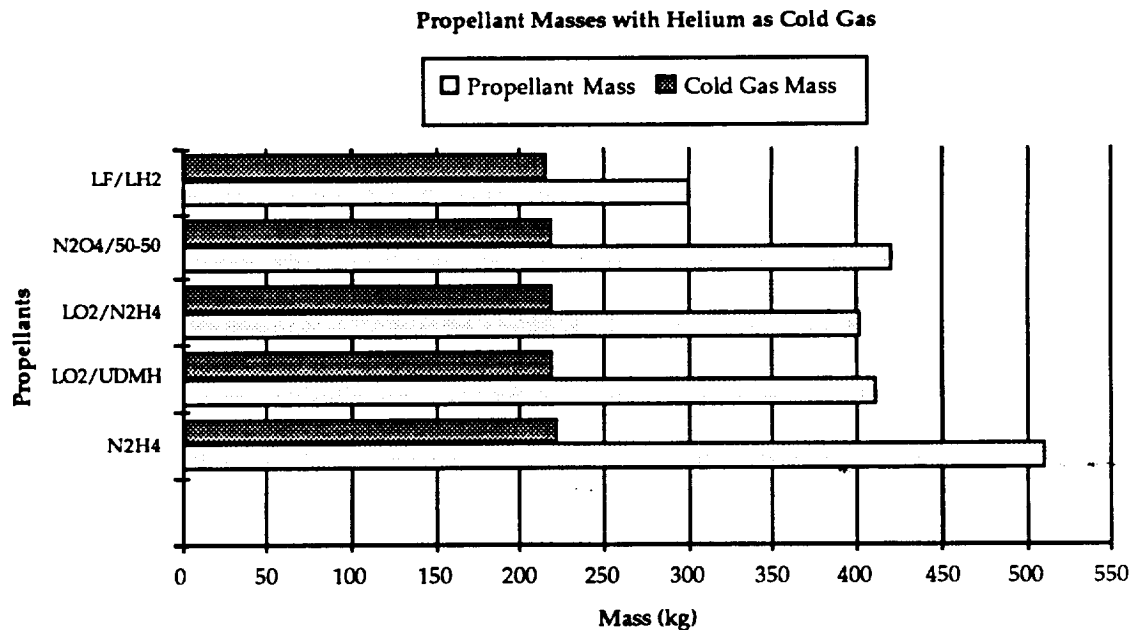


Figure 5.11.a  Primary and Secondary RCS Propellant Mass Requirements
Utilizing Helium as Cold Gas for Secondary RCS

## Propellant Masses with Nitrogen as Cold Gas
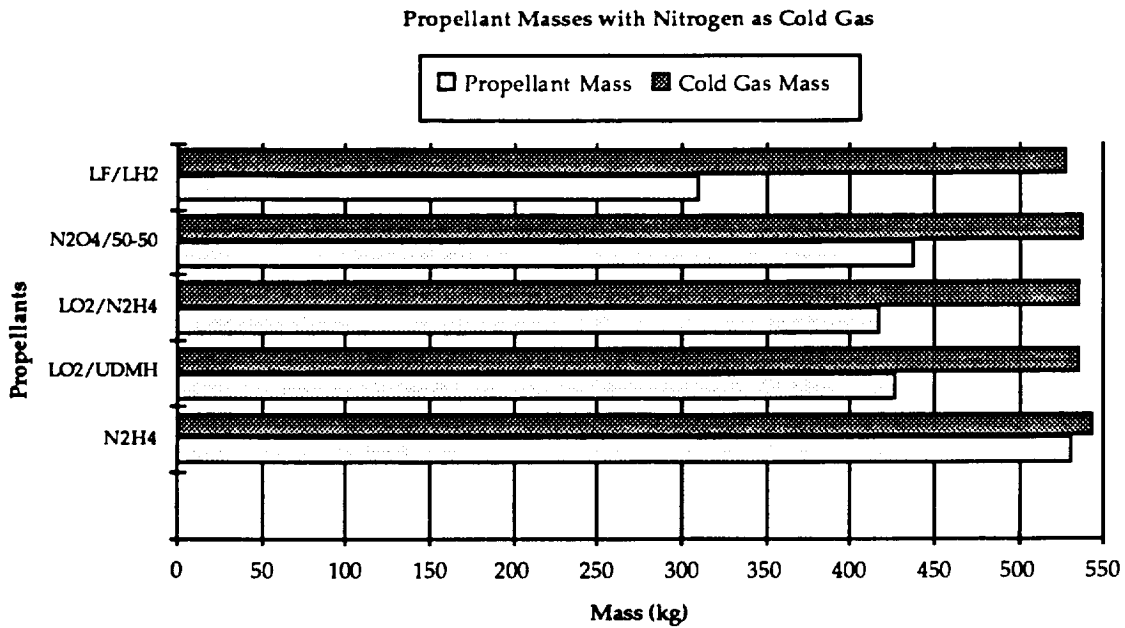


Figure **5.11.b** Primary and Secondary RCS Propellant Mass Requirements
Utilizing Nitrogen as Cold Gas for Secondary RCS

Figure 5.11.c shows the variation in initial vehicle mass in relation to the Cold Gas Secondary RCS propellants used. The dry mass of the vehicle was assumed to be 3000kg.

## Relationship between Total Vehicle Mass and Cold Gas Utilized
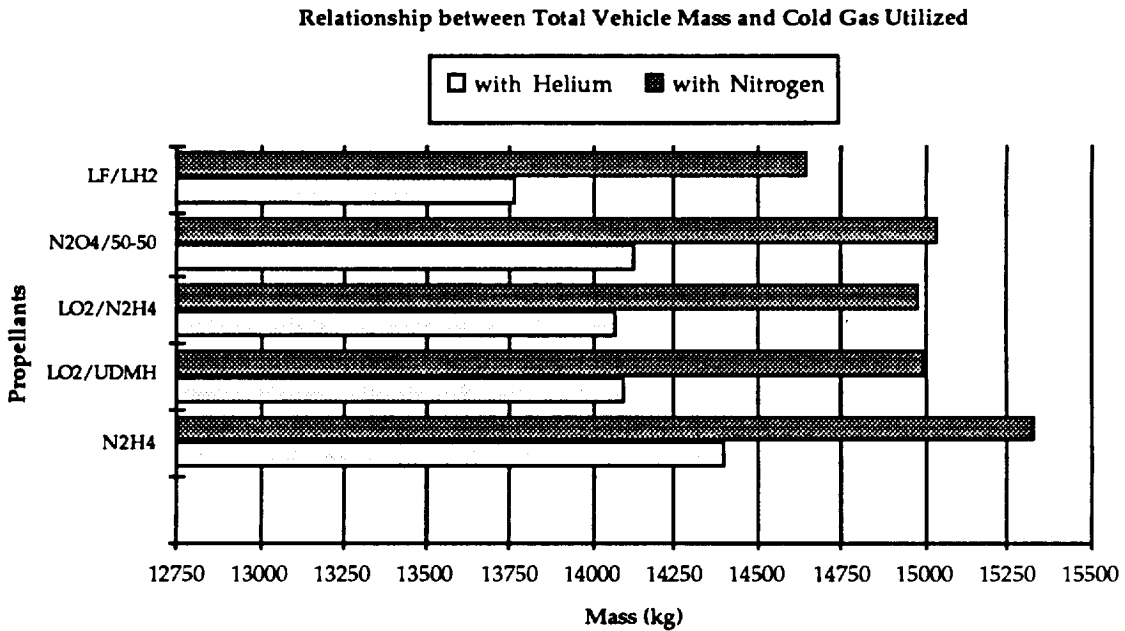


Figure **5.11.c**  Total Vehicle Mass In Relation to (Cold Gas) Secondary RCS Propellant Utilized

One of the driving factors in selecting the Primary and Secondary RCS propellants is mass, but it is not the only factor, thus, further consideration is given to how well the potential propellants uphold most, if not all, aspects of the mission and RCS requirements. The results of Figures 5.11.a,b,c do not fully demonstrate the most appropriate Primary RCS propellants to use for MOOSE, as various aspects of the mission requirements are violated by the bipropellants demonstrating the lowest individual propellant and total vehicle mass requirements.

Utilizing liquid fluorine as an oxidizer was avoided because it is a highly toxic, reactive, and corrosive substance which threatens not only the material integrity of MOOSE, but also that of the satellite. Although it has a high specific gravity and specific impulse, its threat of contamination and reaction with the MOOSE vehicle and satellite surfaces, in addition to it only being used in experimental thrusters, discounts its use as a Primary RCS oxidizer. Systems with lower specific impulse were favored due to their less harmful exhaust products.

The remaining potential Primary RCS propellants were placed into either the bipropellant or the monopropellant group. The total mass requirements for the propellant combinations in the bipropellant group are approximately 410 kg, while the hydrazine monopropellant mass is approximately 100 kg greater. Due to the difficulty of storing cryogens in space, liquid oxygen as an oxidizer for the two bipropellant combinations shown in the above three figures was not favored since storability could be achieved with the other two potential propellants.

Based on the magnitude of the environmental torques and the worst-case slew calculations, found in appendix A.5.8, the maximum required thrust for a given thruster is on the order of 500 N with coupled thruster firings. This magnitude of thrust is at a level where monopropellant hydrazine thrusters have proven reliability, but also, hydrazine thrusters are advantageous because of the simplicity of the thruster design and propellant feed system, relatively clean exhaust plume than many of the other propellants in contention, and minimal contamination of the catalyst bed with the use of high purity grade hydrazine containing less than 0.003% aniline and 0.005% carbonaceous materials. Its standard use as RCS thrusters on most satellites makes it readily available and has proven reliability on satellites orbiting for more than five years. Also, the technology is available for refueling hydrazine tanks on-orbit which will eliminate tank replacement costs for refueling.

### 5.11.5 Hydrazine Monopropellant Thrusters

The Primary RCS thrusters utilize liquid anhydrous hydrazine ($N_2H_4$) operating in a blow down mode with helium (He) as the pressurant gas. The blow down mode means the pressurant gas and the monopropellant are stored in the same tank and as the propellant is expelled from the tank the pressure decreases and causes a gradual decrease in the net thrust. The advantage of this feed system is the simplicity of the design.

As a monopropellant requiring no oxidizer for combustion, $N_2H_4$ spontaneously decomposes when passed over a catalyst, like substrate pellets of iridium on alumina, and produces hot gases which are expelled through the nozzle. The reaction is a two step process with the first being highly exothermic and the second being endothermic:

$$3N_2H_4 \quad -> \quad 4NH_3 + \quad N_2 \qquad \text{(step 1)}$$
$$4NH_3 \quad -> \quad 2N_2 + \quad 6H_2 \qquad \text{(step 2)}$$
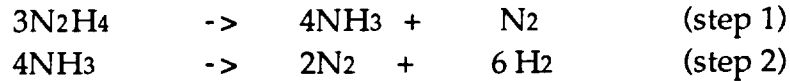
The first step always goes to completion but only a fraction of the ammonia is dissociated in step 2. As a result, these two steps can be combined into one reaction as a function of ammonia dissociation (x = 0.0 - 1.0):

$$3N_2H_4 \quad -> \quad 4(1-x)NH_3 + \quad (2x+1)N_2 + \quad 6xH_2$$

Based on the configuration of the hydrazine thrusters selected, the maximum Isp = 240 seconds relates to an ammonia dissociation of x=0.6, typical for RCS thrusters. Table 5.11.d shows the operating parameters at this value of x.

| | |
|---|---|
| Ammonia Dissociation (x) | 0.6 |
| Adiabatic Reaction Temperature | 1200 °K |
| Vacuum Specific Impulse | 240 seconds |
| Characteristic Exhaust Velocity | 1300 (m/s) |

Table 5.11.d Relationship between Ammonia Dissociation and Thruster Operating Parameters [10]

In order to verify that the mass budget determined by the ΔV budget would meet the requirements of the mission, a 20 hour (72,000 sec) estimated on-time for the primary RCS system was considered. When firing either of the two RCS's, thruster firings will be coupled and occurring at 33 second intervals with one second pulse time. This relates to 1091 pulses and a mass requirement of 249 kg per coupled thruster. To determine the maximum mass requirement, the equation Thrust = mass flow * specific impulse was utilized assuming maximum possible thrust of 500 N and minimum specific impulse of 223 seconds. The total impulse was determined to be 399,306 Ns. Details of the calculations are in A.5.10. Table 5.11.e describes the operational parameters of the Rocket Research Company's MR-104C thruster.

| | |
|---|---|
| Propellant | Hydrazine |
| Catalyst | Shell 405/LCH-202 |
| Thrust/Steady State | 572-205 N |
| Feed Pressure | 420-100 psia |
| Chamber Pressure | 155-56 psia |
| Expansion ratio | 53:1 |
| Mass Flow Rate | 0.241-0.0907 kg/s |
| Weight | 1.864 kg |
| Total Pulses | 1742 |

| | |
|---|---|
| Number per spider truss | 4 |
| Total mass per spider truss | 7.456 kg |
| Number per lower truss | 1 |
| Total mass per lower truss | 1.864 kg |
| Total number of thrusters | 24 |
| Total mass of thrusters | 44.74 kg |

Table 5.11.e  Individual Hydrazine Monopropellant Thruster Information
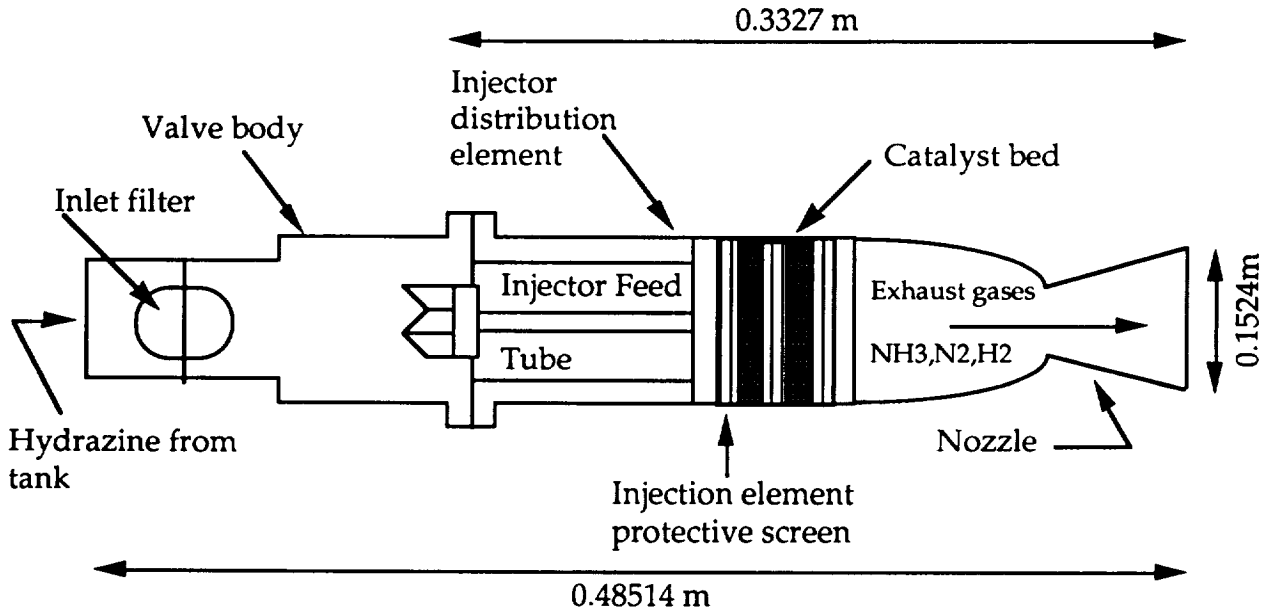


Figure 5.11.d  Hydrazine Thruster Schematic

## 5.11.6 Secondary Cold Gas Thrusters

The secondary RCS thrusters are utilized during maneuvers where avoidance of SSF or satellite hardware contamination and corrosion is critical. These maneuvers include separation and docking with the SSF and all GEO operations about a malfunctioning satellite. The use of helium as both a pressurant and a cold gas thruster is based on the mass calculation totals and the average savings of 1000 kg in overall vehicle mass. The specific impulse of the helium is 179 seconds as opposed to nitrogen which is only 76 seconds. This variation in masses offsets the advantage of nitrogen's higher density.

Based on one hour operations for satellite grappling and six hours for satellite repairing, 10 hours (36,000 sec) of continuous pulse on-time was considered in order to determine the mass budget for the secondary RCS thrusters. The rise and decay time of the thruster is 9.87 msec with a one second pulse and a ten second interval between firings. Coupled thruster firings will place an 1800 second pulse and a 91 kg mass

requirement per thruster. The final mass requirement is 182 kg with a 22% reserve. Table 5.11.f outlines Moog Inc. 89 N thruster and Figure 5.11.e is a schematic of a single seat cold gas thruster engine.[11]

| | |
|---|---|
| Thrust | 89 N |
| Service Fluid | Helium |
| Pressure @ Thrust | 1000 psi |
| Expansion Ratio | 25:1 |
| Exit Diameter | 3.175 cm |
| Response Time | 5.95 msec |
| Pitot Closing | 3.92 msec |
| Power Requirements | 38 W @ 28 VDC |
| Cycle life | 10 000 min |
| Temperature Range | 277-322 K |
| Weight (each) | 85 g |
| | |
| Number per spider truss | 7 |
| Total mass per spider truss | 0.595 kg |
| Number per lower truss | 3 |
| Total mass per lower truss | 0.255 kg |
| Total number of thrusters | 40 |
| Total mass of thrusters | 3.4 kg |

**Table 5.11.f** Individual Cold Gas Thruster Information
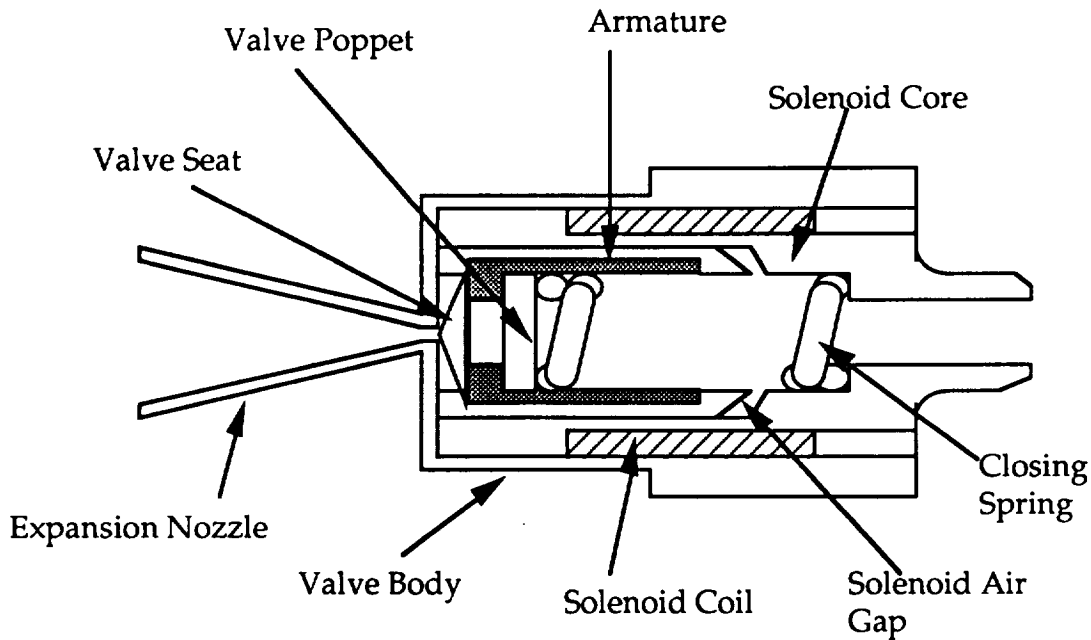


**Figure 5.11.e** Single Seat Cold Gas Thruster[12]

## 5.11.7 Propellants, Tanks and Masses

The equation used to properly size the primary RCS propellant tanks was

$$R = ( V_{gi} + V_p )/ V_{gi}$$

where R is the blow down ratio, $V_{gi}$ is the initial pressurant gas volume and $V_p$ is the propellant volume. To find the initial helium pressurant volume, R was derived from the ratio of beginning of life to end of life pressure of the hydrazine thrusters as noted in Table 5.11.e, and the value is 4.2. The volume of the propellant was determined from the product of propellant mass (m) and propellant density ($\rho$ ), where $V_p$ = m* $\rho$. The mass of the hydrazine propellant is 512 kg and the density is 1.023 g/cm$^3$. The total volume for hydrazine propellant is 0.5005 m$^3$ and the backed out total pressurant helium volume is 0.1564 m$^3$ with a total helium mass of 10.83 kg. To maintain some symmetry about the long axis of the vehicle and decrease the size of the tanks, two hydrazine/pressurant tanks were designed to be placed within the spider truss structure at a radius of 0.428 m, excluding tank thickness. The hydrazine and helium mass within each tank is 261.42 kg.

The helium secondary RCS thrusters function in a pressure regulated mode. The equation of state, P*V= m*R*T was utilized to determine the helium tank volume. Variations in tank pressure were considered to drive down the tank volume and radius. At P=6000 psi, R= 2077.3 J/kg K, T = 300 K, and m= 223 kg, the volume is 3.357 m$^3$ which is distributed among four tanks with each tank's volume being 0.8392 m$^3$ and a radius of 0.585 m each, excluding tank thickness.

## 5.11.8  RCS Spider Truss

The RCS Spider truss serves as a platform for the MOOSE RCS. It houses the RCS tanks within its members and acts as a boom for the reaction control nozzles to ensure their operation as far away from the c.g. of the MOOSE vehicle as possible. The RCS Spider Trusses extend approximately 2.6 meters from the center line of the MOOSE vehicle. The trusses and the avionics box are an integrated structure which attaches to the bottom of the MOOSE crew cabin. This integrated structure stays with the crew cabin after separation from the main spine truss and aero-brake modules for service missions concerning the Space Station itself. During this utilization of MOOSE, the reaction control system will serve as the main engine and provide mobility and maneuverability for the vehicle.

## 5.11.8.1  Requirements

As with the main propulsion tanks and with all of the structural components of the MOOSE system, the RCS Spider Truss must withstand the loading induced by both the launch from Earth and the actual operations while integrated with the rest of the

MOOSE system. However, for the spider truss, the loading from its delivery from Earth will not be the critical load. The spider truss can be positioned horizontally in the launch vehicle and is therefore not susceptible to buckling along its major axis. The critical requirements for the RCS Spider Truss will be created during MOOSE operations. First, the spider truss must contain the RCS tanks within its framework. It also must provide hard points for the RCS nozzle attachments. Most importantly, the spider truss must maintain its integrity performing the above mentioned tasks under a 2 g loading sustained during the third burn while MOOSE performs its orbital transfer. Also, the spider truss must not deflect more than 1 mm at its tip to prevent difficult corrections while the reaction control system is active. And finally, the spider truss must sustain the vibration loading created by the MOOSE propulsion system which has been set at 35 Hz as mentioned in the analysis of the main propulsion tanks. As with all MOOSE systems, mass is another critical issue for the design of the spider truss. Optimizing to the least possible mass while still working within the above requirements will be a primary goal of the spider truss design.

**5.11.8.2 Analysis**

Before continuing with a description of the analysis performed on the spider truss structure, it will be helpful to refer to Figure 5.11.f for the geometric configuration of the spider truss and the nomenclature used throughout the description of its analysis.
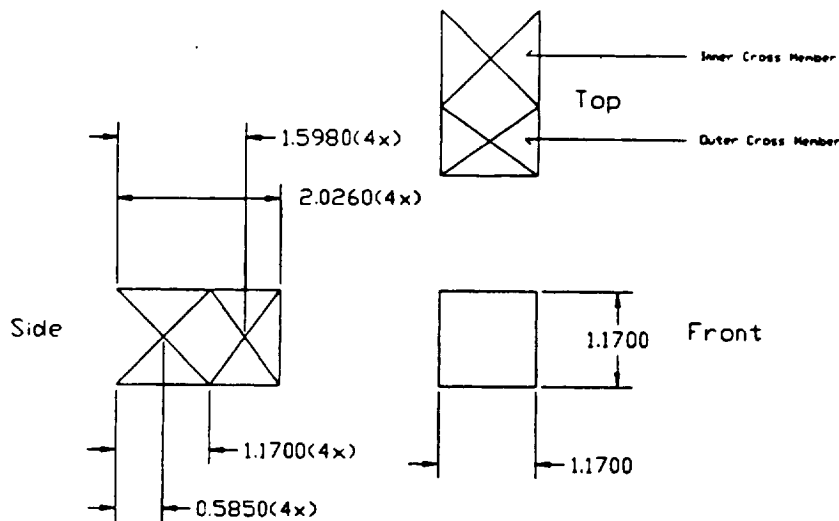


Figure 5.11.f Spider Truss Geometry and Nomenclature

The worst case loading scenario has been developed to be a combination of the third burn 2 g inertial loading and a simultaneous firing of a 500 N RCS nozzle in a direction parallel to the inertial loading. A factor of safety of 1.5 will be used in this

5 - 31

analysis. Material selection has been made to be high-strength graphite/epoxy with a 45 degree fiber orientation to ensure the composites strength in bending. Bending will be the primary concern for the spider truss loading scenario since it is similar to a cantilever beam problem. The maximum stress will not exceed two-thirds of the material's ultimate load strength as specified by Raymer.[13] The maximum deflection should not exceed the value given in the requirements section.

Figure 5.11.g illustrates the loading diagram for the spider truss.
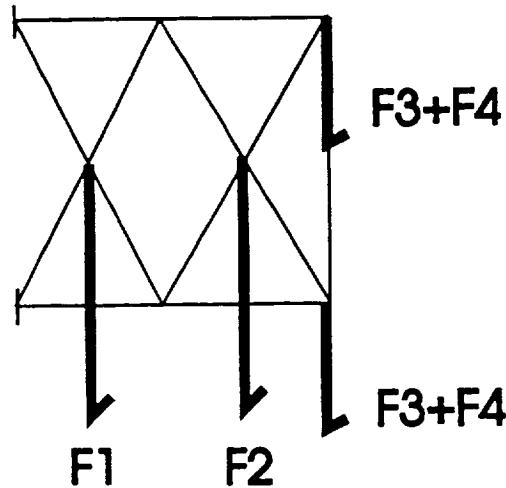


**Figure 5.11.g** Spider Truss Loading Diagram

Table 5.11.g is the corresponding load table for the spider truss.

| | Loads[14] | Source |
|---|---|---|
| F1 | 4352 N | RCS helium tank (2 g's) |
| F2 | 4215 | RCS fuel tank (2 g's) |
| F3 | 250 N | RCS nozzle firing |
| F4 | 136 N | RCS nozzle (2 g's) |
| Inertia | 3 g's | Orbital 3rd Burn |

**Table 5.11.g** Spider Truss Loading Table

## 5.11.8.3 Results

The resulting configuration for the spider truss consists of two different cross sections. The inner and outer cross members both have circular cross sections of outer radius 1.25 cm and inner radius of 1.0 cm. The remaining spider truss members have circular cross sections of outer radius 7 mm and inner radius 5 mm. The resultant maximum stress using this configuration can be found in the upper inside corner of the inner cross member. Its value is 39.57 MPa. This stress is well below the recommended two-thirds of the ultimate strength of the spider truss's material. The maximum tip

deflection is 1.15 mm. This value is also an acceptable value for the maximum tip deflection. Although exceeds the value described in the spider truss requirements section, there is a very small difference considering the rarity of such a worse case loading scenario. With this configuration, the mass per spider truss is 9.36 kg. Therefore, the total mass for all four spider trusses is 37.5 kg.

Actual configuration trade studies can be found in appendix A.5.13. Also included in appendix A.5.13 is a more detailed description of the analysis procedure used to arrive at the final design configuration for the RCS Spider Truss.

### 5.11.8.4 RCS Spider Truss Integration with MOOSE Vehicle

The RCS Spider Truss integrates directly with the avionics box. The ends of the spider truss are fixed to this box by means of aluminum sleeves welded to the avionics box itself. The composite rods of the spider truss are bonded within the aluminum sleeves and, hence, fixed at their ends. The avionics box is then pinned to the bottom of the MOOSE crew cabin. This is a permanent attachment point. The bottom of the avionics box is attached to the main spinal truss of the MOOSE vehicle. This attachment point serves as the detach point for MOOSE operations around Space Station where it need not employ its main propulsion system or aero-brake.

### 5.11.9 Primary and Secondary RCS Feed Systems

Hydrazine freezes at $0^\circ$ C, so line heaters will be placed where the fuel lines split to each individual thrust chamber. The thrusters themselves will also require heaters to maintain operating temperatures, which will be measured by thermocouples in each thruster (see Figure 5.11.i).
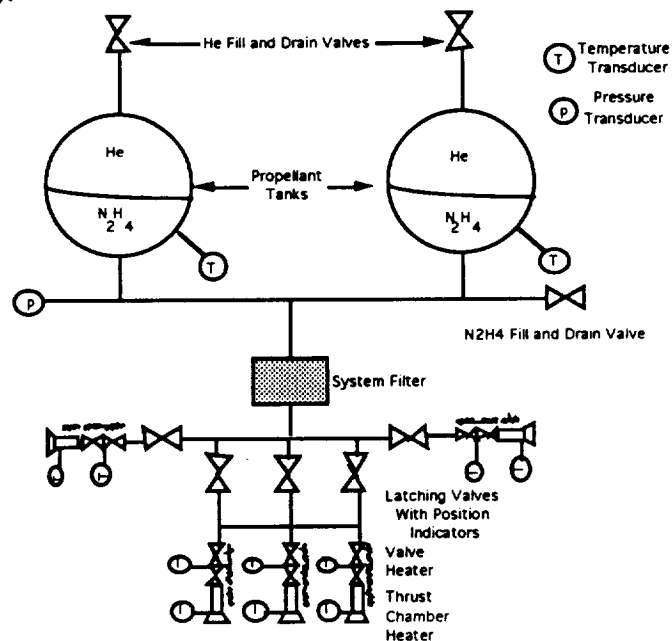


Figure 5.11.i  Hydrazine RCS Thruster and Tank Configuration

There will be a total of 64 thrusters, 24 Primary Hydrazine thrusters and 40 Secondary Helium thrusters. The Hydrazine primary RCS tanks will be cross-linked to allow fuel from either of the two tanks to flow to any thruster, regardless of location, in the event that a problem arises with either of the tank's valves or there is a fuel level difference between the tanks.

Fuel will flow from the tank, through a filter to extract any pressurant helium gas, and through two valves to reach the thruster reaction chamber. On each spider truss boom, there is a pressure transducer between the filter and the first valve to estimate the fuel remaining in the tanks.

An additional valve will be associated with each thruster. The valve is at the reaction chamber interface, as shown in Figure 5.11.d, to allow immediate cutoff of any fuel to the thruster reaction chamber for absolute, fine control of the thrust level. Thus, during operation the valve will be opened and the fuel flowing to the chamber will be controlled with this valve on each of the individual thrusters.

In the Secondary RCS tanks, the helium is stored at 6000 psi and is self pressurizing, thus, heaters are not required because the helium is a gas at low pressure for any temperature likely to be encountered in operation. The helium will feed to a pressure regulator that will maintain a combustion chamber pressure of 1000 psi in each thruster.

## 5.11.10 Thruster Configurations

The primary and secondary RCS thrusters will be integrated into a thruster pod on the spider truss structure. On each pod will be 7 cold gas and 5 hydrazine thrusters. Nozzle and chamber dimensions are given in sections 5.11.5 and 5.11.6. Figure 5.11.j shows a bottom view of the spider truss structure enclosing the helium and hydrazine tanks with the thruster pods integrated at the ends of each boom.
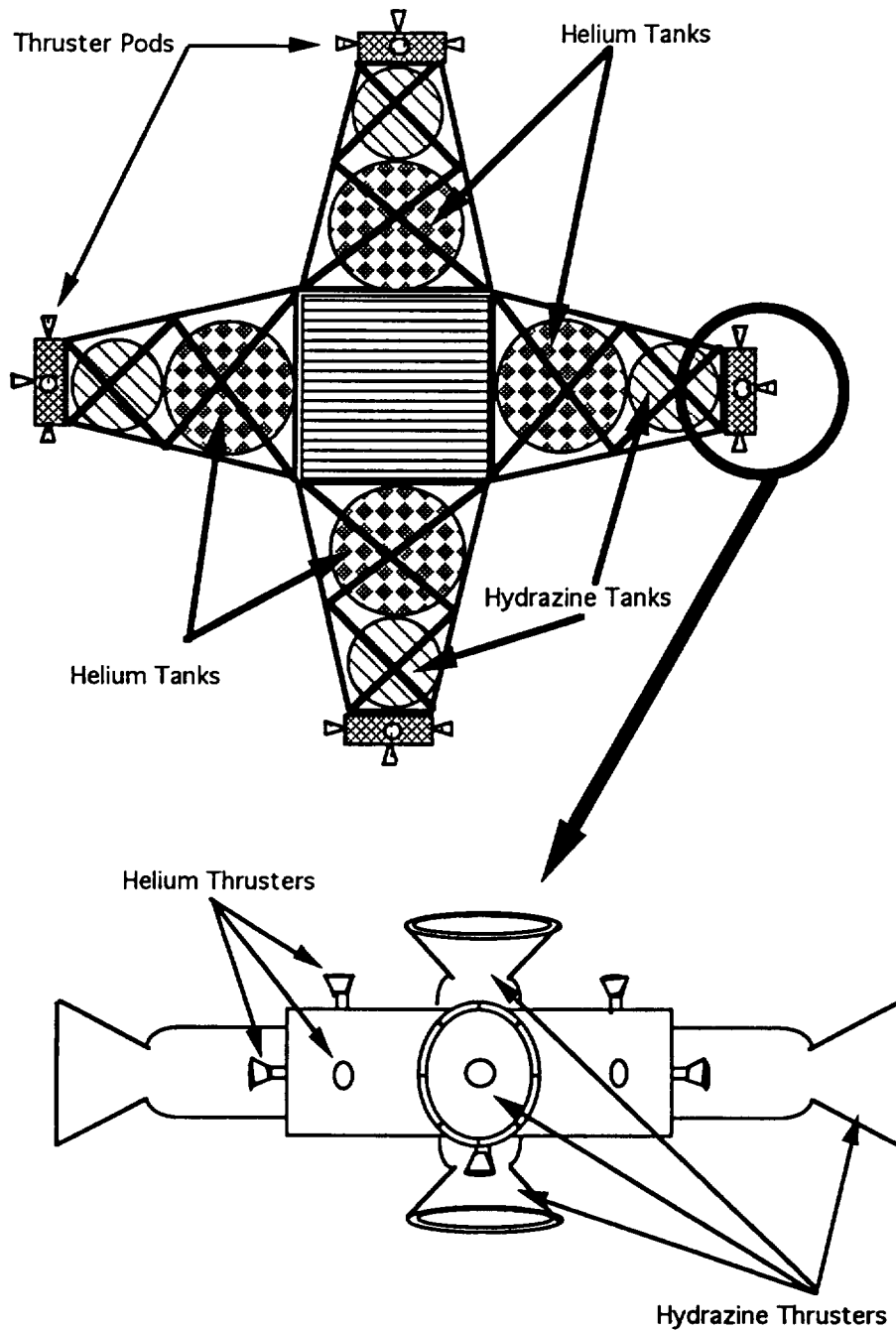
**Figure 5.11.j** Spider Truss with Primary and Secondary RCS

The configuration shown in Figure 5.11.k is of the lower truss where there will be one hydrazine and three cold gas thrusters. Again, the dimensions of the thrusters are given in sections 5.11.5 and 5.11.6.
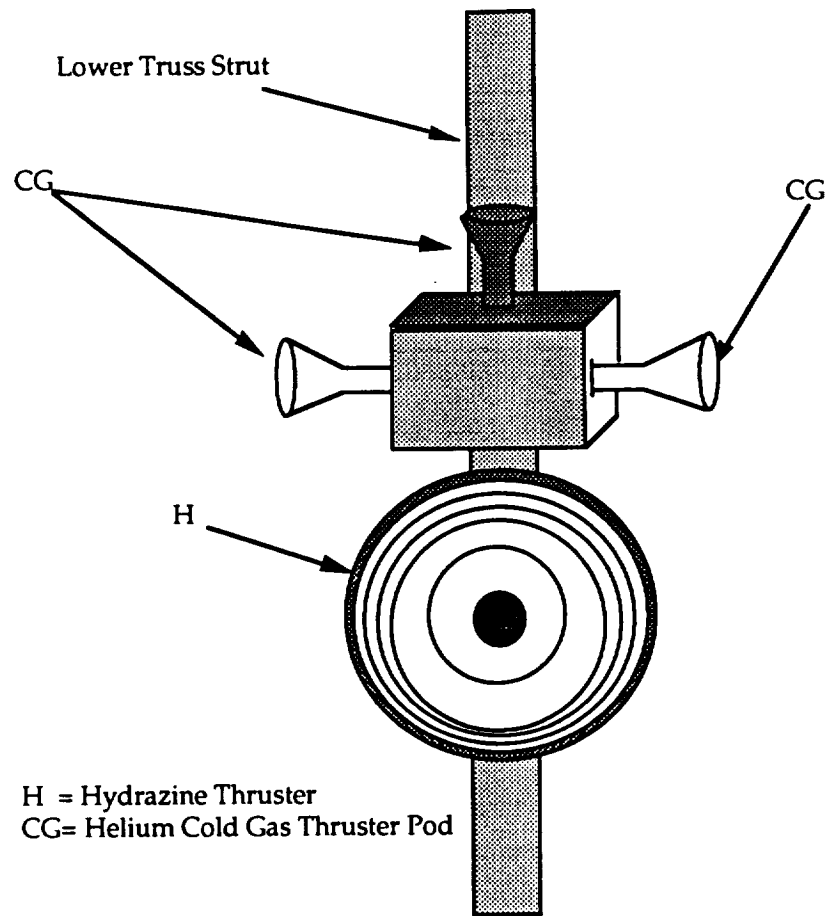
**Figure 5.11.i** Lower Truss Strut RCS Configuration

Lower Truss Strut

CG

CG

H

H = Hydrazine Thruster
CG= Helium Cold Gas Thruster Pod

---

[1] Picture taken from: Sutton, George. *Rocket Propulsion Elements: An Introduction to the Engineering of Rockets.* John Wiley & Sons, Inc. New York. 1992.

[2] Picture taken from: Huzel, D. and D. Huang. *Modern Engineering for Design of Liquid-Propellant Rocket Engines.* Progress in Astronautics and Aeronautics, V. 147. 1992.

[3] Stress stiffening beyond the scope of this tank analysis. Stress stiffening analysis recommended for final design/manufacturing iteration.

[4] Actual vibration loading induced by MOOSE operations not known. The value of 35 Hz used as general norm for safe space operation.

[5] 140 dB loading for MOOSE operation chosen to at least match Shuttle environment since launch vehicle will induce critical acoustic loading.

[6] Tank radii are derived from the volume needed to contain required propellant mass.

[7] Wertz, James R. and Wiley J. Larson, ed. *Space Mission Analysis and Design.* Kluwer Academic Publishers. Boston. 1991. p. 194.

[8] Wertz, James R. ed. *Spacecraft Attitude Determination and Control.* Boston: Kluwer Academic Publishers. Boston. 1978. p. 575.

[9] Sutton, George P. *Rocket Propulsion Elements: An Introduction to the Engineering of Rockets.* John Wiley & Sons, Inc, New York. 1992, p. 194.

[10] Rocket Research Company. *Hydrazine Handbook.* Aerospace Division, Olin Defense Systems Group.

[11] Bzibziak, R., "Miniature Cold Gas Thrusters," AIAA Paper 92-3256, July 1992, 8 pages.

[12] ibid

[13] Raymer, Daniel P. *Aircraft Design: A Conceptual Approach.* American Institute of Aeronautics and Astronautics. Washington, D.C. 1989.

[14] Factor of Safety of 1.5 used to scale loads on spider truss.

[15] Huzel, D. and D. Huang. *Modern Engineering for Design of Liquid-Propellant Rocket Engines.* Progress in Astronautics and Aeronautics, V. 147. 1992.

[16] Sutton, George. *Rocket Propulsion Elements: An Introduction to the Engineering of Rockets,* 6ed. John Wiley & Sons, Inc. New York. 1992.

[17] Wertz, James R. and Wiley J. Larson, ed. *Space Mission Analysis and Design,* 2ed. Kluwer Academic Publishers. Boston. 1991.

[18] Aero-brake maneuver thought to induce greatest G-loading at time of analysis. Actual aero-brake g-loading around 1.5 g's.

# 6.0 Avionics

## 6.1 Introduction

There are five major subsystems of the MOOSE avionics package:

1. Attitude Determination and Control System (ADCS)
2. Navigation and Tracking
3. Communications
4. Data Acquisition and Storage
5. Computation and Data Management

## 6.2 Attitude Determination and Control System (ADCS)

### 6.2.1 Selection of Spacecraft Control Type

It was determined that a three-axis control technique was required to fullfill the high accuracy pointing requirements. A combination of 40 small cold gas thrusters and 20 hydrazine thrusters (covered in section 5.12 ), along with three Control Moment Gyros (CMGs) will be used to meet this requirement. Trade studies on pointing requirements considered several areas: (1) controlling vehicle pointing, (2) determining attitude, and (3) computing trajectory. The manned module must be able to maneuver around and approach the satellite from any angle to capture and repair it. Attitude determination is measured with Inertial Measurement Units (IMUs) which are talked about in section 6.2.4.

Passive control techniques such as gravity gradient, magnetic, or spin control were studied. It was found that these techniques can not fullfill the mission requirements for attitude control of the MOOSE spacecraft.

### 6.2.2 Quantifying the Disturbance Environment

External torques are torques caused by or produced by solar pressure radiation from the sun, aerodynamic forces, magnetic dipole moments from the spacecraft, and gravity gradient torques produced by the earth's gravity.

Internal torques are mostly caused by positional uncertainty of the center of gravity (cg), usually on the order of 1-3cm, thruster misalignment, on the order of 0.1-0.5 deg., mismatched thruster outputs, on the order of +/- 5%, rotating machinery (pumps, tape recorders, etc...), liquid sloshing, and dynamics of flexible bodies. Misalignments in the center of gravity and in thrusters will show up during thrusting only and are self-correcting in a closed-loop control system. The sloshing due to fuel will be corrected by baffle plates inside of the fuel tanks.

### 6.2.2.1 Considerations of External Torques

The four sources of torques which affect for Earth-orbiting spacecraft are gravity-gradient effects, magnetic field torques, impingement by solar radiation (i.e. solar radiation pressure), and aerodynamic torques. Although the gravity-gradient and magnetic torques were not considered for attitude control, they were considered for influences during assent and descent phases. For our mission, external torques from satellite capture and maneuvering must be considered. Calculations for this is shown in section 6.2.3

### 6.2.2.2 Considerations of Internal Torques

Principle internal disturbance torques come from general mass movement, human movement, uncertainty of center of gravity (cg), thrust misalignment, mismatch of thruster outputs, rotating machinery (pumps, taped recorders, etc...), liquid sloshing, dynamics of flexible bodies, and thermal shocks on flexible appendages.

### 6.2.3 Selection and sizing of ADCS Hardware

For a three-axis control, the MOOSE vehicle will use three double gimballed control moment gyroscopes (CMGs), located near the c.g. , to allow for maximum performance. Three CMGs are used for redundancy -- if one should fail the other two will be able to maintain three axis control. The primary RCS will be used to desaturate the wheels. Sizing of the CMG wheels were based on the angular impulse for a 180 degrees slew in 60 seconds around each principle axis x, y, z. The impulse torques caused by gravity gradient, solar pressure, and aerodynamic effects are well below the impulse torque that the control moment gyros were designed for, therefore, any torque from these three environmental factors will be corrected by the CMGs.

The wheels are designed to be used mostly at GEO, so the moments of inertia that were used in the impulse calculations were the moments of inertia for the MOOSE spacecraft at GEO. These moments of inertia can be found in Appendix A1.4.

The model used to design the wheels was a thin rim high-speed flywheel. The maximum permissible speed of the flywheels is limited by the stresses induced in the rim. These stresses result from the effect of the centrifugal force, causing a hoop

tension by the tendency of the wheel to expand. Using the maximum tensile strength for each material studied and a 1.5 margin of safety , a trade study was done using three types of materials, AISI 4340 steel, AISI 302 stainless steel, and PH15-7 MO steel. The trade studies showed that AISI 4340 (normalized at 1600 °F , quenched in oil from 1525 °F) would give the smallest wheel radius while giving maximum performance. The graphs below show how the velocity and radius of the wheels vary with the mass. As the mass of the wheels decreases, the velocity needed to produce a given impulse increases. On the other hand, as the mass increases the radius of the wheels will increase but the velocity will decrease. (Keep in mind that the width of the wheel stays the same.) There is a trade off between the velocity and the radius of the wheel. The optimum point is defined as the point where the two lines intersect. This point represents an average trade off between the velocity and radius of the wheel. If the wheel mass were to decrease, the radius would decrease too, but the velocity would have to increase to keep the same angular impulse. If the decrease in mass were too far left of the optimum point (i.e. there is too little mass), the wheel velocity would approach the maximum allowable limits and would most likely fail. On the other hand, if the mass of the wheel were to increase the velocity required to maintain the same angular impulse would go down but the radius of the wheel would increase and a bigger housing unit would be needed to hold the CMG, thus increasing the total mass of the vehicle.
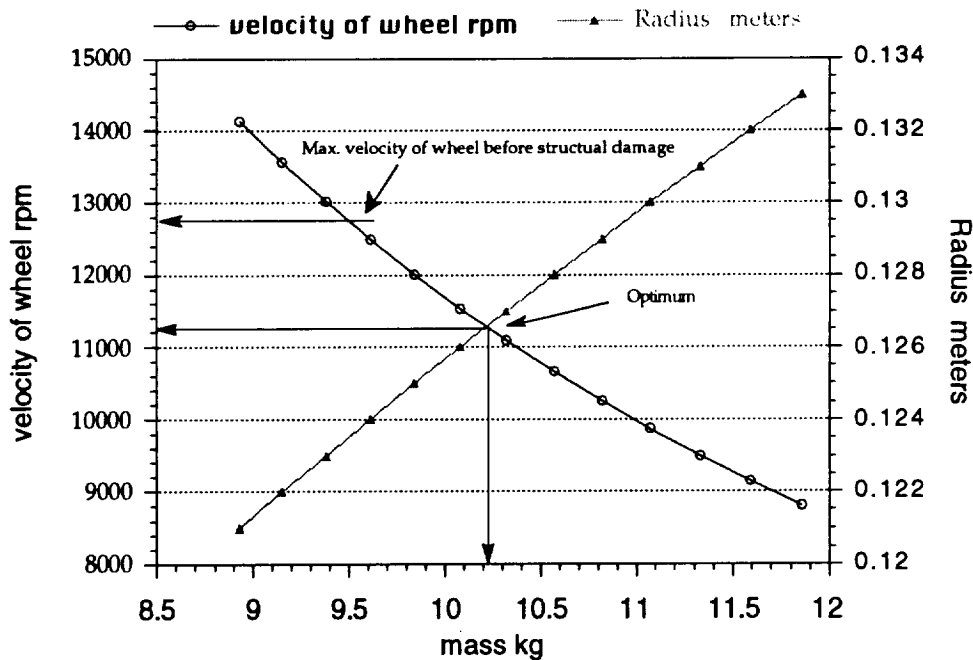


Figure 6.2.a Plot of wheel velocity RPM and radius (m) vx. mass of wheel (kg) for an angular impulse of 96.67 Nms around the X axis
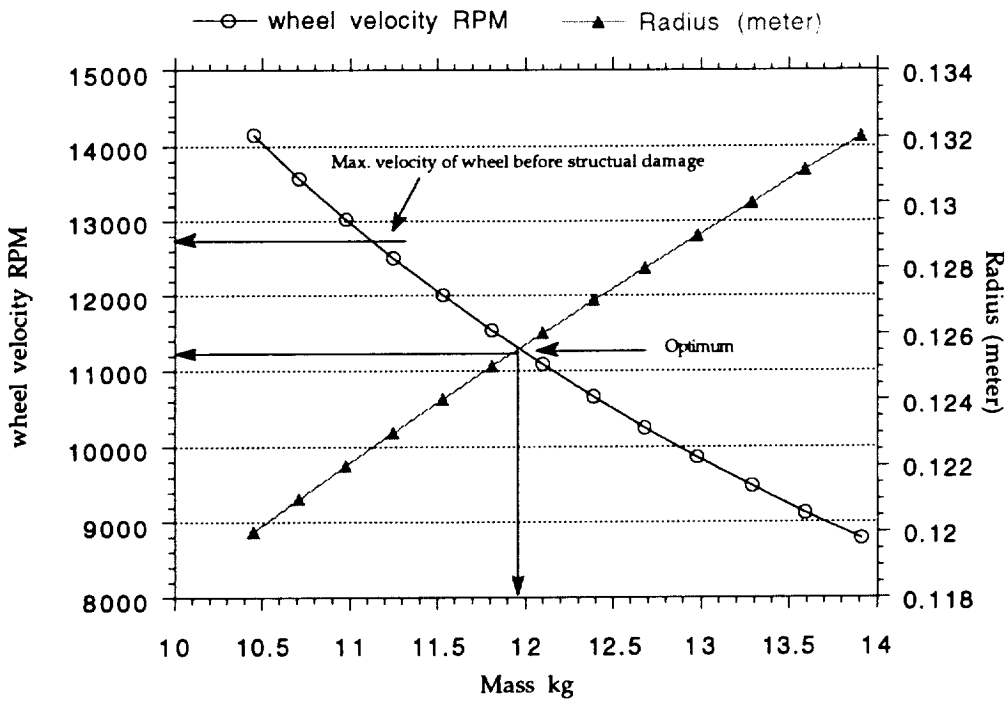
**Figure 6.2.b** Plot of wheel velocity RPM and radius (m) vx. mass of wheel (kg)
for an angular acceleration of 111.5 Nms around the z axis
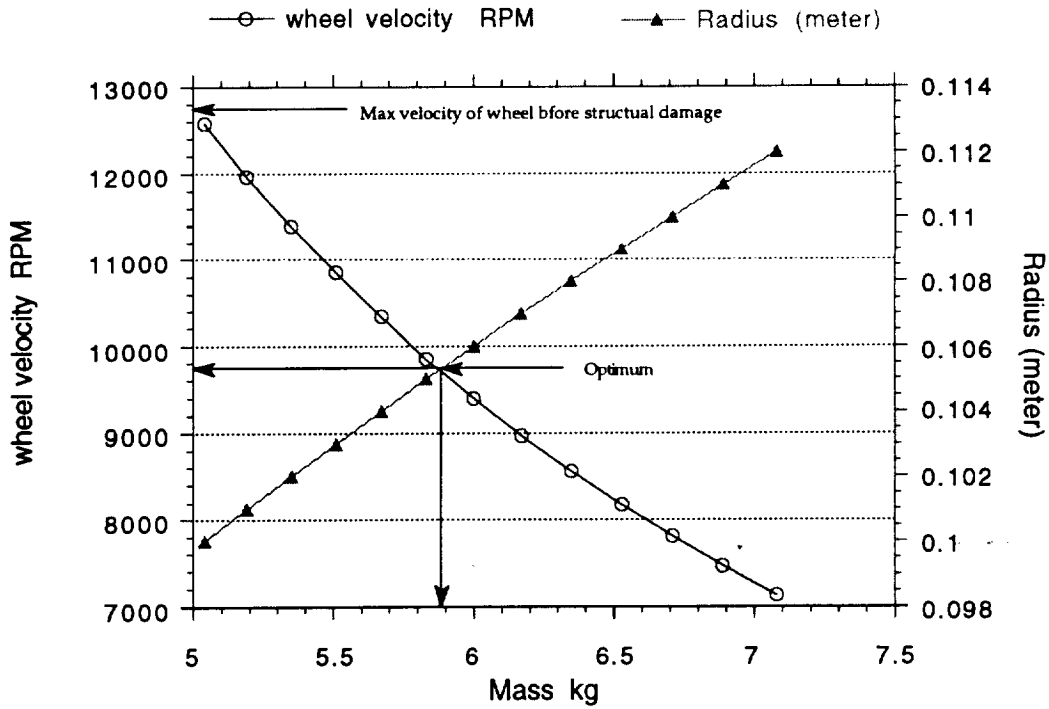


**Figure 6.2.c** Plot of wheel velocity RPM and radius (m) vs. mass of wheel (kg)
for an angular impulse of 33.16 Nms around the Y axis

6 - 4

|  | X axis wheel | Z axis wheel | Y axis wheel |
|---|---|---|---|
| Angular Momentum    N m s | 96.67 | 111.5 | 33.18 |
| Wheel speed    (rpm) | 11100 | 11100 | 9750 |
| Mass of wheel    (kg) | 10.25 | 11.95 | 5.9 |
| Radius   (meters) | 0.1265 | 0.1255 | 0.1055 |
| Power usage   (watts) |  |  |  |
| steady state | 15-30 | 15-30 | 15-25 |
| maximum | 45 | 45 | 40 |

**Table 6.2.a** Characteristics of the CMGs

Total mass of the three CMGs = 76 kg  
Total power consumption  
    steady state = 45 - 85 watts  
    maximum = 130 watts during torquing

Design considerations for the CMGs includes materials/construction, lubrication for the bearing, types of drive motors, and types of tachometers. Typical housing assemblies used for CMGs are made from magnesium with aluminum used for larger wheels. Smaller housings are typically machined hogouts and larger housings may be made from aluminum investment castings. External magnesium surfaces are copper, nickel, or tin plated and painted black. Internal and aluminum surfaces are anodized or chemically treated. For high speed bearings (>3000 rpm), a closed loop oil system should be used to give an active flow through lubrication system which will enhance the bearing life by continuously supplying additional new oil to the spinning ball bearing at a controlled rate. A DC brushless motor will be used because of its high torquing capability. A tachometer will be used to monitor the wheel speed.

A trade-study was done on the mass of fuel it would take to maneuver the spacecraft for a typical three day mission compared to the mass of the CMGs that would do the same job. The total fuel mass needed is 392 kg (150 kg for cold gas thrusters and 242 kg of hydrazine for RCS) compared to 76 kg needed for the CMGs. The CMGs were picked primarily because of mass savings.

### 6.2.4 Types of Sensors and Selection

### 6.2.4.1 Inertial Measuring Units

Two IMUs will be used on the MOOSE spacecraft and will consist of sensors that measure both rotational motion using gyroscopes and translational motion using accelerometers. Strapdown units will be used instead of gimbaled platforms because they have less mechanical complexities, weight, power requirements, and their accuracies are comparabable to gimbaled systems. The unit that was selected was the Litton Zero Lock Laser Gyro which is a "non-dithered" RLG (Ring Laser Gyro). It is a multi-oscillator type RLG that effectively circumvents the frequency-locking phenomenon by removing it (within the optical system) from the gyro's angular-rate input operation region. Low noise, high bandwidth, low quantization and immunity to transients under high dynamic environments are features of the ZLG that make it especially applicable to space satellite attitude and control systems, and pointing and tracking applications. Trade studies were done on three different types of gyros which include the Honeywell GG 334, and Bendix 64 (both single degree of freedom Rate- Integrated Gyros), and the Litton Zero-Lock Laser Gyro. Characteristics of each are shown below.

| Gyro | vol. diameter (cm) | mass (kg) | power (W) | random drift (deg./hr) | input range (deg./s) | angular momentum (cm^2/s) |
|---|---|---|---|---|---|---|
| Honeywell | 5.89 11.94 | .77 | 17 max | 0.003 | +/- 5.6 | 185000 |
| Bendix | 6.35 27.94 | .77 | 8-16 | 0.006 | +/- 2.5 | 430000 |
| Litton | 4.58 | .38 | 2-5 | .0015-.0018 | N/A | 0.0 |

Table 6.2.b Comparison of the Zero-Lock Laser Gyro vs Rate-Intergrated Gyros

The Litton Gyro was pick over the Honeywell and Bendix not only for the aformentioned reasons, but also for its lower weight, size, and power consumption. Other advantages of the Zero-Lock Laser Gyro over the others are:

- No moving parts
- No mechanical noise
- Quantization to within nanoradian resolution
- An extremely accurate scale factor
- A high slew rate capability
- Excellent long-term drift stability
- Excellent reliability/life
- Typically no requirement for temperature control

- Negligible acceleration sensitivity
- Rapid reaction

### 6.2.4.2 Sensors to update IMUs

There will be three types of sensors used to update the IMUs. A Dual Cone sensor will be used from approximately 8000 nmi to GEO. It has an altitude error of .05° at LEO, maximum error of .07° at 4500 km and a minimum error of .02° at GEO. More detail is given in section 6.3.6.1 The second type of sensor is a star tracker which will be used for updating the IMUs once every 12 hours to give the inertial navigation system the most precise positioning coordinates and attitude determination. Accuracy range for a typical star sensor is about 1 arcsec to 1 arcmin or .0003° to .01°. The weight range is 3 to 7 kg and the power requirements are 5 to 20 W. A Global Positioning System is the third type of sensor to be used, primarily for getting the best accuracy prior to, and after, the maneuvers, more on this is covered in the navigation and telemetry in section 6.3.3.

### 6.2.5 Define the Control Algorithm

A typical diagram of an inertial attitude-measurement system is shown below. There are two kinds for feedback control systems. They are the continuous-data and the sampled-data systems. The MOOSE spacecraft will use the sampled-data system so as to free up cpu time for other tasks that are required to be done.

## 6.3 Navigation and Tracking

### 6.3.1 Navigation and Tracking Requirements

The Navigation and Tracking subsystem has three main requirements:
- Orbit and Attitude Determination
- Computational Determination of Delta V requirements
- Target Detection, Tracking, and Rendezvous Guidance

### 6.3.1.1 Orbit and Attitude Determination

This system must provide for an accurate determination of the vehicle's orbit and attitude. Orbit information must be accurate enough at geostationary orbit to bring the vehicle within tracking distance of the destination target. The working range of the selected rendezvous system will be 4.5 nmi (8334 m). The error in position at GEO added to the error in the target's known position must therefore be less than this range. Using a 3/4 safety factor, the requirement for GEO position determination accuracy will therefore be 6 km.

At LEO and below, the main positioning requirement will be determined by the aerobraking maneuver. Non-inertial navigation systems will be blacked out during this maneuver, so inertial guidance will need to be accurately calibrated before the

maneuver. From GEO, an accuracy of 2 km will be required for the aerobrake window. On approach to the maneuver, the window will become smaller and an accuracy of 100 m will be required for any necessary course adjustments.

Attitude determination requirements are listed in the avionics ADCS section (6.2).

### 6.3.1.2 Computational Determination of Delta V

This system must provide the computational power necessary to determine the specific course of the vehicle. This system must be able to collect information about:

- The current orbit of the vehicle,
- The destination orbit of the target,
- Information about known satellites and/or debris in projected
    transfer path,
- Mid-course positioning information,

The navigation system must provide for redundancy in calculations to verify the computed delta Vs and timing of the burns. The system will be responsible for computing delta Vs required for orbit transfers and rendezvous. Actual delta Vs are monitored and are compared to the planned delta Vs. The vehicle's current course information is then updated using this information. The navigation system must also monitor the current course to verify that it matches the planned course and compensate for any differences. The computer must also be able to decide what information from each system is most accurate, depending on the orbit or mission phase. All computations must be done with the highest amount of precision as possible. A more detailed list of requirements is listed in the Computation and Data Management System (section 6.6).

### 6.3.1.3 Target Detection, Tracking, and Rendezvous Guidance

This system must provide a method for detecting a target and guiding the vehicle to rendezvous. As stated above, the principle requirement is the tracking range is greater than the total error in relative distance to the target. The system must provide information for range, range rate, and angle measured to the target. This information must be provided until the target's range to the vehicle is within reach of the vehicle's primary grappling arm.

### 6.3.2 Orbit and Attitude Determination

### 6.3.2.1 Primary Navigation System - Inertial Navigation

This system was chosen due to its potential for high accuracy. The only drawback to using IMU (inertial measurement units) is that their accuracy degrades with time. To keep their accuracy, position and orientation information must be updated before the accuracy degrades past the necessary requirements. Immediate updates

would also be required after a large delta V.  A more detailed listing of the inertial navigation system is provided in the avionics ADCS section (6.2).

### 6.3.2.2 Updating Inertial Navigation

### 6.3.2.2.1 Linear Position and Velocity Updates

Global Positioning System - Provides 25 m accuracy at LEO.  The system is ideal for use in LEO (9.72 x 5 x 2 cubic inches, 1.37 kg, 3 W) however this system is not designed to work above 8000 nmi altitude.  This system will be necessary to meet the 100 m aerobrake accuracy requirement.

Microcosm Autonomous Navigation System (MANS) - This system provides 600m to 1.5km accuracies using 2 sensors.  This system will be necessary for long term navigation in GEO and meeting the 2 km aerobrake window requirement.

For a more detailed description of these systems, consult Appendix A6.2.1.

### 6.3.2.2.2 Orientation Updates

MANS Sensors (Modified Dual Cone Sensors) - This system can provide orientation updates to an accuracy of 0.01 degrees. To have this accuracy, the sensor must be able to use the sun as a reference and becomes blacked out 16% of the time in GEO. For 11.4% of this blackout time, horizon sensor information will still be available and can give an accuracy of 0.1 to 0.25 degrees. For the other 4.6% of the time, no orientation updates are possible.

Star Trackers - This system can provide orientation updates to an accuracy of 0.01 degrees when the sun's glare does not affect the sensor. Although it can be used at other points, the star trackers will definitely be able to be used during the 16% of MANS blackout time.

For a more detailed description of these systems, consult Appendix A6.2.2.

### 6.3.3 Navigational Update Determination

Navigational update information will be mission phase dependent.

### 6.3.3.1 LEO Updates

At LEO, the navigational updates will always be provided for by the GPS receiver. GPS will be used in LEO for calibration and critical information for re-entry. All LEO orbits and LEO to GEO transfer orbits will be calculated using GPS and Kalman filtering software. A single GPS reading can determine the orbit to within 100 meters. With Kalman filtering, this accuracy should improve and meet the 100 m aerobrake accuracy requirement. A GPS position update takes place at the rate of 2 updates per second. This gives the navigation computer plenty of information to determine an accurate orbit in a short amount of time (less than the 25 seconds required by MANS).

GPS will be important in verifying the re-entry orbit. The vehicle will have time to make any mid-course corrections necessary to ensure that it will make the re-entry window. This provides an accurate method to ensure that the aerobraking maneuver will be successful.

The mass and power requirements of GPS are small compared to the overall vehicle mass and power requirements, therefore GPS will be used.

### 6.3.3.2 GEO Updates

GEO updates will be decided on by the navigation system. For the first 20 hours after GPS updates are lost, the inertial navigation system will be more reliable than the MANS system. After this point, however, MANS must begin linear navigation

updates at its return frequency of 0.5 Hz.

## 6.3.3.3 Overall Performance

The following accuracies will result from the different mission phases, using a GPS accuracy of 25 m, a MANS accuracy of 1.5 km (assuming MANS cannot use the moon as a reference), and a linear IMU accuracy degradation of 68 meters per hour:

| GEO Mission Phase | Best Accuracy | Update Accuracy/Frequency |
|---|---|---|
| LEO Orbit | 25 m | 25 m / 2 Hz |
| Transfer LEO to GPS | 25 m | 25 m / 2 Hz |
| Transfer GPS to GEO | 25 - 180 m | No Updates / None |
| GEO Orbit/First 18 Hours | 180 - 1500 m | No Updates / None |
| GEO Orbit/18+ Hours | 1500 m | 1500 m / 0.5 Hz |
| Transfer GEO to GPS | 1500 m | 1500 m / 0.5 Hz |
| GPS to Aerobrake | 25 m | 25 m / Hz |
| Aerobrake (each pass) | ~25 m | No Updates / None |

**Table 6.3.a** Overall Performance of Orbit and Attitude Determination System during GEO missions

## 6.3.4 Computational Determination of ΔVs

The software for the navigation system will utilize all navigational data collected from GPS in LEO and from MANS in GEO. The system will initially compute all ΔVs and their timings based on mission parameters. All transfer orbits will be pre-computed based on initial GPS readings and assuming perfect burns. During the mission, the system will constantly check this computed course against current navigational readings. Course corrections will occur in the event that actual course has deviated from the computed course by more than the accuracy of the data source (GPS or MANS). Course corrections will also be necessary in the event the course plotted intersects with any known satellites (to within a certain degree of tolerance).

In all other aspects, the software should meet all requirements stated in 6.3.1.2.

The computer system hardware will be described in detail in section 6.6.

## 6.3.5 Target Detection, Tracking, and Rendezvous Guidance

For rendezvous, this system must be able to accurately determine the range, range rate, angle and angle rate to the target. Several methods were looked at to accomplish this autonomously.

### 6.3.5.1 Systems for Autonomous Rendezvous Tracking

Star Trackers - Useful in increasing the the accuracy of measuring attitude, star trackers are also useful in determining the angle and angle rate to a target for rendezvous purposes. It can determine the angle to a target to within 0.02 degrees.

IRACS (Space Shuttle Rendezvous Radar) - This system provides fairly accurate range and range rate information at a long range (12 nmi range, 80 - 300 ft range accuracy, 1 ft/sec range rate accuracy). However, the system has a mass of 75 kg and requires 460 watts of power. Because of these restrictions, this system was rejected.

OMV Rendezvous Radar - Although the OMV project has been cancelled, the rendezvous radar for it has been fully designed. This system was specifically designed to do the rendezvous we intend to use it for. It has a lower range (4.5nmi), however, it provides range accuracy of the greater of 20ft or 2% of the range. It also provides greater range rate accuracy of the greater of 0.1 ft/sec or 2% of the range rate. This system's mass of 35kg and power requirement of <60 W, makes this a more attractive choice for a rendezvous radar system.

### 6.3.5.2 Rendezvous Hardware Operations Requirements

Two restrictions will be placed on rendezvous from a hardware standpoint. To maintain navigational updates as long as possible, rendezvous from a higher energy orbit (above) will be required. The vehicle will also have to be rotated such that the radar antenna (mounted on the RCS spider truss, near the crew cabin window) will be facing toward the target satellite, along with the star tracking sensor.

More specific information on rendezvous will be given in the operations section (section 8.9)

### 6.3.6 Mounting of Navigation Sensors and Tracking Hardware

### 6.3.6.1 MANS Sensor (Dual Cone Sensor) Mounting

The MANS sensors for the GEO mission must be mounted with the sensor spin axis pointing 69.5 degrees from nadir. For maximum performance, the sun angle cone must be able to see past the aerobrake as much as possible. This is accomplished by mounting 2 sensors on retractable platforms connected to the lower truss.

In addition, for future missions in LEO where the separable vehicle is used, 2 normal dual cone sensors must be mounted on the RCS spider truss at an angle of 80 degrees from nadir. Since these sensors would only be used in LEO for orientation updates, they would not need to be modified MANS sensors.

### 6.3.6.2 Rendezvous Hardware Mounting

The rendezvous hardware will be mounted on the RCS spider truss, near the crew cabin window. This arrangement will allow the rendezvous system to provide information on any object that can be seen by the astronaut. In this way, radar and optical information can still be given to the astronaut during the manual phase of rendezvous.

The star tracking system will be placed in a passive and fixed position. The radar, as it is currently designed, provides for an extending mechanism for the antenna, as well as all servo mechanisms required to move it.

More information on sensor mounting requirements is presented in Appendix A6.2.3.

## 6.4 Communications

### 6.4.1 Requirements and Constraints

The communication requirements for MOOSE are divided into four sections.

### 6.4.1.1 Range

The assumption is made that MOOSE will not communicate with the space station directly during the mission, but that all communication will be sent first through ground control. This assumption was made because the earth will sometimes block MOOSE's signal from the space station and relay satellites will have to be used. Also if the space station was to be used as a space relay link between MOOSE and earth, some of its communication system only would be used entirely for this mission. Direct contact with earth will enable ground control to monitor the vehicle, releaving the space station of the added burden. In addition, the owners of the satellite or satellites to be repaired will be able to give first hand information to the astronaut on board during the repair. MOOSE will therefore need a communication system that will enable it to communicate with earth from altitudes ranging from LEO ( 250 km) to GEO ( 38,756 km ).

### 6.4.1.2 Links

Moose is an interactive vehicle and therefore will need to have two-way communications with ground control. The uplink, from ground to MOOSE, will consist of both voice and command. Voice will be used when communicating with the astronaut, and the ground control's computer will communicate with the computer system on-board MOOSE using commands. Voice will be primarily used when servicing a satellite and docking at the space station, and commands will be received for course and velocity corrections. In the case of an emergency where ground control needs to control the ship, such as failure of life support systems,

command communication will be essential.

The downlink, from MOOSE to ground, will transmit voice, video, and telemetry. As with the downlink, voice will be used mainly during the satellite repair phase and docking. Video will be transmitted during the repair phase. It will help to show the personal on the ground what is wrong with the satellite and how it can be fixed. With use of the video they can assist the astronaut with the technical aspects. This will limit the training that will be required by the astronaut. The telemetry that will be transmitted down will essentially be housekeeping data. Unlike other space vehicles, there will be no experiments conducted on board MOOSE, therefore, the telemetry data rates will not be as high as other spacecraft.

### 6.4.1.3 Data Rates

Digital communications will be used instead of analog for various reasons. The two most important being, one there is a less chance of error and second, multiple digital signals can be combined onto one rf signal. For example, voice, video, and telemetry can be sent along one link. Voice will use 64 kilo bits per second (kbps) to be communicated. Commands will use 2000 bps. Video will need to have 6 Mbps to be transmitted. These values are estimates based on other communication systems. The voice and command data rates seem to be constant through many applications ranging from the space shuttle to communication satellites. 6 Mbps for video is a greater estimate but falls into a usable range.

The data rate for telemetry is 307 kbps if all the sensors were being read at one time. The value of 307 kbps was reached after it was estimated how many sensors were needed to monitor MOOSE and the individual data rates each required. A complete breakdown and analysis is given in appendix A6.3.2. The breakdown total data rates for each subsection of MOOSE is given below.

| | |
|---|---|
| Structure (aerobrake) | 6400 bps |
| Life Support | 540 bps |
| Man/Grap | 5080 bps |
| Propulsion | 288 kbps |
| Attitude Control System | 3380 bps |
| Navigation/Tracking | 180 bps |
| Reaction Control System | 2900 bps |

Table 6.4.a Subsystem Communication Data Rate Requirements

The data rates were estimated by sub-section because some sections will not be active the entire mission. For instance, during the actual repair of a satellite, the propulsion and structure sensors don't need to be monitored. That is a 95% reduction in telemetry data that is processed and transmitted. On the other hand, the high video data rate required during the satellite repair phase calls for more transmit power. A data rate of 1000 bps must also be added to the telemetry value so that the orbit, course, acceleration, and velocity vectors computed by the on- board

computer can be transmitted.

### 6.4.1.4 Frequency Band

Because of the data rate values, Ku-band will be used as the rf (radio frequency) carrier. The uplink frequency ranges from 14.0 - 14.5 GHz. The downlink ranges from 12..0 to 12.75 GHz.

### 6.4.2 Communication Subsystems

There are two communication systems that will be employed, either the Tracking and Data Relay Satellite System (TDRSS) or a direct space to ground link, depending on the altitude.

TDRSS consists of two satellites that are in geostationary orbit. There is also a third satellite in GEO which acts as a spare for the system. The two relay satellites are spaced 130° apart, one over the Atlantic ocean and the other over the Pacific ocean. Because the relay satellites are in GEO they can virtually maintain constant contact with the ground stations situated around the earth. One station for TDRSS is located at White Sands,New Mexico. TDRSS is operational for vehicles operating at altitudes below 12000 km. It is possible to communicate with an orbiting spacecraft 85% of the time. If the spacecraft is orbiting at altitude between 1200 km and 12000 km, communication is nearly 100% except for regions near the poles (Stark). At altitudes below 1200 km, communication becomes less efficient because the vehicle will sometimes loose sight of the TDRSS satellites.

The direct space to ground link will be used when MOOSE is orbiting at altitudes between 12,000 km to 38756 km. The reason the space to ground link was not used for all altitudes is because at lower altitudes there are longer periods of communication blackouts. At lower altitudes it is difficult for a spacecraft to lock on to ground stations. Also the ground sweeping velocity increases as the altitude decreases, therefore the actual communicating time at a particular ground station decreases.

### 6.4.3 Compatibility

Since a Ku-band frequency will be used for both the uplink and downlink, the communication subsystems must be compatible with Ku-band. TDRSS uses both Ku-band and S-band and therefore is compatible with the preliminary design. The problem occurs with the ground stations. Not all ground stations can communicate using a Ku-band frequency. Therefore there might be a higher ratio of communication blackouts than normal for the direct space to ground link. Normal blackouts are based on using S-band.

## 6.4.4 Link Equations

The link budgets are used to determine whether or not a signal will be receivable. The equations used were taken from *Space Mission Analysis And Design* (p 536). In the equations all values are converted to decibels for ease of calculating. The link equations used are:

$$E_b/N_o(dB) = P+L_l+G_t+L_s+L_a+G_r+228.6-10\log T_s-10\log R$$

where $E_b/N_o$ = received energy-per-bit to noise-density
       P (dB)= power
       $L_l$(dB)= transmitter line loss
       $G_t$(dB)= $G_{pt} + L_{pt}$    transmit antenna gain
$$G_{pt} = 44.3 - 10.0\log (P)$$
$$L_{pt} = -12.0 * (e_t^2/\theta_t^2)$$

             $\theta_t$(deg) = transmit antenna beamwidth
             $e_t$ (deg)= transmit antenna pointing offset
    EIRP = $P + L_l + G_t$ = equiv. isotropic radiated power
    $L_s$(dB)= -92.44 - 20.0 log(s) - 20.0log f = space loss
             s(km) = propagation path lenght
             f(GHz) = frequency
    $L_a$(dB) = propagation and polarization loss
    $G_r$(dB)= $G_{rp} + L_{pr}$   receive transmit antenna gain
$$G_{rp} (dB) = 20.40 + 20\log D_r + 20\log f$$

             $D_r$ = receive antenna diameter
$$L_{pr} = -12.0 * (e_r^2/\theta_r^2)$$

             $\theta_r$(deg) = receive antenna beamwidth
             $e_r$(deg)= receive antenna pointing error
$T_s$(k) = system noise temperature
R(bps) = data rate
$C/N_o$( dB-Hz) = EIRP + S + $L_a$ + $G_r/T_s$ + 228.6
BER = bit error rate
Req $E_b/N_o$(dB-Hz) = required
Implementation Loss (dB)

    Margin(dB)= $E_b/N_o$ - Req $E_b/N_o$ - Imploss

## 6.4.5 Link Budgets

In designing the link budgets, the desired result is a margin of about three decibels. This will allow for error free communication over the propagated path length. In a preliminary design such as this, a link margin of six decibels is desired to allow for miscalculations. Therefore in the following link designs, the parameters were

chosen to give a margin of around six.

The direct space to ground downlink was chosen as the first link designed because its requirements were the most stringent. The propagated path length was longer than the link to TDRSS and had a higher data rate than the uplink, 66 kbps compared to 6.4 Mbps. The previous link equations were solved with the input parameters listed in Figure 6.4.6:

| | |
|---|---|
| • Frequency | 12.0 GHz |
|    determined by Ku-band | |
|    downlink frequency | |
| • Transmitter power | 20.0 W |
|    estimated from existing Ku transmitters | |
| • Transmitter line loss | 1.0 dB |
|    estimated | |
| • Transmitter antenna beamwidth | 1.0-3.0 deg |
|    variable | |
| • Transmit antenna pointing offset | 0.2 deg |
|    estimated | |
| • Propagation path loss | 38756 km |
|    GEO altitude | |
| • Propagation and polarization loss | -0.5 dB |
|    form table on atmospheric loss [2] | |
| • Receive antenna diameter | 5.3 m |
|    estimated | |
| • Receive antenna pointing error | 0.2 deg |
|    estimated | |
| • System noise temperature | 552.0 k |
|    from Ku-band | |
| • Data Rate | 6.4 Mbps |
|    due to data requirements | |
| • Bit Error Rate | 1E-7 |
|    probable value for error free | |
|    communication at this data rate | |
| • Required Eb/No | 15.0 dB-Hz |
|    based on bit error rate | |
| • Implementation loss | -2.0 dB |
|    estimated | |

**Table 6.4.b** Input Parameter for Link Equation

A program( appendix A6.3.1) was used to calculate the link equations. All the input parameters were held constant except for the transmitter antenna beamwidth which was varied from 1.0 - 3.0 dB. A beamwidth of 2.3 was chosen giving a margin of 7.0 dB( 7.04781) and a transmitter antenna diameter of .77(.76087) meters. A margin of 7.0 dB as compared to 6.0 dB was chosen to give more room for errors for the input values that were used.

The above analysis was done for the worst case scenario. That is, the farthest propagation path length (38756 km) and the highest data rate ( 64E6 Mbps). The next

step was to back the power out of the link equations for different altitudes and data rates. For example, if MOOSE was transmitting only voice back to earth at an orbit of 15,000 km, the power consumption should be considerable less than the initial conditions described before. The following graph gives the change in power consumption for four different data rates in the altitude range where a direct space to ground link will be used. See appendix A6.3.3 for a table of calculated values.
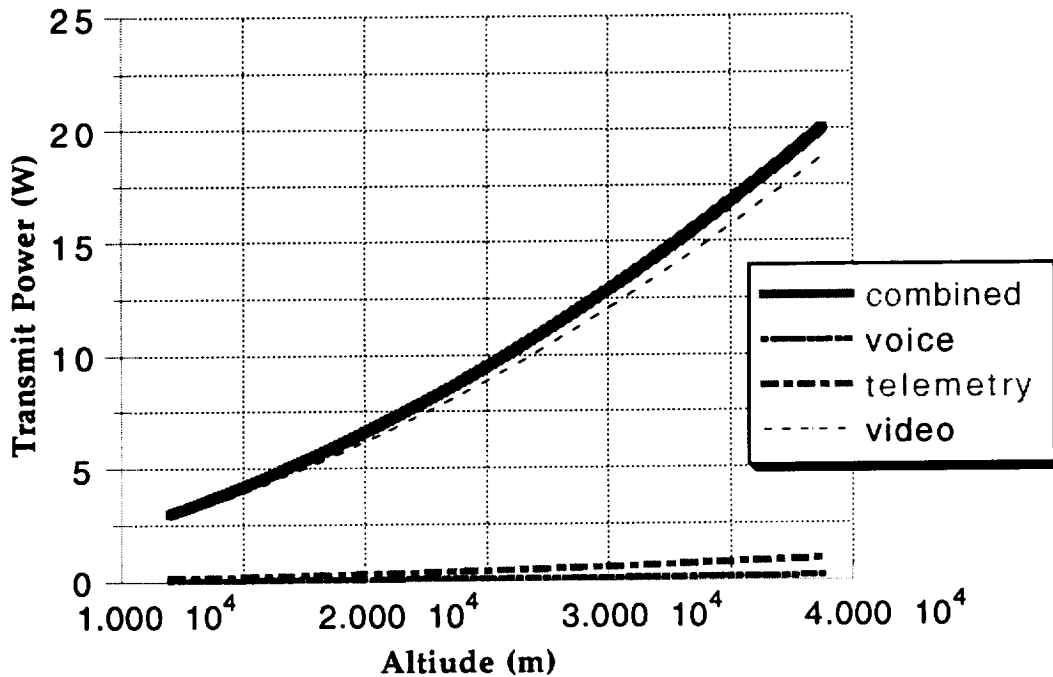


**Figure 6.4.a** Power Requirements-vs-Altitude for Direct Space to Ground Link

Therefore, MOOSE will only be using 20.0 watts of transmitting power when it is at a GEO orbit and sending back voice, telemetry ,and video. This could either occur when actually servicing the satellite, or sending back stored data that was accumulated during a communication blackout.

The uplink budget was designed with a max data rate of 66 kbps , a transmit power of 5 watts, and a frequency 14.0 GHz. The margin was 7.7 dB.

### 6.4.6 Communication Subsystem Parameters

Since the parameters for communicating with TDRSS are less than those of the direct space to ground link, the following communication system will work for both systems.

Downlink
      frequency = 12.0 GHz
      data rate = 6.4 Mbps

transmit power = 20.0 W
link margin = 7.0 dB
transmit antenna diameter = .77 m


Uplink
frequency = 14.0 GHz
data rate = 66 kbps
transmit = 5.0 W
link margin = 7.7 dB
receive antenna = .77 m

The antenna will function as both a receiver and transmitter. The antenna will be a steerable - parabola with a 37.0 dB gain, a 2.3 deg beamwidth, and a mass of 5.8 kg. The mass of the entire communication system will way 15.0 kg.

### 6.4.7 Reliability

The communication system will consist of two transponders for redundancy. If there is a problem communicating with TDRSS a direct link can always be used but it won't be as efficient and there will be longer blackout periods. If there is a problem when at altitudes greater than 12,000 km there is no backup for the direct space to ground link. The two transponders should help to shield against this. The single point failure is with the antenna. If the antenna is damaged there is no backup for both transmitting and receiving. If the steering mechanism is jammed or damaged the antenna can always be aimed by directing the spacecraft.

## 6.5 Data Acquisition and Storage Systems

### 6.5.1 Data Handling Capability Requirements for Data Recording and Telemetry

The first requirement to be determined for both data recording and telemetry are the data rates that will be needed. The data that needs to be considered include: navigation, ADCS , rendezvous, audio, video, and housekeeping data. For the process of data recording, instead of recording every data element from each subsystem ( i.e. the star tracker or the dual cone sensors ), only the finial calculated values of interest will be recorded. Those being the three components of position, velocity, acceleration, and a time stamp. To determine the allocation of space necessary to handle this data, formatting the data using C has been considered. The double float format in C allots 48 bits for the mantissa and 16 bits for the exponent, for a total of 64 bits per element of data. The systems requiring the highest accuracy will use this format. These systems include the navigation and the attitude control systems. The float format will be used for the data returned from the rendezvous radar system. The float allots 24 bits for the mantissa and 8 bits for the exponent; 32 bits per data element. The time stamp can be stored with the long integer format.

The long integer is capable of holding 10 characters and uses 32 bits. These breakdown as follows.

| | | |
|---|---|---|
| Navigation: | Latitude, Longitude, Altitude | X 64 = 192 |
| | X, Y, and Z Velocity | X 64 = 192 |
| | X, Y, and Z Acceleration | X 64 = 192 |
| | Time | X 32 = 32 |
| | Total | 608 bits |
| | | |
| Attitude Control: | X, Y, and Z Position | X 64 = 192 |
| | X, Y, and Z velocity | X 64 = 192 |
| | X, Y, and Z Acceleration | X 64 = 192 |
| | Time | X 32 = 32 |
| | Total | 608 bits |
| | | |
| Rendezvous: | X, Y, and Z Position | X 32 = 96 |
| | X, Y, and Z Velocity | X 32 = 96 |
| | X, Y, and Z Acceleration | X 32 = 96 |
| | Time | X 32 = 196 |
| | Total | 320 bits |

Figure 6.5.a  Avionics Subsystem Storage Breakdown

When the spacecraft is in LEO, navigational data will be received from the GPS system. The GPS is capable of updating the data at 2 Hz. This value of 2 Hz will be used as an upper limit in computing the data rates for the navigation system.

For the purpose of telemetry, data from each subsystem will be telemetered in the same form that it is received by the on board computer. These data rates for each subsystem including all the sensors have been tabulated in appendix A6.3.4.

The frequency of the human voice is approximately 3.5 kHz. It has been demonstrated that original signals can be duplicated if the sampling rate is at least twice that of the highest frequency in the original signal. Filter limitations suggest sampling rates greater than 2.2 times the original signal. Therefor, for digitized voice, sampling should occur at approximately 8000 times per second. Using 8 bits per sample results in 64 Kbps.

Commercial video has a frequency of approximately 4 MHz, therefor requiring samples at 8.8M per second. Using 5 bits per sample leads to a data rate of 44 Mbps. This is fine to input into the displays, but becomes very costly when trying to store or transmit that amount of data. In order to limit the cost, the picture quality can be sacrificed to that of a picturephone for the purpose of telemetry and data recording, approximately 6 Mbp.

| Analog Information | Max Hz | samples/sec. | Bits/Sample | Data Rate (bps) |
|---|---|---|---|---|
| voice | 3600 | 8000 | 8 | 64K |
| color TV | 4.0M | 8.8M | 5 | 44M |
| picturephone | 900K | 2M | 3 | 6M |

Table 6.5.a  Data Storage Requirements

## 6.5.2  Telemetry

The main requirement is to commutate all the data that needs to be telemetered as efficiently as possible. A basic mission can be broken down into four operational modes: 1. Main engine operation, 2. Repair operations, 3. Post aerobrake, and 4. On orbit or standby operation. The data to be telemetered during each mode is as follows:

Main engine mode: Propulsion (290 Kbps), Structure (64 bps)
     Life support (460 bps), ACS (3380 bps)
     Total: 300 Kbps
Repair mode: Life support (460 bps), Man/Grap ( 5080 bps)
     ACS (3380 bps ), RCS (2900 bps), Audio (64 Kbps)
     Video (6 Mbps)
     Total: 6.08 Mbps
Post aerobrake mode: Structure (6400 bps), ACS (3380 bps),
     RCS (2900 bps), Life support (460 bps),
     Navigation (180 bps)
     Total: 13.4 Kbps
Standby mode:  Audio (64 Kbps), ACS (3380 bps), RCS (2900 bps)
     Life support (460 bps), Navigation (180 bps)
     Total: 74 Kbps

Figure 6.5.b  Telemetry Requirements

The data from the current operating mode will be commutated into a single stream to facilitate the telemetry process. Each format mode will be arranged into major and minor frames, with each major frame containing the minimum number of minor frames required for one complete cycle of all subcommutators. The number of minor frames needed for that complete cycle is determined by the degree of supercommutation and subcommutation in each format mode. The data sampled at higher rates will be allotted several minor frame words, i.e. supercommutated, while the slower sampled data will be subcommutated. That is, a certain word position in one minor frame will contain data from one sensor, while that same word position will contain data from a different sensor in another minor frame. Minor frame words will also be allotted for frame counters and for frame synchronization. Each format mode will have some variability to allow for audio, video, and other systems that may not be in continuous operation during that given operational mode.

## 6.5.3  Data Storage

Voice, video, navigation, ACS, rendezvous, and housekeeping data all need to be considered for on board recording. To record everything at full operation, the data recorder would have to be capable of recording at 6.07 Mbps.

Magnetic tape, magneto-optical, and pure optical recording technology have been investigated for potential use as the on board data recorders. Magnetic tape recorders have always been the standard recording equipment on spacecraft, and are available with storage capacities and record rates in excess of 750 Gbits and 300 Mbps respectively.

Magneto-optical recorders can store 8 Gbits to 16 Gbits per disk side. Current technology produces record rates that are only about one-third that of conventional hard disk drives. The main drawback on magneto-optical recorders is that they are not currently available as space rated equipment. The high cost of developing a new space rated hardware leaves magnetic tape recorders as the logical choice for our system.

Audio and video represent the highest data rates that need to be recorded, but also the shortest recording duration time. If a typical repair operation takes 5 hours, and three repairs are performed per mission, audio and video recording time would accumulate to 15 hours. With a data rate of 6 Mbps the video alone would require a recorder with a storage capacity of 325 Gbits. The Odetics model 10000 can handle this storage, but has a mass of 181 Kg. This large mass is more than has been allotted for the entire avionics package. Therefor, the decision at this point is to not record the video digitally, but to record it using a rad hardened VHS type recorder. Allotting 15 hours of audio and 120 hours of repair mode data per mission (that being the mode with the highest data rate) comprises 3.72 Gbits. The Odetics model 5000EC will easily meet these demands with a reasonable mass and volume.

| | |
|---|---|
| Tape width (mm) | 12.7 |
| Record rates (Mbps) | 1-100 |
| Playback rates (Mbps) | 100 |
| Capacity (Gbit) | 45 |
| Record times (min) | 750/7.5 |
| Packing density (Kbit/cm) | 17 |
| Record power (W) | 114/117 |
| Playback power (W) | 178/182 |
| Mass (Kg) | 28.1 |
| | |
| Size (cm) | |
| Transport unit | 33X38X30 |
| Electronics unit | 28X34X28 |

Table 6.5.c  Odetics Model 500EC Specifications

Data compression and error control schemes will be fully employed for both telemetry and data recording. The reduced data rates which result from the compression have been omitted from this analysis as a factor of safety. The extra

space resulting from the compression will allow for added redundancy and permit the use of smaller band widths for the telemetry.

## 6.5.4 Video And Information Displays

Status of on board systems, conditions in the cabin and external tanks, and video during rendezvous and satellite repair all need to be accessible to the pilot. It would be desirable to minimize the size and weight of the displays when consideration is taken for the limited space inside the manned module. The capability of displaying both status type information and video signals on the displays is also of importance.

The displays considered for use in the capsule include cathode ray tubes (CRT), liquid crystal displays (LCD), electroluminescent, and plasma-address liquid crystal displays. With current technology, electroluminescent and plasma-address liquid crystal displays are not capable of handling the high frequency required for video input. LCD's include active matrix (AMLCD), passive matrix (PMLCD), and supertwist-nematic (STN) LCD's. A Type of interference, called cross talk, as well as slow pixel speed, are inherent in the PMLCD design, which results in low contrast and poor image quality. STN LCD technology has yet to achieve even high levels of gray, which leaves the focus on CRT's and AMLCD's. CRT's are bulky, typically ten times as deep as the flat AMLCD screens. CRT's can have a problem with flicker since the screen constantly needs to be refreshed with zaps from an electron gun, and are also known to have electromagnetic emissions. AMLCD's, since they are continuously backlit, do not have the flicker problem, nor do they have any emissions or screen static. AMLCD's do though cost 50% to 60% more than CRT's.

| | CRT | AMLCD | PMLCD | STN-LCD |
|---|---|---|---|---|
| Contrast | 40:1 to 100:1 | 50:1 to 100:1 | 12:1 to 40:1 | 50:1 to 100:1 |
| Pixel speed | on: 0.5ms to 2ms | on: 20ms to 50ms | on: 120ms to150ms | n/a |
| | off: 15ms | off: 50ms | off: 50ms | |
| Resolution | 1024X768 | 640X480 | 640X480 | 640X480 |
| Flicker | 72 Hz | none | none | none |
| Emissions | 1 to 75* | none | none | none |
| Viewing Angle | 135° | 90° | 40° | n/a |

* microteslas

**Table 6.5.d** Display Options

For their low power consumption, small volume, and high picture quality, AMLCD's are presently the best choice for the video and information displays. Three screen will be used in the manned module. Status and data information can be displayed among all the AMLCD's, then, as video needs to be displayed, information from the middle screen can be combined to the other information screens in a windows type format, leaving the pilot with a clear view of the video screen and still allowing access to the status of the on board systems.

### 6.5.5 Video Cameras

The video cameras will be located on each of the two manipulator arm for use during satellite repair. Another camera will be inside the manned module so the pilot can be viewed by those at earth based telemetry sites. The camera inside the cabin will operate continuously for telemetry purposes, but will not be recorded. Those on the manipulator arms will be able to be turned on by the pilot during satellite repair. These manipulator arm cameras will be both recorded and telemetered.

## 6.6 Computation and Data Management System (CDMS)

### 6.6.1 Requirements

#### 6.6.1.1 CDMS Functional Requirements

The CDMS shall provide:

• sufficient processing power for all subsystems, including propulsion, manipulators/grapplers, life support, communications, tracking, navigation, guidance, and control.

• command and status indications to/from all subsystems for overall control, fault detection and isolation, and maintenance scheduling.

• acquisition, encoding, scaling, formatting, and displaying/transmitting physical parameters from other subsystems to support real-time operations, trend analysis, and maintenance.

• data transfer between subsystems through a data network with high transfer rates.

• a man/machine interface, that is fully interactive with required CDMS elements. The crew person shall have total command capabilities and data verification into each system.

• system security to protect the crew and vehicle's safety. This includes measures to prevent unauthorized access to MOOSE's control functions, and prevention of execution of false/erroneous commands.

#### 6.6.1.2 CDMS Design Considerations

• Degree of decentralization

• Extent of automation

• Interface Options

- Equipment technology options

- Redundancy/degree of fault tolerance

- Overall data system architecture

### 6.6.1.3 CDMS Design & Performance Requirements

The CDMS shall:

- be distributed and modular on the hardware level, and "object-oriented" on the software level. This will enable the replacement of individual subsystems without adversely impacting the whole system.

- employ a redundant scheme as part of the fault tolerant architecture. CDMS elements that control critical systems/subsystems shall be fail-operational/fail-safe.

- employ built-in test equipment that diagnoses failures. Artificial intelligence/expert system techniques shall be used to aid in the maintenance of the vehicle.

- employ security techniques to preclude the reception of data/command by unauthorized persons.

- have software that supports flight operations, control of subsystems, redundancy management, monitoring of functions, and fault isolation.

- have a high degree of autonomy in its default operation mode.

- have a highly reliable "core" sub-system that can support a minimum of tasks vital to crew survival.

- have a suitable combination of redundancy and radiation-hardness to operate nominally for the length of a standard mission.

### 6.6.2 CDMS Subsystems & Tasks

- Communications
    Command Processing
    Telemetry Processing
    Data Compression/Expansion
    Antennae Control

- Attitude Sensor Processor
    - Rate Gyro Interface
    - Global Positioning System
    - Horizon Scanner Interface
    - Star-Tracker Interface

- Attitude Determination & Control
    - Kinematic Integration
    - Error Determination
    - Thruster Control
    - Reaction Wheel System Control
    - Center of Mass Calculations

- Propulsion
    - Main Engine Control (Sensors & Actuators)
    - Fuel Tank Monitoring
    - Orbit Trajectory Calculations

- Autonomy Functions
    - Simple Autonomy
    - Complex Autonomy

- Manipulator/Grappler Control
    - Kinematic/Inverse Kinematic Equations
    - Man/Manipulator Interface
    - Control Law Calculations
    - Sensor Integration

- Fault Detection
    - Monitors
    - Fault Corrections
    - Emergency Procedure Initiator
    - Critical Data Recording

- Power Management
    - Distribution/Allocation of Electrical Power
    - Monitoring Fuel Cell Capacity
    - Automatic Shutdown of Unused/Unnecessary Systems

- Climate Monitoring/Control
    - Radiation Detection/Warning
    - Thermal Control
    - Lighting Control
    - Pressure Vessel Monitoring/Control
    - Atmosphere Monitoring/Control
    - Expendables Monitoring

- General Man/Machine Interface
    Touch Screens
    Joysticks
    Voice Command/Feedback Interface
    Indicator Interface

## 6.6.3 CDMS Hardware

### 6.6.3.1 Distributed Processing

Distributed processor architectures offer attractive benefits such as reliability, ease of growth, and parallel processing. Combining modular programming practices with distributed processor architectures allows for increases flexibility in mission-specific hardware configurations.

### 6.6.3.1.1 Distributed Computing Functionality

Distributed processor architectures allows for computers with various capabilities and requirements to work together with ease. The physical distribution of hardware on the MOOSE, combined with the natural delineations and relations of tasks, makes distribution of processes and processors a natural alternative to a centralized system.

Most subsystem processing will be invisible to other subsystems, but some operations (such as orbital transfer and attitude control, attitude control and manipulator/grappler, etc.) will span several subsystems. This would require coordination of some highly complex computing processes over various processors. This could place a heavy burden on the lone crew member, so the level of automation that is required is high, regardless of whether the computer system is centralized or decentralized.

### 6.6.3.1.2 Distributed System Reliability and Security

Reliability has many facets, including probability of correct function over a period of time, probability of recovery (and recovery time) from minor, localized, or major system breakdowns, gracefulness of degradation when full service is impossible, and assurance that critical calculations will be computed in the face of unusual computing loads.

A carefully designed distributed processing system has intrinsic benefits for reliability and secure design, including:
1. enhanced physical, electrical, and logical isolation of faults,
2. convenience of configuration for redundant computing resources,
3. well-defined and protectable constraints on information flow,

4. easy redelegation of tasks as computational priorities shift in the face
   of changing requirements.

### 6.6.3.1.3 Distributed System Growth and Evolution

MOOSE's CDMS must be able to evolve and grow over time to meet different and more complicated mission requirements. Distributed processing provides uniform physical and logical techniques for interconnecting diverse processing activities.

### 6.6.3.1.4 Technical Problems of Distributed Processing

- How can continuity of control and preservation of critical data be
  ensured when processors fail and network connectivity is
  broken?

- How can data replicated in multiple locations be kept consistent with
  low overhead cost?

- How can the design provide for rapid recovery for minor errors and
  maximum preservation of resources under major error
  conditions?

- How can time and sequentiality constraints be honored for safety-
  critical computations, under conditions of high load or system
  failures?

- How can the architecture support dynamic relocation of data,
  programs, and computation site to meet large changes in
  computational load or system breakdown?

### 6.6.3.1.5 Principles for Distributed Design

Modules should be relatively independent of each other, and should be sharply constrained as their side-effects on other modules. A clear order of dependence that relates both functionality and criticality should be established.

The most critical modules should be the most sound, and should be isolated from from less critical ones.

The interface to each module, and its implementation, should isolate all data and internal knowledge that need not be visible to users of the interface.

Components that operate concurrently should have a high degree of independence from one another, except through a carefully constrained communication link.

No untrusted communication, or trusted communication from an untrusted

component, should be allowed to undermine the trust of a given component

### 6.6.3.1.6 A Cost-Effective Strategy for Evolving a High-Performance Distributed System—THE KERNAL APPROACH

An initial effort should be expended to develop a portion of the system that exhibits a high degree of all the desired properties such as fault tolerance, dynamic process management, etc. Such high-quality, mission critical subsystems are called *kernals*.

As technology advances, the overhead costs of producing the high-quality solutions used in kernals can be reduced so that they can be used in a growing fraction of the MOOSE's CDMS.

### 6.6.3.2 Fault Tolerance

There are many types of faults—transient, intermittent and permanent, hard and soft, and including both hardware failures and design and programming errors. A system that can tolerate such faults must provide for:
- *fault detection*, to reduce the likelihood of two or more simultaneous faults that can be difficult to identify,
- *fault location*, to determine the smallest replaceable unit in which the fault is occurring,
- *fault handling*, for manual or automatic reconfiguration and repair,
- and *fault recovery*, to return the system to an acceptable level of operation.

This requires that the system design:
- be appropriately redundant,
- and consist of modules with some degree of self-diagnosis, cross-diagnosis, and interchangability,

### 6.6.3.2.1 Fault Tolerant Design Principles

Economical and effective fault tolerance for large systems requires a "hierarchical" design approach, with fault tolerance distributed over several design levels.

In addition fault tolerance requires the use of modules, with limited information interfaces (for fault isolation), and as high a degree of replication as possible (for effective diagnosis, reconfiguration, and recoverability).·

Lastly, fault tolerant designs tend to be simple and conservative, with strong emphasis on organization and structure as opposed to features such as intricacy and minimality.

### 6.6.3.3 Processor Interconnection

Designing the CDMS for the MOOSE is a complicated affair. A distributed processor scheme is to be used, as follows from the discussion in section 6.6.3.3.1. This raises the issue of processor interconnection.

### 6.6.3.3.1 Bus Standards

Since MOOSE will require high-speed processors with high calculation accuracy and speed in order to perform its tasks, only busses with 32-bit data paths were considered. This narrowed down the field of candidates to the VMEbus and the MultibusII. Though more and more products are coming out, FutureBus technology is too new and unstable to be considered at this time. (NOTE: MUST STILL LOOK INTO USING SBUS--data rates of 160Mbytes/s).

The VMEbus has a sustained data transfer rate of 40 Mbyte/s. Its data and address lines are not multiplexed, meaning it has separate data and address lines. It utilizes an asynchronous protocol, which allows for easy implementation of systems with parallel processors operating at different speeds. Lastly, the VMEbus implement conventional IRQ-type interrupts, allowing for standard programming interfacing with peripherals/co-processors.

Multibus has a sustained data transfer rate of 20Mbyte/s, and a "block-transfer mode" capability of 40Mbyte/s. Its data and address lines are multiplexed. A 10MHz clock is used for synchronization, and conventional interrupts are not used, making operation of parallel processors at different clock speeds and interfacing with peripherals more difficult than would be with the VMEbus.

### 6.6.3.3.2 Network Standards

There are several design requirement for the connection scheme. One is that the system have low radio-frequency and electromagnetic interference (RFI/EMI). The other is that it be free of inherent noise. A third is that data transfer rates and reliability be high. And a fourth requirement is that the interconnection be of low weight. Figure 6.6.a shows a table with typical characteristics of four types of network transmission media--twisted wire pair, baseband coaxial cable, broadband coaxial cable, and fiber-optic cable.

| | Twisted Pair Wire | Baseband Coaxial Cable | Broadband Coaxial Cable | Fiber Optic Cable |
|---|---|---|---|---|
| Partial Bandwidth | 1.5Mbps | 10Mbps | 40Mbps | >150Mbps |
| Media Expense ($/km) | 300 | 1500-5000 | 1500-5000 | 300-6000 |
| Couple/Terminal Hardware Expense | Low | Mod | Mod | High |
| Installation Expense | Low | Mod | High | Low |
| Cable Weight (kg) | 50 | 75-750 | 150-1500 | 30-170 |
| RFI/EMI Susceptibility | High | Mod | Low | None |
| Freedom from Inherent Noise | Low | Mod | High | Very high |
| Spark Hazard | High | High | High | None |
| Data Transfer Reliability | Low | High | High | Very high |
| Transmission Security | Low | Low | Low | High |

**Table 6.6.a** Characteristics of Network Transmission Media

It is clear from the table that fiber optic networks have the best overall characteristics. As the cost of fiber comes down, it is becoming more prevalent in computer networking. Several standards have been developed to handle the transmission of data over fiber optic lines.

### 6.6.3.3.2.1 Fiber Distributed Data Interface (FDDI)

FDDI, as currently defined, only transfers about 12.5Mbits/s, or about 12.5 Mbytes/s, but developing is proceeding to scale FDDI up an order of magnitude to the Gbit/s rate. It has a bit error rate (BER) of $2.5 \times 10^{-10}$.

FDDI has a practical interface, that puts as much of the network protocol intelligence onto a separate intelligent subsystem, to off load protocol management from the host.

FDDI is currently defined as a fiber optic interface, requiring LED lasers and photodiode/phototransistor receiver, in addition to special connectors and splicing. But the FDDI committee has worked out the final details to implement FDDI on low-cost, twisted-pair copper fiber at the 100Mbit/s standard. This can be kept in mind as an option, but with the caveat that using copper wire introduces problems with RFI/EMI that does not occur when fiber optic cables are used.

### 6.6.3.3.2.2 Fiber Channel

In its current incarnation, Fiber Channel is not a network interface. It was designed as primarily a method to provide point-to-point links in a channel type environment, and to map existing interfaces such as High Performance Parallel Interface (HiPPI) and Small Computer Serial Interface (SCSI) into a single standard. Still, work is being done to develop high-performance Fiber Channel switches, and to incorporate standard network protocols such as TCP/IP (Transmission Control Protocol/Internet Protocol) and OSI (Open Systems Interconnect) to it. In addition, studies are being conducted to put the Asynchronous Transmission Mode (ATM) on Fiber Channel, but since ATM is still in the specification phase, it is hard to evaluate this technology.

The primary design goal of HiPPI is to provide a point-to-point channel between CPUs, and from CPUs to storage systems, printers, and other peripherals. Its specification calls for 32 data lines, four parity lines, and an assortment of parity lines in each direction. It was initially designed to be implemented with relatively inexpensive, readily available components to facilitate its acceptance.

HiPPI is a very convenient way of interconnecting major subsections of a system with the kind of transfer rate needed for thing such as real-time graphics.

With HiPPI, transfer rates of 100Mbytes/s have been demonstrated, using conventional parallel HiPPI schemes with copper cables. The Fiber Channel option has been defined to include different rates, from the lowest of 133Mbits/s, doubling through 266, 531, and on to 1.062 Gbits/s, the fastest rate currently specified. The varied transfer rates allows a user to implement the standard that is specific to their needs. In addition, the different rates provides for the most efficient operation, given some combinations of data rates and distance. The Fiber Channel standard makes provision for lower-speed copper interconnections. The ideal solution is some "mix-and-match" combination of speed, medium, and distance to provide the most economical result.

The first boards (from IBM) measure 1.5"x4.5", costs $300-$400, and provides full "byte-to-light" interface at transmission rates of 266 Mbits/s. This includes optical link, encoder, clock recovery unit, and laser safety circuitry. Price are expected to drop to <$100 by mid-decade.

Broadband Communications developed a product that receives standard parallel HiPPI signals and converts them to serial fiber optic output. The unit multiplexes data and control signals to a 1.1Gbaud serial link; the signals are then demultiplexed and reconstructed at the receiving end. It provides transmit capabilities of up to 15km, compared to 25m of conventional HiPPI. It has reduced bulk and high reliability (the typical BER is $10^{-14}$)

## 6.6.3.3.3 Discussion of Network Topologies

### Star Configuration

- Common topology for fiber optic networks.
- All traffic passes through a central switch or router.
- Obvious single point of failure of central switch.
- Control software is complex.
- Sensitive to timing.
- Easily overloaded.

### Ring Configuration

- Typical for communications dominated system.
- Data and control may flow in one or both directions.
- Each processor is connected to its adjacent neighbors only.
- Control software is simple, and maintenance low.

## 6.6.3.3.4 MOOSE Processor Interconnection

The proposed MOOSE Processor Interconnection Scheme is shown below (Figure 6.6.b and Figure 6.6.c).



━━ VME Bus #1

── VME Bus #2
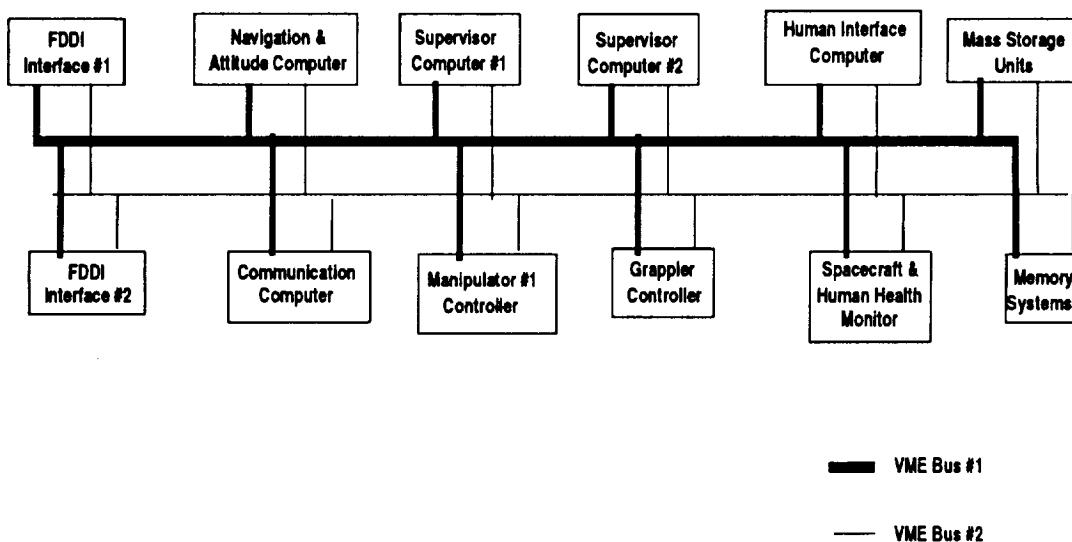
**Figure 6.6.a** Main Processor Bus Interconnection Scheme

The figure above shows the main processor bus interconnection. These subsystems can be contained in the main electronics box, and represents the bulk of the computing processing power. It is not mandatory that there be ten separate computers, as indicated in the figure above. Depending on the processing power of the microprocessors, many of the tasks can be "doubled up". Note the "double-bus"

architecture, used to create a fault-tolerant design.
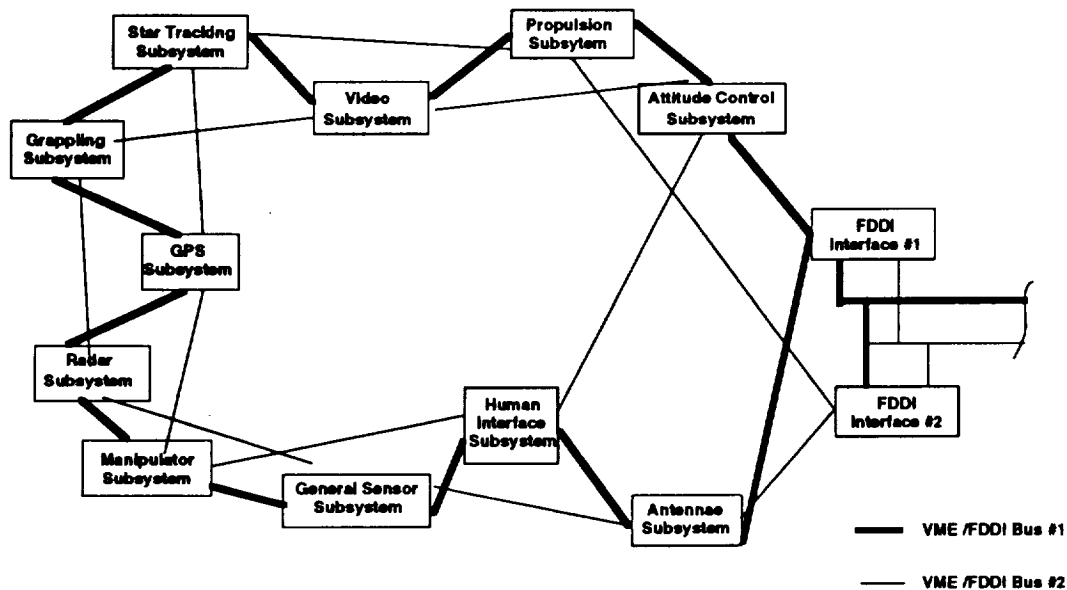


Figure 6.6.b Distributed Processor Bus Interconnection Scheme

The figure above demonstrates how processors dispersed throughout the MOOSE structure will be connected together via a FDDI interface. The ring bus is made more fault-tolerant by doubling it. Note that outer ring connects the subsystems in a straight forward progression, while the inner ring "skips" every two subsystems, until every processor is connected. This allows for multiple failures to occur, while still maintaining a continuous ring topology.

## 6.6.4 CDMS Software

### 6.6.4.1 Systems/Subsystems Breakdown and Requirements

The code size and peformance requirements for the various subsystems are listed in Figure 6.6.d below:

| SYSTEMS/SUBSYSTEMS | CODE SIZE (word) | Throughput (KIPS) |
|---|---|---|
| Communications | | |
| • Command Processing | 50K | 35 |
| • Telemetry Processing | 50K | 15 |
| • Data Compression/Expansion | 100K | 1000 |
| • Antennae Control | 50K | 45 |
| | | |
| Attitude Sensor Processing | | |
| • Rate Gyro Interface | 4K | 45 |
| • Global Positioning System | 4K | 5 |
| • Sun/Horizon Scanner Interface | 10K | 65 |
| • Star-Tracker Interface | 10K | 10 |

| Attitude Determination and Control | | |
|---|---|---|
| • Kinematic Integration | 160K | 80 |
| • Error Determination | 20K | 60 |
| • Precession Control | 17K | 150 |
| • Magnetic Control | 5K | 5 |
| • Thruster Control | 3K | 6 |
| • Reaction Wheel System Control | 5K | 30 |
| • Center of Mass Calculations | 8K | 75 |
| • Ephemeris Control | 6K | 30 |
| • Trajectory Calculations | 13K | 100 |
| | | |
| Autonomy Functions | | |
| • Simple Autonomy | 10K | 5 |
| • Complex Autonomy | 75K | 100 |
| | | |
| Manipulator Control | | 16000 |
| • Kinematic/Inverse Kinematic | 100K | |
| • Man/Manipulator Interface | 25K | |
| • Control Law Calculations | 150K | |
| • Sensor Interface | 50K | |
| | | |
| Fault Detection | | |
| • Monitors | 20K | 75 |
| • Fault Corrections | 10K | 25 |
| • Emergency Procedure Initiator | 30K | 15 |
| • Critical Data Recording | 20K | 60 |
| | | |
| Other Functions | | |
| • Power Management | 6K | 25 |
| • Thermal Control | 4K | 15 |
| • Environmental Control | 25K | 25 |
| | | |
| General Man/Machine Interface | | |
| • Physical Interface | 185K | 500 |
| • Voice Interface | 150K | 2500 |
| | | |
| TOTAL | | 21001 |

Table 6.6.b Subsystems CMDS Requirements Breakdown

## 6.6.4.2 Object-Oriented Programming (OOP) -vs- Procedural Programming

### 6.6.4.2.1 The Structure of OOP Programs

Programming in an OOP language (such as C++, ObjectC, Smalltalk, etc.) entails a programmer to deal with *classes* and *objects*. A class specifies a particular set of characteristics, behaviors, and skills used to define an "unborn" object, much like a DNA template can specify the nature of an organism. When one creates a class, one specifies a set of features and a library of behaviors, called *attributes* and *methods* of the class. Every *instance* (i.e. "born" object") created in that class is defined with the same attributes, although specific attribute values can vary from instance to

6 - 35

instance.

Every instance in a class can access the library defined in that class. But, every instance need not access every method. So, an OOP object is basically its attributes and its know-how, relating pieces of data and code.

One creates a *sub-class* when one needs a slightly different set of attributes or methods than an existing class. Subclasses can add their own unique methods and attributes to those inherited from the parent class. It can also *overshadow* attributes and methods already defined in the parent class. It is easy to see how this feature of *inheritance* can make the creation of new code easier for the programmer.

Rather then having to create a new module from scratch, then test and debug it extensively, the programmer can find a class that that has most of the characteristics that are needed, and specify merely those attributes and methods that are new. This creates a big savings of effort in all phases of development, from code generation to testing, debugging, and maintenance of the code.

It is easy to see how OOP languages force programmers to implement their software design in an extremely modular manner. Failure to properly utilize the features of OOP design would result in a lot of frustration on the part of the programmer as code reuse and software updating issues are addressed. OOP languages demands modular software design in a way that no procedural language can.

## 6.6.4.2.2 Communication Between Objects

A programmer creates a program by selecting/creating objects and passing messages between them. When one sends a message to an object, one communicates with that object as if it were a black box. The black box is trusted to carry out the tasks expected of it, or arrange for the task to be carried out by passing messages to other objects that have the methods necessary to carry out the task. One need not know how the work got done. This information hiding (the storage of the objects' methods and attributes in a "black box") is called *encapsulation,,* a feature that was discussed as necessary for fault tolerant design (section 6.6.3.2)

## 6.6.4.2.3 Real-time Programming Issues

There is a misconception that real-time systems need to be "fast and lean", with no overhead. In reality, real-time systems need to be "fast enough". If one is limited by one's hardware throughput, the software does indeed have to have low overhead. However, this "low-overhead" software comes at the expense of creating software that is easily tested, maintained, modified, and reused.

When "traditional" procedural programming practices are used to develop complicated software system, a trade-off of development and maintenance overhead is substituted for software execution overhead. MOOSE is expected to operated in a

less that ideal environment. It must be easy to operate, test, and maintain. Changes to its operational configuration needs to be able to be made easily and reliably, with a minimum of man-hour expenditure. One of the major driving forces in the MOOSE design is that a minimum support crew be necessary to maintain the MOOSE's software.

Objected-Oriented Programming principles (OOP) allows a real-time programmer to:
- deal more effectively with complexity,
- create a library of readily reusable code,
- begin the design at a higher level of abstraction, allowing trade-offs to be effectively examined before committing to prototype development.

As stated before, raw speed does not necessarily equate to better performance. Most problems with large systems have to do with the complexity of the software. Programmers are not good at predicting performance bottlenecks that can limit the throughput of the computing system.

OOP combats these problems with fast development times, allowing performance data to be collected early in the development cycle. The well-defined module interfaces that result from OOP practices allow for easy elimination of performance problems.

The features of OOP create better systems then the use of optimizing compilers within the framework of the traditional procedural paradigm. Optimizing compilers generally lag far behind hardware technology. They also create side effects that render performance measurements difficult, and can create situations where testing, debugging, and maintenance of software is difficult.

### 6.6.4.2.4 Speed of Development

In a procedural language such as C, one has a relatively small set of key words and a group of syntax rules. The skill is in being able to combine these key words and syntax rules to build elaborate applications.

A OOP language has a large library of classes that can be instantiated as objects to do specifics. The programmer's skill lies in browsing through the class libraries, selecting the right classes, and creating an application out of them, along with new classes that are added to the library for reuse.

OOP also produces a system design and architecture that permits experts who are not programmers to contribute to the development process. While recognizing that objects are still pieces of code, Object Oriented Design (OOD) concentrates more on what processes do rather than how they work internally.

### 6.6.4.2.5 The Inherent Modularity of OOP Languages

The use of "modules" in procedural programming is a practice that is encouraged. However, enforcing a module design framework in traditional language (such as C, Pascal, etc.) is a difficult task at best. There are no well-defined guidelines for module development in these languages, nor are there standard module interfacing. Creating isolated, stand-alone modules that are secure in their execution is difficult. It is frequently not clear where one module begins, and another ends, so quality of the independence of the modules is questionable.

To ensure that the software development task is proceeding in a manner consistent with the requirements of distributed processing and fault tolerant design would require a significant investment in logistical overhead, in the form of "software design & style enforcers". This group of people would be charged with reviewing all code, making sure that the proper design was implemented, and looking for lapses in the design principles.

The use of OOP principles would make the implementation of the Principles of Distributed Design (section 6.6.3.1.5) and of the Fault Tolerant Design Principles (section 6.6.3.2.1) trivial. The interfaces between objects and object types are clearly defined, so the main task is to select proper objects and combine them into larger objects that aim toward the goal of the design. Once the larger objects are built and tested, they are added to the stockpile of library classes for reuse in other applications.

### 6.6.4.3 Artificial Intelligence and Expert Systems (AI/ES)

### 6.6.4.3.1 System Monitoring and Diagnosis

It is not unreasonable to expect that there will be a shortage of man-hours to do maintenance, modifications, and repairs of systems on Space Station. Such tasks will have to be done with by a minimum crew complement in as short a time-span as possible. In addition, any problems that occur while the MOOSE is operational must be manageable by one crew member.

To facilitate such operations, it will be necessary to implement AI systems that can help maintain MOOSE by diagnosing problems and suggesting repair procedures. Such systems would relieve the crew of more routine duties, reduce the need for ground support, and decrease down time.

In addition, expert systems can by used to control MOOSE subsystems. Such an expert system could monitor and control a subsystem, conduct routine tests, provide expert analysis when a problem arises, and suggest and/or implement a courses of action. This would free the sole crew member of MOOSE from the more mundane chores, and allow him/her to concentrate on critical issues. A highly autonomous system would provide a stress-reduced environment in which the MOOSE operator

can work.

Lastly, expert systems can be used as "assistants" to the crew member, when difficult tasks are undertaken or equipment used. Knowledge about the repairs to be attempted during a mission can be stored in an expert system for the astronaut to recall if need be.

# 7.0 Power

## 7.1 Introduction

This chapter outlines the power requirements of the MOOSE vehicle, the power sources analyzed, and the final selection for the primary and backup power systems.

## 7.2 Requirements

The following is a list of power requirements for each of the subsystems.

| System | Power Required (W) | Time | Energy Required (kW hr) |
|---|---|---|---|
| Data Recording | 0120 | all | 8.64 |
| Optical Sensors | 0022 | all | 1.584 |
| *Computer | 0200 | all | 14.4 |
| *Control Station and LCD Screens | 0008 | all | 0.576 |
| lights | 0040 | all | 2.88 |
| *Inertial Measuring Unit | 0030 | all | 2.16 |
| *Life Support | 0350 | all | 25.2 |
| *Smoke Detector | 0005 | all | 0.36 |
| Communications | 0025 | all | 1.8 |
| *Rendezvous Radar (Rendezvous) | 0060 | 1 hr | 0.06 |
| *GPS Sensors (LEO) | 0006 | 72 hr | 0.432 |
| *Main Fuel Valves and Pumps (burns) | 0020 | 12 min | 0.004 |
| *Star Sensor (every 8 hrs) | 0003 | 1 hr | 0.003 |
| *Control Moment Gyros (drifting & working) | 0030 | 4 hrs | 0.72 |
| Grappler Arm (grappling satellite) | 1000 | 1 hr | 1.0 |
| Manipulator Arm (repairing satellite) | 1000 | 6 hr | 6.0 |
| *Reaction Control System | 0072 | 10 hr | 0.72 |

| | | | |
|---|---|---|---|
| Maximum Power Required | 1.830 kW | Total Energy Required | 66.539 kW hr |
| Backup Power Required | 0.746 kW | Backup Energy Required | 7 kW hr |

Systems marked with an * are essential for the safe return of the astronaut. If a failure of the primary power system occurs, the longest time for return to the station

is 11 hours. In order to supply power to those systems, 746 W of power and 7 kW hr of energy are needed.

## 7.3 Primary Power Source

Fuel cells weigh less than the other power sources. Since weight is the driving factor in the design of this vehicle, fuel cells are used for the primary power source. A fuel cell producing a maximum output of 2 kW allows a 10% loss due to power conditioning and full power for the mission. The fuel cells will operate on gaseous hydrogen and oxygen stored as cryogens. This is a more mature technology and is more efficient than other fuel cell designs (similar to the fuel cells in the space shuttle). It also allows the 7.1 kg of oxygen needed for life support to be stored in the same tanks as the oxygen for the fuel cell. The weight of the fuel, tanks, and fuel cell will be about 63 kg (including life support's oxygen).[1] The fuel cell and fuel will be stored in the avionics box of the vehicle.

## 7.4 Backup Power System

The lightest weight power source for the 7 kW hr needed for backup was nickel cadmium batteries. At an energy density of 0.4 kW/kg, 17.5 kg of batteries are needed.[23]

The two figures that follow demonstrate the relation of power and energy needs to power source mass.
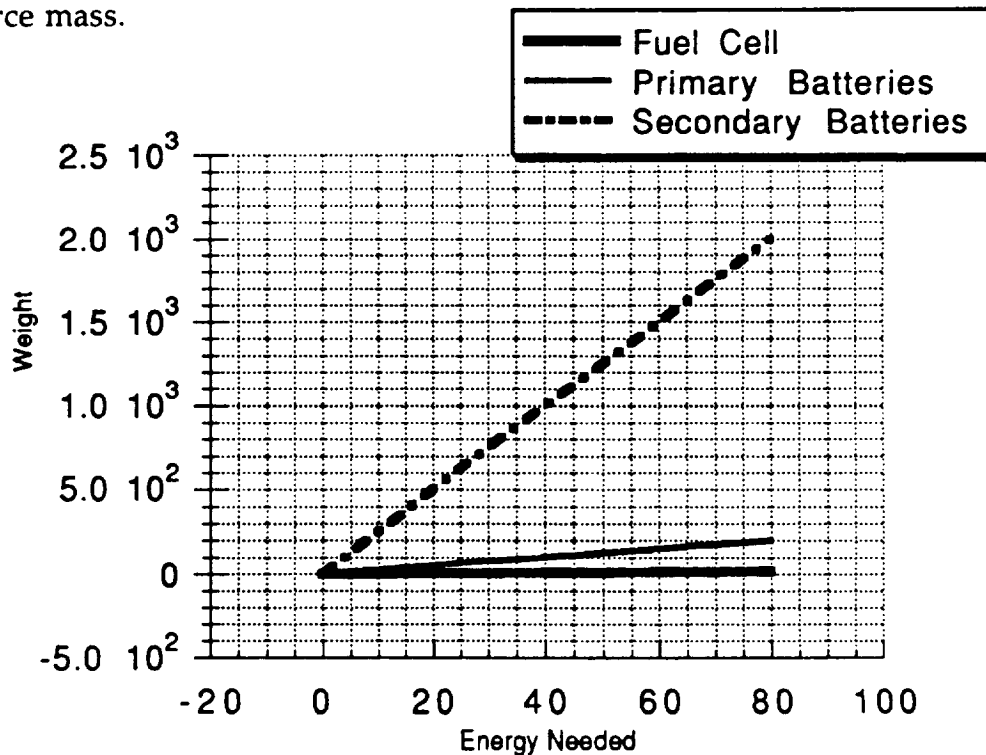


Figure 7.4.a Mass of Power Source in Relation to Energy Needed

7-2
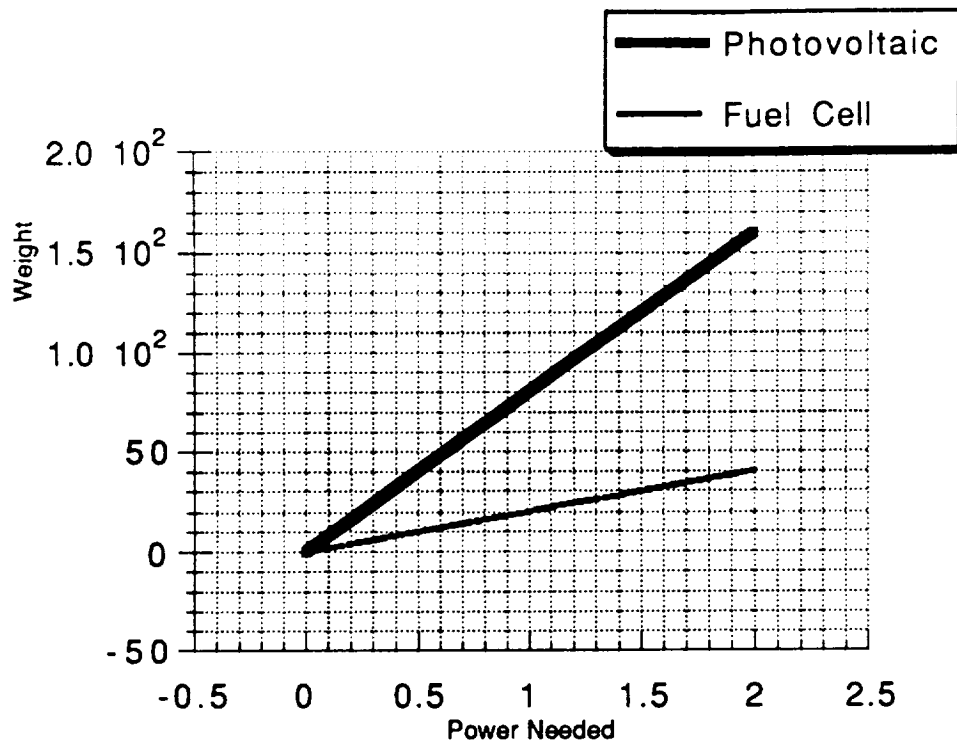
**Figure 7.4.b** Mass of Power Source in Relation to Power Needed

---

[1] Source for weight estimates: *Handbook of Batteries and Fuel Cells.* McGraw-Hill. 1984.

[2] ibid.

[3] Wertz, James R. and Wiley J. Larson, ed. *Space Mission Analysis and Design.* Kluwer Academic. Boston. 1991.

# 8.0 Operations & Production

This report represents the Operation & Production Group's baseline operations plan for the Manned Satellite Servicing System (MSSS) popularly known as "MOOSE" (Natasha, blow up moose and squirrel....and get me taco...). It describes the basic operating concepts to support the MSSS and the facilities required. Also addressed are MSSS capabilities, training and simulation facilities, and missionplanning/flight design procedures, and Operational interfaces with Space Station Freedom and ClientSpacecraft Operations Control Centers (CSOCC's).

### 8.1.1 Purpose

The OPS/PROD group has the responsibility of providing a supervisory environment within which MSSS missions can be successfully executed. This environment includes MSSS ELV, ground, and airborne support for design, implementation, and operation of the MSSS.

Once the particulars of the environment are known, the MSSS vehicle may be designed to operatewithin the realistic infrastructure, aiding the ENAE 412 design class in it's vision of what the MSSSvehicle should be.

### 8.1.2 Approach

The MSSS baseline operating plan will provide a complete operating scheme as it is currentlyunderstood by the OPS/PROD Group. Section 1 establishes the purpose of the plan and theoperational tasks which will be covered. Section 2 provides background and description on the MSSS. Also described are basic design philosophies and a breakdown of responsibilities between the MSSS Project Office, NASA centers, and other facilities. Section 3 explains the capability which the MSSS Operations Support Center (MOSC) will provide. The MOSC and ground/Pilot/Flight Control Officer control interface capabilities are discussed in section 3 with specifics operational concept with realtime support teams. Section 5 describes pre-mission support

activites for the flight planning process. Section 6 outlines realtime support teams and their tasks. Section 7 describes MSSS/SSF crew training requirments and schedules. Section 8 describes how SSF/MSSS operations will be conducted. Appendix A8.1 contains the acronym list.

## 8.1.3 Assumptions

The MSSS mission concept is based upon the premise of satellite repair as an alternative toreplacement. In order to validate the concept financially, a relatively high frequency of MSSS activity must be maintained such that "economy of scale" advantages become realized. MSSS will have theability to service a satellite in any attainable orbit; to only design for GEO missions exclusively would be impractical. MSSS will be able to provide SSF servicing as required. Alternative missions include DoD, anti-satellite operations, and surveillance/ferret operations with the appropriate ORU fits. Others arepotential STS co-operative missions, and possible STS emergency assistance.

The amount of propellant consumed on a per-mission basis will vary considerably. A large amount ofpropellant will be stored on-station; uncoupling MSSS schedules from ELV-delivered tanker schedules. The on-orbit depot concept is the key which will make the MSSS system flexible and responsive to transient mission opportunities.

Prior to the first flight of the MSSS and the start of integrated MSSS simulations, the Mission Control Center (MSS) at Johnson Spaceflight Center will house a support room for MSSS operations. This room will be referred to as the MSSS Operations Support Center (MOSC). Within the MOSC are 2 identical ground control consoles (GC's) and several mission support workstations. A MSSS pilotstation will be provided, so that remote pilotage may be accomplished from the MOSC. The workstations must be allow for rapid reconfiguration and processing of data for OMV planning and support. The goal is to provide quality flight support while minimizing flight planning and rehearsal time, allowing a high tempo of MSSS operations to be maintained.

STS facilities may be used when practical in order to minimize cost. However, STS facilities are designed for many months (even years) of premission planning and such a scheme invalidates the inherent MSSS concept of rapid, flexible mission planning and execution.

## 8.2.0 MSSS PROGRAM

This Section gives a General Overview of the MSSS Project. It includes a physical description of thevehicle, the suggested responsibilities of several NASA centers and supporting sites, and severaloperational modes MSSS may operate in.

### 8.2.1 Background

With the growing utility of Earth-orbiting spacecraft, Satellites have become indispensable parts of modern life. Satellite useful life can be extended beyond the life of it's propellant, ORU components, or cryo dewar, thus forestalling the eventual need for replacement with a new platform.This growing requirement for satellite on-orbit servicing will be met by the MSSS. Any Mission requiring orbit transfer capability, precision manipulation or maneuvering, and man-in-the-loop control can be accomplished using MSSS.

The MSSS is a reusable, single-place, aerobraking spacecraft designed to refuel, repair, and otherwise service orbiting spacecraft. The MSSS will be deployed from SSF, where it will be stored, resupplied,and refurbished.

The MSSS development and procurement are being managed by the MSSS Project Office (MSSSPO)located at the University of Maryland Space Systems Laboratory. MSSSPO has the responsibility of the design and sustained engineering support of MSSS. JSC has the primary responsibility of operation of the MSSS. The principal contractor has yet to be selected. Competitive bids should be routed to Systems Integration Group, ENAE 412, UMCP.

## 8.2.2 MSSS Description

The MSSS overall dimensions have yet to be finalized; yet some aspects of the design have beenestablished.

The main propulsion system for MSSS is an RL-10 derivative engine fueled by cryogenic LO2/LH2. It is similar to the re-usable RL-10A4-N to be flown on the DC-Y SSRT vehicle. The MSSS combines cold-gas and bi-propellant RCS capacity in a single Aerojet GH2/GO2 system also similar to the DC-Y. The system operates in the bi-propellant mode producing an Isp of 350 and in the hydrogen-only vernier mode providing contamination-free attitude and directional control. Propellant for ACS use is drawn from the joint APU/ACS cryogenic storage tanks.

MSSS subsystems are designed as orbital replacement units (ORU's) which can be changed out via the SSF RMS. All significant systems are configured to make access, test, and change-out as simple as possible.

The MSSS primary communications and data interfaces are S-band links with the Tracking and Data Relay Satellite System, STS communication system, and ground network sites. MSSS will also haveKu-band capability in order to communicate with the space station.

## 8.2.3 Program Roles & Responsibilities

The MSSS program will require support from several NASA centers and their contractors. The centerswill have various responsibilities which are mission dependant. The exact nature of these responsibilities will be finalized after primary contractor selection and the final MSSS vehicle design and operational concept.

### 8.2.3.1 University of Maryland Space Systems Laboratory (SSL)

The SSL is the location of the MSSS Project office. The MSSSPO manages the entire MSSS program and is responsible for the design, procurement, and the sustaining engineering requirements or the program. The SSL will provide engineering and crew staffing support to all OMV operations during MSSS flight DEM/VAL testing. The SSL shall also provide real-time engineering support, as required, from the Client Spacecraft Operations Control Center (CSOCC).

The primary contractor, once selected, will be responsible for the final design and manufacture of 2 MSSS flight vehicles. Other contractor responsibilities include ground control facilities and software to be used for MSSS pilot, realtime support team, and SSF crew training. Additionally, the design and manufacture of all ASE and SSF-based flight hardware (to include propellant depot, and storage/refurbishment facility) will be contractor duties.

### 8.2.3.2 Johnson Spaceflight Center (JSC)

JSC has been designated as the NASA center responsible for MSSS flight operations. Throughout the MSSS design process, JSC will provide operational design inputs to the MSSSPO. JSC will also identify any SSF requirements affecting MSSS design. It will also be JSC's task to develop the ground facilities requiem to support MSSS operations in accordance to guidelines presented in this document. Preflight, and during the course of a mission, JSC will conduct all necessary integration with SSF, CSOCC, and their respective control and support teams. JSC primary responsibility must be operating the MSSS and achieving mission goals. JSC will conduct all aspects of MSSS flight operations including manifest assessments, mission planning, crew training, systems management, and missionmanagement and direction. JSC will evaluate all flight feasibility assessments presented to the MSSSPO by potential users of MSSS. MSSSPO, however, will have final approval authority over all potential missions.

### 8.2.3.3 Kennedy Spaceflight Center (KSC)

KSC, as the primary launch site for STS and PMV tankers, is responsible for ground support required by MSSS assembly, MSSS resupply, MSSS mission-specific payloads, and PMV "tanker" flights before and during launch. KSC will perform all prelaunch interface verification testing between tankers, MSSS resupply components, and mission dependant hardware and the STS or ELV. In addition, KSC will participate in the end-to-end testing of MSSS, STS, and client spacecraft payload communication links. KSC will further support the program by serving as a storage and maintenance facility MSSS flight components.

### 8.2.3.4 Cape Canaveral Air Force Station (CCAFS)

As the primary launch site for Titan IV, Delta, and Atlas ELV's, CCAFS will provide launch services forPMV tankers. Pre-launch checkout and storage of PMV's and integration will also be provided by CCAFS.

### 8.2.3.5 Other NASA Centers

Various other support services will be performed by other NASA centers on a TBD basis. These services include NASCOM network support provided by Goddard Spaceflight Center (GSFC) and aerobraking technical support provided by Langley Research Center (LaRC).

### 8.2.3.5 Other Facilities

Bulk propellant delivery to the SSF Cryogenic Storage Facility will be accomplished by ELV (and possibly STS) delivery of PMV tankers. The tempo of MSSS missions may require additional launch support. Candidate sites for supplemental propellant support include Vandenberg Air Force Base/WTR (Titan IV, Delta, Atlas, STS(?)), Kourou (Ariane 4,5), Tanegashima (H-II), and Baikonur/Tyuratam (Proton/Energiya).

### 8.2.4 SSF-Based Operations

MSSS operations increase the frequency of SSF departing/arriving spacecraft. PMV's, Shuttles, and MSSS will be utilizing SSF airspace, possibly simultaneously. A SSF traffic management scheme has been developed based upon the JSC Orbital Maneuver Vehicle (OMV) plan for SSF terminal controlzone management. The space around SSF is divided into 3 regions. The Proximity Operations Zone extends in a 1 km radius around the station. All docking/release activities occur within the SSPOZ. The Command and Control Zone (CCZ) is a rectangular space that extends 37 km ahead, above, 37 km below, and +/- 9 km out of plane of SSF. The Flight Control Officer (FCO) on station has responsibility for all traffic entering the CCZ. The Departure/Arrival Zone extends 147 km in front of the station. Entering/Exiting the outer zones must be cleared by the FCO and MOSC. Transfer among the inner zones must be cleared by the FCO.

Dedicated MSSS support personnel on-station are not required. MSSS maintenance, check-out, andrefurbishment tasks will be as automated as possible. Dedicated IVA/EVA activities would be performed by available crew. During flight operations within the CCZ, the FCO console, located at the cupola workstation, will be manned at all times. FCO responsibilities would be rotated in 4 hour shifts during lengthy operations. A second crewperson is required to operate the RMS during grapple, docking, berthing and de-berthing operations.

A SSF-based MSSS mission begins with the Moose Project Office (MSSSPO) and the Space Station Program Office (SSPO) identifying mission objectives and requirements. The PMV Project Office then presents projected propellant delivery data/initiates launch preparation of additional tanker flights. A joint team of JSC/UMCP ENAE personnel then initiate detailed mission planning. Upon completion of mission planning, the MSSS preparation requirements can be communicated to the SSF crew. MSSS pilot training and rehearsals are included as an integral part of the mission plan.

Premission Preparation at SSF includes pilot training, vehicle check-out and servicing, battery charging, APU and RCS fueling, and primary propulsion

fueling. The MSSS Operations Support Center (MOSC) will then uplink the initial software load (I-loads) to the MSSS flight computers (MFC).

After vehicle check-out, any mission payloads (ORU's, liquid tanks, pumps, etc) are mated to MSSS and interface verification tests will be performed. SSF state vector and attitude alignment data will then be transmitted to MSSS via a data umbilical. The MSSS then conducts a self-test as commanded by the Flight Control Officer (FCO). Concluding a successful self-test the MSSS is placed in a stand-by mode. The MSSS cabin is then pressurized and the pilot may board the spacecraft.

The pilot then commands a second self-test and initiates the berthing removal checklist. The FCO authorizes a SSF crewperson to secure the pressurized docking  assembly and remove the MSSS from the berthing facility using the SSF RMS. The MSSS is the placed in position for deployment.

Prior to release, the MSSS will command the MSSS to the primary hold mode, enabling the ACS and receiving continuous GPS/IMU state vector updates from SSF via downlink. When the Space StationControl Center (SSCC) mission director receives a "go-for-release" from the MSSS director and relays it to the FCO, the MSSS will be released.

The MSSS pilot will have primary responsibility for safety-critical monitoring and dynamic control of MSSS while it is departing from the Command and Control Zone (CCZ). Any maneuvers must be cleared by the FCO before execution.

Upon Completion of the mission, the pilot will return MSSS to a predefined location outside the CCZ. When directed by the SSCC Mission Director, the FCO will assume operational command of the MSSS at the CCZ boundary. The FCO then controls the MSSS approach to SSF. Prior to retrieval, the MSSS  will be maneuvered to the proper attitude and commanded into primary hold mode with attitude control maintained by the vernier (cold gas) ACS. A space station crewmember then grapples the MSSS with the RMS.

The MSSS pilot commands MSSS into a standby mode, disabling the ACS system. The MSSS is then placed into the berthing facility and the egress checklist initiated. The PDA is secured and pressurized, and airlock integrity checks executed. After receiving a "go-for-egress" from the FCO, the MSSS pilot may exit the spacecraft.

ELV operations are essential to the MSSS mission. Regular propellant delivery must be maintained if flexibility is desired. PMV's would be delivered to SSF from their prospective launch sites. Launch Sites for tanker flights will include ETR and WTR, and possibly foreign sites. Candidate sites include Kourou, Tanegashima, and Baikonur/Tyuratam.

A PMV tanker delivery would enter the Departure/Arrival area and there the PMV would be cleared into the CCZ by the FCO and SSCC. Ground Control of PMV's is excersized from the MOC and PMV Mission Director.

# Operations & Production
# Propellant Maneuvering Vehicle

## Chris Lash

## 8.2.5            Propellant Re supply

8.2.5.1 The success of project MOOSE is directly linked to the ability to supply propellant to the vehicle in the most efficient way. Neglecting development costs ,propellant supply is the most expensive operating factor . An analysis of potential methods of delivering propellants to LEO shows that the minimum $/Kg value that can be expected is on the order of $10,000 / Kg of fuel delivered. As a result of this analysis the MOOSE operational design must have a propellant supply reserve located on or near space station Freedom . This fuel reserve will give the system the operational flexibility to utilize the most cost effective means available to lift propellants into LEO without relying on any one specific launch vehicle.

MOOSE Support Vehicles

Figure 8.2.5.1 shows the capabilities of launch-systems supporting MOOSE operations.
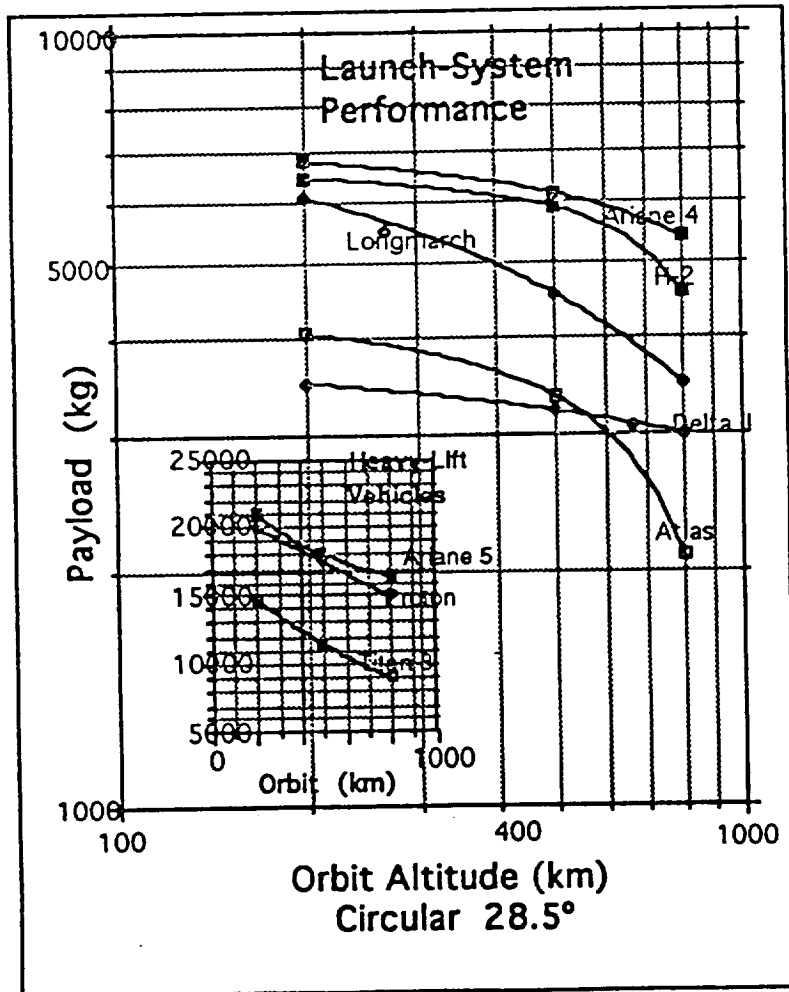


fig.8.2.5.1. Launch System Performance

8.2.5.2 Extensive study of launch systems capable of supporting MOOSE reveals the following :   • Average lead time for launch  30-36 months.
• Average three sigma injection accuracy to 440 km  altitude +/- 5 km at apogee and .01 ° inclination .
• All systems  are capable of handling large amounts of Cryogenic fuels.


8.2.5.3                                     Propellant Maneuvering Vehicle


8.2.5.3.1 The following sections describe the <u>PROPELLANT MANEUVERING VEHICLE</u> OR PMV. This  unmanned vehicle will be  used to transport fuel  from   the ground to the propellant storage facility at the space station.  The PMV consists of four major components:

• Oxygen tank
• Hydrogen tank
• Orbital Correction And Maneuvering Set  (OCAMS)
• Payload Container


The PMV operational requirements are:

• Multiple propellant tank sizes
• Reusable OCAMS
• Tele-operated from ground and space station
adaptable to all launch support vehicles
• Capable of rendezvous with the space station within 24 hrs of launch

The PMV is shown in figure 8.2.5.2
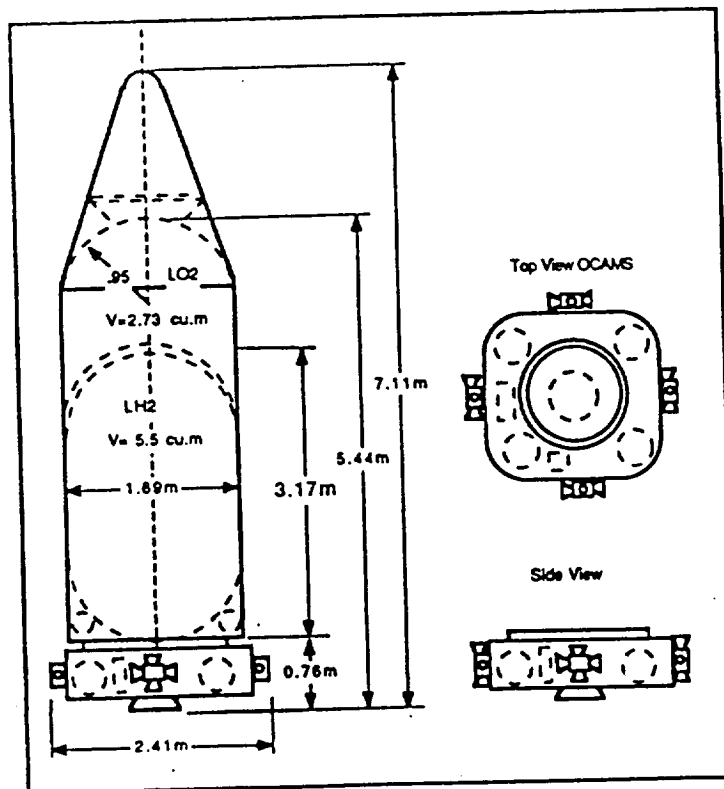


fig.8.2.5.2

8.2.5.3.2 The operational goal of the PMV is to deliver as much usable payload to the space station as possible. The concept of the MOOSE has been based on a flight system that can pay for itself in the commercial market . Study has shown that a single MOOSE sortie to GEO and back will require 13,000 kg of fuel and other payloads. As a best estimate launch support costs will average $7,000/kg delivered. At this $/kg rate a single sortie will cost $91 million just for propellants and Orbital Replacement Units (ORU).

8.2.5.4                                    PMV Tank Design

8.2.5.4.1The MOOSE uses liquid Hydrogen and liquid Oxygen as main propellants. The initial thought was to make a tank set made up of multiple common tanks stacked together to make the required volume.. Analysis of this approach showed two important design elements . The first was that the current launch systems available fall into three distinct payload ranges and the second was that the additional structure weight of a piggy-back tank arrangement is not exceptable. The results of the analysis from section 8.2.5.1 shows the need for three PMV tank sizes ; Small (Atlas type ) volume of 8 cubic meters , Medium (Ariane type) volume of 18 cubic meters and Large(Titan 3 type ) volume of 36 cubic meters. Figure 8.2.5.3 shows a typical installation of a PMV with a Atlas type tank.
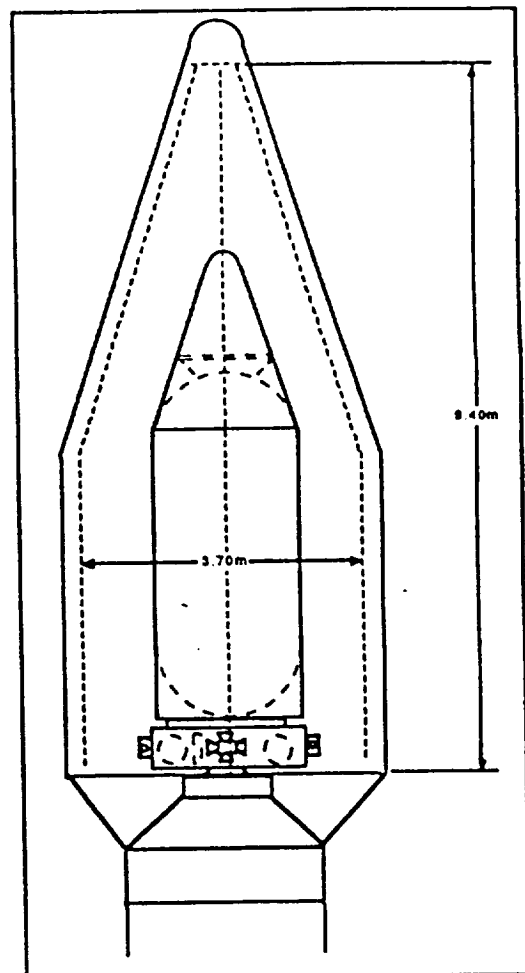


fig.8.2.5.3 Atlas type PMV

8.2.5.4.2 The tank design for the PMV chosen is a common bulkhead design , with liquid oxygen stored in the upper tank and liquid hydrogen in the lower. The upper tapered portion of the PMV is a payload support structure used for delivery of ORUs or small amounts of liquid helium or Hydrazine. The cryogenic liquids are expelled from the tanks by a pressure fed nitrogen gas system. The Atlas type shown in figure 8.2.5.3 requires 35 kg of liquid nitrogen to expel the full volume of cryogen's stored.
8.2.5.4.3 The common bulkhead design is easy to build and has a low weight to volume ratio 18.75 kg/cubic meter. The tanks are designed to operate at low pressures with a max. pressure of 50 psig used as the design upper limit.

8.2.5.5                           Orbital Correction And Maneuvering Set

8.2.5.5.1 The OCAMS is a reusable propulsion module designed to move the PMV short distances while in orbit. From the analysis of launch system injection accuracy a maximum likely error of 5% of the desired orbital altitude was chosen as a worst case parameter. Since the OCAMS must push varying size payloads of 3500 kg to ·15000 kg the largest payload was used for the design study.
8.2.5.5.2 The results of the design study show to push a Titan type PMV from a insertion altitude of 418 km circ. to the desired altitude of 440 km requires a $\Delta V$ of 13 m/s combined burn. The phasing maneuvers will require an additional $\Delta V$ of 7 m/s per degree out of phase. The combined maneuver plus a reserve will require the OCAMS to carry 100 kg of fuel.
8.2.5.5.3 The engine for the OCAMS is a single Marquardt R-40A engine developed for the space shuttle orbit control system. The R-40A has a dry mass of 10.25 kg has multi-start capability and supplies a 289N-sec min. impulse. The mass budget for the OCAMS is listed in table 8.2.5.1

## OCAMS Mass Budget

| Item | No. | Mass (kg.) | Mass Total |
|---|---|---|---|
| RCS thrusters | 16 | 0.34 | 5.44 |
| MMH tanks | 1 | 20 | 20 |
| Main Engine | 1 | 10.25 | 10.25 |
| He tanks | 2 | 12 | 24 |
| Pressure feed Sys. | 1 | 7.2 | 7.2 |
| Guidance | 1 | 4 | 4 |
| Tank suspension Frame | 1 | 20 | 20 |
| Honeycomb Main Frame | 8 | 4 | 32 |
| Thrust Structure | 1 | 5 | 5 |
| Separation Ring | 1 | 10 | 10 |
| Thermal Control Sys. | 1 | 10 | 10 |
| Nitrogen Tet. tank | 1 | 20 | 20 |
| | | Structure Tot. | 167.89 |

table.8.2.5.1

[1]     Dennis R. Jenkins (1992).  Space Shuttle  The history of Developing the National Space Transportation System.  Missouri:Walsworth Publishing.

[2]     James R. Wertz and Wiley J. Larson  (1991).  Space Mission Analysis and Design  Netherlands : Kluwer Academic.

[3]     Klaus D. Timmerhaus and Thomas M. Flynn (1989). Cryogenic Process Engineering.  New York: Plenum Pub.

[4]     Hanns Kellermeier,D.E. Koelle, R. Barbera(1984).  A Standardized Propulsion Module for Future Communications Satellites.  AIAA paper  84-0727.

[5]     Andrew Wilson  (1989-90). Intervia Space Directory  Virginia: Jane's Information Group inc.

[6]     Steven J. Isakowitz (1991).  International Reference Guide to Space Launch Systems.  Washington D.C. : AIAA  publication.

## 8.3.0 Operations Support Facilites

This section describes the capability which exists in the MSSS Operations Support Center (MOSC) to be located at Johnson Spaceflight Center. Included is an overview of the MOSC interfaces with the MCC, SSCC, Ground Control (GC), Space Station Mission Simulator (SSMS), POCC, and the CSOCC.

### 8.3.1 Support Responsibilities

The MOSC will be located at JSC in the MCC near the STS Flight Control Room (FCR). The MOSC will house two GC (a primary and a secondary pilot station) and several controller facilities will also be required for MOSC personnel. MOSC reconfiguration and maintenance interfaces will also be provided. The OSC will share STS facilities when possible to reduce system development cost. STS facilities will be utilized for the engineering and payload support teams to monitor MSSS operations.

JSC is responsible for all aspects of the OSC including design, development, operations, and maintenance. JSC will also provide training and flight support team personnel. JSC has responsibility for design, development, and integration of the GC.

### 8.3.2 MOSC Design

The preliminary design of the MOSC is described in this section. MSSS MOSC assumptions and guidelines are influenced by management, the MOSC development budget, and existing MCC floor space available for MSSS use. Existing and planned MCC and SMS capabilities will be used where possible, to enhance data systems integration, reduce sustained engineering costs, and reduce MOSC controller training time. The new hardware/software technology being developed for the MCC will also be utilized in the MSSS MOSC. Listed below are key assumptions made in the MOSC design:

8-16

(1) The MCC and MOSC data system may be limited to one critical phase at a time. Hence, while
one vehicle (Orbiter or MSSS) is engaged in a critical phase, the other can not be. Critical
phases include launch, rendezvous, proximity operations, EVA, or entry.
(2) The MSSS ground navigation and GPS monitoring will utilize the STS navigation software,
processors and personnel to the extent practical.
(3) The MSSS workstations will possess the capability to build command loads to be sent by the
avionics position, but the GC will automatically give priority to pilot commanding.
(4) The GC capabilities will be utilized to the maximum extent practical to reduce MOSC requirements.
(5) Classified operations may be required.

The MOSC contains all required hardware for integrating individual operators into a coordinated Flight Control Team. This includes, but is not limited to, multi-bay workstations, voice, electronic communication and data transfer equipment, room displays, and room clocks for mission events.

## 8.3.3 GC Design

The G is completely redundant including the power source, video monitoring, pilot hand controllers, and commands exiting the GC.

There are two GC's inside the MOSC. Each GC is independent and complete with the capability to control the MSSS. Each GC contains a Pilot Station, a terminal for command generation (Command Support Terminal), and a terminal to interface with the RISC computer (Ground Configuration Terminal). There are no single point failures which would result in the loss of both GC'S.
However, single components required for piloting operations do exist outside the GC, one of which is TDRSS.

The MOSC workstations are required to support the GC. However, the GC will have all commanding and monitoring capability necessary to control the MSSS In the event of a temporary loss of the MOSC workstations. Permanent loss of the MOSC workstations can not be tolerated because it contains capabilities which are critical for mission success. Those capabilities include system health monitoring, failure analysis, trajectory analysis, mission activity planning and anomaly evaluation.

## 8.3.3.1 Pilot Station

Only one Pilot Station is required for vehicle control and mission completion. The redundant console isrequired for backup capability if the primary console fails. The redundant pilot station will have command capability and can assist the pilot to ease his work load. Its primary task, however, is to serve as an on-line backup during time-critical phases.

Both Pilot Stations contain an area for time-critical commands and an area for non-time-critical commands. The time-critical area contains all functions required for the final phase of docking when the MSSS is manually piloted. This includes hardware for hand controllers, video monitors, latching commands, autopilot commands, and an assortment of single function switches. An area for sending non-time-critical commands is also provided to give the pilot station a complete command capability. This area consists of a terminal, keyboard, and some desktop work space.This terminal is identical in function to the Command Support Terminal

## 8.3.3.2 Command Support Terminal (CST)

The Command Support Terminal, which is identical to the pilots non-critical command terminal, allows another operator besides the GC PILOT and the PROXO to send commands. This terminal will be located near or in the MOSC and supported by an MOSC operator. The Avionics position will be able to send commands from this terminal. The system must be user friendly, easily accessible, and understandable. All commands will be programmed and placed on a call-up menu for commanding ease and to

eliminate errors. This call-up will be structured to allow command grouping, mission to mission reconfiguration, and operational efficiency. The system must also provide a safety check for critical commands to prevent untimely execution.

## 8.3.3.3 Ground Configuration Terminal (GCT)

The GC contains a terminal to interface with the RISC computer inside the MOSC. Ground personnel will use this interface for reconfiguration and maintenance of the GC hardware. This interface will also allow configuration control of the GC for check-pointing. Check-pointing is required to assure, in the event of a GC failure, previous configuration changes are not lost. Check-pointing may also be used to assure that each GC is identically configured.

## 8.3.4 MOSC Training

In addition to supporting real-time mission operations, The MOSC will also support training of the MOSC controller personnel. The MOSC interfaces with the MSSS Training Facility (MSSSTF) and the SSFMS simultaneously. The MSSSTF generates MSSS systems models, visual scenes of MSSS operations, and simulates the MSSS telemetry downlink. The MOSC simulated data is distributed throughout the MOSC to all support positions. The MSSSTF generated data will be used to train MSSS teams for MSSS free-flight operations which are independent of STS operations.

The MSSSTF will provide all MSSS simulation data to the MOSC and MCC as required to support Full-up and Integrated simulations. During SSF berthing and RMS operations the MSSS full-up simulation shall provide MSSS data to the SMS fororbiter on-board use. The MSSSTF will simulate MSSS systems, MSSS video, MSSS responses to commands, and the MSSS telemetry downlink. Preliminary facility architecture reflects an MSSS host computer which correctly models the MSSS computer commands systems performance, and responses. The MSSS host also solves equations of motion and provides the MSSS visual simulation system data needed to accurately simulate MSSS video scenes. The MSSS host interfaces with the MSSS

network simulation to output simulated MSSS telemetry downlink, including TDRSS and ground network. The MSSSTF also contains an instructor/development station which interfaces with the MSSS host. This station may be used during MSSS model development to test newly developed software and allow theinstructor to initialize and control the simulations.

The MOSC also interfaces with the STS Shuttle Mission Simulator (SMS). The SMS simulates STS systems, the MSSS in the payload bay, and STS visual scenes. The SMS will simulate MSSS component removal from the cargo bay and operations in close proximity of the STS. This includes simulations of the RF link between MSSS, STS, MCC, and MOSC. Both STS and MSSS personnel will be trained using the SMS simulated data.

## 8.3.5 MOSC Reconfiguration

The MOSC will be reconfigured as required before each light to reflect mission unique telemetry and commands. MOSC reconfiguration can also be performed in real-time if necessary. MOSC processors and tables which utilize these mission unique parameters are reconfigured to reflect the changes. Some items which are reconfigured in the MOSC are: telemetry definition tables, calibration curves, engineering unit conversion factors, limit sensing tables, limit sets, special computations, display processing parameters, and command tables. Software necessary to reconfigure the MOSC will be provided by JSC.

## 8.3.6 Software Verification

The GC may be used to test software modifications and isolate problems in either the MOSC or
light software without utilizing the MSSS. This support may be required during an MSSS mission.

Mission-unique data software updates are in two categories, vehicle configuration data and mission profile data. The vehicle configuration data

consists of all the hardware and software unique parameters associated with a particular MSSS (i.e., calibration and alignment data, equipment lists, etc). Calibration data will be required for gyros, accelerometers, and radar equipment. Alignment data will be required for sensors, and thrusters. Mission profile data consists of all the information necessary to perform orbital maneuvers. Profiles, such as MSSS mass properties, payload mass properties, and control gains are included. Thruster selection, software telemetry, and redundancy management tables are included. Other data in this category are MFC mission sequence, ephemeris (target, TDRS, Orbiter) piloting data, collision avoidance maneuver (CAM) data, attitude control data sets, guidance target sets, and software command blocks.

The MFC flight program is the mission common software consisting of write-protected code and constants, and unprotected variables. It provides the mission-unique flight design data for incorporation into a memory which can be updated. The real time variable portion of the MFC memory map will be verified to a range of values.

The MFC software will be verified and placed under configuration control. JSC flight design I-loads may be tested at the JSC possible using the MSSSTF. Verification and control will be managed by the SSL for the first flight and possible for subsequent flights. This may requprovide software functions for reconfiguration and verification.

Realtime software changes are avoided because of the risk of inadvertent changes; However, events will eventually mandate realtime software changes. All software changes will require
validation. The type of validation will depend upon what software
is involved:

(1) I-Loads   - mission unique unprotected variables typically changed during a mission,
(2) K-Loads  - generic write protected constants not typically changed during a mission
(3) CODE    - write protected code.

I-Loads are supported by special software which provides routine changes to be made without risk of damaging other software. These I-Load changes may be validated using the MOSC prior to

K-Loads reside in protected code and are not as easily changed as the validated by the SSL prior to implementation.

CODE changes are only made as a last resort because of the risk of damaging other software. Any code changes requires validation by the principal contractor.

### 8.3.7 Communications and Data Services

MSSS will interface with the GC through the Ground Network, TDRSS, or the SSF communication systems. In turn, the GC will interface with the MOSC. The MOSC will interface with the SSCC, SSL, CSOCC, POCC, the MCC for STS Orbiter data, the MSSSTF, and SMS as required. Note that MSSS piloted operations for the GC will be performed through TDRSS communication link only and that Space Station interfaces have not been identified.

### 8.3.7.1 Voice

Direct voice communication will be provided between the MSSS PILOT and the SSF crew. This will allow the SSF crew to relay information should contingency commanding from the FCO or MSSS Pilot be necessary. Voice communication will also be provided between the Space Station, MSSS PILOT and the MOSC GC PILOT. This will allow quick response by the GC PILOT.

The digital voice communication system used in the MCC will also be used in the MOSC. Communication will be provided between the MOSC (which includes the GC) and the STS FCR, SSCC, CSOCC, the Engineering Support Team, the Customer Support Room (CSR), the POCC, and the SSL.

The GC will be designed such that the pilot can control the MSSS and still have person-to-person communication with all operators. During piloting operations, the MSSS director is the interface between the pilot and the MOSC operators.

## 8.3.7.2 Telemetry

Interfaces will be provided to accommodate telemetry data from the MSSS through TDRSS, Ground Network, or strip and ship data from the Orbiter telemetry stream. Should an attached payloads's data be interleaved into the MSSS data stream, the GC will be responsible for the subsequentdeinterleaving.

The GC will provide data processing capabilities for the MOSC. It may be possible to utilize one of three STS real-time host computers as a dedicated computer for trajectory, Near-realtime retention,and reduction. In the future, as MSSS manifesting and scheduling demands increase, additional MSSS dedicated hardware may be provided to avoid impacting the STS or SSF MCC schedule.

## 8.3.7.3 Video

MSSS video is critical for MSSS piloting and mission success. Video decompression, if needed, will be provided by the GC. Distribution of video will be to the GC and the MOSC. Video data will be used fordocking and MSSS checkout by the pilot, FCO, and MOSC operators.

## 8.3.7.4 Commanding

Commanding from the GC to the MSSS can be by either one or two paths. The first path is direct from the GC through TDRSS. The second path is from the GC to the MSSS through the Radio Frequency (RF) systems similar to STS systems.

Commands to the MSSS can originate from three specific locations, the GC, MOSC workstation, or the CSOCC. The CSOCC can only issue payload/client spacecraft commands. Regardless of origination,all MSSS commanding will be processed by the GC.

## 8.3.7.4.1 GC Commanding

The GC command processor will ensure that manual (hand block (MOSC workstation or POCC) commands. The processor will also perform a "reasonableness" check on all commands.

The pilot station will have the capability to send the full range of MSSS commands, including both control and block commands. No other station will possess control command capability. Both GCs have the capability to command. Procedurally, only one GC will be commanding at a time. The capability will exist to switch to the back-up GC instantaneously if the primary GC fails.

## 8.3.7.4.2 SSF Command

## 8.3.7.4.3 MOSC Command

The MOSC workstations will build, verify, and send the required block commands to GC. Block commands cover a wide range, such as system configurations, checkout, trajectory loads, and initiation of orbit adjust maneuvers.

Commands generated by the MOSC can be inhibited by the MSSS Pilot. During critical phases, GC commands are used in conjunction with MSSS Pilot activity. During non-critical phases, such as orbit coast, the MSSS Pilot can shift command privilege to the MOSC. MOSC-issued commands are always formatted and hazard-checked by GC before being uplinked.

## 8.3.7.4.4 CSOCC Command

### 8.3.7.5 Command Time Delay

The time delay created by network, transfer, and GC processing must be minimized to provide the MSSS Pilot and GC PILOT with quick response to command strings and reaction totransients. Long time delays reduce the ability of MSSS to be remote commanded and hinderGC supervision. All time delays will be modeled during simulations in the MSSSTF and SSFMS.Command Encryption

### 8.3.7.6 Command Encryption

The policy for the application of communications security (COMSEC) is to be set by military standards on a per-mission basis. DoD servicing or Ferret/ASAT
operations require command
encryption. Planning must support the MSSS command and
telemetry links in either encrypted
or unencrypted mode.

### 8.3.7.7 Command Validation

A two-stage command capability provides the option for selected commands to be buffered priorto transfer to destination software applications or ORU or payload for execution. This capability ensures critical command integrity for such information as computer memory modifications and SSF or target state vectors. It also provides a command system troubleshooting tool. Two-stage buffering is part of the GC command process and features:

(1) downlink telemetry of the buffer contents
(2) execution of buffered commands on GC go-ahead
(3) removal of erroneous commands from the buffer via GC screening
(4) sufficient buffer size to allow review and storage of multiple block command strings

### 8.3.8 Project Integration Schedule

The project development integration schedule for MSSS would reflect both SSF and STS heritage. A template integration schedule should be developed showing meetings and events MSSSPO require for support.MSSS will require expanded JSC MOD facilities. These facilities must be designed and built; therefore, in addition to meetings held for the first test missions, the MSSS Project Office will be required to support meetings concerning facilities development.

## 8.4.0 MSSS FLIGHT OPERATIONAL CONCEPTS

The MSSS will be controlled from the MSSS cockpit. MSSS flight control and remote pilotage will be implemented utilizing this baseline operational concept. The goal is to provide a MOSC flexible enough to accommodate a variety of tasks in support of MSSS missions. MOSC flight operations must be simplified and standardized without unduly compromising SSF crew/MSSS pilot safety or missionsuccess.

### 8.4.1 Guideline Fundamentals

The fundamental guidelines for establishing this operational concept were based upon existing STS concepts. The MSSS must perform rendezvous/docking with SSF which will retain (assumed by the author) the same fail operational/fail safe requirements as the STS. The MSSS must operate closelywith SSF especially during proximity operations, as does the STS. The STS operational concept has grown out of many years of flight control experience; the same operational concept will be applied to the MSSS.

Most of the MSSS mission will be performed outside the CCZ separate from SSF. Because of complex and time-critical rendezvous maneuvers, the flight controllers will be located in a dedicated room in the MCC, called the MOSC. The MOSC will be located near the MCC FCR because of the critical information which must be exchanged for joint SSF/STS/MSSS/PMV operations. Additional support, such as sub-system managers and contractor hardware experts will be available for contingencies. Customer support will

also require an interface. Voice communications and data transfer interfaces will be established between these support facilities to provide an efficient means of exchanging information in the event of a contingency. Operator positions will be established to maintain these criticalinterfaces.

The following guidelines are provided to ensure the success of MOSC Flight Operations:

(1) During MSSS operations, The MSSS vehicle is independent of either SSF and/or STS. Therefore,
    the need for dedicated flight control areas are apparent.
(2) Standardized flight phases will be defined where feasible and convenient.
(3) MSSS procedures will be standardized to the maximum extent possible. Procedure development
    during realtime flight support for coping with systems failures will be reduced from the STS
    precedent due to the limited amount of redundancy and the electrical power of the vehicle.

## 8.4.2 Flight Support Teams

Realtime operations will be broken up into four major teams; the SSF flight control team, MSSS flight control team, engineering support team, and customer support team.

The MSSS flight control team residing in the MOSC is a dedicated unit. This team is on duty 24 hour a day for the duration of each mission. This group will provide direct, realtime support to ensure mission success. This team controls all aspects of the mission and has primary responsibility for mission success. The MSSS Director, with SSCC concurrence, will determine mission priorities and final actions to be taken. This team will control the vehicle through telemetry monitoring, video, and direct vehicle commands sent via the GC to either the pilot or the spacecraft systems during all mission phases. The flight control team will consist of the positions outlined in section 8.6.

The SSF flight control team resides in the SSCC; however, the principal member is the Flight Control Officer, who is an SSF crewmember. This team is responsible for MSSS deployment, retrieval, and berthing. A close interface is required during the MSSS mission to plan retrieval rendezvous with the allocated resources. The primary interface will be the FCO, who is under the authority of the SSF FlightDirector.

The Engineering Support Team will follow the MSSS's activates and mission progress. Additional data and information can be provided by the flight control team on request. The Flight Control Team will operate the MSSS within the limits and constraints set by the MSSS Operational Data Book. Operations exceeding these limits require engineering support team evaluation and approval.

The Customer Support Team will have representatives located in the Customer Support Room (CSR) and additional support from the remote CSOCC. The CSOCC has the ability to send payload and client spacecraft commands through the MOSC when required.

8.4.3 Concurrent Flight Support

Due to the nature of MSSS operations and the many critical phases involved with other systems (SSF,STS), Standalone capability is required. Interfaces with the mission control and training simulations of the other systems will occur often. and may impact upon the ability of the other systems to provideadequate support of their own operations. Most simulation resource conflicts can be resolved through scheduling. However, during periods of high activity, such as simultaneous STS, MSS, SSF andpossibly other programs, MCC capacity, at it's present level, would be unable to support all of theoperations simultaneously. The MOSC can only support one MSSS flight at a time.

8.5.0 Mission Planning

This section addresses the MSSS flight planning process concentrating on the major areas of flightdesign, operations, and training. It also describes the control plan for flight design developmentdocumentation.

## 8.5.1 Background

MSSS Preflight mission planning will be performed, essentially, the same as STS flight planning. The process, however, has been streamlined in order to expedite mission planning in accordance with therapid mission tempo precept. The planning will be conducted by the flight designers and missionoperators at JSC.

Several layers of planning must be accomplished before an MSSS mission can be executed. STS planning software could be used to reduce development of code. In order to accomplish the flight-specific mission design, modifications to existing STS mission design software will be required. These modifications include models of MSSS sensor systems, maneuver limits, ACS system, launch window, and deploy window routines along with the changes necessary to accommodate the massproperties of the MSSS.

## 8.5.2 Flight Definition

Before a detailed mission design can begin, the goals and objectives of the mission must be formulated and specific requirements identified. When the mission goals and objectives have been agreed upon bythe MSSSPO, the SSFPO, and the Client, JSC will be directed to begin planning the mission.

The MSSS flight planning will be coordinated with SSF operations planning to ensure that MSSS activityis compatible with Space Station crew timelines, re-boost schedules, and proximity operations planning. The SSFPO is responsible for mission planning compatibility.

### 8.5.2.1 Project Integration Plan

The Project Integration Plan is an agreement between the MSSSPO and the SSFPO and the Client. It defines the requirements of each party. It contains the objectives, constraints, roles and responsibilities, and the general NASA/Client interfaces.

### 8.5.2.2 MSSS Program Requirements Documents

All MOSC services to the CSOCC such as voice, video, trajectory services, and facsimile services will be defined in the MSSS Program Requirements Document, to be generated by the MSSSPO and theClient organization.

### 8.5.2.3 Flight Definition and Requirements Directive (FDRD)

The FDRD defines the mission goals and objectives and directs JSC to begin mission planning and flight design process on the proposed mission. The FDRD contains such information as proposedmission date, propellant delivery schedules, STS/ELV Special Payload Deliveries (if required), MSSS payload manifest, and mission constraints. It will be generated by the MSSSPO and will be delivered to JSC at approximately launch minus 5 months (L-5m).

### 8.5.2.4 Trajectory Planning Data Package (TPDP)

The TPDP is delivered to JSC at approximately the same time as the FDRD and contains the technicaldata necessary to perform the trajectory design. The package will contain such information as MSSS and Payload mass properties and propulsion performance data. The MSSSPO is responsible to fordelivering the TPDP to JSC.

### 8.5.2.5 Flight Requirements Document (FRD)

The FRD is produced by JSC using inputs from the FDRD and the Payload Integration Plan. The FRD states the mission objectives and specifies flight requirements. The preliminary flight requirements document is produced

approximately 4 months (L-4m) before the mission. The requirements specified in the FRD will be used to subsequent flight profiles.

## 8.5.3 MSSS Flight Planning Process

The actual long-range flight planning process begins several years before any particular mission with the projected mission profiles study. The results of the study are used to determine ELV-based propellant delivery schedules. The resulting schedules ensure sufficient propellant availability for a given tempo of MSSS operations. Any deviance from the projected mission profiles study may require supplemental ELV support. It is imperative that enough contingency propellant be available to handle a tanker loss or forego a dedicated tanker mission. Such contingency storage prevents ELV timelines from interfering with MSSS timelines.

The MSSS preliminary mission flight planning process begins as soon as the Project Integration Plan is drafted. A number of mission templates will be available and initial mission estimates made based upon the templates. The templates produce preliminary assessment data which identifies the necessary elements to complete the proposed mission. This includes shared STS flight cargo, rendezvous assessments, crew, mission, and training timelines. Trade studies will be undertaken to maximize system performance between SSF, MSSS, target, and STS as needed. Optimum profiles are determined based upon mission constraints, and previous and following sortie requirements. The MSSS profile chosen will satisfy the desired mission constraints, rendezvous windows, and multiple MSSS deployment windows to the fullest extent possible.

The flight Design Team's first opportunity to develop an integrated (MSSS, SSF, target) profile and timeline is the Assessment Flight Profile (AFP) design cycle. The AFP is drafted as soon as possible after the FDRD and TPDP are delivered to JSC. This cycle allows the MSSSPO and other parties to critique the flight design at an early stage. The Conceptual Flight Profile (CFP) cycle runs from launc minus 4 (L-4m) to (L-3m). In this cycle, a detailed assessment is made in preparation for the PayloadIntegration Review (PIR). The final

detailed analysis of the flight is performed during the two Operational Flight Profiles (OFP) cycles which run from the end of CFP to launch. During these cycles, the flight products and on-board data loads are generated. Due to the nature of SSF/MSSS flight design, MSSS data loads (I-loads) will be produced in parallel with SSF data loads and flght products.

### 8.5.3.1 Assessment Flight Profile (AFP)

During the AFP cycle, a preliminary profile, timeline, propellant budget, power budget, and deploy/launch window are developed primarily using desktop computing techniques. Several profiles are considered during this planning phase.

### 8.5.3.2 Conceptual Flight Profile (CFP)

In the CFP profile, a set of ground rules and constraints are developed to better define the flight. Analyses are performed which result in a trajectory profile, timeline, propellant budget, power budget, deploy/launch window and other flight design items. The level of detail must be sufficient to support the PIR.

### 8.5.3.3 Operational Flight Profile (OFP)

In the two OFP cycles, actual flight products are developed. These include a more refined set of ground rules and constraints, an activity plan, a pilot procedures book, critical windows, and I-loads. The analyses done in this phase use the most complex tools available including Monte Carlo dispersion analysis and pilot simulations to define procedures. Analysis of off-nominal launch and deploy times are performed to ensure the trajectory sequence will function throughout the launch/deploy windows.Crew training is performed during the OFP cycle using data generated in the flight design process.

### 8.5.4 Flight Design

MSSS flight design consists of the development of maneuver profiles, SSF deploy windows, and MSSS attitude timelines which satisfy mission objectives while staying within the power, propellant, and time constraints. Flight design is dependant on SSF capabilities and mission objectives. The flight is designed such that the MSSS will operate as independently as possible.

Certain phases of MSSS flight design will be standardized due to their repeatable nature (design templates). For maneuver profile design, several areas exist which may be the same on most missions.
These standard mission phases will probably include rendezvous approach to the target (from several kilometers to a few meters), proximity operations approach, MSSS checkout, deberthing and separationfrom SSF. For an off-nominal flight, any/all of these phases may be modified to accommodate uniquemission requirements.

Other area will be unique for almost every mission. These include launch/deploy windows and phasing requirements in the rendezvous maneuver profile. Many trade-offs exist in SSF/MSSS capabilities; e.g.a SSF re-boost may be rescheduled to enlarge a MSSS launch window.

Throughout the design process a working knowledge of the power, timeline, and propellant impacts of the design will be used. Once a preliminary profile is developed, a detailed analysis of windows, trajectory dispersions, power profile, and propellant usage will be completed. The profile is then modified to overcome any shortcomings discovered in the analysis. The basic process is repeated during each cycle of the flight design template. Any changes to the mission objectives or payload requirements are integrated during these cycles. During the OFP, the mission data loads are generated for the vehicle.

During each flight design cycle, a number of products will be delivered. These include, but are not limited to, propulsive and non-propulsive consumables budgets and flight charts, attitude timelines, antenna communications availability analyses, ground rules and constraints, event sequences, day/night timelines, deploy windows, on-board data loads, Monte Carlo

dispersions, rendezvous targeting plans, relative motion plots, plume torque disturbance assessments, surface damage assessments, flight rules, and pilot procedures.

## 8.5.5 Operations Planning

Flight operations planning is the set of tasks which must be accomplished to ensure that MSSS systems, pilots, and flight controllers can adequately support the flight. It also includes planning performed to ensure smooth execution of the flight itself. All of these task will be accomplished by the JSC staff.

The Client PIP and its annexes and the results of analyses performed during flight design are the primary inputs to operations planning activity. These inputs are used in the production of SSF and MOSC Flight Data Files (FDF's) and operations support documentation. For the MSSS, the MOSC documentation under the Crew Procedures and Control Board (CPCB). Some SSF FDF documents pertinent to MSSS operations are the Crew Activity Plan (CAP), MSSS Deploy and Retrieval checklists, and MSSS/Payload Systems Malfunction Procedures. MOSC FDF will include a Mission Activity Plan (MAP) and MSSS/Payload Contingency Procedures. The MAP is the major mission timeline and includes all mission events, trajectory profiles, day/night cycles, and NASCOM support schedules.

Several other types of support documents will be required as a result of detailed mission planning. These are:

(1) MOSC FDF
(2) SSF FDF
(3) MOSC/MCC/SSCC/CSOCC Network Support Plans
(4) MOSC/MCC/SSCC/CSOCC Command Plans
(5) MSSS Communications and Data Plan
(6) MSSS Flight Rules
(7) Console Handbooks and System Briefs
(8) MSSS systems schematics

(9)  MSSS Operational Maintenance Instructions

(10) Flight Software Documentation

(11) Payload Handling Characteristics Handbook

(12) MSSS Man Rating Safety Assessment

Also accomplished during this planning period are detailed MSSS systems and consumables analyses for the flight, using the flight profile and MAP as the basis for the studies. As s result, detailed maneuver plans, attitude plans, mass properties history, consumables budgets, and redlines for the flight are produced. These analyses and plans are converted to their I-Load equivalents and compiled on an I-load data optical disk or other storage medium. The I-Loads are sent to the MSSS approximately 3 days prior to the mission date. I-load update after mission start will performed on-orbit.

## 8.5.6 Training Planning, Development, and Implementation

The early training planning task involves evaluation of the upcoming flight to determine mission training requirements, plus facilities required to accomplish said training. Other activates include determining the MSSS, SSF, and payload skills required, and determining the skill level and availability of pilots.

Once detailed operations planning is well underway, the training planning, development, and implementation task will consist of  developing any unique training, scheduling training facilities, and performing the training to support pilots and ground controller personnel.

MSSS and SSF related training are the responsibility of JSC for pilots, SSF crew, and flight control personnel. The client organization is responsible for payload related training for the flight control team and pilots. Integrated MSSS/payload training operations is the responsibility of JSC with inputs from the client.  In order to organize a balanced training plan, client personnel will be an integral part of training development.Section 7 contains detailed descriptions of training activities.

## 8.5.7 Payload Integration

Payload Integration is performed premission with several organizations coordinating with one another. These organizations are the NSTS Integration and Operations Office, SSFPO, the MSSSPO, and the MOSC and SSCC. JSC manages the entire operation and coordinates formal agreements and requirements. The NSTS Integration and Operation Office integrates the customers payload into theSTS using the STS/PIP. This PIP describes the interfaces between the STS and the payload. TheSSFPO integrates the customers payload into SSF using the SSF/PIP. This PIP describes theinterfaces between the SSF and the payload. The MSSSPO integrates the customers payload into the MSSS using the MSSS/PIP. This PIP describes the interfaces between the MSSS and the payload. All PIP's include handling and mate/demate information, and all services provided to the payload. The MOSC and JSC flight planners use the PIP's to plan flight activates and procedures. Flight control team members coordinate closely with the client to develop payload and servicing operations procedures and to become as familiar as possible with the MSSS and client payloads and spacecraft. The client provides realtime support via the CSOCC and/or the Customer Support Room (CSR) located on the second floor of the MCC.

## 8.5.8 Crew Procedures and Control Board (CPCB)

A well organized, effective CPCB is in place for the STS, the MSSS will be represented as an integral part of a CPCB based upon the STS CPCB in use for SSF. Many STS procedures will be modified to form MSSS procedures. Rendezvous and deployment activates especially benefit from using already existing STS procedure. However, additional standalone procedures will be developed for the MSSS. These procedures will impact the SSF CPCB as additional time allocation needed to address MSSS operations.

The CPCB shall be operated under authority of the JSC MOD for development, validation, and change control of all MSSS FDF.

The responsibility of the CPCB is to insure the orderly development and control of MOSC FDF and pilot procedures from their inception through mission completion. Specifically, CPCB activities include:

(1) Directing the development, publication,and distribution process to be utilized for the MOSC FDF

(2) Determine FDF and pilot procedures requirements for each mission including alternate and

contingency situations. Identify preparation responsibilities, Maintain the status of each MOSC

FDF item for traceability and control.

(3) Establish and implement procedures to validate MOSC FDF. Ensure timely and complete review of

MOSC FDF by appropriate technical personnel from NASA, contractors, and the client.

(4) Coordinate and provide MOSC FDF development schedules compatible with training requirements

and applicable mission events.

(5) Determine requirements and reference data; i.e. hardware operational characteristics, system

parameters, trajectory parameters, and constraints for use in development of MOSC FDF.

(6) Provide and Coordinate pilot procedures development with other program activates such as

engineering simulations, SSF/MSSS avionics integration laboratories, and major hardware

testing and provide feedback of test data which impacts the current MOSC FDF.

The CPCB reviewing of all MSSS documentation shall be chaired by the DIrector of Mission Operations. A MSSSPO representative will be on the CPCB.

## 8.6.0 MOSC REALTIME SUPPORT

Realtime MSSS Operations will be performed by the MOSC Flight Control Team. Support will be provided by the Mission Management Team, the Engineering Support Team, and the Payload/Client Support Team. This section describes the MSSS Flight Control Team positions and responsibilities. The other support teams are also described.

## 8.6.1 Flight Control Team

The MSSS Flight Control Team performs all realtime MSSS operations in support of the MSSS Pilot, and is responsible for the mission. The Flight Control Team consists of the MSSS Director, the Ground Control Pilot (GC PILOT), the Proximity Operations Officer (PROXO), Guidance/Navigation/Control (GNAC), Propulsion/Propellant Engineer (PPE), Avionics System Analyst (AVIONICS), Flight Dynamics Officer (FDO), the Flight Support Systems Officer (FSSO),and the Mission Activites/Payload Officer (MAPO).

The MOSC will maintain close interfaces with the MCC but MSSS support will remain independent of other programs. This independence allows the MSSS support team to operate intact regardless of other simultaneous MCC activates (STS, ELV, or SSF support). Position responsibilities remain the same during all phases of the MSSS mission.

### 8.6.1.1 MSSS Director

The MSSS Director is the controlling authority for all MSSS realtime operations. All decisions regarding the safe and expedient conduct of the mission is the OMV Directors responsibility. The MSSS Director does not have the responsibility for operating systems or performing any particular task. This frees the MSSS Director to manage the MOSC positions. In a contingency situation, the MOSC positions will present their status to the MSSS Director. Although individual MOSC positions can build and send commands through the avionics position, the MSSS Director will coordinate the flow and execution of these commands. The MSSS DIrector must design which options presented to him by the other members of the Flight Control

Team are consistent with the established mission flight rules and bestserves mission objectives.

When in the CCZ or the vicinity of STS, the MSSS DIrector must coordinate with the SSCC Mission Director and FCO or STS Flight Director.

A lead MSSS Director will be assigned to each MSSS mission and will operations documentation pertinent to that mission and developing the MSSS Flight Rules. This Director will represent the MSSS Flight Control Team at the MSSS Flight Readiness Review which will take place approximately 1 week prior to an MSSS mission.

## 8.6.1.2 MSSS GC PILOT (GC PILOT)

The GC PILOT is responsible for total dynamic control of the MSSS during contingency operationswhich incapacitate the MSSS Pilot or communications failure. The GC PILOT may assume partial control of the MSSS vehicle to aid the MSSS pilot during demanding control operations such as aerobraking and grappling/secure operations at CCZ-2.

During GC control of the MSSS Vehicle, the GC PILOT will have full control and authority. Mission Directives can be recommended by the MOSC support positions but the MSSS DIrector shall be the final authority.

Communications to the MSSS Pilot during operations will be controlled by the MSSS Director. The GC layout provides the capability for the MSSS Pilot, GC PILOT, FCO, and MSSS Director to conduct person-to-person conversations with the PROXO and other positions while piloting the vehicle.

The GC PILOT and PROXO consoles will have all required command capability. The AVIONICS position is the only MOSC position with a command execution capability. Thus all remote commands must be routed through the AVIONICS position.

The GC PILOT will support during all flight operations. Support of these phases allows the GC PILOT to status the systems and trajectory, check procedural changes, and configure the console while the MSSS pilot actually operates the MSSS. Such support allows immediate control handover to the GC PILOT as needed. The MSSS Director has authority to handover MSSS flight control.

### 8.6.1.3 Proximity Operations Officer (PROXO)

The PROXO has responsibility for onboard guidance and navigation application software and procedures. The PROXO position is manned during all phase of the mission. PROXO assess all impacts to proximity operations due to vehicle anomalies or off-nominal performance, performs replanning (of proximity procedures) and coordinates overall profile execution with the FDO. PROXO's primary responsibility is the development of the proximity operations profile, I-loads, and procedures to be utilized by the PILOTS and the FCO during flight operations.

The PROXO participates in overall MSSS mission profile generation insuring conformity with MSSS capability. PROXO is responsible for the development of contingency protocols and workarounds concerning proximity operations. The PROXO is certified and proficient to remote pilot the vehicle and may assist the GC PILOT or MSSS Pilot during operations.

### 8.6.1.4 Guidance, Navigation, Control (GNAC)

Then GNAC is responsible for realtime analysis and control of the following systems:

(1) Inertial Measurement Units
(2) GPS hardware
(3) Rate Gyro hardware
(4) Guidance and control system software
(5) ACS system

This position will build all necessary commands and is required during all MOSC shifts.

### 8.6.1.5 Avionics Systems Analyst (AVIONICS)

The AVIONICS position is responsible for the realtime analysis and control of the following systems:

(1) Command and data handling system (C&DH)
(2) Onboard computer hardware and systems software
(3) Video Camera systems
(4) High gain/Omni/GPS antenna positioning
(5) Redundancy Management
(6) Communications relate software
(7) Computer operating systems software
(8) Data bus
(9) Radar system and antenna

The AVIONICS position will manage the MSSS command link. This position coordinate offline support and provides subsystem health, status, and anomaly assessment to the MSSS Director. System reconfiguration commands would originate from this location. However, during time-critical operations, the GC PILOT station will send all commands. Communications with the payload and client spacecraft will be managed by this position.

The AVIONICS position is required during all MOSC shifts for commanding and system monitoring. This station will have access to the CST which interfaces directly with GC for commanding. This terminal will support the MSSS Pilot and GC PILOT as required. The MOSC workstations will have the ability to build and send commands via AVIONICS during non-time-critical operations. The AVIONICS position will be responsible for establishing the communication links used for troubleshooting communication link problems.

### 8.6.1.6 Propulsion and Propellant Engineer (PPE)

The PPE is responsible for realtime assessment and monitoring of the following systems:

(1) Primary Propulsion Engine(s)

(2) Gas-generators for engine and tank pressurization

(3) Cryogenic Bi-Propellant storage

(4) Pressure control electronics

(5) Propellant budget and redline margins analysis

(6) Propulsion-related application software

(7) Propellant status for mass properties

### 8.6.1.6 Flight Support Systems Officer (FSSO)

The FSSO has the responsibility for monitoring and managing the following systems:

(1) Thermal control system

(2) Manipulator hardware

(3) Manipulator control electronics

(3) Electrical power systems

(5) APU units

(6) Propellant Storage for APU/ACS system

(7) APU/ACS propellant status for mass properties

(8) APU/ACS propellant budgets and redline margins

(9) Exterior lighting system

(10) cabin lighting system

(11) Life support system

(12) Atmospheric management, storage and composition

(13) Atmosphere budget and redline margins

(14) docking hardware

(15) hatch integrity

The FSSO position coordinates offline support and provides subsystem health, status, and anomalyassessment to the MSSS DIrector. The

management of power to MSSS and payload and client spacecraft are the responsibility of this station. The FSSO station will be manned at all times during a mission. The FSSO has command building authority over the above systems. FSSO commands are routed through the AVIONICS console.

## 8.6.1.7 Flight Dynamics Officer (FDO)

The FDO has overall trajectory responsibility for premission and realtime definition,design,planning, monitoring, and execution of impulsive MSSS maneuvers. Specific areasinclude:

(1) launch and rendezvous window analysis

(2) Orbit adjust and rendezvous profile

(3) Maneuver planning, targeting, monitoring, and confirmation terminating at the proxops phase

(4) SSF/STS/MSSS trajectory profile coordination

(5) ground navigation coordination

(6) Attitude/pointing requirement for burn support

(7) Contingency analysis and replanning including time to ignition slips

(8) Predicted acquisition parameters

(9) trajectory database management

(10) trajectory tool maintenance and console reconfiguration

(11) relative motion analysis

(12) collision avoidance analysis and coordination

(13) ground radar tracking and site scheduling

(14) state vector command preparation

## 8.6.1.8 Flight Control Officer (FCO)

The FCO is an SSF crewmember and occupies the FCO station in the cupola workstation. This stationprovides the FCO a clear view of all spacecraft cleared to grapple/docking positions. The FCOcoordinates with and supervises the MSSS Pilot during operations in the Proximity Operations Zone.

## 8.6.1.9 Mission Activities and Payloads Operations (MAPO)

MAPO is responsible for the development and maintenance of the MSSS mission activity plan, payload-related attitude and pointing profiles, and payload related MSSS FDF's. MAPO coordinates between the MSSS flight control team and the client support teams/CSOCC. TheMAPO represents the client payload/servicing requirements to the MSSS Flight Control Team and represents the MSSS to the client.

## 8.6.2 Mission Management Team

The mission management team will monitor SSF/STS and MSSS operations and is responsible for making any necessary programmatic decisions; e.g. whether or not to proceed with servicing if a warning indicator in the grappler arm is present. The mission management team will supporthe SSF and MSSS flight control teams prelaunch and for the duration of the mission. The MSSS Program director will chair the team, and the SSF program manager will be present.Other members include the customer management, the payload integration manager, and the JSC mission operations Director. The Mission Management Team will monitor MSSS operations from the customer support room and will interface with the flight control team via the MOSCDirector.

## 8.6.3 Engineering Support Team

The flight control team is supported by the engineering support team. for analyzing situationswhich occur in realtime which are outside the scope of the MSSS operational data book. This engineering support will be provided by the MSSS system design engineers of the ENAE department and the principal contractors.

## 8.6.3.1 Spacecraft Analysis (SPAN) Team

The SPAN team will be located within the MCC complex near the MOSC. The SPAN coordinatesrequests for engineering evaluations from the MSSS and

SSF flight control teams. Any request for engineering analysis of MSSS systems will be routed to the SPAN team. The SPAN analysis recommendations are communicated to the MOSC director for approval and execution.

8.6.3.2 CSOCC Support

8.6.4 Payload Support Team

Payload support teams consist of remote CSOCC personnel and/or customer support teams sent to JSC to monitor and participate in payload and servicing operations. Payload support teamsinterface with the flight control team via the MAPO position. customer support teams sent to JSC will monitor MSSS operations from the customer support room in the MCC.

8.6.5 MSSS Training Facility Support

The MSSSTF primary function is for personnel training premission and possible I-load software verification activity premission. However, the MSSSTF could be utilized for procedure validation during a mission.

8.7.0 PREMISSION TRAINING

This section covers the various types of training required for the MSSS Mission and the trainingschedule.

8.7.1 Initial Training

The First phase of MSSS training for pilots, MOSC controllers, and SSF and STS crews will consist of self-study workbooks and computer-aided instruction describing MSSS systems, flight operations, GC systems and operations, workstation operations, and MSSS/SSF interfaces and operations. These materials will be prepared by the JSC Training Division. A training brief will be delivered to JSC controllers and crew members to address item of

interest which are flight specific and to allow interactive discussions with MSSS clients, engineers, and support teams.

Additional classroom/video training will be required. The GC will provide simulation software for the pilot and subsystem positions.

### 8.7.1.1 Standalone Training

MSSS Standalone training will be used to provide initial simulation training for pilots and controllers. This training will consist of 1-2 students and an instructor. Pilot core training will include vehicle maneuvering, GC familiarization, MSSS systems commanding, spacecraft approach and docking, payload handling, SSF traffic management and controlled airspace procedures, and contingency protocols. MOSC controller core training will consist of workstation familiarization, dynamic data display familiarization during typical flight phases, commanding, system familiarization, and contingency protocols. The training will be available for proficiency maintenance of students who have already completed core training.

### 8.7.1.2 SSF Crew Initial Training Excersizes

The SSF deployment/retrieval crew will consist of the FCO and an RMS operator. Core training willconsist of MSSS-related generic training (rendezvous and proximity operations, RMS operations in MSSS docking/berth/deberth, payload handling, servicing, and turnaround, vehicle and hardwareretention systems, and communications) in generic JSC facilities.An MSSS-shaped mockup will be required to support RMS training in the JSC Manipulator Development Facility. Additionally, if any EVA's are planned in support of MSSS operations, a mockup will be required to support EVA training in the JSC Weightless Environment Training Facility (WETF).

### 8.7.2 Advanced Training

Upon completion of core training, subsequent training is required. Training is both generic and mission specific.

## 8.7.2.1 MOSC Training Exercises

A MOSC team consisting of MSSS Flight Director, GC PILOT, PROXO, and controllers who have completed at least core training will proceed with advanced training using the consoles and hardware/software tools in-place at the MOSC. This training will be driven by the MSSS Full-Up Simulation capability located within the MSSSTF. During these training exercises the MOSC will interface with the MSSSTF for MSSS data and interface with the OTF or SSTF for data which may be needed during proximity operations and docking. This training will exercise the MOSC team members in their respective discipline and in coordinating between other disciplines during simulated discrete flight phases and full MSSS free-flight duration. These training exercises can be either generic or flight specific in nature.

## 8.7.2.2 MOSC/Remote Facility Training Exercises

During specific MOSC training exercises, data and voice links to CSOCC, SSCC, contractors, and/or POCC will be established in order to exercise interfacility operations that will be necessary for MSSS flight. This training will also be driven by the Full-Up Simulation capability located within the MSSSTF and will most often be flight specific.

## 8.7.2.3 SSF Crew Advanced Training Exercises

The MSSS deployment/retrieval crew will receive advanced training for MSSS operations in the existing SSF Mission Simulator (SSFMS). An MSSS functional model resident in the SSFMS or provided by the MSSS Full-Up simulator will allow the SSF crew to exercise MSSS predeploy checkout, deployment, separation, rendezvous, grappling, berthing, and powerdown and safing.

## 8.7.2.4 Integrated MOSC/SSF Training Exercises

The MSSS Full-Up Simulation will be capable of performing a MOSC training exercise while integrated with the SSFMS and MSSSTF simulators simultaneously. Duringthese exercises the SMS may also be integrated with the MCC. These simulations will exercise the MOSC/SSF and MOSC/MCC interfaces and operational handovers during discrete mission phases and during the entire MSSS free flight duration. Data and voice links from the MOSC to CSOCC, contractors, POCC, or the SSCC will be established, as appropriate, during these simulations.

### 8.7.3 First Flight Training Schedule

Instructive materials and flight procedures will be available for MSSS pilots and controllers approximately 18 to 24 months before first flight. These materials will be updated as the MSSS operations and/or systems are modified.

The Standalone simulation capability will be available 18 months before first flight for instructor checkout and certification. MSSS pilot and controller core training will begin at approximately L-16 months. The standalone training software load will be representative of the anticipated first flight missioncharacteristics.

The MOSC will support personnel training and console procedure development starting at L-18 months. This is required prior to the first flight for development of the team communications, team timing, display, special computations, and standard console procedures.

The MSSS full-up simulation capability will be operational at L-9 months for instructor checkout and certification. MOSC and MOSC/Remote Facility simulations will begin at L-8 months for integrated training with MOSC teams which have completed their core training. The software load for this training will be representative of the anticipated first mission characteristics.

STS crew members responsible for deploy and retrieval on the first MSSS mission will follow the 12 weeks a final, first flight specific software load will

be delivered for both the standalone and full-up simulations. All MOSC teams supporting the first flight will participate in MOSC simulations using this final load. Also in this time frame the SSFMS training software load for the MSSS deploy/retrieval mission will become available for SSF crew advanced training and SSF/MOSC joint training. The MSSS flight specific software load will support SSFMS development milestones.

## 8.7.4 Subsequent Flights

Previous flight simulator loads will be used for core training of new MSSS personnel and proficiency maintenance of existing Flight Control Teams. At L-4 weeks before each MSSS mission a flight specificload for the MSSS full-up simulation and for the SSFMS will be delivered for flight specific advancedtraining. Training will began at L-3 weeks.

## 8.8.0 Space Station Operations

This section addresses planning, training, and execution of MSSS tasks to be performed at or in conjunction with Space Station Freedom. The proposed SSF traffic management plan may be revised as the SSF design evolves resulting from Clinton Administration redesign mandates.

## 8.8.1 Assumptions

MSSS Personnel will not be located in the SSCC. The SSF cupola workstation will contain the FCO
station and a MSSS pilot station with sufficient flight controls such that MSSS could be piloted remotely
by the FCO from the CCZ to the SSFPOZ to docking/berth. MSSS, STS, and PMV docking operations
will not occur simultaneously.

## 8.8.2 MSSS and SSF Overview

The extent to which MSSS could be utilized by SSF is largely a function of the MSSS design. MSSScould perform dexterous manipulation tasks at SSF as well as in GEO, further increasing mission options.

MSSS can only become operational after PMC. MSSS operations require:

(1) cupola workstation with FCO/Pilot station

(2) servicing/berthing facility which houses automated systems which refuel/refurbish/inspect MSSS and MSSS payloads. It must also be able to store MSSS and payload consumables such as H2O, GN2, Hydrazine products, NTO, various cryogens, and tools/end effectors

(3) Cryogenic storage facility which can store large amounts (exact requirement TBD) of LO2 and LH2 to be fueled by regular delivery from the surface via ELV-delivered PMV tankers.

8.8.3 Control Center Interactions

The MOSC will operate independently during operations outside the CCZ. Prior to approaching the station MSSS director will notify the SSCC Operations Director of the intent to enter the RDZ, and then coordinate operations between the MOSC and SSCC as required. Following a joint decision, the MSSS by the SSCC Ops Director and the MSSS Director inform the SSF FCO and MSSS approach is initiated under MOSC guidance. The SSCC and FCO will be advised of the progress of the approach. At the CCZ boundary, dynamic control safety critical system monitoring of MSSS will transfer to the FCO and authority for the direction of the mission will be handed off from the MOSC Director to the SSCC Operations Director. The MOSC will continue systems monitoring and provide recommendations to the FCO as needed. The MSSS pilot will excersize physical control of the vehicle during all phases of operations, acting under the guidance of the current control authority. The MOSC or FCO can assume command and dynamic control of the MSSS in the event of communications failure or SSF/MSSS crew incapacitation. Proximity procedures for a MSSS total radio-

out situation must be developed, but will probably consist of remote piloting from MOSC and the FCO.

This plan should be consistent with the distributed control center approach used by NASA to operates STS and SSF. The MOSC facilities and user tools should be compatible with STS, MCC, SSCC, and SSF with respect to control team communications, data displays, telemetry processing, command processing, and other user tools.

## 8.8.4 Rendezvous & Proximity Procedures

MSSS release and recovery could be from either a positive or negative V-bar. The + V-bar approach would be preferable for it provides good target visibility. The rendezvous phase ends and proximity operations begin when MSSS enters the Space Station Proximity Operations Zone (1 km radius around SSF).

The MOSC will continue to perform overall system monitoring and provide recommendations during operations within the CCZ. The FCO has overall responsibility for operations within the Proximity Operations Zone. The Pilot will execute all proximity maneuvers under guidance from MOSC and theFCO. MOSC support will continue on an as-needed basis until MSSS is berthed.

During departure operations, the MSSS Pilot will control the spacecraft within the CCZ. Control authority passes from the FCO to MOSC when MSSS exits the CCZ. The FCO advises MOSC and the SSCC Operations Director of mission progress until MSSS exits the Rendezvous/Departure Zone.

## 8.8.5 Training

The Space Station Training facility will be able to conduct MSSS piloting simulations from a space station cupola workstation mockup. Software simulations will be available for the SSF crew and FCO to conduct in-orbit

simulations from the cupola workstation and possibly a dedicated console. Maximum level of similarity between GC, FCO, and SSF Training Facility should be attempted. The purpose of this is to limit pilot/controller retraining required due to dissimilar facilities; i.e. different control locations

## 8.8.6 Crew Responsibilities

The FCO will monitor the MSSS approach trajectory only to the extent required for a successful hand-over at the CCZ boundary. Upon CCZ entry, the FCO will assume dynamic control and command authority, providing the MSSS pilot with approach corrections and possibly flying the MSSS to grapple/dock position in the event of pilot incapacitation or communications failure. The FCO will monitor safety-critical systems during approach. When the MSSS is berthed, the SSF crew is responsible for ensuring proper operation of on-board systems required to meet MSSS utility needs. Safety-critical systems monitoring and fault detection will be as automated as possible in order to SSF crew MSSS-related IVA to be minimized.

## 8.8.7 Payload Responsibilities

The MOSC will operate independently when conducting payload/servicing operations outside CCZ-2 unless the target is a SSF element. In this case, operations with the appropriate Space Station Element Control Center will be coordinated by the SSCC.

For MSSS payload loading/unloading operations conducted at SSF the SSCC will have the primary responsibility for integration and check-out, and verification operations conducted by the SSF crew and on-board systems. The above activates will be monitored by the CSOCC, which will provide realtime engineering support and guidance to the SSCC and SSF crew.

## 8.8.8 MSSS Refueling and Servicing

Refueling of primary cryogenic propellant will be accomplish by a Common Cryogenic Transfer Coupling (CCTC) located on the SSF RMS or in the MSSS

refurbishment facility. LH2 and LO2 will be drawn from the depot located on-station Refueling of secondary propellant (APU/ACS) shall also be accomplished via the CTCC, and will be accomplished automatically but supervised by the SSF crew.

MSSS cryogenic propellant tanks will be filled as part of the preflight checklist and top-off fuelingconducted until removal from the berthing/servicing facility.Other MSSS servicing operations include battery charging(?), Atmosphere replenishment, LiO2 replacement, and ORU replacement.

### 8.8.9 Transport into Orbit

One space shuttle flight will be enough to MOOSE into Orbit. A suggested arrangement is given in figure 8.10.4 The usable dimensions of the of



8.8.1b: Side View

8.8.1a: Perspective View          8.8.1c: Front view
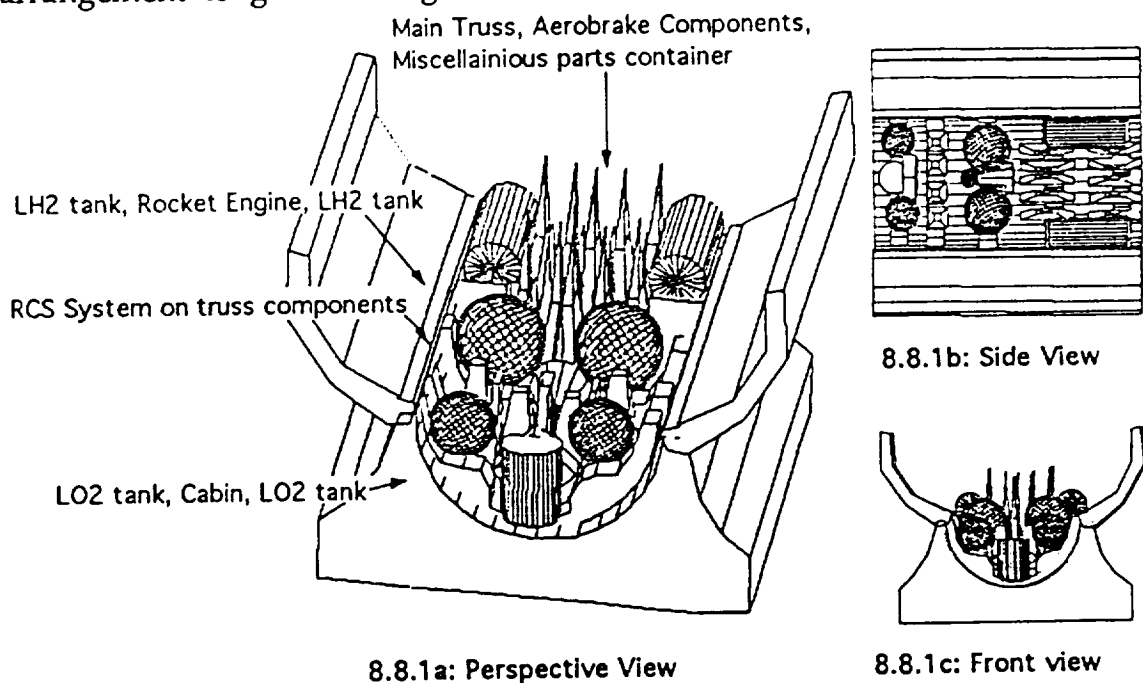
## Figure 8.8.1 Conceptual Shuttle Bay Arrangement

the space shuttle's cargo bay are a length of 18.2 m and a diameter of 4.5 m. Typical launch load estimates for doing the finite analysis design on the truss are 11 gees in all directions, and 85 rad/s about the space shuttle's velocity

vector. Geometry is used to lessen the forces on the vehicles. These are conservative numbers based on a standard hitchhiker platform estimates, will more than likely lead to overdesign and the weight problems associated with overdesign. For this reason, NASA specialists are usually called in to help. Using past flights and some testing, better approximations are made, to which the platform structure is than designed. This analysis still needs to be done. At the present time, MOOSE will need to be assembled on-orbit by EVA. The RCS truss will need to be attached to the cabin, and the tanks and main rocket engine will have to be connected to the main truss. The aerobrake will then be assembled and attached to the vehicle.

## 8.9.0 Satellite Proximity Operations

### 8.9.1 General Considerations

Proximity operations cover all operations within a one kilometer radius of the target satellite. The final phasing maneuver should bring MOOSE within this radius. After the final phasing maneuver, MOOSE should have enough daylight to complete its mission. Such light will help the pilot as he/she performs the tasks of satellite repair. Also before MOOSE is within the one kilometer radius, the satellite should be deactivated. This is to prevent any unforeseen accidents. Example: the satellite's attitude adjustment system comes on as MOOSE grabs the satellite. Before beginning terminal rendezvous, the pilot should be made aware of any potential debris hazards from ground operations. This is necessary because with current technology, a debris detector of any worth on board the spacecraft would be a dominate part of the vehicle[1], thus hindering the vehicles performance. Using IMU's, and rendezvous radar, the computer should keep the vehicle on course without any help from the pilot. However, the pilot should keep an eye on what should be and what actually is during the final approach. Should the automatic guidance system malfunction, the pilot will have to guide the craft manually. When performing manual proximity maneuvers, the pilot should be off course by no more then ten percent of the distance from the target satellite. This value is arbitrary, and should be changed according to the conditions found on-orbit. It effectively gives the pilot a cone of approach to stay within (figure 8.9.1). With regards to plume impingement, most any satellite will have an overpressure sphere of influence between five and four-hundred meters[2]. If the overpressure sphere of influence is unknown, all operations shall be under the assumption that it is four-hundred meters. Whenever MOOSE needs to maneuver within this sphere, with its engines towards the satellite, the thrust shall come from the cold gas thrusters.

### 8.9.2 General Equations

Once MOOSE is within one kilometer of the target satellite, all thrust vectors shall be determined from the following equations, derived in reference 3:
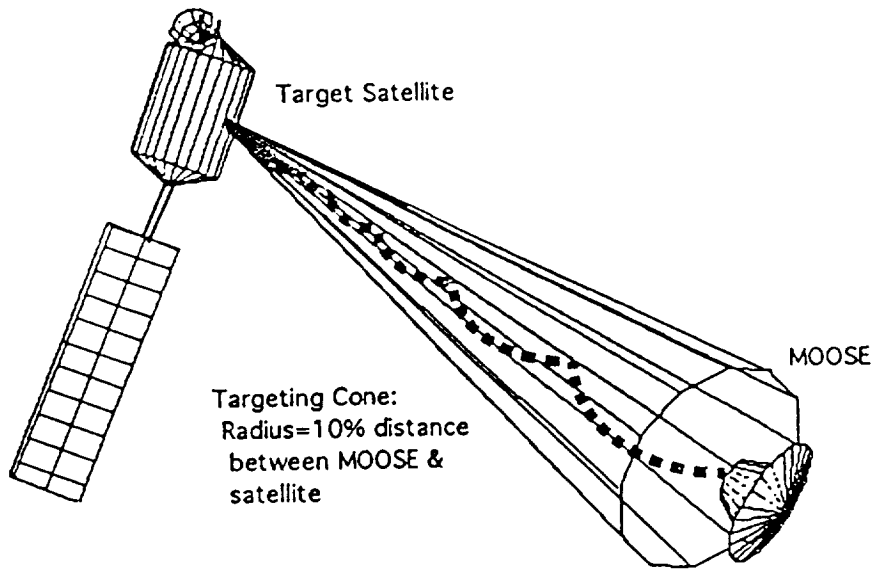
Figure 8.9.1: Approach Concept

$$\{8.9.1\} \qquad \frac{\dot{x}_{0r}}{w} = \frac{x_0 \sin wt + y_0(6wt\sin wt - 14(1 - \cos wt))}{3wt \sin wt - 8(1 - \cos wt)}$$

$$\{8.9.2\} \qquad \frac{\dot{y}_{0r}}{w} = \frac{2x_0(1 - \cos wt) + y_0(4 \sin wt - 3wt\cos wt)}{3wt \sin wt - 8(1 - \cos wt)}$$

$$\{8.9.3\} \qquad \frac{\dot{z}_{0r}}{w} = \frac{-z_0}{\tan wt}$$

$$\{8.9.4\} \qquad DV_1 = [(x_{0r} - x_0)^2 + (y_{0r} - y_0)^2 + (z_{0r} - z_0)^2]^{1/2}$$

The variables for these equations are as follows:

- $\overset{\text{Æ}}{r_0}$ : position vector of MOOSE relative to target satellite

- $x_0, y_0, z_0$ : components of $\overset{\text{Æ}}{r_0}$

- $\overset{\text{Æ}}{x_0}, \overset{\text{Æ}}{y_0}, \overset{\text{Æ}}{z_0}$: initial velocity compon-ents of $\overset{\text{Æ}}{r_0}$

- $x_0, y_0, z_0$ : components of $\overset{\text{Æ}}{r_0}$

8-56

- $\ae_{x_0}, \ae_{y_0}, \ae_{z_0}$: initial velocity compon-

ents of $\ae_{r_0}$

- $\ae_{x_{0r}}, \ae_{y_{0r}}, \ae_{z_{0r}}$: desired velocity

components of $\ae_{r_0}$

- w : angular velocity of target satellite
- t : desired time of maneuver



Figure 8.9.2 : Coordinate System

•• $DV_1$ : magnitude of velocity change

The coordinate system for the above equations is found in Figure 8.9.2.

### 8.9.3 Terminal Rendezvous

There are three general types of approaches that can be followed, depending on where MOOSE will grapple the satellite. The first is known as R-bar (Figure 8.9.3). This is an approach vector along the target satellites radius with respect to the earth. An R-bar maneuver shall be done whenever the target satellite's point of grappling is best reached along the target satellites radial axis. The second type of general approach is V-bar (Figure 8.9.4). A V-bar approach is performed along the satellites velocity vector. This maneuver is to be performed whenever the target satellite's grappling point is best reached along this axis. The final general type of approach is a direct approach This approach will be done whenever either an R-bar or a V-bar approach will bring MOOSE within grappling range. In all cases, the optimal DV is found whenever MOOSE is positioned initially above and behind the target satellite, or ahead and below the target satellite, relative to the satellites radial axis (above and below), and the satellites velocity axis (ahead and behind).

Figure 8.9.3: R-bar Approach          Figure 8.9.4: V-bar Approach
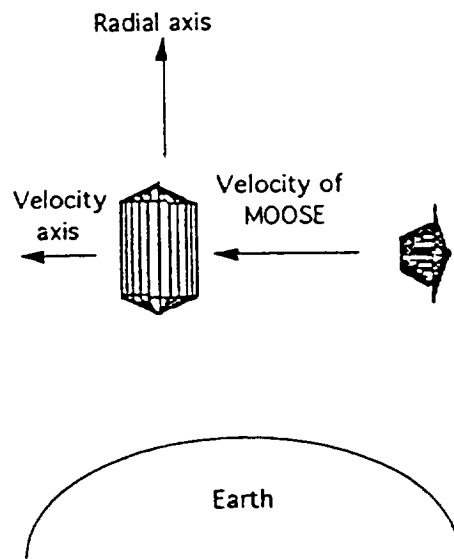
Before beginning the final approach, MOOSE must be placed along the correct satellite axis. This will be done within the 1000m - 400m radial range. As MOOSE moves to within one kilometer of the target satellite, the on board computer should have made the calculation for the optimum velocity vector (ie. based on desired time, t, for smallest DV) for the pilot to use to get within 400m of the target satellite and on the correct axis. The computer will tell the pilot how to orient the craft with respect to the satellite and the necessary DV, and the pilot will then make the necessary attitude adjustments to MOOSE, firing the thrusters at the appropriate time. As MOOSE approaches the 400m mark, another calculation should be made that will put MOOSE on the proper axis at a distance of 200m from the target satellite. The pilot then prepares to execute the maneuver. When the vehicle is +/- 20m of the 200m mark, the pilot then initiates the proper DV, making whatever corrections necessary to remain on target axis enroute, per figure 1. The next target distant is 50m. After that the range will be grappling range (within 5m), at which point MOOSE should have zero velocity relative to

the satellite. The pilot then prepares for grappling. An example numerical analysis for a geosynchronous satellite is found in appendix A8.2.

### 8.9.4 Grappling Satellite

The exact procedure for grappling a satellite shall vary from mission to mission, depending on such things as what is being grappled, were it is located on the satellite, and whether or not the satellite is spinning. In general, once MOOSE is within grappling range, the pilot maneuvers the grappling arm toward the predetermined grappling point, grappling when he/she is able. The pilot will accomplish this task using his/her own visual ability, a range sensor, a video monitor of camera mounted on arm, with cross hairs, and another camera on the arm of the manipulator arm. Of concern once MOOSE has grappled the satellite is the vehicle crashing into some portion of the satellite MOOSE maneuvers about the satellite using the grappling point.

### 8.9.5 Repositioning MOOSE

During a given mission, it may be necessary to reposition MOOSE on the relative to the satellite. During such maneuvers, there is a danger of MOOSE colliding with the satellite. To prevent this, MOOSE will use a collision avoidance system based built within the computer (see avionics section). If possible this is to be done using the grappling arm. If this is not feasible, then MOOSE must maneuver around the satellite using its cold gas thrusters. More often then not, a standard fly-around maneuver would take excessive time. A fly-around being when one spacecraft goes into an orbit resulting in it relatively circling another spacecraft[4] (figure 8.9.5). Again, this generally will take excessive time due to the time it takes the vehicle to complete the desired portion of the orbit, but it is a pre-mission consideration. Therefore,

Actual Orbit          Relative Motion



**Figure 8.9.5**
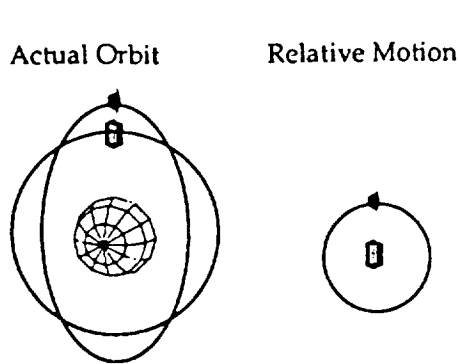


Regrapple
Starting
point
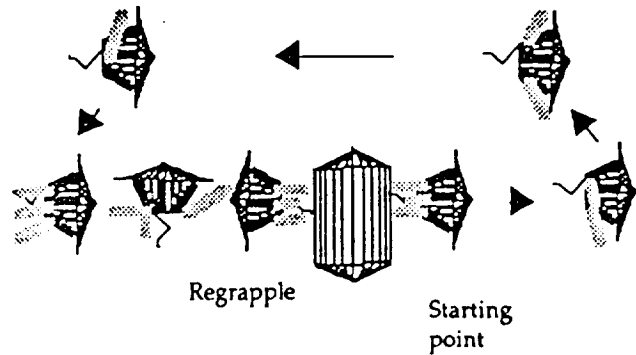
**Figure 8.9.6**

the equations {8.9.1}-{8.9.4} mentioned above shall be used. In general, the pilot first releases the grappler, bringing it to a rest position, and moves away from the satellite the minimal clearance distance with a relative velocity no greater then 0.20 m/s. Using the computer to determine the necessary velocity changes, the pilot makes the necessary translations to put MOOSE along the next approach axis for the next grappling point. The pilot then moves in and grapples the satellite as before (figure 8.9.6).

## 8.9.6 Leaving Satellite

Once the satellite servicing tasks are completed, MOOSE should make any necessary orbital adjustments to the satellite that it can. Ground operations makes any checks it can before the satellite is reactivated. Should any problem be found that can be fixed, it will be repaired if time allows. Otherwise, it will be left alone. As soon as the satellite can be reactivated, the pilot releases the grappler, bringing it to a rest position, and moves away from the satellite with a relative velocity no greater then 0.20 m/s. When MOOSE is 100m from the satellite (more if safety deems necessary), the repaired satellite is reactivated. If a problem is found that MOOSE fix in the given time, it shall be done. Otherwise, MOOSE will increase its relative velocity to about 1 m/s. At the 1 km mark, the pilot should be prepared to begin the return flight.

## 8.10.0 Satellite Servicing

Satellite servicing refers to what MOOSE does to the satellite. It includes exchange of ORU's, consumable replenishment, and satellite deorbiting. To accomplish these tasks, MOOSE will need exterior lighting and two cameras[5]. The exterior lighting should be on the ends of the two arms, for spot lights, and just below the canopy, for flood lights. The cameras are located on the arms.

## 8.10.1 ORU's ( Orbital Replacement Units)

ORU replacement shall be a major servicing task that MOOSE will perform. These devices comprise the most all the components of a satellite with modular design. Typical ORU's are listed in appendix A8.3. A conservative estimate of failed ORU's on typical satellites indicate about 5 on average over the first two years of a satellites life[6]. Through various methods these satellites are made to operate, but they still are in need of repair. It should noted that payload restrictions may prevent complete repair of a satellite since not all of the necessary ORU's may be taken into orbit with MOOSE.

## 8.10.1.1 Transport Palette

ORU's will be brought up into orbit during the routine shuttle visits to the space station. They shall be transported on the palette that will be attached to

MOOSE. The palette (Figure 8.10.1) is a removable truss structure attached to



8.10.2a: Front view

8.10.2b: Side View
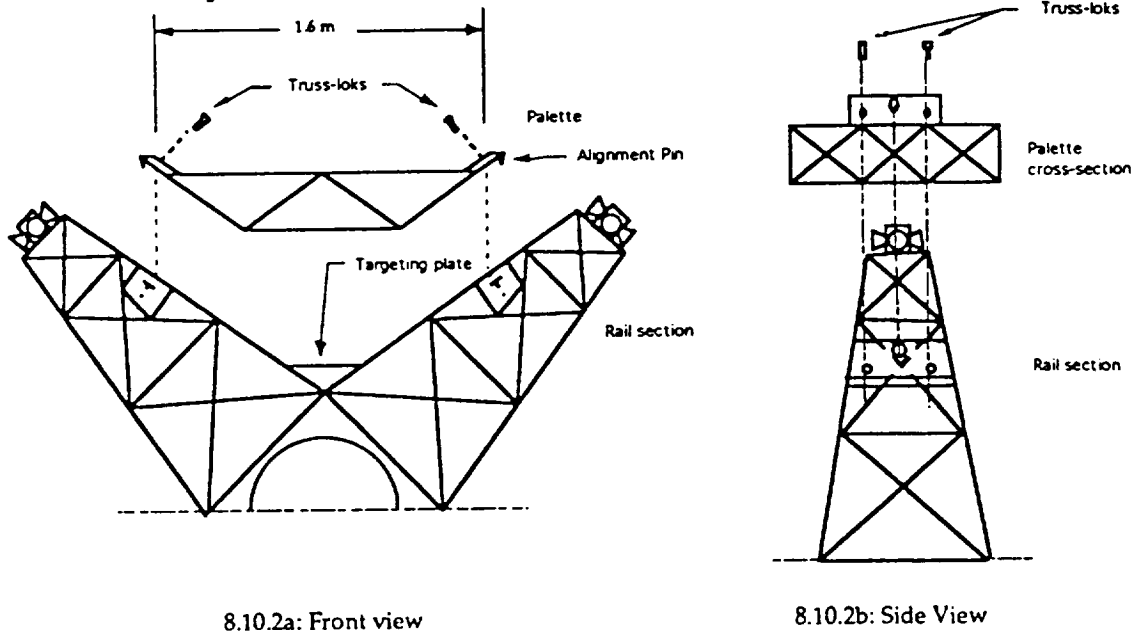
## Figure 8.10.1: Palette Attachment Concept

MOOSE using truss-loks[6] and located behind the canopy. Although attachment to MOOSE shall be standardized, palette configuration will have to be mission specific to accommodate the different needs of different satellites. ORU's should be removable and attachable using one manipulator arm, since this is the situation encountered on-orbit at the satellite. The simplest way to accomplish this would be to attach the ORU to the palette however it is attached to the satellite. The attached ORU should be able to withstand the shuttles launch loads of 11 gees and rotation of 85 rad/s (conservative estimates for hitchhiker payloads used by NASA) and the combined system should be able to withstand the 7.5 gees encountered during the aerobrake maneuver (no rotation there)

During a repair, satellite insulation may be destroyed, and provisions must be made to replace the insulation. The simplest way to accomplish this would be to store individually stored precut sheets on the palette (figure 8.10.2).
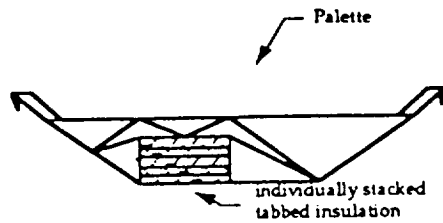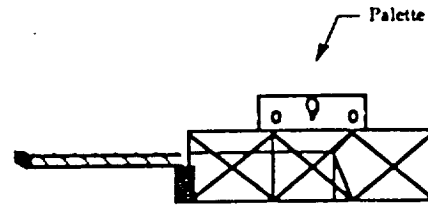
8.10.2a Front View                                    8.10.2b: Side view

**Figure 8.10.2: Insulation Stacks on Palette**

Should the insulation peices prove to be to large to store in this manner, they can be stored as roll on the palette. Similar considerations are given for the transport and storage of solar panels.

### 8.10.1.2 On-orbit Handtools

MOOSE will use the currently available handtools for EVA repair. Specialty tools shall be made as needed. Hand tools shall be found in a tool box right below the pilot's arms and they are to be tethered to the box to prevent accidental loss (figure 8.10.4). The box will be attached using truss-loks[6.] so it can be replace at station, allowing it to be easily modified or replaced to accommodate specific missions. To prevent any problems while on-orbit, any tool that could be possibly be needed should be brought.

### 8.10.1.3 Generalized ORU Exchange

8.10.3a: Front view    8.10.3b: Side view
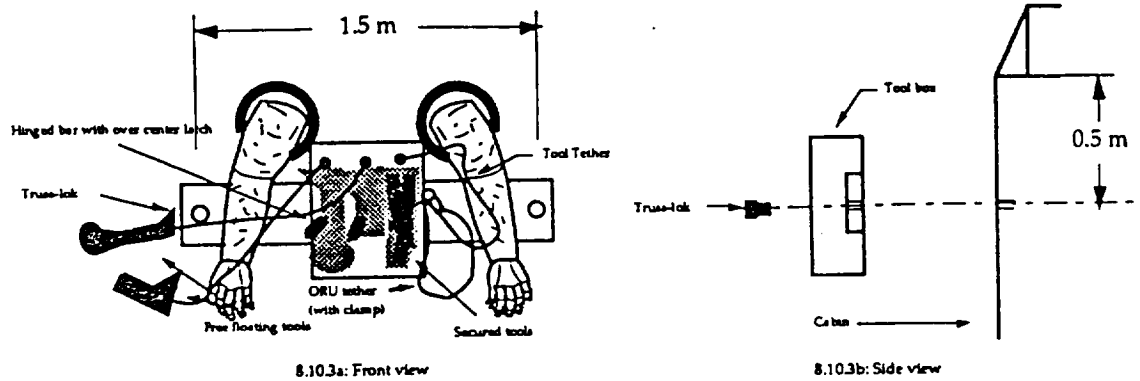
**Figure 8.10.3: Tool-box**

Once MOOSE is in position, a typical exchange of ORUs for a satellite will look something like this:

- Remove insulation/ open area surrounding old ORU (~10-20min)[5].
- Remove old ORU fastening devices on satellite (~45-60min)[5].
- Connect a tether from the toolbox to the old ORU (~10min)[5].
- Move tethered old ORU safely out of the way (~5min)[5].
- Using manipulator arm, remove new ORU fastening devices on MOOSE (~35min)[5].
- Using manipulator arm, maneuver new ORU from palette to a workable location (~15min)[5].
- Mount new ORU onto satellite (~40-50min)[5].
- Secure new ORU bolts onto satellite (~15min)[5].
- Grasp old ORU with manipulator arm and remove tether (~20min)[5].
- Using manipulator arm, maneuver old ORU to palette (~35-45min)[5].
- Mount old ORU to palette and attach truss-loks (~50-65min)[5].
- Checkout system, fixing anything that needs to be and can be fixed .
- Replace insulation/close up area surrounding ORU (~25-30min)[5].
- Move to next ORU or leave satellite.

### 8.10.2 Consumables

Consumables refer to items that the satellite loses as they are used, generally fluids such as fuels. Typical consumables are listed in appendix A8.4. Resupply of consumables requires special attachment devices and pumps.

Also, the satellite will need an easily accessible nipple or similar opening that allows the fluids to be transfered. Most satellites have such a device.

Exact methodology for replenishing consumables will vary from mission to mission, but a typical procedure would something like this:
- Make sure the consumable supply interface is accessible (~10-30min)[5].
- Attach resupply docking mechanism (~10-20min)[5].
- Transfer consumable (~30-60min)[5].
- Remove resupply docking mechanism (~10-20min)[5].
- Make supply interface is sealed[5]
- Check as far as safety will allow.
- Move onto next task.

The hose for transfer of fuel should be attached to the toolbox, thereby being readily accessible to the pilot.

### 8.10.7 Satellite Deorbiting

One important task that MOOSE can fulfil is the removal of useless satellites from orbit, or the transfer of these satellites to less troublesome orbits. Satellites are designed to do this themselves, but some are unable to do this due to lack of fuel or a malfunction. MOOSE can fix this one of three ways:
- Repair malfunction.
- Refuel satellite.
- Attach kick motor.

Choice of method is based on whichever proves most cost effective.

## 8.25 Vehicle Servicing Facility (VSF)

### 8.25.1 Vehicle Servicing Facility Requirements

The VSF shall be mounted at Space Station Freedom (SSF) on a truss structure in the form of a keel.

A maintenance dock shall be located on the of the keel structure.

The VSF shall provide a fluids storage and transfer system located at or near the maintenance dock; this will include a cryogenic storage system as well as storable fluids capability.

The VSF shall utilize the SSF Remote Manipulator System (RMS) in conjunction with the MOOSE Manipulation System to perform normal vehicle turnaround. EVA shall not be a part of normal turnaround operations.

A VSF control station, integrated with the SSF control station, will be the command center for all servicing operations.

The VSF shall have a cargo and ORU storage area located on the maintenance dock.

The VSF will be powered by an additional SSF solar array wing pair.

A debris and radiation shield shall be integrated about the VSF maintenance dock.

### 8.25.2 VSF Configuration

The VSF is located at the Space Station Freedom, occupying a modified SSF expansion capability keel truss (see Figure 8.2-1). The VSF consists of seven main
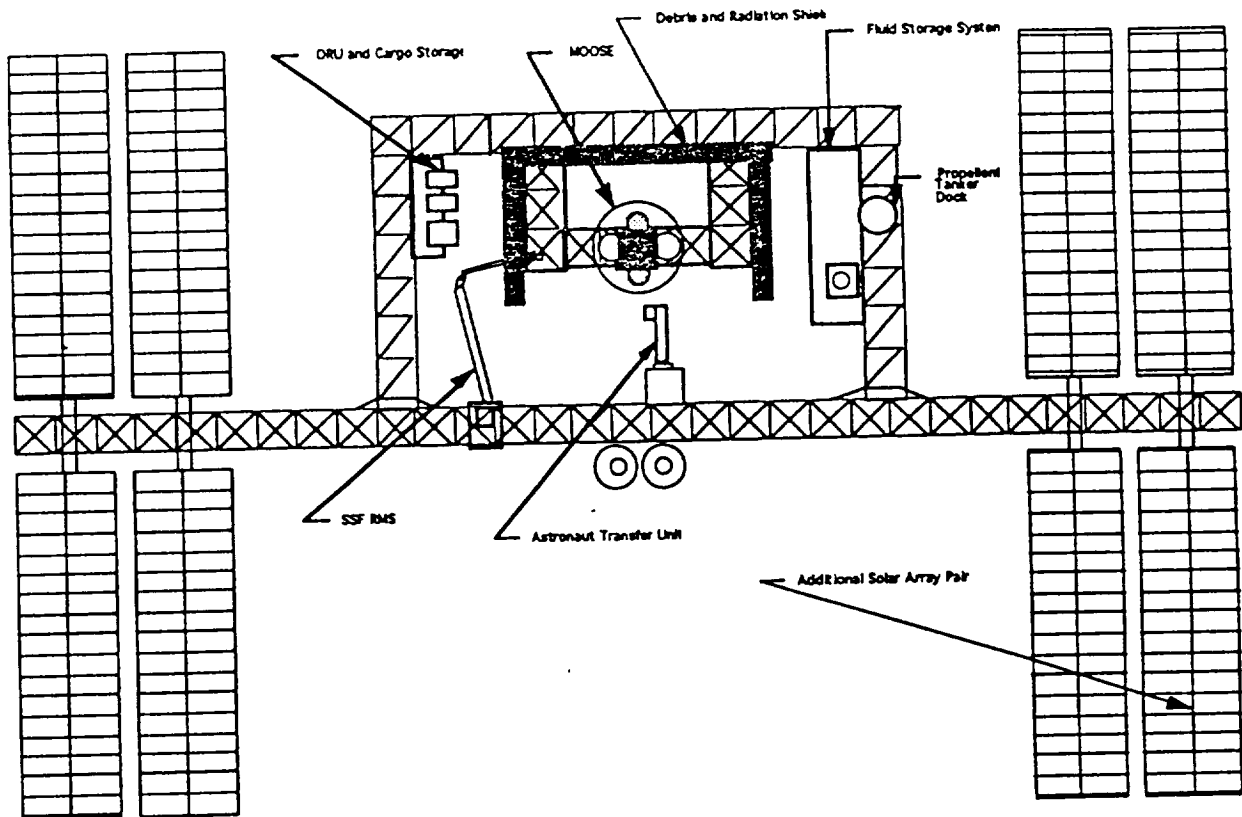


Figure 8.2-1. Vehicle Servicing Facility Configuration

elements: the Keel Truss Structure, the Maintenance Dock, the Debris and Radiation Shield, the ORU/Cargo Storage Area, the Fluid Storage System, the Astronaut Transfer System, and the Control Station.

### 8.25.2.1 Keel Truss Structure

The keel structure is made up of six main sections. All section consist of a 3.5 m box cross section, with one stabilizing member across each unit. The cross section is modeled after the SSF Integrated Truss Assembly. The keel consists of two 29m by 3.5 m links rising perpendicularly from the SSF main truss. A 52 m by 3.5 m truss then connects these links to form the keel. To support the maintenance dock there is small secondary keel that is mounted off the main keel. It consists of two 11.5 m by 3.5 m links connected by a 22m by 3.5 m truss. The keel provides the structural stability for all the maintenance facility elements.
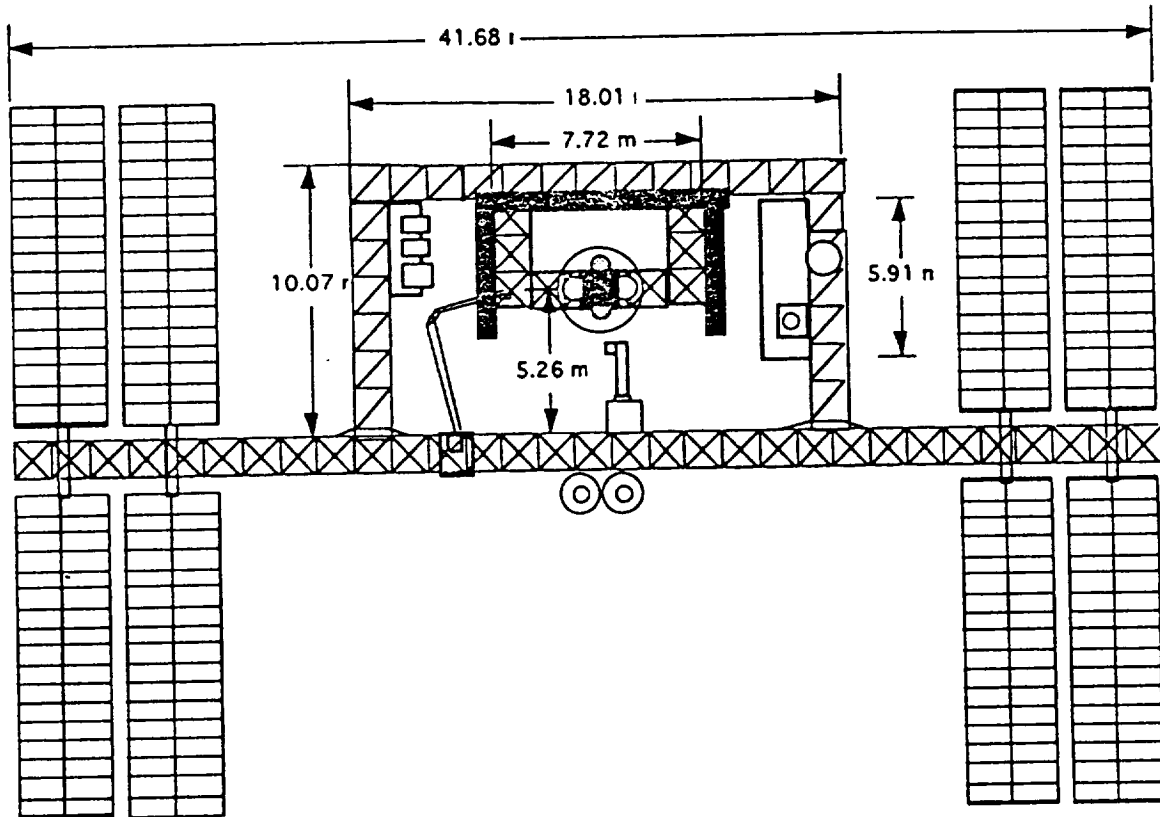


Figure 8.2-2. VSF Dimensions

### 8.25.2.2 Maintenance Dock

The maintenance dock consists essentially of a vehicle berthing interface. The interface, shown in Figure 8.2-3, consists of a base that is connected to the keel truss. Four grasping units run perpendicularly from the interface base. These grasping units mate to the MOOSE at four hard points located on the MOOSE thrust structure. These grasping units also connect power and communication lines to the MOOSE during servicing. The interface base has a rotating mechanism that will allow rotation of the MOOSE during servicing. This will
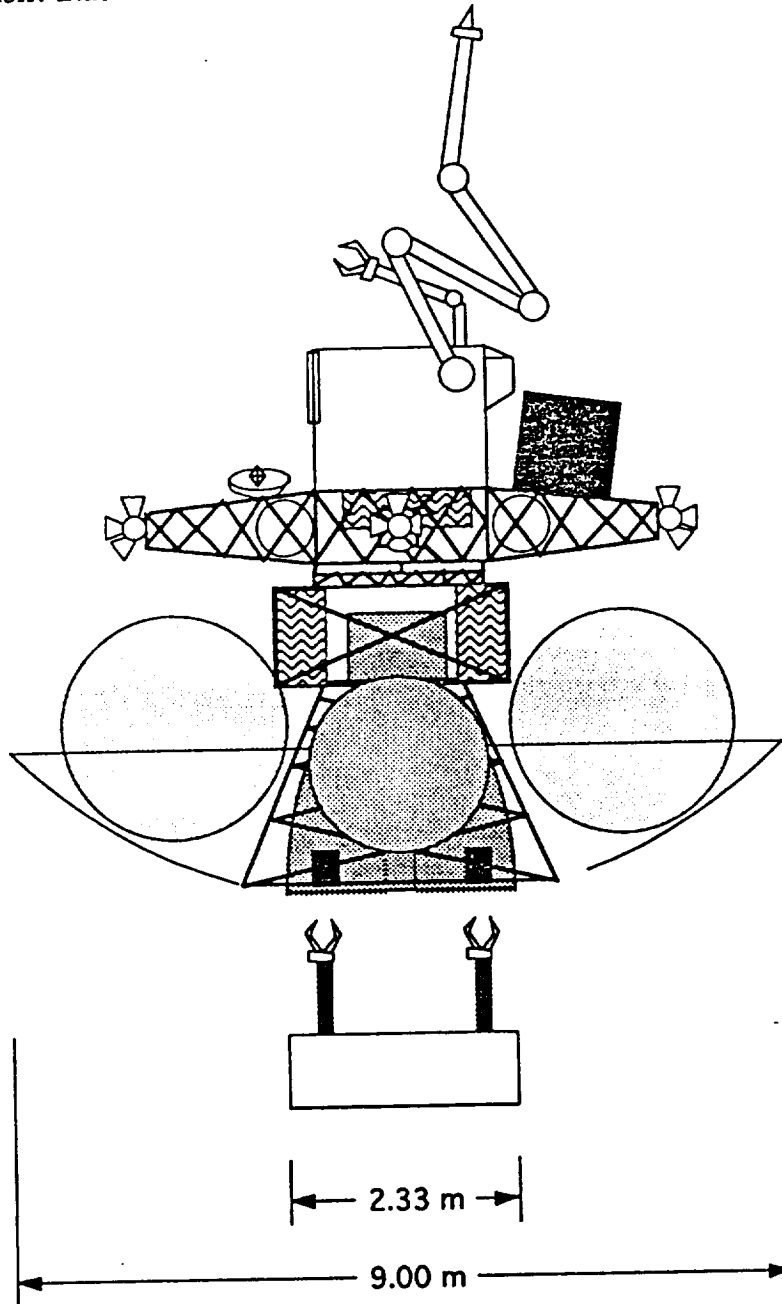


Figure 8.2-3. VSF Vehicle Berthing Interface

allow the SSF RMS to reach all points on the MOOSE during vehicle turnaround. The RMS requires this rotation due to its limited reach capability (18 meters).

### 8.25.2.4 Debris and Radiation Shield (DRS)

The DRS will consist of a three piece structure that will shield the MOOSE from micrometeoroid debris and solar radiation. The structure will be mounted on the VSF keel structure on the solar side of the vehicle, thus shielding it from solar radiation approching from that direction. The MOOSE is only radiation shielded for up to 3 day missions, therefore the it requires additonal radiation shielding during storage and turnaround times ( approx. 120 days).

### 8.25.2.5 ORU/Cargo Storage Area (OCSA)

The OCSA will consist of a platform containing holding fixtures to store MOOSE and satellite ORU's, ACS modules, spare MOOSE parts (engine, tanks, fuel cells), and satellite replenishment tanks.

### 8.25.2.6 Fluids Storage System (FSS)

The FSS will consist mainly of a 17 m by 5 m fluid storage unit. This unit will contain the tanks for all fluids being stored at the VSF. The unit will store enough fluids to resupply the MOOSE for 3 missions. The MOOSE has schedule of 3 missions per year.

Fluid storage Requirements per mission:

| | |
|---|---|
| Liquid Hydrogen (LH2) | 10500 kg |
| Liquid Oxygen (LO2) | 1500 kg |
| Gaseous Helium (GHe) | 450 kg |
| Hydrazine | 618 kg |

To accomodate storage for 3 missions the storage tanks were sized for the following amounts:

| | | | |
|---|---|---|---|
| LH2 | 33000 kg | ---> | 2.19 meter radius |
| LO2 | 5000 kg | ---> | 1.90 meter radius |
| GHe | 1500 kg | ---> | 1.84 meter radius |
| Hydrazine | 1900 kg | ---> | 1.88 meter radius |

To accomodate these tanks a 17 m by 5 m unit was designed to hold all of these fluids (see Figure 8.2-4).

Lox Tank   LH2 Tank   He Tanks (2)   Pump Unit

He Pressurant Tanks (5)

Refrigeration Unit

Hydrazine Tank

Fluid Transfer Hose
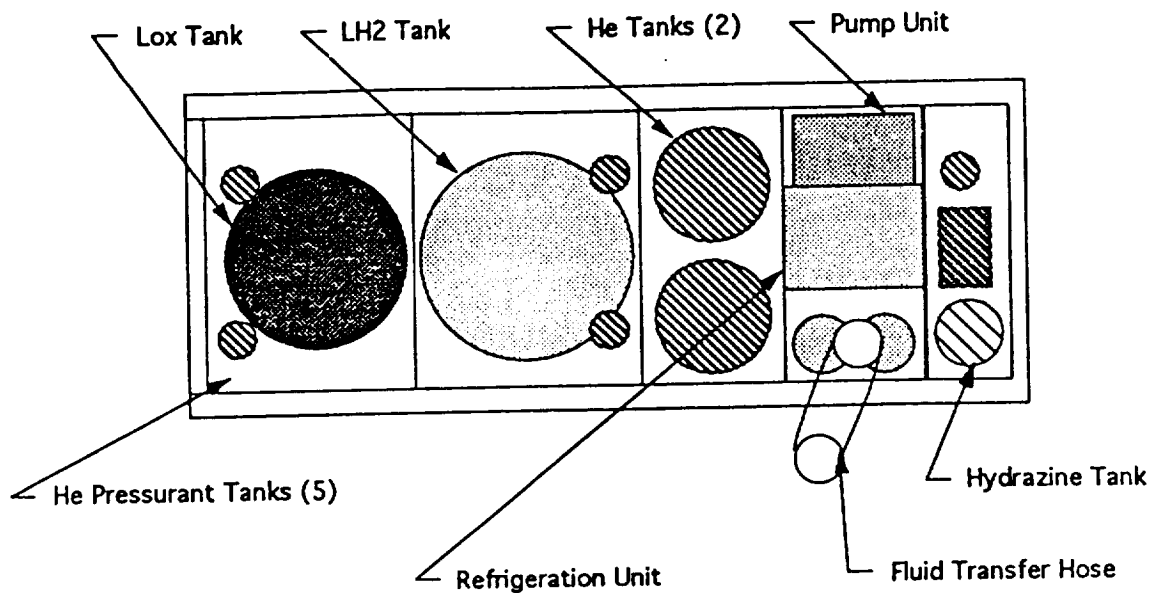
Figure 8.2-4.    Fluids Storage Unit

The fluid storage unit consists of a tank for each fluid, one pressurant system which will be used for transferring all fluids. There will be a separate GHe pressurant tank for each fluid. There will be separate plumbing coming out of each fluid tank, consisting of valves, pump connections, and sensor devices. Each fluid will have plumbing that runs to the refrigeration unit to reliquify fluid boil-off. Each fluid will also have a line running to the fluid transfer hose, which will contain four insulated fluid lines, one for each fluid. The storage system will also have an extensive thermodynamic control scheme. This will consist of vapor-cooled shields, multi-layer insulation (MLI) blankets, a venting system, and as mentioned before a refrigeration unit. An option for this refrigeration unit is the Stirling refrigerator, manufactured by Phillips-Magnavox; it offers good thermodynamic efficiency for our temperature range (50 -100 K). A reliquifier will also be used to control boil-off loses. The reliquifier will take gases that are formed during cryogenic boil-off and convert them back to liquid, much the way a humidifier converts moisture in aroom back to liquid. This will limit the losses that occur due to cryogenic boil-off. The storage system will also have its own protection from micrometeoroids and other debris. This will consist of an outer structural shell on the unit.

The FSS will needa thermal control system to regulate heat accumulated from the refrigeration unit, the reliquifier, and the plumbing system. As seen in Figure 8.2-5 the FSS will have its own thermal radiator to dispatch excess heat.
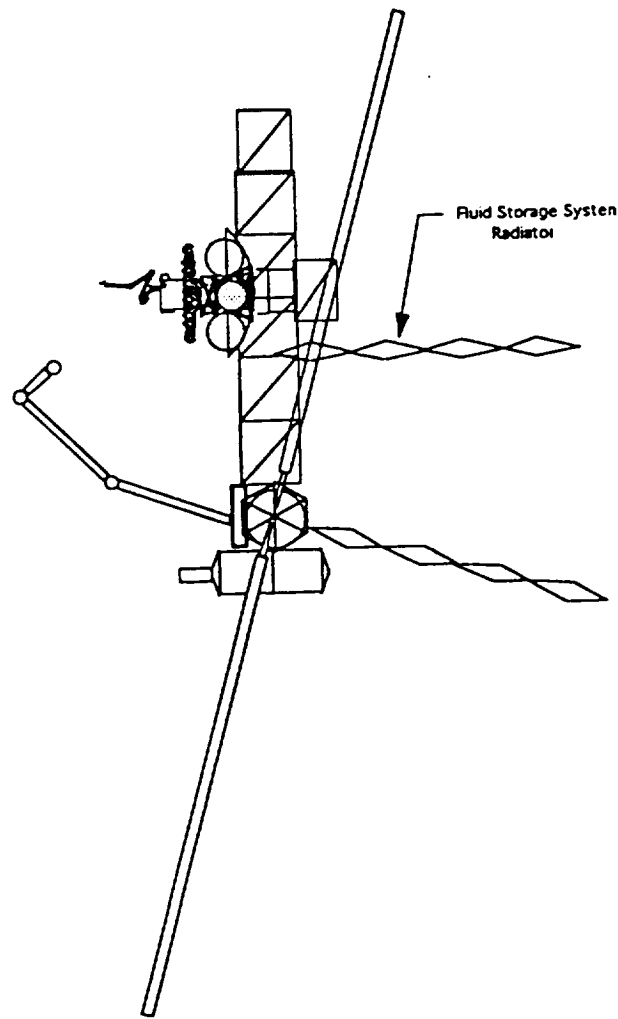
Figure 8.2-5.    VSF Side View

### 8.25.2.7  Astronaut Transfer System (ATS)

The ATS consists of a SSF module, SSF airlock, and a transfer tube. The configuration for the ATS is illustrated in Figure 8.2-1. The ATS requires an SSF module to mount a SSF airlock. The custom made transfer tube will mount on the airlock and shall have a prismatic type joint for extension to the MOOSE docking ring.

### 8.25.2.8  Control Station

The VSF control station will be located in the addition SSF module that is required for the ATS. The control station will work in close conjunction with the SSF control station due to the fact that all most turnaround procedures will be done using the SSF RMS.

### 8.25.3 VSF Power Requirements

The VSF power requirements will stem from the Fluids Storage System and the Maintenance Dock interface. The FSS will draw a large amount of power to store the cryogenic liquids. The Maintenance Dock interface will supply power to the MOOSE during turnaround operations.

The maximum power requirement should be on the order of 5-10 kW. This sizable requirement probably will require the addition of a solar array pair to SSF (see Figure 8.1-1). This would supply the station with an additional 18.75 kW of power, more than enough to support the VSF.

### 8.25.4 Vehicle Maintenance Guidelines

Three-level maintenance hierarchy based on level-of-rapair analyses.

- Level I consists of vehicle local maintenance; such as removal and replacement (R/R) activities using components that are stocked in the spare storage area. These repairs are accomplished directly with manned EVA or telerobotics.
- Level II consists of maintenance at SSF of components removed during level I maintenance.
- Level III maintenance incorporates sending unrepairable components back to earth via the logistics module that is returned to earth from SSF on every shuttle flight.

Spare parts will be stocked based on reliability, criticality and cost. Shuttle flights are scheduled for every 90 days to resupply SSF. Modular construction of the MOOSE was stressed to simplify vehicle turnaround.

## Bibliography (sections 8.9-10 & A8.2-4)

1) "Space Mission Analysis and Design, 2nd. edition," Wiley Larson & James Wertz, editors; Kluwer Academic Publishers, Netherlands & Microsm, Inc,Torrance, California; 1992, Pg 764.

2) "Rendezvous/ Proximity operations Workbook," NASA, LBJSC, March, 1983, RNDZ 2102, pg 4-2.

3) "Orbital Mechanics," Chobotov, editor, AIAA, 1992, pgs 179-180

4) "Orbital Mechanics," Chobotov, editor, AIAA, 1992,

5) "The Human Role in Space:Technology, Economics, Optimization," Stephen Hall, editor; Noyes Publications, Park Ridge, NJ, 1985.

6) "Reliability Prediction for Spacecraft," Hecht, H. & M., Dec, 1985, RADC report RADC-TR-85-229.

7) "Accessing Space: a catalogue of process, equipment and resources for commercial users," Office of Commercial Programs, NASA, 1990.

8) "Proposed Design for On-Orbit Servicing Handbook," AIAA, 1992

9) "Space Mission Analysis and Design, 2nd. edition," Wiley Larson & James Wertz, editors; Kluwer Academic Publishers, Netherlands & Microsm, Inc,Torrance, California; 1992, pgs 331-335.

References (sections 8.9-10 & A8.2-4)

1) AIAA, "Proposed Design for On-Orbit Servicing Handbook," 1992

2) Chobotov;"Orbital Mechanics," editor, AIAA, 1992, pgs 179-180

3) Hall, Stephen;"The Human Role in Space:Technology, Economics, Optimization," editor; Noyes Publications, Park Ridge, NJ, 1985.

4) Hecht, H. & M; "Reliability Prediction for Spacecraft," , Dec, 1985, RADC report RADC-TR-85-229.

5)Larson, Wiley & James Wertz, editors;"Space Mission Analysis and Design, 2nd. edition," Kluwer Academic Publishers, Netherlands & Microsm, Inc,Torrance, California; 1992, Pg 764.

6) NASA,"Accessing Space: a catalogue of process, equipment and resources for commercial users," Office of Commercial Programs, 1990.

7) NASA, "Rendezvous/ Proximity operations Workbook," LBJSC, March, 1983, RNDZ 2102, pg 4-2.

## 7.4 MOOSE MISSION MODELS

Jason Budinoff, Operations & Production

### 7.4.1 Location of Target Spacecraft

Artificial Satellites are generally located in 5 orbit types:

(1) LEO in-plane
(2) GEO
(3) LEO mid-latitude
(4) HEO mid-latitude
(5) LEO Polar/Synchronous
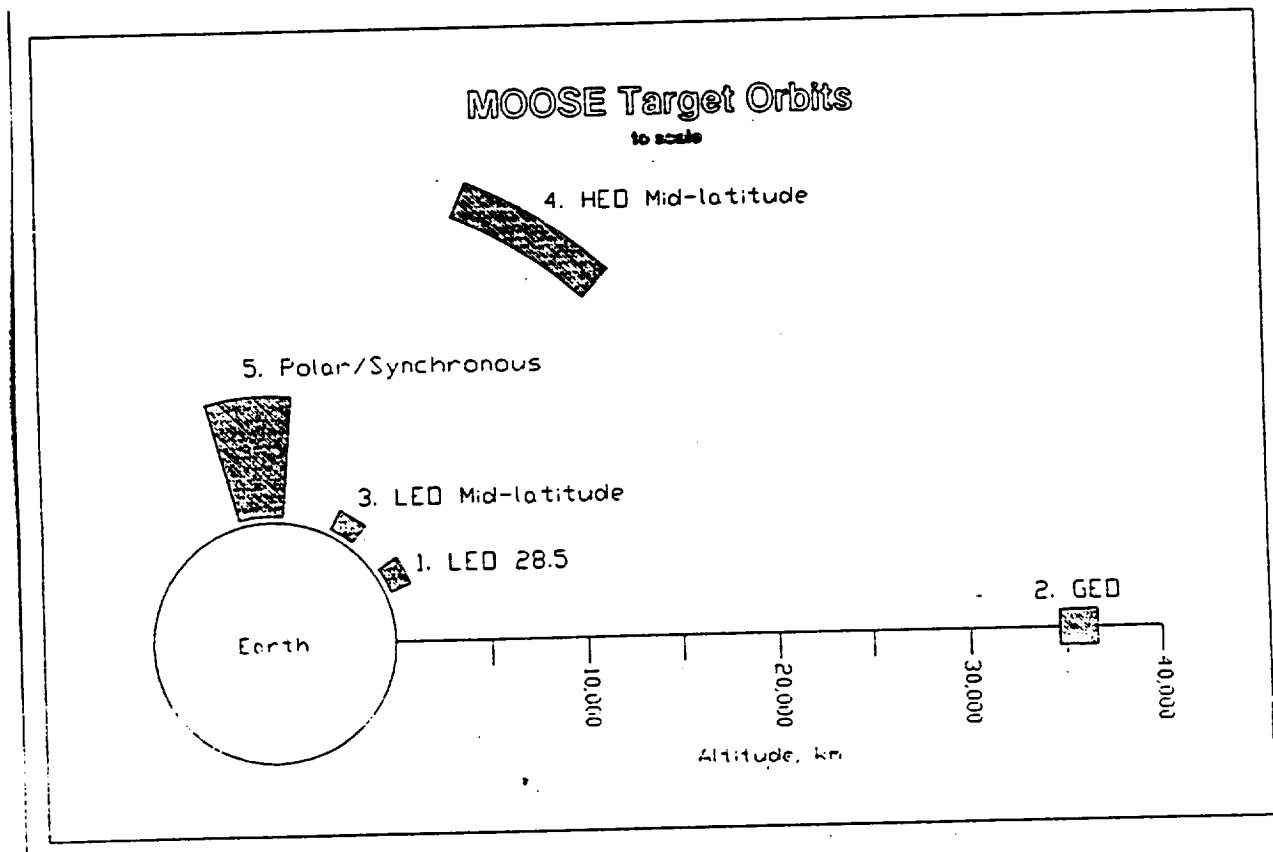


Figure 7.4.1

Figure 7.4.1 shows the orbits by region. The MOOSE vehicle can rendezvous with spacecraft in type (1) orbits with negligible amounts of propellant. The vehicle separates and relies on attitude control thrusters for impulse on these missions. Local missions (which do not leave the SSF proximity operations zone) also do not require primary propulsion and use little propellant. Type (1) spacecraft include NASA science/application spacecraft (GRO, HST, UARS, XTE, Space Station).

Type (2) orbits are Geosynchronous and include DoD (Milstar, FLTSATCOM), NASA and commercial spacecraft (TDRSS, Intelsat, COMSAT).

Type (3) orbits are low-altitude mid-range inclination orbits. Primarily DoD ELINT and surveillance satellites are in this orbit.

Type (4) orbits contain older Soviet communication satellites (Molniya) and DoD surveillance spacecraft.

Type (5) orbits are repeating and/or synchronous. Survey spacecraft (Landsat, SEASTAR, TOPEX/Poseidon) and DoD ELINT and surveillance satellites are in LEO type 5 orbits. The type (5) orbit is not attainable by the MOOSE vehicle.

Orbits requiring inclination change (type (2), (3), (4)) are reached via trans-GEO plane change trajectories. Aerobraking is used to decelerate only and 2 aerobraking passes must be made for each inbound transfer. See figure 7.4.2.



MOOSE Inbound Aerobraking Geometry
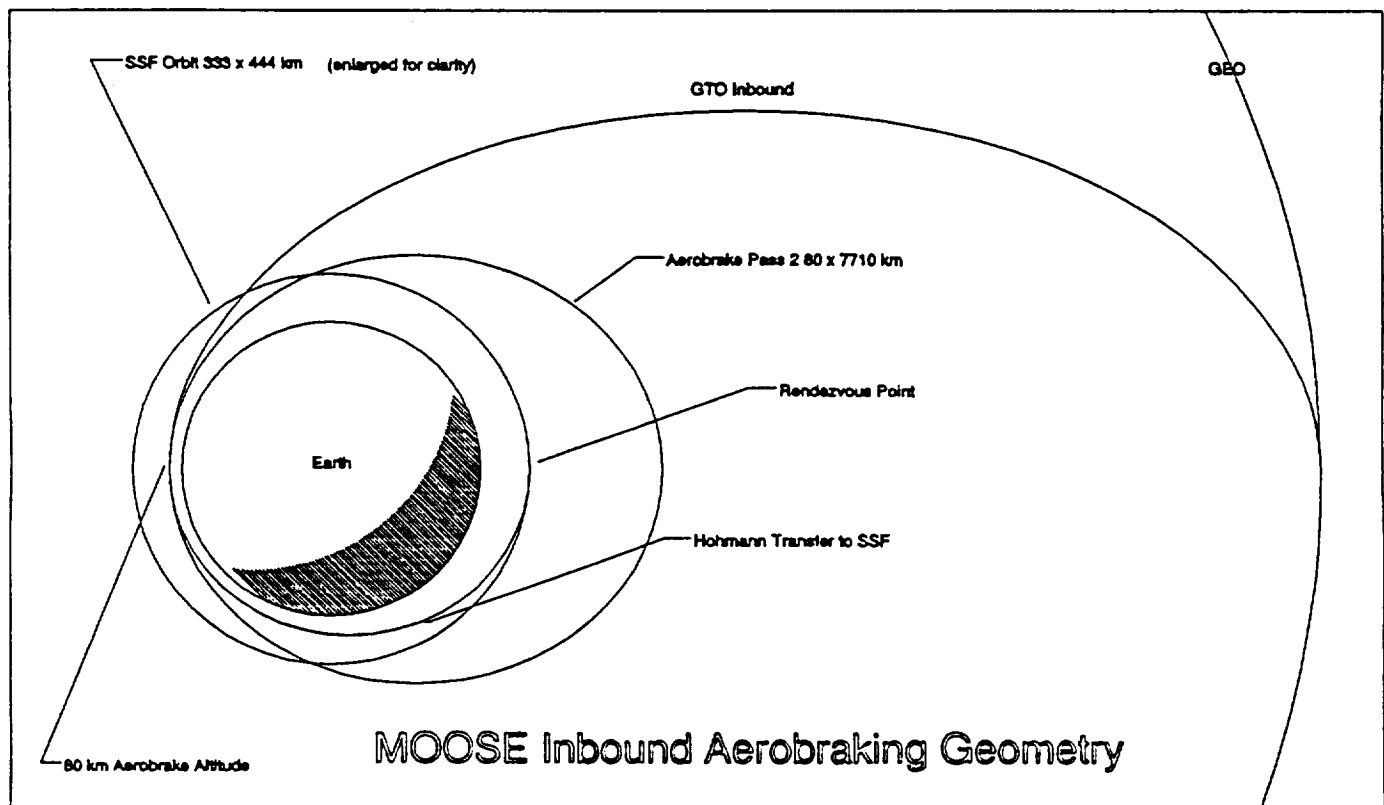
Figure 7.4.2

### 7.4.1.1 Spacecraft Density Per Orbit Type

The tonnage launched into each type of orbit for the 1991-2000 period is approximately 400/500/91/304/291 thousand kg for type 1/2/3/4/5 orbits respectively, based upon the

Rockwell "Medium" model. It can be inferred that the frequency of servicing missions to the various orbits will follow these ratios. The MOOSE Medium and High mission models were constructed using these ratios.

Servicing 2 (or more) spacecraft in a single sortie is possible, but restricted and subject to many conditions. Double servicing missions will be rare at best and propellant requirements may exceed the MOOSE maximum load. While significant customer cost savings result, double servicing missions will be transient opportunities; considered exceptions to normal operating modes. Double servicing missions have not been included in typical mission modelling and must be considered on a case-by-case basis.

All costing models in this section reflect 85% learning curve effects and yearly discounting of 10%.

7.4.2 Mission Models

3 mission models have been analyzed reflecting differing levels of MOOSE mission tempos.

7.4.2.1 LOW Mission Model (ENAE 412 CDR)

The LOW mission model represents the mission frequency presented at CDR and reflects a sortie rate of 1/4 months. 3 GEO (type (2)) missions are performed. This model is not based upon orbit mass ratios.

7.4.2.2 MEDIUM Mission Model

The MEDIUM mission model entails 6 MOOSE sorties per year (1/2 months). The missions are divided into: 2 type (2) GEO in-plane, 2 type (2) GEO, 1 type (3) LEO mid-latitude, and 1 type (4) HEO mid-latitude.

7.4.2.3 HIGH Mission Model

This model represents the maximum operational tempo for a single MOOSE vehicle without significant expansion of current space support infrastructure. The High mission model entails 13 MOOSE sorties per year (1/4 weeks). This is the minimum time acceptable for mission planning, training and preparation. The missions are divided into: 4 type (2) GEO in-plane, 5 type (2) GEO, 2 type (3) LEO mid-latitude, and 2 type (4) HEO mid-latitude.

7.4.3 MOOSE Flight Operational Launch Support

MOOSE Flight Operations Launch Support is divided into 3 phases:

(1) Delivery, Assembly, and Verification
(2) Flight Engineering Evaluation
(3) Servicing Operations

(1) and (2) will utilize US launch vehicles only in order to prepare domestic manufacturers for future international open-bid competition, and to allow maximum communications during critical assembly and testing. The 2-year phase 1 and 2 process requires a block purchase of 4 dedicated STS, 2 Titan IV SRMU (ETR) and 4 Delta 7920 (ETR) vehicles. See figure 7.4.3.
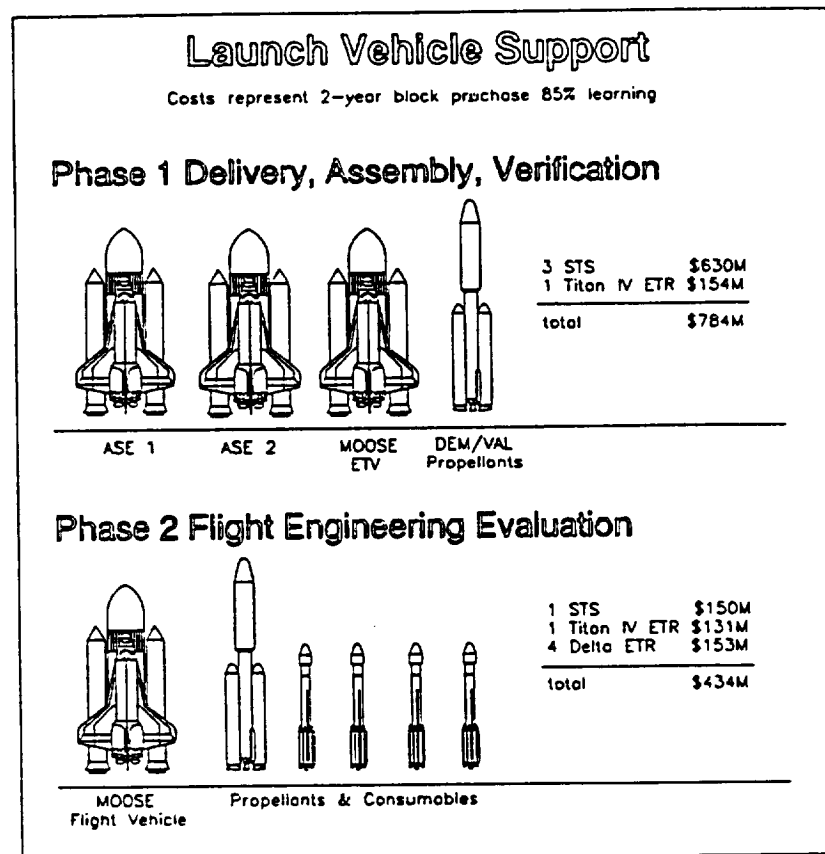


figure 7.4.3


## 7.4.3.1 Phase (1) Delivery, Assembly, and Verification

Phase 1 is the assembly stage of MOOSE verification. Phase 1 requires 1 year. An Engineering Test Vehicle (ETV) is delivered to space station after ASE (Airborne Support Equipment, including berthing facilities and cryogenic propellant depot) is assembled and checked-out. The ETV verifies assembly, vehicle handling, safing, docking/release, and berthing schemes. Phase 1 launch vehicle support requires:

(1) 2 STS delivery flights of ASE
(2) 1  STS Delivery of MOOSE Engineering Test Vehicle
(3) 1 Titan IV delivery of cryogenic  propellants and consumables for ASE checkout & verification

## 7.4.3.2 Phase (2) Flight Engineering Evaluation

Upon successful completion of Phase (1), Phase (2) is initiated. This phase is 1 year long and provides flight testing of the unmanned, instrumented ETV. The ETV is flight-prepared and undergoes a battery of orbit transfer and flight mechanics verification tests. Any residual problems are accounted for. The MOOSE Flight Vehicle is delivered and assembled, run through "shakedown" trials and prepared for Phase (3), MOOSE Servicing Operations.

ETV flight testing entails 3 "local" systems verification flights of the cab-separated vehicle, 3 type (1) LEO in-plane missions, 2 type (2) GEO missions, and 2 type (3) LEO mid-latitude missions. The propellant required is delivered from Delta PMV's and the left-over from ASE demonstration/validation (DEM/VAL) testing. This phase will also validate SSF Terminal Control Zone traffic management protocols, and command dynamics.

Phase 2 requires 1 STS, 1 Titan IV, and 4 Delta launches. The first STS flight delivers the MOOSE flight vehicle. The Delta and Titan IV (ETR) deliver Propellant/Consumables to support flight test operations. See figure 7.4.3.

## 7.4.3.3 Phase (3) Servicing Operations

The third phase covers operational deployments of the MOOSE flight vehicle. 3 models of Phase (3) operations reflect different mission tempos, and each require varying levels of ELV support.

Cost per delivered kg is too simplistic of a model for MOOSE lift requirements. The nature of the mission requires frequent delivery of specific satellite components to SSF. The Shuttle will support MOOSE operations with 4 deliveries of payloads and consumables per year, during regular SSF support missions. Individual launch vehicles are limited in terms of availability and long-lead times (years); therefore a large degree of foresight is required in ELV support procurement.

The trade-off is between 4 factors:
(1) ELV $/kg
(2) ELV dedicated availability
(3) Many small deliveries (rapid mission response requiring special payloads)
(4) Infrequent bulk load delivery (cost savings)       ·

The ELV models are described in section 7.4.4.1.

MEDIUM/HIGH mission models will be the largest single consumer of ELV's. Open bids industry-wide and purchase of large ELV lots will be required and drive launch costs down. The US-only support requirement is dropped after completion of phase 1 and 2.

## 7.4.4 MOOSE Operations Launch Support

Launch support considers vehicles operational in the 1998-2005 timeframe. Surveyed

vehicles include:

(1) Titan IV SRMU (Martin Marietta)
(2) Delta 7920 (General Dynamics)
(3) Ariane AR 44L (Arianespace)
(4) Ariane 5 (Arianespace)
(5) H-II (Rocket Systems Corporation/NASDA)
(6) Proton SL-13 (Lockheed/Khrunichev/Energia (LKE))
(7) Energiya (Energia USA)

Atlas is not surveyed due to high specific cost ($/kg delivered to SSF), dated nature of design and current string of failures threaten program cancellation

The STS is currently prohibited from carrying large quantities of propellants (Centaur G-prime restriction) and therefore not considered in propellant support models.

## 7.4.4.1 Support Model

Based upon MOOSE propellant usage of 12,000 kg of cryogenic LO2/LH2 per type (2), (3), and (4) mission, the LOW, MEDIUM, and HIGH models require delivery of 36,000, 72,000, and 156,000 kg to SSF, respectively. Propellant delivery is containerized in Propellant Maneuvering Vehicles's (PMV) for orbit correction and controlled proximity operations in the SSF Proximity Operations Zone. PMV's exhibit typical payload mass fractions of 0.85 - 0.9. The PMV mass has been accounted for in lift capacity required.

## 7.4.4.2 Mixed Manifest

Bulk propellant delivery shall not be centered around any single ELV. Opening the launch requirements to industry bids induces competitive market practice and enhances the reliability of propellant delivery. Using a variety of systems avoids bottlenecks should any single system become grounded, similar to the Challenger incident and current Atlas grounding. Contingency planning must foresee lift requirements and factor in launch vehicle failures.

## 7.4.4.2.1 Assumptions

In determining which ELV's would contribute to each model's support requirement, many factors were considered. The model assumes:

(1) STS delivery of mission-specific payloads to SSF 4 times per year in ALL models.
   Normal SSF support operations require delivery of resource nodes and crew rotations every 90 days. MOOSE mission specific payloads are relatively small and low mass (> 1000 kg) and can accompany SSF support payloads without jeopardizing STS mission success.

(2) 100% of servicing missions require dedicated payload deliveries
   All MOOSE missions are assumed to require special payloads: Hydrazine products,

ORU, MLI , manipulator end effectors. The number of launches required to provide these payloads is given as

$$\frac{Minimum\ Launches}{Year} = \frac{Number\ of\ Sorties}{Year} - 4$$

Minimum launches indicates the smallest number of single ELV launches required. Number of sorties depends on mission model; LOW = 3, MEDIUM = 6, HIGH = 13. The 4 represents the 4 STS deliveries.

PMV deliveries include propellant AND special payloads. Delivery of payloads to SSF occurs on a year-round basis and provides flexible scheduling of flight opportunities.

(3) ELV available flights indicate the number of vehicles current space manufacturing and launch facilities can provide to MOOSE support. MOOSE operations cannot deprive other launch activity; e.g. MOOSE purchase of every Delta vehicle in a single year would delay other programs requiring Delta support. Use of a wide base of launchers alleviates this problem. Available flights reflects 50% of maximum launch rate in most cases, and 25% in others.

(4) ELV available flights are MOOSE dedicated
No other payloads piggyback PMV payloads. Payloads have been designed to utilize the maximum amount of ELV lift capacity.

(5) ELV support costs per year divided by the number of MOOSE sorties yield the ELV support cost / sortie. The ELV cost / sortie is the major operational cost for MOOSE flight missions. Mean cost per sortie represents the average of many different possible ELV combinations.

(6) ELV lift capacity, launch cost, flights available, and other information is given in figure 7.4.4.

7.4.4.2.2 ELV Groups

In order to provide 36,000/72,000/156,000 kg of lift to the Phase 3 LOW/MEDIUM/HIGH models respectively, and maintain mixed manifest under the above assumptions, many groups of ELV's were considered: High, Low, US+Various. French CIS, and US Japan CIS. Groups were more than 1 of a single type of ELV are used reflect 85% learning curve cost effects for additional vehicles.

(1) High
The High group represents the ELV combination exhibiting the highest launch cost
(2) Low
The Low group represents the ELV combination exhibiting the lowest launch cost.
The High and Low group establish the bounds of possible launch costs.

# MOOSE Launch Support Vehicles
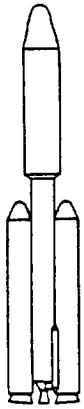
## Titan IV SRMU
17,800 kg to SSF ETR
15,000 kg to SSF WTR
$154M/launch
1 available flight/year ETR
1 available flight/year WTR
$8.7K/kg ETR
$10.3K/kg WTR
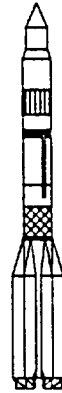
## Proton SL-13
15,000 kg to SSF
$70M/launch
5 available flights/year
$5K/kg

## Delta 7920
5100 kg to SSF ETR
4000 kg to SSF WTR
$48M/launch
5 available flights/year ETR
2 available flights/year WTR
$9.3K/kg ETR
$12K/kg WTR

## H-2
9,800 kg to SSF
$120M/launch
1 available flight/year
$12.3K/kg
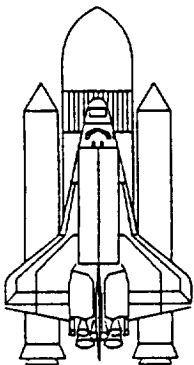
## STS / ASRM
20,100 kg to SSF
$245M/launch
3 available flights/year
$12.2K/kg
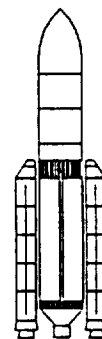
## Ariane 5
18,000 kg to SSF
$110M/launch
4 available flights/year
$6.1K/kg
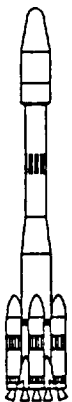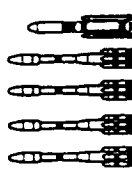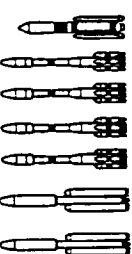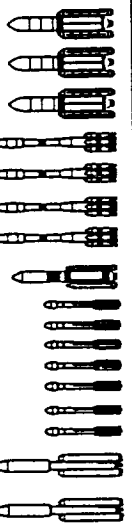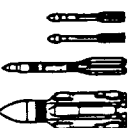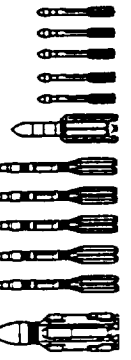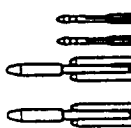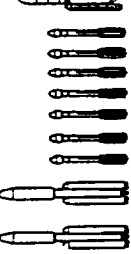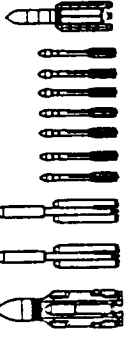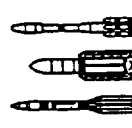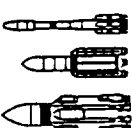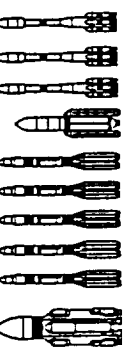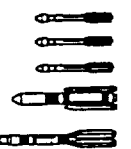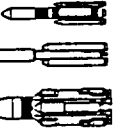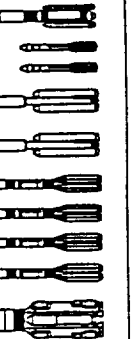
## Ariane AR-44L
8300 kg to SSF
$110M/launch
5 available flights/year
$13.2K/kg
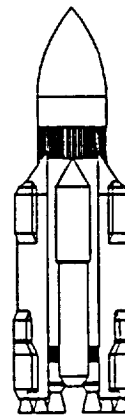
## Energiya
52,800 kg to SSF
$110M/launch
1 available flight/year
$2.1K/kg

# Phase 3 MOOSE Mission Model ELV Support Costs



| | LOW | MEDIUM | HIGH |
|---|---|---|---|
| HIGH | $390M<br>$130M/sortie | $715M<br>$119/sortie | $1,141M<br>$88M/sortie |
| LOW | $110<br>$37M/sortie | $269M<br>$45/sortie | $480M<br>$37M/sortie |
| US +<br>VARIOUS | $389M<br>$130M/sortie | $623M<br>$104/sortie | $852M<br>$65M/sortie |
| FRENCH<br>CIS | $290M<br>$97M/sortie | $330M<br>$55/sortie | $641M<br>$49M/sortie |
| US<br>JAPAN<br>CIS | $292M<br>$97M/sortie | $384M<br>$64/sortie | $790M<br>$61M/sortie |
| MEAN | $98M/sortie | $72M/sortie | $60M/sortie |

8-83

(3) US+Various

The US+ Various group reflects using the maximum US ELV available support with supplemental support from the lowest cost foreign ELV's (if required).

(4) French CIS

The French CIS model incorporates using at least 1 CIS ELV and 1 French vehicle and supplementing remaining lift with appropriate lowest-cost combinations of French and CIS launchers. This tends to be among the lower cost alternatives.

(5) US Japan CIS

The US Japan CIS group utilizes 1 H-2, 1 US, and 1 CIS vehicle and supplements remaining lift with additional US and CIS launches.

Other groups are possible; Detailed combinatoric analysis may be done at a later date. The mean cost/sortie of the above groups represents the resulting cost/sortie. Figure 7.4.5. Shows the results of the 5 groups in support of the mission models.

### 7.4.4.3 Cost summary (Cost/sortie)

The resulting cost / sortie of the MOOSE ELV Support Models are given as:

| Mission Model | Cost / Sortie in Millions |
|---------------|---------------------------|
| LOW           | $98                       |
| MEDIUM        | $72                       |
| HIGH          | $60                       |

### 7.4.4.3.1 Discounting Effects

Applying a 10% discount to future MOOSE ELV operations support models show significant cost effects after 3 years of phase 3 operations and drastic reductions after 6 years.



8-84
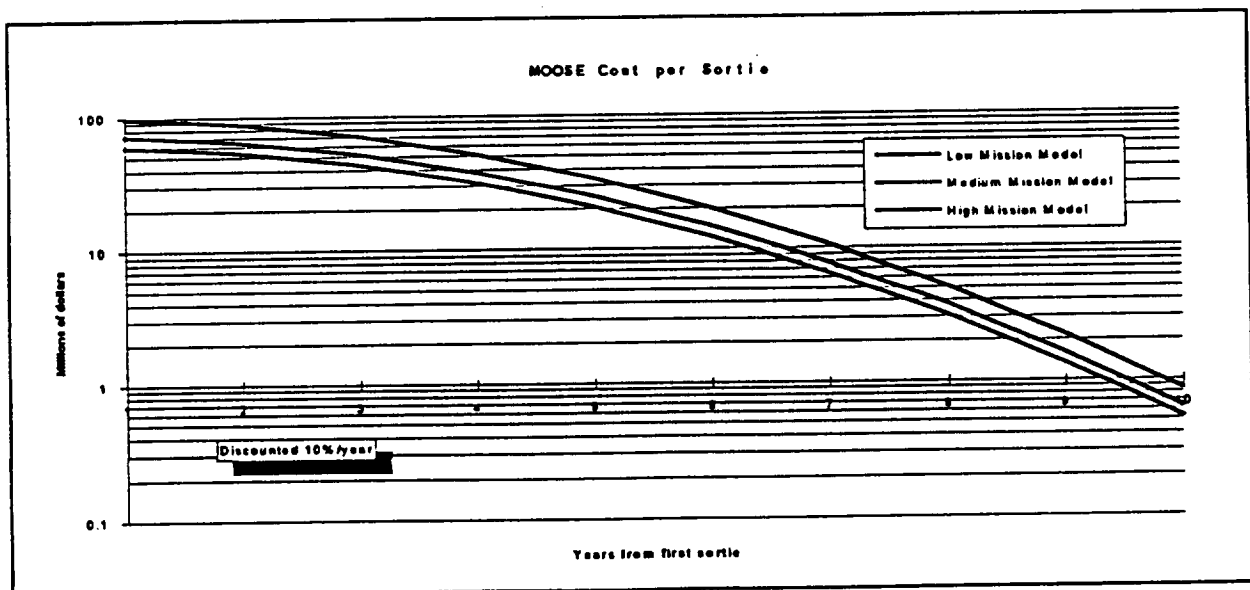
# BIBLIOGRAPHY

COLD-SAT Cryogenic On-Orbit Liquid Depot-Storage, Acquisition, and Transfer
NASA TM-102308 July 1989

Cole, E.G.
Service Role of a Space Station: System Approach to Requirements at the Transportation Node
Shuttle Integration and Satellite Systems Division, Rockwell International
from
Space Station Policy Planning and Utilization
AIAA Aerospace Assesment Series Volume 10
Proceedings of the NASA/AIAA Symposium on the Space Station
Arlington, VA, July 1983

de Ste. Croix
Space Technology
Second Edition
Orion Books, NY, NY, 1989

Definition of Satellite Servicing Technology Development Missions for Early Space Stations
Final Report Volume II - Technical
TRW Space and Technology Group
NASA CR-170844 May 1983

Fisher, H.T.
Satellite Platform Service and Maintenence
Lockheed Missiles and Space
Sunnyvale, CA
from
Space Station Policy Planning and Utilization
AIAA Aerospace Assesment Series Volume 10
Proceedings of the NASA/AIAA Symposium on the Space Station
Arlington, VA, July 1983

Iskawitz, Steven J.
Inernational Guide to Space Launch Systems 1991 Edition
AIAA, Washington D.C. 1991

Jezewski, D.J.
A Survey of Rendezvous Trajectory Planning
AAS 91-505

McHenry, Stevn T, and Yost, James M.
COLD-SAT Feasibility Study Safety Analysis
NASA CR-187042 January 1991

OTV Concept Definition and Evaluation - Subsystem Trade Studies
Volume II, Book 3, Orbital Transfer Vehicle Concept Definition and System Analysis Study
Martin Marietta Aerospace
NASA CR 183544

Repa, K.P.

Trajectory Design for Design Reference Missions of Space-Based Vehicles
TM-FM8-EE-11, Mcdonnel Douglas Astronautics Company Engineering Services, June 1988

Space Launch - Cost Increases and schedule delays in the Air Force's Titan IV Program
Report to the Chairman, Subcommitee on Defense, Commitee on Appropriations, House of Representatives
Government Accounting Office
GAO/NSIAD-90-113 May 1990

Space Station Definition and Preliminary Design Work Package 3
Automation and Robotics Plan
Contract No. NAS5-29300
General Electric Space Systems Division Philidelphia, PA, January 1987

Space Station Freedom User's Guide
Office of Space Flight
Spacelab/Space Station Utilization Program
User Integrstion Division
Code MG
NASA Washington D.C. August 1992

A study of Concept Options for the Evolution of Space Station Freedom
Langley Research Center
NASA TM 102675 May 1990

Turnaround Operations Analysis for OTV
Final Report Volume III  Technology Development Plan
General Dynamics Space Systems Division
NASA CR 179318 Febuary 1988

Turnaround Operations Analysis for OTV
Final Report Volume IV  WBS,Dictionary, and Cost Methodology
General Dynamics Space Systems Division
NASA CR 179319 Febuary 1988

Woodcock, Gordon
Space Stations and Platforms
Orbit Books 1990

# Appendix 1.1.5 ΔV - Vehicle Mass Trade Study

## Sample Calculation

Assumptions:

| | | |
|---|---|---|
| $\Delta V_{mission}$ | = 6 568 m/s | Baseline one sattellite at GEO mission |
| $I_{sp}$ | = 450 sec | |
| $Mdry_o$ | = 3000 kg | dry vehicle, mass budget ceiling |
| | | **does not** include propellant tank dry ma |

## Mass Estimation

Initial dry mass , $Mdry_o$ , is plugged into the rocket equation,

$$(1) \quad e^{-\frac{\Delta V}{I_{sp} \, g_o}} = \frac{M_{dry_0}}{M_{initial}}$$

to yield $Minitial_o$. From this relation the propellant mass is found:

$$(2) \quad M_{propellant} = \left( 1 - \frac{M_{dry_0}}{M_{initial_o}} \right) M_{initial_o}$$

Tank mass is estimated using the empirical equation given in ENAE 488D:

$$(3) \quad M_{tank_0} = 0.1 \left( M_{propellant_0} \right)^{0.9}$$

A new dry mass is calcualated by adding $Mdry_o$ to $Mtank_o$, $Mdry_{n+1}$

$$(4) \quad M_{dry_{n+1}} = M_{dry_n} + M_{tank_n}$$

The new value is then plugged back into equation (1), and the procedure is repeated. A final value is decided as reached when the n+1 value is within e = 0.001 kg of the n value. A full iteration yields the following results:

| | | |
|---|---|---|
| $Mdry_{final}$ | = | 4247 kg |
| $M_{tank}$ | = | 1145 kg |
| $M_{vehicle}$ | = | 18806 kg |
| $M_{propellant}$ | = | 14559 kg |

# Appendix 1.2

| Event | High Energy | Spiral | ΔV (m/s) Low Thrust | Hohmann | Aerobrake |
|---|---|---|---|---|---|
| Separate | 3 | 3 | 3 | 3 | 3 |
| GEO Transfer Inject | 3000 | 6052 | 592x4 burns | 2400 | 2400 |
| Midcourse | 15 | - | 60+75 | 15 | 15 |
| GEO Circ | 2514 | - | 550x5 burns | 1762 | 1762 |
| Orbit Trim | 9 | 9 | 9 | 9 | 9 |
| GEO Ops | 208 | 208 | 208 | 208 | 208 |
| LEO Transfer Inject | 2514 | 6052 | 550x5 burns | 1762 | 1844 |
| Midcourse | 20 | - | 75+60 | 20 | 20 |
| Aeromaneuver | - | - | - | - | 67 |
| LEO Circ | 3000 | - | 592x4 burns | 2400 | 122 |
| Rend & Dock | 18 | 18 | 18 | 18 | 18 |
| Reserves | 565 | 616 | 537 | 532 | 532 |
| | | | | | |
| Total ΔV | 11866 | 12958 | 11281 | 9129 | 7000 |
| | | | | | |
| Total Transfer Times(hours) | 8.4 | 686 | 165 | 10.6 | 15.2 |

The high energy transfer offers the shortest mission transfer times and the lowest total radiation exposure to the astronaut. However, there are high h loads placed on the astronaut. It can be seen that the energy expenditure is not worth the few hours saved from the mission time. Both the spiral and low thrust transfers have considerably less g loads but it can be seen that both of these transfers have prohibitive mission transfer times at no energy savings. The hohmann transfer offers one of the best solutions by having low mission times, minimal energy expenditure, and g loads in the range of 1 to 2g's. Further energy savings can be obtained if an aerobrake is used for one to the transfer burns. Utilizing a hohmnann transfer to GEO and then using the aerobrake for one of the transfer burns back to LEO will minimize both the total ΔV and mission times.

## Appendix 1.2.6

Phasing Orbit Study - Sample Calculation

$\Phi = 45°$

$\omega = 4.166$ E-3 °/sec      (angular rate of Earth)

$\mu = 398604$ km$^3$/sec$^2$      (GM of Earth)

$\Delta T$ = Difference between GEO circular and Transfer Orbit periods

$$\Delta T = \frac{\Phi}{\omega} = \frac{45°}{4.166\text{E-}3} = 10800 \text{ sec}$$

$T_{GEO}$ = GEO circular Orbit period

$$T_{GEO} = \sqrt{\frac{4\pi^2}{\mu}a^3_{GEO}} = 85661 \text{ sec}$$

$T_{transfer} = T_{GEO} - \Delta T = 85661 - 10800 = 74861 \text{ sec} = 20.8 \text{ hours}$

$a_{transfer}$ = semi-major axis of transfer orbit

$$a_{transfer} = \sqrt[3]{T^2_{transfer}\frac{\mu}{4\pi^2}} = \sqrt[3]{74861^2\frac{\mu}{4\pi^2}} = 38391 \text{ km}$$

$\Delta V = \Delta V$ required for the transfer orbit

$$\Delta V = 2\Delta V_{transfer} = 2\sqrt{\frac{\mu}{R_{GEO}}}\left[\sqrt{2 - \frac{R_{GEO}}{a_{transfer}}} - 1\right] = 2\sqrt{\frac{398604}{42000}}\left[\sqrt{2 - \frac{42000}{38391}} - 1\right] = -0.297 \text{ km/sec}$$

| Appendix | 1.2.6 continued | | | | | |
|---|---|---|---|---|---|---|
| ω = | 0.004166667 | °/sec | T geo = | 85660.97 | sec | |
| μ = | 398604 | km^3/sec^2 | R geo = | 42000 | km | |
| (°) | (sec) | (sec) | (hrs) | (km) | (km/sec) | (km) |
| Φ | ΔT | T transfer | T trans. | a transfer | ΔV transfer | perigee alt. |
| -360 | -86400 | 172061 | 47.8 | 66862 | 1.055 | 91725 |
| -345 | -82800 | 168461 | 46.8 | 65927 | 1.032 | 89853 |
| -330 | -79200 | 164861 | 45.8 | 64984 | 1.007 | 87968 |
| -315 | -75600 | 161261 | 44.8 | 64034 | 0.982 | 86069 |
| -300 | -72000 | 157661 | 43.8 | 63078 | 0.955 | 84156 |
| -285 | -68400 | 154061 | 42.8 | 62114 | 0.928 | 82228 |
| -270 | -64800 | 150461 | 41.8 | 61143 | 0.899 | 80285 |
| -255 | -61200 | 146861 | 40.8 | 60163 | 0.869 | 78327 |
| -240 | -57600 | 143261 | 39.8 | 59176 | 0.837 | 76352 |
| -225 | -54000 | 139661 | 38.8 | 58181 | 0.804 | 74361 |
| -210 | -50400 | 136061 | 37.8 | 57176 | 0.770 | 72353 |
| -195 | -46800 | 132461 | 36.8 | 56163 | 0.733 | 70327 |
| -180 | -43200 | 128861 | 35.8 | 55141 | 0.695 | 68282 |
| -165 | -39600 | 125261 | 34.8 | 54109 | 0.655 | 66218 |
| -150 | -36000 | 121661 | 33.8 | 53067 | 0.612 | 64135 |
| -135 | -32400 | 118061 | 32.8 | 52015 | 0.567 | 62031 |
| -120 | -28800 | 114461 | 31.8 | 50953 | 0.519 | 59905 |
| -105 | -25200 | 110861 | 30.8 | 49878 | 0.469 | 57757 |
| -90 | -21600 | 107261 | 29.8 | 48793 | 0.415 | 55586 |
| -75 | -18000 | 103661 | 28.8 | 47695 | 0.357 | 53390 |
| -60 | -14400 | 100061 | 27.8 | 46584 | 0.296 | 51168 |
| -45 | -10800 | 96461 | 26.8 | 45460 | 0.230 | 48920 |
| -30 | -7200 | 92861 | 25.8 | 44322 | 0.159 | 46643 |
| -15 | -3600 | 89261 | 24.8 | 43169 | 0.083 | 44337 |
| 0 | 0 | 85661 | 23.8 | 42000 | 0.000 | 42000 |
| 15 | 3600 | 82061 | 22.8 | 40815 | -0.090 | 39630 |
| 30 | 7200 | 78461 | 21.8 | 39612 | -0.189 | 37225 |
| 45 | 10800 | 74861 | 20.8 | 38391 | -0.297 | 34782 |
| 60 | 14400 | 71261 | 19.8 | 37150 | -0.416 | 32301 |
| 75 | 18000 | 67661 | 18.8 | 35888 | -0.549 | 29777 |
| 90 | 21600 | 64061 | 17.8 | 34604 | -0.698 | 27208 |
| 105 | 25200 | 60461 | 16.8 | 33295 | -0.866 | 24590 |
| 120 | 28800 | 56861 | 15.8 | 31960 | -1.059 | 21920 |
| 135 | 32400 | 53261 | 14.8 | 30596 | -1.282 | 19192 |
| 150 | 36000 | 49661 | 13.8 | 29201 | -1.544 | 16403 |
| 165 | 39600 | 46061 | 12.8 | 27773 | -1.858 | 13545 |
| 180 | 43200 | 42461 | 11.8 | 26306 | -2.248 | 10612 |
| 195 | 46800 | 38861 | 10.8 | 24797 | -2.752 | 7594 |
| 210 | 50400 | 35261 | 9.8 | 23241 | -3.456 | 4482 |
| 225 | 54000 | 31661 | 8.8 | 21631 | -4.673 | 1262 |
| 240 | 57600 | 28061 | 7.8 | 19959 | #NUM! | -2083 |
| 255 | 61200 | 24461 | 6.8 | 18213 | #NUM! | -5574 |
| 270 | 64800 | 20861 | 5.8 | 16379 | #NUM! | -9242 |
| 285 | 68400 | 17261 | 4.8 | 14436 | #NUM! | -13129 |
| 300 | 72000 | 13661 | 3.8 | 12351 | #NUM! | -17297 |
| 315 | 75600 | 10061 | 2.8 | 10073 | #NUM! | -21854 |
| 330 | 79200 | 6461 | 1.8 | 7498 | #NUM! | -27005 |

| | | | | | | |
|---|---|---|---|---|---|---|
| 345 | 82800 | 2861 | 0.8 | 4356 | #NUM! | -33288 |
| 360 | 86400 | -739 | -0.2 | 1767 | #NUM! | -38467 |

Appendix 1.3.1: NASA JSC Cost Model Summary (revised to FY92 and metric system)

### RDT&E Costs

| System | A ($M92) | B | Parameter |
|---|---|---|---|
| ECLSS/Crew Accomodations | 32.691 | 0.414 | system mass (kg) |
| Avionics | 24.817 | 0.579 | system mass (kg) |
| Control Moment Gyros | 5.553 | 0.468 | system mass (kg) |
| Structures/TPS | 5.226 | 0.491 | system mass (kg) |
| Electrical Power | 1.821 | 0.584 | system mass (kg) |
| Docking Module | 1.366 | 0.524 | system mass (kg) |
| RCS/Propulsion System | 0.411 | 0.876 | dry mass (kg) |
| Cryogen Tanks | 0.120 | 0.885 | dry mass (kg) |
| | | | |
| Software | 0.576 | 1.000 | kloc |
| Systems Engineering & Integration | 0.084 | 1.000 | RDT&E Costs ($M91) |
| Project Management | 0.030 | 1.000 | Total Direct Costs ($M91) |
| Subsystems Development Test | 0.073 | 1.000 | Total Direct Costs ($M91) |
| Support Equipment | 0.090 | 1.000 | Total Direct Costs ($M91) |
| Integration, Assembly and Checks | 0.596 | 0.832 | First Unit Costs ($M91) |

### First Unit Costs

| System | A ($M92) | B | Parameter |
|---|---|---|---|
| ECLSS/Crew Accomodations | 2.373 | 0.502 | system mass (kg) |
| Avionics | 0.212 | 0.917 | system mass (kg) |
| Control Moment Gyros | 0.256 | 0.531 | system mass (kg) |
| Structures/TPS | 1.204 | 0.440 | system mass (kg) |
| Electrical Power | 0.150 | 0.784 | system mass (kg) |
| Docking Module | 0.167 | 0.508 | system mass (kg) |
| RCS/Propulsion System | 0.342 | 0.550 | dry mass (kg) |
| Cryogen Tanks | 0.060 | 0.625 | dry mass (kg) |

Cost ($M92)=A*Parameter^B
Cost ($M93)=Cost ($M92)*1.043    (from DoD standard inflation factor tables)

## Modifications to NASA JSC Model

| Component | Reference System | Complexity Factor |
|---|---|---|
| Cabin Insulation and Shielding | Structures | 1.25 |
| Aerobrake Structure | Structures | 1.50 |
| Aerobrake TPS | Structures | 1.50 |
| Aerobrake Truss (Lower Truss) | Structures | 1.25 |
| Grappler & Robotic Arm | Structures | 2.50 |

Component Cost ($M93) = Reference System Cost ($M93)*Complexity Factor

Note:  The complexity factors were derived from judgements about relative system complexity and technology level.

## Appendix 1.3.2: Cost Discounting Analysis

| Year | Annual Cost % | Annual Cost $M93 | Discounted Annual Cost % | Discounted Annual Cost $M93 |
|------|------|------|------|------|
| 1993 | 6.4 | 166.0 | 8.2 | 166.0 |
| 1994 | 17.6 | 452.6 | 20.3 | 411.4 |
| 1995 | 23.8 | 612.8 | 25.0 | 506.5 |
| 1996 | 23.7 | 610.7 | 22.6 | 458.8 |
| 1997 | 17.9 | 461.6 | 15.6 | 315.3 |
| 1998 | 9.0 | 232.6 | 7.1 | 144.4 |
| 1999 | 1.6 | 42.3 | 1.2 | 23.9 |
| Totals | 100.0 | 2578.6 | 100.0 | 2026.3 |

| Year | Cumulative Annual Cost % | Cumulative Annual Cost $M93 | Cumulative Discount Cost % | Cumulative Discount Cost $M93 |
|------|------|------|------|------|
| 1993 | 6.4 | 166.0 | 8.2 | 166.0 |
| 1994 | 24.0 | 618.6 | 28.5 | 577.5 |
| 1995 | 47.8 | 1231.4 | 53.5 | 1083.9 |
| 1996 | 71.4 | 1842.1 | 76.1 | 1542.7 |
| 1997 | 89.3 | 2303.7 | 91.7 | 1858.0 |
| 1998 | 98.4 | 2539.3 | 98.8 | 2002.4 |
| 1999 | 100.0 | 2578.6 | 100.0 | 2026.3 |
| Totals | 100.0 | 2578.6 | 100.0 | 2026.3 |

Cumulative and annual costs and their respective percentages were computed using the time spreading of cost algorithm developed by Wynholds and Skratt (1977). The relevant equation is:

$$F(s) = As^2 [10+s((15-4s)s-20)] + Bs^3 [10+s(6s-15)] + [1-(A+B)]s^4 (5-4s)$$

where  A = 0.32
B = 0.68
s = fraction of total time elapsed
F(s) = fraction of cost consumed in time s

The values for the constants A and B were selected such that 60% of the costs will be incurred during the first three to four years. These values are consistent with typical projects in industry today. In order to obtain discounted costs, the following correction equation is necessary:

$$P = (1+d)^{-(n-1)}$$

where   P = discount factor
           d = discount rate
           n = year of the project

Then:

$$\text{Discount Cost} = \text{Annual Cost} * P$$

A standard discount rate of 10% was utilized in these calculations. As expected, costs are front loaded due to heavy RDT&E spending in the early stages of the project. Finally, since there is only one vehicle currently being considered for production and operation learning curve effects were not considered. Figures 1.3.1 and 1.3.2 present a graphical comparison of discounted and regular cost distributions.

| component | model | mass kg | status | height | length | radius/width | f part | component | model | Zcg stat=0 | m*Zc.g. | Izz | Iyy |
|---|---|---|---|---|---|---|---|---|---|---|---|---|---|
| LH2 TANK | sphere | 4853 | calculated | | 2.34 | 2.34 | 1.17 | LH2 TANK | sphere | 1.5823 | 7581.8419 | 2657.30868 | 2657.30868 |
| LH2 TANK | sphere | 4852 | calculated | | 2.34 | 2.34 | 1.17 | LH2 TANK | sphere | 1.5623 | 7580.2796 | 2656.76112 | 2656.76112 |
| main prop tank | sphere | 772 | calculated | | 1.84 | 1.84 | 0.92 | main prop tank | sphere | 1.2452 | 961.2944 | 261.36832 | 261.36832 |
| main prop tank N2H4 | sphere | 772 | calculated | | 1.84 | 1.84 | 0.92 | main prop tank N2H4 | sphere | 1.2452 | 961.2944 | 261.36832 | 261.36832 |
| RCS tank N2H4 | sphere | 261 | calculated | | 0.856 | 0.856 | 0.428 | RCS tank N2H4 | sphere | 3.6 | 939.6 | 19.1244096 | 19.1244096 |
| RCS tank | sphere | 261 | calculated | | 0.856 | 0.856 | 0.428 | RCS tank | sphere | 3.6 | 939.6 | 19.1244096 | 19.1244096 |
| cold gas tank H | sphere | 61 | calculated | | 1.17 | 1.17 | 0.585 | cold gas tank H | sphere | 3.6 | 219.6 | 8.35029 | 8.35029 |
| cold gas tank | sphere | 61 | calculated | | 1.17 | 1.17 | 0.585 | cold gas tank | sphere | 3.6 | 219.6 | 8.35029 | 8.35029 |
| crew module | cylinder | 240 | calculated | | 1.3 | 1.75 | 0.875 | crew module | cylinder | 4.85 | 1164 | 91.875 | 79.7375 |
| aerobrake w/ TF | ellipsoid | 650 | est | | 1 | 9 | 4.5 | aerobrake w/ TF | ellipsoid | 0.375 | 243.75 | 2632.5 | 1381.25 |
| grappler/ arm | beam w/rect x | 250 | est | | | | | grappler/ arm | prism (approx) | 5.5 | 1375 | 130.2083333 | 48.17708333 |
| insulation/shield | | 75 | est | | | | | insulation/shield | | 4.85 | 363.75 | 8.9392125 | 4.46960625 |
| spider upper | cylinder | 100 | est | | | | | spider upper | cylinder | 4.2 | 420 | | |
| (end effector,gld point) | | 200 | est | | | | | (end effector,gld point) | point | | | | |
| window | | 10 | est | | | | | window | | 5.6 | 56 | | |
| lower truss | | 100 | est | | | | | lower truss | | 2.97 | 297 | | |
| interior of cabin | | 213 | est | | | | | interior of cabin | | 4.75 | 101.75 | | |
| upper sun sensor 1 | | 1 | est | | | | | upper sun sensor 1 | | 4.2 | 4.2 | | |
| gps | | 7 | est | | 0.05 | 0.13 | 0.25 | gps | | 3.6 | 25.2 | | |
| upper sun sensor 2 | | 1 | est | | | | | upper sun sensor 2 | | 4.2 | 4.2 | | |
| lower sun sensors | | 1 | est | | | | | lower sun sensors | | 1 | 1 | | |
| cntrl moment gy | point | 56 | calc | | | | | cntrl moment gy | point | 3.6 | 201.6 | | |
| accelerometers | point | 1 | calc | | | | | accelerometers | point | 3.6 | 3.6 | | |
| star trackers | | 3 | est | | | | | star trackers | | 4.2 | 12.6 | | |
| lower sun sensor | | 1 | est | | | | | lower sun sensor | | 1 | 1 | | |
| rendezvous radar | | 34 | est | | | | | rendezvous radar | | 4.2 | 142.8 | | |
| data recorders | | 28 | est | | | | | data recorders | | 3.6 | 100.8 | | |
| antenna | prism | | | | 0.025 | 0.36 | 0.38 | antenna | prism | | | | |
| fuel cells | cone | 52 | calc | | | | | fuel cells | cone | 0.31 | 93 | 34.187842 | |
| Thrust chamber | cone | 300 | est | | | | | Thrust chamber | cone | 3.6 | 219.6 | 33.489 | |
| cold gas | | 61 | calc | | 1.17 | 1.17 | 0.585 | cold gas | | 3.6 | 219.6 | 8.35029 | 8.35029 |
| cold gas | | 61 | calc | | 1.17 | 1.17 | 0.585 | cold gas | | 3.6 | 219.6 | 8.35029 | 8.35029 |
| N2H4 & He thrusters | | 8.1 | calc | | | | | N2H4 & He thrusters | | 3.6 | | | |
| N2H4 & He thrusters | | 8.1 | calc | | | | | N2H4 & He thrusters | | 3.6 | | | |
| N2H4 & He thrusters | | 8.1 | calc | | | | | N2H4 & He thrusters | | 3.6 | | | |
| N2H4 & He thrusters | | 8.1 | calc | | | | | N2H4 & He thrusters | | 3.6 | | | |
| N2H4 & He thrusters | | 1.985 | calc | | | | | N2H4 & He thrusters | | 1.38 | | | |
| N2H4 & He thrusters | | 1.985 | calc | | | | | N2H4 & He thrusters | | 1.38 | | | |
| N2H4 & He thrusters | | 1.985 | calc | | | | | N2H4 & He thrusters | | 1.38 | | | |
| N2H4 & He thrusters | | 1.985 | calc | | | | | N2H4 & He thrusters | | 1.38 | | | |
| | Σmass= | 14378.34 | | | | | | | | | | | |

| bx | component | model | Z | Y | | |
|---|---|---|---|---|---|---|
| 2657.~ | LH2 TANK | sphere | | 1.5623 | 2.1914 | 0 |
| 2656.78112 | LH2 TANK | sphere | | 1.5623 | -2.1914 | 0 |
| 261.36832 | main prop tank | sphere | | 1.2452 | 0 | 2.19 |
| 261.36832 | main prop tank N2H4 | sphere | | 1.2452 | 0 | -2.19 |
| 19.1244096 | RCS tank N2H4 | sphere | | 3.6 | 0.0643 | 0 |
| 19.1244096 | RCS tank | sphere | | 3.6 | -0.0643 | 0 |
| 8.35029 | cold gas tank H | sphere | | 3.6 | 1.145 | 1.145 |
| 8.35029 | cold gas tank | sphere | | 3.6 | 1.145 | -1.145 |
| 79.7375 | crew module | cylinder | | 4.85 | 0 | 0 |
| 1361.25 | aerobrake w/ T | ellipsoid | | 0.375 | 0 | 0 |
| 130.2083333 | grappler/ arm | beam w/rect x | | 5.5 | 0 | 0 |
| 4.46960625 | insulation/shield | | | 4.85 | 0 | 0 |
| | spider truss | cylinder | | 4.2 | 0 | 0 |
| | (end effector,gid | point | | | | |
| | window | | | 5.6 | 1.05 | 0 |
| | lower truss | | | 2.97 | 0 | 0 |
| | interior of cabin | | | 4.75 | -0.04 | 0.66 |
| | upper sun sensor 1 | | | 4.2 | 1.03 | 0 |
| | gps | | | 3.6 | 0 | 0 |
| | upper sun sensor 2 | | | 4.2 | -1.03 | 0 |
| | lower sun sensor | | | 1 | 4.45 | 0 |
| | cntrl moment gy | point | | 3.6 | 0 | 0 |
| | accelerometers | point | | 3.6 | 0 | 0 |
| | star trackers | | | 4.2 | 0.95 | 0 |
| | lower sun sensor | | | 1 | -4.45 | 0 |
| | rendezvous radar | | | 4.2 | 0 | 1.03 |
| | data recorders | | | 3.6 | 0 | 0 |
| | antenna | prism | | | | |
| | | | | | | |
| 34.1878842 | fuel cells | cone | | 0.31 | 0 | 0 |
| 8.35029 | Thrust chamber | cone | | 3.6 | -1.145 | 1.145 |
| 8.35029 | cold gas | | | 3.6 | -1.145 | -1.145 |
| | cold gas | | | 3.6 | 2.06 | 0 |
| | N2H4 & He thrusters | | | 3.6 | -2.06 | 0 |
| | N2H4 & He thrusters | | | 3.6 | 0 | 2.06 |
| | N2H4 & He thrusters | | | 3.6 | 0 | -2.06 |
| | N2H4 & He thrusters | | | 1.38 | 3.36 | 0 |
| | N2H4 & He thrusters | | | 1.38 | -3.36 | 0 |
| | N2H4 & He thrusters | | | 1.38 | 3.36 | 3.36 |
| | N2H4 & He thrusters | | | 1.38 | -3.36 | -3.36 |

| Z'm | Y'm | X'm | dist to Zcg | dist to Ycg | dist to Xcg | 2 w/y&z | hycg w/ xcg | bxcg w/ xcg | Ixzcg | Ixycg | Iyzcg |
|---|---|---|---|---|---|---|---|---|---|---|---|
| 7581.8410 | 10634.8542 | 0 | 0.210585987 | 2.1909117 | 0.0122120 | 25952.16524 | 2872.52204 | 2659.032517 | 1023.680977 | 10632.65967 | 10681.49659 |
| 7580.2796 | -10632.6728 | 0 | 0.210585987 | 2.1918863 | 0.0122128 | 25967.58532 | 2871.030134 | 2657.484806 | 1023.490037 | 10635.20711 | 10684.01231 |
| 961.2944 | 0 | 1690.66 | 0.527685987 | 0.0004883 | 2.1777872 | 261.3685041 | 476.3336505 | 3922.776792 | 1729.901896 | 1681.251761 | 407.3737563 |
| 961.2944 | 0 | -1690.66 | 0.527685987 | 0.0004883 | 2.2022128 | 261.3685041 | 476.3336505 | 4005.366539 | 1748.233796 | 1700.108323 | 407.3737563 |
| 939.6 | 251.6823 | 0 | 1.827114013 | 0.9638117 | 0.0122128 | 261.5759208 | 890.4326157 | 19.1633384 | 476.8674104 | 251.5750481 | 539.1579418 |
| 939.6 | -251.6823 | 0 | 1.827114013 | 0.8647883 | 0.0122128 | 262.0675067 | 890.4326157 | 19.1633384 | 476.8674104 | 251.8299203 | 539.276141 |
| 219.6 | 69.845 | 69.845 | 1.827114013 | 1.1445117 | 1.1327872 | 88.25461892 | 211.9893726 | 86.62590727 | 131.1365574 | 98.22920501 | 131.5148209 |
| 219.6 | 69.845 | -69.845 | 1.827114013 | 1.1445117 | 1.1572128 | 88.25461892 | 211.9893726 | 90.03791933 | 131.927432 | 99.28297665 | 131.5148209 |
| 1164 | 0 | 0 | 3.077114013 | 0.0004883 | 0.0122128 | 91.87505722 | 2352.208656 | 79.7732966 | 738.5131797 | 2.933413887 | 738.5073725 |
| 243.75 | 0 | 0 | 1.397885987 | 0.0004883 | 0.0122128 | 2632.500155 | 2651.405401 | 1381.346949 | 908.6605678 | 7.944682611 | 906.6259469 |
| 1375 | 0 | 0 | 3.727114013 | 0.0004883 | 0.0122128 | 130.2063929 | 3521.0218 | 130.2456215 | 931.7835056 | 3.055639466 | 931.7785113 |
| 363.75 | 0 | 0 | 3.077114013 | 0.0004883 | 0.0122128 | 8.039230353 | 714.616905 | 4.490702686 | 230.7853687 | 0.91669184 | 230.7835539 |
| 420 | 0 | 0 | 2.427114013 | 0.0004883 | 0.0122128 | 2.38437E-05 | 589.0882433 | 0.014915248 | 242.7144739 | 1.222255786 | 242.7114062 |
|  |  |  |  |  |  |  |  |  |  |  |  |
| 56 | 10.5 | 0 | 3.827114013 | 1.0495117 | 0.0122128 | 11.01474808 | 146.4660167 | 0.001491525 | 38.27133499 | 10.49582756 | 39.68409817 |
| 297 | 0 | 0 | 1.197114013 | 0.0004883 | 0.0122128 | 2.38437E-05 | 143.3081961 | 0.014915248 | 119.7176308 | 1.222255786 | 119.7114113 |
| 1011.75 | -8.52 | 140.58 | 2.977114013 | 0.0004883 | 0.6477872 | 0.349171419 | 1887.863271 | 89.38081863 | 648.9630122 | 138.2479218 | 634.1839247 |
| 4.2 | 1.03 | 0 | 2.427114013 | 1.0295117 | 0.0122128 | 1.05989434 | 5.890082433 | 0.010149152 | 2.427144739 | 1.029584136 | 2.636432585 |
| 25.2 | 0 | 0 | 1.827114013 | 0.0004883 | 0.0122128 | 1.669062433 | 23.36841832 | 0.010144067 | 12.7900838 | 0.065557905 | 12.78979855 |
| 4.2 | -1.03 | 0 | 2.427114013 | 1.0304883 | 0.0122128 | 1.061806136 | 5.890082433 | 0.000149152 | 2.427144739 | 1.030560667 | 2.636814095 |
| 1 | 4.45 | 0 | 0.772885987 | 4.4495117 | 0.0122128 | 19.79815437 | 0.597352749 | 0.000149152 | 0.772982471 | 4.449528461 | 4.516138518 |
| 201.6 | 0 | 0 | 1.827114013 | 0.0004883 | 0.0122128 | 1.33525E-05 | 166.9473546 | 0.008352539 | 102.3206704 | 0.68446324 | 102.3183684 |
| 3.6 | 0 | 0 | 1.827114013 | 0.0004883 | 0.0122128 | 2.38437E-07 | 3.338345617 | 0.000149152 | 1.827154829 | 0.012222558 | 1.827114078 |
| 12.6 | 2.85 | 0 | 2.427114013 | 0.9495117 | 0.0122128 | 2.704717405 | 17.6726473 | 0.000447457 | 7.281434218 | 2.848770715 | 7.818701562 |
| 1 | -4.45 | 0 | 2.427114013 | 4.4504883 | 0.0122128 | 19.80684611 | 0.597352749 | 0.000149152 | 0.772982471 | 4.450505057 | 4.517100714 |
| 142.8 | 0 | 35.02 | 0.772885987 | 0.0004883 | 1.0177872 | 8.10685E-06 | 200.2900027 | 35.22026667 | 89.48379652 | 34.60476878 | 82.52187812 |
| 100.8 | 0 | 0 | 2.427114013 | 0.0004883 | 0.0122128 | 6.67623E-06 | 93.47367728 | 0.00417627 | 51.16033522 | 0.34223162 | 51.1591942 |
|  |  |  | 1.772885987 | 0.0004883 | 0.0122128 | 0 | 0 | 0 | 0 | 0 | 0 |
|  |  |  | 1.772885987 | 0.0004883 | 0.0122128 | 0 | 0 | 0 | 0 | 0 | 0 |
|  |  |  | 1.772885987 | 0.0004883 | 0.0122128 | 0 | 0 | 0 | 0 | 0 | 0 |
| 93 | 0 | 0 | 1.772885987 | 0.0004883 | 0.0122128 | 1.23997E-05 | 163.4424856 | 0.007755929 | 92.19225866 | 0.635573009 | 92.19007481 |
| 219.6 | -69.845 | 69.845 | 1.462885987 | 1.1454883 | 1.1327872 | 33.48907153 | 676.1985073 | 34.23262995 | 438.8610894 | 3.666767359 | 438.8658205 |
| 219.6 | -69.845 | -69.845 | 1.827114013 | 1.1454883 | 1.1572128 | 88.39104017 | 211.9893726 | 86.62590727 | 131.1365574 | 98.27155445 | 131.5464549 |
| 29.16 | 16.696 | 16.696 | 1.827114013 | 2.0595117 | 0.0122128 | 34.35686638 | 27.0405995 | 0.001206135 | 14.79995412 | 16.68233807 | 22.30066083 |
| 29.16 | -16.696 | -16.696 | 1.827114013 | 2.0604883 | 2.0477872 | 34.38945748 | 27.0405995 | 0.001206135 | 14.79995412 | 16.69024839 | 22.3057888 |
| 29.16 | 0 | 0 | 1.827114013 | 0.0004883 | 2.0722128 | 1.93134E-06 | 27.0405995 | 33.96680257 | 22.22970888 | 16.58707679 | 14.79962404 |
| 29.16 | 0 | 0 | 1.827114013 | 0.0004883 | 0.0122128 | 1.93134E-06 | 27.0405995 | 34.7819337 | 22.37772372 | 16.78492415 | 14.79962404 |
| 2.7393 | 6.6696 | 6.6696 | 0.392885987 | 3.3595117 | 0.0122128 | 22.41637 | 0.306403406 | 0.000296068 | 0.780255379 | 6.666674788 | 6.714078232 |
| 2.7393 | -6.6696 | -6.6696 | 0.392885987 | 3.3604883 | 0.0122128 | 22.41637 | 0.306403406 | 0.000296068 | 0.780255379 | 6.670613327 | 6.716003664 |
| 2.7393 | 0 | 6.6696 | 0.392885987 | 0.0004883 | 3.3477872 | 4.73297E-07 | 0.306403406 | 22.24724309 | 6.690963181 | 6.645357663 | 0.779879286 |
| 2.7393 | 0 | -6.6696 | 0.392885987 | 0.0004883 | 3.3722128 | 4.73297E-07 | 0.306403406 | 22.57306105 | 6.739119894 | 6.693842478 | 0.779879286 |

Zcg= 1.772885987  Ycg= 0.000488332  Xcg= 0.012212815

| Izzc.g.= | Iyyc.g= | Ixxc.g.= | Ixzc.g.= | Ixyc.g.= | Iyzc.g.= |
|---|---|---|---|---|---|
| 56385.79579 | 22819.01881 | 15503.62327 | 11756.15422 | 25961.04273 | 28523.79383 |

Page 4

FOR SEF

| LE PORTION | mass | Z | Y | X | Z*M | Y*M | X*M | Zdist to c.g. | Ydist to c.g. | Xdist to c.g. | Izz | Iyy |
|---|---|---|---|---|---|---|---|---|---|---|---|---|
| LH2 TANK | | | | | | | | | | | | |
| LH2 TANK | | | | | | | | | | | | |
| main prop tank LOX | | | | | | | | | | | | |
| main prop tank LOX | | | | | | | | | | | | |
| RCS tank N2H4 | 261 | 3.6 | 0.9643 | 0 | 939.6 | 251.6823 | 0 | -0.2464 | 0.961908 | -0.08704 | 19.1244086 | 19.1244086 |
| RCS tank | 261 | 3.6 | -0.9643 | 0 | 939.6 | -251.6823 | 0 | -0.2464 | -0.966694 | -0.08704 | 19.1244086 | 19.1244086 |
| cold gas tank H | 61 | 3.6 | 1.145 | 1.145 | 219.6 | 69.845 | 69.845 | -0.2464 | 1.142606 | 1.05796 | 8.35029 | 8.35029 |
| cold gas tank | 61 | 3.6 | 1.145 | -1.145 | 219.6 | 69.845 | -69.845 | -0.2464 | 1.142606 | -1.23204 | 8.35029 | 8.35029 |
| crew module | 240 | 4.85 | 0 | 0 | 1164 | 0 | 0 | 1.0036 | -0.002394 | -0.08704 | 91.875 | 79.7375 |
| aerobrake w/ TPS | | | | | | | | | | | | |
| grappler/ arm | 250 | 5.5 | 0 | 0 | 1375 | 0 | 0 | 1.6536 | -0.002394 | -0.08704 | 130.208333 | 46.17708333 |
| insulation/shield | 75 | 4.85 | 0 | 0 | 363.75 | 0 | 0 | 1.0036 | -0.002394 | -0.08704 | 8.9392125 | 4.46960625 |
| spider truss | 100 | 4.2 | 0 | 0 | 420 | 0 | 0 | 0.3536 | -0.002394 | -0.08704 | 0 | 0 |
| (end effector,gic | 200 | | | | | | | | | | | |
| window | 10 | 5.6 | 1.05 | 0 | 56 | 10.5 | 0 | 1.7536 | 1.047606 | -0.08704 | 0 | 0 |
| lower truss | | | | | | | | | | | | |
| interior of cabin | 213 | 4.75 | -0.04 | 0.66 | 1011.75 | -8.52 | 140.58 | 0.9036 | -0.042394 | 0.57296 | 0 | 0 |
| upper sun senso | 1 | 4.2 | 1.03 | 0 | 4.2 | 1.03 | 0 | 0.3536 | 1.027606 | -0.08704 | 0 | 0 |
| gps | 7 | 3.6 | 0 | 0 | 25.2 | 0 | 0 | -0.2464 | -0.002394 | -0.08704 | 0 | 0 |
| upper sun senso | 1 | 4.2 | -1.03 | 0 | 4.2 | -1.03 | 0 | 0.3536 | -1.032394 | -0.08704 | 0 | 0 |
| lower sun sensors | | | | | | | | | | | | |
| cntrl moment gy | 56 | 3.6 | 0 | 0 | 201.6 | 0 | 0 | -0.2464 | -0.002394 | -0.08704 | 0 | 0 |
| accelerometers | 1 | 3.6 | 0 | 0 | 3.6 | 0 | 0 | -0.2464 | -0.002394 | -0.08704 | 0 | 0 |
| star trackers | 3 | 4.2 | 0.95 | 0.95 | 12.6 | 2.85 | 2.85 | 0.3536 | 0.947606 | -0.08704 | 0 | 0 |
| lower sun sensor | | | | | | | | | | | | |
| rendezvous rad | 34 | 4.2 | 0 | 0 | 142.8 | 0 | 35.02 | 0.3536 | -0.002394 | -0.08704 | 0.94296 | 0 |
| data recorders | 28 | 3.6 | 0 | 0 | 100.8 | 0 | 0 | -0.2464 | -0.002394 | -0.08704 | 0 | 0 |
| antenna | | | | | | | | | | | | |
| | | | | | | | | | | | | |
| fuel cells | | | | | | | | | | | | |
| Thrust chamber assembly | | | | | | | | | | | | |
| cold gas | 61 | 3.6 | -1.145 | 1.145 | 219.6 | -69.845 | 69.845 | -0.2464 | -1.147394 | 1.05796 | 8.35029 | 8.35029 |
| cold gas | 61 | 3.6 | -1.145 | -1.145 | 219.6 | -69.845 | -69.845 | -0.2464 | -1.147394 | -1.23204 | 8.35029 | 8.35029 |
| N2H4 & He thru | 8.1 | 3.6 | 2.06 | 2.06 | 29.16 | 16.686 | 16.686 | -0.2464 | 2.057606 | 1.97296 | 0 | 0 |
| N2H4 & He thru | 8.1 | 3.6 | 2.06 | -2.06 | 29.16 | 16.686 | -16.686 | -0.2464 | -2.062394 | 1.97296 | 0 | 0 |
| N2H4 & He thru | 8.1 | 3.6 | -2.06 | 2.06 | 29.16 | 0 | 16.686 | -0.2464 | -0.002394 | 1.97296 | 0 | 0 |
| N2H4 & He thru | 8.1 | 3.6 | -2.06 | -2.06 | 29.16 | 0 | -16.686 | -0.2464 | -0.002394 | -2.14704 | 0 | 0 |
| N2H4 & He thrusters | | | | | | | | | | | | |
| N2H4 & He thrusters | | | | | | | | | | | | |
| N2H4 & He thrusters | | | | | | | | | | | | |
| N2H4 & He thrusters | | | | | | | | | | | | |

Zcg 3.846406265  Ycg 0.002394171  Xcg 0.087042728

APPR

C-4.

| Ixx | Izzc.g. | Iyyc.g. | Ixx c.g. | Ixzc.g. | Ixyc.g. | Iyzc.g. |
|---|---|---|---|---|---|---|
| | | | | | | |
| | | | | | | |
| 19.1244096 | 260.6180625 | 34.97049216 | 367.7203685 | 68.20490912 | 252.0831873 | 259.163421 |
| 19.1244096 | 263.0282022 | 34.97049216 | 367.7203685 | 68.20490912 | 253.327954 | 260.3741873 |
| 8.35029 | 87.98874675 | 12.05378056 | 138.0033841 | 68.2674541 | 94.98633605 | 71.30118362 |
| 8.35029 | 87.98874675 | 12.05378056 | 162.3206193 | 76.64269552 | 102.4904425 | 71.30118362 |
| 79.7375 | 91.8763755 | 321.4696104 | 6359.887137 | 241.7681573 | 20.89750003 | 240.8646653 |
| | | | | | | |
| 130.2083333 | 130.2097661 | 731.7753233 | 16956.10408 | 413.9722900 | 21.78822919 | 413.4404332 |
| 4.46060625 | 8.039642343 | 80.01057825 | 20.54557715 | 75.55254916 | 6.530486758 | 75.27021415 |
| 0 | 0.000573124 | 12.503296 | 0.757569616 | 36.41550791 | 8.707291678 | 35.3609104 |
| | | | | | | |
| 0 | 10.97478331 | 30.7511296 | 0.075759616 | 17.55758788 | 10.51215626 | 20.42692168 |
| | | | | | | |
| 0 | 0.382814513 | 173.9130005 | 69.92431342 | 227.6976697 | 122.3740914 | 192.678511 |
| 0 | 1.055974091 | 0.12503296 | 0.007575962 | 0.384155079 | 1.031285631 | 1.086741483 |
| 0 | 4.01187E-05 | 0.42490072 | 0.053031731 | 1.829250436 | 0.609510417 | 1.724881408 |
| 0 | 1.085837371 | 0.12503296 | 0.007575962 | 0.384155079 | 1.036056626 | 1.091270054 |
| | | | | | | |
| 0 | 0.000320949 | 3.39992676 | 0.42425385 | 14.63400349 | 4.876083339 | 13.79905126 |
| 0 | 5.73124E-06 | 0.06071296 | 0.007575962 | 0.261321491 | 0.087072917 | 0.24641163 |
| 0 | 2.693871394 | 0.37509988 | 0.022727885 | 1.092465237 | 2.854785077 | 3.034289179 |
| | | | | | | |
| 0 | 0.000194962 | 4.25112064 | 30.23190109 | 34.24065915 | 32.08074332 | 12.02267554 |
| 0 | 0.000160475 | 1.69996286 | 0.212126925 | 7.317001745 | 2.43804167 | 6.899525631 |
| | | | | | | |
| | | | | | | |
| 8.35029 | 88.65756247 | 12.05378056 | 138.0033841 | 68.2674541 | 95.20285366 | 71.586715 |
| 8.35029 | 88.65756247 | 12.05378056 | 162.3206193 | 76.64269552 | 102.6982702 | 71.586715 |
| 0 | 34.29331386 | 0.491774976 | 0.061365289 | 2.116704076 | 16.68151375 | 16.78566496 |
| 0 | 34.45309999 | 0.491774976 | 0.061365289 | 2.116704076 | 16.72026198 | 16.82419327 |
| 0 | 4.6423E-05 | 0.491774976 | 31.52082641 | 16.10512251 | 15.96998776 | 1.9959342 |
| 0 | 4.6423E-05 | 0.491774976 | 37.39224417 | 17.50517332 | 17.39103481 | 1.9959342 |
| | | | | | | |
| Izzc.g.= | 1192.885819 | Iyyc.g.= 1481.007022 | Ixxc.g.= 24843.34174 | Ixzc.g.= 1533.331179 | Ixyc.g. = 1203.357002 | Iyzc.g. 1860.821574 |

| component | model | mass kg | status | height | length | radius/width | c.g. of part | o | part | model | Zcg start=0 | m*Zcg | Izz | lzz | by | lby | box |
|---|---|---|---|---|---|---|---|---|---|---|---|---|---|---|---|---|---|
| LH2 TANK | sphere | 999 | calculated | 2.34 | 2.34 | 2.34 | 1.17 | 1.17 | LH2 TANK | sphere | 1.5623 | 1545.1147 | 541.53684 | 541.53684 | 541.53684 | 541.53684 | 541.53684 |
| LH2 TANK | sphere | 999 | calculated | 2.34 | 2.34 | 2.34 | 1.17 | 1.17 | LH2 TANK | sphere | 1.5623 | 1545.1147 | 541.53684 | 541.53684 | 541.53684 | 541.53684 | 541.53684 |
| main prep tank | sphere | 220 | calculated | 1.84 | 1.84 | 1.84 | 0.92 | 0.92 | main prep tank | sphere | 1.2452 | 273.944 | 74.4632 | 74.4632 | 74.4632 | 74.4632 | 74.4632 |
| main prep tank | sphere | 220 | calculated | 1.84 | 1.84 | 1.84 | 0.92 | 0.92 | main prep tank N2H4 | sphere | 1.2452 | 273.944 | 74.4632 | 74.4632 | 74.4632 | 74.4632 | 74.4632 |
| RCS tank N2H4 | sphere | 84 | calculated | 0.856 | 0.856 | 0.856 | 0.428 | 0.428 | RCS tank N2H4 | sphere | 3.6 | 338.4 | 8.6877184 | 8.6877184 | 8.6877184 | 8.6877184 | 8.6877184 |
| RCS tank | sphere | 95 | calculated | 0.856 | 0.856 | 0.856 | 0.428 | 0.428 | RCS tank | sphere | 3.6 | 342 | 8.960992 | 8.960992 | 8.960992 | 8.960992 | 8.960992 |
| cold gas tank H | sphere | 17 | calculated | 1.17 | 1.17 | 1.17 | 0.585 | 0.585 | cold gas tank H | sphere | 3.6 | 61.2 | 2.32713 | 2.32713 | 2.32713 | 2.32713 | 2.32713 |
| cold gas tank | sphere | 17 | calculated | 1.17 | 1.17 | 1.17 | 0.585 | 0.585 | cold gas tank | sphere | 3.6 | 61.2 | 2.32713 | 2.32713 | 2.32713 | 2.32713 | 2.32713 |
| crew module | cylinder | 240 | calculated | 1.3 | 1.75 | 0.876 | 0.876 | 0.65 | crew module | cylinder | 4.65 | 1164 | 1164 | 91.875 | 79.7375 | 79.7375 | 79.7375 |
| aerobrake w/ TF | ellipsoid | 650 | est | 1 | 8 | 4.5 | 0.375 | 0.375 | aerobrake w/ TF | ellipsoid | 0.375 | 243.75 | 2832.5 | 1361.25 | 1361.25 | 1361.25 | 1361.25 |
| grappler/ arm | beam w/net x | 250 | est | | | | | | grappler arm | prism (approx) | 5.5 | 1375 | 130.2083333 | 130.2083333 | 49.17706333 | 130.2083333 | 130.2083333 |
| insulation/shield | cylinder | 75 | est | | | | | | insulation/shield | | 4.85 | 363.775 | 8.3392125 | 8.3392125 | 4.4696025 | 4.4696025 | 4.4696025 |
| spider upper | point | 100 | est | | | | | | spider upper | cylinder | 4.2 | 420 | | | | | |
| (end effector,grp) | | 200 | est | | | | | | (end effector,grp) | point | | 0 | | | | | |
| window | | 10 | est | | | | | | window | | 5.6 | 56 | | | | | |
| lower truss | | 100 | est | | | | | | lower truss | | 2.97 | 297 | | | | | |
| interior of cabin | | 213 | est | | | | | | interior of cabin | | 4.75 | 1011.75 | | | | | |
| upper sun sensor 1 | | 1 | est | | | | | | upper sun sensor 1 | | 4.2 | 4.2 | | | | | |
| gps | | 7 | est | | 0.05 | 0.13 | 0.25 | | gps | | 3.6 | 25.2 | | | | | |
| upper sun sensor 2 | | 1 | est | | | | | | upper sun sensor 2 | | 4.2 | 4.2 | | | | | |
| lower sun sensors | | 1 | est | | | | | | lower sun sensors | | 1 | 1 | | | | | |
| cntrl moment gy | point | 56 | calc | | | | | | cntrl moment gy | point | 3.6 | 201.6 | | | | | |
| accelerometers | point | 1 | calc | | | | | | accelerometers | point | 3.6 | 3.6 | | | | | |
| star trackers | | 3 | est | | | | | | star trackers | | 4.2 | 12.6 | | | | | |
| lower sun sensor | | 1 | est | | | | | | lower sun sensor | | 1 | 1 | | | | | |
| rendezvous radar | | 34 | est | | | | | | rendezvous radar | | 4.2 | 142.6 | | | | | |
| data recorders | | 20 | est | | | | | | data recorders | | 3.6 | 100.8 | | | | | |
| antenna | prism | | | 0.025 | 0.36 | 0.38 | 0.38 | 0.38 | antenna | prism | | 0 | | | | | |
| | | | | | | | | | | | | 0 | | | | | |
| fuel cells | cone | 82 | calc | | | | | | fuel cells | cone | | 0 | | | | | |
| Thrust chamber | cone | 300 | est | | | | | | Thrust chamber | cone | 0.31 | 93 | 33.499 | 34.187842 | 34.187842 | 34.187842 | 34.187842 |
| cold gas | | 17 | calc | 1.17 | 1.17 | 0.585 | 0.585 | 0.585 | cold gas | | 3.6 | 61.2 | 2.32713 | 2.32713 | 2.32713 | 2.32713 | 2.32713 |
| cold gas | | 17 | calc | 1.17 | 1.17 | 0.585 | 0.585 | 0.585 | cold gas | | 3.6 | 61.2 | 2.32713 | 2.32713 | 2.32713 | 2.32713 | 2.32713 |
| N2H4 & He thrusters | | 8.1 | calc | | | | | | N2H4 & He thrusters | | 3.6 | | | | | | |
| N2H4 & He thrusters | | 8.1 | calc | | | | | | N2H4 & He thrusters | | 3.6 | | | | | | |
| N2H4 & He thrusters | | 8.1 | calc | | | | | | N2H4 & He thrusters | | 3.6 | | | | | | |
| N2H4 & He thrusters | | 8.1 | calc | | | | | | N2H4 & He thrusters | | 3.6 | | | | | | |
| N2H4 & He thrusters | | 1.985 | calc | | | | | | N2H4 & He thrusters | | 1.36 | | | | | | |
| N2H4 & He thrusters | | 1.985 | calc | | | | | | N2H4 & He thrusters | | 1.36 | | | | | | |
| N2H4 & He thrusters | | 1.985 | calc | | | | | | N2H4 & He thrusters | | 1.36 | | | | | | |
| N2H4 & He thrusters | | 1.985 | calc | | | | | | N2H4 & He thrusters | | 1.36 | | | | | | |
| Σmass= | | 5039.34 | | | | | | | | | | | | | | | |

| component | model | Z | Y | X |
|---|---|---|---|---|
| I2 TANK | sphere | 1.5623 | 2.1914 | 0 |
| H2 TANK | sphere | 1.5623 | -2.1914 | 0 |
| main prop tank | sphere | 1.2452 | 0 | 2.19 |
| main prop tank | sphere | 1.2452 | 0 | -2.19 |
| RCS tank N2H4 | sphere | 3.6 | 0.9943 | 0 |
| RCS tank | sphere | 3.6 | -0.9943 | 0 |
| cold gas tank He | sphere | 3.6 | 1.145 | 1.145 |
| cold gas tank | sphere | 3.6 | 1.145 | -1.145 |
| crew module | cylinder | 4.85 | 0 | 0 |
| aerobrake w/ TR | ellipsoid | 0.375 | 0 | 0 |
| grappler/ arm | beam w/rect x | 5.5 | 0 | 0 |
| insulation/shield | | 4.85 | 0 | 0 |
| spider truss | cylinder | 4.2 | 0 | 0 |
| (end effector,gtc) | point | | | |
| window | | 5.6 | 1.05 | 0 |
| lower truss | | 2.97 | 0 | 0 |
| interior of cabin | | 4.75 | -0.04 | 0.66 |
| upper sun sensor 1 | | 4.2 | 1.03 | 0 |
| gps | | 3.6 | 0 | 0 |
| upper sun sensor 2 | | 4.2 | -1.03 | 0 |
| lower sun sensors | | 1 | 4.45 | 0 |
| cntrl moment gyro | point | 3.6 | 0 | 0 |
| accelerometers | point | 3.6 | 0 | 0 |
| star trackers | | 4.2 | 0.95 | 0 |
| lower sun sensor | | 1 | -4.45 | 0 |
| rendezvous radar | | 4.2 | 0 | 1.03 |
| data recorders | | 3.6 | 0 | 0 |
| antenna | prism | 0 | | |
| | | 0 | | |
| fuel cells | cone | 0 | 0 | 0 |
| Thrust chamber | cone | 0.31 | 0 | 0 |
| cold gas | | 3.6 | -1.145 | 1.145 |
| cold gas | | 3.6 | -1.145 | -1.145 |
| N2H4 & He thrusters | | 3.6 | 2.06 | 0 |
| N2H4 & He thrusters | | 3.6 | -2.06 | 0 |
| N2H4 & He thrusters | | 3.6 | 0 | 2.06 |
| N2H4 & He thrusters | | 3.6 | 0 | -2.06 |
| N2H4 & He thrusters | | 1.36 | 3.36 | 0 |
| N2H4 & He thrusters | | 1.36 | -3.36 | 0 |
| N2H4 & He thrusters | | 1.36 | 0 | 3.36 |
| N2H4 & He thrusters | | 1.36 | 0 | -3.36 |

| Z'm | Y'm | X'm | dist to Zcg | dist to Ycg | dist to Xcg | Izcg w/ kke | Iyrcg w/ rcg | Ixr | Ixrcg | Izcg | Iyrcg | Iyrcg | Iyrcg |
|---|---|---|---|---|---|---|---|---|---|---|---|---|---|

# Appendix A2.1 Robotic Terminology

## A2.1.1 Basic Parameters

There are several basic parameters that can be used to define the capabilities of a robotic manipulator. These are

- Payload
- Mobility
- Workspace
- Agility
- Accuracy
- Structural Dynamics
- Economics

*Payload* is the maximum mass that the manipulator can handle in any configuration of its linkages. This mass is likely to be less than the maximum load-carrying capacity of the system, which can be much higher in certain configurations. The payload capacity of the arm is a function of the size and shape (moments of inertia) of the payload, as well as its mass. Therefore, wrist interface torques are sometime specified instead of, or in addition to, the payload rating.

*Mobility* is determined by the total number of independent "degrees of freedom" (DOF), or motions, that can be performed by all the links. The degree of mobility of the end effector is equal to the sum of independent degrees of freedom all the intermediate links. However, because of possible "degeneracies" of major and minor wrist linkages, some link configurations may have a reduced number of guaranteed degrees of mobility. Six DOF is needed (theoretically) for an arm to reach any point within its three-dimensional workspace. Despite programming and control problems, a seventh DOF is sometimes added to help deal with degeneracy issues.

The *workspace* of a manipulator is the space composed of all points that can be reached by the end of the arm, or some point on the wrist, but not by the the end effector or tool tip. This is because the size and shape of different end effectors can significantly alter the dimensions of the workspace. Some segments of the theoretical workspace can be excluded if required velocity, payload, etc., specifications can not be performed in these regions. Degeneracy in the major and minor wrist linkages can also eliminate workspace points. As stated above, redundant DOFs can help overcome degeneracy problems.

*Agility* is the speed at which prescribed motions can be executed. To accurately characterize robot performance, the maximum speed and the maximum rates of acceleration and deceleration have to be specified. These

may not be enough to accurately characterize a system, since, typically, the more deceleration a link experiences, the longer the required settling time is, thus reducing the effective speed.

*Accuracy* can be defined as the difference between the desired coordinate and actual coordinate. *Repeatability* can be characterized by the deviation of the actual coordinate from the desired coordinate in multiple instances. Typically, one sees either: [1] good accuracy, high repeatability, [2] high accuracy, poor repeatability, or [3] poor accuracy, high repeatability. Both of these factors can be influenced by friction, hysteresis, backlash, compliance in links, joints, or drives, settling times, etc.

*Structural dynamics* is characterized as having many components and considerations. For instance, large *inertia* values lead to a need for high-torque (thus heavy, not very responsive) motors, and for high forces to execute a motion with a given speed and acceleration/deceleration profile, thus resulting in lower performance. Low *stiffness* (or high *compliance*) values lead to low natural frequencies, resulting in longer stabilization times and reduced speed, accuracy, and repeatability, and may cause large path deviations, and induce dynamic instabilities. *Natural frequencies* should be the highest possible, in order to reduce the transient times and overshoot factors.

Basic *economic* factors include investment cost and operating expense. These factors are largely dependent on structural design. Operating expense includes power requirements, ratio between operating time and down time, and difficulty of maintenance.

## A2.1.2 Structural Configurations

Robot motion can be broken down into three different parts. *Global* motions involve traveling distances that exceed the overall dimensions of the manipulator (i.e. traversing of the spacecraft). *Regional* motions involves the placement of an end effector into various points of the workspace. *Local* motions cover the fine or small adjustment movements of the end effector.

A mechanism needs to have at least six degrees of freedom to move and orient a body in three-dimensional space: three DOF to place the object in the proper region of space (execute regional motions by the arm), and three DOF to properly orient the body (execute local motions by wrist/end effector).

Robotic arms are characterized by the first three elementary joints of the arm. There are two types of elementary joints: prismatic and revolute joints. A *prismatic* joint translates along an axis, while a revolute joint rotates around an axis. In order to move the end point of the arm in three-dimensional space, at least one of the following obvious conditions have to be satisfied:

- There are two revolute joints with non-parallel axes.
- There are two revolute joints with parallel axes, and one prismatic joint whose axis is not perpendicular to the revolute joint axes.
- There are two prismatic joints with nonparallel axes and one revolute joint whose axis is not perpendicular to the plane containing axes of the prismatic joints or the third prismatic joint whose axes is nonparallel to that plane.

## A2.1.3 Coordinate Frame Selection

Robots moving in the *rectangular* or *cartesian frame* are used for relatively simple applications. These robots have three main joints that are prismatic. Rectangular frame robots are the easiest to program because the joint coordinates are completely independent. However, it is difficult to protect the sliding surfaces, the structure is very large and bulky, as it must completely encompass the workspace, and it is difficult to access enclosed areas.

*Cylindrical coordinate system* robotic arms have two translational motions (radial and vertical), with telescopic radial motion. These robots are more versatile then cartesian frame robots. They require relatively small space, and can have faster transients and reduced dynamic loads. One disadvantage of the cylindrical frame robots is their reduced work zone, since the arm cannot reach below the bed of the structure.

Many robotic arms are designed to work in *spherical coordinate frames*. These arms are very complicated and require more sophisticated control systems, but they have the advantage of servicing a larger workspace. Anthropomorphic robot designs have only revolute joints (RRR), and are called *jointed* or *articulated*. The Space Shuttle Remote Manipulator System (RMS) is an example of a jointed manipulator.

Jointed arms have large workspaces in comparison to the required hardware. They have a high degree of accessibility, and have no sliding surfaces. Rotary bearings are easier to seal then sliding bearings, and have lower inertia and friction losses. Jointed robots have lower energy requirements and lower required joint force (torques).

One disadvantage to jointed arms is the degenerate behavior of the near the workspace boundaries. Another is that conventional jointed robots have shoulder and elbow joint axes that are parallel and orthogonal to the waist axes, which results in relatively low stiffness.

Another significant disadvantage of the jointed configuration is the need to move the elbow joint motor when the upper arm or waist is moving. Conventional motor-transmission units or direct-drive motors are very

heavy, impairing system dynamics. One way to overcome this problem is to locate the motors closer to the base and use a special light transmission system to transmit power to the shoulder joint. But, transmission systems introduce compliances, backlashes, and energy losses.

## Appendix A2.2  Jointed Manipulator Models

### A2.2.1  Simplified Jointed Manipulator (2D)

To simplify the initial analysis, first consider a 2D (planar) jointed manipulator.
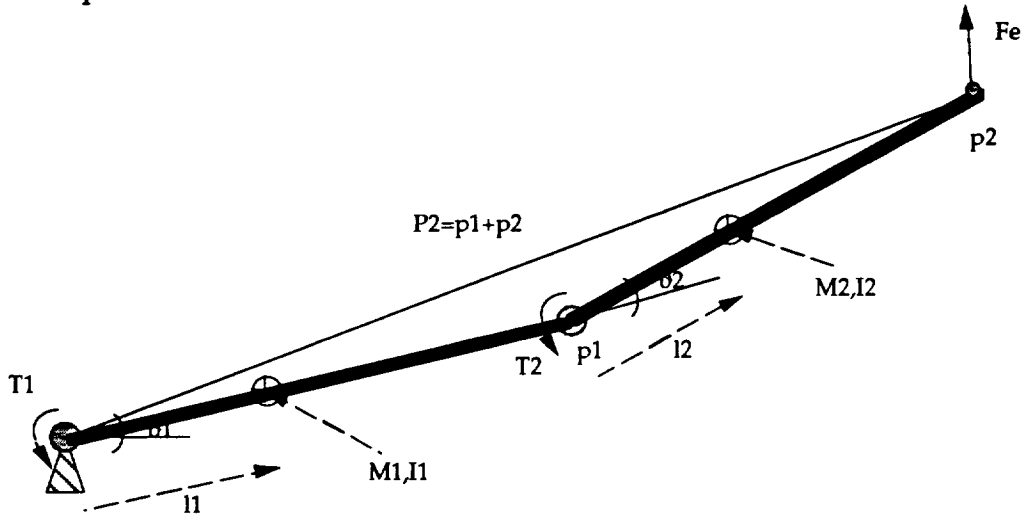


**Figure A2.2.a**  A 2D Jointed Manipulator

### A2.2.1.1 Statics

Each link has to be in equilibrium under the influence of action and reaction forces and joint torques.  So, one vector equation for the balance of forces and one equation for the balance of torques can be made for each link.

for link 1:

$$F_{1e} = F2e$$
$$\overline{T_1} - \overline{T_2} - \overline{p}_1 \times \overline{F}_{2e} = 0$$

for link 2:

$$F_{2e} = \overline{F}_e$$
$$\overline{r}_2 - \overline{p}_2 \times \overline{F}_e = 0$$

So,

$$\overline{F}_{1e} = \overline{F}_{2e} = \overline{F}_e$$
$$\overline{T}_1 = (\overline{p}_1 + \overline{p}_2) \times \overline{F}_e$$
$$\overline{T}_2 = \overline{p}_2 \times \overline{F}_e$$

To analyze the roles of T1 and T2, first assume T2=0.  This means that
$$\overline{T}_2 = \overline{p}_2 \times \overline{F}_e = 0$$

or that p2 and Fe are parallel. So, the motor at joint 1, creating torque T1, can only create a force Fe which is directed along link 2.

Now, assume that T1 = 0. Then

$$\overline{T}_1 = (\overline{p}_1 + \overline{p}_2) \times \overline{F}_e = 0$$

or Fe is parallel to p1+p2.

Analytically, this can be represented by the equations

$$T_1 = [l_1 c_1 + l_2 c_2] F_{ey} - [l_1 s_1 + l_2 s_2] F_{ex}$$
$$T_2 = l_2 c_{12} F_{ey} - l_2 s_{12} F_{ex}$$

or

$$\begin{bmatrix} T_1 \\ T_2 \end{bmatrix} = \overline{J}^{T} \begin{bmatrix} F_{ex} \\ F_{ey} \end{bmatrix}$$

From the above equations, the torques required from each motor joint to develop the needed force at the arm's end point can be determined for each linkage (assuming that the friction forces in the joints are zero...).

The reverse can be done easily, as well. The magnitudes and directions of the arm end force can be determined from given torques, via the following equations

$$F_{ex} = \frac{1}{l_1 l_2 s_2} [l_2 c_{12} T_1 - (l_1 c_1 + l_2 c_{12}) T_2$$
$$F_{ey} = \frac{1}{l_1 l_2 s_2} [l_2 s_{12} T_1 - (l_1 s_1 + l_2 s_{12}) T_2$$

To figure out the torques required for an arm to move 6000 kg at an acceleration of 1m/s/s in all points of 2-d space, one would use the equations

$$F_{ex} = mac_{12}$$
$$F_{ey} = mas_{12}$$

Note that when links 1 and 2 are parallel (J2=0 or p, or sinJ2=0), the joint motors do not have any control over the radial (link 2) force component. This cooresponds to a *degeneracy* condition.

If gravity forces need to be accounted for, they can be handled in a manner similar to the arm-end force. Payload gravity force is treated exactly like the force Fe, and can be considered to be part of this force. Because of the linear relationship of force and torque in the equations above, superposition applies. So, only gravity forces of links are considered.

The equilibrium equations for two links considered as free bodies loaded with gravity forces W1 and W2, and reation forces and driving torques Fg and Tg are as follows:

$$\overline{F}_{1g} - \overline{F}_{2g} - \overline{W}_1 = 0$$
$$\overline{F}_{2g} - \overline{W}_2 = 0$$
$$T_{1g} + W_1 l_{1c} c_1 - T_{2g} + F_{2g} l_1 c_1 = 0$$
$$T_{2g} + W_2 l_{2c} c_{12} = 0$$

or

$$\overline{F}_{1g} = (m_1 + m_2)\overline{g}$$
$$\overline{F}_{2g} = m_2 \overline{g}$$
$$T_{1g} = -m_1 l_{1c} g c_1 - m_2 g[l_1 c_1 + l_{2c} c_{12}]$$
$$T_{2g} = -m_2 l_{2c} g c_{12}$$

It is assumed that the effects of gravity is negligible on the arm (for now, at least). If it becomes a factor, the gravity forces can be reduced by shifting the locations of the center of gravity closer to the joint pivots.

## A2.2.1.2 Dynamics

These equations allow for the computation of acceleration and velocity when the forces are known (direct), or of forces when the acceleration and velocities are specified (indirect).

The kinetic and potential energy expressions for the first link are:

$$K_1 = \frac{1}{2} m_1 l_{1c}^2 \dot{\theta}_1^2 + \frac{1}{2} I_1 \dot{\theta}_1^2$$
$$V_1 = m_1 g_1 l_{1c}$$

Note that the potential energy of the links equals zero, since it is assumed that gravity has a negligible effect on the system.

For the second link, the coordinates and velocities of the center of gravity must first be determined. First, the coordinates:

$$x_{2c} = l_1 c_1 + l_{2c} c_{12}$$
$$y_{2c} = l_1 s_1 + l_{2c} s_{12}$$

Now, the velocities:

$$\dot{x}_{2c} = -l_1 \dot{\theta}_1 s_1 - l_{2c}(\dot{\theta}_1 + \dot{\theta}_2)s_{12}$$
$$\dot{y}_{2c} = l_1 \dot{\theta}_1 c_1 + l_{2c}(\dot{\theta}_1 + \dot{\theta}_2)c_{12}$$

The angular velocity of link 2 is $\dot{\theta}_1 + \dot{\theta}_2$. So, the kinetic and potential energies for link 2 are:

$$K_2 = \tfrac{1}{2}m_2(\dot{x}_{2c}^2 + \dot{y}_{2c}^2) + \tfrac{1}{2}I_2(\dot{\theta}_1 + \dot{\theta}_2)^2$$

$$K_2 = \tfrac{1}{2}m_2 l_1^2 \dot{\theta}_1^2 + \tfrac{1}{2}m_2 l_{2c}^2(\dot{\theta}_1^2 + 2\dot{\theta}_1\dot{\theta}_2 + \dot{\theta}_2^2) + m_2 l_1 l_2(\dot{\theta}_1^2 + \dot{\theta}_1\dot{\theta}_2)c_2 + \tfrac{1}{2}I_2(\dot{\theta}_1^2 + 2\dot{\theta}_1\dot{\theta}_2 + \dot{\theta}_2^2)$$

and

$$V_2 = m_2 g l_1 s_1 + m_2 g l_{2c} s_{12}$$

Note, again, that the potential energy V2 = 0 for this case.

Therefore, the kinetic energy of the payload is

$$K_0 = \tfrac{1}{2}m_0 l_1^2 \dot{\theta}_1^2 + \tfrac{1}{2}m_0 l_2^2(\dot{\theta}_1^2 + 2\dot{\theta}_1\dot{\theta}_2 + \dot{\theta}_2^2) + m_0 l_1 l_2(\dot{\theta}_1^2 + \dot{\theta}_1\dot{\theta}_2)c_2$$

The Lagrangian L = K - V can be constructed easily, since there is no V term.

$$L = \tfrac{1}{2}m_1 l_{1c}^2 \dot{\theta}_1^2 + \tfrac{1}{2}I_1 \dot{\theta}_1^2 + \tfrac{1}{2}m_2 l_1 \dot{\theta}_1^2 + \tfrac{1}{2}m_2 l_{2c}^2(\dot{\theta}_1^2 + 2\dot{\theta}_1\dot{\theta}_2 + \dot{\theta}_2^2)$$

$$+ m_2 l_1 l_{2c}(\dot{\theta}_1^2 + \dot{\theta}_1\dot{\theta}_2)c_2 + \tfrac{1}{2}I_2(\dot{\theta}_1^2 + 2\dot{\theta}_1\dot{\theta}_2 + \dot{\theta}_2^2) + \tfrac{1}{2}m_0 l_1^2 \dot{\theta}_1^2$$

$$+ \tfrac{1}{2}m_0 l_2^2(\dot{\theta}_1^2 + 2\dot{\theta}_1\dot{\theta}_2 + \dot{\theta}_2^2) + m_0 l_1 l_2(\dot{\theta}_1^2 + \dot{\theta}_1\dot{\theta}_2)c_2$$

The derivative of the Lagrangian are as follows:

$$\frac{\partial L}{\partial \dot{\theta}_1} = m_1 l_{1c}^2 \dot{\theta}_1 + I_1 \dot{\theta}_1 + m_2 l_1 \dot{\theta}_1 + m_2 l_{2c}^2(\dot{\theta}_1 + \dot{\theta}_2)$$

$$+ m_2 l_1 l_{2c}(2\dot{\theta}_1 + \dot{\theta}_2)c_2 + I_2(\dot{\theta}_1 + \dot{\theta}_2) + m_0 l_1^2 \dot{\theta}_1$$

$$+ m_0 l_2^2(\dot{\theta}_1 + \dot{\theta}_2) + m_0 l_1 l_2(2\dot{\theta}_1 + \dot{\theta}_2)c_2$$

$$\frac{\partial}{\partial t}\frac{\partial L}{\partial \dot\theta_1} = (m_1 l_{1c}^2 + I_1 + m_2 l_1^2 + m_2 l_{2c}^2 + 2m_2 l_1 l_{2c} c_2 + I_2 + m_0 l_1^2 + m_0 l_2^2 + 4m_0 l_1 l_2 c_2)\ddot\theta_1$$

$$+ (m_2 l_{2c}^2 + m_2 l_1 l_{2c} c_2 + I_2 + m_0 l_2^2 + m_0 l_1 l_2 + 2m_0 l_1 l_2 c_2)\ddot\theta_2$$

$$\frac{\partial L}{\partial \theta_1} = 0$$

$$\frac{\partial L}{\partial \dot\theta_2} = m_2 l_{2c}^2(\dot\theta_1 + \dot\theta_2) + m_2 l_1 l_{2c}\dot\theta_1 c_2 + I_2(\dot\theta_1 + \dot\theta_2) + m_0 l_2^2(\dot\theta_1 + \dot\theta_2) + m_0 l_1 l_2 \dot\theta_1 c_2$$

$$\frac{\partial}{\partial t}\frac{\partial L}{\partial \dot\theta_2} = (m_2 l_{2c}^2 + m_2 l_1 l_{2c} c_2 + I_2 + m_0 l_2^2 + m_0 l_1 l_2 c_2)\ddot\theta_1$$

$$+ (m_2 l_{2c}^2 + I_2 + m_0 l_2^2)\ddot\theta_2 - (m_2 l_1 l_2 + m_0 l_1 l_2)\dot\theta_1\dot\theta_2 s$$

$$\frac{\partial L}{\partial \theta_2} = -[m_2 l_1 l_{2c}(\dot\theta_1^2 + \dot\theta_1\dot\theta_2) + m_0 l_1 l_2(\dot\theta_1^2 + \dot\theta_1\dot\theta_2)]s_2$$

Using the above equations, it is possible to determine expressions for joint motor torques:

$$T_1 = \frac{\partial}{\partial t}\frac{\partial L}{\partial \dot\theta_1} - \frac{\partial L}{\partial \theta_1}$$

$$T_2 = \frac{\partial}{\partial t}\frac{\partial L}{\partial \dot\theta_2} - \frac{\partial L}{\partial \theta_2}$$

Note: These equations do not take the force Fe into account. The appropriate expressions can be added to the above torque equations.

The torque equations can be rewritten as:

$$T_1 = D_{11}\ddot\theta_1 + D_{12}\ddot\theta_2 + D_{111}\dot\theta_1^2 + D_{122}\dot\theta_2^2 + D_{112}\dot\theta_1\dot\theta_2 + D_{121}\dot\theta_1\dot\theta_2 + D_1$$

$$T_2 = D_{11}\ddot\theta_1 + D_{22}\ddot\theta_2 + D_{211}\dot\theta_1^2 + D_{222}\dot\theta_2^2 + D_{211}\dot\theta_1\dot\theta_2 + D_{221}\dot\theta_1\dot\theta_2 + D_2$$

Dii is the "effector inertia" of link i, since angular acceleration $\ddot\theta_i$ at the proximal joint i causes torque $D_{ii}\ddot\theta_i$. A coefficient of the form Dij is the

"coupling inertia", since acceleration at joint j on i causes torque $D_{ij}\ddot{\theta}_j$ or $D_{ji}\ddot{\theta}_i$ at joint i or j respectively. A term of form $D_{ijj}\dot{\theta}_j$ or $D_{iii}\dot{\theta}_i$ is the "centripetal force" acting at joint i due to rotation at joint j and i respectively.

# Appendix A2.3 Telerobotic Manipulator Arm (TMA) Appendix

## A2.3.1 Materials Selection

Materials for the TMA were selected based on the following criteria: stiffness, strength, density (weight), thermal expansion, thermal conductivity, and corrosive resistance.

Beryllium was eliminated due to its toxic nature. This material would have been unsafe to use in conjunction with the Manned Manipulation System (MMS).

Magnesium was also eliminated due to its susceptibility to corrosion. Many of the fluids the TMA will be transferring to satellites will be of a very corrosive nature. The other materials listed in Table A2.2.a were all considered as materials for the TMA.

Graphite/Epoxy was chosen as the link material due to its large strength to density ratio. Another factor was that it has one of the higher Young's Modulus (E) values, which lends to a good stiffness (EI) for the link. A resistance to corrosion is a factor due to the corrosive fluids (hydrazine) that will be transferred to satellites. This composite also has no thermal conductivity and a very small negative thermal expansion coefficient. No thermal conductivity means that less insulation will be needed. The minimal thermal expansion coupled with a low equilibrium temperature will avert any material expansion problems.

| Material | Ult. tensile strength(x e6 N/sq. m) | Density (x e3 kg/ cub.m) | Specific(E/rho) stiffness(x e3 N•m/kg) | Thermal Expansion (x e6)/K | Equilibrium Temperature ( K ) |
|---|---|---|---|---|---|
| Aluminum 7075-T6 | 523 | 2.8 | 25.4 | 28.9 | 700 |
| Beryllium | 620 | 1.85 | 158.4 | 11.5 | N/A |
| Boron/epoxy | 1337 | 2.01 | 102.9 | 4.2 | 300 |
| Graphite/ epoxy | 1337 | 1.49 | 101.7 | -0.36 | 300 |
| Magnesium | 221 | 1.77 | 25.3 | 25.2 | N/A |
| Steel Ph15-7 MO | 1309 | 7.6 | 26.3 | 11 | 500 |
| Titanium | 1034 | 4.43 | 24.9 | 8.8 | 450 |

Table A2.3.a. Properties of Spacecraft Materials

The next material selection was for the arm joints. The critical factor in this choice was thermal expansion compatibility with the Graphite/Epoxy. Titanium was selected mainly because it has a small coefficient of thermal expansion (see Table A2.3.a above). This will allow the links and joints to be designed with minimum tolerances for material expansion. If expansion is not allowed for, then the temperature gradients the arm will experience could cause the mechanics of the arm to bind. Titanium also has a very large strength to density ratio for robustness.

## A2.3.2 TMA Mechanical Drive Analysis

In designing the TMA two drive methods were explored, geared drive and direct drive. Direct drive consist of motors using no gears to drive the arm. This results in a much larger torque being required from the motors, resulting in more massive motors and larger housing for the motors. Geared drive on the other hand uses gears to multiply its supplied torque and gives a considerable mass savings over direct drive (see Figure A2.3.a).

To estimate the mass of the TMA and its components a computer program was formed from a manipulator scaling model (Lecture 2/18/93. Dr. R. Howard). The model allows the calculation of total manipulator mass given the desired payload mass, tip acceleration, link length, and an estimated mass of the outer-most link.

Another input parameter that was necessary was the transmission ratio of the gear system; this parameter was set at a ratio of 500:1. The model consisted of a 3 link arm with one degree of freedom at each joint. An adaptation of the 2 link Shuttle RMS to this model was illustrated in Dr. Howard's lecture. A similar adaptation was done for the 2 link TMA. The computer programs containing the models for both direct drive and geared drive are listed at the end of this appendix section in Tables A2.3.c and A2.3.d.

The first analysis done with this program was to compare the model for geared drive to that for direct drive. The graph of total arm mass vs. tip acceleration (Fig. A2.3.a) shows the mass savings gained by using a geared drive system.
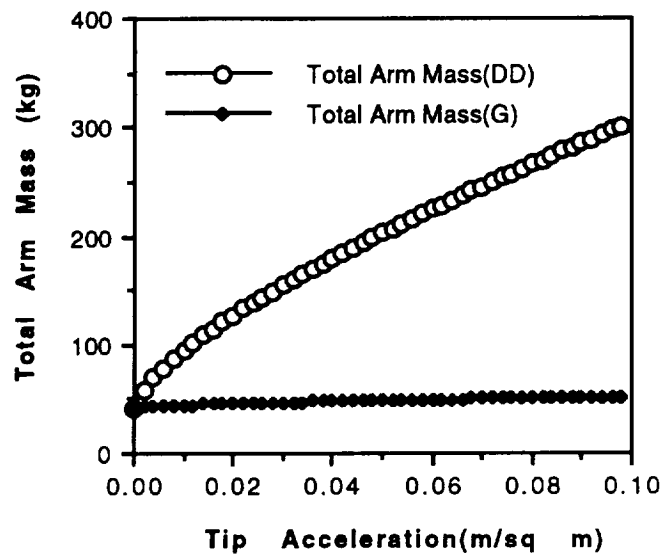
**Figure A2.3.a** Drive Mechanism Comparison

It is readily apparent that constructing the TMA using a geared drive mechanism was the best way to work toward meeting the total arm mass requirement of 50 kg.

## A2.3.3 Application of Manipulator Arm Model

The first analysis done with the manipulator arm model was to set 3 of the independent parameters (payload mass, tip acceleration, link length), and to explore the relationship between total arm mass and outer link mass. This analysis would give us an estimate of outer link mass related to keeping the total arm mass below 50 kg. The results shown in Figure A2-2 are based on a the following set independent parameters: payload mass = 425 kg, tip acceleration = .05 m/s/s, and link length = 1.33 m. The trade-off between total arm mass and outer link mass shows that to keep the total arm mass below 50 kg, the outer link mass will have to be approximately 3 kg or less.
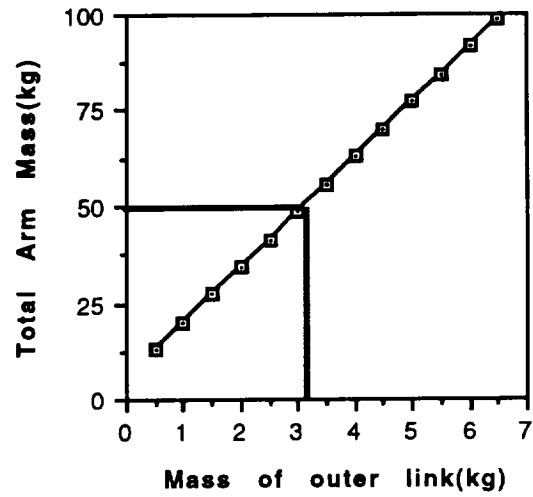
**Figure A2.3.b**   Results of Total Arm Mass vs. Outer Link Mass Trade-off

The next step taken with the arm model was to determine the optimum tip acceleration. To determine this quantity the total arm mass was plotted against tip acceleration, seen in Figure A2.3.c. The initial tip acceleration used in the last
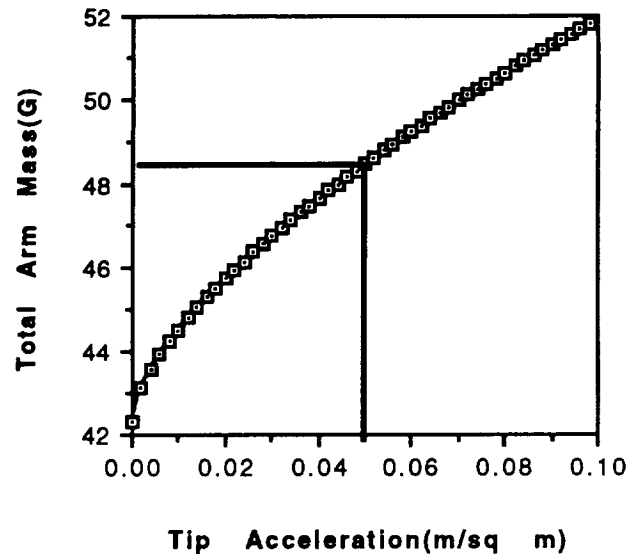
**Figure A2.3.c** Results of Total Arm Mass vs. Tip Acceleration Trade-off

step (0.05 m/s/s) is located in the optimum range just below 50 kg total arm mass.

## A2.3.4  Structural Analysis of Link 2

The next step in the arm design was to determine the radius of link 2 (outer link). Factors affecting this parameter were: link skin thickness, longitudinal stress, tip deflection, and space available inside link. The decision on what skin thickness to use was also dependent on longitudinal stress and tip deflection, evident in Figures A2.3.c, A2.3.d, and A2.3.e, as well as on buckling strength of the link. The goal is to minimize skin thickness, as this in turn minimizes mass as well as maximizes space in the link due to an increase in link diameter for the same amount of mass. The link radius should be as large as possible to increase the moment of inertia (I), and thus have maximum stiffness (EI). A range of link radii from 0.05 m to 0.09 m was considered as a range with appropriate inner link space. A final choice of link radius = .07 m and skin thickness = .002 m was made after iterating the analysis. This analysis included link 2 mass vs. link 2 radius, shown in Figure 2.3.c, which considered several skin thicknesses. It is
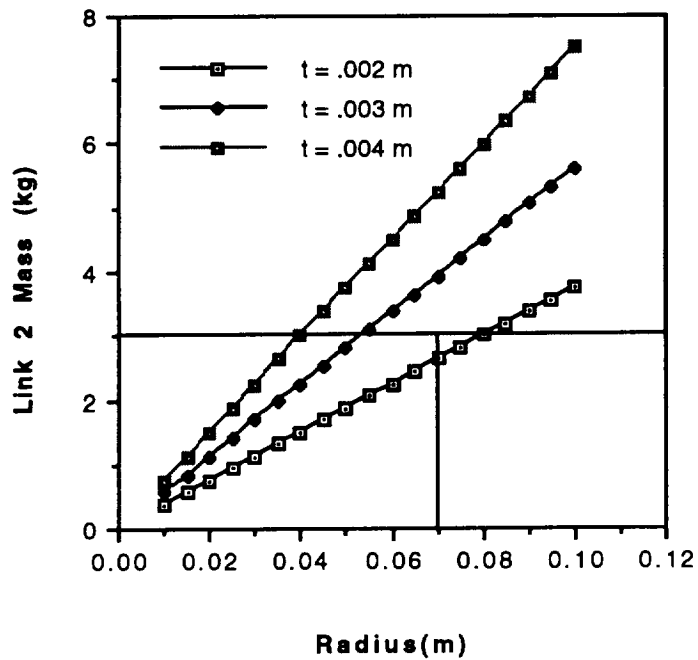
**Figure A2.3.d** Results of Link 2 Mass vs. Link 2 Radius Trade-off

evident from this graph that link 2 mass decreases as skin thickness decreases and link 2 mass increases as the radius increases. The analysis of longitudinal stress vs. link 2 radius, illustrated in Figure A2.4.d, showed that our radius and
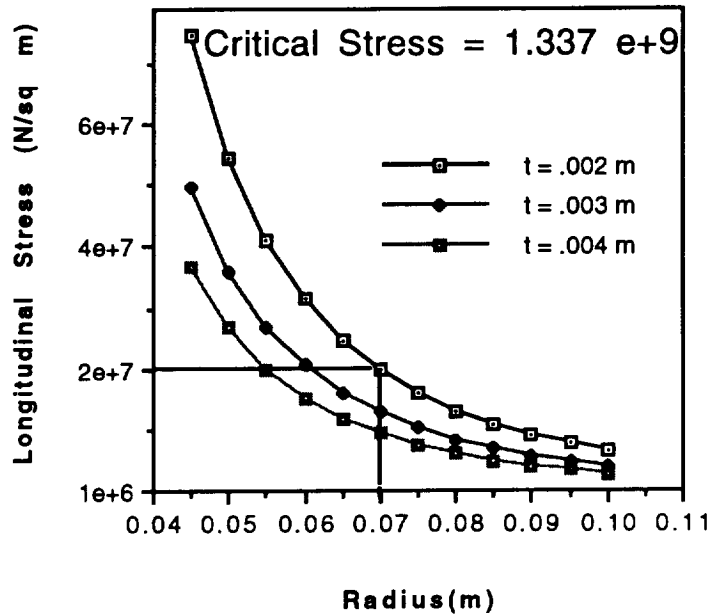
**Figure A2.3.e** Results of Longitudinal Stress vs. Link 2 Radius Analysis

skin thickness were easily within safe stress levels; having a factor of safety of more than 10. The next factor considered in our link radius decision was the tip deflection of link 2 in relation to link 2 radius. The analysis is shown in Figure A2.3.e, where we can see that the
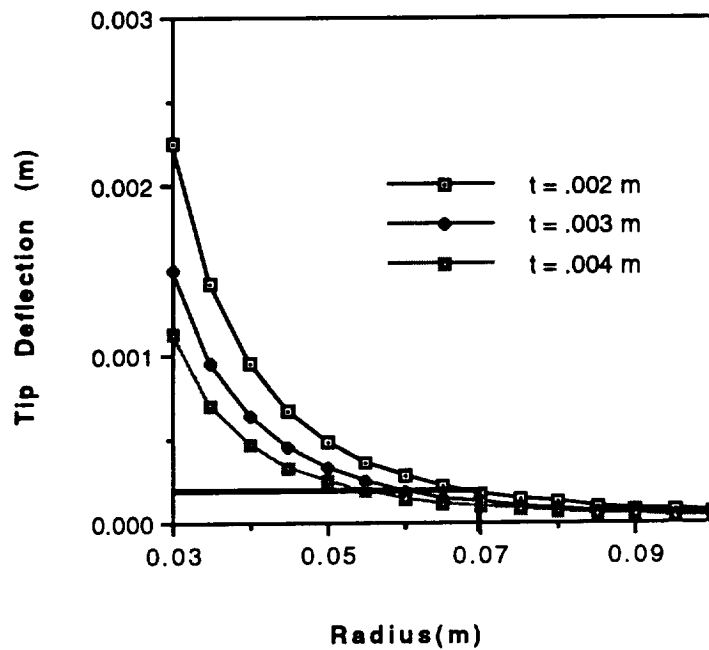
**Figure A2.3.f** Results of Tip Deflection vs. Link Radius Trade-off

tip deflection will be less than 0.0005 m for a radius of 0.07 m. A tip deflection of 0.0005 m is well within acceptable limits.
The equations and the basic parameters used in the above structural analysis are listed in the following paragraph.

Manipulator Link Structural Analysis

Graphite/Epoxy
   $E = 151 \times e9$
   Ultimate Tensile Strength = sigma cr. = $1337 \times e6$ N/m sq.
   Density = rho = 1490 kg/cu. m

   Mass payload = Mpay = 425 kg
      mass of largest ORU + 3 dof wrist + end effector
   Tip accel. = Ay = .05 m/s sq.
   Length of link = L = 2
   Angular accel. = wdot = Ay/2 = .025 rad/s sq.
   Max Angular velocity = 1 rad/sec
   Angular velocity = w = wdot • time = .025 • 40 = 1 rad/sec
   Radial accel. = Ax = $w^2$ • L = 2 m/s sq.
   Moment about z-axis = Mz = Mpay•Ay•L = 42.5 N•m

Axial Load = Px = Mpay • Ax = 850 N

Model: circular thin wall beam
      r = radius of beam
      t = thickness of beam wall

      Moment of Inertia = I = pi • R^3 • t

      Tensile Stress = P/A + M•y / I

      Deflection = d = L^3 • (.333 • Mpay) / (E • I)

The last factor checked was the danger of the link buckling. The following is the list of equations and the order of their analysis to determine the maximum compressive load the link can take.

Buckling Analysis
      R = radius of link = .07 m
      t = thickness of link wall = .002 m
      ø = geometric parameter = 1/16 * sqrt(R/t) = 0.370
      gam = reduction factor = 1.0 - 0.901 * (1.0 - e(-ø)) = 0.722
      E = Young's Modulus = 151 x e9 N/m sq.
      Critical Stress = sigcr = 0.6 * gam * E *t / R = 1.86 x e9 N/m sq.
      Cross Sectional Area = A = 0.000879
      Critical Load = Pcr = A * sigcr = 1,641,677 N (ultimate)

The critical load of 1.641 x e6 N is well above any expected compressive loads that act on link 2 of the arm.

So the parameters that result are:
                Link 2 radius =     0.07 m
                Link 2 skin thick. =     0.002 m

## A2.3.5 Link 1 Sizing

The sizing of link 1 of the TMA was done by matching the stiffnesses of links 1 and 2. The basic process that this was done by was to increase the skin thickness by a large amount (to approx. 0.01m ) and to set the radius of the link at about 0.08 m. Then iteration was done with the equations presented in the structural analysis of link 2 until the tip deflection was similar to that for link 2.
The parameters that resulted for link 1 are:
                Link 1 radius =     0.08 m
                Link 1 skin thick. =     0.01 m

## A2.3.6 Manipulator Arm Model

The model that was used to estimate the parameters of the TMA is given in Tables A.2.3.c and A2.3.d. There is a model for direct drive system (A2.3.b) as well as for a geared drive system (A2.3.c). The two model have been formulated in the C computer language. The programs give the estimated masses of arm links, motor masses, and gearbox masses for the geared case. Torques to be supplied by the motors are computed as well. A sample output of the geared manipulator model is given in Table A2.3.2 below.

```
Total arm mass is  50.715729  kg
  Motor 1 mass is  1.525671  kg
  Motor 2 mass is  1.145030  kg
  Motor 3 mass is  0.706037  kg
   Link 1 mass is  27.316391  kg
   Link 2 mass is  12.042868  kg
   Link 3 mass is  3.000000  kg
Gearbox 1 mass is  2.170088  kg
Gearbox 2 mass is  1.694247  kg
Gearbox 3 mass is  1.115397  kg
   Torque M3 is  0.113316  kg
   Torque M2 is  0.227441  kg
```

**Table A2.3.b** Sample output from Geared Drive Manipulator Model

```c
/* this program calculates the parameters for a direct drive robotic arm using four independent
input variables. These input variables are the link length, mass of arm payload, tip
acceleration, and the mass of the outer-most link. The program calculates the other link
masses, and the motor masses. */
#include <math.h>
#include <stdio.h>

main ()

{
        float L, Mpay, A, Ml3, Ml2, Ml1, K, wdot1, wdot2, wdot3, N1, N2,N3;
        float Tm1, Tm2, Tm3, M1, M2, M3, T1, T2, T3, Mtot;
        float Aa, Ba, Am, Bm, Ag, Bg, expo1, expo2;

        FILE *datafile_ptr;

        /* Given input parameters */

        L    = 1.33;
        Mpay = 425;
        A    = .05;
        Ml3  = 3;

        /* Direct drive motor parameters */

        Aa   = .000111;
        Ba   = 1.33;
        Am   = 3.2;
```

```
Bm  = .694;
Ag  = .15;
Bg  = .6;

expo1 = (1-Ba) / (2-Ba);
expo2 = 1 / (2-Ba);

datafile_ptr = fopen("launch.dat","w");
fprintf(datafile_ptr,"\ntime of transfer\t\n");

K    = Mpay / Ml3 +.333;

wdot1 = A / (3 * L);
wdot2 = A / (2 * L);
wdot3 = A / L;

/*  Values for LINK 3
    ---------------------   */

T3   = A * L * K * Ml3;

M3   = Am * pow(T3, Bm);

Ml2  = Ml3/Mpay *(4*Mpay + 7/3 * Ml3 + M3);

/*  Values for LINK 2
    ---------------------   */

T2   = .5 * A * L * K * Ml2;

M2   = Am * pow(T2, Bm);

Ml1  = Ml3/Mpay *(9*Mpay + 19/3*Ml3 + 7/3*Ml2 + 4 * M3 + M2);

/*  Values for LINK 1
    --------------------   */

T1   = .333 * A * L * K * Ml1;

M1   = Am * pow(T1, Bm);

/*  Total all component masses to get Mtot
    --------------------------------------   */

Mtot = M1 + M2 + M3 + Ml1 + Ml2 + Ml3;

         fprintf(datafile_ptr,"%f\n",Mtot);

                   printf ("total arm mass is  %f  kg \n", Mtot);
                   printf ("Motor 1 mass is  %f  kg \n", M1);
                   printf ("Motor 2 mass is  %f  kg \n", M2);
                   printf ("Motor 3 mass is  %f  kg \n", M3);
                   printf ("Link 1 mass is  %f  kg \n", Ml1);
                   printf ("Link 2 mass is  %f  kg \n", Ml2);
```

```c
        printf ("Link  3 mass is  %f  kg \n", Ml3);
        printf ("Gearbox 1 mass is  %f  kg \n", Mg1);
        printf ("Gearbox 2 mass is  %f  kg \n", Mg2);
        printf ("Gearbox 3 mass is  %f  kg \n", Mg3);
        printf ("torque M3 is  %f  kg \n", Tm3);
        printf ("Torque M2 is  %f  kg \n", Tm2);


    fclose( datafile_ptr );


    }
```

**Table A2.3.c** Computer Program Modeling a Geared Drive Manipulator

```c
/* this program calculates calculates the parameters for a geared robotic arm using  four
independent input variables. These input variables are the link length, mass of arm payload,
tip acceleration, and the mass of the outer-most link. The program calculates the other link
masses, the motor masses, and the gearbox masses. */
#include <math.h>
#include <stdio.h>


main ()


    {
        float L, Mpay, A, Ml3, Ml2, Ml1, K, wdot1, wdot2, wdot3, N1, N2,N3;
        float Tm1, Tm2, Tm3, M1, M2, M3, T1, T2, T3, Mg1, Mg2, Mg3;
        float Aa, Ba, Am, Bm, Ag, Bg, expo1, expo2,Mtot;


        FILE *datafile_ptr;


        /* Given input parameters */


        L   = 1.33;
        Mpay = 425;
        A   = .05;
        Ml3 = 3;


        /* Geared drive motor parameters */


        Aa   = .000111;
        Ba   = 1.33;
        Am   = 3.2;
        Bm   = .694;
        Ag   = .15;
        Bg   = .6;


        /* Transmission Ratios */


        N1   = 500;
        N2   = 500;
        N3   = 500;


        expo1 = (1-Ba) / (2-Ba);
        expo2 = 1 / (2-Ba);
```

```c
datafile_ptr = fopen("launch.dat","w");
fprintf(datafile_ptr,"\ntime of transfer\t\n");

K    = Mpay / Ml3 +.333;

wdot1 = A / (3 * L);
wdot2 = A / (2 * L);
wdot3 = A / L;

/* Values for LINK 3
-------------------- */

wdot1   = pow(2*A*L*K*Ml3,expo1) * pow(L/(2*A*Aa), expo2);

Tm3  = 2 * A * L * K * Ml3 / N3;

M3   = Am * pow(Tm3, Bm);

T3   = A * L * K * Ml3;

Mg3  = Ag * pow(T3, Bg);

Ml2  = Ml3/Mpay *(4*Mpay + 7/3 * Ml3 +.04 * (M3 + Mg3));

/* Values for LINK 2
-------------------- */

wdot1   = pow(A*L*K*Ml2, expo1) * pow(L/(A*Aa), expo2);

Tm2  = A * L * K * Ml2 / N2;

M2   = Am * pow(Tm2, Bm);

T2   = .5 * A * L * K * Ml2;

Mg2  = Ag * pow(T2, Bg);

Ml1  = Ml3/Mpay *(9*Mpay + 19/3*Ml3 + 7/3*Ml2 +1.44 *(M3 +
       Mg3)+.04*(M2 + Mg2));

/* Values for LINK 1
-------------------- */

wdot1   = pow(2*A*L*K*Ml1 / 3, expo1) * pow(3 * L/(2*A*Aa),
    expo2);

Tm1  = 2 * A * L * K * Ml1 / (3 * N1);

M1   = Am * pow(Tm1, Bm);

T1   = .333 * A * L * K * Ml1;

Mg1  = Ag * pow(T1, Bg);
```

```
/*  Total all component masses to get Mtot
    ---------------------------------------  */

Mtot  = M1 + M2 + M3 + Mg1 + Mg2 + Mg3 + Ml1 + Ml2 + Ml3;

        fprintf(datafile_ptr,"%f\n",Mtot);


                printf ("total arm mass is  %f  kg \n", Mtot);
                printf ("Motor 1 mass is  %f  kg \n", M1);
                printf ("Motor 2 mass is  %f  kg \n", M2);
                printf ("Motor 3 mass is  %f  kg \n", M3);
                printf ("Link  1 mass is  %f  kg \n", Ml1);
                printf ("Link  2 mass is  %f  kg \n", Ml2);
                printf ("Link  3 mass is  %f  kg \n", Ml3);
                printf ("Gearbox 1 mass is  %f  kg \n", Mg1);
                printf ("Gearbox 2 mass is  %f  kg \n", Mg2);
                printf ("Gearbox 3 mass is  %f  kg \n", Mg3);
                printf ("torque M3 is  %f  kg \n", Tm3);
                printf ("Torque M2 is  %f  kg \n", Tm2);

    fclose( datafile_ptr );

    }
```

**Table A2.3.d**     Computer Program Modeling Direct Drive Manipulator

# Appendix A2.4 Simulation Code

## A2.4.1 Power Transmission

```
/******************************************************************/
/*      Program:              TransRatioTS                        */
/*      File Name:            TransRatioTS2.c                      */
/*      Author:               Rommel                              */
/*      Creation Date:        4.26.93                             */
/*      Last Modification:    4.27.93                             */
/*                                                                */
/*      Modules:                                                  */
/*                                                                */
/*      Notes: TransRatioTS is a trade study to compare masses of direct-drive */
/*                     arms versus geared arms.                   */
/*                                                                */
/*                     This program builds upon TransRatioTS1.c.  It writes the */
/*                     calculated values out to *.out files, and does iterative */
/*                     calculations.                              */
/*                                                                */
/*                     This program iterates arm mass values based upon varying */
/*                     tip accelerations.                         */
/******************************************************************/

#include <stdio.h>
#include <math.h>

#define LINKLGTH_FILE_NAME "LinkLength.out"
#define ACCTIP_FILE_NAME "AccTip.out"
#define AMASSDD_FILE_NAME "ArmMassDD.out"
#define AMASSG_FILE_NAME "ArmMassG.out"
#define PARAM_FILE_NAME "ArmParam.out"

main ()
{
        FILE    *out_file1;        /* Output file number one.         */
        FILE    *out_file2;
        FILE    *out_file3;
        FILE    *out_file4;
        FILE    *out_file5;

        float   aA,aG,aM;          /* Some inertial scaling parameters. */

        float   acctip;            /* Accel. at end-effector.         */
        float   bA,bG,bM;          /* More inertial scaling parameters. */
        float   k;                 /* Some sort of constant.          */
        float   ln;                /* Length of links.                */
        float   maxacc,minacc;     /* Tip acceleration maximum and minimum
                                         value.                      */
        float   accinc;            /* Tip acceleration increment.     */
        float   mG1,mG2,mG3;       /* Mass of gear boxes for motors 1, 2, & 3 */
        float   mL1,mL2,mL3;       /* Mass of links 1, 2, & 3 (direct-drive). */
        float   mL1g,mL2g,mL3g;    /* Mass of links 1, 2, & 3 (geared). */
```

```c
float    mM1,mM2,mM3;        /* Mass of motor one (direct-drive).           */
float    mM1g,mM2g,mM3g;     /* Mass of motor one (geared).                 */
float    mTot, mTotg;        /* Mass of whole arm (direct-drive and geared)*/
float    massPL;             /* Mass of payload (kg).                       */
float    n1,n2,n3;           /* Gear ratios for motors 1, 2, & 3 (geared).  */
float    tm1,tm2,tm3;        /* Torques of motors 1, 2, & 3 (direct-drive). */
float    tm1g,tm2g,tm3g;     /* Torques of motors 1, 2, & 3 (geared).       */

int         accval;          /*     Counter value to increment tip accel.   */

out_file1 = fopen(LINKLGTH_FILE_NAME, "w");
out_file2 = fopen(ACCTIP_FILE_NAME, "w");
out_file3 = fopen(AMASSDD_FILE_NAME, "w");
out_file4 = fopen(AMASSG_FILE_NAME, "w");
out_file5 = fopen(PARAM_FILE_NAME, "w");

ln        = 4;
massPL = 4000;
acctip   = 0.0;
mL3      = 10;
mL3g     = 10;
aA       = 0.000111;
bA       = 1.33;
aM       = 3.2;
bM       = 0.694;
aG       = 0.15;
bG       = 0.6;
n1       = 5000;
n2       = 5000;
n3       = 5000;

minacc = 0.0;
maxacc = 0.10;
accinc  = 0.002;

//      Calculate the values for the constant, k.

k = massPL/mL3 + 1/3;

fprintf (out_file5, "Length of each link %f.\n", ln);
fprintf (out_file5, "Mass of payload %f.\n", massPL);
fprintf (out_file5, "Mass of link 3 %f.\n", mL3);
fprintf (out_file5, "Gear ratio for motor 1 %f.\n", n1);
fprintf (out_file5, "Gear ratio for motor 2 %f.\n", n2);
fprintf (out_file5, "Gear ratio for motor 3 %f.\n", n3);
fprintf (out_file5, "Minimum tip acceleration %f.\n",minacc);
fprintf (out_file5, "Maximum tip acceleration %f.\n",maxacc);
fprintf (out_file5, "Acceleration increment %f.\n",accinc);

fprintf (out_file2, "Mass of payload %f.\n", massPL);
fprintf (out_file2, "Mass of link 3 %f.\n", mL3);

fprintf (out_file3, "Mass of payload %f.\n", massPL);
fprintf (out_file3, "Mass of link 3 %f.\n", mL3);
```

```c
fprintf (out_file4, "Mass of payload %f.\n", massPL);
fprintf (out_file4, "Mass of link 3 %f.\n", mL3);

for (accval = minacc; accval <= maxacc/accinc; accval++)
{
        //  Do the calculations for a direct-drive arm first.

        //  Calculate the required torque for motor 3...

        tm3 = acctip * ln * k * mL3;

        //  Calculate the mass for motor 3...

        mM3 = aM * pow(tm3,bM);

        //  Calculate the mass of link 2...

        mL2 = mL3/massPL * (4*massPL + 7/3*mL3 + mM3);

        //      Calculate the required torque for motor 2...

        tm2 = acctip * ln * k * mL2 / 2;

        //      Calculate the mass for motor 2...

        mM2 = aM * pow(tm2,bM);

        //      Calculate the mass for link 1...

        mL1 = mL3/massPL * (9*massPL + 19/3*mL3 + 7/3*mL2 + 4*mM3 + mM2);

        //  Calculate the required torque for motor 1...

        tm1 = acctip * ln * k * mL1 / 3;

        //      Calculate the mass for motor 1...

        mM1 = aM * pow(tm1,bM);

        //  Calculate the total mass for the direct-drive arm...

        mTot = mM1 + mL1 + mM2 + mL2 + mM3 + mL3;

        //  Now, calculate the equivalent for the geared arm.

        //  Calculate the torque that motor 3 must supply...

        tm3g = 2 * tm3 / n3;

        //      Calculate the mass of motor 3...

        mM3g = aM * pow(tm3g,bM);
```

```
//      Calculate the mass of motor 3 gear box...

mG3 = aG * pow(tm3,bG);

// Calculate the mass of link 2...

mL2g = (mL3g / massPL) * (4*massPL + 7/3*mL3g + 0.04*(mM3g+mG3));

// Calculate the torque that motor 2 must supply...

tm2g = tm2 / n2;

//      Calculate the mass of motor 2...

mM2g = aM * pow(tm2g,bM);

//      Calculate the mass of motor 2 gear box...

mG2 = aG * pow(tm2,bG);

//      Calculate the mass of link 1...

mL1g = (mL3g/massPL) * (9*massPL + 19/3*mL3g + 7/3*mL2g +
               1.44*(mM3g+mG3) + 0.04*(mM2g+mG2));

// Calculate the torque that motor 1 must supply...

tm1g = 2 * tm1 / 3 / n1;

//      Calculate the mass of motor 1...

mM1g = aM * pow(tm1g,bM);

//      Calculate the mass of motor 1 gear box...

mG1 = aG * pow(tm3,bG);

//      Calculate the total mass for the geared arm...

mTotg = mL1g + mM1g + mG1 + mL2g + mM1g + mG2 + mL3g + mM3g + mG3;

//      Print the results to file...

fprintf (out_file2, "%f\n", acctip);

fprintf (out_file3, "%f\n", mTot);

fprintf (out_file4, "%f\n", mTotg);

// Increment acctip to the next value...

acctip = acctip + accinc;
```

```
        }        /* end for       */


        fclose(out_file1);
        fclose(out_file2);
        fclose(out_file3);
        fclose(out_file4);
        fclose(out_file5);


}        /* end main     */
```

## A2.4.2 Joint Motor Torque Requirement

```
/*******************************************************************************/
/*      Program:                StaticTorque1                                  */
/*      File Name:              StaticTorque1.c                                 */
/*      Author:                 Rommel                                         */
/*      Creation Date:          4.16.93                                        */
/*      Last Modification:      4.16.93                                        */
/*                                                                            */
/*      Modules:                                                              */
/*                                                                            */
/*      Notes:                                                                */
/*******************************************************************************/

#include <stdio.h>
#include <math.h>

#define THETA1_FILE_NAME "CalcTheta1.out"
#define THETA2_FILE_NAME "CalcTheta2.out"
#define TORQ1_FILE_NAME "CalcSTorqs1.out"
#define TORQ2_FILE_NAME "CalcSTorqs2.out"

#define      PI      3.14159265359   /* Constant value for pi.              */

float   len1, len2;             /* Lengths of links 1 and 2 (meters).       */
float   theta1, theta2;         /* Angles of links 1 and 2 (degrees).       */
float   forcex, forcey;         /* Forces in x and y direction at end-eff (N). */
float   torq1, torq2;           /* Torques at joints 1 and 2.               */

main ()
{
        FILE    *out_file1;     /* Output file number one.                  */
        FILE    *out_file2;
        FILE    *out_file3;
        FILE    *out_file4;

        float   accx, accy;     /* Accel. at end-effector in x & y direction. */
        float   plmass;         /* Mass of payload (kg).                    */

        int     numang1;        /* Number of angles to calculate for joint 1. */
        int     numang2;        /* Number of angles to calculate for joint 2. */
        int     anginc;         /* Incremental value of angles.             */
```

```c
int     maxang;              /* Maximum angle to be used in calculations.   */
int     minang;              /* Minimum angle to be used in calculations.   */

out_file1 = fopen(THETA1_FILE_NAME, "w");
out_file2 = fopen(THETA2_FILE_NAME, "w");
out_file3 = fopen(TORQ1_FILE_NAME, "w");
out_file4 = fopen(TORQ2_FILE_NAME, "w");


len1    = 2.5;
len2    = 2.5;
plmass  = 6000;
accx    = 1;
accy    = 1;


anginc  = 5;
maxang  = 90;
minang  = 0;


//      Calculate x- and y- forces at end-effector from payload mass and
//  acceleration values.

forcex = plmass * accx;
forcey = plmass * accy;

for (numang1 = minang; numang1 <= maxang/anginc; numang1++)
{
        for (numang2 = minang; numang2 <= maxang/anginc; numang2++)
        {

                //      Convert angles from degrees to radians.

                theta1 = 2*PI * (anginc * (numang1 - 1)) / 360;
                theta2 = 2*PI * (anginc * (numang2 - 1)) / 360;

                // Calculate static torques at joints 1 and 2.

                torq1 = (len1*cos(theta1) + len2*cos(theta1+theta2))*forcey -
                                (len1*sin(theta1) + len2*sin(theta1+theta2))*forcex;
                torq2 = len2*cos(theta1+theta2)*forcey -
                                len2*sin(theta1+theta2)*forcex;


                // Print the calculated values.

                fprintf (out_file1, "%f\n", theta1);
                fprintf (out_file2, "%f\n", theta2);
                fprintf (out_file3, "%f\n", torq1);
                fprintf (out_file4, "%f\n", torq2);

        }       /* end for       */

}       /* end for       */

fclose(out_file1);
```

```
        fclose(out_file2);
        fclose(out_file3);
        fclose(out_file4);

}       /* end main    */
```

# Appendix A2.5  Other Trade Studies

## A2.5.1 Target Satellites

1. Advanced X-Ray Astrophysics Facility (AXAF)
   - 4.5m diameter
   - 15m long
   - 8650 kg
   - LEO
   - 2 solar arrays, 10'x32', on traverse axis
   - 2 antennae, 6' long, on axis perpendicular to arrays.
   - Designed for in-orbit servicing by Shuttle

2. Cosmic Background Explorer (COBE)
   - 13' diameter
   - 18' length
   - 10000 lbs
   - 12 solar arrays form perimeter
   - antennae & propulsion subsystems extend outward

3. X-Ray Timing Explorer (EXP)
   - 4.5m wide
   - 2.5m high
   - 1.5m long
   - 3000 kg
   - altitude = 400 km
   - 2 solar arrays, 7'x8'
   - Mandatory payload changeout every 2 years

4. Gravity Probe-B
   - Conical geometry, 6' diameter to <1' diameter
   - 2900 lbs
   - 4 solar arrays, attached symmetrically. Diameter -> 15'

5. Gamma Ray Observatory (GRO)
   - 4.6 m diameter
   - 7.3 m length
   - 15000 kg
   - altitude = 4450 km
   - 2 solar arrays, 70' tip-to-tip
   - 21' antenna
   - Designed for Shuttle servicing.  Irregular surface.

5. GeoPotential Research Mission (GRM)
   - 1 m diameter
   - 6.4 m length

- 2800 kg
- LEO, altitude=4450 km
- 2 satellites, large fuel consumption to maintain odd orbit.

6. Hubble Space Telescope (HTS)
    - 4.2 m diameter
    - 13.1 m length
    - 11360 kg
    - LEO, altitude = 590 km
    - Designed for Shuttle servicing

7. INTELSAT VI
    - 4.0 m diameter
    - 6.4 m length
    - 2255 kg
    - LEO, altitude = 460 km
    - covered with "solar drums"
    - spin stabilized, 30 to 55 rpm

8. LANDSAT
    - 2.1 m diameter
    - 4.0 m length
    - 2000 kg
    - LEO, altitude = 709km
    - On-board propulsion system can boost the LANDSAT D from a nominal Shuttle orbit to 709 km and back

**A2.5.2. Survey of Satellite Failures** (Shockey 1984)

| Spacecraft Subsystem Anomaly | Number | Percent |
|---|---|---|
| Timing, Control and Command | 55 | 9.1 |
| Telemetry and Data Handling | 112 | 19.1 |
| Power Supply | 56 | 9.2 |
| Attitude Control and Stabilization | 123 | 20.3 |
| Propulsion | 26 | 4.3 |
| Environmental Control | 16 | 2.6 |
| Structure | 6 | 1.0 |
| Payload/Experiment | 208 | 34.3 |
| TOTAL | 602 | 100% |

| Degree of Failure | Number | Percent |
|---|---|---|
| Negligible Effect | 447 | 74.3 |
| Noticeable Effect | 117 | 19.4 |
| 1/3 to 2/3 Loss | 32 | 5.3 |

| | | |
|---|---|---|
| 2/3 to Nearly Total Loss | 5 | 1 |
| Total Mission Loss | 1 | --- |
| TOTAL | 602 | 100% |

## A2.5.3 Typical Mission Parameters

GEO (immediately after circularization maneuver)

delta i = 20.5 degrees
altitude = 42000 km
payload mass = 200 kg
vehicle mass = 7216 kg

LEO

delta i = 0 degrees
altitude = 500 km
payload mass = 400 kg
vehicle mass = 1600 kg

# Appendix A3.1 Carbon Dioxide Removal

The Carbon Dioxide Removal system will be responsible for the removal of odors, trace contaminants in the atmosphere, and $CO_2$. Several types of systems were looked into for the removal of $CO_2$, but the most efficient removal system for a 3 day mission was chemical absorption. No trade studies were done on other removal systems because all sources agreed that other systems were inefficient for a mission duration under two weeks. A trade study was conducted to determine the most efficient chemicals to use to remove $CO_2$ from the atmosphere. The four chemicals that were studied were Lithium Hydroxide (LiOH), Soda Lime, Sodium Hydroxide (NaOH), and Baralyme. Below is a table comparing the efficiency of these four chemicals.

## A3.1.1 Removal Amounts

LiOH        removes 0.614 kg of $CO_2$ per 1 kg of LiOH
Soda Lime   removes 0.241 kg of $CO_2$ per 1 kg of Soda Lime
NaOH        removes 0.37  kg of $CO_2$ per 1 kg of NaOH
Baralyme    removes 0.13  kg of $CO_2$ per 1 kg of Baralyme

## A3.1.2 Amount of Chemical Needed

For a 3 day mission

LiOH        – 24.3 kg
Soda Lime   – 61.2 kg
NaOH        -- over 70 kg because of baking of the chemical
Baralyme    -- 104.4 kg‹

## A3.1.3 Storage Volume

For a 3 day canister

LiOH        needs 46.8 liters
Soda Lime   needs 75.6 liters
NaOH        needs over 110 liters due to baking of the material
Baralyme    needs 108 liters

As can be seen from these figures the most efficient chemical to use is LiOH. Therefore canisters of LiOH will be placed in the system.

# Appendix A3.2 Radiation Environment

The radiation environment of Earth orbit include three major areas: galactic cosmic radiation, trapped particle radiation, and solar particle event radiation.

## A3.2.1 Galactic Cosmic Radiation (Cosmic Rays)

Cosmic rays consist of extremely high energy particles that have traveled trillions of light years to reach Earth. Most particles are of such high energy, that they pass through a human body without doing appreciable damage. However, some cosmic ray radiation is harmful and should be shielded against, but this radiation is only damaging when accumulated, and is not dangerous in a single dose. 5-10% of effective radiation doses in all Earth orbits are due to cosmic rays.

## A.3.2.2 Trapped Particle Radiation (Van Allen Belts)

The Van Allen belts consist of trapped proton and electron particles caught in the Earth's magnetic field. These particles form an inner belt reaching 2.8 Earth radii (17,500km) and an outer belt stretching to 12 Earth radii (75,000km). The inner belt is made up of Mev protons and kev electrons. The outer belt only contains charged electrons. The largest radiation doses are received between 1,000 to 10,000km altitude, especially around the South American Anomaly. The belts only concentrate around the central orbits of the Earth, and do not exist in any intensity at polar orbits.

## A3.2.3 Solar Particle Events (Solar Flares)

Solar flares are composed of proton, helium, and some heavier ions. They are the most unsteady form of Earth orbit radiation, varying with the sun's eleven year cycle. The largest solar flares can deliver more than 10,000 rem in 24 hours. It is because of this massive dosage that solar flares are usually the limiting factor in determining radiation shielding. With 3 $gm/cm^2$, two large flares delivered the following doses:
October 1989- 73.29 rem
August 1972- 113.5 rem

## A3.2.4 Radiation Dosage

The standard unit of measuring radiation damage in humans is the rem. The rem is equivalent to the dose (usually measured in rads) multiplied by the RBE coefficient (relative biological effectiveness). The RBE accounts for the varying degrees of damage inflicted by different forms of radiation.

When considering the acceptable dosage limits for an astronaut, these factors should be studied. One, the dose should not affect the astronaut's immediate

health and performance to insure the astronaut can carry out his mission properly and return safely to base. Two, the dose should not exceed cumulative limits to avoid latent cancer threats. The probability of cancer death in astronauts must be comparable to Earth occupations. Additionally, genetic damage to the reproductive organs must be kept to a minimum.

## A3.2.5 Health Effects

For a single emergency radiation dose, here are some probable effects:

| Dose(rem) | Probable effect |
|---|---|
| 0-50 | No obvious effects, possible blood changes |
| 50-100 | Radiation sickness in 5-10% of people, no serious disability |
| 100-150 | Radiation sickness in 25% of people |
| 150-200 | Radiation sickness in 50% of people, no immediate deaths |
| 200-350 | Radiation sickness in nearly all people, 20% death rate |

**Table A3.2.a** Radiation Affects

## A3.2.6 NASA Dose Limits

| Exposure Time | Dosage for Vital Organ (rem) |
|---|---|
| Career | 100-400* |
| Annual | 50 |
| 30 Days | 25 |

*Varies with age and gender, based on the following equations:

male=200rem + 7.5rem(age of astronaut - 30)

female=200rem +7.5rem(age of astronaut - 38)

## A3.2.7 Radiation Dosage for Three Missions

Assuming the recommended thickness of 1 cm aluminum shielding, here is the average radiation hazards expected at low orbit inclination, polar orbit, and geostationary orbit.

### A3.2.7.1 Low Orbit Inclination (Space Station Orbit)

This orbit includes regions between the altitudes 200-500 km, and an inclination up to 28.5 degrees. In this region, the majority of radiation comes from trapped protons from the Van Allen belts. The total daily dose is approximately .11rem including trapped proton radiation and galactic cosmic

radiation. The Earth's geomagnetic field effectively shields most solar particle events,so the dosage does not reach significant levels.

## A.3.2.7.2 High Orbit Inclination (Polar Orbit)

Including regions from 450-1000 km, this region stretches from 85-90 degrees orbit inclination. Since the Earth' s magnetic field is not very strong here, the dosage received from trapped particles is much less significant. However, because of the weak magnetic field, solar flares and cosmic rays can cause much more significant radiation doses in humans. For large solar flares the dosage will reach 30-50 rem. The average daily dose including trapped protons and cosmic rays amounts to about .082 rem.

## A3.2.7.3 Mission to Geostationary Earth Orbit (GEO)

The approximate altitude of the satellite belt MOOSE will be servicing is around 36,000 km. The majority of the daily radiation at this altitude will be from trapped electrons and cosmic rays. Additionally, the radiation incurred in traveling through the Van Allen belts must be figured in. For a two day mission, the average total dose including all these factors can be from 4 to 8 rem. However, the most serious radiation threat at GEO is the random large solar flare. The largest flares can deliver between 130-200 rem at the shielding recommended without considering evasive maneuvers.

# Appendix A3.3 Smoke Detector Trade Study

In considering a smoke detector for the MOOSE, special needs must be addressed due to the small size of the craft. In the MOOSE, open fires or a rapid rise in heat will almost instantly be detected by the astronaut in his shirt sleeve surroundings. Also, temperature and humidity will probably fluctuate to some extent because the vehicle is not a large craft, therefore a smoke detector must be relatively insensitive to these changes to avoid excessive false alarms. Also, the largest fire threat aboard MOOSE will be smoldering fires, because these cannot be readily detected by human sense. Finally, cost, size, and ease of installation should be considered on a cost conscious project like MOOSE.

| Type of Detector | Characteristics |
|---|---|
| Thermal | Uses a heat expansion metal sensor that closes a contact when the sensor is heated, setting off the alarm. This device will not detect a smoldering fire that does not put out a lot of heat. |
| Ionization | Has an internal fan to blow air particles to detector. A small amount of radioactive material in the device ionizes the air and the level of conductive of the air is then measured. Smoke particles lower the conductance of air and set off the alarm. However, other airborne particles can also lower conductance such as dust particles, halon, etc. This device can also be set off by electrical equipment, humidity and temperature changes, and radiation exposure that changes the conductance of the air. |
| Photoelectric | Uses light sources and photodetectors to measure the light scattering and obscuration levels in the air. When smoke particles affect these levels enough, the alarm is set off. Because this device uses light detection, it is insensitive to other environmental changes. This device can be made very sensitive to smoldering fires. |

# Appendix A3.4 Fire Extinguisher Trade Study

A fire extinguisher aboard the MOOSE must be small, light, and easily used. It should put out the fire immediately, and not allow it to rekindle later. The extinguishing agent should be relatively safe to the astronaut, or a system should be in place so as to avoid prolonged exposure to a toxic extinguishing agent. Additionally, the agent should not damage sensitive electrical equipment while still being effective in extinguishing chemical fires.

| Substance | Amount Needed | Characteristics |
|---|---|---|
| Water | 3-5 kg | Quickly extinguishes flame, but is not only ineffective in extinguishing chemical and electrical fires, but also damaging to electrical equipment. Mass necessary to extinguish fires is larger than other agents |
| Carbon Dioxide | 3.75 kg | Non-conductive, so effectively smothers electrical and chemical fires. Does not leave a residue, so it will not damage equipment. However, after $CO_2$ dissipates, flame may reignite because the agent does not cool a fire effectively. Also prevents oxygen from reaching lungs in addition to smothering flames. Produces a thick white fog during use that may obscure vision |
| Halon 1301 | 1.13 kg | Effective for chemical, electrical fires, will not damage equipment. Works quickly, cools and smothers fires. Lightest of the three agents. Semi-toxic to humans. Breathable for five minutes at 7% concentration without ill health effects. Can cause dizziness and nausea from 5-10 minutes and fainting after 10 minutes. |

# Appendix A3.5 Waste Management Options

The necessity to collect, treat and store/dispose solid waste is as important as providing oxygen. A simple bag is not acceptable because microorganisms, within the waste, produce gas unless controlled. The controlling methods are given below.

## A3.5.1 Incineration

The incineration of waste will not only destroy microorganisms, but will bring down the volume of waste stored or expelled. The compact waste can then be expelled easier or stored taking very little space. However the cost burning oxygen for this process is its major disadvantage. Also the carbon dioxide and other residues from the process will have to be treated, filtered, or eliminated in some other way.

## A3.5.2 Heat Sterilization

The microorganisms can be controlled by applying heat. Wet-heat sterilization occurs for 15 minutes when the waste is exposed to 121°C steam. Dry heat can also be used. However the process is longer, one hour, and occurs at higher temperature, 160°C. Once sterilized the waste will remain stable unless somehow microorganisms are again introduced. Therefore non sterilized and treated waste can not be stored together. Also, the treated waste should be occasionally checked making sure of its condition.

## A3.5.3 Freezing

Materials can be controlled by keeping it at a temperature of -10 C. For the duration of the mission, the containment facility will have to be keep at this level. A monitoring system would be needed to insure that freezing is maintained.

## A3.5.4 Desiccation or Expulsion

Waste can be dumped into space or a chamber can expel all current waste a few times a day. This will lower the total mass of the vehicle negligibly, but during long duration a sufficient mass can be eliminated this way. Desiccation merely exposes the waste to the vacuum of space. Without moisture the microorganisms can not grow. The treated waste can be held on the vehicle and used as radiation shielding. The major disadvantage is the part of the cabin atmosphere will be vented every time the waste is desiccated or expelled.

## A3.5.5 Chemical Treatment

Destroying the microorganisms with chemicals has been used in many space missions. Chemicals needed are not exotic, therefore this system is very simple. The treatment can be ongoing; introduction of new waste to the past treated waste is standard procedure. Bio-oxidation is an idea used on earth, which with development may be adapted to space. Bacteria are used, which feeds of the microorganisms in the waste, thus treating it. Part of the waste is consumed by the bacteria, and the rest can be stored safely. However, this process needs a gravitational force not easily available in space missions.

# Appendix A4.1 Trajectory Program

```
:        Program to determine aerobraking loads
:
      dimension y(4,401)
      double precision y,drd,decel,p,po,hs,g,alt,k,q
        teger n1,m
      ~ouble precision gamma,b
      common/blk/gamma,b
      n1=401


:                        * INITIAL CONDITIONS *
:
:
      write (*,*) 'Enter initial velocity (m/s) '
      read (*,*) y(1,1)
      write (*,*) 'Enter initial altitude (m) '
      read (*,*) y(2,1)
      write (*,*) 'Enter initial flight path angle (deg) '
      read (*,*) gamma
      y(3,1)=-gamma*3.141592654/180.0
      write (*,*) 'Enter ballistic coefficient (kg/m/m) '
      read (*,*) b
      y(4,1)=0.0

:
:
      k=0.0
      drd= 0.0
      po=1.22
      hs=7100.0
      p=po*exp((-y(2,1)/hs))
      q=0.5*p*(y(1,1)**2)
      g=9.81
      alt=y(2,1)/1000.0
        ~=(-0.5*p*(y(1,1)**2))/b-g*dsin(y(3,1))
         el = -acc
      write (*,1) k,alt,y(1,1),gamma,q,decel
1     format (f8.4,2x,f10.4,2x,f14.8,2x,f8.4,2x,f10.4,2x,f14.8)
      call runkut(y,n1,4)
      stop
      end

:
:

      double precision function f(y,m,p,g,r)
      dimension y(4)
      double precision y,p,po,hs,pi,g,r,a,r1
      integer m
      double precision gamma,b
      common/blk/gamma,b
      po=1.22
      g=9.81
      hs=7100.0
      pi=3.1415927
      r1=6378000.0
      r=y(2)+r1
      p=po*dexp((-y(2)/hs))
       if (m.eq.1) then
         f=(-0.5*p*(y(1)**2)/b)-g*dsin(y(3))
      else
          if (m.eq.2) then
            f=y(1)*dsin(y(3))
         else
            if (m.eq.3) then
              a=1-(y(1)**2)/(g*r)
              f=((0.122*p*y(1))/b)-(g*cos(y(3))/y(1))*a
         else
             if (m.eq.4) then
               f=(-y(1)*cos(y(3)))/(r)
```

```fortran
              end if
            end if
          end if
        end if
         return
        end


        subroutine runkut(y,n1,m)
        dimension y(m,n1),v(4),t(4,4)
        double precision deltat,y,v,t,f,p,g,acc,r,dr,drd,alt
        double precision decel,time,q
        integer j,i
        double precision gamma,b
        common/blk/gamma,b
c
        deltat=1.25
        n1=401
c
        do 1 i=2,n1
c
           do 2 j=1,m
               v(j)=y(j,i-1)
2          continue
c
           do 3 j=1,m
               t(j,1)=f(v,j,p,g,r)
3          continue
c
           do 4 j=1,m
               v(j)=v(j) + 0.5*deltat*t(j,1)
4          continue
c
           do 5 j=1,m
               t(j,2)=f(v,j,p,g,r)
5          continue
c
           do 6 j=1,m
               v(j)=y(j,i-1)+0.5*deltat*t(j,2)
6          continue
c
           do 7 j=1,m
               t(j,3)=f(v,j,p,g,r)
7          continue
c
           do 8 j=1,m
               v(j)=y(j,i-1)+deltat*t(j,3)
3          continue
c
           do 9 j=1,m
               t(j,4)=f(v,j,p,g,r)
?          continue
c
           do 10 j=1,m
        y(j,i)=y(j,i-1)+deltat*(t(j,1)+2.0*t(j,2)+2.0*t(j,3)+t(j,4))/(6.0)
10         continue
           if (y(2,i).le.0) go to 60
           acc =(-0.5*p*(y(1,i)**2))/b-g*dsin(y(3,i))
           decel=-acc
           q=0.5*p*(y(1,i)**2)
           gamma =(y(3,i)*180.0)/3.1415927
           dr=-(y(4,i)/360.0)*2.0*3.1415927*r
           drd=dr/1000.0
```

```
        alt=y(2,i)/1000.0
        time=((real(i-1))*deltat)/60.0
        write (*,50) time,alt,y(1,i),gamma,q,decel
0    format (f8.4,2x,f10.4,2x,f14.8,2x,f8.4,2x,f10.4,2x,f14.8)
      ntinue
    .eturn
0    end
```

## Appendix A4.2 Aerobrake Structural Analysis

Hexcel Aerospace's *Mechanical Properties of Hexcel Honeycomb Material* was used for all of the following honeycomb structural analysis.

At a temperature of 300 deg F (the back surface temperatue of the TPS) aluminum retains only approximately 70% of its original room temperature strength. This was taken into account when sizing the structural members against failure.

### A4.2.1 Plates

Each of the curved trapezoidal plates was modeled as a flat rectangular plate subjected to a distributed normal load. The model had the following characteristics:

    simply supported plate : 9.3 ft x 16 ft
    distributed load : w = 0.215 psi

The selected materials are as follows :

    Honeycomb face sheets :

    7075-T6 Al alloy                 $E_f = 9.5 \times 10^6$ psi

    $F_y = 67000$ psi                $w_f = .101 \dfrac{lb}{in^3}$


    Honeycomb core :

    $\dfrac{3}{16}$ in.  5052H39-.001P  Hexagonal Honeycomb

        $w_c = 0.00179$ lb/in$^3$
         $G_{ca} = 22000$ psi
         $G_{cb} = 41800$ psi
          $F_s = 124$ psi
          $F_c = 282$ psi

Through successive iterations, the thickness of the face sheets ($t_f$) and the thickness of the core ($t_c$) were obtained. Only the final results are presented here.

The maximum bending moments that would occur for a given distributed loading were given by the handbook to be

$$M_a = \frac{16pb^2}{\pi^4}(C_3 + \mu C_2) = \frac{16(.215)(12454.56)}{\pi^4}(.15 + .3(.52)) = 134.60 \text{ in-lb/in}$$

$$M_b = \frac{16pb^2}{\pi^4}(C_2 + \mu C_3) = 248.50 \text{ in-lb/in.}$$

The stresses in the face sheets are determined by

$$f_a = \frac{2M_a}{t(d+t_c)} = \frac{2(134.60)}{.006(.632 + .62)} = 3.58 \times 10^4 \text{ psi}$$

$$f_b = \frac{2M_b}{t(d+t_c)} = 6.61 \times 10^4 \text{ psi.}$$

These stresses are both below the yield stress for aluminum 7075-T6.

The shear forces in the honeycomb plates are determined by

$$S_b = \frac{16 \, pb}{\pi^3}(0.75) = \frac{16(.215)(111.6)}{\pi^3} = 8.79 \text{ lb/in}$$

$$S_a = \frac{16pb}{\pi^3}(.84) = 10.40 \text{ lb/in.}$$

The stresses due to the shear forces in the core are determined by

$$f_a = \frac{2S_a}{d+t_c} = 16.61 \text{ psi}$$

$$f_b = \frac{2S_b}{d+t_c} = 14.04 \text{ psi.}$$

These stresses are also well below the maximum allowable shear stress of 124 psi.

## A4.2.2 Arches

The 4.88m long curved arches were modeled as straight beams subjected to both the distributed load and the g-loads. From a free body diagram, the following loads were determined.

Dynamic Pressure :
    Maximum moment = $2.75 \times 10^4$ lb-in
    Maximum shear = 685.13 lbs

Acceleration loads :
    Maximum moment = $2.31 \times 10^4$ lb-in
    Maximum shear = 238.71 lbs

Try solid aluminum I-beams ( S3 x 5.7)
$$\sigma = \frac{My}{I} = \frac{2.75 \times 10^4 (1.5)}{2.52} = 16369.05 \text{ psi}$$

This is well below the limit for aluminum. However, the weight is calculated as follows : $w = Al\rho = 316.27$ lbs/10 beams. This is well beyond the mass budget.

Try honeycomb beam with the following characteristics :

Face sheets :

7075-T6 Al
$F_y$ = 67000psi
$w_f$ = .101 lb/in$^3$

Core :

3/16 cell 5052-.003 Al
$w_c$ = .00179 lb/in$^3$
$G_c$ = 40000 psi
$F_s$ = 180 psi
$F_c$ = 250 psi

After several iterations, the following dimensions were decided upon

beam width (b) = 6 in
face sheet thickness ($t_f$) = .055 in
core thickness ($t_c$) = 3.172 in.

The stress in the face sheets due to the moment is given by

$$f_f = \frac{M}{bt_f(d-t_f)} = 2.6 \times 10^4 \text{ psi.}$$

This is well below the yield stress for 7075-T6 Al.

The shear stress in the core is given by

$$f_s = \frac{2S}{b(d+t_c)} = 35.56 \text{ psi.}$$

The compressive stress in the core is given by

$$f_c = \frac{2f_f^2}{E_f(\frac{d}{t_c} - 1)} = 2.47 \text{ psi.}$$

These stresses are also well below the stress limits for the core material.

**A4.2.3 Rods**

From a free body diagram, it was seen that the rods would be subjected to both tensile and compressive loads.

Maximum compressive load = 2051.73 N
Maximum tensile load = 699.38 N

Compressive test

Try aluminum rod of radius .018 m

$$I = \frac{1}{4}\pi r^4 = 8.24 \times 10^{-8} \text{m}^4$$

$$P_{cr} = \frac{\pi^2 EI}{L^2} = 2320.0 \text{ N}$$

Maximum compressive load < $P_{cr}$   Buckling will not occur

Tensile test

$$P = 699.38 \text{ N}$$
$$A = \pi r^2 = 1.02 \times 10^{-3} \text{ m}^2$$
$$\sigma = \frac{P}{A} = 6.9 \times 10^5 \frac{N}{m^2}$$

$\sigma < \sigma_y$   :   Rod will not fail in tension

## A4.2.4 Deflections

Since both the rods and arches are pinned at both ends, the deflection of these members was not considered to be a major problem. However, the plates will have a tendency to deflect under the dynamic pressure loading. This deflection is found as follows

$$D = \frac{E_f}{12\lambda}(d^3 - t_c^3) = 30803.75$$

$$\delta = \frac{16pb^4(.5)}{\pi^6 D} = \frac{2.7 \times 10^8}{961.4(30803.75)}$$

$$\delta = 9 \text{ in.}$$

This is a somewhat large deflection. It is hoped that the TPS will provide some additional stiffness. If not, the plates may have to be thickened which will produce additional weight.

# Appendix A4.3 Torque Spreadsheet

| mu | 3.99E+14 |
|---|---|
| theta | 45 |

| Radius of orbit km | lz to GEO | lz from GEO | ly to GEO | ly from GEO | Torque to GEO | Torque from GEO |
|---|---|---|---|---|---|---|
| 80 | 56385.8 | 14085.3 | 22819 | 15084.7 | 35043.2544 | 1043.35917 |
| 100 | 56160.8 | 14310.3 | 22777.9 | 15125.8 | 17843.8479 | 435.901554 |
| 600 | 55935.8 | 14085.3 | 22736.8 | 15166.9 | 82.1553221 | 2.67656244 |
| 1100 | 55710.8 | 14310.3 | 22695.7 | 15208 | 13.258641 | 0.36051025 |
| 1600 | 55485.8 | 14535.3 | 22654.6 | 15249.1 | 4.28441233 | 0.09314961 |
| 2100 | 55260.8 | 14760.3 | 22613.5 | 15290.2 | 1.88431644 | 0.03058444 |
| 2600 | 55035.8 | 14985.3 | 22572.4 | 15331.3 | 0.98727562 | 0.01052254 |
| 3100 | 54810.8 | 15210.3 | 22531.3 | 15372.4 | 0.57917015 | 0.00290846 |
| 3600 | 54585.8 | 15435.3 | 22490.2 | 15413.5 | 0.36770747 | 0.00024975 |
| 4100 | 54360.8 | 15660.3 | 22449.1 | 15454.6 | 0.24749294 | 0.00159532 |
| 4600 | 54135.8 | 15885.3 | 22408 | 15495.7 | 0.1742332 | 0.00213949 |
| 5100 | 53910.8 | 16110.3 | 22366.9 | 15536.8 | 0.12710695 | 0.00231093 |
| 5600 | 53685.8 | 16335.3 | 22325.8 | 15577.9 | 0.09545011 | 0.00230529 |
| 6100 | 53460.8 | 16560.3 | 22284.7 | 15619 | 0.07341702 | 0.00221668 |
| 6600 | 53235.8 | 16785.3 | 22243.6 | 15660.1 | 0.05762157 | 0.002092 |
| 7100 | 53010.8 | 17010.3 | 22202.5 | 15701.2 | 0.04601052 | 0.00195507 |
| 7600 | 52785.8 | 17235.3 | 22161.4 | 15742.3 | 0.0372899 | 0.00181796 |
| 8100 | 52560.8 | 17460.3 | 22120.3 | 15783.4 | 0.03306169 | 0.00168662 |
| 8600 | 52335.8 | 17685.3 | 22079.2 | 15824.5 | 0.025542665 | 0.00156376 |
| 9100 | 52110.8 | 17910.3 | 22038.1 | 15865.6 | 0.021331107 | 0.00145034 |
| 9600 | 51885.8 | 18135.3 | 21997 | 15906.7 | 0.01805757 | 0.00134643 |
| 10100 | 51660.8 | 18360.3 | 21955.9 | 15947.8 | 0.015541091 | 0.00125161 |
| 10600 | 51435.8 | 18585.3 | 21914.8 | 15988.9 | 0.013324884 | 0.00116525 |
| 11100 | 51210.8 | 18810.3 | 21873.7 | 16030 | 0.01146602 | 0.00108664 |
| 11600 | 50985.8 | 19035.3 | 21832.6 | 16071.1 | 0.00998336 | 0.00101507 |
| 12100 | 50760.8 | 19260.3 | 21791.5 | 16112.2 | 0.0087407 | 0.00094985 |
| 12600 | 50535.8 | 19485.3 | 21750.4 | 16153.3 | 0.00769175 | 0.00089034 |
| 13100 | 50310.8 | 19710.3 | 21709.3 | 16194.4 | 0.00680048 | 0.00083596 |
| 13600 | 50085.8 | 19935.3 | 21668.2 | 16235.5 | 0.00603858 | 0.00078619 |
| 14100 | 49860.8 | 20160.3 | 21627.1 | 16276.6 | 0.00538363 | 0.00074055 |
| 14600 | 49635.8 | 20385.3 | 21586 | 16317.7 | 0.00481765 | 0.00069863 |
| 15100 | 49410.8 | 20610.3 | 21544.9 | 16358.8 | 0.0043262 | 0.00066005 |
| 15600 | 49185.8 | 20835.3 | 21503.8 | 16399.9 | 0.00389752 | 0.00062449 |
| 16100 | 48960.8 | 21060.3 | 21462.7 | 16441 | 0.003522 | 0.00059165 |
| 16600 | 48735.8 | 21285.3 | 21421.6 | 16482.1 | 0.00319175 | 0.00056127 |

| | | | | | |
|---|---|---|---|---|---|
| 17100 | 48510.8 | 21510.3 | 21380.5 | 16523.2 | 0.00290022 | 0.00053312 |
| 17600 | 48285.8 | 21735.3 | 21339.4 | 16564.3 | 0.00264197 | 0.00050699 |
| 18100 | 48060.8 | 21960.3 | 21298.3 | 16605.4 | 0.00241243 | 0.0004827 |
| 18600 | 47835.8 | 22185.3 | 21257.2 | 16646.5 | 0.00220779 | 0.00046009 |
| 19100 | 47610.8 | 22410.3 | 21216.1 | 16687.6 | 0.0020248 | 0.000439 |
| 19600 | 47385.8 | 22635.3 | 21175 | 16728.7 | 0.0018607 | 0.00041931 |
| 20100 | 47160.8 | 22860.3 | 21133.9 | 16769.8 | 0.00171316 | 0.00040089 |
| 20600 | 46935.8 | 23085.3 | 21092.8 | 16810.9 | 0.00158018 | 0.00038365 |
| 21100 | 46710.8 | 23310.3 | 21051.7 | 16852 | 0.00146002 | 0.00036748 |
| 21600 | 46485.8 | 23535.3 | 21010.6 | 16893.1 | 0.0013512 | 0.0003523 |
| 22100 | 46260.8 | 23760.3 | 20969.5 | 16934.2 | 0.00125245 | 0.00033803 |
| 22600 | 46035.8 | 23985.3 | 20928.4 | 16975.3 | 0.00116263 | 0.00032461 |
| 23100 | 45810.8 | 24210.3 | 20887.3 | 17016.4 | 0.00108078 | 0.00031196 |
| 23600 | 45585.8 | 24435.3 | 20846.2 | 17057.5 | 0.00100605 | 0.00030002 |
| 24100 | 45360.8 | 24660.3 | 20805.1 | 17098.6 | 0.0009377 | 0.00028876 |
| 24600 | 45135.8 | 24885.3 | 20764 | 17139.7 | 0.00087508 | 0.00027811 |
| 25100 | 44910.8 | 25110.3 | 20722.9 | 17180.8 | 0.0008176 | 0.00026803 |
| 25600 | 44685.8 | 25335.3 | 20681.8 | 17221.9 | 0.00076477 | 0.00025849 |
| 26100 | 44460.8 | 25560.3 | 20640.7 | 17263 | 0.00071612 | 0.00024945 |
| 26600 | 44235.8 | 25785.3 | 20599.6 | 17304.1 | 0.00067127 | 0.00024087 |
| 27100 | 44010.8 | 26010.3 | 20558.5 | 17345.2 | 0.00062986 | 0.00023272 |
| 27600 | 43785.8 | 26235.3 | 20517.4 | 17386.3 | 0.00059157 | 0.00022497 |
| 28100 | 43560.8 | 26460.3 | 20476.3 | 17427.4 | 0.00055612 | 0.00021761 |
| 28600 | 43335.8 | 26685.3 | 20435.2 | 17468.5 | 0.00052325 | 0.00021059 |
| 29100 | 43110.8 | 26910.3 | 20394.1 | 17509.6 | 0.00049275 | 0.00020391 |
| 29600 | 42885.8 | 27135.3 | 20353 | 17550.7 | 0.00046441 | 0.00019754 |
| 30100 | 42660.8 | 27360.3 | 20311.9 | 17591.8 | 0.00043805 | 0.00019147 |
| 30600 | 42435.8 | 27585.3 | 20270.8 | 17632.9 | 0.00041349 | 0.00018566 |
| 31100 | 42210.8 | 27810.3 | 20229.7 | 17674 | 0.0003906 | 0.00018012 |
| 31600 | 41985.8 | 28035.3 | 20188.6 | 17715.1 | 0.00036924 | 0.00017482 |
| 32100 | 41760.8 | 28260.3 | 20147.5 | 17756.2 | 0.00034928 | 0.00016975 |
| 32600 | 41535.8 | 28485.3 | 20106.4 | 17797.3 | 0.00033061 | 0.0001649 |
| 33100 | 41310.8 | 28710.3 | 20065.3 | 17838.4 | 0.00031315 | 0.00016025 |
| 33600 | 41085.8 | 28935.3 | 20024.2 | 17879.5 | 0.00029678 | 0.00015579 |
| 34100 | 40860.8 | 29160.3 | 19983.1 | 17920.6 | 0.00028144 | 0.00015152 |
| 34600 | 40635.8 | 29385.3 | 19942 | 17961.7 | 0.00026704 | 0.00014741 |
| 35100 | 40410.8 | 29610.3 | 19900.9 | 18002.8 | 0.00025352 | 0.00014348 |
| 35600 | 40185.8 | 29835.3 | 19859.8 | 18043.9 | 0.00024081 | 0.00013969 |
| 36100 | 39960.8 | 30060.3 | 19818.7 | 18085 | 0.00022885 | 0.00013606 |
| 36600 | 39735.8 | 30285.3 | 19777.6 | 18126.1 | 0.00021759 | 0.00013256 |
| 37100 | 39510.8 | 30510.3 | 19736.5 | 18167.2 | 0.00020699 | 0.0001292 |
| 37600 | 39285.8 | 30735.3 | 19695.4 | 18208.3 | 0.00019699 | 0.00012596 |
| 38100 | 39060.8 | 30960.3 | 19654.3 | 18249.4 | 0.00018756 | 0.00012285 |
| 38600 | 38835.8 | 31185.3 | 19613.2 | 18290.5 | 0.00017865 | 0.00011984 |
| 39100 | 38610.8 | 31410.3 | 19572.1 | 18331.6 | 0.00017024 | 0.00011695 |
| 39600 | 38385.8 | 31635.3 | 19531 | 18372.7 | 0.00016229 | 0.00011416 |
| 40100 | 38160.8 | 31860.3 | 19489.9 | 18413.8 | 0.00015477 | 0.00011147 |
| 40600 | 37935.8 | 32085.3 | 19448.8 | 18454.9 | 0.00014766 | 0.00010887 |

| 41100 | 37710.8 | 32310.3 | 19407.7 | 18496 | 0.00014092 | 0.00010636 |
|---|---|---|---|---|---|---|
| 41600 | 37485.8 | 32535.3 | 19366.6 | 18537.1 | 0.00013453 | 0.00010393 |
| 42100 | 37260.8 | 32760.3 | 19325.5 | 18578.2 | 0.00012848 | 0.00010159 |
| 42600 | 37035.8 | 32985.3 | 19284.4 | 18619.3 | 0.00012273 | 9.9328E-05 |
| 43100 | 36810.8 | 33210.3 | 19243.3 | 18660.4 | 0.00011729 | 9.7139E-05 |
| 43600 | 36585.8 | 33435.3 | 19202.2 | 18701.5 | 0.00011211 | 9.5021E-05 |
| 44100 | 36360.8 | 33660.3 | 19161.1 | 18742.6 | 0.00010719 | 9.2972E-05 |
| 44600 | 36135.8 | 33885.3 | 19120 | 18783.7 | 0.00010252 | 9.0988E-05 |
| 45100 | 35910.8 | 34110.3 | 19078.9 | 18824.8 | 9.8077E-05 | 8.9067E-05 |
| 45600 | 35685.8 | 34335.3 | 19037.8 | 18865.9 | 9.385E-05 | 8.7205E-05 |
| 46100 | 35460.8 | 34560.3 | 18996.7 | 18907 | 8.9826E-05 | 8.5402E-05 |
| 46600 | 35235.8 | 34785.3 | 18955.6 | 18948.1 | 8.5994E-05 | 8.3654E-05 |

# Appendix A.5

## A.5.1 Choosing the Optimum Propulsion System

Five different propulsion systems were considered for the MOOSE project. These propulsion systems included three different chemical propulsion systems (liquid, solid, and hybrid), a nuclear fission reactor, and a laser absorption process. It has been determined by the design group that the optimum propulsion system for the MOOSE project is a chemical system with liquid propellants. This section of the appendix details the four propulsion systems that were analyzed but not chosen for the MOOSE project. In addition to this section, Section 5.1.2 (Propellant Transport Cost for Chemical Propulsion Systems) details the major factor in determining the optimum propulsion system for the MOOSE project.

### A.5.1.1 Solid Rocket Systems

Solid rocket motors provide a wide range of applications with a relatively simple design, as compared to liquid rocket systems. A typical solid motor assembly consists of a propellant grain, igniter, motor case, and exhaust nozzle. The propellant grain is typically bonded to the motor case and once ignited the propellant burns to completion. Some degree of thrust variation can be achieved by selecting an appropriate grain configuration or by bonding propellants of different burn rates in the motor. Typical solid rocket motors deliver Isp values of 180-300 seconds which is lower than typical liquid rocket engines which deliver Isp's of 300-450 seconds.

In addition to the operational simplicity of the solid rocket systems, solid propellants have storability advantages over other systems, usually lasting from 5-25 years. Also, the higher densities associated with solid propellants result in reduced overall volume for a given design. Solid rocket systems are generally reliable systems available at low cost compared to other rocket systems. One major problem associated with solid systems is the possibility of spontaneous ignition or even detonation in some propellants; for manned applications this is a critical safety issue which would dismiss the use of that particular propellant. Also, the tendency of solid systems to produce smoky and caustic exhaust products is extremely undesirable for the MOOSE as the exhaust may contaminate the satellites to be serviced.

Various general types of propellant grains are available depending on the desired thrust-time history of the rocket. Neutral grain configurations, such as the common

star shaped grain, provide thrust which is relatively constant with time. Progressive grain configurations, such as a simple circular bore, offer increasing thrust with time. Regressive grain configurations, such as a solid core that burns from the outside, provide decreasing thrust with time. Pulse rockets have two or more distinct burning periods separated by an off time. Step thrust rockets have two or more thrust levels; this can be done by having fuels of different types or by allowing a drastic change in burn area at a given point in the mission.

Solid propellants are available in several general categories: Double Base (DB), Composite Modified Double Base (CMDB), and Composite (C). The DB propellants were common in the early solid rockets, generally a homogeneous combination of nitrocellulose (NC) dissolved in nitroglycerin (NG). DB propellants are typically low performance, Isp < 200 seconds, but have relatively smokeless and non-toxic exhaust. The CMDB propellants are DB propellants improved by adding composites such as crystalline oxidizers like ammonium perchlorate (AP) and aluminum fuel. Performance of CMDB systems is higher than DB, Isp ~ 250 seconds, higher density is also achieved; however the CMDB propellants can have smoky and toxic exhaust. Composite propellants are heterogeneous mixtures of oxidizer crystals and powdered aluminum fuel held in a matrix of plastic binder material. Conventional composites are reliable, perform as well as CMDB but have toxic and smoky exhaust. The best performing solid fuels, the modified composites, have crystalline nitramines (explosives) such as RDX, HMX added to boost the Isp to 270 and above. However, these systems are expensive, have toxic, smoky exhaust, and are dangerous due to their explosive contents.

## A.5.1.2 Chemical Propulsion with Hybrid Propellants

A chemical system with hybrid propellants has many advantages over other propulsion systems. A few of these advantages include: storable propellants which are readily available, stop - start - restart capabilities, operation without the possibility of explosion or detonation, and the need for only half of the pumps and plumbing of a liquid propellant system. A hybrid propulsion system also has several disadvantages. These disadvantages include nominal steady-state combustion efficiencies ranging from 93% to 97 %, which are slightly lower than liquid or solid systems, and the performance level of a hybrid system is typically 21% lower than that of a liquid system.

The following analysis was completed on both hybrid and liquid propellant propulsion systems to determine the optimum system for the following design criteria:

Note: The following criteria was determined based on the initial design of the MOOSE project. This criteria was changed as the design of the vehicle changed.

• single stage design
• structural mass of 10,000 kg

- tank size restrictions - determined so the dry tanks can fit into the shuttle cargo bay

    - 1 oxidizer tank & 4 fuel tanks
        - max radius of oxidizer tank is 2.25 m
        - max radius of fuel tanks are 1.00 m
    - 2 oxidizer tanks & 2 fuel tanks
        - max radius of oxidizer tanks are 1.00 m
        - max radius of fuel tanks are 1.00 m

- $\Delta V$ values

    - $\Delta V$ = 9.13 km/s without aerobraking
    - $\Delta V$ = 5.74 km/s with aerobraking

- cylindrical or spherical tanks
- max cylindrical tank length of 10.00 m
- flexibility to increase or decrease structural mass while maintaining tank size restrictions

Three different hybrid propellant combinations and two liquid propellant combinations were considered for the analysis, these propellant combinations include:

Hybrid:
- LOX / HTPB
- N20 / HTPB
- ClO2 / HTPB

Liquid:
- LOX / LH2
- LOX / RP-1

The results of the analysis are as follows:

- optimum system with 1 oxidizer & 4 fuel tanks without aerobraking
    - LOX / HTPB
- optimum system with 2 oxidizer & 2 fuel tanks without aerobraking
    - no system meets the trade study criteria
- optimum system with 1 oxidizer & 4 fuel tanks with aerobraking
    - LOX / HTPB or LOX / LH2
- optimum system with 2 oxidizer & 2 fuel tanks with aerobraking
    - LOX / HTPB or LOX / LH2

The results can be summarized as follows:

- single stage mission is possible with both hybrid & chemical systems
- hybrid system can be efficient with or without aerobraking
- chemical system can only be efficient with aerobraking design
- LOX is the optimum oxidizer for both hybrid and chemical systems
- LH2 is the optimum fuel for the chemical systems
- two different tank configurations can be considered
- if aerobraking design is not considered then limited to hybrid system with 1 oxidizer & 4 fuel tanks
- if aerobraking design is considered then plenty of flexibility in increasing or decreasing structural mass while maintaining tank size restrictions

Data for the 2 LOX tanks and 2 HTPB tanks are tabulated below, these results give a good representation of the propulsion characteristics calculated in this analysis. Based on the current design requirements, it is apparent from these figures that this system is no longer feasible.

| $\Delta V$ | 5.74 Km/s | Mi | 62000 Kg |
|---|---|---|---|
| Isp | 340 s | Mf | 11092 Kg |
| mass ratio | 5.59 | Mpl | 1000 Kg |
| mixture ratio | 2.2 | Mst | 10092 Kg |
| 1ST Unit Cost | 57.4 $M93 | Mprop | 50908 Kg |

| LOX | | HTPB | |
|---|---|---|---|
| density | 1140 Kg/m^3 | density | 913 Kg/m^3 |
| mass | 34999 Kg | mass | 15909 Kg |
| # of cyl. tanks | 2 | # of cyl. tanks | 2 |
| mass of each tank | 260 Kg | mass of each tank | 167 Kg |
| volume | 15.4 m^3 | volume | 8.7 m^3 |
| surface area | 37.2 m^2 | surface area | 23.9 m^2 |
| radius | .99 m | radius | 0.96 m |
| length | 5.00 m | length | 3.00 m |

The two tank configurations considered are shown below in Figure A.5.1.a.

4 Fuel Tanks

1 Oxidizer Tank

2 Oxidizer Tanks

2 Fuel Tanks

Truss Structure
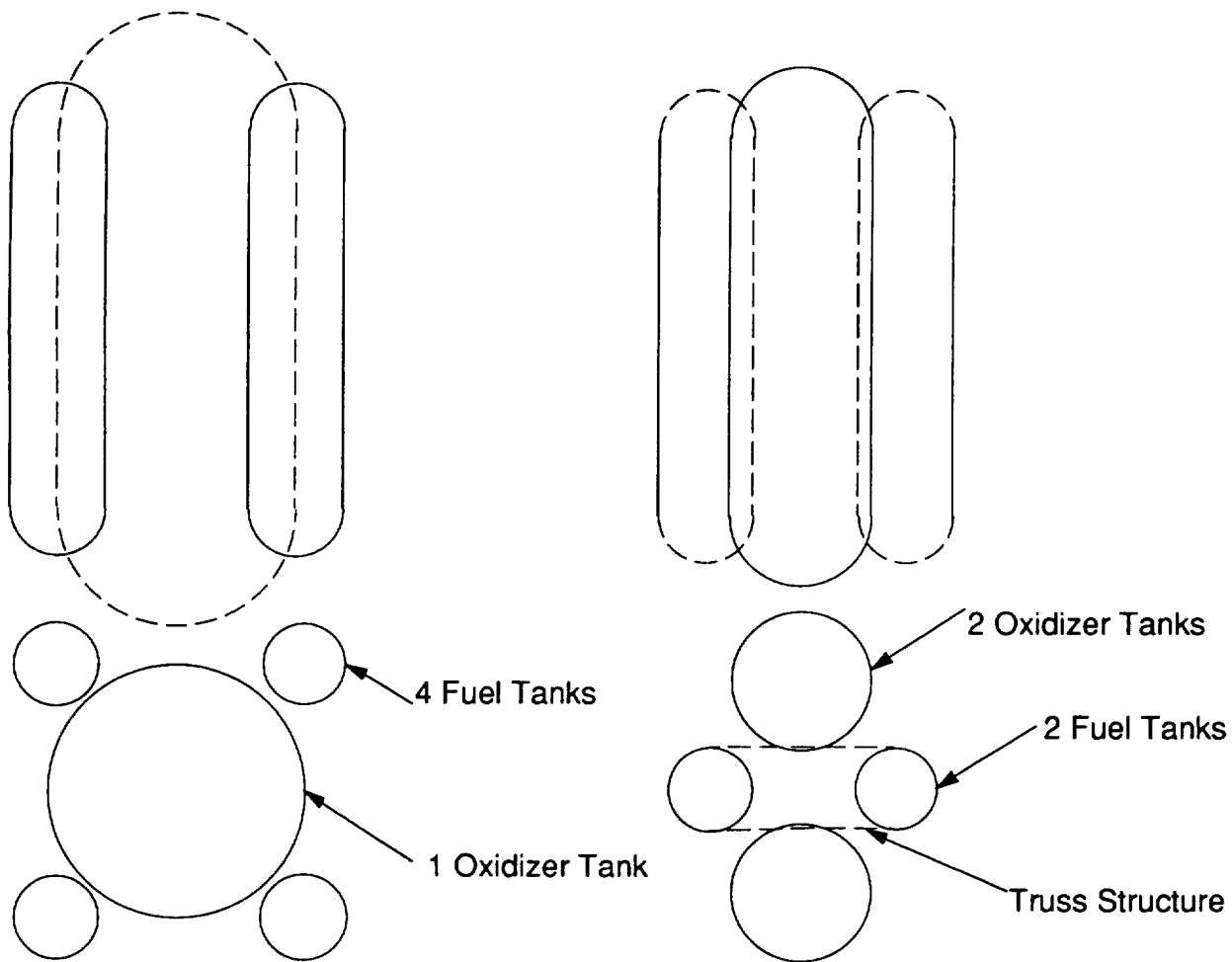
**Figure A.5.1.a** Schematic of Two Different Tank Configurations
Used in an Analysis for Hybrid and Liquid Propulsion.

## A.5.1.3 Nuclear Propulsion

A nuclear propulsion system, like every propulsion system, has several advantages
and disadvantages when compared to other propulsion systems. A couple of these
advantages include high specific impulse and high thrust to weight ratio. In addition,
a nuclear system doesn't need any oxidizing propellants. The major disadvantage of a
nuclear system is that proven technology is unavailable at this time and therefore
doesn't meet the 1993 technology cut-off date. Other disadvantages include the
massive radiation shield that is necessary to protect the astronaut, the expensive core
construction, and that there is no instantaneous engine shut down since the working
fluid is used to help cool the core.

An analysis was completed on the nuclear propulsion system. The results from this
analysis, which are tabulated below, give a good representation of the propulsion
characteristics for a nuclear system. It is apparent from the results that a nuclear

system will one day be a feasible system for space flight, however, the design group has decided to enforce the 1993 technology cut off date for the main propulsion system of the MOOSE project.

This analysis was based upon a vehicle structural mass of 50,000 kg and cylindrical tank sizes shorter than 10 meters.

| | | | |
|---|---|---|---|
| Isp | 750 s | # of Tanks | 3 |
| mass ratio | 3.459 | mass of each tank | 1247 kg |
| Mpl | 1000 kg | volume | 105.8 m^3 |
| Mi | 50000 kg | radius | 2.034 m |
| Mf | 14455 kg | length | 8.136 m |
| Mst | 13455 kg | | |
| Mprop | 35545 kg | | |

## A.5.1.4 Laser Propulsion

A laser propulsion system can be divided into four main components; beam collection optics, propellant tanks, a thrust chamber, and one or more laser beam generators. The advantages of using a laser propulsion system include: no on board prime power system, no conditioning systems with corresponding weight penalties, a low vehicle mass allowing for higher payload mass, and high exhaust velocities. The major disadvantage, as explained with the nuclear system, is that proven technology is unavailable at this time and therefore doesn't meet the 1993 technology cut-off date. Other disadvantages include: combustion chamber must withstand temperatures at 20,000 K, space rated technology is unavailable for space or ground based transmitting stations, proven technology is unavailable for the precise accuracy needed to orient the laser beam to the combustion chamber, and it is a low thrust system so travel time to GEO exceeds 2 days.

An analysis was completed on the laser propulsion system. The results from this analysis, which are tabulated below, give a good representation of the propulsion characteristics for a laser system. Even though the results may demonstrate a feasible system, it is apparent from the statements above that a laser propulsion system is not an optimum propulsion system at this time. The design group has decided to enforce the 1993 technology cut-off date for the main propulsion system.

This analysis was based on an initial mass of 50,000 kg and the flexibility of a one or two tank system for the fuel.

| | | | | |
|---|---|---|---|---|
| mass ratio | 1.86 | | Cylindrical Tanks | |
| Mi | 50000 kg | 1 Tank | | |
| Mf | 26885 kg | radius | 2.00 m | 3.00 m |
| Mst | 25885 kg | height | 16.42 m | 7.30 m |
| Mpl | 1000 kg | 2 Tanks | | |
| Mprop | 23115 kg | radius | 2.00 m | 3.00 m |

| Tank mass | 2539 kg | | height | 8.21 m | 0.91 m |

Tank volume    206 m^3

Spherical Tanks

1 Tank
     radius     3.67 m

2 Tanks
     radius     2.91 m

## A.5.2 Cooling Schemes

Regenerative Cooling

Regenerative cooling, the most widely applied method, utilizes one or possibly both of the propellants fed through passages in the thrust-chamber wall for cooling, before being injected into the combustion chamber.

Dump Cooling

With this principle, a small percentage of the propellant, such as the hydrogen in a LOX/LH$_2$ engine, is fed through passages in the thrust chamber wall for cooling and is subsequently dumped overboard through openings at the rear end of the nozzle skirt. due to performance losses, this method has only limited application.

Film Cooling

The exposed combustion chamber wall surfaces are protected from excessive heat by a thin film of coolant or propellant introduced through orifices around the injector or through orifices in the chamber wall near the injector. This method has been used, particularly for high heat fluxes, either alone or in combination with regenerative cooling.

Transpiration Cooling

Transpiration cooling introduces a coolant (either gaseous or liquid propellant ) through porous chamber walls at a rate sufficient to maintain the desired temperature of the chamber wall. This method is essentially a special type of film cooling.

Ablative Cooling

In an ablative cooling scheme, the combustion-gas-side wall material is melted, vaporized, and chemically altered to dissipate the heat load. Ablative cooling has been used in numerous designs, mainly for solid-propellant systems, or for short duration and or low chamber pressure liquid systems.

Radiation Cooling

The heat is radiated away from the surface of the outer chamber wall. It has been applied to very small, high temperature material combustion chambers and to low heat flux regions, such as nozzle extensions.

## A.5.3 Conical vs. Bell Shaped Nozzles

The following analysis is to determine whether or not the losses produced by a conical nozzle are negligible compared to a bell nozzle. For the conical nozzle I will assume a uniform exit velocity, Ue. That is, the flow down the centerline of the nozzle is Ue and the flow tangent to the nozzle wall is also Ue. This assumption will result in a worse case scenario because the viscous effects at the wall will actually slow the flow down, that is, the flow near the wall is actually less than Ue. Therefore, the conical nozzle will perform slightly better than what is determined by this analysis. A schematic of the conical nozzle is shown below in Figure A.5.3.a.
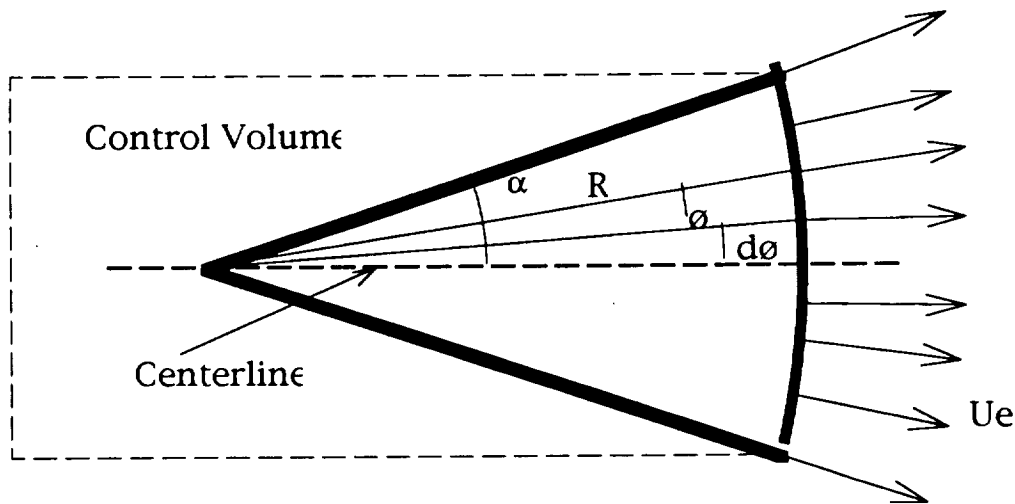


Figure A.5.3.a Schematic of a Conical Nozzle.

The force component parallel to the centerline is:

$$F_x = \int_{c.s.} \rho(\vec{U}\cdot\vec{n})U_x dA$$

Using a spherical geometry the cross sectional area can be divided into concentric rings and the incremental area can be determined by:

$$dA = 2\pi R \sin\theta R d\theta$$

where R is a constant due to the geometry.

$$\vec{U} \cdot \vec{n} = U_e$$
$$U_x = U_e \cos \theta$$

By substituting into the force equation the thrust can be determined by:

$$T = \int_0^\alpha \rho U_e \cdot U_e \cos \theta \, 2\pi R^2 \sin \theta \, d\theta$$
$$= 2\pi R^2 \rho U_e^2 \left( \frac{1 - \cos^2 \alpha}{2} \right)$$

The exit area of the nozzle as determined from the geometry is:

$$A_e = 2\pi R^2 (1 - \cos \alpha)$$

The mass flow rate is defined and rearranged by the equation for the exit area:

$$\dot{m} = \rho U A = \rho U_e \, 2\pi R^2 (1 - \cos \alpha)$$

From trigonometry:

$$1 - \cos^2 \alpha = (1 - \cos \alpha)(1 + \cos \alpha)$$

By substituting the mass flow rate into the thrust equation and applying the trigonometry identity:

$$T = \dot{m} U_e \left( \frac{1 + \cos \alpha}{2} \right)$$

The thrust for an ideal bell nozzle is defined as:

$$T = \dot{m} U_e$$

Therefore the ratio of conical nozzle thrust to ideal bell nozzle thrust is:

$$\frac{T_{conical}}{T_{bell}} = \left( \frac{1 + \cos \alpha}{2} \right)$$

Table A.5.3.a lists the percent losses of a conical nozzle compared to an ideal bell nozzle for various half angles of the conical nozzle.

| $\alpha$ | $\left(\dfrac{1+\cos\alpha}{2}\right)$ | % Loss |
|---|---|---|
| 10° | 0.992 | 0.8% |
| 15° | 0.983 | 2.0% |
| 20° | 0.970 | 3.0% |

**Table A.5.3.a** Percent Losses of a Conical Nozzle Compared to an Ideal Bell Nozzle for Various Half Angles of the Conical Nozzle

At a conical half angle of 10° the losses are negligible, however, a longer and thus heavier nozzle would be needed for such a small half angle in order to avoid overexpansion. At a conical half angle of 20° the nozzle must be shorter and thus lighter in order to avoid underexpansion, however, the thrust losses at this half angle are of concern. At a conical half angle of 15° the losses can be neglected for the ease of fabrication. Even though conical nozzles are easier and cheaper to fabricate than bell shaped nozzles, the cost of a bell shaped nozzle is not significant when compared to the entire vehicle cost. In fact, a bell shaped nozzle would not represent more than 5% of the entire vehicle cost.

The material for this section has been referenced from a Rocket Propulsion Lecture, ENAE 462, by Dr. Mark Lewis.

## A.5.4 Results of the Method of Characteristics

The following data gives a good representation of the data calculated from the method of characteristics technique. Only the properties for the first 33 grid points are shown below. The properties at 152 grid points were calculated when developing the contour of the nozzle.

| Point # | K - | K + | ø | v | M | μ | Comments |
|---|---|---|---|---|---|---|---|
| 1 | 2.868 | 0.000 | 1.434 | 1.434 | 1.10 | 65.4 | |
| 2 | 8.868 | 0.000 | 4.434 | 4.434 | 1.22 | 55.1 | |
| 3 | 14.868 | 0.000 | 7.434 | 7.434 | 1.32 | 49.3 | |
| 4 | 20.868 | 0.000 | 10.434 | 10.434 | 1.41 | 45.2 | |
| 5 | 26.868 | 0.000 | 13.434 | 13.434 | 1.50 | 41.8 | |
| 6 | 32.868 | 0.000 | 16.434 | 16.434 | 1.58 | 39.3 | |
| 7 | 38.868 | 0.000 | 19.434 | 19.434 | 1.66 | 37.0 | |
| 8 | 44.868 | 0.000 | 22.434 | 22.434 | 1.75 | 34.8 | |
| 9 | 50.868 | 0.000 | 25.434 | 25.434 | 1.83 | 33.1 | |
| 10 | 56.868 | 0.000 | 28.434 | 28.434 | 1.92 | 31.4 | |
| 11 | 62.868 | 0.000 | 31.434 | 31.434 | 2.00 | 30.0 | |
| 12 | 68.868 | 0.000 | 34.434 | 34.434 | 2.08 | 28.7 | |
| 13 | 74.868 | 0.000 | 37.434 | 37.434 | 2.17 | 27.4 | |
| 14 | 80.868 | 0.000 | 40.434 | 40.434 | 2.26 | 26.3 | |

| 1 5 | 86.868 | 0.000 | 43.434 | 43.434 | 2.35 | 25.2 | |
|---|---|---|---|---|---|---|---|
| 1 6 | 92.868 | 0.000 | 46.434 | 46.434 | 2.44 | 24.2 | |
| 1 7 | 92.868 | 0.000 | 46.434 | 46.434 | 2.44 | 24.2 | Wall Pt. |
| 1 8 | 8.868 | -8.868 | 0.000 | 8.868 | 1.36 | 47.3 | |
| 1 9 | 14.868 | -8.868 | 3.000 | 11.868 | 1.45 | 43.6 | |
| 2 0 | 20.868 | -8.868 | 6.000 | 14.868 | 1.54 | 40.5 | |
| 2 1 | 26.868 | -8.868 | 9.000 | 17.868 | 1.62 | 38.1 | |
| 2 2 | 32.868 | -8.868 | 12.000 | 20.868 | 1.7 | 36.0 | |
| 2 3 | 38.868 | -8.868 | 15.000 | 23.868 | 1.79 | 34.0 | |
| 2 4 | 44.868 | -8.868 | 18.000 | 26.868 | 1.87 | 32.3 | |
| 2 5 | 50.868 | -8.868 | 21.000 | 29.868 | 1.96 | 30.7 | |
| 2 6 | 56.868 | -8.868 | 24.000 | 32.868 | 2.04 | 29.4 | |
| 2 7 | 62.868 | -8.868 | 27.000 | 35.868 | 2.13 | 28.0 | |
| 2 8 | 68.868 | -8.868 | 30.000 | 38.868 | 2.21 | 26.9 | |
| 2 9 | 74.868 | -8.868 | 33.000 | 41.868 | 2.3 | 25.8 | |
| 3 0 | 80.868 | -8.868 | 36.000 | 44.868 | 2.39 | 24.7 | |
| 3 1 | 86.868 | -8.868 | 39.000 | 47.868 | 2.48 | 23.8 | |
| 3 2 | 92.868 | -8.868 | 42.000 | 50.868 | 2.57 | 22.9 | |
| 3 3 | 92.868 | -8.868 | 42.000 | 50.868 | 2.57 | 22.9 | Wall Pt. |

Table A.5.4.a  Results of the Method of Characteristics,
Properties for the First 33 Grid Points

## A.5.5 Engine Materials[15]

| Material | Applications | Temp. Range | Comments |
|---|---|---|---|
| Austenitic stainless steels | Nozzle tubing, ducts bolts, bellows, hydraulic tubing, washers, shims, turbine discs, injectors. | -423F to 600F | Susceptible to pitting and stress corrosion. |
| Martensitic stainless steels | Bearing-balls, races. | -423F to 300F | Susceptible to all forms of corrosion. |
| PH stainless steels | Valve parts-stems. | -110F to 200F | Susceptible to Hydrogen environment embrittlement. Stress corrodes in high strength tempers, marginal for cryogenic applications. |
| Nickel base superalloys | Impellers, inducers pump housing, valves, ducts, manifolds, bolts, turbine blades, turbine discs, shafts, bellows, stators, injectors. | -423F to 1500F | Susceptible to Hydrogen environment embrittlement. |

| | | | |
|---|---|---|---|
| Iron base superalloys | Struts, ducts, bellows, bolts, turbine, discs. | -423F to 1100F | Resistant to Hydrogen environment embrittlement. |
| Aluminum alloys | Pump housings, impellers, injectors, gear cases, brackets, valve bodies. | -423F to 200F | Often used as castings. |
| Copper alloys | Thrust chambers, injector rings, baffles. | -423F to 1000F | High oxygen grades susceptible to hydrogen reaction environment. |
| Titanium alloys | Impellers, inducers, pump housings, valve bodies, ducts, gimbal blocks, pressure bottles, hydraulic tubing. | -423F to 600F | Pyrophoric reaction in LOX, pure GOX, red fuming nitric acid. May absorb hydrogen above -110F. |
| Beryllium | Small thrust chambers | 70F to 1200F | Brittle, avoid all notches in design. Hazardous material, not weldable. |
| Cobalt alloys | Injector posts, ducts, springs, turbine blades. | -320F to 2100F | Vary in susceptibility to hydrogen environment embrittlement. |
| Low alloy steels | Thrust mounts, frames reinforcing bands, gears, shafts, bolts, bearings. | 70F to 300F | Susceptible to corrosion, marginal for cryogenic applications. |
| Fluorocarbon polymers | Seals, coatings, electrical insulation | -423F to 200F | Generally compatible with liquid oxygen. |
| Elastomers | O-rings, gaskets, sealants, electrical insulation, adhesives. | 70F to 300F | Not compatible with liquid oxygen. |
| Nickel | Nozzle tubing, electrodeposited close outs of coolant channels for combustion chambers. | -423F to 1000F | Susceptible to hydrogen environment embrittlement. |
| Carbon | Combustion chamber throat inserts, dynamic turbine seals. | -423F to 600F | Brittle Material |
| Ceramics | Protective coatings on turbine blades, nozzles, thrust chambers. | -423F to 1500F | High temperatures, brittle materials. |

## A.5.6 Representative LOX/LH$_2$ Engines[16] [17]

| System | Manufacturer | T(kN) | Isp(s) | O/F ratio | Mass(kg) |
|--------|-------------|-------|--------|-----------|----------|
| SSME | Rocketdyne | 2296 | 455 | 6.0 | 3150 |
| J2S | Rocketdyne | 1180 | 435 | 5.5 | 1560 |
| LE-5A | MHI (Japan) | 127 | 452 | 5.0 | 242 |
| HM-7B | SEP (France) | 62.7 | 444 | 4.8 | 155 |
| RL10A3-3 | Pratt & Whitney | 67.0 | 444 | 5.0 | 132 |
| RL10A3-3A | Pratt & Whitney | 73.4 | 446 | 5.0 | 138 |

## A.5.7 Structural Analysis

A finite element model using ANSYS version 44a was constructed to calculate the critical buckling and vibration loads for the main propulsion tanks. ANSYS STIF 63 shell elements were used to model the tanks. A plot of the finite element model and its boundary conditions is show below in Figure A.5.7.a.
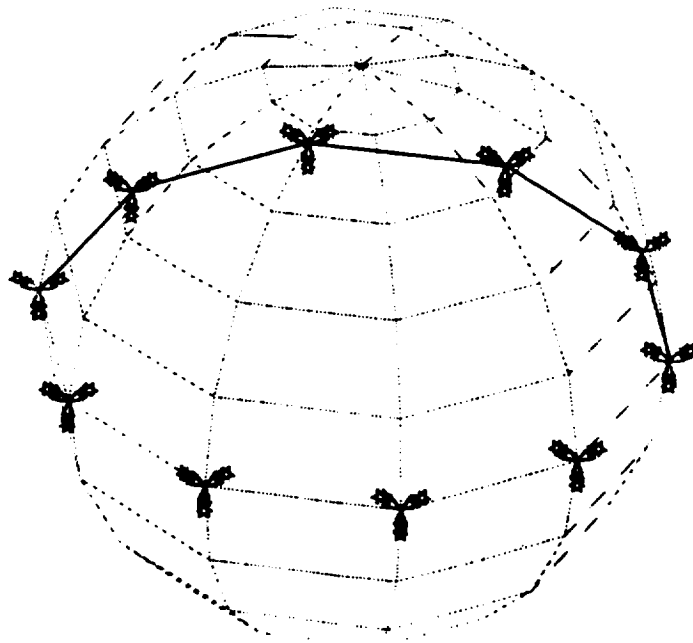


Figure A.5.7.a ANSYS Finite Element with Constraints

The ANSYS /BUCKLE routine was used to determine the critical G-load that the tanks could withstand without buckling. The ANSYS free vibration modal analysis routine was used to determine the fundamental frequency of the tanks. For safe operation the

fundamental frequency of the tanks should meet or exceed the natural frequency of the launch vehicle. Factors of safety were not applied to the G-Load and vibration values because of the use of pressure to stiffen the tanks upon launch. Figure A.5.7.b and Figure A.5.7.c below show the trade study between Al-1100 and Ti-6Al-4V respectively in the form of allowable G-load versus tank thickness. The following plots were used at an earlier design iteration to determine the critical loading for tanks of 0.410 meters in radius. The results of these analyses have been used in later iterations as the basis for which load and material to analyze in a more detailed manner for the final design presentation as found in section 5.10.
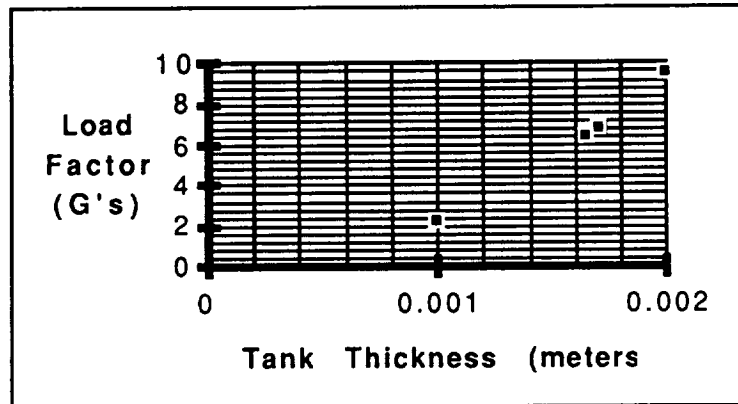


Figure A.5.7.b  Load Factor versus Tank Thickness (Al-1100 Alloy)
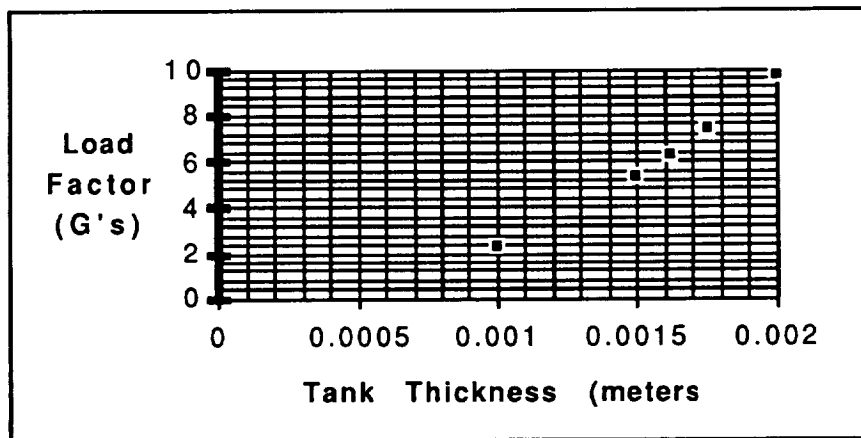


Figure A.5.7.c  Load Factor versus Tank Thickness (Ti-6Al-4V Alloy)

Figures A.5.7.b and A.5.7.c show that for launch load buckling the Al alloy only lags behind that of the Ti alloy by very little. Although the graphs of load factor versus tank thickness are not linear, a linear interpolation was used to get a tank thickness for the upper load limit of 6.5 g's by using a reiterative process through which two points closely surrounding this upper limit were found. From Figures A.5.7.b and A.5.7.c, the interpolation yields a required tank thickness for the Ti alloy of 1.65 mm while the required tank thickness for the Al alloy is only slightly larger at 1.67 mm. Because Al 1100-0's density is smaller than Ti-6Al-4V's density by nearly a factor of two, it is clear

that Al 1100-0 offers a significant mass savings. Mass for the 1.65 mm thick Ti alloy tank was 16 kg and the mass for the 1.67 mm thick Al alloy tank was 10 kg. Although the numbers are small, this is over a 25% savings.

After starting the vibration analysis for the tank configurations, it was soon found that, in fact, vibration launch loads will drive the thicknesses of the tanks. A comparison of the two candidate materials used in the above analysis showed that (although extremely close) an Al 1100-0 tank had a higher natural frequency than a Ti-6Al-4V tank of equal thickness and radius. Figures A.5.7.d and A.5.7.e show the plots of fundamental frequency versus tank thickness for the Al-100 Alloy and the Ti-6Al-4V Alloy respectively. Figure A.5.7.d shows that the necessary thickness to achieve a frequency of 35 Hz is 4 mm. A Al 1100-0 tank of this thickness has a mass of 24 kg. An equivalent tank constructed of our Ti alloy would have a mass of 39 kg. The mass savings seen here is much more significant than that realized in the buckling analysis because the numbers are now larger and the percent savings has risen to about 40%.

These results were used to provide a starting point for the final tank design iteration. The results showed the best material selection to continue analysis with, and they showed that in fact the vibration load induced by the launch platform is the critical load for the MOOSE main propulsion tanks. Tank structures for these types of systems are generally higher. It is thought that because of the empty configuration at launch, the MOOSE design has seen considerable tank mass savings since buckling is more of a critical load with full tanks. Because of the large propellant masses used in such systems, high G-loads imposed by launch platforms can create large tank thicknesses to withstand buckling. Because of the relatively low G-loading during MOOSE operation (2 g's maximum) and the near empty configuration of the tank at this time, it is clear that launch vibration loading is still the critical load for the tank structures.
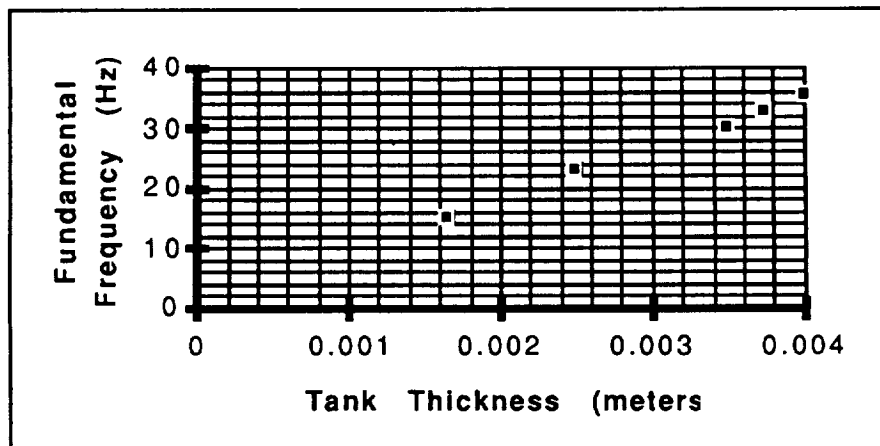


Figure A.5.7.d  Fundamental Frequency versus Tank Thickness (Al-1100 Alloy)
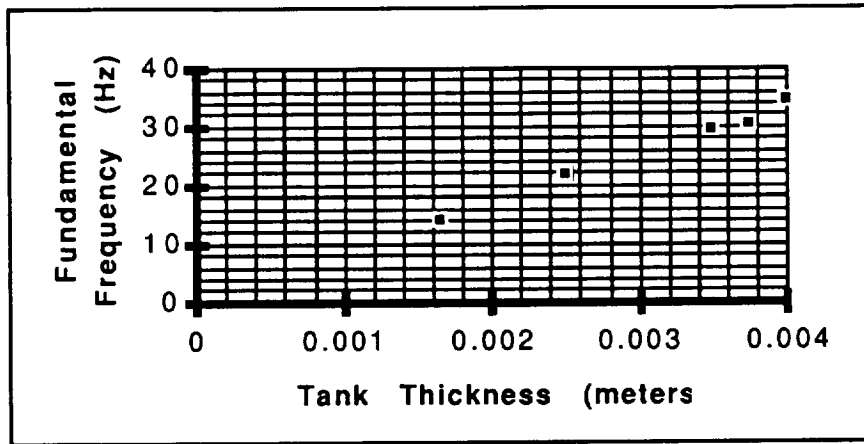
**Figure A.5.7.e** Fundamental Frequency versus Tank Thickness (Ti-6Al-4V)

## A.5.8 Slew Torque Calculations

Calculations of worst case torques showed that slew torques would apply the largest magnitude torques on the MOOSE vehicle. The figures listed below show the calculations made along each principal axis.

Figure A.5.8.a Worst Case Slew Torques about Ixx, prior to GEO Transfer Injection Burn
Figure A.5.8.b Worst Case Slew Torques about Iyy, prior to GEO Transfer Injection Burn
Figure A.5.8.c Worst Case Slew Torques about Izz, prior to GEO Transfer Injection Burn

Figure A.5.8.d Worst Case Slew Torques about Ixx, after GEO Satellite Servicing Operations
Figure A.5.8.e Worst Case Slew Torques about Iyy, after GEO Satellite Servicing Operations
Figure A.5.8.f Worst Case Slew Torques about Izz, after GEO Satellite Servicing Operations

Figure A5.8a Worst Case Slew Torques about Ixx, prior to GEO Transfer Injection Burn

Figure A5.8b Worst Case Slew Torques about Iyy, prior to GEO Transfer Injection Burn

Figure A5.8c Worst Case Slew Torques about Izz, prior to GEO Transfer Injection Burn

Legend:
- 15
- 20
- 30
- 40
- 50
- 60
- 120
- 180
- 240
- 300
- 360
- 420

Torque (Nm)

Maximum Attitude Excursion (rad)

Figure A5.8d Worst Case Slew Torques about Ixx, after GEO Satellite Servicing Operations
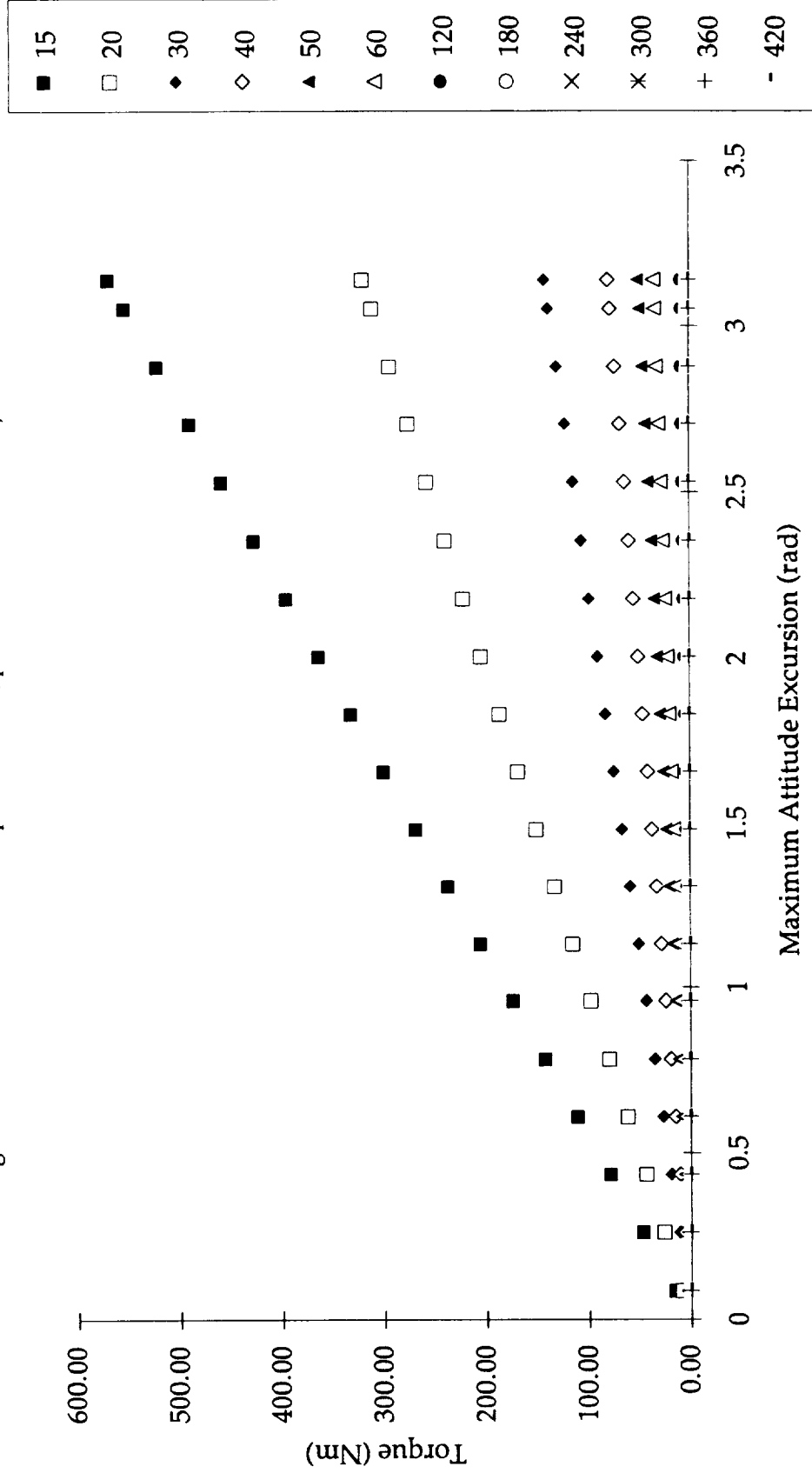
Figure A5.8e Worst Case Slew Torques about Iyy, after GEO Satellite Servicing Operations

Figure A5.8f  Worst Case Slew Torques about Izz, after GEO Satellite Servicing Operations

## A.5.9 Propellant Mass Calculations

Utilizing the baseline ΔV budget shown in Table 5.11.a with the main propulsion system consisting of LOX/LH2, a mass budget was derived for the potential primary RCS propellants consisting of a single monopropellant and five bipropellants. The potential cold gases for the secondary RCS were helium and nitrogen. The mass calculations were a two step process with the cold gas utilized in the secondary RCS varied for each process.

| | |
|---|---|
| A.5.9.1 | Hydrazine and Helium |
| A.5.9.2 | Oxygen / UDMH and Helium |
| A.5.9.3 | Oxygen / N2H4 and Helium |
| A.5.9.4 | N2O4 / 50-50 UDMH & N2H4 and Helium |
| A.5.9.5 | Fluorine / Hydrogen and Helium |
| | |
| A.5.9.6 | Hydrazine and Nitrogen |
| A.5.9.7 | Oxygen / UDMH and Nitrogen |
| A.5.9.8 | Oxygen / N2H4 and Nitrogen |
| A.5.9.9 | N2O4 / 50-50 UDMH & N2H4 and Nitrogen |
| A.5.9.10 | Fluorine / Hydrogen and Nitrogen |

## A.5.9.1 Hydrazine and Helium

| Assumptions | | All of the reserved fuel is used | | | |
|---|---|---|---|---|---|
| | | All of the reserved ΔV is used | | | |
| | | | | | |
| Isp | MAIN | LOX/LH2 | | 450 | sec |
| | rcs | HYDRAZINE | | 240 | sec |
| | COLD | HELIUM | | 179 | sec |
| Final Mass | | | | 3000 | Kg |
| | | | | | |

| Maneuvers | | Δ V | Final mass | Initial mass | Propellant mass used | Propulsion System |
|---|---|---|---|---|---|---|
| | | (m/s) | (kg) | (kg) | (kg) | used |
| Attitude Control Reserve | | 10 | 3000 | 3017 | 17 | COLD |
| Rendezvous & Docking | | 18 | 3017 | 3048 | 31 | COLD |
| Attitude Control Reserve | | 20 | 3048 | 3074 | 26 | rcs |
| LEO Circularization | | 122 | 3074 | 3160 | 86 | MAIN |
| Attitude Control Reserve | | 20 | 3160 | 3187 | 27 | rcs |
| Aerobraking Maneuver | | 67 | 3187 | 3279 | 92 | rcs |
| Attitude Control Reserve | | 5 | 3279 | 3286 | 7 | rcs |
| Mid Course Correction | | 20 | 3286 | 3314 | 28 | rcs |
| Main Propulsion Reserve | | 30 | 3314 | 3337 | 23 | MAIN |
| LEO Transfer Injection | | 1844 | 3337 | 5067 | 1730 | MAIN |
| GEO Operation | | 54 | 5067 | 5185 | 118 | rcs |
| GEO Operation | | 50 | 5185 | 5334 | 150 | COLD |
| GEO Operation | | 54 | 5334 | 5458 | 124 | rcs |
| Orbit Trim | | 9 | 5458 | 5479 | 21 | rcs |
| Main Propulsion Reserve | | 30 | 5479 | 5516 | 37 | MAIN |
| GEO Circularization | | 1762 | 5516 | 8222 | 2706 | MAIN |
| Attitude Control Reserve | | 5 | 8222 | 8240 | 17 | rcs |
| Mid Course Correction | | 15 | 8240 | 8293 | 53 | rcs |
| Main Propulsion Reserve | | 30 | 8293 | 8349 | 57 | MAIN |
| GEO Transfer Injection | | 2400 | 8349 | 14380 | 6031 | MAIN |
| Separation from Station | | 3 | 14380 | 14404 | 25 | COLD |
| | | | | | | |
| Total ΔV | | 6568 | m/s | | | |
| Initial Mass | | | | | 14404 | kg |
| Total Propellant Mass | | | | | 11404 | kg |
| Total Main Propellant Mass | | | | | 10669 | kg |
| Total RCS Propellant Mass | | | | | 512 | kg |
| Total Cold Gas Propellant Mass | | | | | 223 | kg |

## A.5.9.2 Oxygen and UDMH

| Assumptions | | All of the reserved fuel is used | | | | |
|---|---|---|---|---|---|---|
| | | All of the reserved ΔV is used | | | | |
| | | | | | | |
| Isp | MAIN | LOX/LH2 | | 450 | sec | |
| | rcs | OXYGEN/UDMH | | 295 | sec | |
| | COLD | HELIUM | | 179 | sec | |
| Final Mass | | | | 3000 | Kg | |
| | | | | | | |
| Maneuvers | | Δ V | Final mass | Initial mass | Propellant mass used | Propulsion System |
| | | (m/s) | (kg) | (kg) | (kg) | used |
| Attitude Control Reserve | | 10 | 3000 | 3017 | 17 | COLD |
| Rendezvous & Docking | | 18 | 3017 | 3048 | 31 | COLD |
| Attitude Control Reserve | | 20 | 3048 | 3069 | 21 | rcs |
| LEO Circularization | | 122 | 3069 | 3155 | 86 | MAIN |
| Attitude Control Reserve | | 20 | 3155 | 3177 | 22 | rcs |
| Aerobraking Maneuver | | 67 | 3177 | 3252 | 74 | rcs |
| Attitude Control Reserve | | 5 | 3252 | 3257 | 6 | rcs |
| Mid Course Correction | | 20 | 3257 | 3280 | 23 | rcs |
| Main Propulsion Reserve | | 30 | 3280 | 3302 | 22 | MAIN |
| LEO Transfer Injection | | 1844 | 3302 | 5014 | 1712 | MAIN |
| GEO Operation | | 54 | 5014 | 5109 | 94 | rcs |
| GEO Operation | | 50 | 5109 | 5256 | 148 | COLD |
| GEO Operation | | 54 | 5256 | 5355 | 99 | rcs |
| Orbit Trim | | 9 | 5355 | 5372 | 17 | rcs |
| Main Propulsion Reserve | | 30 | 5372 | 5409 | 37 | MAIN |
| GEO Circularization | | 1762 | 5409 | 8062 | 2653 | MAIN |
| Attitude Control Reserve | | 5 | 8062 | 8076 | 14 | rcs |
| Mid Course Correction | | 15 | 8076 | 8118 | 42 | rcs |
| Main Propulsion Reserve | | 30 | 8118 | 8173 | 55 | MAIN |
| GEO Transfer Injection | | 2400 | 8173 | 14077 | 5904 | MAIN |
| Separation from Station | | 3 | 14077 | 14101 | 24 | COLD |
| | | | | | | |
| Total ΔV | | 6568 | m/s | | | |
| Initial Mass | | | | | 14101 | kg |
| Total Propellant Mass | | | | | 11101 | kg |
| Total Main Propellant Mass | | | | | 10469 | kg |
| Total RCS Propellant Mass | | | | | 412 | kg |
| Total Cold Gas Propellant Mass | | | | | 220 | kg |

## A.5.9.3 Oxygen and N2H4

| Assumptions | | All of the reserved fuel is used | | | |
|---|---|---|---|---|---|
| | | All of the reserved ΔV is used | | | |
| | | | | | |
| Isp | MAIN | LOX/LH2 | | 450 | sec |
| | rcs | OXYGEN/N2H4 | | 301 | sec |
| | COLD | HELIUM | | 179 | sec |
| Final Mass | | | | 3000 | Kg |
| | | | | | |

| Maneuvers | | Δ V | Final mass | Initial mass | Propellant mass used | Propulsion System used |
|---|---|---|---|---|---|---|
| | | (m/s) | (kg) | (kg) | (kg) | |
| Attitude Control Reserve | | 10 | 3000 | 3017 | 17 | COLD |
| Rendezvous & Docking | | 18 | 3017 | 3048 | 31 | COLD |
| Attitude Control Reserve | | 20 | 3048 | 3069 | 21 | rcs |
| LEO Circularization | | 122 | 3069 | 3155 | 86 | MAIN |
| Attitude Control Reserve | | 20 | 3155 | 3176 | 21 | rcs |
| Aerobraking Maneuver | | 67 | 3176 | 3249 | 73 | rcs |
| Attitude Control Reserve | | 5 | 3249 | 3255 | 6 | rcs |
| Mid Course Correction | | 20 | 3255 | 3277 | 22 | rcs |
| Main Propulsion Reserve | | 30 | 3277 | 3299 | 22 | MAIN |
| LEO Transfer Injection | | 1844 | 3299 | 5010 | 1711 | MAIN |
| GEO Operation | | 54 | 5010 | 5102 | 92 | rcs |
| GEO Operation | | 50 | 5102 | 5250 | 147 | COLD |
| GEO Operation | | 54 | 5250 | 5347 | 97 | rcs |
| Orbit Trim | | 9 | 5347 | 5363 | 16 | rcs |
| Main Propulsion Reserve | | 30 | 5363 | 5399 | 37 | MAIN |
| GEO Circularization | | 1762 | 5399 | 8048 | 2649 | MAIN |
| Attitude Control Reserve | | 5 | 8048 | 8062 | 14 | rcs |
| Mid Course Correction | | 15 | 8062 | 8103 | 41 | rcs |
| Main Propulsion Reserve | | 30 | 8103 | 8158 | 55 | MAIN |
| GEO Transfer Injection | | 2400 | 8158 | 14051 | 5893 | MAIN |
| Separation from Station | | 3 | 14051 | 14075 | 24 | COLD |
| | | | | | | |
| Total ΔV | | 6568 | m/s | | | |
| Initial Mass | | | | | 14075 | kg |
| Total Propellant Mass | | | | | 11075 | kg |
| Total Main Propellant Mass | | | | | 10452 | kg |
| Total RCS Propellant Mass | | | | | 403 | kg |
| Total Cold Gas Propellant Mass | | | | | 220 | kg |

| A.5.9.4 N2O4 and 50-50 UDMH and N2H4 | | | | | |
|---|---|---|---|---|---|
| **Assumptions** | | All of the reserved fuel is used | | | |
| | | All of the reserved ΔV is used | | | |
| | | | | | |
| **Isp** | **MAIN** | LOX/LH2 | | 450 sec | |
| | rcs | N2O4/50-50UDMH | | 288 sec | |
| | COLD | HELIUM | | 179 sec | |
| **Final Mass** | | | | 3000 Kg | |
| | | | | | |
| **Maneuvers** | | Δ V | Final mass | Initial mass | Propellant mass used | Propulsion System used |
| | | (m/s) | (kg) | (kg) | (kg) | |
| Attitude Control Reserve | | 10 | 3000 | 3017 | 17 | COLD |
| Rendezvous & Docking | | 18 | 3017 | 3048 | 31 | COLD |
| Attitude Control Reserve | | 20 | 3048 | 3070 | 22 | rcs |
| LEO Circularization | | 122 | 3070 | 3156 | 86 | **MAIN** |
| Attitude Control Reserve | | 20 | 3156 | 3178 | 22 | rcs |
| Aerobraking Maneuver | | 67 | 3178 | 3255 | 76 | rcs |
| Attitude Control Reserve | | 5 | 3255 | 3260 | 6 | rcs |
| Mid Course Correction | | 20 | 3260 | 3284 | 23 | rcs |
| Main Propulsion Reserve | | 30 | 3284 | 3306 | 22 | **MAIN** |
| LEO Transfer Injection | | 1844 | 3306 | 5020 | 1714 | **MAIN** |
| GEO Operation | | 54 | 5020 | 5117 | 97 | rcs |
| GEO Operation | | 50 | 5117 | 5265 | 148 | COLD |
| GEO Operation | | 54 | 5265 | 5366 | 102 | rcs |
| Orbit Trim | | 9 | 5366 | 5383 | 17 | rcs |
| Main Propulsion Reserve | | 30 | 5383 | 5420 | 37 | **MAIN** |
| GEO Circularization | | 1762 | 5420 | 8079 | 2659 | **MAIN** |
| Attitude Control Reserve | | 5 | 8079 | 8093 | 14 | rcs |
| Mid Course Correction | | 15 | 8093 | 8136 | 43 | rcs |
| Main Propulsion Reserve | | 30 | 8136 | 8192 | 55 | **MAIN** |
| GEO Transfer Injection | | 2400 | 8192 | 14109 | 5917 | **MAIN** |
| Separation from Station | | 3 | 14109 | 14133 | 24 | COLD |
| | | | | | |
| Total ΔV | | 6568 | m/s | | | |
| Initial Mass | | | | | 14133 | kg |
| Total Propellant Mass | | | | | 11133 | kg |
| Total Main Propellant Mass | | | | | 10490 | kg |
| Total RCS Propellant Mass | | | | | 422 | kg |
| Total Cold Gas Propellant Mass | | | | | 220 | kg |

## A.5.9.5 Fluorine and Hydrogen

| Assumptions | | All of the reserved fuel is used | | | |
|---|---|---|---|---|---|
| | | All of the reserved ΔV is used | | | |
| | | | | | |
| Isp | MAIN | LOX/LH2 | | 450 | sec |
| | rcs | FLUORINE/HYDROGEN | | 398 | sec |
| | COLD | HELIUM | | 179 | sec |
| Final Mass | | | | 3000 | Kg |
| | | | | | |
| Maneuvers | | Δ V | Final mass | Initial mass | Propellant mass used | Propulsion System used |
| | | (m/s) | (kg) | (kg) | (kg) | |
| Attitude Control Reserve | | 10 | 3000 | 3017 | 17 | COLD |
| Rendezvous & Docking | | 18 | 3017 | 3048 | 31 | COLD |
| Attitude Control Reserve | | 20 | 3048 | 3064 | 16 | rcs |
| LEO Circularization | | 122 | 3064 | 3150 | 86 | MAIN |
| Attitude Control Reserve | | 20 | 3150 | 3166 | 16 | rcs |
| Aerobraking Maneuver | | 67 | 3166 | 3221 | 55 | rcs |
| Attitude Control Reserve | | 5 | 3221 | 3225 | 4 | rcs |
| Mid Course Correction | | 20 | 3225 | 3241 | 17 | rcs |
| Main Propulsion Reserve | | 30 | 3241 | 3263 | 22 | MAIN |
| LEO Transfer Injection | | 1844 | 3263 | 4956 | 1692 | MAIN |
| GEO Operation | | 54 | 4956 | 5025 | 69 | rcs |
| GEO Operation | | 50 | 5025 | 5170 | 145 | COLD |
| GEO Operation | | 54 | 5170 | 5242 | 72 | rcs |
| Orbit Trim | | 9 | 5242 | 5254 | 12 | rcs |
| Main Propulsion Reserve | | 30 | 5254 | 5290 | 36 | MAIN |
| GEO Circularization | | 1762 | 5290 | 7884 | 2595 | MAIN |
| Attitude Control Reserve | | 5 | 7884 | 7895 | 10 | rcs |
| Mid Course Correction | | 15 | 7895 | 7925 | 30 | rcs |
| Main Propulsion Reserve | | 30 | 7925 | 7979 | 54 | MAIN |
| GEO Transfer Injection | | 2400 | 7979 | 13742 | 5763 | MAIN |
| Separation from Station | | 3 | 13742 | 13766 | 23 | COLD |
| | | | | | |
| Total ΔV | | 6568 | m/s | | | |
| Initial Mass | | | | | 13766 | kg |
| Total Propellant Mass | | | | | 10766 | kg |
| Total Main Propellant Mass | | | | | 10248 | kg |
| Total RCS Propellant Mass | | | | | 301 | kg |
| Total Cold Gas Propellant Mass | | | | | 217 | kg |

## A.5.9.6 Hydrazine and Nitrogen

| Assumptions | | All of the reserved fuel is used | | | |
|---|---|---|---|---|---|
| | | All of the reserved ΔV is used | | | |
| | | | | | |
| Isp | MAIN | LOX/LH2 | | 450 | sec |
| | rcs | HYDRAZINE | | 240 | sec |
| | COLD | NITROGEN | | 76 | sec |
| Final Mass | | | | 3000 | Kg |
| | | | | | |
| Maneuvers | | Δ V | Final mass | Initial mass | Propellant mass used | Propulsion System |
| | | (m/s) | (kg) | (kg) | (kg) | used |
| Attitude Control Reserve | | 10 | 3000 | 3041 | 41 | COLD |
| Rendezvous & Docking | | 18 | 3041 | 3115 | 74 | COLD |
| Attitude Control Reserve | | 20 | 3115 | 3141 | 27 | rcs |
| LEO Circularization | | 122 | 3141 | 3229 | 88 | MAIN |
| Attitude Control Reserve | | 20 | 3229 | 3257 | 28 | rcs |
| Aerobraking Maneuver | | 67 | 3257 | 3351 | 94 | rcs |
| Attitude Control Reserve | | 5 | 3351 | 3358 | 7 | rcs |
| Mid Course Correction | | 20 | 3358 | 3387 | 29 | rcs |
| Main Propulsion Reserve | | 30 | 3387 | 3410 | 23 | MAIN |
| LEO Transfer Injection | | 1844 | 3410 | 5178 | 1768 | MAIN |
| GEO Operation | | 54 | 5178 | 5298 | 120 | rcs |
| GEO Operation | | 50 | 5298 | 5665 | 367 | COLD |
| GEO Operation | | 54 | 5665 | 5797 | 131 | rcs |
| Orbit Trim | | 9 | 5797 | 5819 | 22 | rcs |
| Main Propulsion Reserve | | 30 | 5819 | 5859 | 40 | MAIN |
| GEO Circularization | | 1762 | 5859 | 8733 | 2874 | MAIN |
| Attitude Control Reserve | | 5 | 8733 | 8751 | 19 | rcs |
| Mid Course Correction | | 15 | 8751 | 8807 | 56 | rcs |
| Main Propulsion Reserve | | 30 | 8807 | 8867 | 60 | MAIN |
| GEO Transfer Injection | | 2400 | 8867 | 15272 | 6405 | MAIN |
| Separation from Station | | 3 | 15272 | 15334 | 62 | COLD |
| | | | | | | |
| Total ΔV | | 6568 | m/s | | | |
| Initial Mass | | | | | 15334 | kg |
| Total Propellant Mass | | | | | 12334 | kg |
| Total Main Propellant Mass | | | | | 11258 | kg |
| Total RCS Propellant Mass | | | | | 532 | kg |
| Total Cold Gas Propellant Mass | | | | | 544 | kg |

| A.5.9.7 Oxygen and UDMH | | | | | |
|---|---|---|---|---|---|
| **Assumptions** | | All of the reserved fuel is used | | | |
| | | All of the reserved ΔV is used | | | |
| | | | | | |
| **Isp** | **MAIN** | LOX/LH2 | | 450 | sec |
| | rcs | OXYGEN/UDMH | | 295 | sec |
| | COLD | NITROGEN | | 76 | sec |
| **Final Mass** | | | | 3000 | Kg |
| | | | | | |
| **Maneuvers** | | Δ V | Final | Initial | Propellant | Propulsion |
| | | | mass | mass | mass used | System |
| | | (m/s) | (kg) | (kg) | (kg) | used |
| Attitude Control Reserve | | 10 | 3000 | 3041 | 41 | COLD |
| Rendezvous & Docking | | 18 | 3041 | 3115 | 74 | COLD |
| Attitude Control Reserve | | 20 | 3115 | 3136 | 22 | rcs |
| LEO Circularization | | 122 | 3136 | 3224 | 88 | **MAIN** |
| Attitude Control Reserve | | 20 | 3224 | 3247 | 22 | rcs |
| Aerobraking Maneuver | | 67 | 3247 | 3323 | 76 | rcs |
| Attitude Control Reserve | | 5 | 3323 | 3328 | 6 | rcs |
| Mid Course Correction | | 20 | 3328 | 3352 | 23 | rcs |
| Main Propulsion Reserve | | 30 | 3352 | 3374 | 23 | **MAIN** |
| LEO Transfer Injection | | 1844 | 3374 | 5124 | 1750 | **MAIN** |
| GEO Operation | | 54 | 5124 | 5220 | 97 | rcs |
| GEO Operation | | 50 | 5220 | 5583 | 362 | COLD |
| GEO Operation | | 54 | 5583 | 5688 | 105 | rcs |
| Orbit Trim | | 9 | 5688 | 5705 | 18 | rcs |
| Main Propulsion Reserve | | 30 | 5705 | 5744 | 39 | **MAIN** |
| GEO Circularization | | 1762 | 5744 | 8562 | 2818 | **MAIN** |
| Attitude Control Reserve | | 5 | 8562 | 8577 | 15 | rcs |
| Mid Course Correction | | 15 | 8577 | 8622 | 45 | rcs |
| Main Propulsion Reserve | | 30 | 8622 | 8680 | 59 | **MAIN** |
| GEO Transfer Injection | | 2400 | 8680 | 14950 | 6270 | **MAIN** |
| Separation from Station | | 3 | 14950 | 15010 | 60 | COLD |
| | | | | | |
| Total ΔV | | 6568 | m/s | | |
| Initial Mass | | | | | 15010 | kg |
| Total Propellant Mass | | | | | 12010 | kg |
| Total Main Propellant Mass | | | | | 11046 | kg |
| Total RCS Propellant Mass | | | | | 428 | kg |
| Total Cold Gas Propellant Mass | | | | | 537 | kg |

## A.5.9.8 Oxygen and N2H4

| Assumptions | | All of the reserved fuel is used | | | | |
|---|---|---|---|---|---|---|
| | | All of the reserved ΔV is used | | | | |
| | | | | | | |
| Isp | MAIN | LOX/LH2 | | 450 | sec | |
| | rcs | OXYGEN/N2H4 | | 301 | sec | |
| | COLD | NITROGEN | | 76 | sec | |
| Final Mass | | | | 3000 | Kg | |
| | | | | | | |
| Maneuvers | | Δ V | Final mass (m/s) | Initial mass (kg) | Propellant mass used (kg) | Propulsion System used |
| Attitude Control Reserve | | 10 | 3000 | 3041 | 41 | COLD |
| Rendezvous & Docking | | 18 | 3041 | 3115 | 74 | COLD |
| Attitude Control Reserve | | 20 | 3115 | 3136 | 21 | rcs |
| LEO Circularization | | 122 | 3136 | 3224 | 88 | MAIN |
| Attitude Control Reserve | | 20 | 3224 | 3246 | 22 | rcs |
| Aerobraking Maneuver | | 67 | 3246 | 3320 | 74 | rcs |
| Attitude Control Reserve | | 5 | 3320 | 3326 | 6 | rcs |
| Mid Course Correction | | 20 | 3326 | 3348 | 23 | rcs |
| Main Propulsion Reserve | | 30 | 3348 | 3371 | 23 | MAIN |
| LEO Transfer Injection | | 1844 | 3371 | 5119 | 1748 | MAIN |
| GEO Operation | | 54 | 5119 | 5214 | 94 | rcs |
| GEO Operation | | 50 | 5214 | 5575 | 362 | COLD |
| GEO Operation | | 54 | 5575 | 5678 | 103 | rcs |
| Orbit Trim | | 9 | 5678 | 5696 | 17 | rcs |
| Main Propulsion Reserve | | 30 | 5696 | 5734 | 39 | MAIN |
| GEO Circularization | | 1762 | 5734 | 8548 | 2813 | MAIN |
| Attitude Control Reserve | | 5 | 8548 | 8562 | 14 | rcs |
| Mid Course Correction | | 15 | 8562 | 8606 | 44 | rcs |
| Main Propulsion Reserve | | 30 | 8606 | 8664 | 59 | MAIN |
| GEO Transfer Injection | | 2400 | 8664 | 14923 | 6258 | MAIN |
| Separation from Station | | 3 | 14923 | 14983 | 60 | COLD |
| | | | | | | |
| Total ΔV | | 6568 | m/s | | | |
| Initial Mass | | | | | 14983 | kg |
| Total Propellant Mass | | | | | 11983 | kg |
| Total Main Propellant Mass | | | | | 11027 | kg |
| Total RCS Propellant Mass | | | | | 419 | kg |
| Total Cold Gas Propellant Mass | | | | | 537 | kg |

## A.5.9.9 N2O4 and 50-50 UDMH and N2H4

| Assumptions | | All of the reserved fuel is used | | | | |
|---|---|---|---|---|---|---|
| | | All of the reserved ΔV is used | | | | |
| | | | | | | |
| Isp | MAIN | LOX/LH2 | | 450 | sec | |
| | rcs | N2O4/50-50UDMH | | 288 | sec | |
| | COLD | NITROGEN | | 76 | sec | |
| Final Mass | | | | 3000 | Kg | |
| | | | | | | |

| Maneuvers | | Δ V | Final mass | Initial mass | Propellant mass used | Propulsion System used |
|---|---|---|---|---|---|---|
| | | (m/s) | (kg) | (kg) | (kg) | |
| Attitude Control Reserve | | 10 | 3000 | 3041 | 41 | COLD |
| Rendezvous & Docking | | 18 | 3041 | 3115 | 74 | COLD |
| Attitude Control Reserve | | 20 | 3115 | 3137 | 22 | rcs |
| LEO Circularization | | 122 | 3137 | 3225 | 88 | MAIN |
| Attitude Control Reserve | | 20 | 3225 | 3248 | 23 | rcs |
| Aerobraking Maneuver | | 67 | 3248 | 3326 | 78 | rcs |
| Attitude Control Reserve | | 5 | 3326 | 3332 | 6 | rcs |
| Mid Course Correction | | 20 | 3332 | 3355 | 24 | rcs |
| Main Propulsion Reserve | | 30 | 3355 | 3378 | 23 | MAIN |
| LEO Transfer Injection | | 1844 | 3378 | 5130 | 1752 | MAIN |
| GEO Operation | | 54 | 5130 | 5229 | 99 | rcs |
| GEO Operation | | 50 | 5229 | 5591 | 363 | COLD |
| GEO Operation | | 54 | 5591 | 5699 | 108 | rcs |
| Orbit Trim | | 9 | 5699 | 5717 | 18 | rcs |
| Main Propulsion Reserve | | 30 | 5717 | 5756 | 39 | MAIN |
| GEO Circularization | | 1762 | 5756 | 8580 | 2824 | MAIN |
| Attitude Control Reserve | | 5 | 8580 | 8595 | 15 | rcs |
| Mid Course Correction | | 15 | 8595 | 8641 | 46 | rcs |
| Main Propulsion Reserve | | 30 | 8641 | 8700 | 59 | MAIN |
| GEO Transfer Injection | | 2400 | 8700 | 14984 | 6284 | MAIN |
| Separation from Station | | 3 | 14984 | 15044 | 60 | COLD |
| | | | | | | |
| Total ΔV | | 6568 | m/s | | | |
| Initial Mass | | | | | 15044 | kg |
| Total Propellant Mass | | | | | 12044 | kg |
| Total Main Propellant Mass | | | | | 11068 | kg |
| Total RCS Propellant Mass | | | | | 439 | kg |
| Total Cold Gas Propellant Mass | | | | | 538 | kg |

| A.5.9.10 Fluorine and Hydrogen | | | | | |
|---|---|---|---|---|---|
| **Assumptions** | | All of the reserved fuel is used | | | |
| | | All of the reserved ΔV is used | | | |
| | | | | | |
| **Isp** | **MAIN** | LOX/LH2 | | 450 sec | |
| | rcs | FLUORINE/HYDROGEN | | 398 sec | |
| | COLD | NITROGEN | | 76 sec | |
| **Final Mass** | | | | 3000 Kg | |
| | | | | | |
| **Maneuvers** | | Δ V | Final | Initial | Propellant | Propulsion |
| | | | mass | mass | mass used | System |
| | | (m/s) | (kg) | (kg) | (kg) | used |
| Attitude Control Reserve | | 10 | 3000 | 3041 | 41 | COLD |
| Rendezvous & Docking | | 18 | 3041 | 3115 | 74 | COLD |
| Attitude Control Reserve | | 20 | 3115 | 3131 | 16 | rcs |
| LEO Circularization | | 122 | 3131 | 3219 | 88 | **MAIN** |
| Attitude Control Reserve | | 20 | 3219 | 3235 | 17 | rcs |
| Aerobraking Maneuver | | 67 | 3235 | 3291 | 56 | rcs |
| Attitude Control Reserve | | 5 | 3291 | 3295 | 4 | rcs |
| Mid Course Correction | | 20 | 3295 | 3312 | 17 | rcs |
| Main Propulsion Reserve | | 30 | 3312 | 3335 | 23 | **MAIN** |
| LEO Transfer Injection | | 1844 | 3335 | 5064 | 1729 | **MAIN** |
| GEO Operation | | 54 | 5064 | 5134 | 71 | rcs |
| GEO Operation | | 50 | 5134 | 5490 | 356 | COLD |
| GEO Operation | | 54 | 5490 | 5567 | 76 | rcs |
| Orbit Trim | | 9 | 5567 | 5580 | 13 | rcs |
| Main Propulsion Reserve | | 30 | 5580 | 5618 | 38 | **MAIN** |
| GEO Circularization | | 1762 | 5618 | 8374 | 2756 | **MAIN** |
| Attitude Control Reserve | | 5 | 8374 | 8384 | 11 | rcs |
| Mid Course Correction | | 15 | 8384 | 8417 | 32 | rcs |
| Main Propulsion Reserve | | 30 | 8417 | 8474 | 57 | **MAIN** |
| GEO Transfer Injection | | 2400 | 8474 | 14595 | 6121 | **MAIN** |
| Separation from Station | | 3 | 14595 | 14654 | 59 | COLD |
| | | | | | |
| Total ΔV | | 6568 | m/s | | | |
| Initial Mass | | | | | 14654 | kg |
| Total Propellant Mass | | | | | 11654 | kg |
| Total Main Propellant Mass | | | | | 10811 | kg |
| Total RCS Propellant Mass | | | | | 312 | kg |
| Total Cold Gas Propellant Mass | | | | | 530 | kg |

## A.5.10 Total Impulse & Mass Calculations for Primary RCS Thrusters

Assume 20 hours on-time

| | |
|---|---|
| 20 hours= | 72000 sec |
| | |
| Pulse time on | 1 sec |
| Pulse interval | 33 sec |
| | |
| On time/ Pulse Intervals | 2182 pulses |

Two thrusters firing at any given time

| | |
|---|---|
| Pulses per firing thruster | 1091 |

| | |
|---|---|
| M=Mass | |
| T=Thrust | 500 N |
| t=on time | 1091 sec |
| Isp=Specific Impulse | 223 N |
| g=Acceleration of gravity | 9.81 m/s^2 |
| | |
| M=T*t/Isp/g | 249 kg |

| | |
|---|---|
| Two thrusters firing at any time requires a mass of | 499 kg |
| | |
| Average Thrust | 366 N |
| Time | 1091 sec |
| | |
| Total Impulse | 399273 Nsec |

## A.5.11 Total Impulse & Mass Calculations for Secondary RCS Thrusters

Assume 10 hours on-time

| | | |
|---|---|---|
| 10 hours= | 36000 | sec |

| | | |
|---|---|---|
| Pulse Rise/Decay | 9.87 | msec |
| Pulse time on | 1 | sec |
| Total Pulse time on | 1.00987 | sec |
| Pulse interval | 10 | sec |
| On time/ Pulse Intervals | 3600 | pulses |

Two thrusters firing at any given time

| | |
|---|---|
| Pulses per firing thruster | 1800 |

| | | |
|---|---|---|
| M=Mass | | |
| T=Thrust | 89 | N |
| t=on time | 1800 | sec |
| Isp=Specific Impulse | 179 | N |
| g=Acceleration of gravity | 9.81 | m/s^2 |

| | | |
|---|---|---|
| M=T*t/Isp/g | 91 | kg |

| | | |
|---|---|---|
| Two thrusters firing at any time requires a mass of | 182 | kg |

| | | |
|---|---|---|
| Average Thrust | 89 | N |
| Time | 1800 | sec |

| | | |
|---|---|---|
| Total Impulse | 160200 | Nsec |

## A.5.12 Hydrazine Tank Volume Calculations

| | |
|---|---|
| Blowdown Ratio | R |
| Pressurant Gas Volume | Vgi |
| Propellant Volume | Vp |

R=(Vgi + Vp)/ Vgi

| | |
|---|---|
| R | 4.2000 |

| | |
|---|---|
| Propellant Mass | 512 kg |
| Propellant Density | 1.0230 g/cm^3 |
| Propellant Volume | 0.5005 m^3 |

| | |
|---|---|
| Pressurant Gas Volume | 0.1564 m^3 |
| Pressurant Gas Density | 69.2600 kg/m^3 |
| Pressurant Gas Mass | 10.8325 kg |

| | |
|---|---|
| Total Volume | 0.6569 m^3 |
| Total Mass | 522.83 kg |

| | |
|---|---|
| Radius-1 Tank | 0.5393 m |
| Radius-2 Tanks | 0.4280 m |

## A.5.12.1 Helium Tank Volume Calculations

| Assuming Ideal Gas | | | | | | | | |
|---|---|---|---|---|---|---|---|---|
| PV=mRT | | | | | | | | |
| R | 2077.3 | J/kgK | | | | | | |
| Temperature | 300 | K | | | | | | |
| | | | | | | | | |
| | | | | | | | | |
| Delta V | 100 | m/s | | | | | | |
| Mass | 377 | kg | | | | Radius with | | Radius with |
| Pressure | | | | | Volume | 2 tanks | | 4 tanks |
| 1000 | psi | | 6.89E+06 | N/m^2 | 34.08 m^3 | 1.596 m | | 1.267 m |
| 2000 | psi | | 1.38E+07 | N/m^2 | 17.04 m^3 | 1.267 m | | 1.006 m |
| 3000 | psi | | 2.07E+07 | N/m^2 | 11.36 m^3 | 1.107 m | | 0.878 m |
| 4000 | psi | | 2.76E+07 | N/m^2 | 8.52 m^3 | 1.006 m | | 0.798 m |
| 5000 | psi | | 3.45E+07 | N/m^2 | 6.82 m^3 | 0.934 m | | 0.741 m |
| 6000 | psi | | 4.14E+07 | N/m^2 | 5.68 m^3 | 0.878 m | | 0.697 m |
| | | | | | | | | |
| Delta V | 50 | m/s | | | | | | |
| Mass | 223 | kg | | | | | | |
| Pressure | | | | | | | | |
| 1000 | psi | | 6.89E+06 | N/m^2 | 20.16 m^3 | 1.340 m | | 1.064 m |
| 2000 | psi | | 1.38E+07 | N/m^2 | 10.08 m^3 | 1.064 m | | 0.844 m |
| 3000 | psi | | 2.07E+07 | N/m^2 | 6.72 m^3 | 0.929 m | | 0.737 m |
| 4000 | psi | | 2.76E+07 | N/m^2 | 5.04 m^3 | 0.844 m | | 0.670 m |
| 5000 | psi | | 3.45E+07 | N/m^2 | 4.03 m^3 | 0.784 m | | 0.622 m |
| 6000 | psi | | 4.14E+07 | N/m^2 | 3.36 m^3 | 0.737 m | | 0.585 m |
| | | | | | | | | |
| Delta V | 40 | m/s | | | | | | |
| Mass | 192 | kg | | | | | | |
| Pressure | | | | | | | | |
| 1000 | psi | | 6.89E+06 | N/m^2 | 17.35 m^3 | 1.275 m | | 1.012 m |
| 2000 | psi | | 1.38E+07 | N/m^2 | 8.68 m^3 | 1.012 m | | 0.803 m |
| 3000 | psi | | 2.07E+07 | N/m^2 | 5.78 m^3 | 0.884 m | | 0.702 m |
| 4000 | psi | | 2.76E+07 | N/m^2 | 4.34 m^3 | 0.803 m | | 0.637 m |
| 5000 | psi | | 3.45E+07 | N/m^2 | 3.47 m^3 | 0.745 m | | 0.592 m |
| 6000 | psi | | 4.14E+07 | N/m^2 | 2.89 m^3 | 0.702 m | | 0.557 m |
| | | | | | | | | |
| Delta V | 30 | m/s | | | | | | |
| Mass | 162 | kg | | | | | | |
| Pressure | | | | | | | | |
| 1000 | psi | | 6.89E+06 | N/m^2 | 14.64 m^3 | 1.205 m | | 0.956 m |
| 2000 | psi | | 1.38E+07 | N/m^2 | 7.32 m^3 | 0.956 m | | 0.759 m |
| 3000 | psi | | 2.07E+07 | N/m^2 | 4.88 m^3 | 0.835 m | | 0.663 m |
| 4000 | psi | | 2.76E+07 | N/m^2 | 3.66 m^3 | 0.759 m | | 0.602 m |
| 5000 | psi | | 3.45E+07 | N/m^2 | 2.93 m^3 | 0.704 m | | 0.559 m |
| 6000 | psi | | 4.14E+07 | N/m^2 | 2.44 m^3 | 0.663 m | | 0.526 m |
| | | | | | | | | |
| Delta V | 25 | m/s | | | | | | |
| Mass | 147 | kg | | | | | | |
| Pressure | | | | | | | | |
| 1000 | psi | | 6.89E+06 | N/m^2 | 13.29 m^3 | 1.166 m | | 0.926 m |
| 2000 | psi | | 1.38E+07 | N/m^2 | 6.64 m^3 | 0.926 m | | 0.735 m |
| 3000 | psi | | 2.07E+07 | N/m^2 | 4.43 m^3 | 0.809 m | | 0.642 m |
| 4000 | psi | | 2.76E+07 | N/m^2 | 3.32 m^3 | 0.735 m | | 0.583 m |
| 5000 | psi | | 3.45E+07 | N/m^2 | 2.66 m^3 | 0.682 m | | 0.541 m |
| 6000 | psi | | 4.14E+07 | N/m^2 | 2.21 m^3 | 0.642 m | | 0.509 m |

# A.5.13 Spider Truss Analysis

Trade studies for the spider truss configuration began with selection of the appropriate cross section for the spider truss members. Through fairly lengthy spread sheet calculations, circular and quadrilateral tubing cross sections were analyzed. It was found that the circular cross section tube is more efficient because of its smaller $c/I_{xx}$ ratio and comparable mass to that of a quadrilateral cross section tube.

A starting point was developed by placing a circular cross section tube in a cantilever configuration and submitting it to a load that the entire spider truss would encounter during actual MOOSE operations. At the time of these trade studies, the spider truss had an overall length of 1.5 m. It was found that for such a beam a $c/I_{xx}$ ratio of approximately $326 \times 10^3$ m$^{-3}$ was needed to bring the beam near the ultimate strength of the graphite composite (158 MPa). From the previous cross section trade study, a cross section of outer radius 2.5 cm and inner radius of 2.2 cm was chosen to begin the cross section configuration trade study. The following four configurations were then analyzed:

In configuration #1, all the spider truss beams were modeled with outer radius 2.5 cm and inner radius 2 cm. Configuration #2 consisted of all members with an outer radius of 1.25 cm and an inner radius of 1 cm. In configuration #3, all the beams of the inner cross member were modeled as in configuration #2 and the rest of the beams had an outer radius of 7 mm and an inner radius of 5 mm. And finally, configuration #4 saw the removal of the outer cross member and cross sections exactly as described for configuration #3.

The loading diagram and the loading table for these trade studies are shown in Figure A.5.13.a and Table A.5.13.a respectively. The results from these four configurations led to the single analysis done in section 5.11.8.2. As will be seen, configuration #3 provided an excellent model from which analyses could take place despite design changes in RCS configuration or operation. Table A.5.13.b shows the results from the analyses of these four configuration in the form of maximum stress and maximum tip deflection.

After preliminary estimations were made for the configurations, ANSYS models were constructed for comparative purposes and to nail down the more difficult maximum tip displacement number.
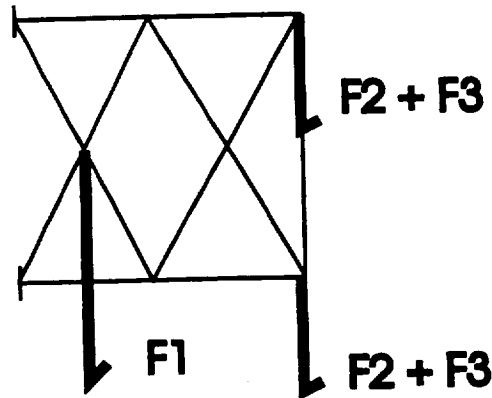
**Figure A.5.13.a Trade Study Loading Diagram**

| | Loads | Source |
|---|---|---|
| F1 | 25,310 N | RCS tank (3 g's) |
| F2 | 250 N | RCS nozzle firing |
| F3 | 136 N | RCS nozzle (3 g's) |
| Inertia | 6 g's | Brake Maneuver[18] |

**Table A.5.13.a Trade Study Loading Table**

| Configuration | s max | End Displacement |
|---|---|---|
| 1 | .49E8 Pa | .304E-3 m |
| 2 | .113E9 Pa | .753E-3 m |
| 3 | .114E9 Pa | .775E-3 m |
| 4 | .122E9 PA | 8.8 mm |

**Table A.5.13.b Trade Study Results**

Based on results shown in Table A.5.13.b, it was clear that at this iteration configuration #3 was the best choice for the MOOSE RCS Spider Truss. The stress results were right around the two-thirds stipulation mentioned earlier and the displacement requirement. Both of these points were introduced in section 5.11.8.2.

Finally, a vibration check was made under the assumption that the four main spider truss beams of 1.5 meters in length were modeled together as one beam with a tip mass simulated by the RCS nozzles. The following equation was used to calculate a natural frequency of 315 Hz.

$$\text{Natural Frequency} = .276 \cdot \sqrt{\frac{AE}{(mL^3 + .236M_BL^3)}}$$

It is recommended that a full vibration analysis be conducted for the spider truss.

## A.5.14 Helium Tank Material and Mass Analysis

Tank Pressure $(P_{tanks})= 4.137 \times 10^7$ N/m$^2$
Radius (R) = 0.585 m
Surface Area = $4\pi R^2$

Stress = $(P_{tanks}R)/2t$

| Material | Stress (1.1 Safety Factor) | Thickness (m) | Mass (kg) |
|---|---|---|---|
| Al 6061 - T6 | $2.806 \times 10^8$ | .04312 | 502 |
| Al 7075 -T6 | $4.689 \times 10^8$ | .0258 | 307 |
| Ti 6 % Al, 4% V | $8.97 \times 10^8$ | .0169 | 243 |
| Ti 8-1-1 | $10.91 \times 10^8$ | .0166 | 234 |

**Table A.5.14.a** Secondary RCS Tank Materials Study

# Appendix A6.1 ADCS

## Torques from cyclic and secular disturbances

### Cyclic disturbances

- **Gravity gradient torque at GEO**

$$Tg = \frac{3\mu}{R^3} |Izz-Iyy| \Theta$$

$\mu$ = earths gravity constant $\quad 3.9x10^3 \frac{km^3}{s^2}$

$\quad \Theta$ = off-axis from nadir = 5 deg.

$\quad R$ = orbital radius = 46028 km

$$Tg = 9.168x10^{-5} \text{ N m}$$

- **Solar Radiation Torque at GEO**

$$Tsp = PsAsLs(1+q) \cos q$$

$Ps$ = solar constant = $4.617x10^{-6}$ N m

$As$ = Area of surface = $10 \text{ m}^2$

$Ls$ = center of press. to center of-mass
     offset = 1 m

$q$ = angle of incidence of sun = 90 deg.

$\quad q$ = reflective factor * .6

$$Tsp = 7.38 \times 10^{-5} \text{ N m}$$

Note: solar radiation press. Tsp is highly dependent
     on the surface being illuminated. For our vehicle
     it will be mostly reflective surfaces.

## Secular Torque Disturbances

• Aerodynamic Torque at GEO

$$Ta = \sum_{i=1}^{n} F_i l_i$$

$$F_i = 0.5\left[rC_d A V^2\right]$$

$C_d$ = coefficient of drag of each part

A = effected area of each part

V = velocity of spacecraft

r = at GEO ≈ 0

so

Ta ≈ 0

li = dist. from c.g. of part
to c.g. of spacecraft.

# Appendix A6.2 Navigation and Tracking

## A6.2.1 Linear Navigation and Velocity Update Systems

Ground Tracking / TDRSS - Provides accuracy from 50m to several hundred meters when tracking objects in LEO. This system, however requires a full ground crew during each vehicle mission and does not work for objects in GEO.

Space Sextant - Provides 250m accuracy. The unit however is large compared to other units (25 kg, 0.4 cubic meters) and requires more power (50 W) than other systems. The unit also requires a 24 hour scan time to achieve the stated accuracy.

Global Positioning System - Provides 25 m accuracy at LEO. The system is ideal for use in LEO (9.72 x 5 x 2 cubic inches, 1.37 kg, 3 W) however this system is not designed to work above 8000 nmi altitude. According to Marc Crotti, product manager for the TANS GPS receiver for Trimmble Navigation, there was talk of a GPS receiver that would work in GEO. However, if such a receiver is developed, such a receiver would not work in LEO and would be GEO specific. If this receiver is developed, the software and hardware interface will already be in place on board the vehicle and a more accurate navigational update system could be implemented.

Microcosm Autonomous Navigation System (MANS) - This system provides 600m to 1.5 km accuracies in GEO using 2 sensors. (The added accuracy comes from using the moon as a source, and any additional GEO accuracy requirements would require the mission to be planned during a week where the moon can be used as a reference.) The system works from LEO to GEO (and beyond). The system uses a dual sun angle/earth horizon sensor that also provides attitude determination. The sensor is a good compromise for mass and power (4.3 kg, 11 W per sensor). In addition, these sensors will also return orientation information. Using two sensors, the system will provide accurate coverage up to 84% of the time at GEO. (The other 16% of the time accounts for eclipses of the moon and the sun which provide navigational information discussed later.)

## A6.2.2 Orientation Update Systems

MANS Sensors (Modified Dual Cone Sensor) - These sensors return the information of both sun angle sensor and a horizon sensor. The sun angle information will determine the vehicle's orientation to an accuracy of 0.01 degrees. The horizon sensors information will determine the vehicle's orientation to an accuracy of 0.1 to 0.25 degrees. In addition, these modified sensors will detect the moon's angle and can be used to return navigational information.

Star Trackers - These sensors can determine a vehicle's orientation to an accuracy of 0.01 degrees. These sensors can also be utilized to determine the angle to a rendezvous target to an accuracy of 0.02 degrees.

# Appendix A6.1 ADCS

## Torques from cyclic and secular disturbances

### Cyclic disturbances

- **Gravity gradient torque at GEO**

$$Tg = \frac{3\mu}{R^3} |Izz-Iyy| \Theta$$

$\mu$ = earths gravity constant $\quad 3.9 \times 10^3 \dfrac{km^3}{s^2}$

$\Theta$ = off-axis from nadir = 5 deg.

R = orbital radius = 46028 km

$$Tg = 9.168 \times 10^{-5} \, N \, m$$

- **Solar Radiation Torque at GEO**

$$Tsp = PsAsLs(1+q) \cos q$$

$Ps$ = solar constant = $4.617 \times 10^{-6} \, N \, m$

$As$ = Area of surface = $10 \, m^2$

$Ls$ = center of press. to center of-mass
offset = 1 m

$q$ = angle of incidence of sun = 90 deg.

$q$ = reflective factor * .6

$$Tsp = 7.38 \times 10^{-5} \, N \, m$$

Note: solar radiation press. Tsp is highly dependent
on the surface being illuminated. For our vehicle
it will be mostly reflective surfaces.

**Secular Torque Disturbances**

• Aerodynamic Torque at GEO

$$Ta = \sum_{i=1}^{n} F_i l_i$$

$$F_i = 0.5\left[ r C_d A V^2 \right]$$

$C_d$ = coefficient of drag of each part

A = effected area of each part

V = velocity of spacecraft

r = at GEO ⁎ 0

so

Ta ⁎ 0

li = dist. from c.g. of part
to c.g. of spacecraft.

## Appendix A6.2 Navigation and Tracking

### A6.2.1 Linear Navigation and Velocity Update Systems

Ground Tracking / TDRSS - Provides accuracy from 50m to several hundred meters when tracking objects in LEO. This system, however requires a full ground crew during each vehicle mission and does not work for objects in GEO.

Space Sextant - Provides 250m accuracy. The unit however is large compared to other units (25 kg, 0.4 cubic meters) and requires more power (50 W) than other systems. The unit also requires a 24 hour scan time to achieve the stated accuracy.

Global Positioning System - Provides 25 m accuracy at LEO. The system is ideal for use in LEO (9.72 x 5 x 2 cubic inches, 1.37 kg, 3 W) however this system is not designed to work above 8000 nmi altitude. According to Marc Crotti, product manager for the TANS GPS receiver for Trimmble Navigation, there was talk of a GPS receiver that would work in GEO. However, if such a receiver is developed, such a receiver would not work in LEO and would be GEO specific. If this receiver is developed, the software and hardware interface will already be in place on board the vehicle and a more accurate navigational update system could be implemented.

Microcosm Autonomous Navigation System (MANS) - This system provides 600m to 1.5 km accuracies in GEO using 2 sensors. (The added accuracy comes from using the moon as a source, and any additional GEO accuracy requirements would require the mission to be planned during a week where the moon can be used as a reference.) The system works from LEO to GEO (and beyond). The system uses a dual sun angle/earth horizon sensor that also provides attitude determination. The sensor is a good compromise for mass and power (4.3 kg, 11 W per sensor). In addition, these sensors will also return orientation information. Using two sensors, the system will provide accurate coverage up to 84% of the time at GEO. (The other 16% of the time accounts for eclipses of the moon and the sun which provide navigational information discussed later.)

### A6.2.2 Orientation Update Systems

MANS Sensors (Modified Dual Cone Sensor) - These sensors return the information of both sun angle sensor and a horizon sensor. The sun angle information will determine the vehicle's orientation to an accuracy of 0.01 degrees. The horizon sensors information will determine the vehicle's orientation to an accuracy of 0.1 to 0.25 degrees. In addition, these modified sensors will detect the moon's angle and can be used to return navigational information.

Star Trackers - These sensors can determine a vehicle's orientation to an accuracy of 0.01 degrees. These sensors can also be utilized to determine the angle to a rendezvous target to an accuracy of 0.02 degrees.

Orientation Determination with GPS - Using 4 GPS antennas, this can be accomplished, however it would only be useful in LEO and useless in GEO.

## A6.2.3 Performance of MANS

MANS performance is based on:
- Mounting Angle
- Availability of the Moon as a Reference
- Altitude of Orbit

### A6.2.3.1 Performance Based on Mounting Angle
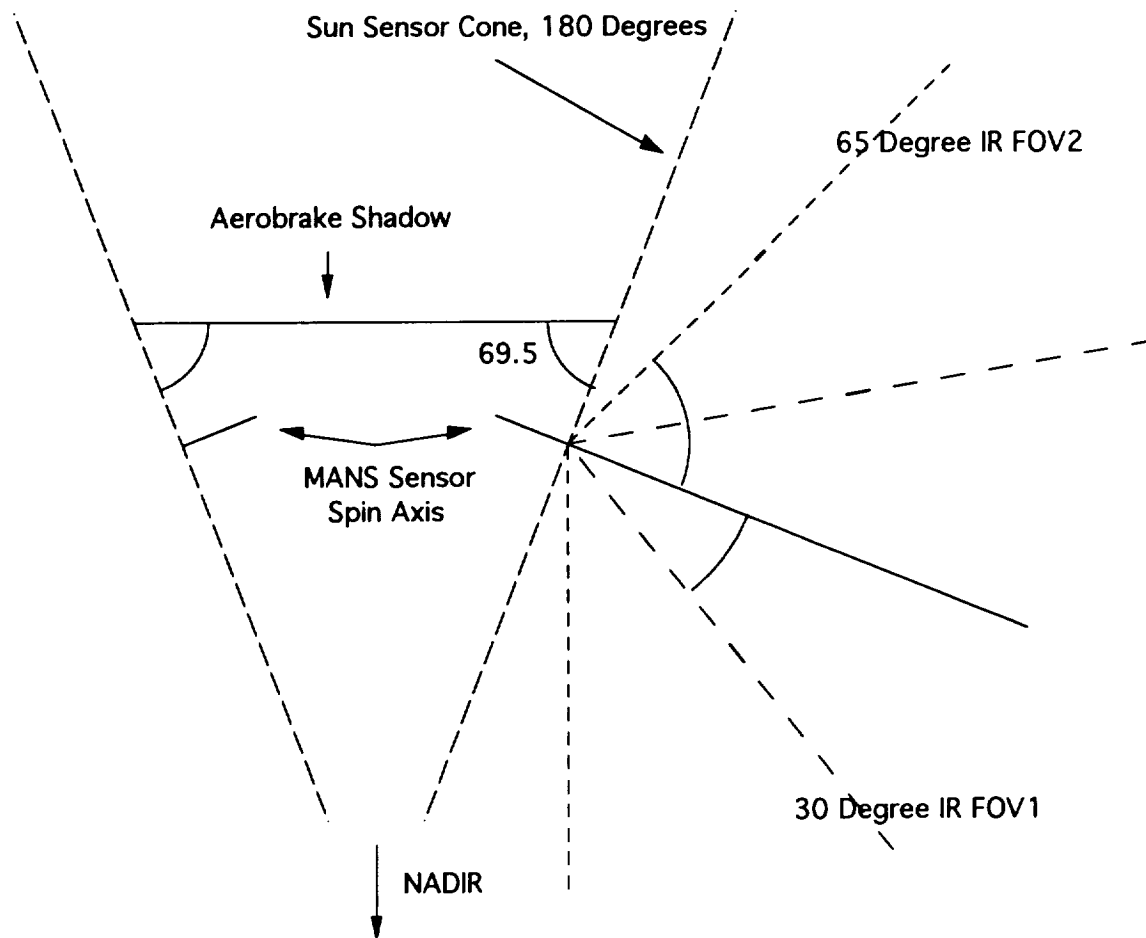


Figure A6.2.a Sensor Mounting and Scan Angles

Two MANS sensors are mounted with the head perpendicular to a 69.5 degree line with respect to the aerobrake shadow. This configuration will allow maximum sun sensor coverage while allowing the horizon sensor (FOV2) to scan the horizon of the earth. The combination of sensors gives 4 horizon crossings. The sensors heads must be mounted so they are outside this 69.5 degree cone to ensure the aerobrake shadow does not increase the blackout time; the shadow should fall outside the sun

sensing cone.



20.5 Degree Half Angle
Blackout due to Mounting Angle

MOOSE

8.5 Degree Half Angle
Blackout due to Eclipse of Sun by Earth
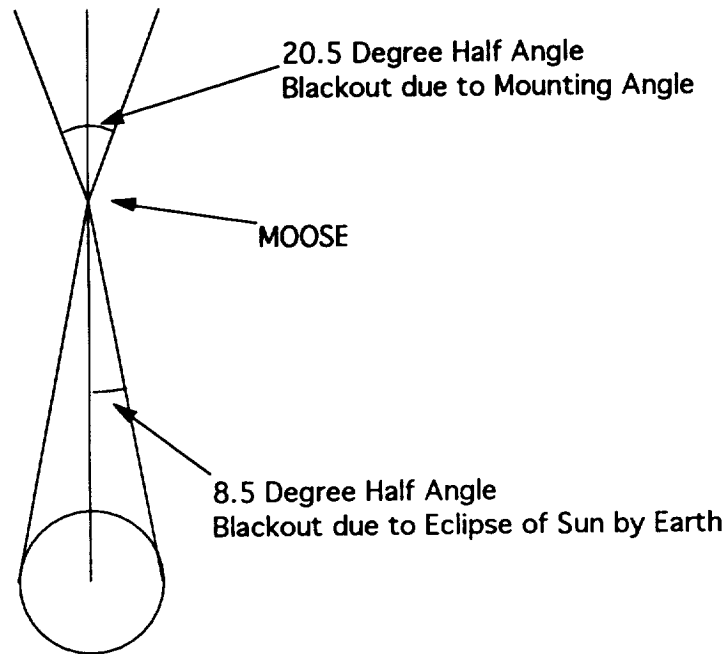
**Figure A6.2.b** Sun Blackout Regions in GEO

With the vehicle orbiting at GEO, the problem of detecting the sun can be approximated as a 2-D problem. In this problem, 2 blackout regions occur. The eclipse of the sun by the earth accounts for a region of 17 degrees lost. The sun sensor blind spot accounts for 41 degrees lost. This gives a total of 16% blackout time. In GEO this results in a blackout of 1.2 hours due to earth eclipsing and 2.6 hours of blackout due to the sun sensor blind spot. However, this blackout time results in a loss of precision, not a total loss of navigation. The altitude accuracy returned by the optical sensors will degrade to an accuracy of over 6 km. The vehicle can rely on inertial navigation until after the blackout, however, the accuracy of re-entry can not be met unless the vehicle can begin before inertial navigation degrades to an unacceptable error level.

The mission can also be planned to minimize the blackout time. The transfer to GEO can be timed such that the sun sensor blind spot is just past the sun when the vehicle switches from GPS to MANS at just under 8000nmi. The transfer orbit will have already been determined at this time by GPS and should be fairly accurate. The next sensor blind spot is then over 10 hours away. This is enough time to accurately compute the vehicle's orbit in GEO using Kalman filtering software.

## A6.2.3.2 Availability of the Moon as a Reference

The MANS system's accuracy can be improved from 1.5 km to 600 m if the moon is available as a reference. The MANS system computes the vehicles orbit by utilizing two scans of the sun or by using one scan of the sun and one scan of the moon. The latter is more accurate, providing 32m accuracy at LEO and 500 - 600 m accuracy at GEO. If greater accuracy is ever required at GEO, the mission could be limited to a week of the month when the moon is available as a reference.

## A6.2.3.3 Effects of Vehicle Altitude on Accuracy

The accuracy of the vehicle's measured altitude decreases in GEO, causing a loss of accuracy overall. The altitude as determined by a horizon sensor can be found using the following equation:

$$\cos \rho = \frac{\sqrt{E^2 - R_E^2}}{E}$$

where $\rho$ is the angular radius of the earth as measured by the sensor, Re is the actual radius of the earth, and E is the distance of the sensor from the center of the earth.

Using 2 MANS sensors, the error in $\rho$ is 0.023 degrees. At GEO, therefore, an error in altitude of 12.5 km is given from one reading. To gain extra accuracy, the MANS system uses kalman filtering, along with sun angle readings to improve accuracy. If navigational course information and current IMU information is used to improve the accuracy, an accuracy of 1.5 km can be achieved. This is assuming that kalman filtering can improve the accuracy by a factor of between 5 and 10. Microcosm claims that a kalman filtering update can be provided every 25 seconds, while still achieving this accuracy.

It is apparent that the navigation system at GEO will be dependent on kalman filtering, and therefore it will be heavily software dependent.

# Appendix A6.3 Communications

## A6.3.1 Computer Program for Link Budget

Program downlink

```
      real  frequency,trpw,trlogpw,trll,trabeam,ptrgain,trapo
      real  trapl,tragain,pploss,propoloss,rad,prag,raploss
      real  rag,snt,datarate,eirp,rho,lambda,ebno,cno,reqebno
      real  imploss,margin,trad,rape,ber,rab,spaceloss,re

      open (unit=8,file="down1",status="new")
      write (8,49)
49    format (1x,'downlink worst case')
      write (8,50)
      write (9,50)
50    format(1x,'frequency')
      read (9,*) frequency
      write (8,65) frequency
65    format (1x,f10.5)
      write (8,51)
      write (9,51)
51    format(1x,'transmit power')
      read (9,*) trpw
      write (8,66) trpw
66    format (1x,f10.5)
      write (8,52)
      write (9,52)
52    format(1x,'transmit line loss')
      read (9,*) trll
      write (8,67) trll
67    format (1x,f10.5)
      write (8,54)
      write (9,54)
54    format(1x,'transmit antenna pointing offset')
      read (9,*) trapo
      write (8,69) trapo
69    format (1x,f10.5)
      write (8,56)
      write (9,56)
56    format(1x,'propagation path loss')
      read (9,*) altitude
      write (8,71) altitude
71    format (1x,f15.5)
      write (8,57)
      write (9,57)
```

```fortran
57    format(1x,'propagation and polarization loss')
      read (9,*) propoloss
      write (8,72) propoloss
72    format (1x,f10.5)
      write (8,58)
      write (9,58)
58    format(1x,'receive antenna diameter')
      read (9,*) rad
      write (8,73) rad
73    format (1x,f10.5)
      write (8,59)
      write (9,59)
59    format(1x,'receive antenna pointing error')
      read (9,*) rape
      write (8,74) rape
74    format (1x,f10.5)
      write (8,60)
      write (9,60)
60    format(1x,'system noise temp')
      read (9,*) snt
      write (8,75) snt
75    format (1x,f10.5)
      write (8,61)
      write (9,61)
61    format(1x,'data rate')
      read (9,*) datarate
      write (8,76) datarate
76    format (1x,f15.5)
      write (8,62)
      write (9,62)
62    format(1x,'bit error rate')
      read (9,*) ber
      write (8,77) ber
77    format (1x,f15.5)
      write (8,63)
      write (9,63)
63    format(1x,'required Eb/No')
      read (9,*) reqebno
      write (8,78) reqebno
78    format (1x,f15.5)
      write (8,64)
      write (9,64)
64    format(1x,'implementation loss')
      read (9,*) imploss
      write (8,79) imploss
79    format (1x,f10.5)
```

```
      do 150 trabeam= 1.0,3.1,0.1

   re = 6378.0
      trad = ( 21.0/ ( frequency * trabeam ))
      trlogpw = 10.0*alog10(trpw)
      ptragain = 44.3 - 10.0*alog10(trabeam**2)
      trapl = -12.0* (trapo**2/trabeam**2)
      tragain = ptragain + trapl
      eirp = trlogpw + trll + tragain

c              find path length from altitude

      rho = asin ( re / ( re + altitude ))
      rho = 57.29577951 * rho
      lambda = 90.0 - rho
      lambda = lambda*.017453292
      pploss = re*tan(lambda)

      spaceloss = -92.44 - 20.0*ALOG10(pploss) -
    + 20.0*ALOG10(frequency)
      prag = 20.40+ 20*alog10(rad)+ 20*alog10(frequency)- 2.5964
      rab = 21.0/(frequency * rad)
       raploss = -12.0*(rape**2/rab**2
      rag = prag + raploss
      ebno = trlogpw + trll + tragain + propoloss + spaceloss
    +     + rag +228.6 - 10*alog10(snt) - 10*alog10(datarate)
      cno = eirp + pploss + propoloss + rag/snt + 228.
      margin = ebno - reqebno + imploss
      write (8,100) trabeam,ptragain,margin,trad
      write (9,100) trabeam,ptragain,margin,trad
100   format(1x,'trabeam',f10.5,1x,'ptragain',f10.5,1x,'margin',
    +     f10.5,1x,'trad',f10.5)

150   continue
      close (unit=8)
      pause
      end
```

## A6.3.2  Solution for Downlink

downlink worst case
 frequency
  12.00000
 transmit power
  20.00000

transmit line loss
-1.00000
transmit antenna pointing offset
.20000
propagation path loss
38756.00000
propagation and polarization loss
-.50000
receive antenna diameter
5.30000
receive antenna pointing error
.20000
system noise temp
552.00000
data rate
6400000.00000
bit error rate
0.00000
required Eb/No
15.00000
implementation loss
-2.00000

| | | | | | | | |
|---|---|---|---|---|---|---|---|
| trabeam | 1.00000 | ptragain | 44.30000 | margin | 13.89308 | trad | 1.75000 |
| trabeam | 1.10000 | ptragain | 43.47215 | margin | 13.14854 | trad | 1.59091 |
| trabeam | 1.20000 | ptragain | 42.71637 | margin | 12.45613 | trad | 1.45833 |
| trabeam | 1.30000 | ptragain | 42.02113 | margin | 11.81020 | trad | 1.34615 |
| trabeam | 1.40000 | ptragain | 41.37744 | margin | 11.20563 | trad | 1.25000 |
| trabeam | 1.50000 | ptragain | 40.77817 | margin | 10.63792 | trad | 1.16667 |
| trabeam | 1.60000 | ptragain | 40.21760 | margin | 10.10320 | trad | 1.09375 |
| trabeam | 1.70000 | ptragain | 39.69102 | margin | 9.59802 | trad | 1.02941 |
| trabeam | 1.80000 | ptragain | 39.19455 | margin | 9.11949 | trad | .97222 |
| trabeam | 1.90000 | ptragain | 38.72493 | margin | 8.66505 | trad | .92105 |
| trabeam | 2.00000 | ptragain | 38.27940 | margin | 8.23248 | trad | .87500 |
| trabeam | 2.10000 | ptragain | 37.85561 | margin | 7.81985 | trad | .83333 |
| trabeam | 2.20000 | ptragain | 37.45155 | margin | 7.42546 | trad | .79545 |
| trabeam | 2.30000 | ptragain | 37.06544 | margin | 7.04781 | trad | .76087 |
| trabeam | 2.40000 | ptragain | 36.69578 | margin | 6.68553 | trad | .72917 |
| trabeam | 2.50000 | ptragain | 36.34120 | margin | 6.33749 | trad | .70000 |
| trabeam | 2.60000 | ptragain | 36.00053 | margin | 6.00261 | trad | .67308 |
| trabeam | 2.70000 | ptragain | 35.67273 | margin | 5.67998 | trad | .64815 |
| trabeam | 2.80000 | ptragain | 35.35684 | margin | 5.36870 | trad | .62500 |
| trabeam | 2.90000 | ptragain | 35.05204 | margin | 5.06805 | trad | .60345 |
| trabeam | 3.00000 | ptragain | 34.75758 | margin | 4.77733 | trad | .58333 |

## A6.3.3 Power Consumption of various data rates at different altitudes

| Altitude | Combined | Voice | Telemetry | Video |
|---|---|---|---|---|
| 1.50e+04 | 4.17 | 0.0417 | 0.19802 | 3.9100 |
| 1.60e+04 | 4.61 | 0.0461 | 0.22110 | 4.3210 |
| 1.70e+04 | 5.07 | 0.0507 | 0.24309 | 4.7510 |
| 1.80e+04 | 5.55 | 0.0555 | 0.26604 | 5.1994 |
| 1.90e+04 | 6.04 | 0.0604 | 0.28995 | 5.6667 |
| 2.00e+04 | 6.56 | 0.0656 | 0.31482 | 6.1520 |
| 2.10e+04 | 7.10 | 0.0710 | 0.34065 | 6.6578 |
| 2.20e+04 | 7.66 | 0.0766 | 0.36745 | 7.1810 |
| 2.30e+04 | 8.24 | 0.0824 | 0.39520 | 7.7240 |
| 2.40e+04 | 8.84 | 0.0884 | 0.42392 | 8.2850 |
| 2.50e+04 | 9.46 | 0.0946 | 0.45360 | 8.8650 |
| 2.60e+04 | 10.1 | 0.101 | 0.48423 | 9.4630 |
| 2.70e+04 | 10.8 | 0.108 | 0.51583 | 10.081 |
| 2.80e+04 | 11.4 | 0.114 | 0.54839 | 10.720 |
| 2.90e+04 | 12.1 | 0.121 | 0.58191 | 11.373 |
| 3.00e+04 | 12.8 | 0.128 | 0.61640 | 12.047 |
| 3.10e+04 | 13.6 | 0.136 | 0.65184 | 12.740 |
| 3.20e+04 | 14.3 | 0.143 | 0.68824 | 13.450 |
| 3.30e+04 | 15.1 | 0.151 | 0.72561 | 14.181 |
| 3.40e+04 | 15.9 | 0.159 | 0.76394 | 14.930 |
| 3.50e+04 | 16.7 | 0.167 | 0.80323 | 15.698 |
| 3.60e+04 | 17.6 | 0.176 | 0.84348 | 16.484 |
| 3.70e+04 | 18.4 | 0.184 | 0.88468 | 17.290 |
| 3.80e+04 | 19.3 | 0.193 | 0.92686 | 18.110 |
| 3.88e+04 | 20.0 | 0.200 | 0.96129 | 18.787 |

## A6.3.4 Sensor Rates

Sensors, sometimes called transducers, are sensing devices which measure a physical parameter. The sensors used on MOOSE are local environment sensors that measure internal measurements. Sensors can either be sensors that measure internal measurements or scientific data. Sensors can either be self-generating or those that need an external voltage supply. Thermocouples are an example of self-generating sensors. Potentiometers, strain gauges, and variable capacitors are examples of dependent sensors.

Sensors will give constant data and the computer will sample the data at certain rates. Therefore the data will not be read sequentially, and any excess data memory on a particular sampling will be allocated to the next sampling This assumption is made so that data that is not sampled every second can be averaged so it can be combined with data rates that are in bits per second. Navigation and tracking data rates are an example.

These are the data rates for all of the sensors on MOOSE. The data rates are read by the computer. The computer then sends the data to either storage, the cockpit, or earth. Some data will be sent to two or three of these areas. These are the estimated sensor data rates by subsection:

## A 6.3.4.1 Structure

1. Back Surface Heat Sensor for Aerobrake
   { Thermocouple }
   - sample only during aerobrake maneuvers
   - range  0°-350° ;  resolution = .085°
   - 12 Bits at 100/s
   - 4 sensors - 1 for each quadrant of aerobrake                            4800 bps

2. Angle Attack Indicator
   { Potentiometer}
   - sample only during aerobrake maneuvers
   - range 0°- 20° ;  resolution .078°
   - 8 Bits at 100/s
   - 2 sensors - 1 for each side of spacecraft                         <u>1600 bps</u>

                                                          <u>Total :         6400 bps</u>

## A6.3.4.2  Life Support

1. Temperature  { Thermocouple }
   - range 60°- 80°
   - 8 Bits at 1/s
   - 2 sensors for redundancy                                        16 bps

2. Oxygen Tank Pressure { Pressure Transducer }
   - 8 Bits at 1/s
   - 2 sensors for redundancy                                        16 bps

3. Nitrogen Tank Pressure { Pressure Transducer }
   - 8 Bits at 1/s
   - 2 sensors for redundancy                                        16 bps

4. Radiation { high-impedance voltmeter monitors ion
              flow between electrodes }
   - range 10E-6 - 10E-4 amps

### A6.3.4.3 Man/ Grap

1. Load Sensor
   - 12 Bits at 2/s
   - 6 for arm                                              144 bps
2. Strain Gauges
   - 12 Bits at 2/s
   - 6 for arm                                              144 bps
3. Motor Decoders { measure rpm digitally }
   - 16 Bits at 20/s
   - 7 sensors                                            2240 bps

4. Power Consumption { Voltmeter }
   - 12 Bits at 1/s                                         12 bps


                                                      Total : 2540 bps

- multiply by two for both manipulators and grappling arms

                                                      Total : 5080 bps


### A6.3.4.4 Propulsion

1. Hydrogen Fuel Pump  { Pressure Transducer }
   - 12 Bits at 100/s                                     1200 bps

2. Hydrogen Fuel Turbine
   - Blade Housing { Thermocouple }
   - 12 Bits at 1000/s                                   12000 bps
   - Shaft { Strain gauge }
   - 12 Bits at 100/s                                     1200 bps
   - Motor Decoders
   - 12 Bits at 100/s                                     1200 bps

3. Oxidizer Fuel Pump  { Pressure Transducer }
   - 12 Bits at 100/s                                     1200 bps

4. Oxidizer Fuel Turbine
   - Blade Housing { Thermocouple }
   - 12 Bits at 1000/s                                   12000 bps
   - Shaft { Strain gauge }
   - 12 Bits at 100/s                                     1200 bps
   - Motor Decoders
   - 12 Bits at 100/s                                     1200 bps

5. Three Shut Off Valves
- On/Off { Switch }
- 1 Bit at 100/s x 3                                          300 bps
- Redundancy
- Up Flow { Pressure Transducer }
- 8 Bits at 100/s x 3                                        2400 bps
- Down Flow { Pressure Transducer }                          2400 bps

6. Nozzle Heat { Thermocouple }
- 12 Bits at 1000/s                                         12000 bps

7. Combustion Chamber
- Chamber Pressure { Pressure Transducer }
- 12 Bits at 10,000/s                                      120,000 bps
- Chamber Temperature { Thermocouple }
- 12 Bits at 10,000/s                                     <u>120,000 bps</u>

8. Tank Pressure { Pressure Transducer }
- 12 bits at 10/s
- 4 tanks ( 2 fuel & 2 oxidizer )                            480 bps

9. Tank Level
- 12 bits at 10/s
- 4 tanks ( 2 fuel & 2 oxidizer )                            480 bps

                                                       = 288060 bps

                                                      <u>Total : 288 kbps</u>

## A6.3.4.5 Navigation/ Tracking

1. Dual Cone Sensor
- 56 Bits at once every 25 seconds
- 2 sensors                                                    5 bps

2. GPS Receiver
- 80 Bits at 2/s                                             160 bps

3. Rendezvous Radar { used only during rendezvous }
- 48 Bits once every 300 seconds                              1 bps

4. Star Tracker
- 30 Bits once every 60 seconds                               1 bps

5. Power Consumption { Volt Meter }
   - 12 Bits at 1/s                                            12 bps

                                                              = 179 bps

                                                          Total: 180 bps

## A6.3.4.6  Attitude Control System

1. Rate Gyro
   - 16 Bits at 100/s                                         1600 bps

2. Accelerometers
   - 16 Bits at 100/s                                         1600 bps

3. Temperature { Thermocouple }
   - Gyros
   - 8 Bits at 10/s                                             80 bps
   - Inertial Measurement Unit
   - 8 Bits at 10/s                                             80 bps
4. Power Consumption { Volt Meter }
   - 12 Bits at 1/s                                            12 bps

                                                             = 3372 bps

                                                         Total: 3380 bps

## A6.3.4.7  Reaction Control System

1. Tank Pressure { Pressure Transducer }
   - 12 Bits at 10/s
   - 4  Tanks x 2 sensors each for redundancy                 960 bps

2. Thruster Temperature  { Thermocouple }
   - 12 Bits at 10/s
   - 16 Thrusters                                            1920 bps

3. Power Consumption { Volt Meter }
   - 12 Bits at 1/s                                            12 bps

                                                             = 2892 bps

                                                         Total: 2900 bps

# Appendix A6.4 CDMS

## A6.4.1 Analogy from the Automotive Industry

The automotive industry faces many of the same challenges that the space systems industry faces. More and more sophisticated electronics must be integrated together as cars become increasingly computerized. Automotive systems have to coordinate the activities of microprocessors, microcontrollers, digital signal processing chips (DSPs), application specific ICs (ASICs), and smart sensors and actuators.

The increasing number of wiring cables and connector contacts is leading to long production times, higher labor costs, cramped body space, and decreased reliability. Another concern is the reliability of complex, interacting functions, which can not be exposed to the weakness of point-to-point wiring.

The obvious solution is to multiplex data through one serial line or bus tied to the vehicle Electronic Control Units (ECUs). Multiplexing allows data from different sources—sensors, switches, and ECUs, to be be sent over a common bus, typically consisting of four wires. Two conductors are used for signal transmission, the other two for power and ground.

Limitations of ring and star networks has led the auto industry to select a linear bus structure for high-speed networking. This scheme gives every network node the same right to access the bus. Arbitration among nodes is done by prioritizing the addresses of the messages.

The Multiplexing Standards Committed of the Society of Automotive Engineers (SAE) has partitioned the data-rate requirements for automotive serial communications into three segments.

Class A defines parameters for body control applications where high data speed and accuracy levels are not critical. These include turn signal, headlights, entertainment systems, etc. Data rates of up to 1 kbit/s are handled, with up to 100 nodes. Latency time between transmission request and transmission initiation is 50 ms.

Class B refers to information shared systems with moderate speed (up to 100 kbits/s) and accuracy requirements that consist of up to 50 nodes. Applications include communication between sensors and instrumentation clusters. Class B data does not control the automotive subsystems, and is not transmitted in real time.

Class C protocols are for real-time control applications with critical speed and accuracy requirements, such as communication between engine and transmission, or between ABS sensors and brake actuators. The higher data rates of Class C (up to 1Mbit/s) reduce the maximum number of nodes allowed to 10, and latency time decreases to under 5 ms.

# Appendix

## 8.1 Acronyms

| | |
|---|---|
| ACS | Attitude Control System |
| AFB | Air Force Base |
| ASE | Airborne Support Equipment |
| ASP | Assessment Flight Profile |
| CAM | Collision Avoidance Maneuvers |
| CAP | Crew Activity Plan |
| CCTC | Common Cryogenic Transfer Coupling |
| CCZ | Command and Control Zone |
| CFP | Conceptual Flight Profile |
| CPCB | Crew Procedures and Control Board |
| CSOCC | Client Spacecraft Operations Control Center |
| CSR | Customer Support Room |
| DEM/VAL | Demonstration & Validation |
| DoD | Department of Defense |
| ELV | Expendable Launch Vehicle |
| ENAE | Department of Aerospace Engineering |
| EVA | Extra-Vehicular Activity |
| FCO | Flight Control Officer |
| FCR | Flight Control Room |
| FDF | Flight Data Files |
| GC | Ground Control |
| GCT | Ground Configuration Terminal |
| GEO | Geosynchronous Orbit |
| GNAC | Guidance/Navigation/Control |
| GN2 | Gaseous Nitrogen |
| GPS | Global Positioning System |
| GSFC | Goddard Space Flight Center |
| GSTDN | Ground Spacecraft Tracking & Data Network |
| GTO | Geosynchronous Transfer Orbit |
| I-Loads | Initial Software Loads |
| IMU | Inertial Measurement Unit |

| | |
|---|---|
| IVA | Intra-Vehicular Activity |
| JSC | Johnson Spaceflight Center |
| KSC | Kennedy Spaceflight Center |
| LH2 | Liquid Hydrogen |
| LiO2 | Lithium Dioxide |
| LO2 | Liquid Oxygen |
| MAP | Mission Activity Plan |
| MCC | Mission Control Center |
| MFC | MSSS Flight Computers |
| MOC | Mission Operations Center |
| MOSC | MSSS Operations Support Center |
| MSC | MSSS Flight Computer |
| MSSS | Manned Satellite Servicing System |
| MSSSPO | MSSS Project Office |
| MSSSTF | MSSS Training Facility |
| NASA | National Aeronautics and Space Administration |
| NASCOM | NASA Communications Network |
| NTO | Nitrogen Tetroxide |
| OFP | Operational Flight Profile |
| OMV | Orbital Maneuvering Vehicle |
| ORU | Orbital Replacement Unit |
| OTF | Orbiter Training Facility |
| PDA | Pressurized Docking Assembly |
| PMC | Permanently Manned Capability |
| PMV | Propellant Maneuvering Vehicle |
| POCC | PMV Operations Control Center |
| PROXO | Proximity Operations Officer |
| PROXOPS | Proximity Operations |
| RDZ | Rendezvous/Departure Zone |
| RMS | Remote Manipulator System |
| SSCC | Space Station Control Center |
| SSL | Space Systems Laboratory |
| SSF | Space Station Freedom |
| SSFMS | Space Station Freedom Mission Simulator |
| SSFPO | Space Station Freedom Program Office |

| SSPOZ | Space Station Proximity Operations Zone |
| TDRS | Tracking and Data Relay Satellite |
| TDRSS | Tracking and Data Relay Satellite System |
| UMCP | University of Maryland, College Park |
| VAFB | Vandenberg Air Force Base |
| V-bar | Velocity Vector Direction |
| WETF | Weightless Environment Training Facility |
| WTR | Western Test Range |

## 8.2 Example Final Approach

Figures A8.1 to A8.3 represent the $\Delta V$'s for various times at different points during the final approach, based upon equations 8.1.1-4. The satellite is assumed to be in a geosynchronous orbit (42160 km) and MOOSE is initilally at $\vec{\rho_0} = [580\hat{i} - 580\hat{j} + 580\hat{k}]m$. The initial relative velocity is assumed to be zero

for figure A8.1a, but for figures A8.1b, A8.1c & A8.1d, the velocities are assumed to be the chosen velocities of the previous gates. Choice of $\Delta V$= 10.02 m/s is based on the lowest $\Delta V$ in figure A8.1a, while in figure A8.1b, the choice $\Delta V$= -9.99 m/s is the limit (approximately) as the $\Delta V$ values level off over time. A $\Delta V$ of -0.33 m/s was chosen from figure A8.1c since, although there are lesser values, 300s (5 min) should give the pilot whatever time he/she needs before executing the next maneuver. In figure A8.1d, a $\Delta V$= -0.11 was chosen since this was the lowest $\Delta V$. Once the pilot is within grappling range (ie. within 5m of the target satellite), he/she uses the cold gas thrusters to bring the vehicle to zero velocity relative to the target satellite.
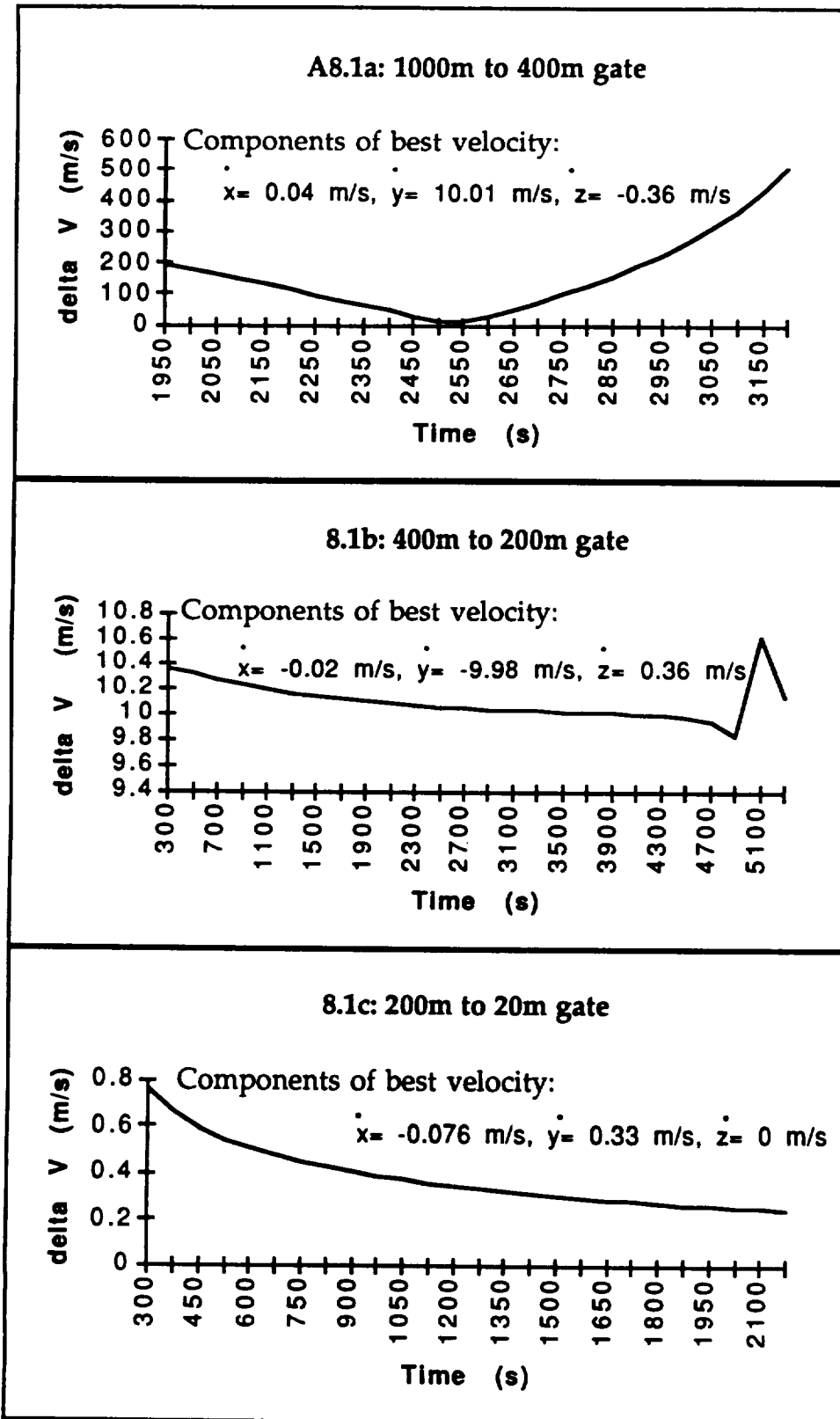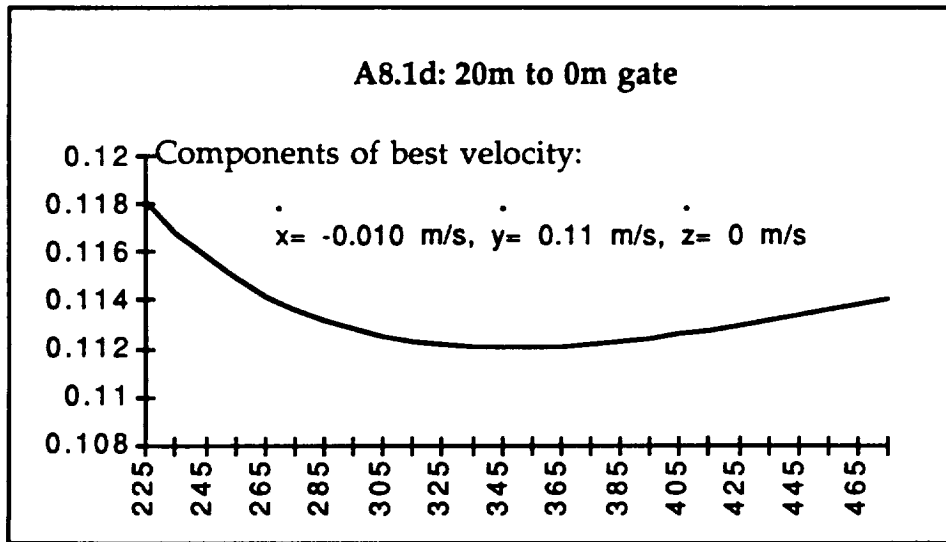
## A8.1a: 1000m to 400m gate

Components of best velocity:

$\dot{x}$= 0.04 m/s, $\dot{y}$= 10.01 m/s, $\dot{z}$= -0.36 m/s

(y-axis: delta V (m/s), values 0, 100, 200, 300, 400, 500, 600)
(x-axis: Time (s), values 1950, 2050, 2150, 2250, 2350, 2450, 2550, 2650, 2750, 2850, 2950, 3050, 3150)

## 8.1b: 400m to 200m gate

Components of best velocity:

$\dot{x}$= -0.02 m/s, $\dot{y}$= -9.98 m/s, $\dot{z}$= 0.36 m/s

(y-axis: delta V (m/s), values 9.4, 9.6, 9.8, 10, 10.2, 10.4, 10.6, 10.8)
(x-axis: Time (s), values 300, 700, 1100, 1500, 1900, 2300, 2700, 3100, 3500, 3900, 4300, 4700, 5100)

## 8.1c: 200m to 20m gate

Components of best velocity:

$\dot{x}$= -0.076 m/s, $\dot{y}$= 0.33 m/s, $\dot{z}$= 0 m/s

(y-axis: delta V (m/s), values 0, 0.2, 0.4, 0.6, 0.8)
(x-axis: Time (s), values 300, 450, 600, 750, 900, 1050, 1200, 1350, 1500, 1650, 1800, 1950, 2100)

Figure 8.1a-c

**A8.1d: 20m to 0m gate**

Components of best velocity:

x= -0.010 m/s,  y= 0.11 m/s,  z= 0 m/s

**Figure 8.1d**

## 8.3 Typical ORU's

* Limited life components requiring routine replacement:

  * Battery Modules[8](~90 kg)[9]
  * Reaction Wheels[8](~10-55 kg)[9]
  * Solar Arrays[8](~70-90 kg , ~9-12 m² rolled sheets)[9]
  * Tape Recorders[8](~14 kg)[9]

* Indefinite life components requiring periodical replacement:

  * Sun Sensor Module[8](~1.5 kg)[9]
  * Command & Data Management[8](~30 kg)[9]
  * Low gain Antenna Assembly[8](~10kg)[9]
  * Power Switching & Distribution[8](~30 kg)

## A8.4 Typical Consumables

- Liquids[8] (~80-140 kg)[9]:

  - Earth Temperature Storables:
    - $N_2O_4$
    - MMH
    - Water

  - Space Temperature Storables:
    - Oxidizers
    - Fuels

- Cryogenic Temperature Storables:
  - $O_2$
  - $H_2$
  - Helium

- Gases[8] (~4kg)[8]:

  - Earth Temperature storables:
    - Oxygen
    - Air
    - Nitrogen

  - Cryogenic Temperature Storables:
    - Oxygen
    - Hydrogen

# References

Asada, Haruhiko and Kamal Youcef-Toumi. *Direct Drive Robots: Theory and Practice.* MIT Press. Cambridge, MA. 1987.

Ault, Norman and Zarobsky. *Fundamentals of Flywheel Design..* 1958.

Avallone, Eugene A. and Theodore Baumeister III. *Marks' Standard Handbook for Mechanical Engineers, ninth edition.* McGraw-Hill Book Company. 1987.

Barnes, Robert and Frank Tai, "The Dual Cone Sensor: An Enhanced Performance, Low Cost Earth Sensor", *Advances in the Astronautical Sciences, Guidance and Control,* 1989

Bleazard, G.B., *Introducing Satellite Communications.* NCC. Publications, England,1985.

Bzibziak, R. "Miniature Cold Gas Thrusters," AIAA Paper 92-3256. July 1992, 8 pages.

Cantafio, Leopold J., *Space-Based Radar Handbook,* Artech House, Inc, 1989.

Chetty, P.R.K., *Satellite Technology and its Applications.* Tab Books, Germantown, Maryland, 1988.

Craig, John J. *Introduction to Robotics: Mechanics & Control.* Addison-Wesley. Reading, MA. 1986.

Elbert, Bruce R., *Introduction To Satellite Communication.* Artech House, Massachusetts,1987.

Foster, LeRoy E., *Telemetry Systems..* John Wiley and Sons, Inc. London. 1965.

Greensite, Arthur L. *Control Theory: Volume II -- Analysis and Design of Space Vehicle Flight Control Systems.* Spartan Books. Washington. 1970.

*Handbook of Batteries and Fuel Cells.* McGraw-Hill. 1984.

Holzbock, Werner G. *Robotic Technology: Principles and Practices.* Reinhold Co. New York. 1986.

Howle, D.H. "Man in Space" *The Space Environment.* University of London Press Ltd., London, 1969.

Jensen, Jurgen, et. al. *Design Guide to Orbital Flight.* McGraw-Hill. NewYork. 1962.

Lopes, Roberto V.F. and Helio K. Kuga, "Optimal Estimation of Local Orbit from GPS Measurements", *AIAA*, Feb. 26, 1987.

McKerrow, Phillip John. *Introduction to Robotics.* Addison-Wesley. New York. 1991.

Merril, Grayson.*Handbook of Satellites and Space Vehicles.* D. Van Nostrand Company,Inc. Princeton, NJ. 1965.

Navtech Seminars, Inc., "Fundamentals of GPS", *Course 101*, Tysons Corner, May 18,1992.

Noerdlinger, Peter D. and Frank Tai, "A Low Cost Autonomous Navigation System", *Advances in the Astronautical Sciences, Guidance and Control*, 1989.

"OTV Concept Definition + Evaluation - Subsystem Trade Studies" Vol II, Book 3,  paper NAS8-36108, 1985.

Pitman, George R., *Inertial Guidance*, Wiley & Sons, New York, 1962.

Rivin, Eugene I. *Mechanical Design of Robots.* McGraw-Hill, Inc. New York. 1988.

Rocket Research Company. *Hydrazine Handbook.* Aerospace Division, Olin Defense Systems Group.

Sciulli, Joseph A., and Wilbur L. Pritchard, " Satellite Communication Systems Engineering," Prentice-Hall, Englewood Cliffs, N.J.,1986.

Stark, John and Peter Fortescue, eds. " Spacecraft Systems Engineering," John Wiley and Sons, England.

Sutton, George P. *Rocket Propulsion Elements: An Introduction to the Engineering of Rockets.* John Wiley & Sons, Inc. New York. 1992.

Van Wylen, Gordon J. and Richard E. Sonntag. *Fundamentals of Classical Thermodynamics.* John Wiley & Sons, Inc. New York. 1986.

Wertz, James R. *Spacecraft Attitude Determination and Control.* Kluwer Academic Publishers. Boston. 1978.

Wertz, James R. and Wiley J. Larson, ed. *Space Mission Analysis and Design.* Kluwer Academic. Boston. 1991.